

THE CONTROLLED RELEASE OF REACTIVE  
DIATOMIC MOLECULES FROM *PERI*- AND  
*PERI*-LIKE SUBSTITUTED DISULFIDES



UNIVERSITY OF  
BIRMINGHAM

By

**CONNOR PRIOR**

A thesis submitted to The University of Birmingham for the degree of

DOCTOR OF PHILOSOPHY

School of Chemistry

The University of Birmingham

October 2022

UNIVERSITY OF  
BIRMINGHAM

**University of Birmingham Research Archive**

**e-theses repository**

This unpublished thesis/dissertation is copyright of the author and/or third parties. The intellectual property rights of the author or third parties in respect of this work are as defined by The Copyright Designs and Patents Act 1988 or as modified by any successor legislation.

Any use made of information contained in this thesis/dissertation must be in accordance with that legislation and must be properly acknowledged. Further distribution or reproduction in any format is prohibited without the permission of the copyright holder.

## Dedication

*This PhD thesis is dedicated to those postgraduate students who have struggled, are struggling and will struggle with their mental health. 70% of us experience symptoms of depression. Academia is changing. I look forward to what is on the horizon.*

## Acknowledgements

Firstly, I would like to thank Dr Richard Grainger. His guidance and mentorship throughout my degree has been invaluable. I have learnt a lot from him, not just chemistry but other aspects of academia which I am extremely grateful for. This project would not have been possible without Dr Ian Pocock. His new synthetic route into the dilithio-acenaphthene, optimisation of the dilithiation of carbazole and general guidance helped me significantly. He was also always happy to proofread any documents I gave to him and spit ball any ideas with me.

Prof. Nicholas Leadbeater, Dr Shelli Miller and the rest of the Leadbeater group at UCONN were fantastic to work with. I wish my time stateside wasn't so short, and I will be visiting again. Shelli is a dear friend who I miss greatly – she is always there for me. I also want to thank her partner Brandon who, with Shelli, allowed me to stay in their home for a month. A truly wonderful and accommodating couple.

Friendship is important during a PhD. I found it difficult, and I did want to give up on some days. On those days Charlotte Farrow, Izzy Barker, Jamie Bradley, Russell Wood, Kesar Jagdev, Matt Wilkinson, George Williamson, Harry Bird, Nick Cundy, Alya Alotaibi, Luke Watson, Richard Mudd, Ed Wilkinson, Alice Sayers, and many others kept me going and made me

laugh. I found that the strong friendship with these people gave me the opportunity to vent and seek advice from them.

Lindsey Dalzell, Josh Herrington, Liam Armstrong, Robert Kyles, Jack Craven, Tom Engel, Conall Borowski, Matt Smith and many of my other friends who are non-chemists gave me a wonderful outlet to relax and not think about my PhD. This is something I am truly grateful for.

There was one month during my PhD, where I had to sleep on sofas, couches, and blow-up beds. Izzy Barker, Alice Sayers, Richard Mudd, George Williams, Jamie Bradley, and Charlotte Farrow opened their doors to me and really helped me out. Thank you so much. You all helped in this project in your own way.

Dr Ian George was a postdoctoral research associate in the Clarke group during my MChem year. He taught me that a reaction not working is good because you learnt something. Throughout this PhD, his friendship, and unique ways of keeping my moral up have been very important to me. He's also been very keen to proofread any materials I have sent him. He also taught me that whilst the yields within this body of work are "low" they are excellent for the field and that my impact has made a change.

The analytical facilities in Birmingham are second to none. Dr Cécile Le Duff, Dr Louise Male, Dr Chris Williamson, Chi Wai Tsang and the late Peter Ashton were absolutely critical to this work. Particularly to Louise and Cécile – I cannot thank you enough.

My family – Mam, Dad, Roisin, and Shay. You've always been there and made me smile. I love Roisin's hugs upon me walking in through the front door in Leeds. During the lonely days in Birmingham, it was hard, but you guys made it easier. As well as the emotional support, the



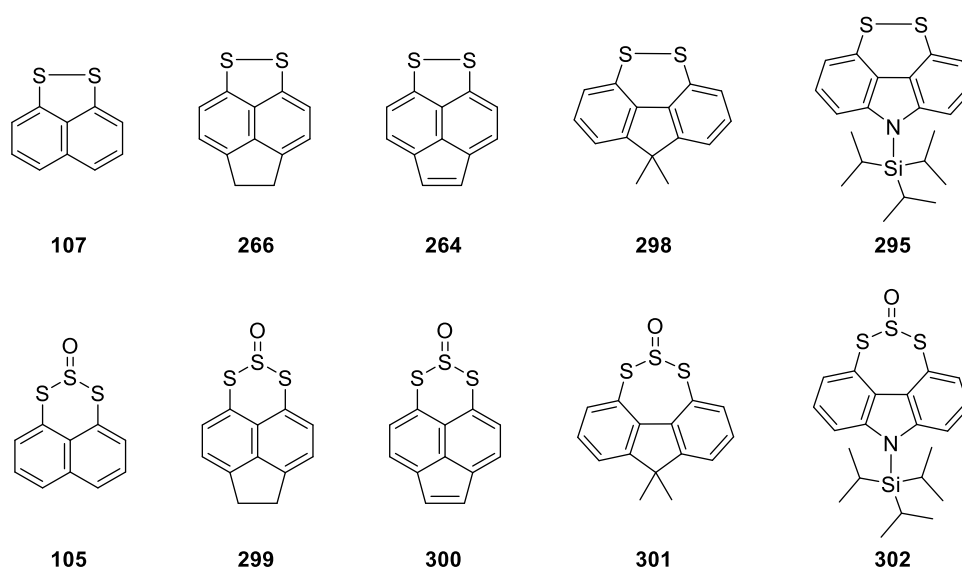
financial support from my parents I am very thankful for. This helped significantly. I could not have completed this degree without you guys. I love you and I always will.

Sulfur is a temperamental element and will happily cause issues wherever possible. Dr Richard Grainger once said to me *“Connor, I didn’t choose sulfur; sulfur chose me”*. I finally understand that. No-one wakes up wanting to be a sulfur chemist, but it becomes a friend which you can eventually rely on, once you get around its annoying quirks. I hate that element, but I am still very fond of it.

## Abstract

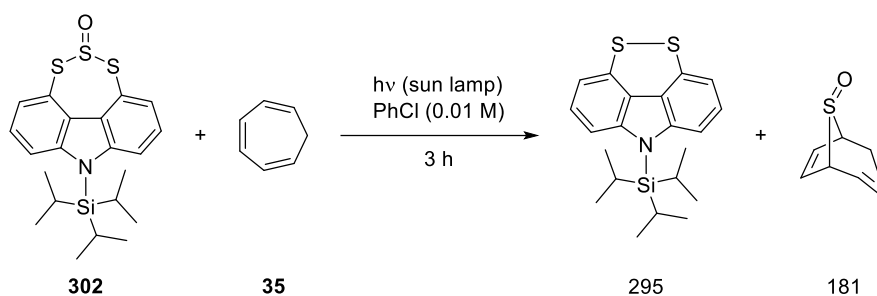
Sulfur monoxide has been known for a little over a century. SO has been known to have 3 electronic configurations in which it exists – two of which have been used in organic synthesis. In the last 70 years it has become a useful reagent in organic synthesis displaying a wide range of reactivities with many different functionalities. That being said, only 2 reports confirm singlet SO has been released and captured. These two papers display a large scope of the reactivity of singlet SO but neither display excellent yields that are reported for triplet SO release and capture. The most efficient triplet SO transfer reagent was reported by Grainger *et al.* in 2001 and 2011. This involved the release from *peri*-substituted trisulfide-2-oxides and capture using a variety of dienes. Therefore, there is still scope for an efficient singlet SO transfer reagent which displays capture of singlet SO.

This thesis reports the synthesis, study and controlled release of SO from 4 novel trisulfide-2-oxides (**299**, **300**, **301**, and **302**). All of the trisulfide-2-oxides were synthesised from the corresponding disulfides (**266**, **264**, **295**, and **298**) *via* the reduction of the disulfide (or disulfide/trisulfide mixtures) to the dithiol in yields comparable to previously reported trisulfide-2-oxides (45 – 50 % yield). The dithiol is subject to either SOCl<sub>2</sub>/pyridine or SO(im)<sub>2</sub>. SO(im)<sub>2</sub> shows a novel method to synthesise trisulfide-2-oxides. All novel trisulfide-2-oxides were crystallised, and the crystallographic data has been compared. The crystallographic data explains how strain within a system can alter the release rate of SO from a trisulfide-2-oxide.



**Figure 1** Top row - proposed disulfides (naphthalene **107**, acenaphthene **266**, acenaphthylene **264**, fluorene **298**, and carbazole **295**) Bottom row - proposed trisulfide-2-oxides (naphthalene **105**, acenaphthene **299**, acenaphthylene **300**, fluorene **301**, and carbazole **302**).

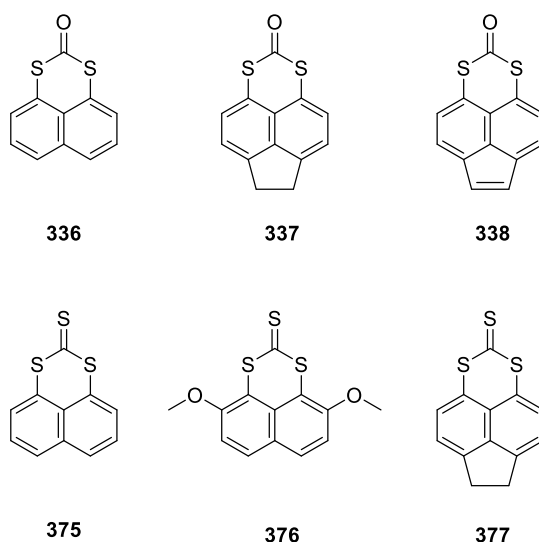
Finally, each of the trisulfide-2-oxides have been pyrolysed in the presence of 2,3-dimethyl-1,3-butadiene in chlorobenzene at reflux. None of the novel trisulfide-2-oxides in this study perform better than the previously developed naphthalene trisulfide-2-oxide **105**. Similarly, none of the trisulfide-2-oxides in this study performed as well as naphthalene trisulfide-2-oxide under photolysis conditions. However, carbazole trisulfide-2-oxide **302** has shown potential to be a singlet SO transfer reagent, with preliminary results indicating that singlet SO has reacted with cycloheptatriene to form bridged sulfoxide **181** (**Scheme 1**).



**Scheme 1** Singlet SO release from carbazole trisulfide-2-oxide **302** to yields disulfide **295** and sulfoxide **181**.

Carbon monoxide and carbon monosulfide are two reactive diatomic molecules. CO has been shown to have extensive uses in organic synthesis and is an important biological signalling molecule (and has also been shown to be a therapeutic despite its potent toxicity). Carbon monosulfide has very little literature on its uses in synthesis. This could be due to the difficulty generating CS.

Naphthalene dithiocarbonate **336** and trithiocarbonate **375** have been synthesised by modified procedures from Ogura *et al.* These same procedures were used to the synthesise acenaphthene dithiocarbonate **337** and trithiocarbonate **377**, acenaphthylene dithiocarbonate **338**, 2,7-dimethoxynaphthalene trithiocarbonate **376**. All the compounds have been crystallised and their diffraction data analysed, and comparisons between each system have been made. The naphthalene, acenaphthene, and acenaphthylene dithiocarbonates (**336**, **337**, and **338**) were subjected to irradiation from a medium pressure Hg lamp – causing photochemical degradation to the corresponding disulfide (**107**, **266**, and **264**).



**Figure 2** Top row - proposed dithiocarboantes (naphthalene **336**, acenaphthene **337** and, acenaphthylene **338**). Bottom row - proposed trithiocarbonates (naphthalene **375**, 2,7-dimethoxy naphthalene **376** and, acenaphthene **377**).

Naphthalene trithiocarbonate was irradiated using 365nm LED strips in the following solvents; toluene, PhF, PhCl, DMF, CH<sub>2</sub>Cl<sub>2</sub>, CHCl<sub>3</sub>, and THF. Decomposition occurred in THF, but in no others. Morpholine (10 eq) was added and the solvent screen was re-trialled. Decomposition occurred in all solvents. The reactions were repeated but 1,3,5-trimethoxybenzene was added as an NMR standard. Percentage yields of all components in the reaction have been determined *via* <sup>1</sup>H NMR integration.

Abbreviation	Definition
2D	2 Dimentional
Å	Ångström
Ac	Acetate
Ad	Adamantyl
An	Anisole ( <i>para</i> -MeO-Ph)
Ar	Aromatic (when attached to a molecule) Argon (under reaction conditions)
Bn	Benzyl
Br	Broad
C	Celsius
CDI	1,1'-Carbonyldiimidazole
Ch	Chalcogen
COD	1,5-Cyclooctadiene
COSY	<sup>1</sup> H - <sup>1</sup> H Correlation Spectroscopy
Cp	Cyclopentadienyl
Cp*	Pentamethylcyclopentadienyl
Cy	Cyclohexyl
d	Days
<i>d</i>	Doublet
DABSO	1,4-Diazacyclo[2.2.2]octane bis(sulfur dioxide) adduct
dba	(1 <i>E</i> , 4 <i>E</i> )-1,5-Diphenylpenta-1,4-dien-3-one
<i>dd</i>	Double doublet
<i>ddd</i>	Double double doublet
DDQ	2,3-Dichloro-5,6-dicyano-quinone
Decomp.	Decomposition
DIPEA	Diisopropylethylamine
DMDO	3,3-Dimethyldioxirane (Murray's Reagent)
DME	1,2-Dimethoxyethane (glyme)
DMF	Dimethylformamide
dppe	1,2-Bis(diphenylphosphino)ethane
Eq	Equivalents
Et	Ethyl
FCC	Flash column chromatography
FGI	Functional Group Interconversion
FLP	Frustrated Lewis Pair
FT-IR	Fourier-transform infrared spectroscopy
g	Gram
h	Hours
hept	Heptet
HMBC	Heteronuclear Multiple Bond Correlation
HSQC	Heteronuclear Single Quantum Coherence Spectroscopy
hν	Light
<i>i</i>	<i>Iso</i> -
im	Imidazole

IR	Infrared
L	Ligand
LED	Light Emitting Diode
M	Molar
<i>m</i>	<i>meta</i>
<i>m/z</i>	Mass/charge
max	Maximum
<i>m</i> CPBA	<i>meta</i> -Chloroperoxybenzoic Acid
Me	Methyl
Mes	Mesityl
min	Minutes
mol	moles
<i>n</i>	<i>normal</i>
NBS	<i>N</i> -Bromosuccinimide
NHC	<i>N</i> -Heterocyclic carbene
NMR	Nuclear Magnetic Resonance
NOESY	Nuclear Overhauser Effect Spectroscopy
PAH	Polyaromatic Hydrocarbon
Ph	Phenyl
ppm	Parts Per Million
Pr	Propyl
q	Quartet
quint	Quintet
R <sub>f</sub>	Retention Factor
RT	Room Temperature
st	stack
<i>t</i>	<i>Tert</i>
t	Triplet
TEMP.	Temperature
Tf	Triflic
THF	Tetrahydrofuran
Thio-CDI	1,1'-Thiocarbonyldiimidazole
TIPS	Triisopropylsilyl
TLC	Thin layer chromatography
TMEDA	<i>N, N, N', N'</i> -tetramethylethane-1,2-diamine
UV	Ultraviolet
Vis	visible
w	Wide
WRT	With respect to
X	Halogen
XRD	X-ray Diffraction
λ	Wavelength
ν	frequency

## Contents

Dedication .....	1
Acknowledgements.....	2
Abstract.....	5
1.1 Sulfur monoxide.....	15
1.1.1 Introduction to sulfur monoxide .....	15
1.1.2 Reactivity of SO.....	16
1.1.2.1 Representative reactivity of both singlet and triplet SO .....	16
1.1.3 Episulfoxides .....	18
1.1.3.1 Decomposition of episulfoxides to $^3\Sigma^-$ SO and alkenes .....	18
1.1.3.2 Episulfoxides and the reaction of SO with dienes and trienes .....	23
1.1.4 Episulfoxides and other traps .....	31
1.1.4.1 Organic traps .....	31
1.1.4.2 Inorganic traps .....	33
1.1.5 Trisulfide-2-oxides as SO transfer reagents.....	37
1.1.6 Small ring strain release SO transfer reagents .....	40
1.1.7 Singlet SO transfer reagents .....	45
1.1.8 Miscellaneous SO transfer reagents.....	51
1.1.9 Inorganic complexes and SO .....	56



1.1.10	Inorganic SO transfer reagents.....	57
1.1.11	Applications of SO release .....	60
1.2	Peri-substitution .....	68
2	The design, synthesis, and evaluation of sulfur monoxide transfer reagents.....	83
2.1	Aims and objectives .....	83
2.2	Synthesis of the disulfide scaffolds.....	86
2.3	Synthesis of the trisulfide-2-oxides .....	105
2.4	Structure analysis and characterisation .....	111
2.4.1	Peri-substitution analysis .....	111
2.4.2	Peri-like structural analysis.....	116
2.4.3	Disulfides .....	119
2.4.4	Trisulfides.....	124
2.4.5	Trisulfide-2-oxides .....	130
2.5	The controlled release of SO from trisulfide-2-oxides.....	138
3	Carbon monochalcogenides .....	149
3.1	Carbon monoxide.....	149
3.1.1	Introduction to Carbon monoxide.....	149
3.1.2	Synthesis of the dithiocarbonates .....	153
3.1.3	Dithiocarbonate structural analysis.....	156
3.1.4	The controlled release of CO from dithiocarbonates.....	160

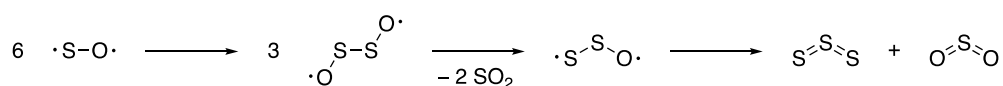
3.2	Carbon monosulfide.....	164
3.2.1	Introduction to carbon monosulfide .....	164
3.2.2	Synthesis of the trithiocarbonates .....	170
3.2.3	Trithiocarbonates structural analysis .....	172
3.2.4	The controlled release of CS from trithiocarbonates .....	177
3.3	Conclusions and future work .....	187
4	Experimental .....	188
5	References .....	255
6	Appendix .....	272

*Chapter 1:*  
Literature review: Sulfur monoxide and  
*peri*-substituted scaffolds

## 1.1 Sulfur monoxide

### 1.1.1 Introduction to sulfur monoxide

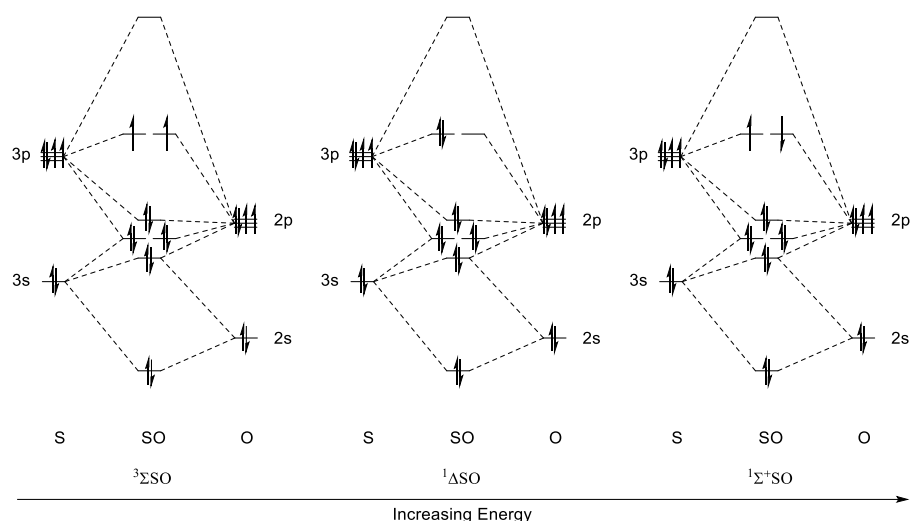
Sulfur monoxide (SO) is a reactive diatomic molecule which is isoelectronic with molecular oxygen. SO is found naturally in the atmosphere of Venus, comets and Jupiter's moons in small quantities.<sup>1-5</sup> On earth it is usually found as a gaseous pollutant from combustion of fossil fuels. SO disproportionates in 20 milliseconds into elemental sulfur and sulfur dioxide (SO<sub>2</sub>) (**Scheme 2**).<sup>6</sup> Due to the rapid disproportionation there has been a need for a method by which SO can be released *in situ* in order to use this versatile building block. This introduction serves to highlight some key information about SO.



**Scheme 2** The disproportionation of SO to sulfur and SO<sub>2</sub>.<sup>6</sup>

The UV band spectrum of SO was first described in 1906 (240 nm to 400 nm).<sup>7</sup> An electrical discharge through an SO<sub>2</sub> matrix was the preferred method of generating SO.<sup>6</sup> This allowed scientists to characterise SO. The excited states of SO have been studied and are well documented. By 1932 the ground state of SO had been shown to be a triplet state.<sup>7</sup> This was later characterised fully using various radiation sources to gain the rotational and vibrational energy levels.

SO is a biradical and the spin multiplicity is critical for the reactivity of the diatomic. SO has two low-lying excited singlet states; the first excited singlet state (<sup>1</sup>ΔSO) and a second excited singlet state (<sup>1</sup>Σ<sup>+</sup>SO) (**Figure 3**).<sup>8</sup>



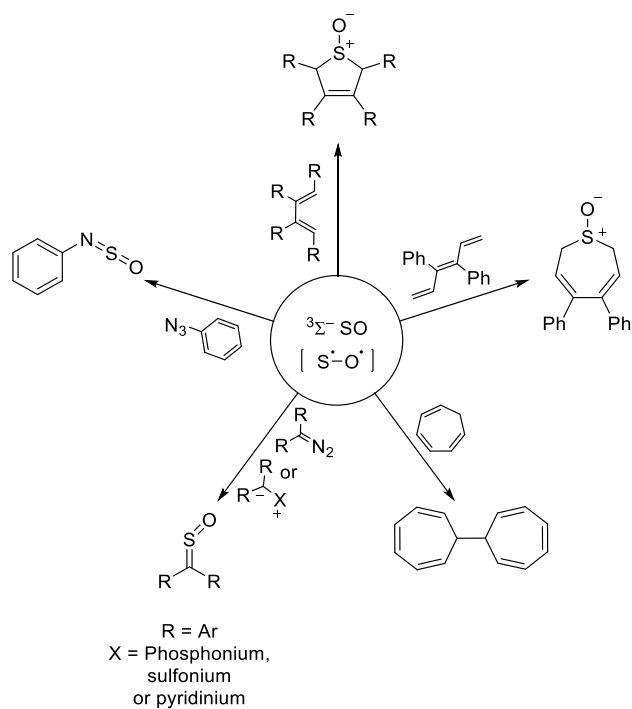
**Figure 3** Molecular orbital diagram of the three electronic configurations of SO.

In this review, the methods in which SO has been generated (by both organic and inorganic chemistry) and trapped will be highlighted. The methods will also be compared, and the potential applications of the products outlined.

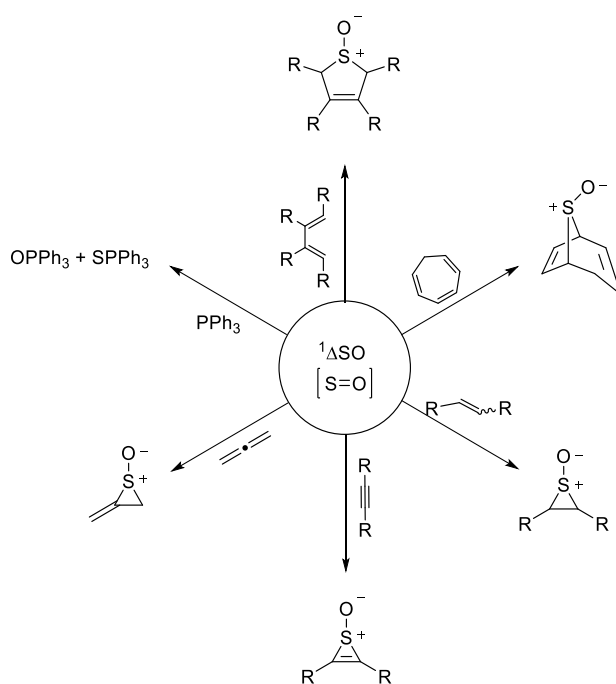
### 1.1.2 Reactivity of SO

#### 1.1.2.1 Representative reactivity of both singlet and triplet SO

Triplet and singlet SO have differing reactivities. Below are two schemes outlining the reactivity of triplet and singlet SO. The reactivity of triplet SO (**Scheme 3**) has been explored significantly more than that of singlet (**Scheme 3** and **Scheme 4**). This has been facilitated by the broader availability of triplet release agents and the high interest in the reactivity of episulfoxides.



**Scheme 3** Representative reactivity of triplet SO ( $^3\Sigma^- \text{SO}$ ).<sup>9-13</sup>



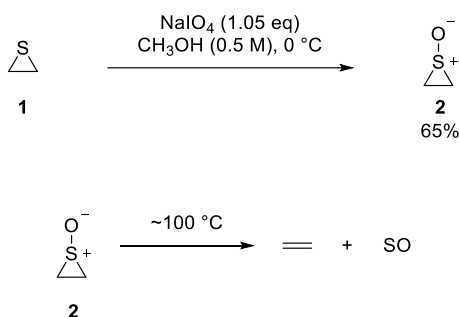
**Scheme 4** Representative reactivity of singlet SO ( $^1\Delta \text{SO}$ ).<sup>14,15</sup>

### 1.1.3 Episulfoxides

#### 1.1.3.1 Decomposition of episulfoxides to $^3\Sigma^-$ SO and alkenes

*Note to reader: During the writing of this thesis Dr Grainger and myself have written a review on SO transfer reagents. In this we outline that strained SO transfer reagents (e.g. episulfoxides, trisulfide-2-oxides, vic-sulfoxides and sultines) release triplet SO. DFT calculations have been done on most of these by Cummin's et al. The singlet SO transfer reagents undergo a different release pathway which is outlined in the stated sections.*

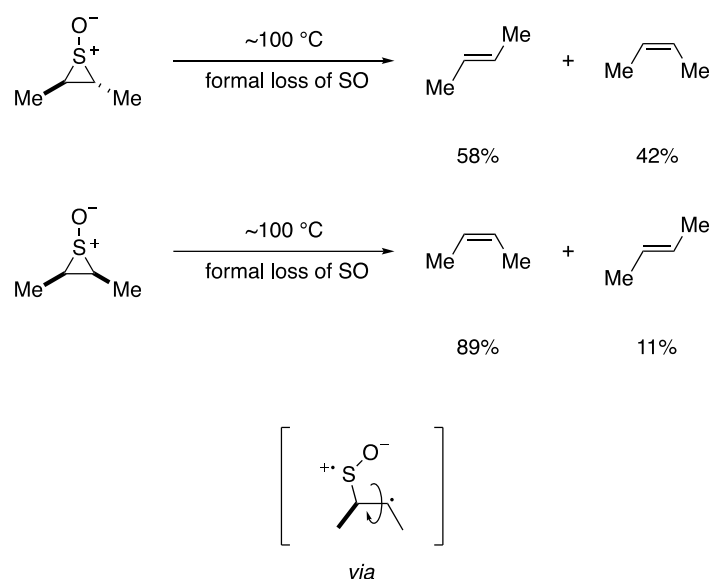
The first method to release SO under mild conditions was reported by Hartzell and Paige in 1966.<sup>16</sup> Thermolysis of ethylene episulfoxide **2** gave ethene and formal loss of SO (**Scheme 5**).



**Scheme 5** Synthesis and decomposition of episulfoxides.<sup>16</sup>

The resultant stereochemistry of the alkene from the decomposition of an episulfoxide became of interest as it could give an insight into the mechanism of release of SO. In 1967, Hartzell and Paige hypothesised that the stereochemistry of episulfoxides **3** and **4** would be retained in the alkene due to the mechanism being concerted – similar to the findings of Matsumura *et. al.* and Neureiter with episulfones.<sup>17,18</sup> However, in practice, stereochemistry was not retained (**Scheme 6**).<sup>17</sup> This indicated a different mechanism of release to that of the analogous  $\text{SO}_2$  adducts. One of the C-S bonds in the episulfoxide must undergo fission first and then a rotation around the C-C bond must occur to form the isomer. In the paper, Hartzell

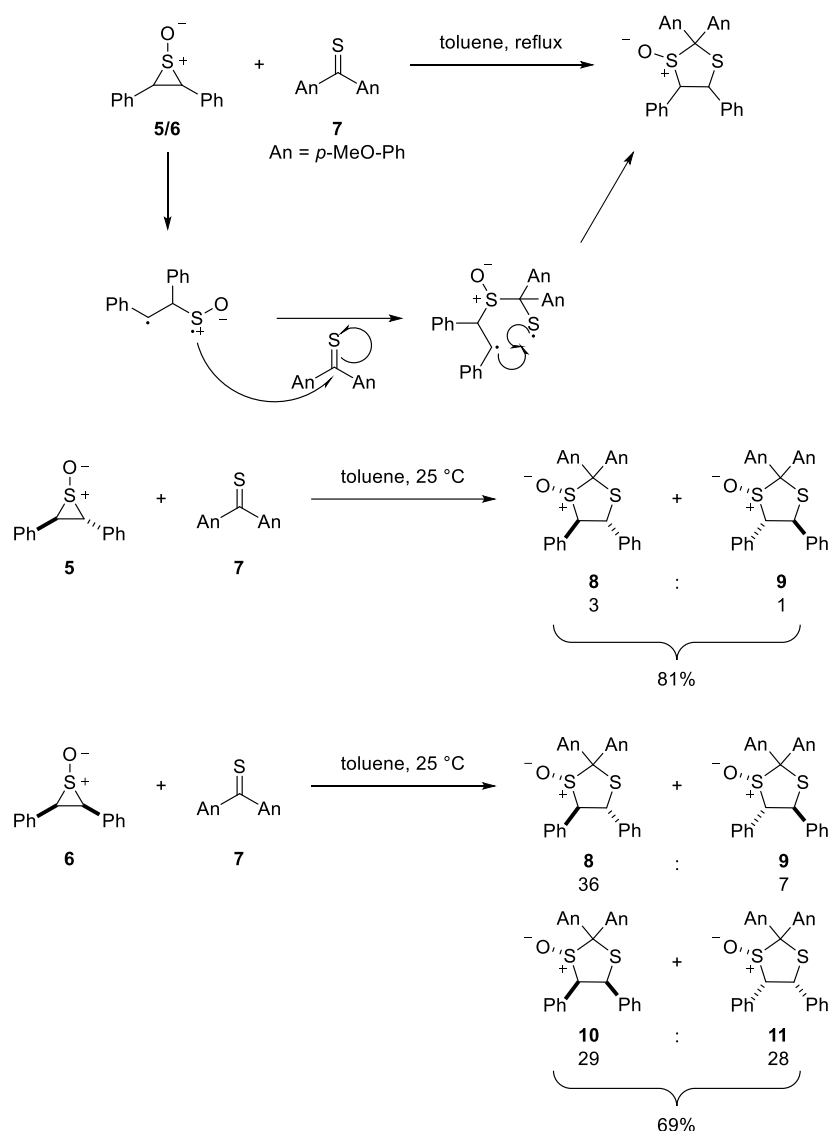
and Paige suggest the reaction may go *via* an ionic intermediate (it was later found to be a radical intermediate).<sup>17</sup>



**Scheme 6** The stereochemical outcomes of the resultant alkenes from the *cis*- and *trans*-episulfoxides and the radical intermediate.<sup>17</sup>

The mechanism of SO release from episulfoxides was probed by Kondo and Negishi in 1972.<sup>19</sup> Stilbene episulfoxides **5** and **6** were pyrolyzed in the presence of 1,3-dipolarophiles, to trap any ionic intermediates. No trapped products were observed. 4,4'-Dimethoxythiobenzophenone **7** – a known carbon radical trap – was then used and dithiolane-1-oxide was observed suggesting a radical mechanism.<sup>19</sup>





**Scheme 7** The reaction of stilbene episulfoxide with a thioketone.<sup>19</sup>

Depending on the starting episulfoxide (*cis*- or *trans*-) different ratios of 4 stereoisomers were isolated from the reaction (**8** – **11**). The clear scrambling of the stereochemistry shows that the reaction must be a two-step non-concerted mechanism involving the breaking of one C-S bond first before the alkene is formed.

When ethylene episulfoxide **2** was subjected to thermolysis, Saito could not identify any singlet SO.<sup>20</sup> Using microwave spectroscopy, only triplet SO was detected. This was consistent with Uehara's results using electron magnetic resonance spectroscopy.<sup>21</sup> The transition from

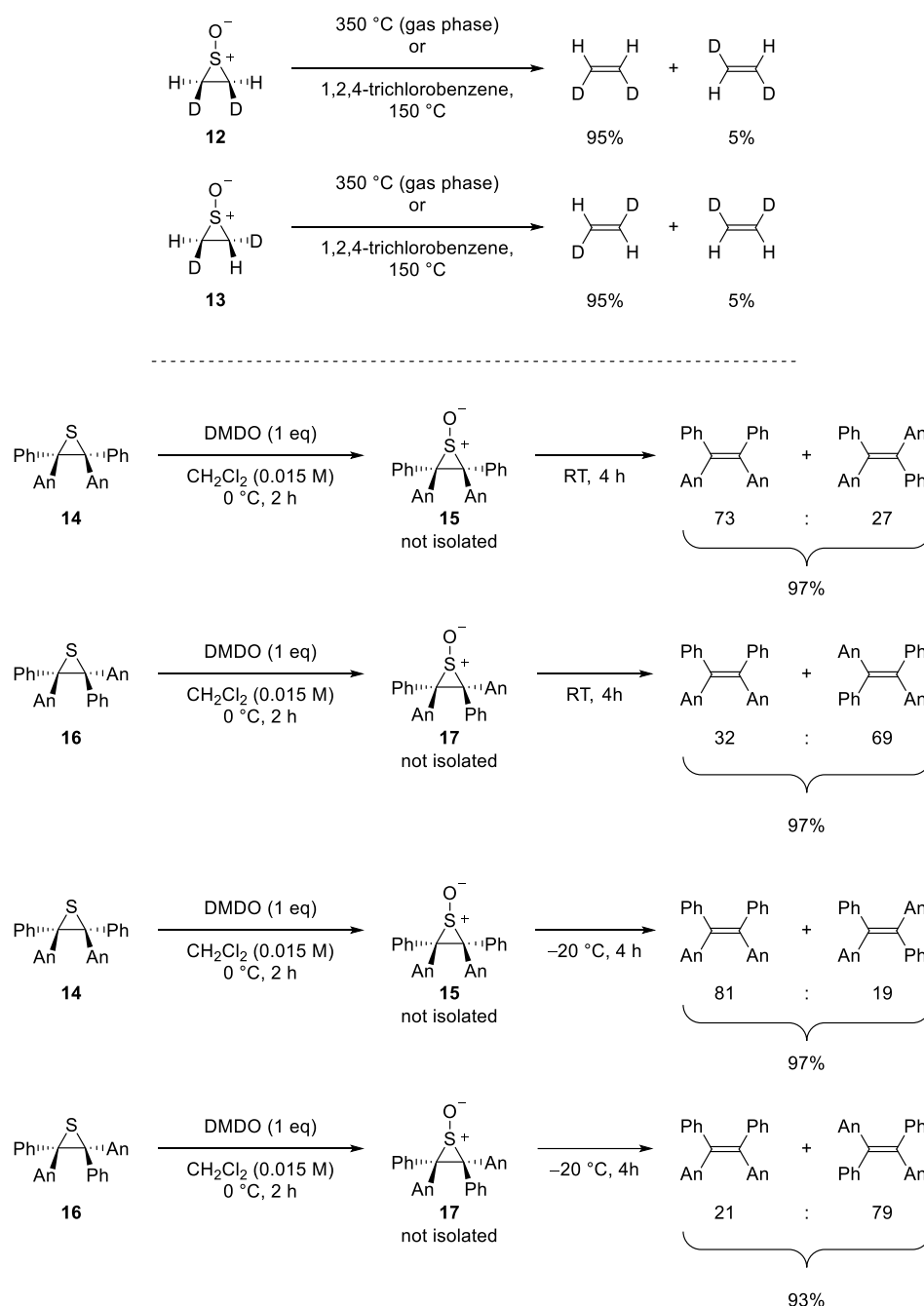
singlet SO to triplet SO should have a long lifetime as the transition is forbidden. The radiative lifetime of O<sub>2</sub> in the singlet state is 45 minutes. Therefore, the SO generated must be released in the triplet electronic configuration.

In 1972, Chao and Lemal provided evidence that episulfoxides release triplet SO and not singlet SO.<sup>22</sup> The standard heat of reaction for episulfoxide → ethylene + <sup>3</sup>Σ<sup>-</sup>SO was calculated and compared with the activation enthalpies of triplet and singlet SO. They found that the episulfoxides release triplet SO selectively.

Dideuteroethylene episulfoxides **12** and **13** were pyrolyzed and the resulting dideuterated alkenes were analysed by Vollhardt and Aalbersberg in 1977 (**Scheme 8**).<sup>23</sup> This was used to evaluate the stereochemical outcome of the reaction with a sterically and electronically unbiased probe. The stereochemistry was not fully retained. 95% was retained but there was 5% of the opposite double bond geometry. A biradical mechanism is therefore present but Vollhardt and Aalbersberg mention that an appreciable amount of the retained product could be obtained from a concerted process and therefore it cannot be ruled out.

The decomposition of tetraarylepisulfoxides to tetraarylalkene and SO were investigated by Glass and Jung in 1994. The tetraarylepisulfoxides used were the *cis*-**15** and *trans*-**17** isomers of 1,2-bis(4-methoxyphenyl)-1,2-diphenyl-episulfoxide. Their findings support the conclusions made by Vollhardt and Aalbersberg. *Cis*- and *trans*-episulfoxides do release SO and retain the stereochemistry of the alkene – as the majority isomer. However, a not insignificant amount of the opposite isomer was found. Therefore, a two-step radical mechanism cannot be ruled out. They investigate the decomposition of the tetraarylepisulfoxides at 0 °C and –20 °C and find the retention of the alkene stereochemistry to be higher at lower temperatures (**Scheme 8**). This could be due to the decreased rate of

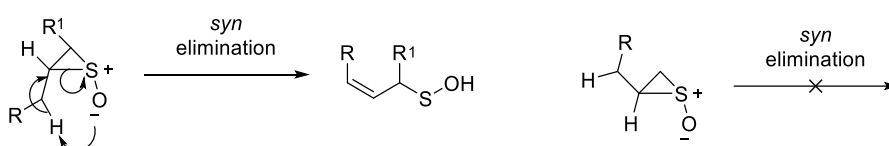
bond rotation upon fission of the S-C bond from the episulfoxide or due to the chelotropic mechanism being favoured at lower temperatures.



**Scheme 8** Top - Vollhardt and Aalberberg's findings on the retention of stereochemistry in dideuterated episulfoxides **12** and **13**.<sup>23</sup> Bottom - Glass et al. finding on the decomposition of *cis*-**15** and *trans*-**17** isomers of 1,2-bis(4-methoxyphenyl)-1,2-diphenyl-episulfoxide at 0 °C and -20 °C.<sup>24</sup>

When the development of episulfoxides began to move toward the different substituents on the ring, it was found that the butene episulfoxide **3** and **4** sometimes degraded at room temperature.<sup>17</sup>

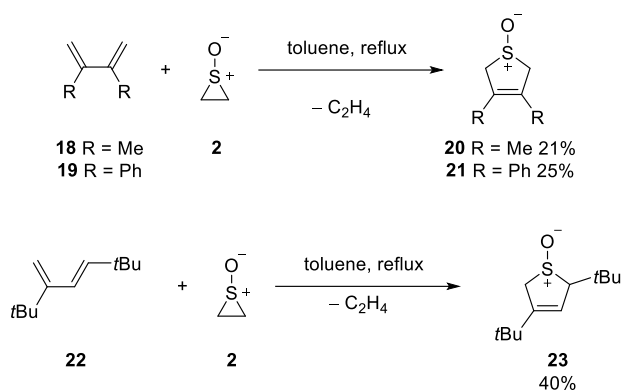
Butene episulfoxides **3** and **4** undergo a *syn* elimination at room temperature if the  $\alpha$ -carbon has a hydrogen on it and is *syn* to the sulfoxide (**Scheme 9**). Degradation leads to the allylic sulfenic acid and the episulfoxide does not release SO.



**Scheme 9** The mechanism of *syn* elimination of episulfoxides to allyl sulfenic acids.<sup>17</sup>

#### 1.1.3.2 Episulfoxides and the reaction of SO with dienes and trienes

Dodson and Sauers then found that SO could be captured.<sup>9</sup> Ethylene episulfoxide **2** was pyrolyzed in the presence of dienes **18**, **19**, and **22** to give cyclic sulfoxides **20**, **21**, and **23** (**Scheme 10**). Although the yields of sulfoxides **20**, **21**, and **23** were poor, it provided the first demonstration that SO can be trapped. The stereochemistry of sulfoxides **20**, **21**, and **23** could not be identified. To prove the sulfoxides were formed, cyclic sulfoxides **20**, **21**, and **23** were oxidised to the cyclic sulfones.

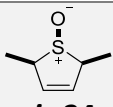
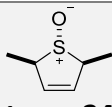
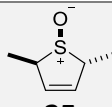

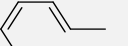
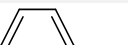


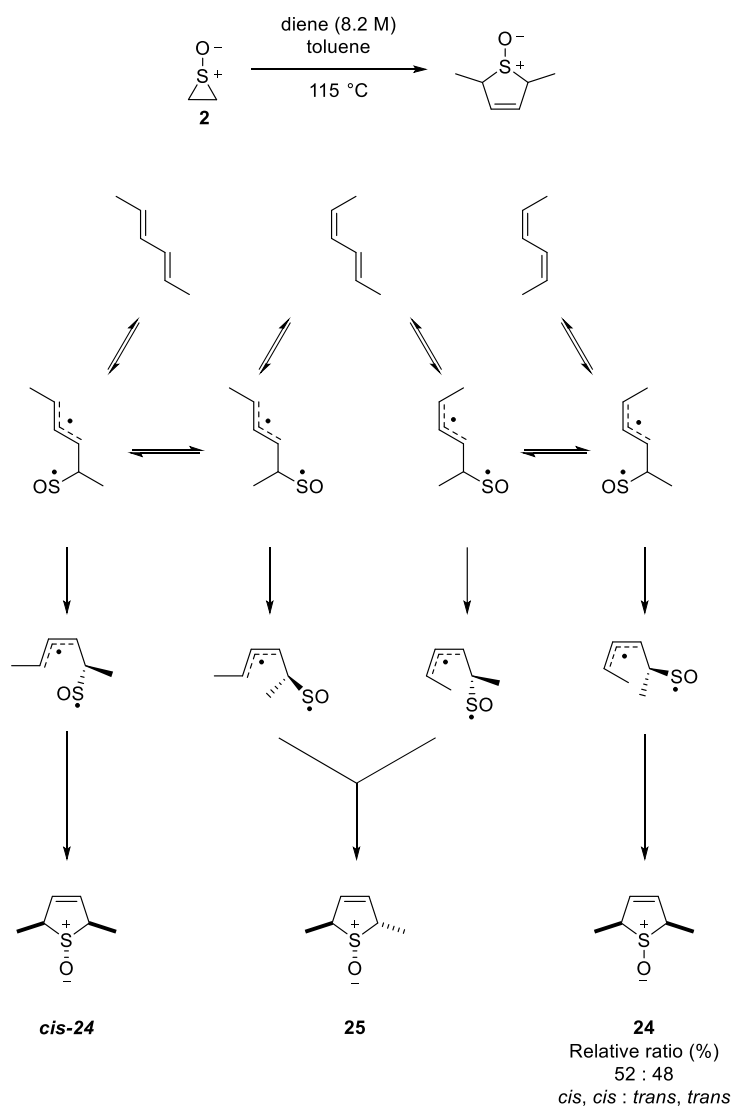
**Scheme 10** The first synthetic trap of SO by Dodson and Sauers using dienes.<sup>9</sup>

A study probing the mechanism of diene-SO cyclisation was published by Lemal and Chao in 1973. The reaction of SO with a diene is not pericyclic.<sup>22,25</sup>

When 2,4-hexadienes react with SO, the 2- and 5- positions of the resulting dihydrothiophene S-oxides **24** are scrambled – the reaction is not stereoselective (**Table 1** and **Scheme 11**). This would indicate a radical mechanism and not a pericyclic mechanism. The different ratios of the different isomers are due to the steric interactions of the system during the radical cyclisation.

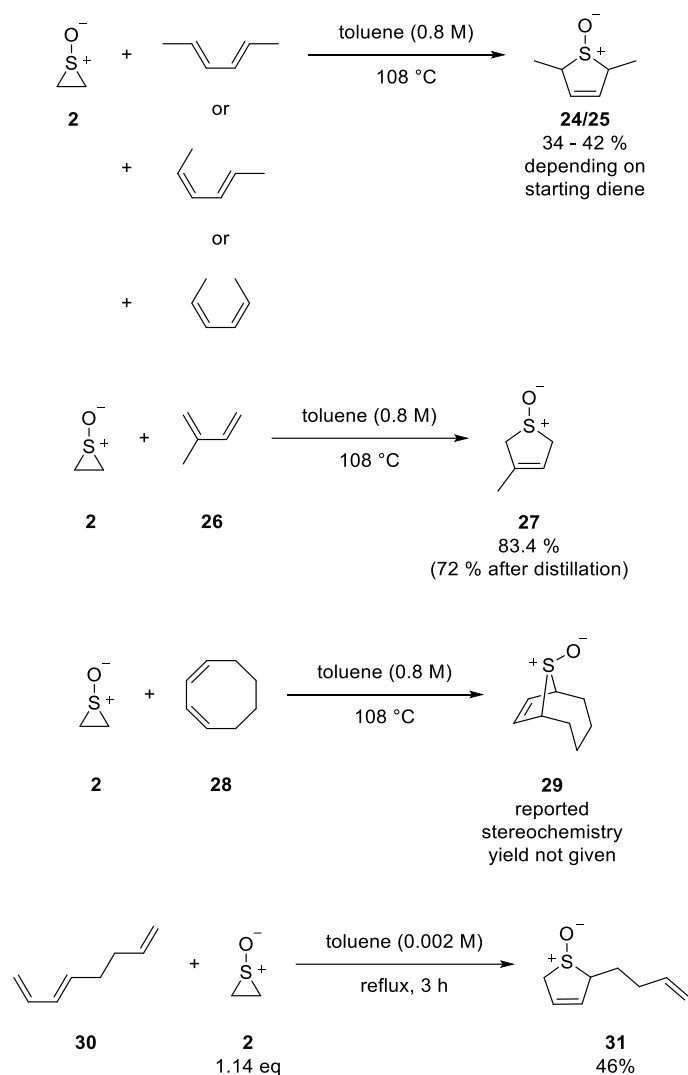
**Table 1** The stereochemical outcomes of the reaction of SO with 1,4-substituted dienes.

Diene	Relative ratios (%)		
	 <b>cis-24</b>	 <b>trans-24</b>	 <b>25</b>
	0	13	87
	Trace	95	5
	20	61	19



**Scheme 11** Lemal and Chao's proposed mechanism for the reaction of SO and a diene.<sup>22,25</sup>

Ethylene episulfoxide **2** reacts with 1,4-dimethyl-butadiene in a 34 – 42% yield dependent on the geometry of the diene. It also reacts with isopropene in excellent yield. Finally, ethylene episulfoxide **2** also reacts with octadiene **28** but no yield was reported (**Scheme 12**). Ethylene episulfoxide **2** was also pyrolyzed in the presence of octa-1,3,7-triene **30** in 1983 by Grigg *et al* (**Scheme 12**).<sup>26</sup> The crude sulfoxide **31** was isolated in a 46% yield and was later used in a hydroformylation reaction.



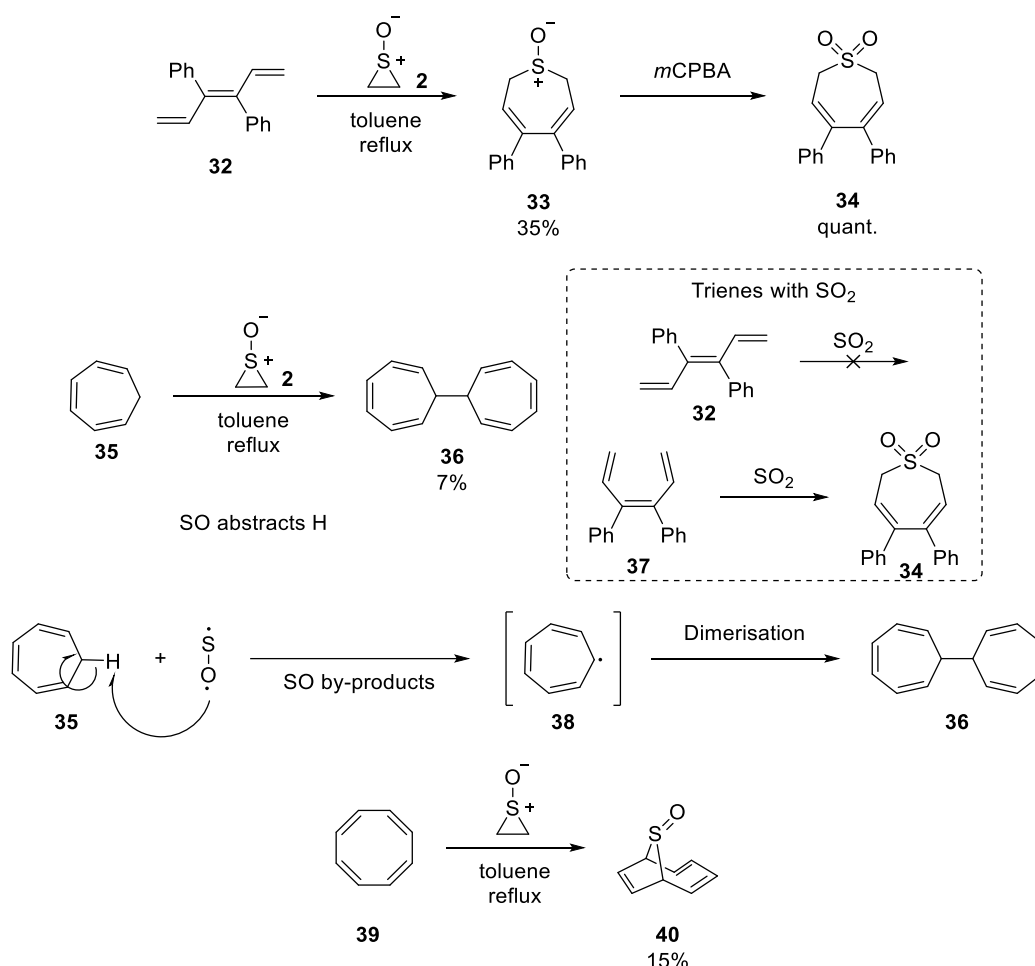
**Scheme 12** Lemal and Chao's reactions of ethylene episulfoxide **2** with dienes and Glass *et al.*

*reaction of ethylene episulfoxide **2** with octa-1,3,7-triene **30**.*<sup>25</sup>

In 1969, Dodson and Nelson published their findings on the reactivity of triplet SO with trienes.<sup>10</sup> They reacted episulfoxide **2** in the presence of different trienes (**Scheme 13**). They found that triplet SO reacts with linear trienes to form 7 membered cyclic sulfoxides. Unlike SO<sub>2</sub>, SO reacts with linear triene **32** to give the cyclic sulfoxide **33**.<sup>10</sup> SO<sub>2</sub>, on the other hand, does not because the central *trans* double bond prevents the pericyclic mechanism. This indicates SO reacts with trienes in a radical mechanism. However, with cycloheptatriene **35**,

triplet SO becomes a hydrogen abstractor, resulting in the stabilised tropylium-radical **38** which consequently dimerises to form dihydroheptafulvalene **36** (**Scheme 13**).<sup>10</sup>

Ethylene episulfoxide **2** was pyrolyzed in the presence of cyclooctatetraene **39** by Anastassiou and co-workers in 1975.<sup>27</sup> Sulfoxide **40** was produced in a 15% yield and selectively yielding the sulfinyl oriented over the diene (**Scheme 13**) – this was determined by lanthanide-induced shift <sup>1</sup>H NMR. The reaction was repeated by Quin and co-workers and a higher yield was obtained (24% and 5% was the opposite diastereomer).<sup>28</sup>

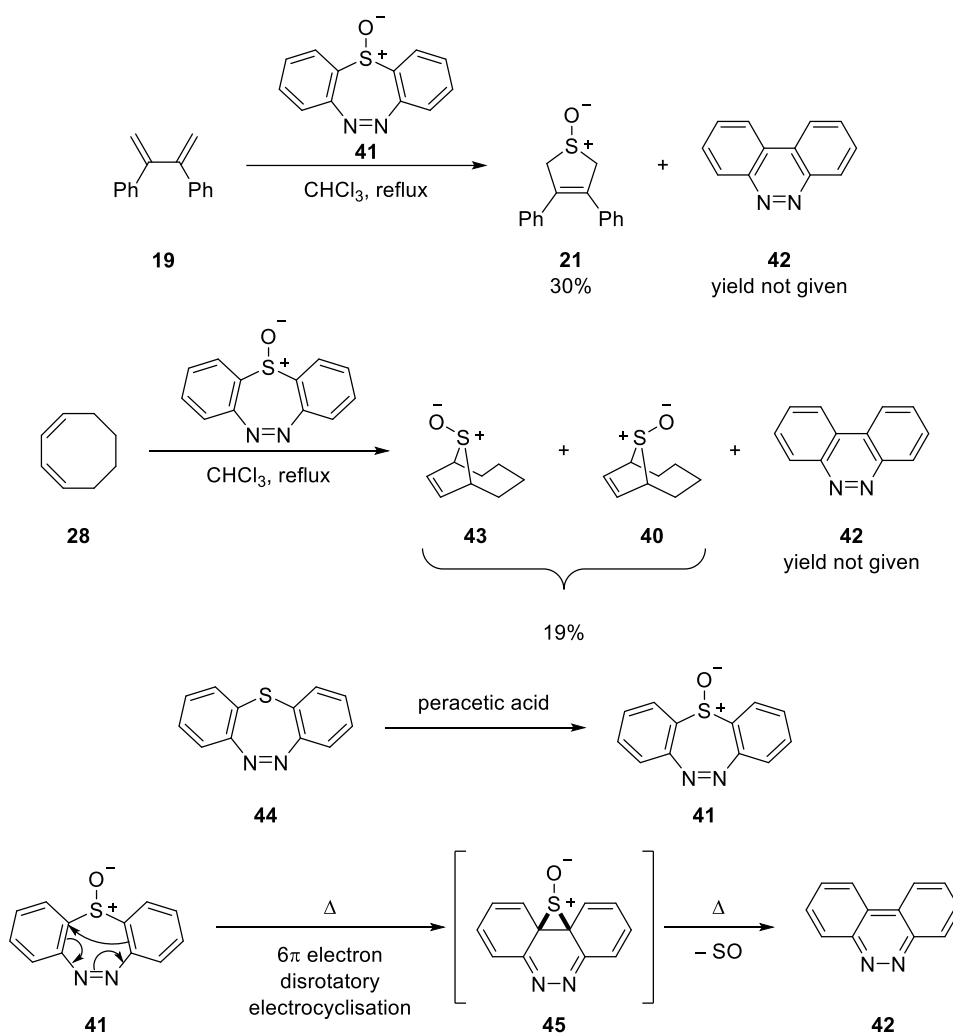


**Scheme 13** The reaction of  $^3\Sigma^+-\text{SO}$  with linear and cyclic trienes and comparison with  $\text{SO}_2$ .<sup>10</sup>

The reaction of  $^3\Sigma^+-\text{SO}$  with cyclooctatetraene **39** to give the syn-sulfoxide **40**.<sup>27</sup>

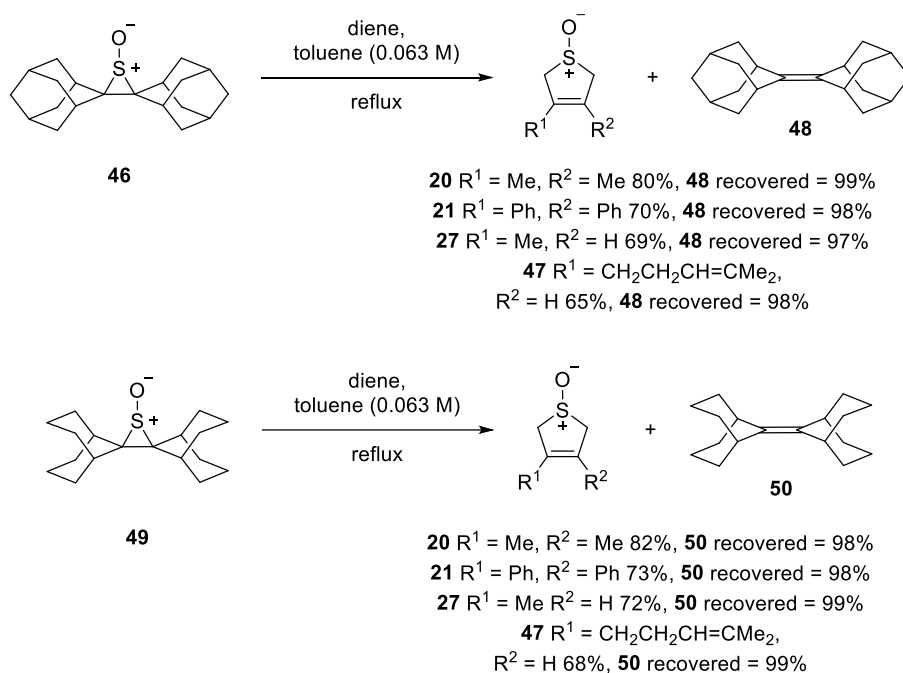


In 1970 Lemal and Chow published a new SO transfer reagent.<sup>29</sup> Dibenzo[*b,f*][1,4,6]thiadiazepin **44** was oxidised to the resulting sulfoxide **41** using peracetic acid. Dibenzo[*b,f*][1,4,6]thiadiazepin **44** and the corresponding sulfone are both stable at high temperatures (decomposition at ~210 °C), whilst the sulfoxide **41** decomposed at much lower temperatures (76 °C). Chow exploited a ring contraction (from a 7-membered ring to a 6-membered ring) and a drive toward aromaticity to extrude SO from sulfoxide **41**, *via* episulfoxide intermediate **45**, and giving aromatic **42** as a by-product. Chow reacts sulfoxide **41** with 2,3-diphenyl-1,3-butadiene **19** and cyclooctadiene **28** – yielding sulfoxide **21** and diastereomeric sulfoxides **40** and **43** (Scheme 14).<sup>29</sup>



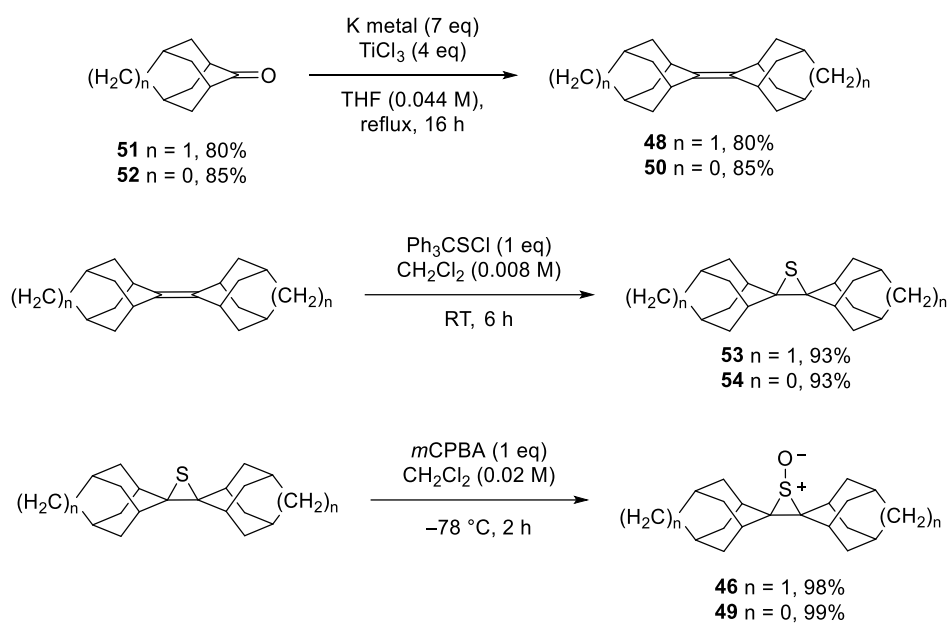
**Scheme 14** The synthesis of dibenzo[b,f][1,4,6]thiadiazepin-1-oxide **41** from dibenzo[b,f][1,4,6]thiadiazepine **44** and the extrusion and trapping of  $^3\Sigma^- \text{SO}$ .<sup>29</sup>

Adamantane-like episulfoxides **46** and **49** both release  $\text{SO}$  in refluxing toluene in 14 h and 24 h, respectively.<sup>30</sup> The release and capture of  $\text{SO}$  occur in moderate to high yields and the alkenes **48** and **50** recovery in excellent yields. The  $\text{SO}$  transfer requires a 3:1 excess of adamantane episulfoxides **46** or **49** and low concentration in solution, presumably to prevent  $\text{SO}$  from reacting with itself in solution (**Scheme 15**).



**Scheme 15** The release and trapping of  $^3\Sigma^-SO$  from strained episulfoxides **48** and **50**.<sup>31</sup>

Harpp and Yousef synthesised adamantane-like episulfoxides **46** and **49** in excellent yields in three steps from ketones **51** and **52**.<sup>30</sup> The ketones are coupled together to give (the recyclable) alkenes **48** and **50**. Episulfidation is performed using  $\text{Ph}_3\text{CSOCl}$  to yield **53** and **54**. Finally, oxidation using *m*CPBA yields episulfoxides **46** and **49** (Scheme 16).<sup>30,31</sup>

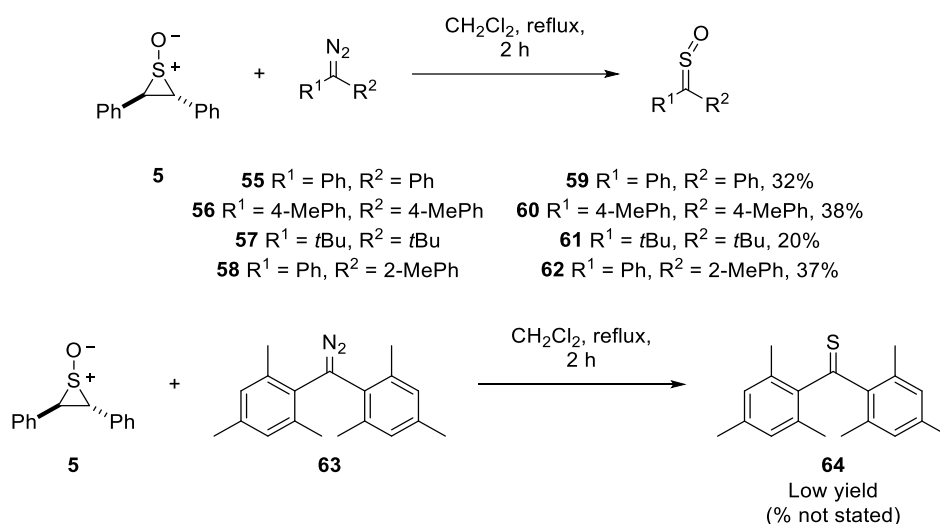


**Scheme 16** The synthesis of episulfoxides **46** and **49** by Yousef and Harpp for  $^3\Sigma^-$ -SO transfer.<sup>30</sup>

#### 1.1.4 Episulfoxides and other traps

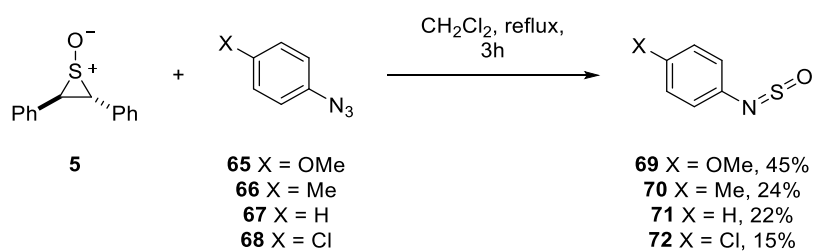
##### 1.1.4.1 Organic traps

Episulfoxide **5** was shown to react with diazoalkanes **55** - **58** to form sulfines **59** - **62** (and in one case a thioketone **64**) and released  $\text{N}_2$  by Maccagnani *et al.* in 1976.<sup>32</sup> Similarly,  $\text{SO}_2$  also reacts with diazoalkanes to form sulfines (**Scheme 17**).<sup>32</sup>



**Scheme 17** Reaction of diazoalkanes with  $^3\Sigma^-SO$  to yield sulfines.<sup>32</sup>

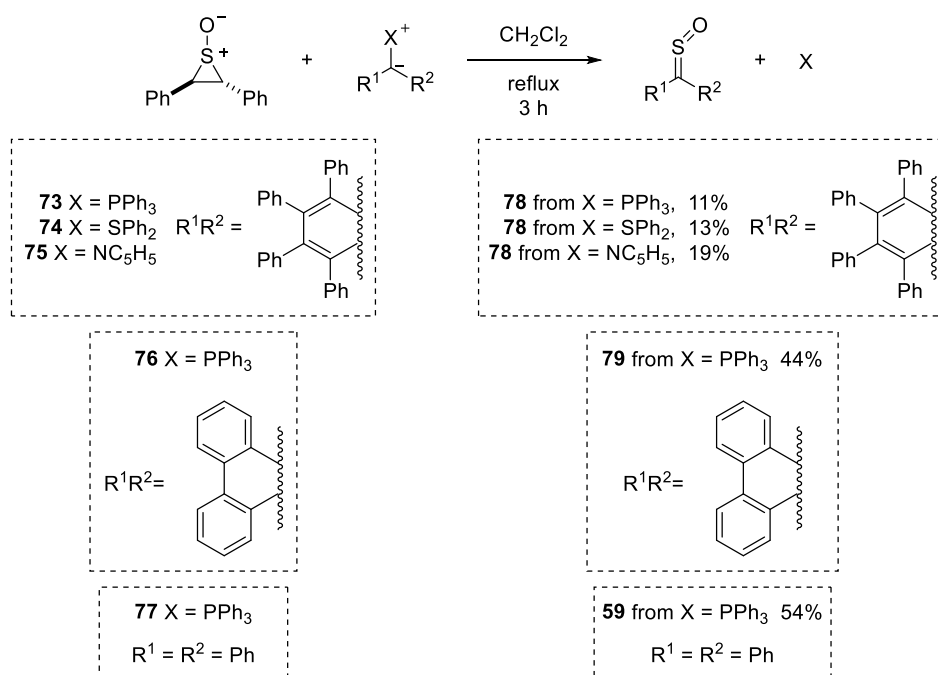
Maccagnani *et al.* also showed episulfoxide **5** reacts with aromatic azides **65** - **68** to yield *N*-sulfinamines **69** – **72**.<sup>12</sup> The reaction proceeds *via* electrophilic attack from SO on the nitrogen  $\alpha$  to the aromatic and extrusion of nitrogen gas (**Scheme 18**). This is proven by a series of controls that show no nitrene is being formed.<sup>12</sup>



**Scheme 18** Reaction of aromatic azides with  $^3\Sigma^-SO$  to yield *N*-sulfinamines.<sup>12</sup>

Stilbene episulfoxide **5** was shown to react with phosphonium, sulfonium and pyridinium ylides to form sulfines by Mazzanti *et. al.* in 1977.<sup>33</sup> SO is electrophilic in nature and is attacked by the nucleophilic position on the ylides – giving loss of neutral X. Moderate yields are

reported but an increase in the equivalents of stilbene episulfoxide **5** gives higher yields (Scheme 19).<sup>33</sup>



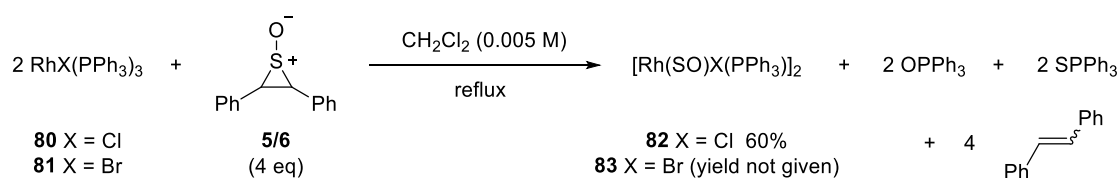
**Scheme 19** The reaction of  $^3\Sigma^-SO$  with phosphonium **73**, **76**, and **77**, sulfonium **74** and pyridinium **75** ylides to yield sulfines **78**, **79**, and **59**.

#### 1.1.4.2 Inorganic traps

There have been several papers where episulfoxides have been used to transfer SO to inorganic metal complexes. The metal traps and stabilises the SO that is released. However, in some cases the episulfoxide is added to the metal at room temperature and the metal traps SO. It could be hypothesised that SO is not strictly released from the episulfoxide as previously proposed. Instead, the episulfoxide can complex to the metal, causing the decomposition of the episulfoxide, and SO co-ordinating to the metal, without formally producing SO at any point (but releasing ethene as the by-product). In this section, reagents which release SO,

transfer it to a metal centre and reagents which migrate the SO from the episulfoxide without thermolysis will be highlighted.

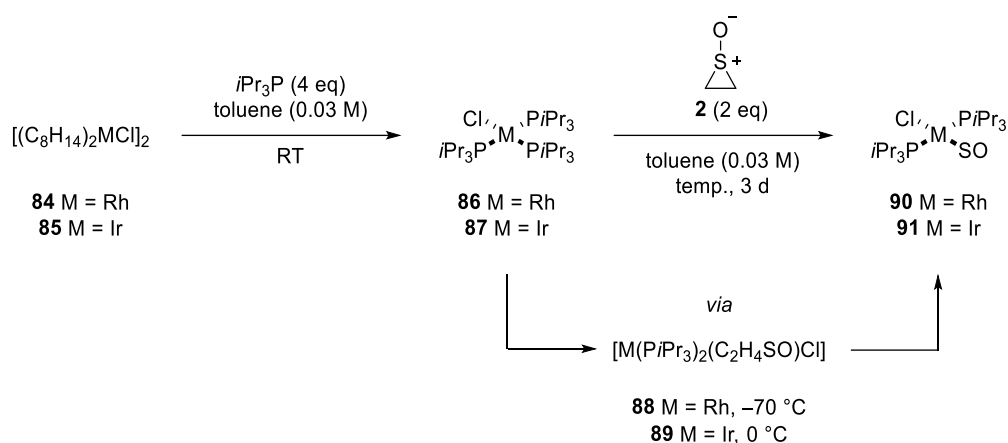
The first example of transfer from an episulfoxide to a metal was from stilbene episulfoxide **5** and **6** to Wilkinson's catalyst **80** and **81** at 40 °C reported by Agarwala *et. al.* in 1981 (**Scheme 20**).<sup>34</sup> As Kondo and Negishi established, stilbene episulfoxide undergoes slow SO release at 0 °C.<sup>19,35</sup> The resultant complex was not fully characterised, but it was determined that SO was co-ordinated to the metal centre by IR (SO stretch) and elemental analysis.<sup>34</sup>



**Scheme 20** The first recorded transfer of SO to a metal complex.<sup>34</sup>

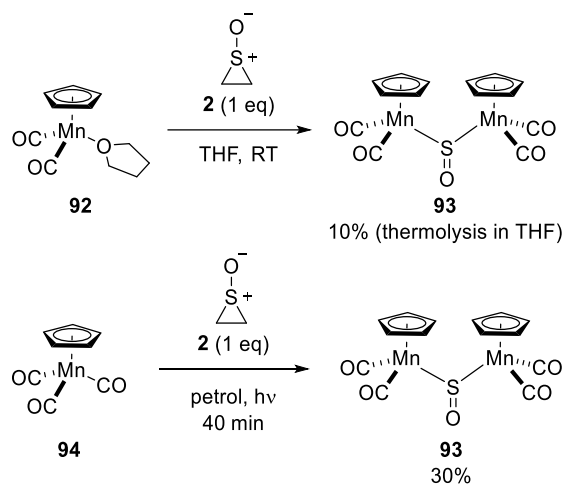
Ethylene episulfoxide **2** was added to platinum group metal complexes **84** and **85** by Schenk *et. al.* in 1984.<sup>36</sup> After 3 days, a ligand exchange occurred with the hindered phosphine, and ethene was released yielding the SO-M complexes **90** and **91**.

However, due to the low temperatures maintained throughout the reaction and the recrystallisation, SO is not strictly being released from the episulfoxide as free SO. Instead, the episulfoxide co-ordinates to the metal centre before release of ethene, leaving SO co-ordinated to the metal. Metal complexes **90** and **91** were made *in situ* from metal complexes **88** and **89** (**Scheme 21**).



**Scheme 21** Schenk *et al.* transfer to iridium and rhodium complexes.<sup>36</sup>

It is well documented that carbon monoxide can co-ordinate to manganese – therefore Lorenz *et al.* attempted SO co-ordination to Mn in 1985.<sup>37</sup> Mn complexes **92** and **94** reacts with episulfide **2** at room temperature or photolytically, respectively, forming an unusual Mn-SO-Mn bridged complex **93** in poor to moderate yields (**Scheme 22**). SO complex **93** was characterised by X-ray diffraction.<sup>37</sup>

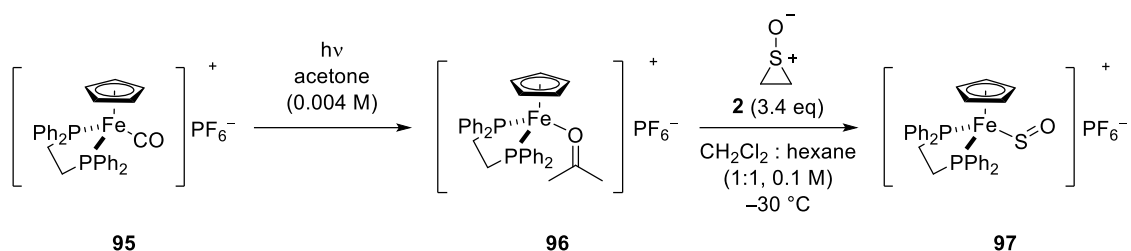


**Scheme 22** Lorenz *et al.* transfer of SO to manganese to produce a bridged SO complex **93**.<sup>37</sup>

SO was co-ordinated to iron by Schenk *et al.* in 1987.<sup>38</sup> Fe-CO complex **95** was irradiated in acetone to give Fe complex **96**. Fe complex **96** was evaporated to dryness, and ethylene

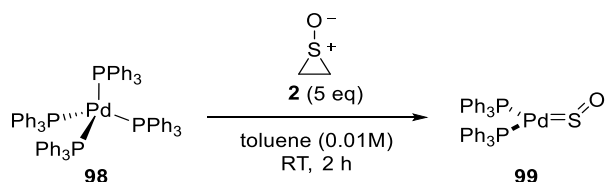


episulfoxide **2** was added and the reactants were dissolved in CH<sub>2</sub>Cl<sub>2</sub>:hexane and cooled to -30 °C to yield Fe-SO complex **97** (**Scheme 23**).



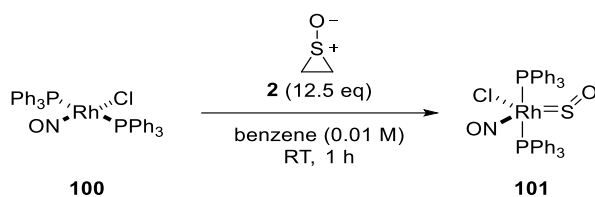
**Scheme 23** Schenk *et. al.* transfer of SO to an Fe complex.<sup>38</sup>

In 1992, a palladium-SO complex **99** was synthesised by Lorenz *et al.* that transferred SO to 2,3-dimethyl-1,3-butadiene **18** (see section 1.1.10).<sup>39</sup> Tetrakis(triphenylphosphine) palladium(0) was reacted with episulfoxide **2** at room temperature which indicates Pd coordination to episulfoxide and not SO release. This produced palladium(II)-SO complex **99** in a 73% yield (**Scheme 24**).<sup>39</sup>



**Scheme 24** Lorenz *et al.* transfer of SO to Pd.<sup>39</sup>

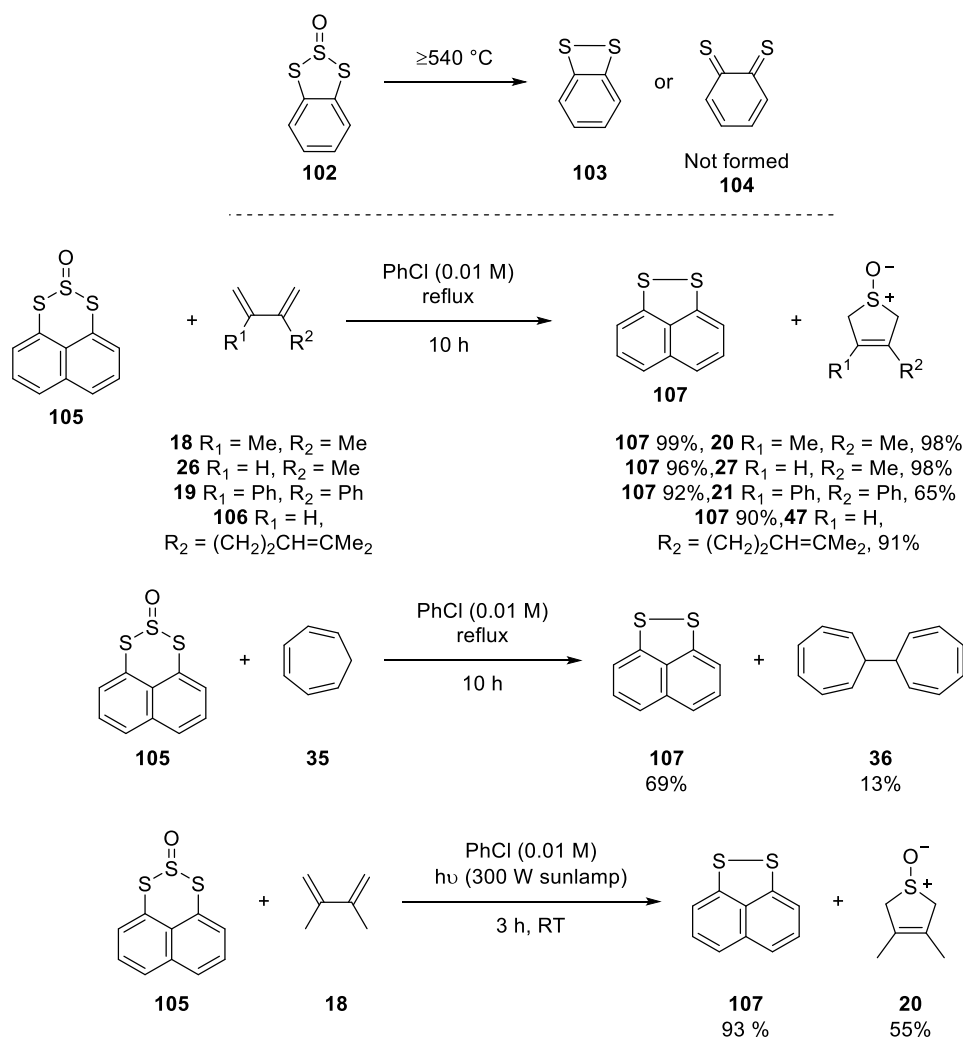
Lorenz *et. al.* also began to explore the possibility of having two reactive diatomic gases attached to a single metal centre.<sup>40</sup> They took rhodium-NO complex **100** and reacted it with episulfoxide **2** to yield the resulting SO complex **101** at room temperature indicating Rh coordination to episulfoxide and not formal SO release (**Scheme 25**).<sup>40</sup>



**Scheme 25** Lorenz *et al.* transfer of SO to Rh-NO complex.<sup>40</sup>

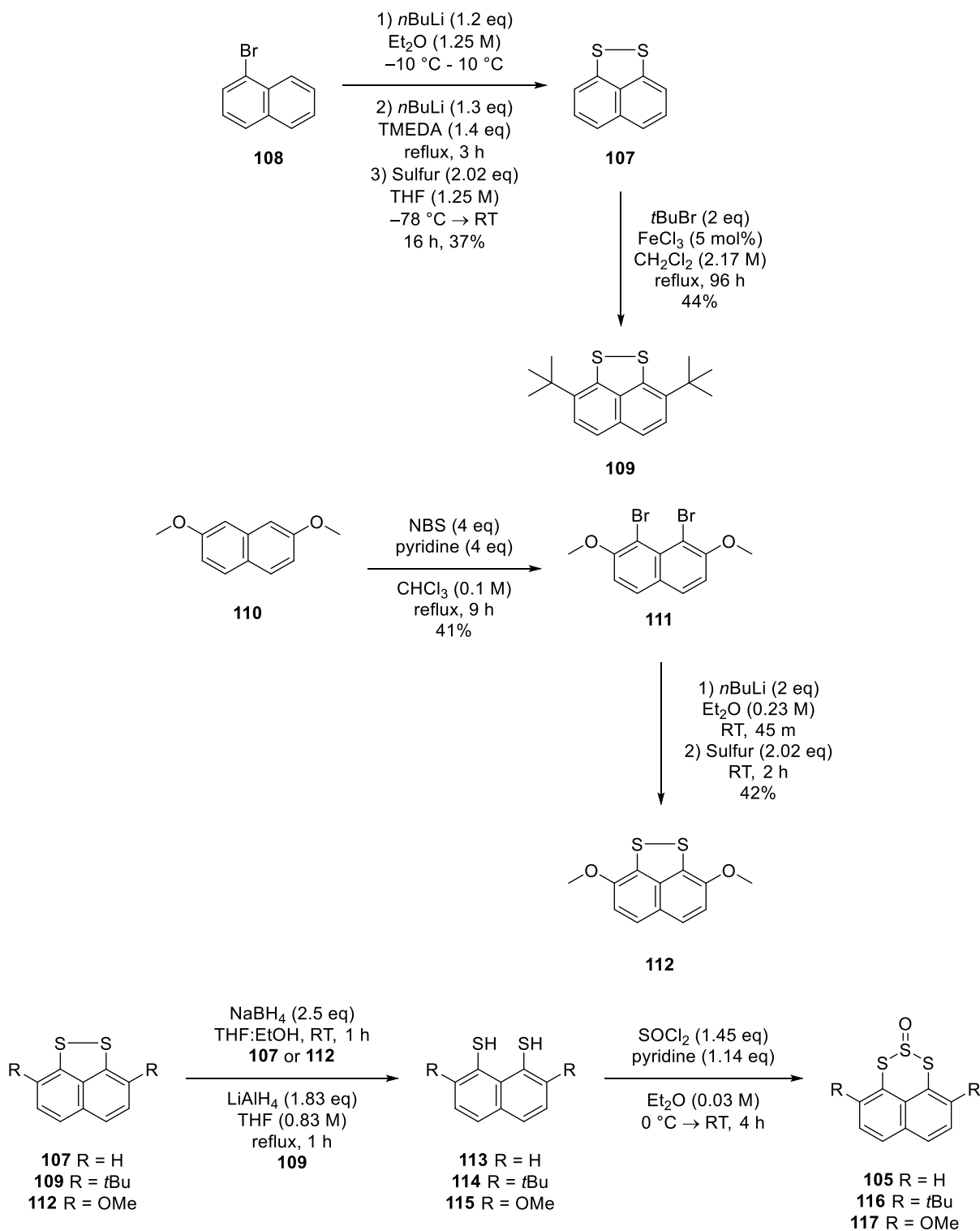
#### 1.1.5 Trisulfide-2-oxides as SO transfer reagents

In 1980, Schweig *et al.* found that pyrolysis of benzene trisulfide-2-oxide **102** releases SO.<sup>41</sup> However, benzene trisulfide-2-oxide **102** required pressures of 0.05 mbar and temperatures of  $\geq 540$  °C. The high temperatures required therefore make benzene trisulfide-2-oxide **102** unsuitable as an SO transfer reagent (**Scheme 26**). Taking inspiration from this, in 2001 Grainger *et al.* published their findings on the release of SO from naphthalene trisulfide-2-oxides **105**. Then in 2011 they published their findings on the release of SO from trisulfide-2-oxides **116**, and **117**. Pyrolysis of trisulfide-2-oxide **105** in the presence of a diene in refluxing chlorobenzene gave excellent yields of the resulting sulfoxide (**Scheme 26**).<sup>42</sup> Pyrolysis of trisulfide-2-oxide **105** in the presence of cycloheptatriene **35** in refluxing chlorobenzene gave dihydroheptafulvalene **36** in a 13% yield (**Scheme 26**).<sup>42</sup> Naphthalene trisulfide-2-oxide **105** undergoes photolysis to disulfide **107**. However, the yield of sulfoxide **20** is significantly lower at 55%. Pyrolysis of naphthalene trisulfide-2-oxide **105** was explored in a variety of other solvents and at lower temperatures. The optimised conditions, however, were found to be chlorobenzene at reflux.



**Scheme 26** Top – Schweig et al. release of SO from benzene trisulfide-2-oxide **102**. Bottom - Grainger et al. trapping of SO from naphthalene trisulfide-2-oxide **105**.<sup>42</sup>

Grainger et al. also synthesised trisulfide-2-oxides **105**, **116** and **117** by first synthesising the respective disulfides via lithiation techniques. Disulfide **112** was particularly challenging to reduce, therefore  $\text{LiAlH}_4$  was used as the reducing agent (**Scheme 27**).



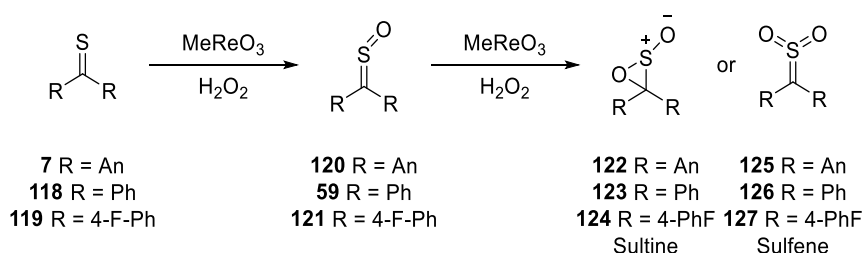
**Scheme 27** Synthesis of naphthalene trisulfide-2-oxides **105**, **116**, and **117** by Grainger et

al.<sup>42,43</sup>

Grainger *et al.* also investigated whether the reaction between trisulfide-2-oxide **105** and diene **18** was a bimolecular transfer of SO from the trisulfide-2-oxide to the diene or was SO itself reacting with the diene.<sup>43</sup> They performed the reaction at a series of different concentrations under *pseudo*-first order conditions and found the reaction to be first order with respect to the trisulfide-2-oxide and zeroth order with respect to the diene. A series of reactions were performed in octane at varying concentrations of both trisulfide-2-oxide **105** and diene and the degradation times was monitored. Plotting  $\ln[105]$  vs time they found the reaction was *pseudo*-first order. This indicated that the diene does not play a role in the rate determining step and the trisulfide-2-oxide must degrade to SO and the disulfide first.

#### 1.1.6 Small ring strain release SO transfer reagents

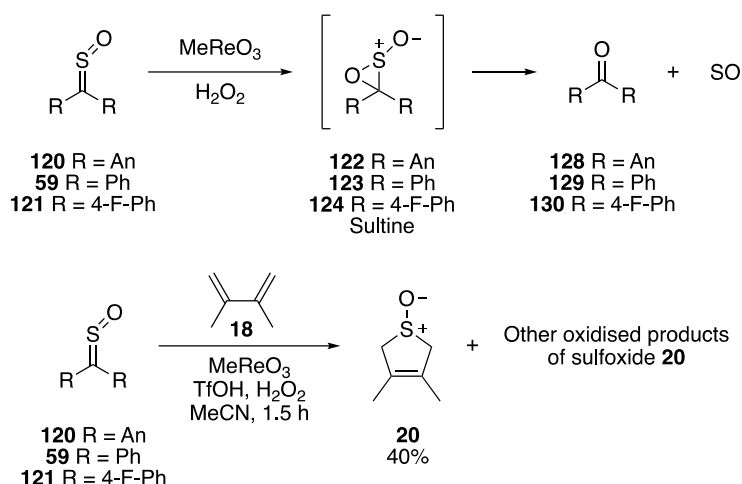
Thioketones were found to react with  $\text{MeReO}_3$  and  $\text{H}_2\text{O}_2$  by Espenson *et al.* in 1999.<sup>44</sup> Oxidation of the thioketones **7**, **118**, and **119** at the sulfur gives the sulfines **120**, **59**, and **121**. The sulfines then undergo oxidation to either the sultines **122** – **124** or the sulfenes **125** – **127** (Scheme 28).



**Scheme 28**  $\text{MeReO}_3$  catalysed oxidation of thioketones to sultines/sulfenes.<sup>44</sup>

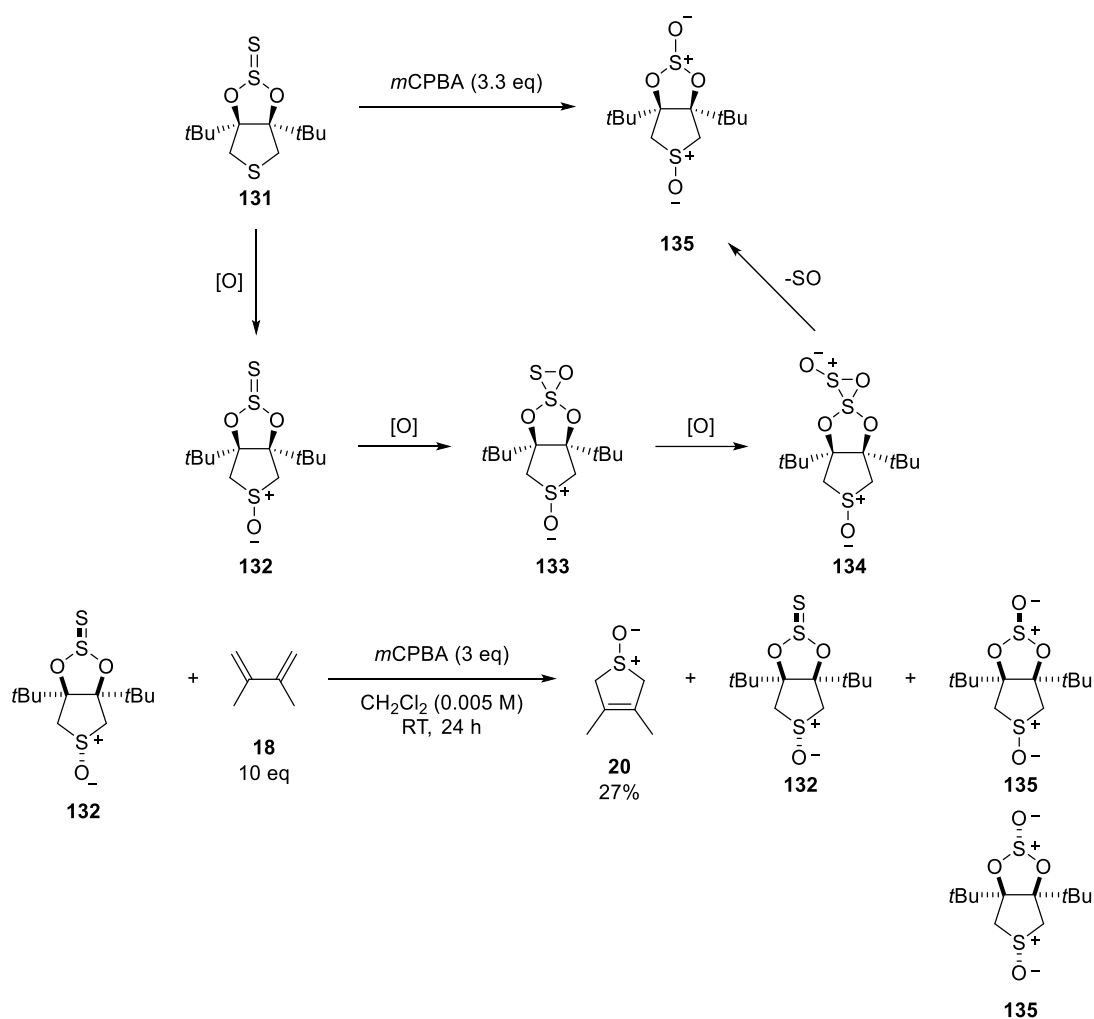
Theoretical studies by Mazzanti *et al.* indicate that the second oxidation does not undergo on the sulfur atom but on the C=S bond (using peroxybenzoic acid) (Scheme 29).<sup>11,45</sup> The resulting sultine undergoes a rearrangement to release SO and give the resulting ketone. The

SO can be trapped using a diene. However, yields are poor as (due to the oxidising reaction media) the SO can be oxidised further to SO<sub>2</sub>, and the cyclic sulfoxide **20** can be oxidised further to give a variety of different products.



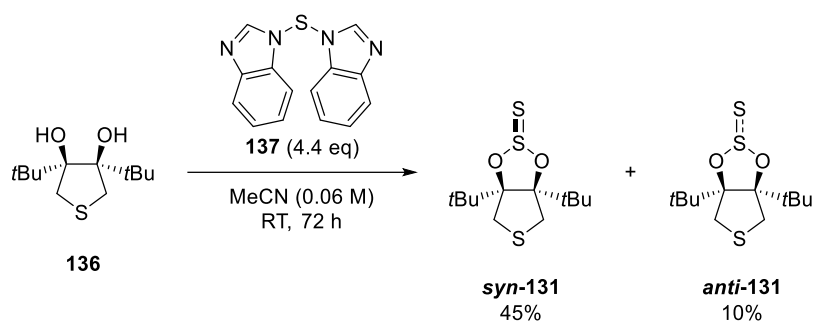
**Scheme 29** The oxidation of sulfine and the rearrangement of the sultine to the ketone and SO release. Reactions of SO in the oxidative media.

Nakayama *et al.* found that oxidation of thiosulfinyl **131** yielded sulfite **135**.<sup>46</sup> Thiosulfinyl **131** firstly oxidises to sulfoxide **132**. Sulfoxide **132** then undergoes oxidation at thiosulfinyl group to yield the three membered ring intermediate **133**. Finally, the three membered ring intermediate undergoes oxidation to give sulfinyl **134**. Sulfinyl **134** undergoes a rearrangement to yield sulfite **135** and SO. SO was captured using diene **18** to yield sulfoxide **20** in a 27% yield and a series of by-products (**Scheme 30**).



**Scheme 30** Oxidation of thiosulfite **131** to sulfite **135** and the release of SO. The capture of SO with diene **18** gives sulfoxide **20** in a 27% yield. No yield is provided of the products **132** and **135** (both isomers) but a ratio of 34:3:63 ratio is given.<sup>46</sup>

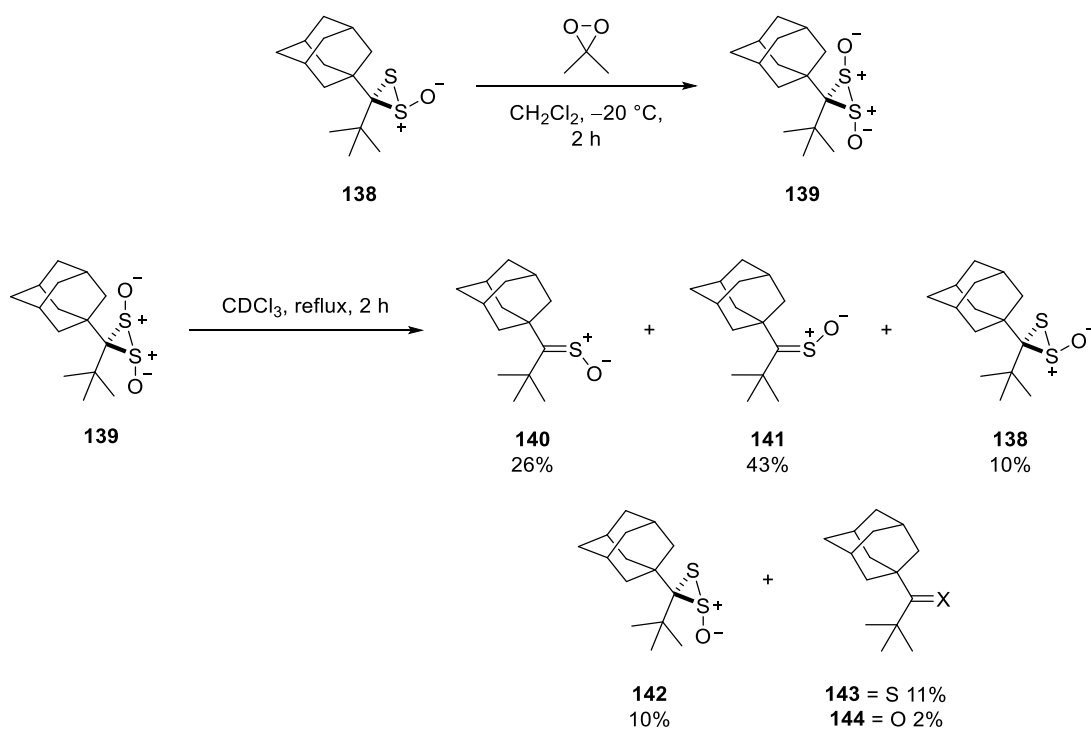
Thiosulfinyl **131** was synthesised by reacting diol **136** with 1,1'-thio-bis(1*H*-benzimidazole) **137** to yield diastereomers **syn-131** and **anti-131** (Scheme 31).



**Scheme 31** Reaction of diol **136** with 1,1'-thiobis-(1H-benzimidazole) to yield thiosulfites **syn-131** and **anti-131**.<sup>46</sup>

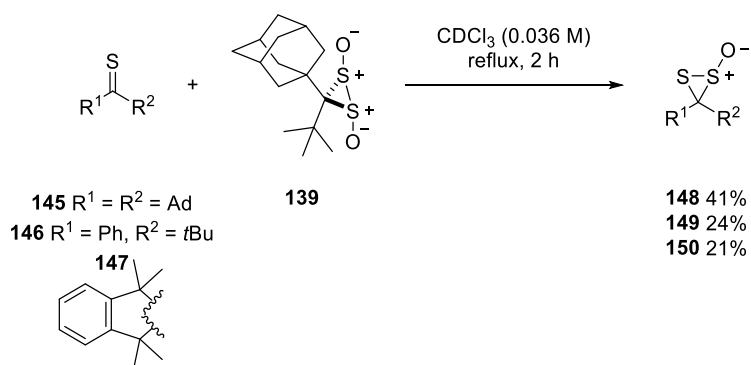
Oxidation of thiosulfinate **138** with DMDO by Ishii *et al.* gave *vic*-disulfoxide **139**.<sup>47</sup> However, if they left *vic*-disulfoxide **139** in solution at room temperature, they found it degraded to several products (**Scheme 32**). After refluxing *vic*-disulfoxide **139** in CDCl<sub>3</sub>, *trans*-sulfine **140** and *cis*-**141** were identified as the main products, indicating loss of SO. The other products were hypothesised to be reactions of SO and the sulfines or the starting material, eventually releasing SO<sub>2</sub>. It was calculated that if SO was being lost, then the SO released from *vic*-disulfoxide **139** should be in the <sup>3</sup>Σ<sup>-</sup>SO state. To prove that SO was being released, they trapped the SO with 2,3-dimethyl-1,3-butadiene **18** in a 19% yield.





**Scheme 32** The decomposition of vic-disulfoxide **139** via the release of  $\text{SO}$ .<sup>48</sup>

Vic-sulfoxide **139** was also reacted with thioketones **145** – **147**, yielding thiosulfinates **148** – **150** (Scheme 33).<sup>48</sup>

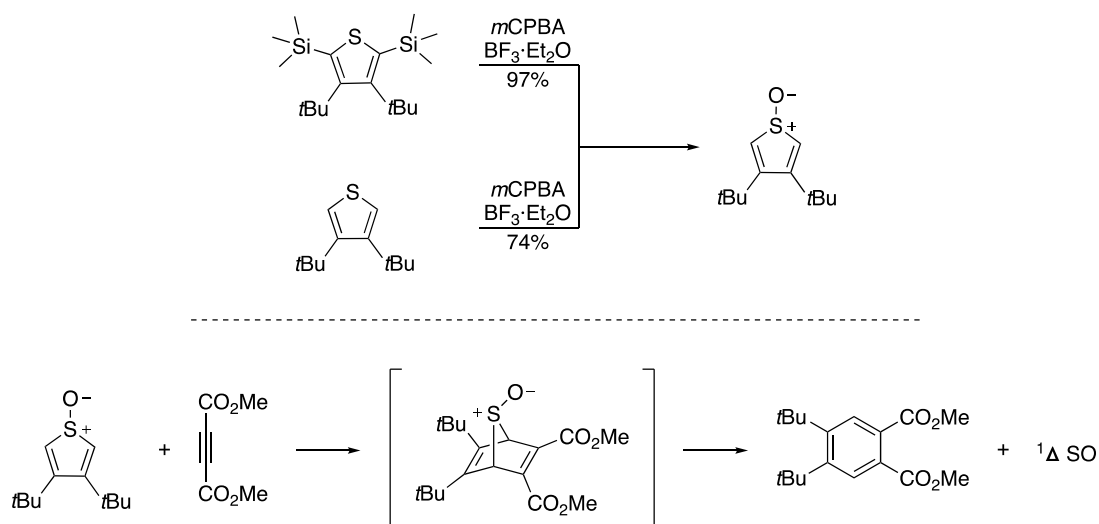


**Scheme 33** Reaction of thioketones **145** – **147** with vic-disulfoxide **139** to yield thiosulfinates

**148** – **150**.<sup>48</sup>

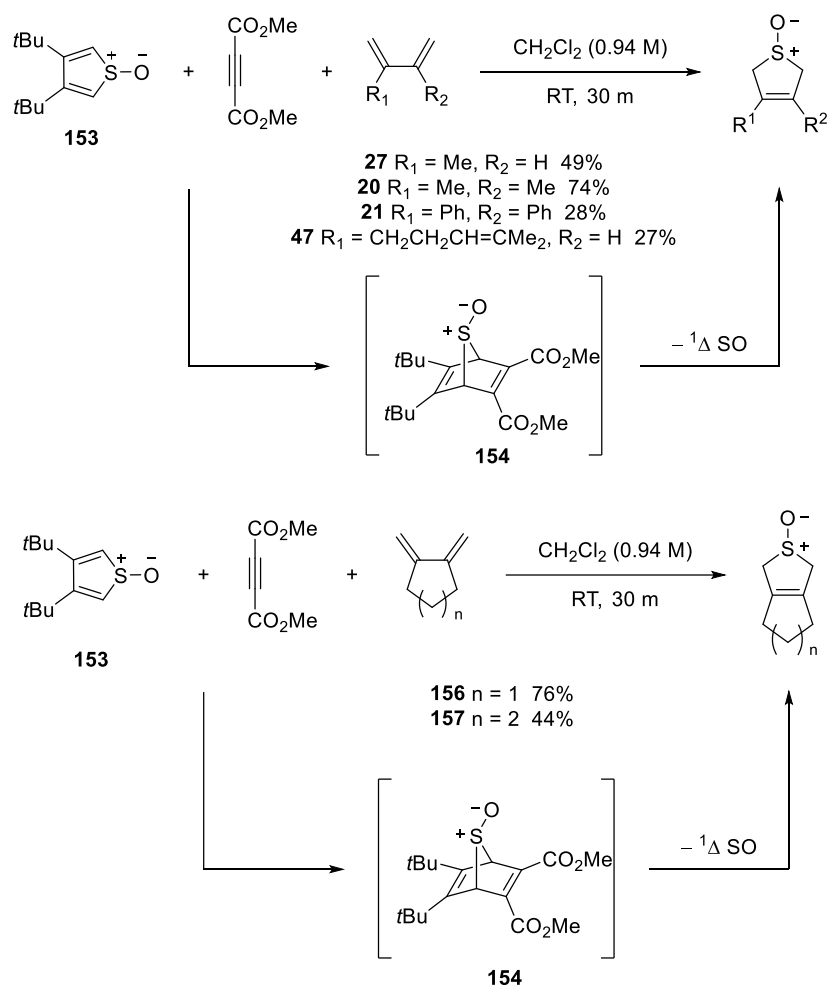
### 1.1.7 Singlet SO transfer reagents

So far, all the SO transfer reagents have either released triplet SO or the electronic configuration of SO was not identified. It has been assumed that the electronic configuration of all previous transfer reagents has yielded triplet SO. All the previously discussed SO transfer reagents have utilised ring strain to release SO – I believe this is a deciding factor in the electronic configuration of release. In the next two cases the systems release singlet SO ( $^1\Delta$  SO) and at the time of writing were the only two known systems to do so. Thiophene-1-oxides tend to be unstable due to the tendency of thiophene-1-oxides to dimerise *via* a Diels–Alder reaction and then a rapid second oxidation of the sulfur.<sup>49–51</sup> Thiophene-1-oxide **153** was found to be stable due to the *t*butyl groups on the 3 and 4 positions by Nakayama *et al.* in 1997.<sup>51–53</sup> Thiophene-1-oxide **153** undergoes a Diels–Alder reaction with dimethyl acetylenedicarboxylate to give bridged sulfoxide **154** (not isolated). However, unlike previous methods, the resulting sulfoxide **154** undergoes a pericyclic cheletropic extrusion of SO to give aromatic **155** (Scheme 34). Due to the unusual reactivity observed, it is hypothesised that  $^1\Delta$  SO is being released.

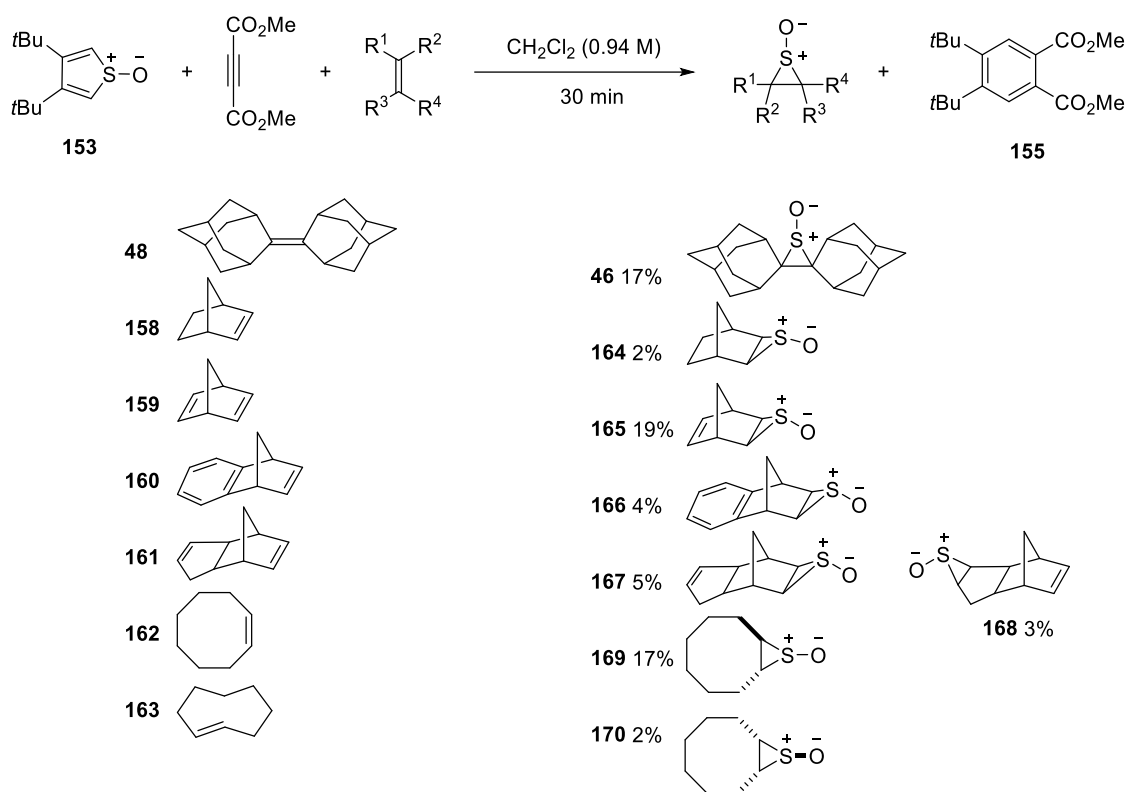


**Scheme 34** Nakayama *et al.* cheletropic extrusion of  $^1\Delta$  SO from Diels-Alder adducts of stable thiophene 1-oxide (or S-oxides).<sup>14,52</sup>

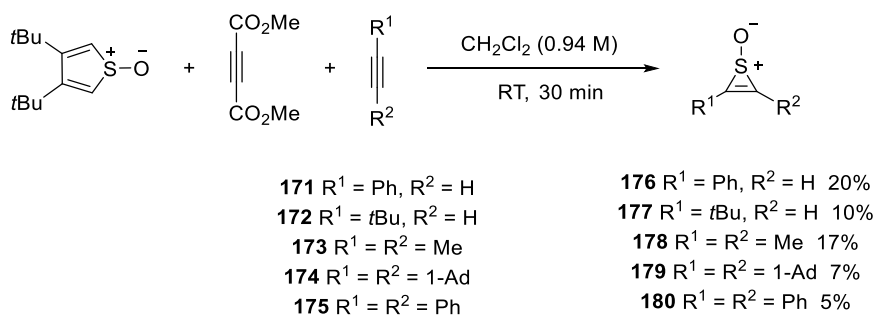
Nakayama *et al.* reports moderate yields when trapping with dienes with the most successful trap 2,3-dimethyl-1,3-butadiene **18** (**Scheme 35**).<sup>14</sup> They also reported low to moderate yields for the reactivity of  $^1\Delta$  SO with alkenes, alkynes, and cycloheptatriene **35** (**Scheme 36**, **Scheme 37**, and **Scheme 38**).<sup>14</sup>  $^1\Delta$  SO reacts with cycloheptatriene **35** acting as a diene to yield sulfoxide **178**.  $^3\Sigma^-$  SO reacts with cycloheptatriene **35** to yield the dihydroheptafulvalene **36** (**Scheme 13**). Therefore, there is a synthetic indication into whether  $^1\Delta$  SO or  $^3\Sigma^-$  SO is being generated.



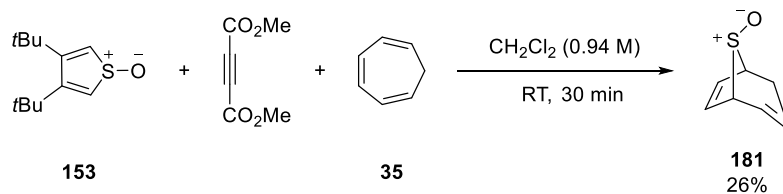
**Scheme 35** The reaction of  $^1\Delta$  SO with dienes.<sup>14</sup>



**Scheme 36** Reaction of alkenes with  $^1\Delta\text{SO}$  to yield episulfoxides.<sup>14</sup>

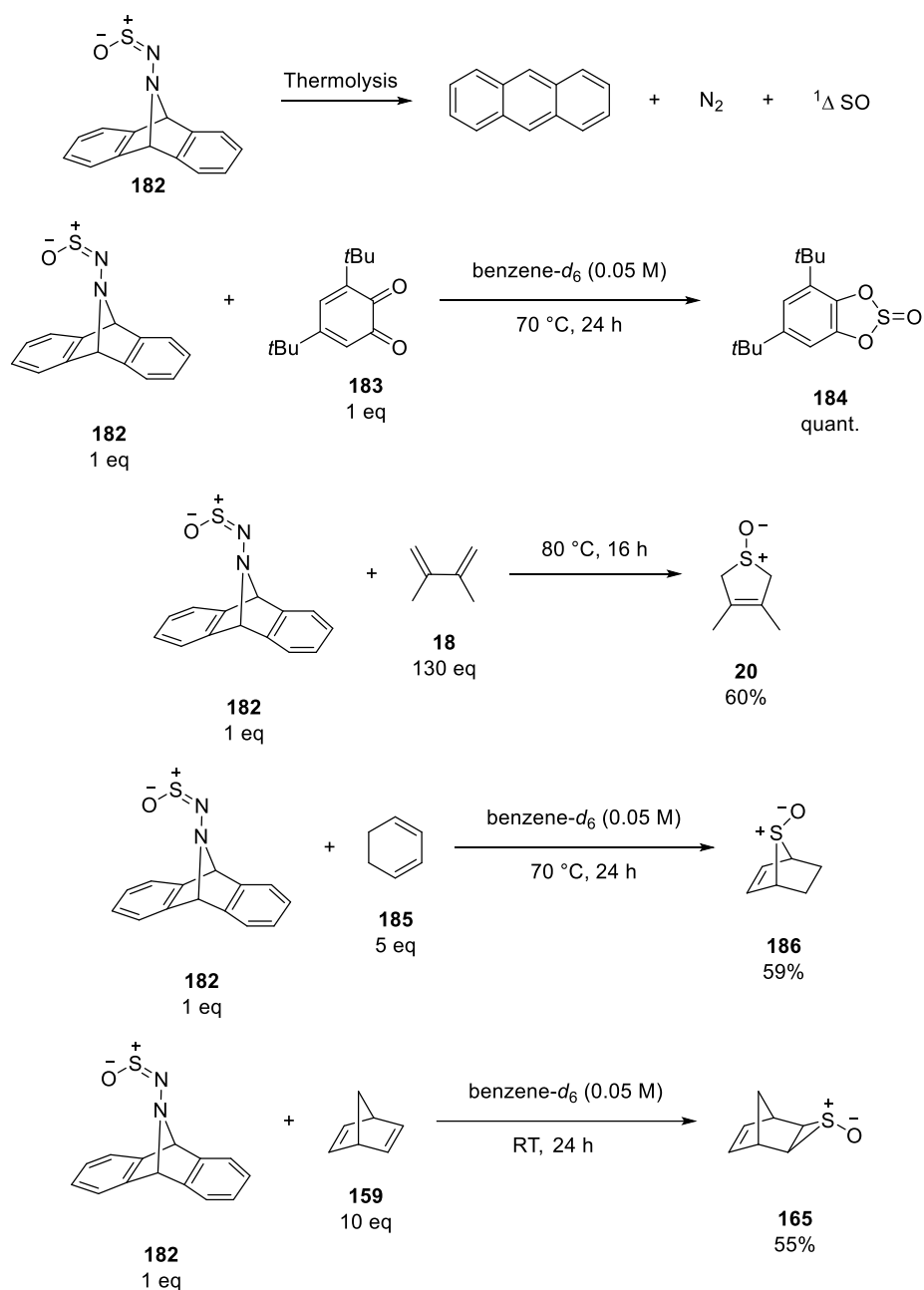


**Scheme 37** Reaction of alkynes with  $^1\Delta\text{SO}$  to yield thiirene-1-oxides.<sup>14</sup>



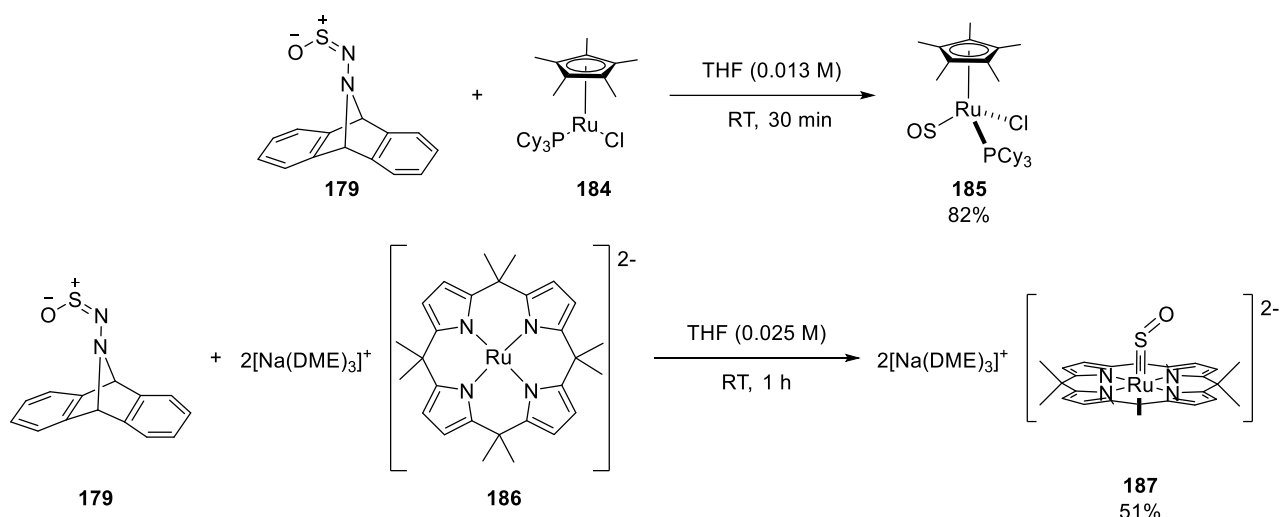
**Scheme 38** Reaction of  $^1\Delta\text{SO}$  with cycloheptatriene to yield cyclic sulfoxide **178**.<sup>14</sup>

Sulfinylhydrazine **182** was synthesised from Carpino's hydrazine by Cummins *et. al* in 2018.<sup>15</sup> Using DFT calculations (RI-B2PLYP-D3(BJ) density functional and Def2-TZVP basis set), sulfinylhydrazine **182** was calculated to release  $^1\Delta$  SO *via* a concerted, asynchronous mechanism.<sup>15</sup> The aminosulfinyl moiety breaks from the anthracene system firstly (C-N bond fission) followed by a concerted, asynchronous breaking of the N-S bond and the other C-N bond. DFT calculations using the RI-B2PLYP-D3(BJ) density functional and the Def2-TZVP basis, found no transition states between the first C-N fission and the final products. The decomposition of sulfonylhydrazine **182** releases SO as well as giving equimolar amounts of N<sub>2</sub> and anthracene.  $^1\Delta$ SO was trapped with 2,3-dimethyl-1,3-butadiene **18** (60%), 1,3-cyclohexadiene **185** (59%), norbornadiene **159** (reacting with one alkene) (55%) and a 1,2-quinone **183** (quantitative) (**Scheme 39**).<sup>15</sup>



**Scheme 39** The transfer of  ${}^1\Delta \text{SO}$  by Cummins et al.<sup>15</sup>

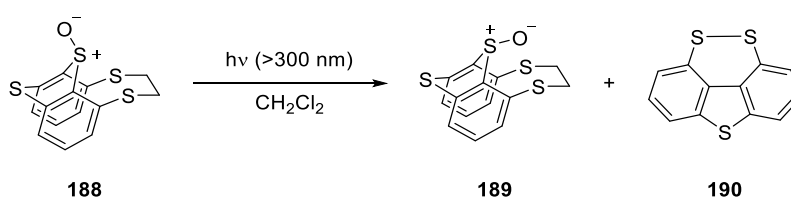
${}^1\Delta \text{SO}$  was also transferred to inorganic metal complexes. The ruthenium complexes were synthesised in moderate to good yields (**Scheme 40**).<sup>15</sup> However, the reactions were performed at room temperature, so it is unclear whether there was formal release of  $\text{SO}$ .



**Scheme 40** The transfer of SO by Cummins et al. to metal complexes.<sup>15</sup>

### 1.1.8 Miscellaneous SO transfer reagents

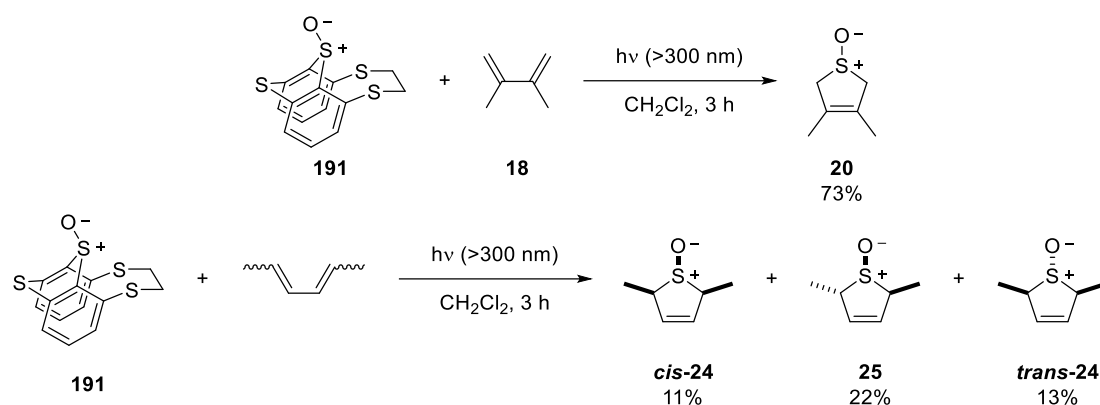
Thianthrene-10-oxide **191** was found to undergo a configurational change, in the presence of light, resulting in sulfoxide inversion.<sup>54</sup> In this case the sulfoxide goes from axial to equatorial. However, with prolonged exposure to light thianthrene-10-oxide **192** decomposes to disulfide **193**. Therefore, there is the formal loss of SO and ethene (**Scheme 41**).



**Scheme 41** Irradiation of thianthrene-1-oxide **191** to give inverted thianthrene-1-oxide **192** disulfide **193**.<sup>54</sup>

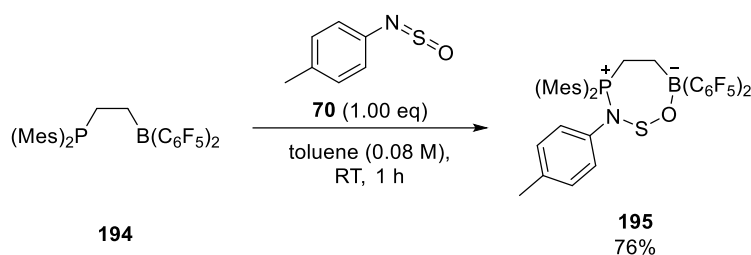
SO was trapped with diene **18** to yield the resulting sulfoxide **20** in a 73% yield, the disulfide **190** in 47% and the equatorial thianthrene-10-oxide **189** in 27% yield. Thianthrene-10-oxide **188** was reacted with 2,4-hexadiene (a mixture of all isomers) in the presence of light to give all possible isomers of the cyclic sulfoxide *cis*-**24**, *trans*-**24**, and **25** (**Scheme 42**).





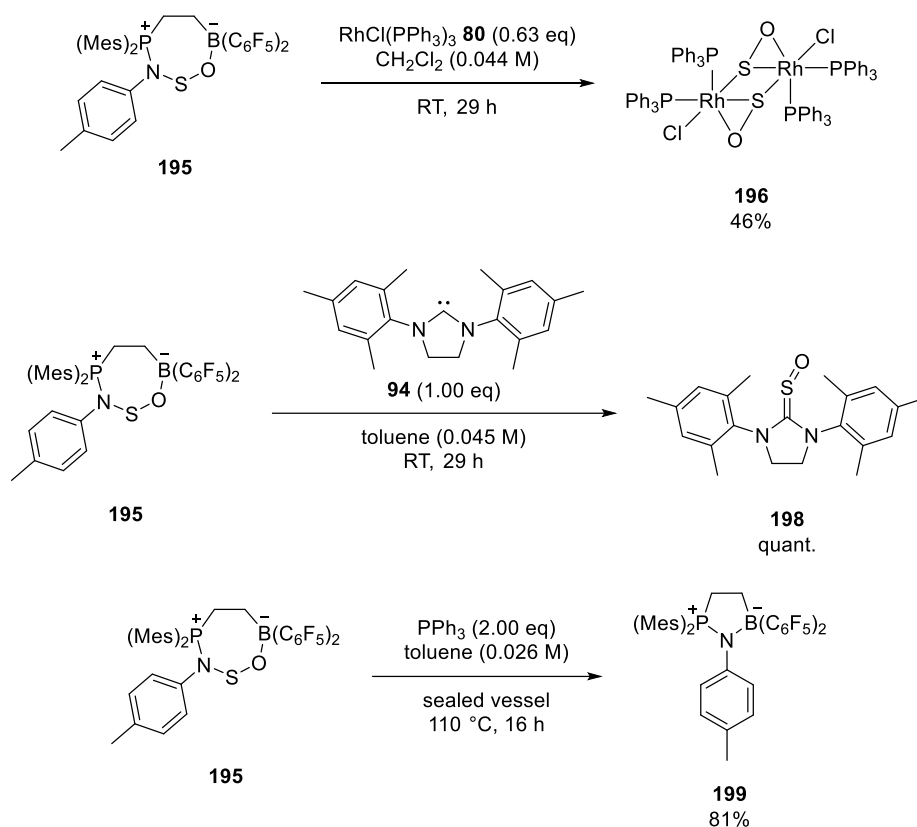
**Scheme 42** SO transfer to dienes from thiantherene-10-oxide **188**.<sup>54</sup>

In 2015, Stephan *et al.* designed a frustrated Lewis pair SO transfer reagent. They reacted frustrated Lewis pair (FLP) **194** with *p*-tolyl-sulfinylamine **70** to give 7-membered ring **195** (**Scheme 43**).<sup>55</sup>



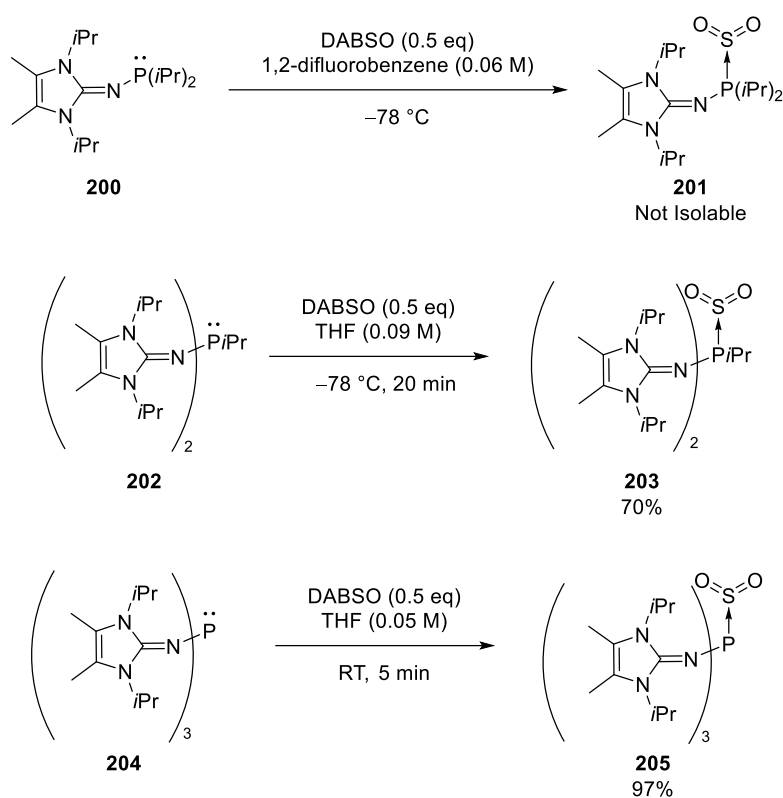
**Scheme 43** Synthesis of FLP-SO **192** transfer reagent by Stephan *et al.*<sup>55</sup>

The FLP-SO **195** reagent was found to have some unusual reactivity. Upon addition to N-heterocyclic carbene (NHC) ligand **197**, sulfine **198** was formed in a quantitative yield.<sup>55</sup> The addition of Wilkinson's catalyst **80** to FLP-SO reagent **195** gave Rh-SO complex **196** in a 46% yield (**Scheme 44**). Finally, the addition of PPh<sub>3</sub> to FLP-SO reagent **195** gave the FLP-N-tolyl **199** in an 81% yield and OPPh<sub>3</sub> and SPPH<sub>3</sub> (yields not stated for phosphine oxide or phosphine sulfide). SO is not formally released but is stabilised by the FLP so it can undergo a reaction with a metal complex.



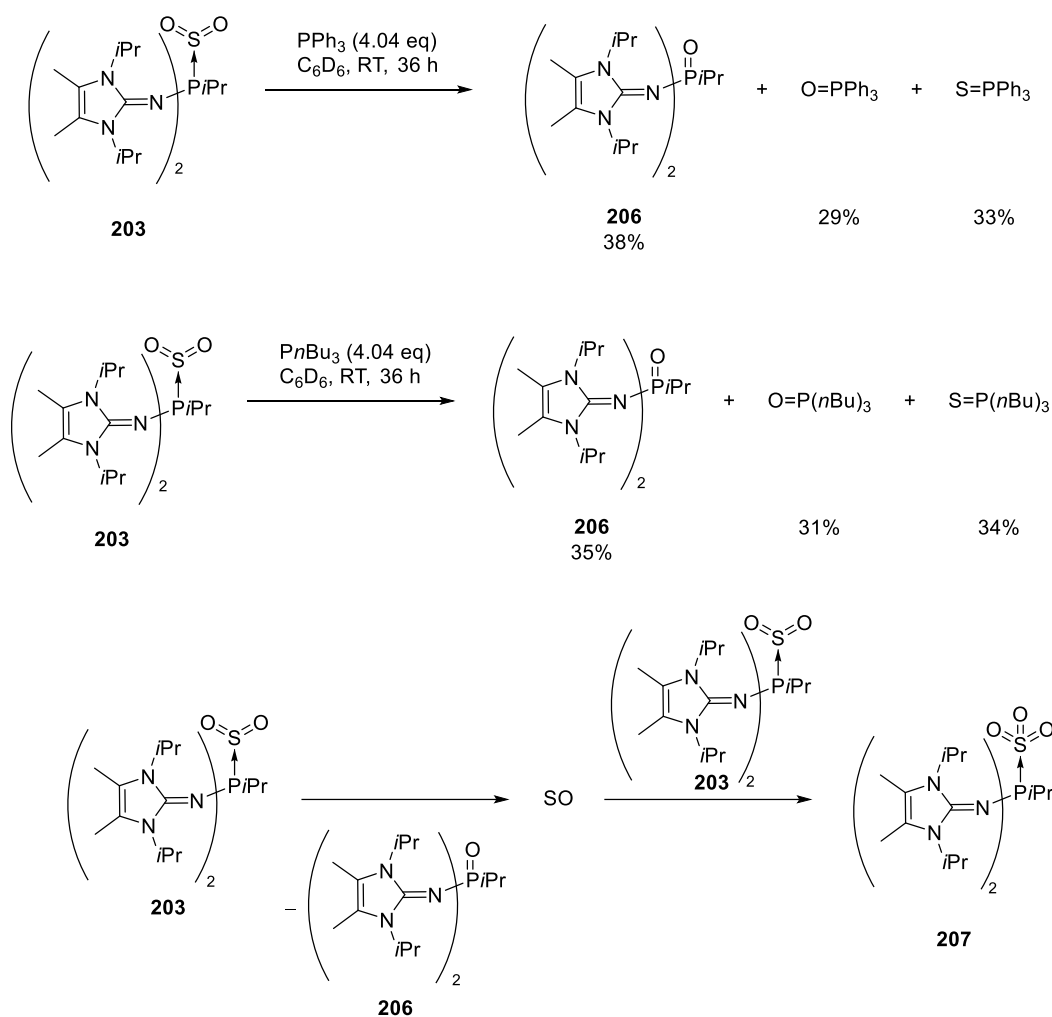
**Scheme 44** FLP-SO 19% transfer of SO to Wilkinson's catalyst **80**, NHC ligand **94** and  $\text{PPh}_3$ .<sup>55</sup>

It has been well documented in the literature that  $\text{SO}_2$  rapidly reacts with both alkyl and aryl phosphines to give 2 equivalents of the phosphine oxide and one equivalent of the phosphine sulfide.<sup>56</sup> In 2018, Dielmann *et al.* found two stable phosphine- $\text{SO}_2$  adducts (**Scheme 45**).<sup>57</sup>



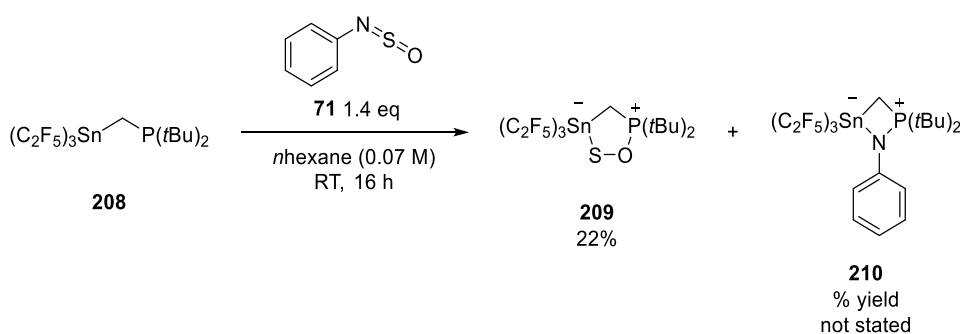
**Scheme 45** Dielmann *et al.* isolable phosphine/SO<sub>2</sub> adducts **201**, **203**, and **205**.<sup>57</sup>

From phosphine-SO<sub>2</sub> adduct **203**, the formation of phosphine-SO<sub>3</sub> adduct **207** was observed (**Scheme 46**). It was hypothesised that the phosphine-SO<sub>2</sub> **203** decomposed to give the phosphine oxide **206** and SO. SO then reacted with phosphine-SO<sub>2</sub> **203** to give phosphine-SO<sub>3</sub> **207** and elemental sulfur. Phosphine-SO<sub>2</sub> **203** was stirred in benzene in the presence of PPh<sub>3</sub> and P(*n*Bu)<sub>3</sub> (Cummins *et al.* confirmed that SO reacts with phosphines to give equimolar amounts of phosphine sulfide and phosphine oxide), and found equimolar amounts of OPPh<sub>3</sub> and SPPH<sub>3</sub> or OP(*n*Bu)<sub>3</sub> and SP(*n*Bu)<sub>3</sub> (**Scheme 46**).<sup>15,57</sup>



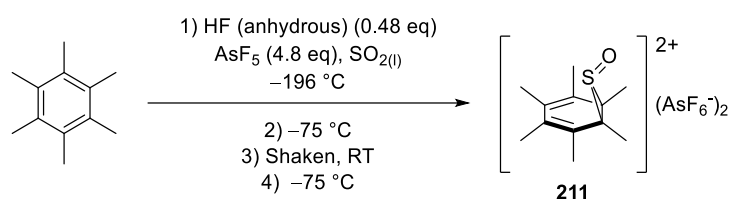
**Scheme 46** Phosphine/SO<sub>2</sub> adduct SO transfer to aryl and alkyl phosphines.<sup>57</sup>

FLP-SO adduct **209** was synthesised using a Sn/P FLP **208** by Mitzel *et al.* in 2020.<sup>58</sup> Using a similar synthesis to that of Stephan *et al.*, they used an aryl sulfinylamine. Instead of creating a 7-membered ring, the sulfinylamine **71** gave a mixture of FLP-SO **209** and an amine-bridged FLP **210**. No SO transfers from this Sn/P FLP **209** have been reported to date.<sup>58</sup>



**Scheme 47** Mitzel et. al. *Sn/P FLP-SO 206 adduct synthesis.*

In 2017, Malischewski and Seppelt created an unusual organic salt which stabilises SO. Whilst investigating a way to synthesise pentagonal-pyramidal hexamethylbenzene, they synthesised  $\text{C}_6(\text{CH}_3)_6\text{SO}^{2+} (\text{AsF}_6^-)_2$  (**Scheme 48**). This shows the unusual reactivity of SO, but the compound rapidly decomposes in organic solvents – suggesting it would not act as a good transfer reagent.<sup>59</sup>

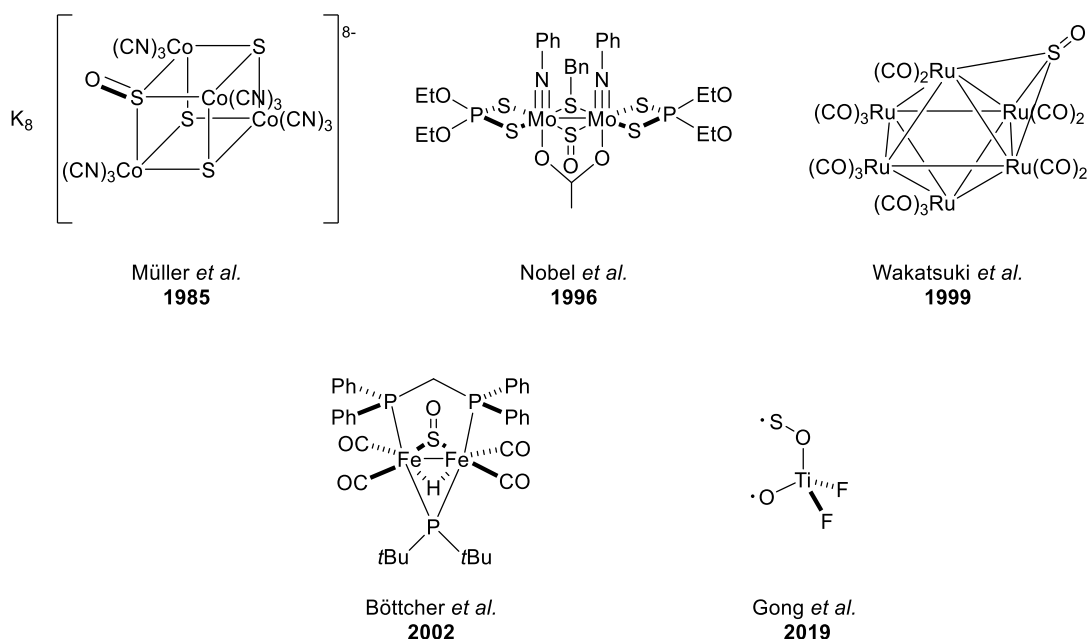


**Scheme 48** Malischewski and Seppelt's  $\text{SO}^{2+}$ /hexamethylbenzene complex.

### 1.1.9 Inorganic complexes and SO

SO has been well explored as a ligand in the literature. A review and a book have been written on this subject alone. This section will show some selective examples including complexes published after the review and book (2011 and 1992 respectively).<sup>8,13,36–38,40,60–73</sup> In these select examples, SO is not transferred to the complex, but rather sulfur has been inserted and an oxidation of the sulfur gives SO, or a SO precursor has been inserted and the precursor has

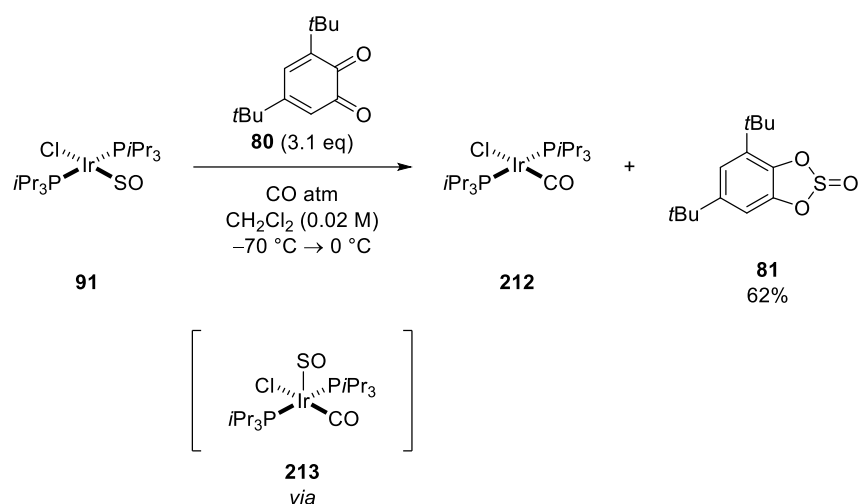
been fully incorporated into the final product. None of the below complexes have been shown to transfer SO (**Figure 4**).



**Figure 4** Some selective examples of M-SO complexes. The titanium complex by Gong *et al.* is displayed with the radicals but no radicals are displayed in the original paper.<sup>60,62,68,71,74</sup>

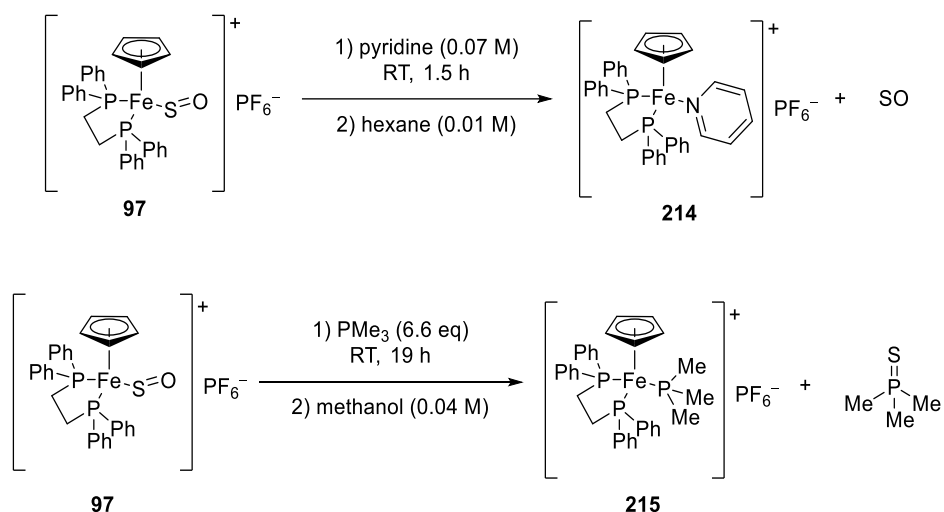
#### 1.1.10 Inorganic SO transfer reagents

There are far fewer examples of inorganic SO transfer reagents. SO was co-ordinated to iridium complex **91** by Schenk *et al.* in 1985 (**Scheme 49**).<sup>36,75</sup> Upon reaction with carbon monoxide (an atmosphere of CO), SO is displaced *via* a 5-membered co-ordinated complex **213**. In 1987 they proved that SO was transferred to 3,5-di-*tert*-butyl-*o*-benzoquinone **81**.<sup>76</sup>



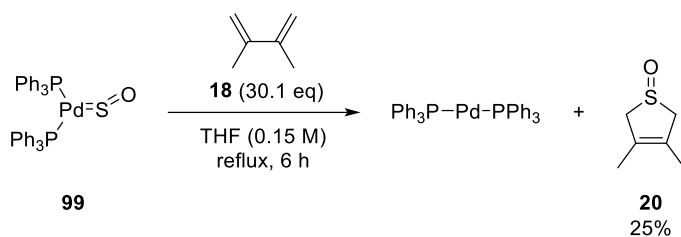
**Scheme 49** The transfer of SO from Ir-SO complex **91** to 1,2-quinone **80** by Schenk *et al.*<sup>75</sup>

[CpFe(II)(dppe)(SO)] **97** was found to formally releases SO upon nucleophilic displacement by both pyridine and PMe<sub>3</sub> by Schenk *et al.* in 1990.<sup>66</sup> In the reaction with PMe<sub>3</sub>, a by-product of the reaction is SPMe<sub>3</sub> – indicating a reaction with PMe<sub>3</sub> with SO, sulfur or SO<sub>2</sub> (the latter two are by-products of SO dimerization) (**Scheme 50**).



**Scheme 50** Formal release of SO from Fe-complex using ligand exchange by Schenk *et al.*<sup>66</sup>

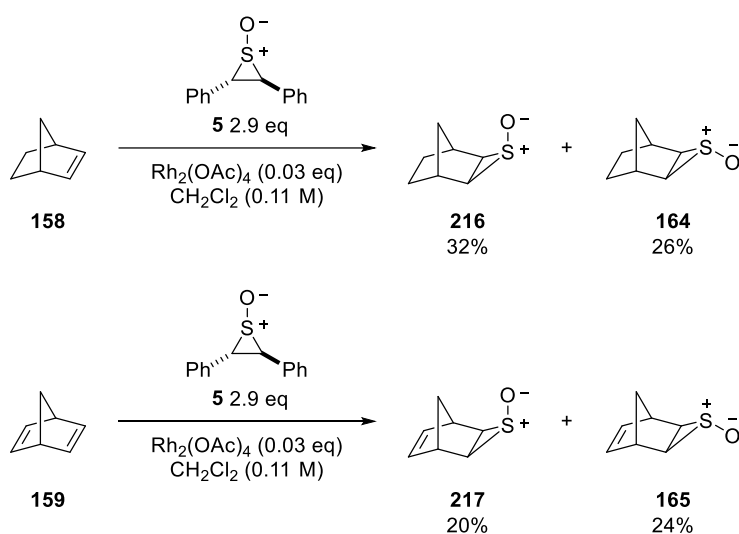
Palladium-SO complex [Pd(PPh<sub>3</sub>)<sub>2</sub>SO] **99** transfers SO. In refluxing THF, it was found that SO transfers to 2,3-dimethyl-1,3-butadiene **18** in a 25% yield (**Scheme 51**).<sup>39</sup>



**Scheme 51** Transfer of SO from Pd-SO complex **99** to 2,3-dimethyl-1,3-butadiene **18** by

Lorenz *et al.*<sup>39</sup>

A Rh-catalysed SO transfer was reported by Simpkins *et al.* in 1999.<sup>77</sup> Stilbene episulfoxide **5** and catalytic amounts of  $\text{Rh}_2(\text{OAc})_4$  were found to transfer SO to two strained alkenes (**158** and **159**) at room temperature. From previous papers, the transfer of SO from stilbene episulfoxide **5** required mild heating and could only be transferred to dienes ( $^3\Sigma$ -SO does not react with alkenes). This indicates the metal is required for the reaction.



**Scheme 52** Simpkins *et al.*  $\text{Rh}_2(\text{OAc})_4$  catalysed SO transfer to strained alkenes **158** and

**159**.<sup>77</sup>

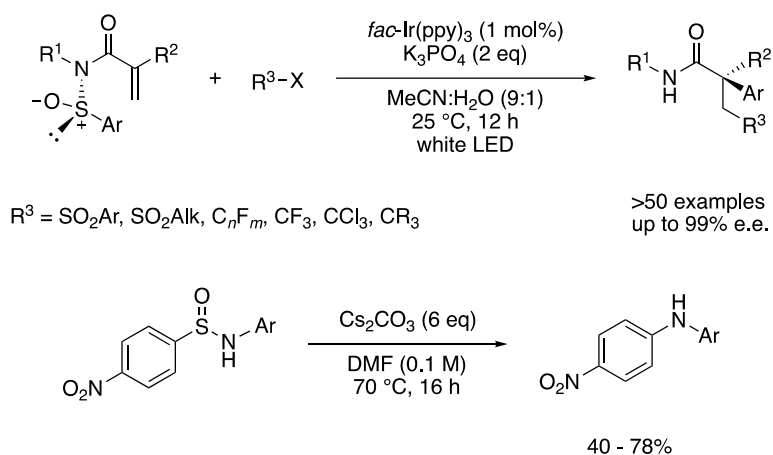


### 1.1.11 Formal loss of SO with no trap

There have been several examples of SO being lost or extruded from a system with the aim of synthesising something not related to SO. Two of the most recent examples are by Greaney *et al.* and Nevado *et al.*

Nevado *et al.* successfully demonstrated an asymmetric visible light-mediated radical sulfinyl-Smiles rearrangement to access all-carbon quaternary stereocentres. SO is lost in the system but is suspected to form H<sub>2</sub>SO<sub>3</sub>. Unfortunately, Nevado *et al.* do not confirm whether SO is released from the system, but their work highlights an excellent example of the Smiles rearrangement (**Scheme 53**).<sup>78</sup>

Greaney *et al.* also demonstrate an example of SO lost in a Smiles rearrangement. In their work, diarylamines are synthesised from diarylsulfinamides. However, it is limited to *p*-nitrosulfinamides (**Scheme 53**).<sup>79</sup>

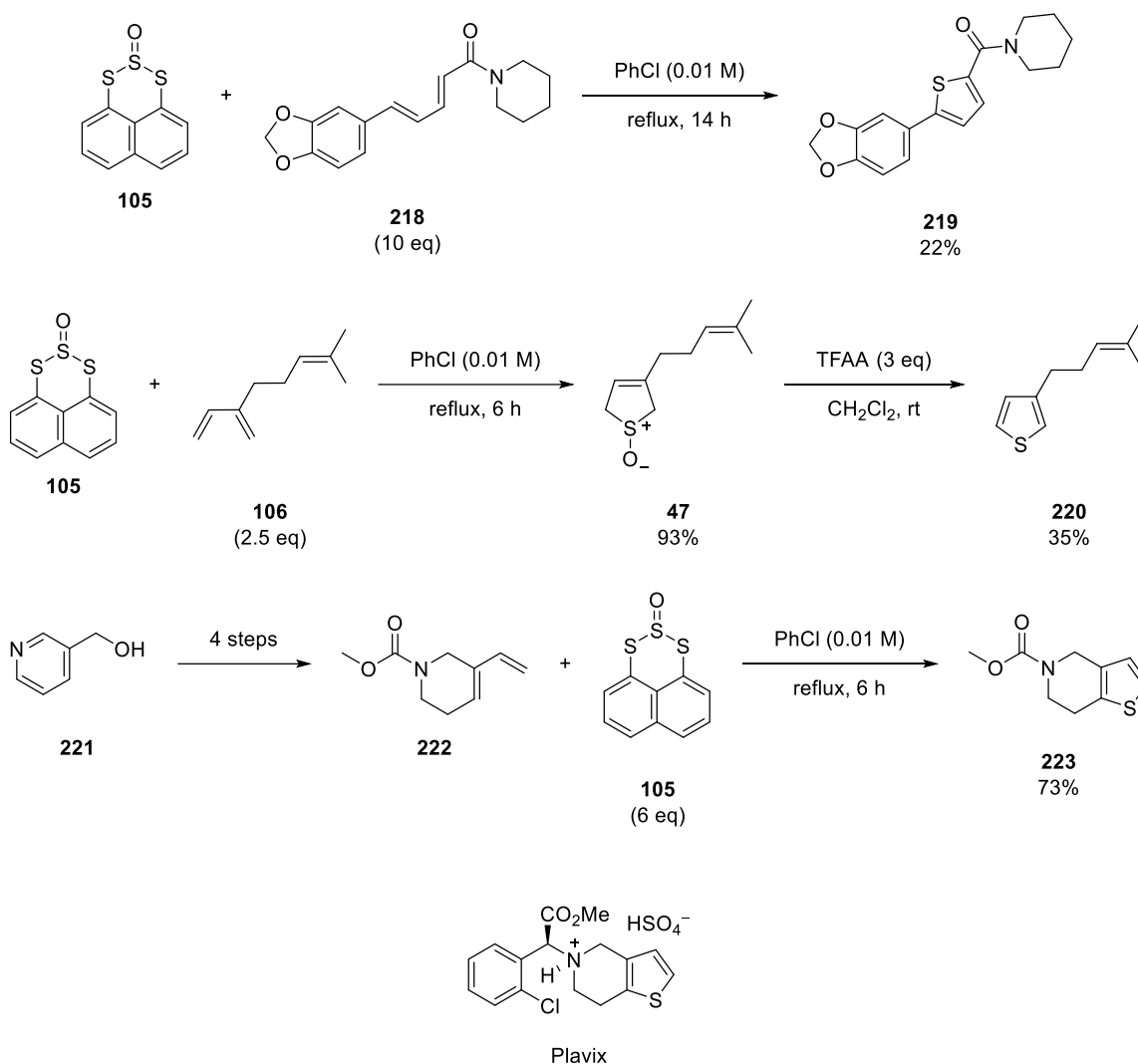


**Scheme 53** Top - Nevado *et al.* synthesis of quaternary all carbon substituted amides. Bottom- Greaney *et al.* synthesis of diarylamines. Both utilise a Smiles rearrangement. Formal loss of SO is observed.

### 1.1.12 Applications of SO release

SO was used, not only to make substituted cyclic sulfoxides, but also to make thiophenes by Grainger *et al.* in 2011. Thiophenes are often found in drug molecules and natural products.

Dihydrothiophene-1-oxides undergo dehydration under Pummerer conditions to give thiophenes. Piperine **218** is a natural product with a diene in the structure and was cyclised to the thiophene **219** directly from its reaction with SO in a 22% yield by Grainger *et al.* using trisulfide-2-oxide **105**. Similarly, myrcene **106** is a naturally occurring terpene and undergoes cyclisation with SO (released from trisulfide-2-oxide **105**) to form sulfoxide **47** in a 93% yield. Sulfoxide **47** undergoes a dehydrative Pummerer in the presence of trifluoroacetic anhydride to yield thioperillene **220**, a natural constituent in hops and rose oil. Plavix is a stroke medication which contains a thiophene. Diene **222** was synthesised from pyridine **221** over 4 steps. In the presence of 6 equivalents of trisulfide-2-oxide **105**, thiophene **223** was synthesised directly from diene **222**, without the need for a dehydrative Pummerer. Thiophene **223** is a precursor to Plavix (**Scheme 54**).

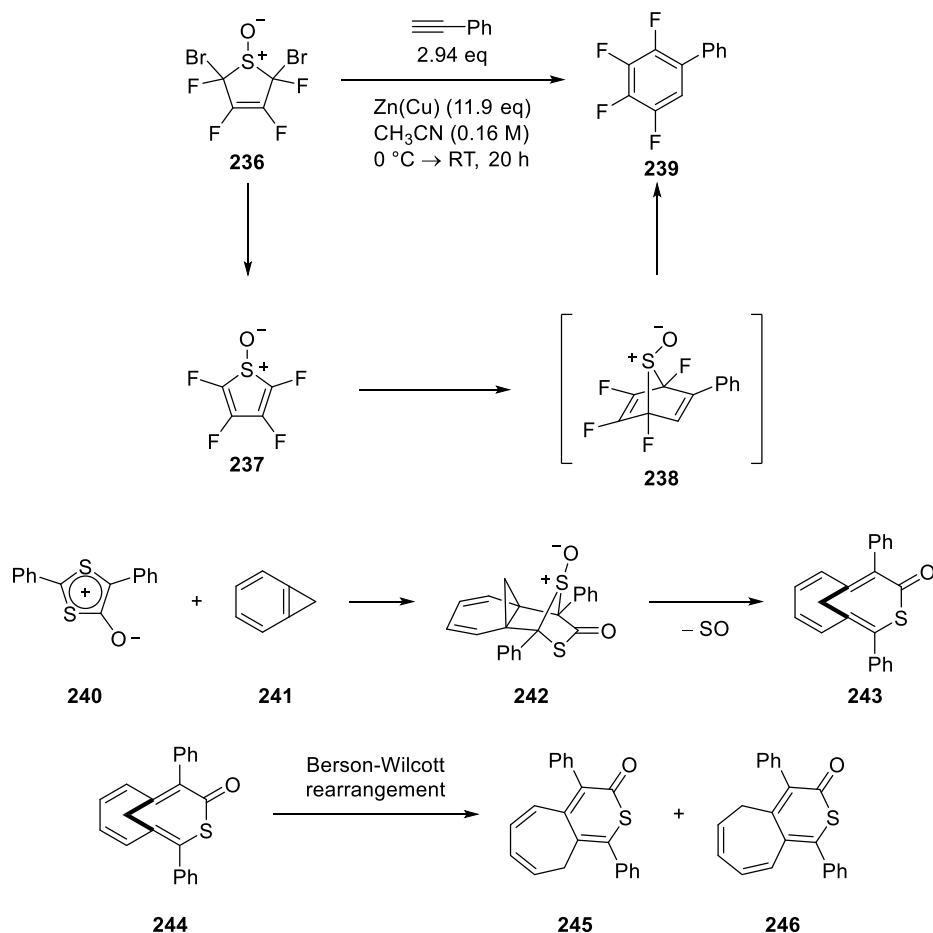
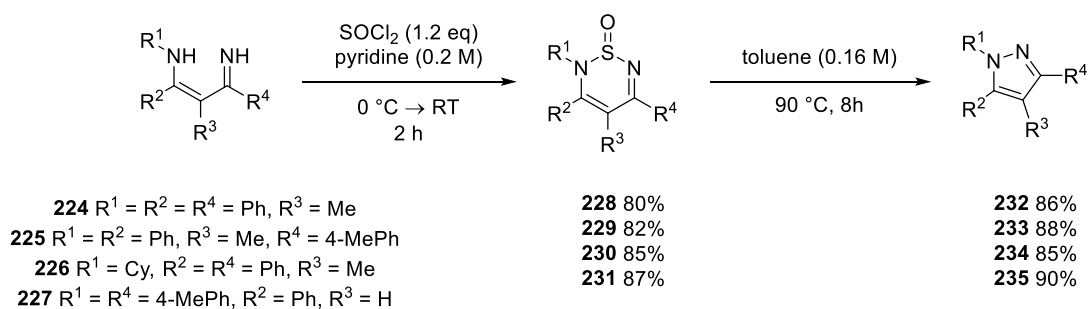


**Scheme 54** Grainger et al. synthesis of **219**, **47**, **220** and **223**.<sup>43</sup>

As SO is a gas, the entropy of a reaction system will increase when SO is released. Therefore, there have been several examples in the literature of SO release being used as an entropic driving force. Often SO release is used to drive towards aromaticity or conjugation. Pyrazoles have been synthesised *via* SO extrusion. In 1981, diimines **224** – **227** were reacted with SOCl<sub>2</sub> in the presence of pyridine to yield thiadiazine S-oxides **228** – **231** by Barluenga.<sup>80</sup> Heating thiadiazines S-oxides to 90 °C in toluene caused N-N bond formation to yield the pyrazole and extrusion of SO. The same reaction could be performed in a one-pot synthesis to form

pyrazoles (**Scheme 55**). In 2013, Lemal *et al.* described the use of thiophene-1-oxides for the synthesis of polyfluorinated aromatics (**Scheme 55**). The biphenyl **239** was achieved in a 41% yield but shows that SO release can be used as a driving force.<sup>81,82</sup>

Similarly, Kato and co-workers investigated the reactivity of mesoionic dithiolone **240**. After reacting mesoionic dithiolone **240** with benzocyclopropene **241**, the bridged sulfoxide **242**, in the presence of light, can undergo the extrusion of SO to conjugated bridged system **243** which can undergo a Berson-Wilcott rearrangement to thioesters **245** and **246** (**Scheme 55**).<sup>83</sup>

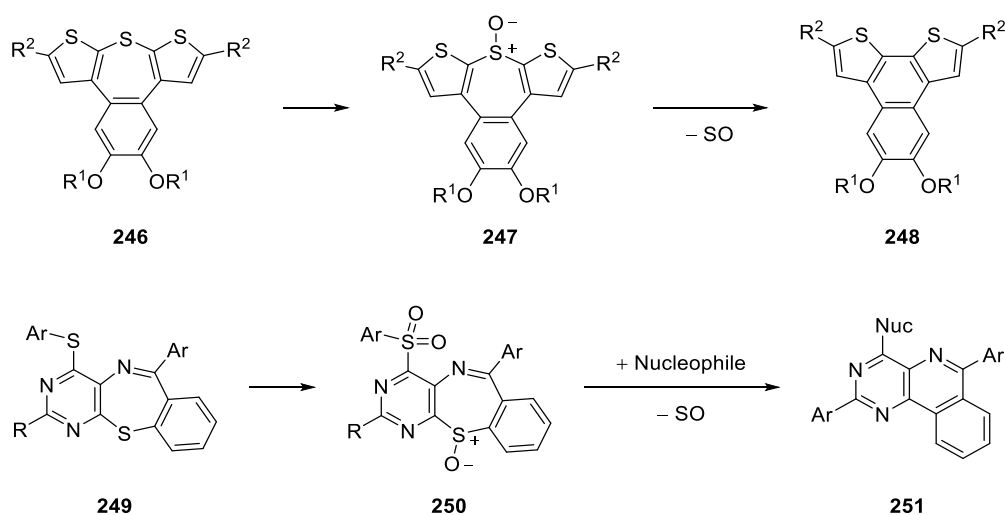


**Scheme 55** Examples of the extrusion of SO to gain aromaticity/conjugation.<sup>82,83</sup>

Another application of SO release is the synthesis of 6-membered rings from 7-membered rings. The conductive properties of thiepin-derived polymers were investigated by Swager and Song in 2010 (**Scheme 56**).<sup>84</sup> Upon oxidation of the thiepin to the 2+ oxidation state they found the compound degraded to the 6-membered benzene ring. If the thiepin sulfur is oxidised to the sulfoxide then the system loses SO. They found the sulfoxide (loss of SO) has

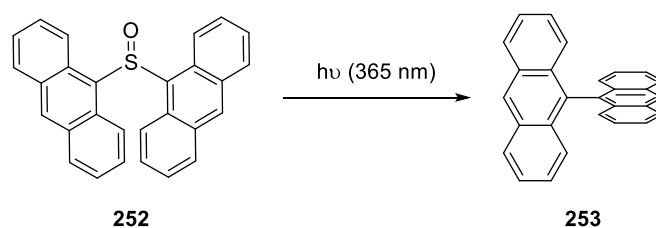
a lower extrusion barrier than the thiopin (loss of sulfur). They applied this as a peroxide sensor, which would lose SO if in oxidising media.

SO release was used to synthesise novel pyrimido[5,4-c]isoquinolines by Bai in 2007. Oxidation of the bridging sulfur atom and addition of the nucleophile caused the molecule to undergo SO loss.<sup>85</sup>



**Scheme 56** Examples of the extrusion of SO to make 6-membered rings from 7-membered rings.<sup>84,85</sup>

Another use for SO extrusion is biaryl bond synthesis. Wolf *et al.* found he could couple two anthracene units together in the 9-positions *via* photolytic extrusion of SO from a sulfoxide bridge to yield **253**.<sup>86</sup> Similarly, Murata *et al.* formed a biaryl bond which closed a fullerene containing molecular hydrogen by SO extrusion. Like Wolf *et al.* they used light to extrude SO.<sup>87</sup>



*Scheme 57 Examples of the extrusion of SO to form biaryl bonds.*<sup>86</sup>

### 1.1.13 Conclusion

The development of SO as a reagent has become of interest over the last 100 years. In the 1960s through to late 1970s the interest was to discover if it could be a viable reagent in organic chemistry. This involved a wide range of screening of organic traps, primarily using episulfoxides as the source of SO. SO has been shown to produce a wide range of different functionalities which were difficult to access prior to these pioneering discoveries. By the 1980s, inorganic chemists had discovered SO as a potential ligand to co-ordinate to metals.

Since then a wide range of SO-metal complexes have been discovered and, notably, 3 which have been shown to transfer SO to a trap. In the last 30 – 50 years there has been a drive to find other methods to release SO, with trisulfide-2-oxides being the most efficient. Whilst pursuing alternative methods of release, Nakayama and co-workers discovered a singlet SO transfer reagent **154**. Since then, the pursuit of another singlet SO transfer reagent has been made by a few groups with little success. Cummins and co-workers reported their singlet SO transfer reagent **182** derived from Carpino's hydrazine. This discovery has certainly piqued the interest of the scientific community and others have now pursued other singlet SO transfer reagents.<sup>55,57,58</sup> The scientific community has yet to discover an efficient singlet SO transfer reagent which can release and trap singlet SO in yields as good as Grainger and co-workers triplet SO transfer reagent **105**.

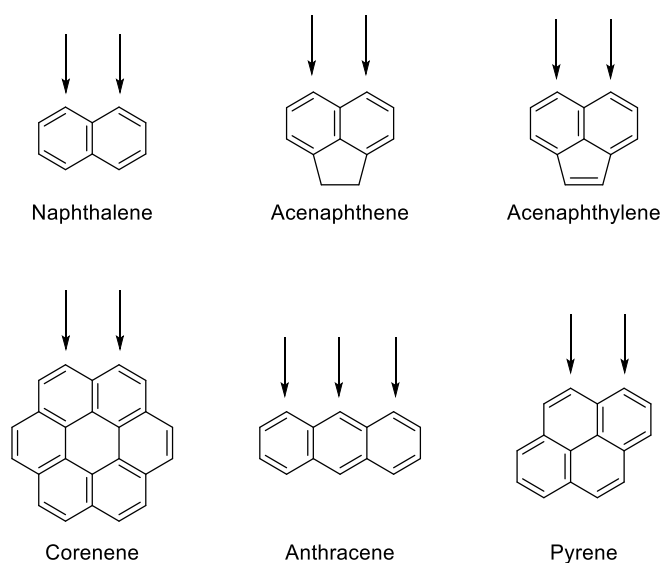
The above are all fundamental principle discoveries and applications in synthesis. The release of SO has also been used by a wide variety of chemists as a method to drive towards aromaticity, form biaryl bonds, synthesise complicated drug-like molecules, synthesise polyfluorinated molecules and the synthesis of fullerenes.

Therefore, there is still a need to discover an efficient singlet SO transfer reagent which can compete with Grainger and co-workers' triplet SO-releasing trisulfide-2-oxide **105**. It would be beneficial to discover alternative reactivities of singlet SO and introduce a similar reagent.



## 1.2 Peri-substitution

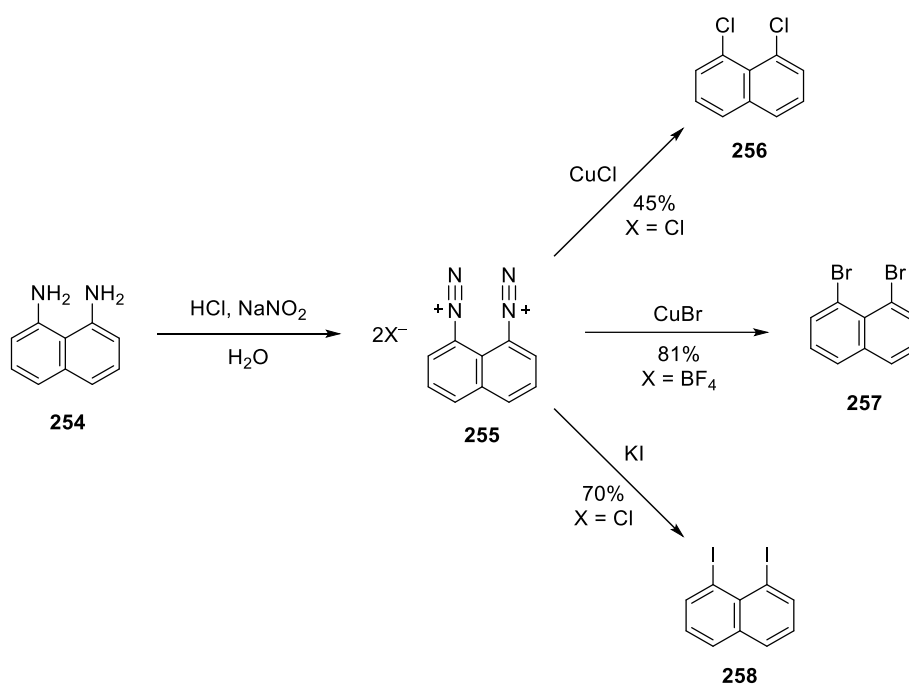
The *peri*-positions are defined as the carbons separated between the connecting carbon between two *ortho*-connected phenyl rings.<sup>88</sup> For example, the 1 and 8 positions of naphthalene are *peri*- with respect to each other. What makes the *peri*-positions unique to other aromatic positions is the inherent strain which is observed when both the C1 and C8 positions are substituted. Typically, functionality at the 1,8-position repel one another due to their close proximity. This is called the “*peri*-effect”. The C1...C8 distance is 2.5 Å.<sup>89</sup> This distance is small and therefore substitution of these positions will cause deviation from the 2.5 Å – either by repulsion (distance is greater than 2.5 Å) or, in some cases, attraction (distance is shorter than 2.5 Å).



**Figure 5** Some examples of PAH with *peri*-positions. The arrows indicate the *peri*-positions.

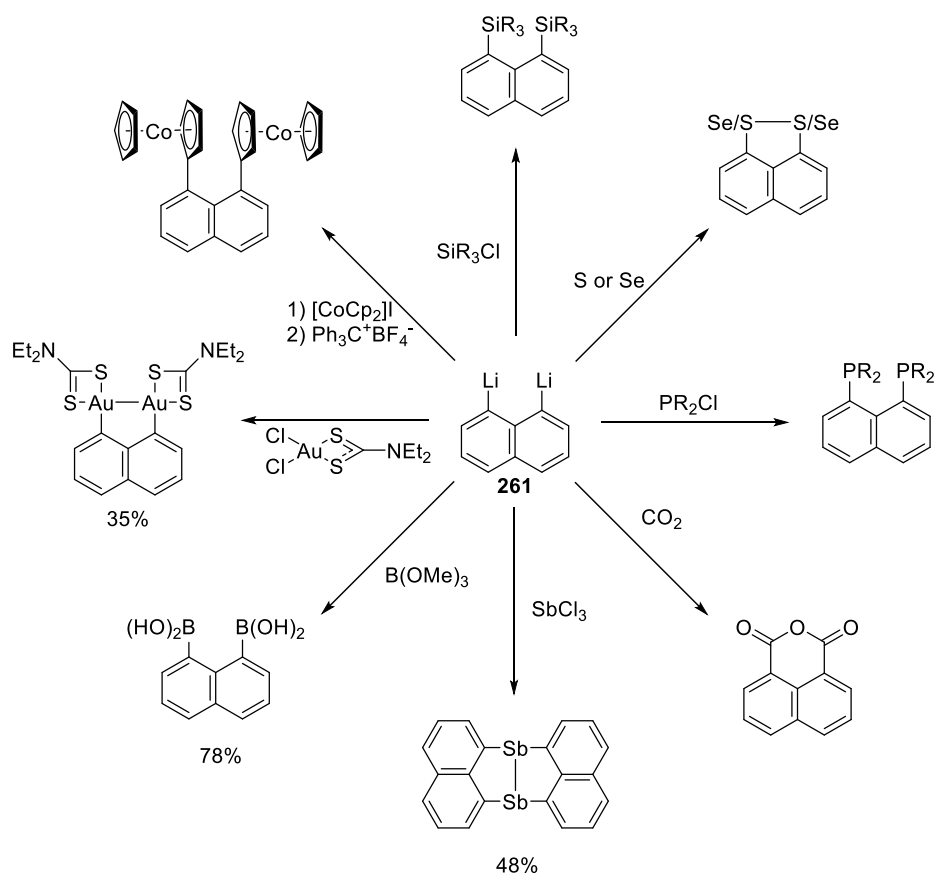
Due to the strain upon substitution, researchers have tried to access the *peri*-positions. This could give unique properties which are highly desired in many areas of chemistry. Accessing these positions is no longer a challenge and there have been several methods of accessing them. One of the most common methods is to start with commercially available 1,8-

diaminonaphthalene **254**, which can be converted into bis-diazonium salt **255**. The bis-diazonium salt allows for a wide range of different  $S_NAr$  reactions, altering the functionality at the 1,8-positions. Installation of halogens allows for a wide range of functional group transformations.



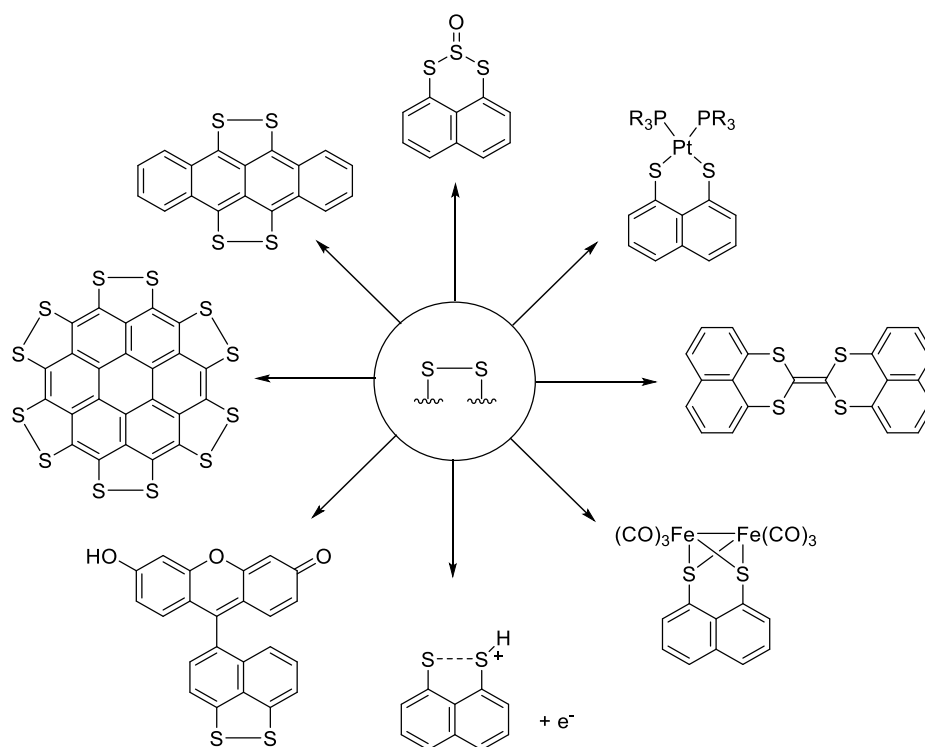
**Scheme 58** Synthesis of dihalogenated naphthalenes from bis-diazo naphthalene salt **255**.

Access to the *peri*-brominated/iodinated naphthalene allows dilithionaphthalene **261** to be accessed. This is obtained from a lithium-halogen exchange using *n*BuLi. Dilithionaphthalene **261** has been quenched with a wide variety of different elements and functional groups used (Scheme 59).



**Scheme 59** Synthesis of a variety of different peri-substituted naphthalenes from 1,8-dilithionaphthalene **261**.<sup>90–100</sup>

Peri-substituted disulfides have been explored for a wide variety of applications since 1928 when naphthalene disulfide **107** was synthesised.<sup>101</sup> Applications include oxidative sensor in cells, charge transfer materials, the controlled release of reactive diatomic molecules, Fe-Fe hydrogenase mimics and many more.<sup>42,43,90–100,102–110</sup>

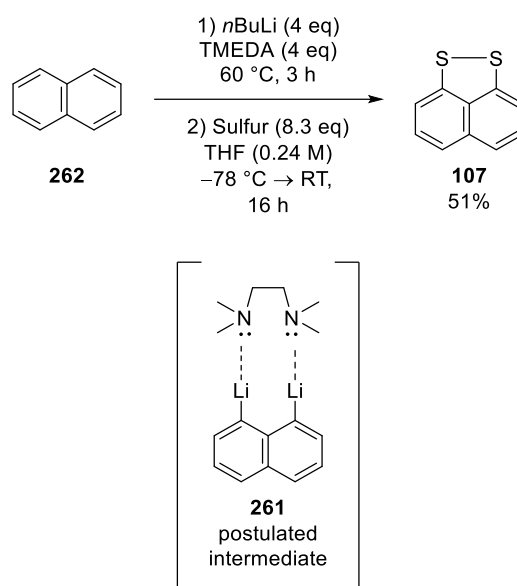


**Scheme 60** Clockwise from the top: Naphthalene trisulfide-2-oxide – a sulfur monoxide transfer reagent<sup>42,43</sup>, platinum co-ordinated naphthalene disulfide by Woollins' and co-workers<sup>108,111–113</sup>, charge transfer molecule by Ogura and co-workers<sup>105,114</sup>, naphthalene disulfide co-ordinated to Fe in an Fe-Fe hydrogenase mimic<sup>104</sup>, naphthalene disulfide as a single electron transfer reagent by Bach and co-workers<sup>91</sup>, naphthalene disulfide covalently bonded to a coumarin as a method to detect ROS in cells by Chang and co-workers<sup>102</sup>, sulflower – the latest generation by Feng and co-workers<sup>103</sup>, tetracene bis-disulfide for functional organic materials by Woodward and co-workers.<sup>109,110</sup>

Once thiols have been installed into the *peri*-positions, the disulfide bond forms readily – due to the *peri*-effect. The *peri*-positions are closer (2.5 Å) than the average sulfur-sulfur bond (3.02 Å) and the combined van der Waals radii of two sulfur atoms (3.2 Å). The thiols undergo thermodynamically favourable air oxidation to the disulfide.<sup>92</sup> This has been well documented not only in naphthalene disulfide but the diselenide *peri*-substituted scaffold.<sup>115–117</sup> Therefore, it is difficult to maintain the dithiol or use the dithiol in a synthetic sequence without the use of an inert gas atmosphere.

Naphthalene disulfides have been synthesised by a variety of methods, but most prominently *via* the lithiation of naphthalene and quenching with sulfur. Other methods include the  $S_NAr$  reaction of the dianion  $Na_2S_2$  with the dichloronaphthalene and synthesis from diazonium salts.<sup>118,119</sup>

The synthesis of naphthalene disulfide **107** is often achieved *via* the method published by Ashe III *et al.* *n*BuLi is added to naphthalene in the presence *N, N, N', N'*-tetramethylethylenediamine (TMEDA) and heated at 60 °C for 3 hours (**Scheme 61**).<sup>92,120</sup> The *n*BuLi first deprotonates the naphthalene at any of the positions around the ring. With the new C-Li bond formed, the high temperature allows the lithium atom to “shuffle/dance” around the ring. When the lithium atom reaches the *peri*-positions of the naphthalene scaffold, the TMEDA co-ordinates to the lithium atom and directs a second lithium into the other *peri*-position. This gives the dilithionaphthalene **261**.<sup>97,120–122</sup> When the dilithio-species is formed, the reaction is cooled to “lock-in” the positions. To combat the poor solubility of the resultant mixture, THF is added because of its stabilising co-ordinating nature. Once solubilised, the reaction is quenched with recrystallised elemental sulfur.

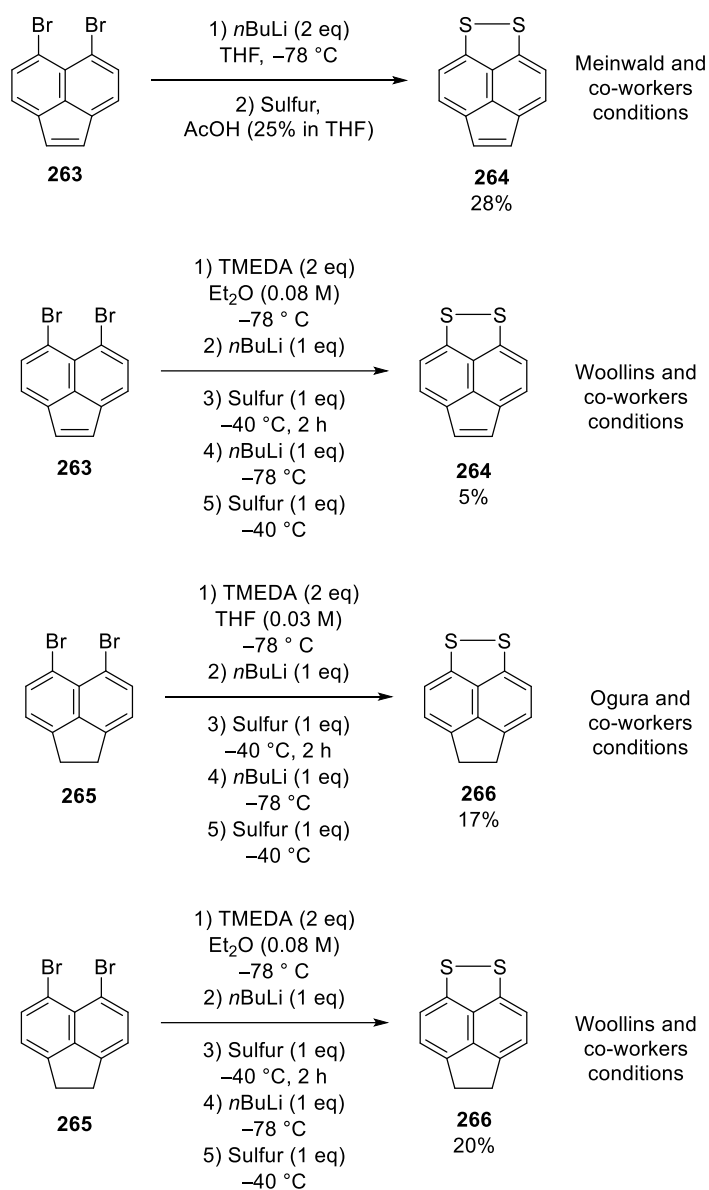


**Scheme 61** Ashe III et al. conditions for the synthesis of naphthalene disulfide **107**. Lithiated species **261** is not the definitive structure merely a simplified version. The actual intermediate has several bridging TMEDA molecules and the lithium atoms are co-ordinate to both *peri*-positions.

Acenaphthene and acenaphthylene are two derivatives from naphthalene that involve a carbon bridge across the *peri*-region. These molecules have an increased amount of strain in the molecule due to the carbon bridge. The carbon bridge of acenaphthylene is a double bond which increases conjugation and therefore gives the compounds containing acenaphthylene a distinctive UV-vis absorbance at approximately 420 nm.<sup>123,124</sup> Whilst there have been quite a few syntheses of acenaphthene and acenaphthylene derived compounds with various substitutions in the *peri*-region, there have been little to no applications of acenaphthene and acenaphthylene disulfides in the literature due to synthetic difficulties.<sup>108,112,118,119,125</sup>

One method of synthesising acenaphthylene disulfide **264** is Woollins' stepwise lithiation, sulfur quench, second directed lithiation and sulfur quench (**Scheme 62**).<sup>108,126</sup> After each addition of sulfur the reaction mixture is warmed from -78 °C to -41 °C. Alternatively, other more "classic" lithiation conditions using ethereal solvents, low temperatures, and air- and water-free atmospheres have been demonstrated to synthesise acenaphthylene disulfide

**261.** Stepwise lithiation and sulfur quenches have also been demonstrated to synthesise acenaphthene disulfide **262**.



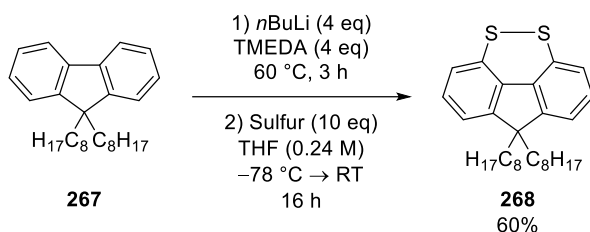
**Scheme 62** Previous literature conditions for the synthesis of acenaphthene and acenaphthylene disulfide **264** and **266**.<sup>108,111,112,118,127,128</sup>

However, all the yields of the reactions to synthesise acenaphthene and acenaphthylene disulfide **264** and **266** are poor (**Scheme 62**). Therefore, there is a need for a synthetic method which can reliably access these compounds.

“*Peri-like*” (or bay-substituted) compounds are defined by the Grainger group as the 4 and 5 positions of a 6-5-6 ring system (sometimes known as bay substitution).<sup>129,130</sup> Compounds that fit this description are fluorene, carbazole, dibenzofuran, dibenzothiophene. There are few examples of accessing the *peri-like* positions of any of these molecules selectively. Often 4 and 5 position functionality is either built into the system or the scaffold is perhalogenated.<sup>131–143</sup>

Some selective 4,5-difunctionality is seen on fluorene.<sup>130,144</sup> Another example is seen from Morita and co-workers to yield dibenzothiophene-4,5-disulfide **193** (Scheme 41).<sup>54</sup>

However, at the time of this writing, there was one known example of a directed lithiation on fluorene. Bonifácio and co-workers synthesised fluorene disulfide **264** in 2010.<sup>144</sup> They also used Ashe III’s procedure in their synthesis. However, there is a requirement to alkylate the methylene unit of the fluorene scaffold prior to the TMEDA directed lithiation to avoid deprotonation by the *n*BuLi. They alkylate the methylene unit with two octyl-chains.<sup>120</sup> Bonifácio and co-workers lithiated 9,9'-dioctylfluorene **267** using TMEDA and *n*BuLi to form 4,5-dilithio-9,9'-dioctylfluorene.<sup>144</sup> The dilithio-species was quenched with sulfur to give disulfide **268** (Scheme 63).

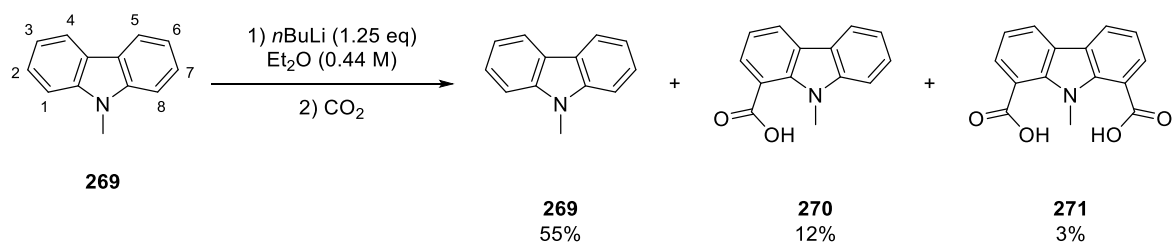


**Scheme 63** Synthesis of fluorene disulfide **264** by Bonifácio et al.

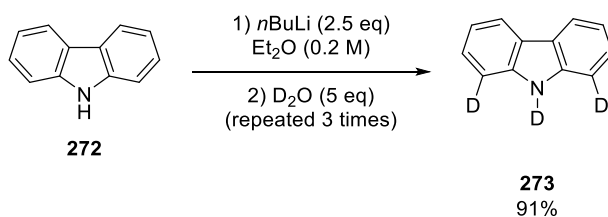
Carbazole **272** is another “*peri-like*” scaffold which has been explored in recent years due to its photophysical properties.<sup>145–150</sup> Previous lithiations of carbazole have selectively lithiated



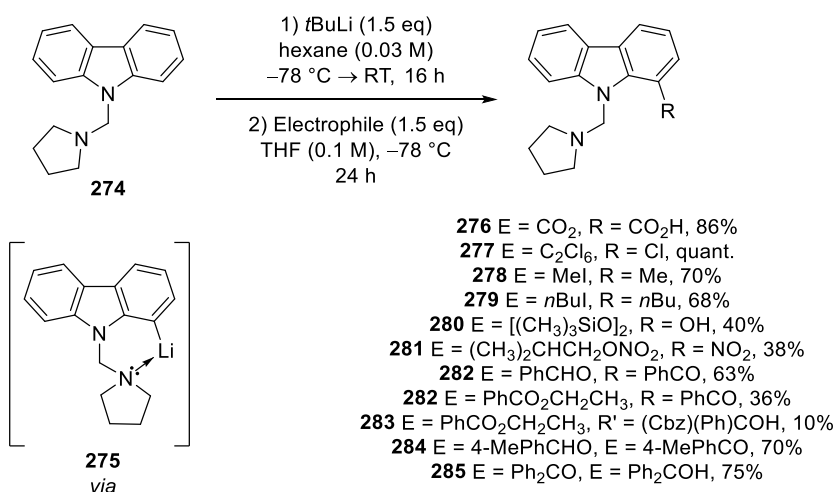
the 1,8-positions (**Scheme 64**). Gilman and Spatz lithiated *N*-methylcarbazole **269** and quenched with CO<sub>2</sub> to give the monoacid **270** in a 12% yield (**Scheme 64**). Hallberg and co-workers lithiated carbazole **272** and quenched with D<sub>2</sub>O to give 1 and 8 dideuterated carbazoles **273** in a 91% yield (**Scheme 64**).<sup>151</sup> They determined from the results that carbazoles naturally direct to the 1 and 8 position. Katritzky and co-workers performed a similar reaction, however, the nitrogen was protected with a methylpyrrolidine group. The nitrogen of the pyrrolidine co-ordinated to the 1 and 8 positions once lithiated. This saw an increase in yields when quenching with a variety of electrophiles (**Scheme 64**).<sup>152</sup>



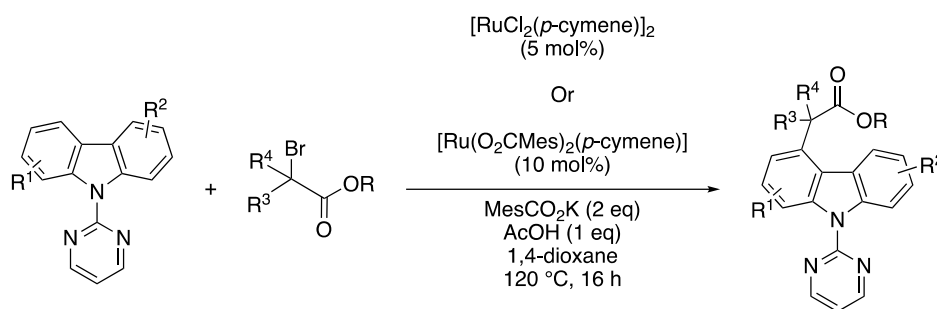
Hallberg and co-workers



Katritzky and co-workers

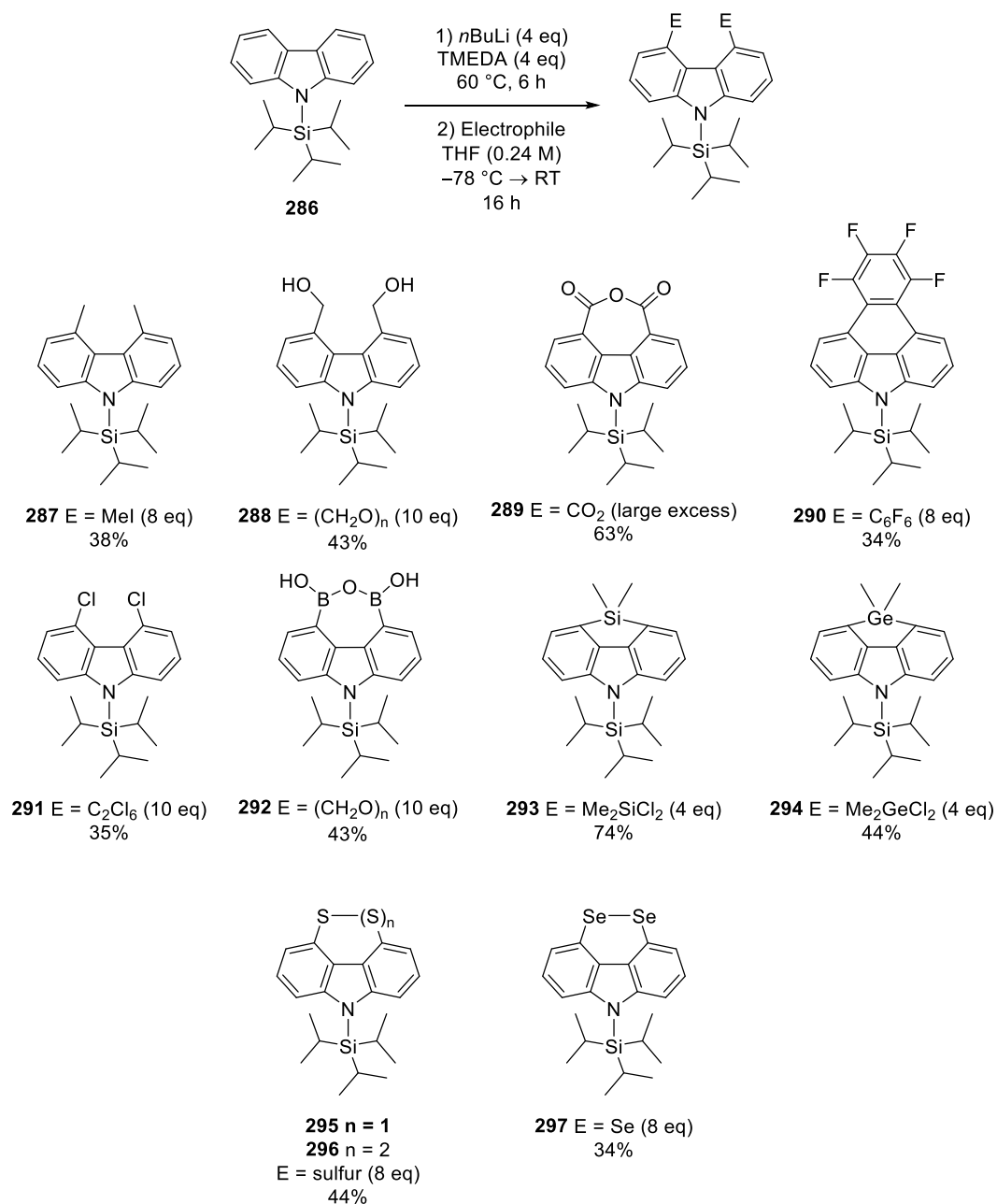
**Scheme 64** Previous lithiation conditions on carbazole - selective for 1 and 8 positions.<sup>151</sup>

There is little literature on accessing the 4,5-positions of carbazole. Carbazole has been directly functionalised in the 4-position.<sup>153</sup> The monofunctionalisation was achieved using ruthenium catalysis by Frost and co-workers.<sup>154</sup> This was achieved by C-H activation of the 1-positions and the substitution of the 4-position. However, the scope is limited to only  $\alpha$ -tertiary esters.



**Scheme 65** 4-position activation using ruthenium by Frost et al.

During this PhD work, the Grainger group published a paper which demonstrated a method to dilithiate the 4,5-positions of carbazole (**Scheme 66**).<sup>129</sup> We hypothesised that a protecting group that can block the 1 and 8 positions of the carbazole and withstand the harsh conditions of *n*BuLi at 60 °C could allow the lithium atoms to migrate the 4,5-positions of carbazole in the presence of TMEDA. Therefore, a tri(isopropyl)silyl protecting group was hypothesised to be large enough to block the 1,8-positions and withstand the harsh conditions and this proved successful (**Scheme 66**). The optimal conditions were found to be 60 °C for 6 hours and not 3 hours, unlike in Bonifácio and co-workers' fluorene disulfide **268** synthesis. A variety of electrophiles were used, including sulfur to make the carbazole disulfide **295**.



**Scheme 66** Grainger et al. conditions to lithiate carbazole **282** to access the 4,5-positions. E = electrophile.

## Conclusion

Over the last 60 years, *peri*-substituted disulfides have become increasingly of interest due to their application in a wide range of different fields. The pursuit of non-naphthalene *peri*-substituted disulfides has been very thorough. However, the syntheses of non-naphthalene disulfides are often difficult due to poor yields or multi-step procedures. Acenaphthene **266**

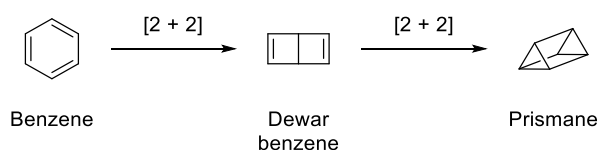
and acenaphthylene disulfides **264** have both been synthesised but little has been done with their application due to their difficulty in the synthesis. Similarly, fluoranthene disulfide has previously been synthesised *via* a 5 – 7 steps synthesis with often low yielding steps.

“*Peri*-like” disulfides have started to become of interest, often mirroring similar applications to the *peri*-substituted scaffolds. However, successful syntheses are rare. Bonifácio and co-workers and Grainger and co-workers have successfully synthesised fluorene disulfides in good yields (~50 – 60%). *Peri*-like functionalisation of carbazole has been demonstrated previously in the literature, including the carbazole disulfide **295**.

The “*peri*-like” scaffolds are rare with only four papers outlining *peri*-like disulfides of fluorene, carbazole and dibenzothiophene.

### 1.3 Valence isomerism

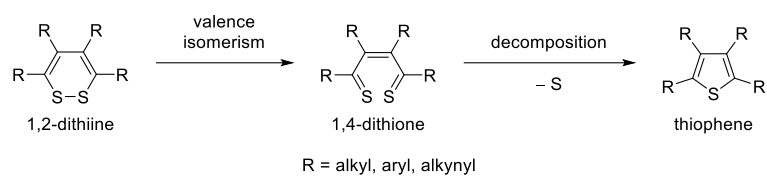
IUPAC defines valence isomerism as “*a constitutional isomer interrelated with another by pericyclic reactions*”.<sup>155</sup> An example of this is the relation of benzene to dewar benzene to prismane. All these valence isomers are related *via* [2+2] pericyclic reactions (**Scheme 67**).



**Scheme 67** The valence isomers of benzene.

There are few examples of valence isomerism involving sulfur. However, a class of natural products called thiarubrines do display valence isomerism.<sup>156</sup> Thiarubrines are found in sunflowers and are usually bright yellow and orange. Thiarubrines contain a 1,2-dithiine ring

system. 1,2-dithiine rings undergo a pericyclic reaction to form 1,4-dithiones.<sup>157</sup> In the case of thiarubrines, 1,4-dithiones rearrange to give thiophenes (**Scheme 68**).



**Scheme 68** 1,2-dithiines and their valence isomerisation to dithiones and subsequent decomposition to thiophenes.

## *Chapter 2:*

The design, synthesis, and evaluation of sulfur monoxide (SO) transfer reagents:

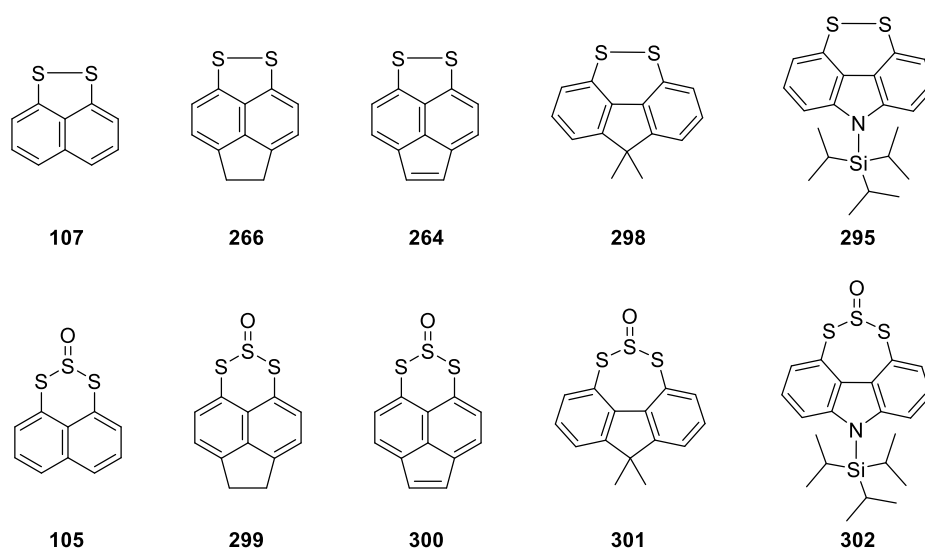
## 2 The design, synthesis, and evaluation of sulfur monoxide transfer reagents

### 2.1 Aims and objectives

The overarching aim of the project is to discover a novel trisulfide-2-oxide which can release SO at lower temperatures and faster times than previous trisulfide-2-oxides that have been reported, and release singlet SO.

In order to achieve the aim of the project, several objectives need to be met. Firstly, to synthesise several disulfides, both novel and known, in order to synthesise the trisulfide-2-oxides of them. The group has an active interest in aromatic disulfides for a variety of reasons. The disulfides/trisulfide-2-oxides of interest are: naphthalene (both disulfide **107** and trisulfide-2-oxide **105** have been previously reported by the Grainger group), acenaphthene (disulfide **266** has previously been reported by several groups and the trisulfide-2-oxide **299** is novel), acenaphthylene (disulfide **264** has previously been reported by several groups and the trisulfide-2-oxide **300** is novel), fluorene (disulfide **268** has previously been reported by Bonifácio, and the trisulfide-2-oxide **301** is novel), and carbazole (disulfide **295** is known and trisulfide-2-oxide **302** is novel). For some of these scaffolds, new synthetic methodology will need to be established in order to access the desired *peri*- or “*peri*-like” positions.





**Figure 6** Top row - proposed disulfides (naphthalene **107**, acenaphthene **266**, acenaphthylene **264**, fluorene **298**, and carbazole **295**) Bottom row - proposed trisulfide-2-oxides (naphthalene **105**, acenaphthene **299**, acenaphthylene **300**, fluorene **301**, and carbazole **302**).

The reason for choosing the aromatic scaffolds listed are due to the difference in the steric interaction across the *peri*- or *peri*-like region. The different steric interactions could cause a difference in the strain in the system potentially leading to different mechanisms of SO release or different rates of SO release.

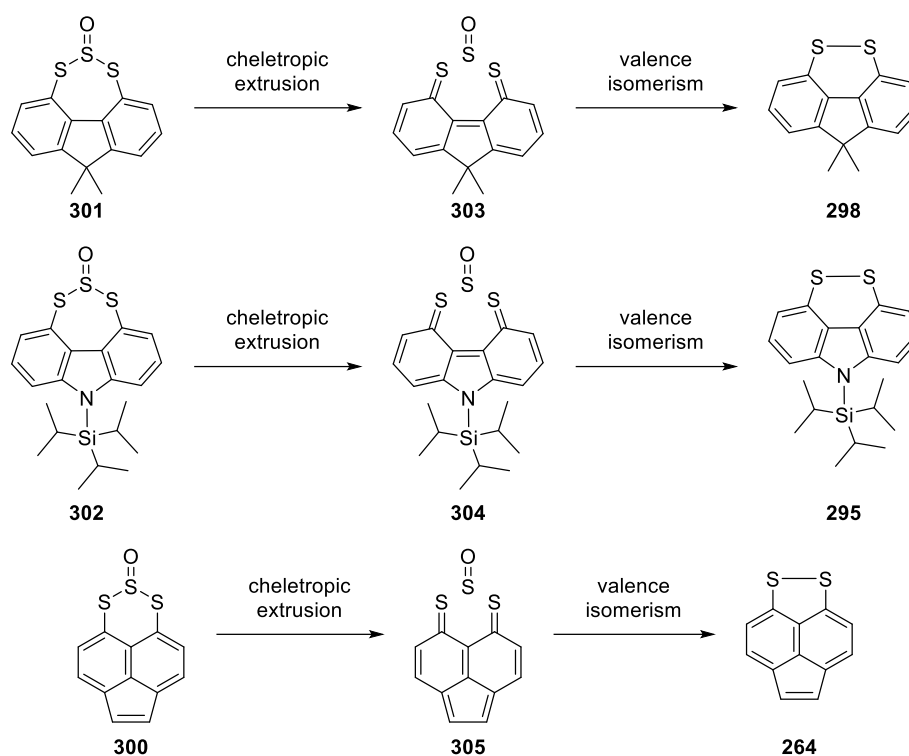
Secondly, due to the poor yields in attempted synthesis of acenaphthene and acenaphthylene disulfide, there needs to be a simple and concise method to access acenaphthene and acenaphthylene *peri*-positions on large scale. This could either be accessed through a directed lithiation as with previous methods or via a  $S_NAr$  approach. The carbazole and fluorene disulfides **295** and **298** can be synthesised from previous known literature.

All disulfides and trisulfide-2-oxides need to be able to crystallise so that structural data can be obtained to give information on the strain of each scaffold. Therefore, small alkyl chains and small protecting groups will often be required in order to allow closer packing in the solid state.

Each trisulfide-2-oxide will require analysis by UV-Vis spectroscopy in order to determine which wavelengths of light are required in order to attempt photochemical release of SO.

Finally, a thorough testing of the release of SO to a diene must be done to show a comparison between the trisulfide-2-oxides. This will include the isolation of the corresponding disulfide and cyclic sulfoxide. Each of the trisulfide-2-oxides will be degraded both photochemically and thermally in the presence of a diene and cycloheptatriene. The formation of the resulting sulfoxide (or no sulfoxide) will give a clear indication of which state of SO is being released.

Acenaphthylene, fluorene, and carbazole are particularly of interest as it is possible that they have an alternative release mechanism. This mechanism proceeds *via* a cheletropic extrusion to a dithione intermediate before undergoing valence isomerism to the disulfide. This proposed mechanism could potentially release singlet SO – like Nakayama's cheletropic extrusion of singlet SO (**Scheme 34** and **Scheme 69**).



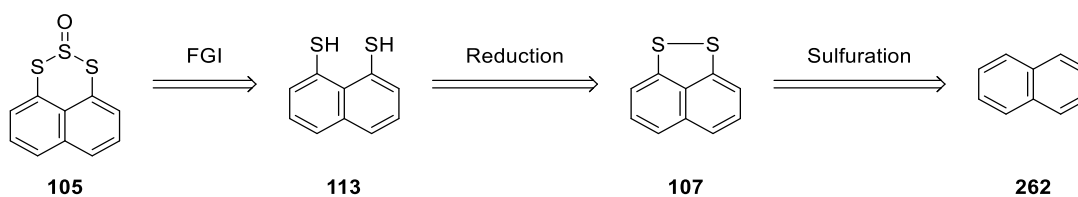
**Scheme 69** Proposed mechanism for the cheletropic extrusion and valence isomerism of fluorene, carbazole and acenaphthylene to release singlet SO.

This alternative mechanism cannot be achieved with naphthalene or acenaphthene due to the lack of conjugation from the carbon bridge.

## 2.2 Synthesis of the disulfide scaffolds

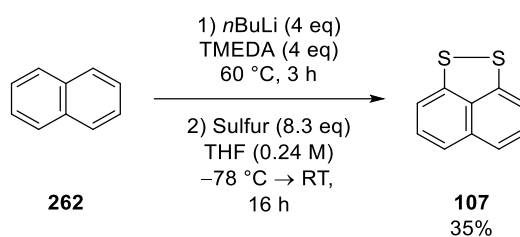
The retrosynthetic analysis connecting the envisaged SO transfer system to naphthalene is shown (**Scheme 70**). The common functional group in the synthesis of our reactive diatomic precursors are the respective disulfides.

Naphthalene:



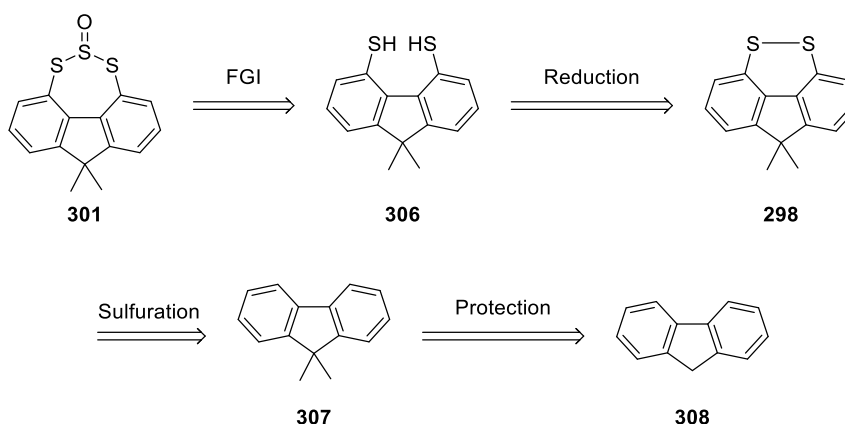
**Scheme 70** Retrosynthetic analysis of the naphthalene trisulfide-2-oxide **107**.

Naphthalene disulfide **105** was prepared using the method published by A. J. Ashe III *et al.* This involves the directed lithiation of naphthalene. *n*BuLi and TMEDA was added to naphthalene and the reaction mixture was quenched with sulfur. Early testing gave naphthalene disulfide **107** in a 5% yield. Further investigation showed that the documented amounts of the *n*BuLi and TMEDA in the original Ashe III paper, were miscalculated and never corrected after publication. The equivalents of *n*BuLi and TMEDA differed between the experimental and the body of the paper. Doubling the number of equivalents of TMEDA to match those in the experimental gave much higher yields (35%) (**Scheme 71**).<sup>120</sup>



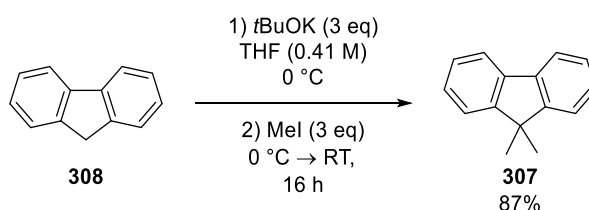
**Scheme 71** Directed lithiation of naphthalene **262**, and quench with sulfur, to yield naphthalene disulfide **107**.<sup>120–122,158</sup>

Focus shifted to the fluorene disulfide **298**. Bonifácio and co-workers synthesised fluorene disulfide **268** in 2010.<sup>144</sup>



**Scheme 72** Retrosynthetic analysis of fluorene trisulfide-2-oxide **301**.

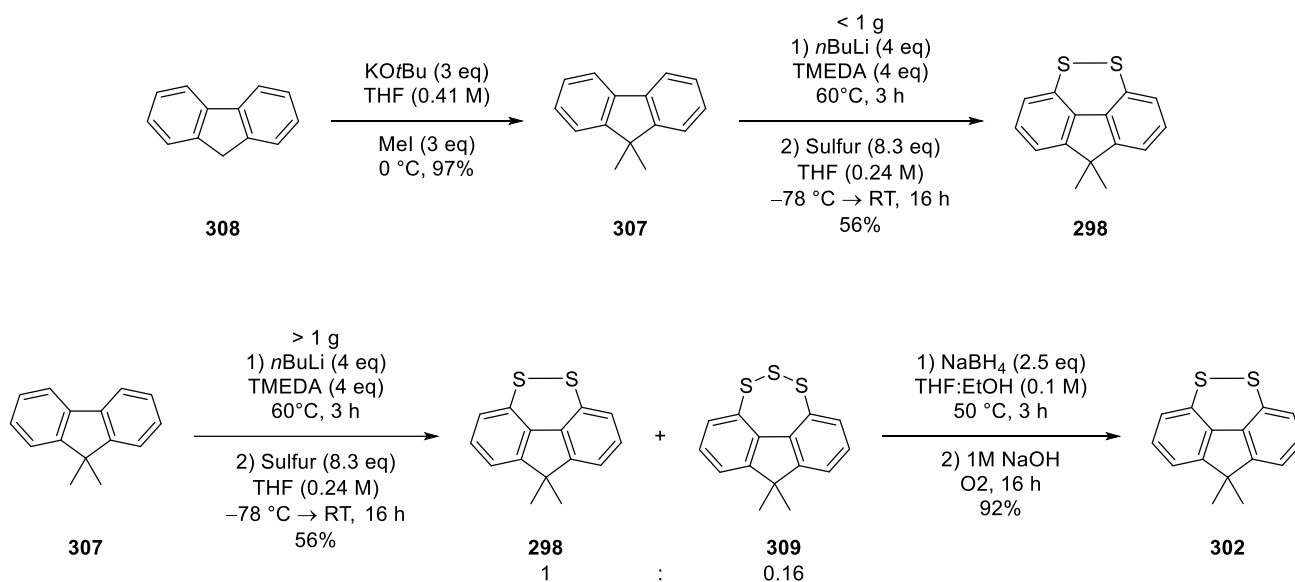
Previously the Grainger group had used *n*butyl chains as the alkyl-group on the methylene unit. However, *n*butyl chains also caused the molecule to become greasy and not very crystalline, making it difficult to obtain a single crystal and X-ray diffraction data (unpublished data). It was proposed that a switch to using methyl groups would increase crystallinity. The smaller chains allowed the molecules to pack closer together (for discussion on the crystal structure see section 2.4.3). The methyl blocking of fluorene is also well known in the literature. A procedure was adapted from 2007; the reaction is exothermic and therefore cooling to 0 °C is required to scale the reaction to 30 g of starting material.<sup>159</sup>



**Scheme 73** Synthesis of 9,9-dimethylfluorene **307**.

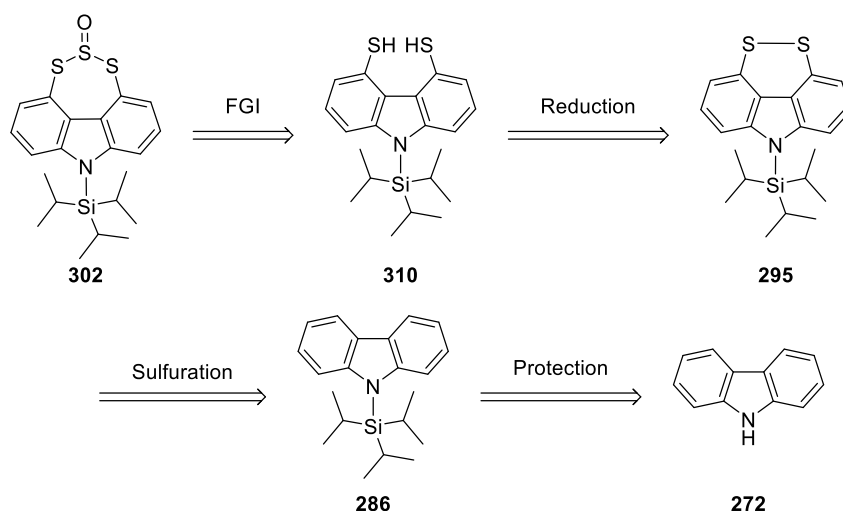
It is important to purify dimethylfluorene **307**. If not, the crude reaction mixture is a yellow/orange solid, indicating the presence of iodine from the iodomethane. The iodine in the compound was found to decrease the yield of the subsequent lithiation step. Once purified dimethylfluorene **307** is a colourless crystalline solid.

Dimethylfluorene **307** was subjected to the Ashe III/Bonifácio lithiation conditions.<sup>120</sup> On a small scale (<1 g) the dimethylfluorene disulfide **298** was produced selectively in yields ranging from 50-60%. However, when the reaction was scaled up to amounts greater than 1 g, an impurity appeared. The impurity ran at nearly the same  $R_f$  as the disulfide (<0.1  $R_f$  difference) and by  $^1\text{H}$  NMR appeared to be a symmetrical fluorene scaffold. Isolation of the impurity was successful, but a wide column is required. Mass spectrometry indicated a molecular ion corresponding to the presence of three sulfur atoms. Crystallisation and subsequent X-ray diffraction analysis allowed us to prove the impurity to be dimethylfluorene trisulfide **309**. Dimethylfluorene trisulfide **309** and disulfide **298** can be reduced as a mixture to yield the dithiol. After a series of tests, it was found that 2.5 equivalents of  $\text{NaBH}_4$  per S-S and  $50^\circ\text{C}$  for 3 hours was enough to fully reduce the di/trisulfide mixture to dithiol **306**. After the addition of base (1 M NaOH), air oxidation of the dithiol gave disulfide **298**.



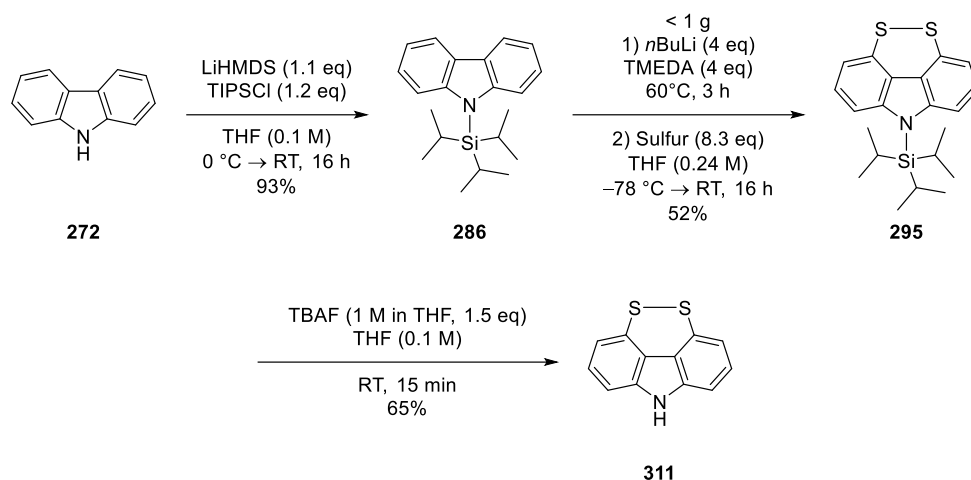
**Scheme 74** Synthesis of fluorene disulfide **298**.

Previous Grainger group work allowed for easy access to the carbazole disulfide **295**.



**Scheme 75** Retrosynthetic analysis of carbazole trisulfide-2-oxide **302**.

First, triisopropylsilyl (TIPS) was used as a protecting group for the nitrogen, achieving the desired product in high yield (93%). Grainger *et al.*'s lithiation conditions and a quench with elemental sulfur gave TIPS-carbazole disulfide **295** in 52% yield (**Scheme 76**). Mass spectrometry showed a  $m/z$  consistent with the desired compound ( $[M + H]$  requires  $386.1432 \text{ g}\cdot\text{mol}^{-1}$ , found  $386.1436 \text{ g}\cdot\text{mol}^{-1}$ ) and confirmed the molecular weight to be of the same mass as  $\text{C}_{21}\text{H}_{27}\text{S}_2\text{NSi}$  ( $385.66 \text{ g}\cdot\text{mol}^{-1}$ ) – a reduction of 2 hydrogens and the addition of two sulfur atoms from TIPS-carbazole **286** ( $\text{C}_{21}\text{H}_{29}\text{NSi}$ ). The  $^1\text{H}$  NMR confirmed only three aromatic peaks – meaning the molecule is symmetrical and again confirming synthesis of the TIPS-carbazole disulfide **295**. Attempts to crystallise the TIPS-carbazole disulfide **295** proved unsuccessful due to the crystal being twinned (i.e. two crystals growing through each other's lattices at the same time and not forming a strongly diffracting sample). Removal of the tri(isopropyl)silyl protecting group allowed the molecules to pack closer together. A simple TBAF deprotection yielded the free amine in a 65% yield.<sup>129,160</sup> Crystallisation and subsequent X-ray crystallography of the free carbazole disulfide **311** proved the structure with the disulfide across the 4 and 5 *peri*-like positions (Section 2.4.3).



**Scheme 76** Synthesis and deprotection of carbazole disulfide **295**.<sup>129</sup>

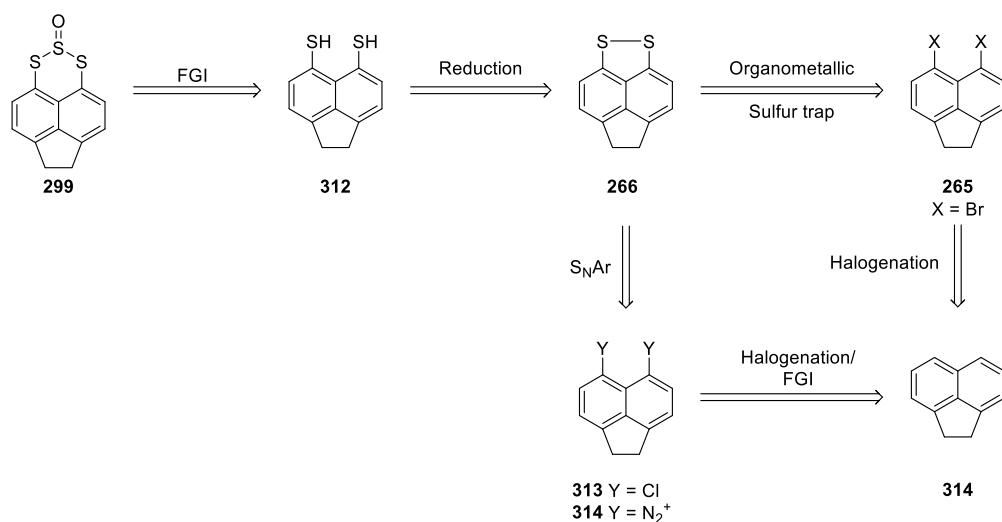
The scaling up of the lithiation of carbazole **286** with a recrystallised sulfur quench proved difficult due to an impurity, similar to that observed for the fluorene scaffold. Isolation of the impurity was achieved in a similar manner to the fluorene scaffold. Mass spectrometry showed a mass ion consistent with  $C_{21}H_{27}S_3NSi$  ( $[M + H]$  requires  $418.1153 \text{ g}\cdot\text{mol}^{-1}$ , found  $418.1150 \text{ g}\cdot\text{mol}^{-1}$ ) and  $^1\text{H}$  NMR confirmed a symmetrical molecule with 3 aromatic peaks, indicating identical functionalisation across both sides of the carbazole. Deprotection of the TIPS group (TBAF in THF – 87% yield) and crystallisation of the product confirmed the synthesis of carbazole trisulfide **296** (for discussion of the crystal structure of carbazole trisulfide **296** see section 2.4.4). Using the same conditions as the fluorene scaffold, the trisulfide/disulfide mixture was reduced to yield the dithiol.

The trisulfides are also interesting as there are relatively very few that are synthesised *via* C-H activation. For the *peri*-like systems the trisulfides were synthesised as a by-product to the disulfides. Often as a minor impurity, the trisulfides run at a  $R_f$  similar to that of the disulfides.



To isolate the trisulfides a column much larger than the standard size is needed (1 g > of sample to 70 mm diameter and 2000 mm).

Acenaphthene and acenaphthylene disulfides **266** and **264** were also targeted due to the similarity to naphthalene and the structural differences imposed by the two carbon bridge. Previous literature synthesised the acenaphthene disulfide **266** in a 5% yield (section 1.2). The chemistry after the synthesis of the disulfide is well known, therefore, the challenge was forming the disulfide in acceptable yields.

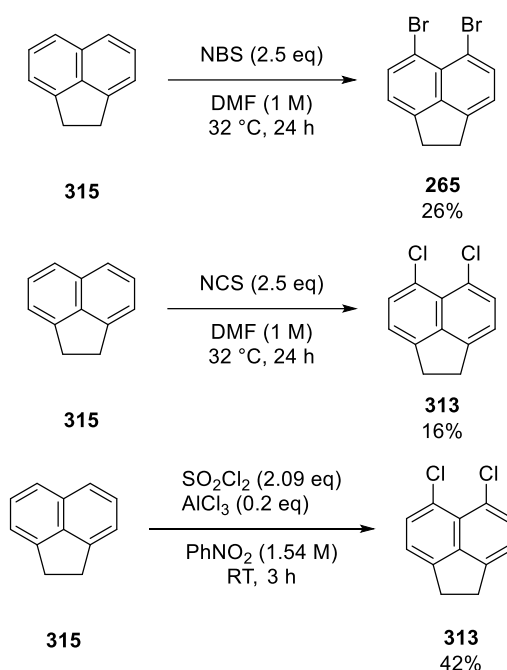


**Scheme 77** Retrosynthetic analysis of the reactive diatomic precursor of acenaphthene.

Two routes into acenaphthene disulfide were hypothesised: 1) an  $\text{S}_{\text{N}}\text{Ar}$  approach or 2) formation of an organometallic compound (from a 5,6- dihalogenated acenaphthene) and quench with elemental sulfur.

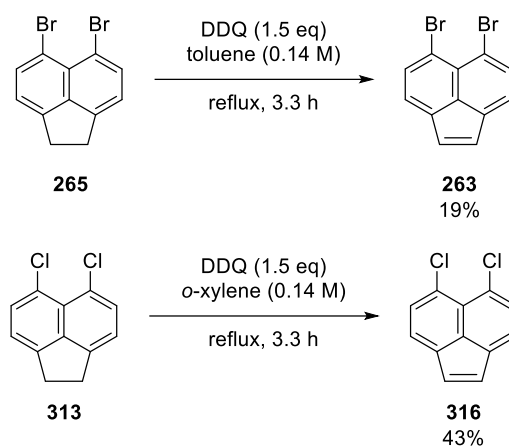
The chlorination and the bromination of acenaphthene are well documented however the yields are poor.<sup>161–163</sup> For the chlorination, the reaction was completed using  $\text{SO}_2\text{Cl}_2$  and  $\text{AlCl}_3$  in nitrobenzene giving yields of 50% in the literature. The yield was slightly lower at 42% (**Scheme 78**).<sup>127,164</sup> The authors of the papers claim that the product is clean enough to use

directly in the next step. However, on attempting the synthesis, further purification by flash column chromatography was required to give a white crystalline solid. Taking inspiration from the bromination procedure, which uses *N*-bromosuccinimide in DMF, the dichloride was also synthesised with NCS without the need for further purification. The product of the reaction precipitated from solution over the course of the 24 h (16%). These procedures were used as the “go to” methods for the synthesis of the dihalogenated acenaphthenes.



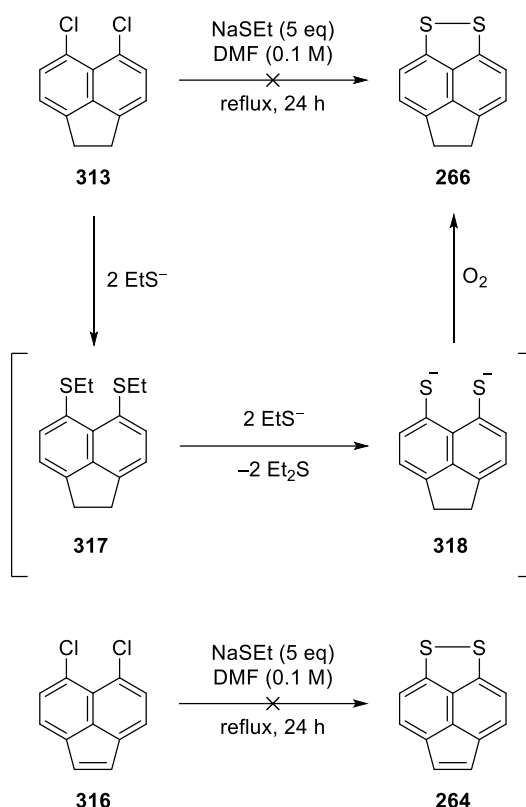
**Scheme 78** Chlorination and bromination of acenaphthene **315**.

Acenaphthene derivatives are classically oxidised to the corresponding acenaphthylene using 2,3-dichloro-5,6-dicyano-*p*-quinone (DDQ) or other quinone-based oxidants. Therefore, a simple DDQ oxidation of the dichloroacenaphthene and dibromoacenaphthene yielded the dichloroacenaphthylene (43%) and dibromoacenaphthylene (19%), respectively (**Scheme 79**).



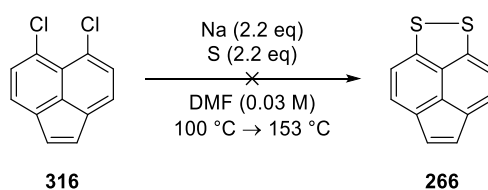
**Scheme 79** Synthesis of dibromoacenaphthylene **263** and dichloroacenaphthylene **316**.

Investigations into the  $S_NAr$  of the *peri*-substituted dichloroacenaphthene **313** were first tried. Sodium ethanethiolate has previously been shown to be a nucleophile towards polychlorinated molecules to yield thiols. However, no reaction occurred in refluxing DMF and degradation occurred in refluxing NMP (**Scheme 80**).<sup>165</sup> This was also found for the dichloroacenaphthylene **316**.



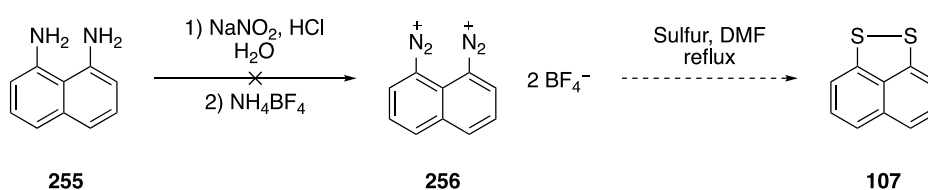
**Scheme 80** Chlorination and attempted sulfur  $S_NAr$  substitution of dichloroacenaphthene **313** and dichloroacenaphthylene **316**.<sup>165</sup>

The failure of sodium ethanethiolate as a nucleophile led to using  $\text{Na}_2\text{S}_2$  as a nucleophile.<sup>127</sup>  $\text{Na}_2\text{S}_2$  is not a stable reagent and must be synthesised *in situ*. This was done by reacting equimolar amounts of elemental sulfur and sodium at 100 °C in DMF.<sup>165,166</sup> A characteristic deep green colour change was observed, indicating the formation of the  $\text{Na}_2\text{S}_2$  nucleophile. Addition of the dichloroacenaphthylene and then an increase in temperature to reflux saw no product formation, only starting material (**Scheme 81**).



**Scheme 81** Attempted  $\text{Na}_2\text{S}_2$   $S_NAr$  reaction with acenaphthylene dichloride **316**.

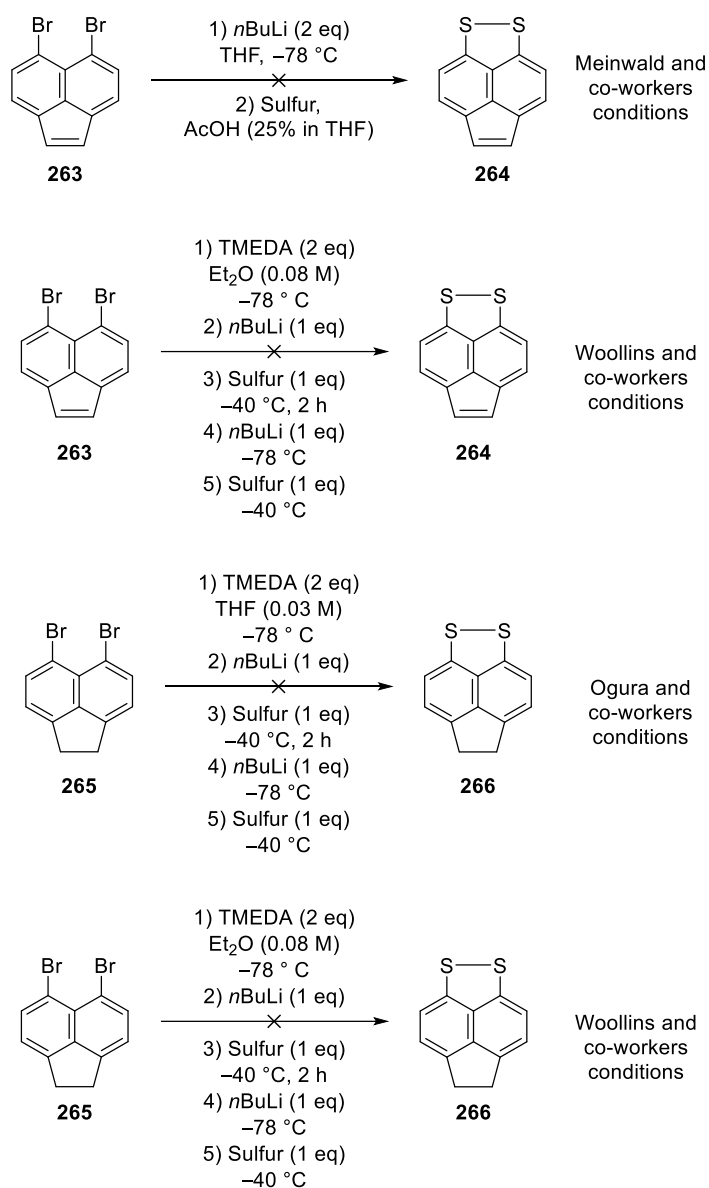
An alternative idea was to use bis-1,8-diazonaphthalene **256** to synthesise naphthalene disulfide **107** through nucleophilic addition of a sulfur electrophile. If successful with naphthalene, it could be possible to perform a similar reaction on acenaphthene. The bis-diazoniumnaphthalene salt synthesis was attempted, however the bis-diazonium naphthalene **256** was not synthesised, 1,8-diaminonaphthalene **255** was recovered and the route was not pursued further (**Scheme 82**).



**Scheme 82** Attempted synthesis of 1,8-bis(diazo)naphthalene **256** and the proposed synthesis of naphthalene disulfide **107**.

The formation of bis-organometallics from acenaphthene dibromide **265** presents alternative opportunities to access the desired scaffolds. Firstly, Woollins' stepwise lithiation, sulfur quench, second directed lithiation and sulfur quench was attempted (**Scheme 83**).<sup>108,126</sup> Unfortunately, when repeating this procedure only complex mixtures were produced, and none of the desired product was observed. Other more "classic" lithiation conditions using

ethereal solvents, low temperatures, and air- and water-free atmospheres did not yield the desired acenaphthene disulfide.

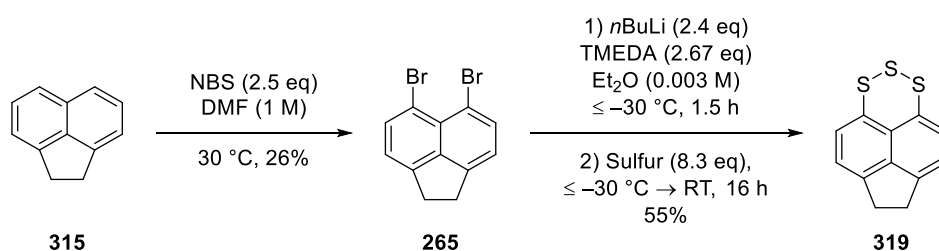


**Scheme 83** Previous literature conditions for the synthesis of acenaphthene and acenaphthylene disulfide **264** and **266**. These were not reproducible.<sup>108,111,112,118,127,128</sup>

A double Grignard formation and sulfur quench was then attempted.<sup>167,168</sup> Firstly, magnesium powder was used. However, no reaction was observed and starting material was recovered. This is probably due to an increased oxide layer and therefore a reduced amount of exposed

elemental magnesium. Magnesium turnings, activated with iodine, were then used to increase the surface area of elemental magnesium present. However, even after increasing the temperature to reflux (THF, 66 °C) but this did not initiate the reaction. To investigate the cause of the reaction failure, an analogous reaction was attempted with 1-bromonaphthalene which worked. This success indicated the dibromoacenaphthene was unsuitable for the Grignard reaction.

Dr Ian A. Pocock, who was working on a similar project, found a method to install the *peri*-substituted sulfur atoms on acenaphthene based on the work from N. Tanaka and T. Kasai.<sup>169</sup> Dibromoacenaphthene is suspended in anhydrous diethyl ether and cooled to  $\leq -30$  °C before the slow addition of a solution of TMEDA and *n*BuLi. Once all the TMEDA: *n*BuLi solution has been added the reaction, the temperature is maintained at  $\leq -30$  °C for a further 1.5 hours. This allowed the TMEDA-stabilised dilithioacenaphthene species to form. Elemental sulfur is added to the dilithioacenaphthene, and the temperature is maintained for a further 0.5 hours. Rather than the anticipated acenaphthene disulfide **266**, acenaphthene trisulfide **319** was isolated in a 55% yield (**Scheme 84**).



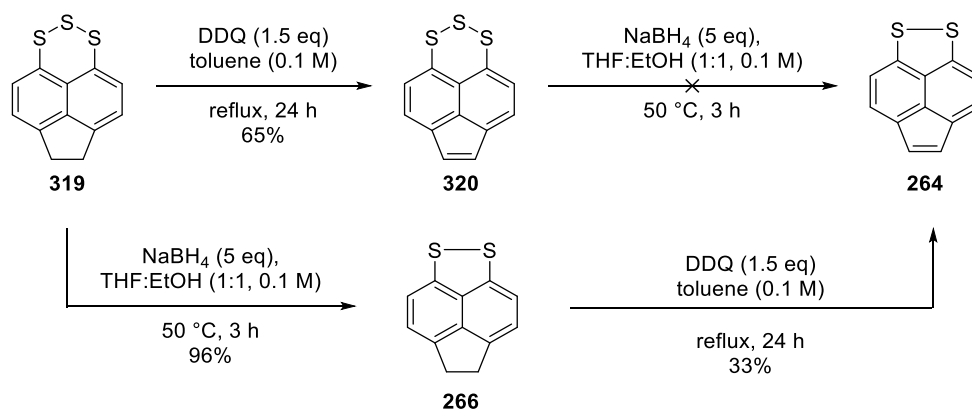
**Scheme 84** Synthesis of acenaphthene trisulfide **319** via acenaphthene dibromide **265**.

The synthesis of acenaphthene trisulfide **319** by Dr Ian Pocock was a key stage in this work and allowed me to continue with the synthesis. Like fluorene and carbazole trisulfides **296** and **309** mentioned previously, acenaphthene trisulfide **319** was easy to reduce to the dithiol.

With the addition of base (1 M NaOH) and in the presence of air the work up of the reduction selectively yields the disulfide **266** – an important intermediate in the synthetic sequence to the acenaphthene and acenaphthylene trisulfide-2-oxides **299** and **300** (**Scheme 85**).

Acenaphthene derivatives are classically oxidised to the corresponding acenaphthylene using 2,3-dichloro-5,6-dicyano-*p*-quinone (DDQ) or other quinone-based oxidants. Acenaphthene trisulfide **319** was oxidised using DDQ (1.5 eq) in refluxing toluene which gave acenaphthylene disulfide and trisulfide **264** and **320** in a combined 30% yield. The work up of the reaction was particularly difficult. The DDQ by-product is extremely insoluble and blocks filter paper and sinter funnels. The disulfide and trisulfide are inseparable, unlike previous fluorene and carbazole disulfide and trisulfide mixtures. This is also true for both the acenaphthene disulfide **266** and trisulfide **319**. However, the yields are moderate at best.<sup>126,170</sup> To aid recovery, the reaction mixture was diluted with CH<sub>2</sub>Cl<sub>2</sub>, dry loaded onto silica, and chromatographed. Dilution with CH<sub>2</sub>Cl<sub>2</sub> prior to dry-loading allowed DDQ by-product aggregates to dissolve and evenly disperse the desired product throughout the silica dry-load. This method of purification gave acenaphthylene trisulfide exclusively in a 65% yield (**Scheme 85**). Acenaphthylene trisulfide **320** was subject to the NaBH<sub>4</sub> reduction condition that were used to reduce the acenaphthene, fluorene, and carbazole trisulfides **319**, **309** and **296**. However, the acenaphthylene trisulfide **320** is more robust than previous trisulfides and can withstand the previous reduction conditions for longer periods of time. Unfortunately, after several attempts no conditions forced the reaction to completion. Alternatively, acenaphthene trisulfide **319** was reduced to the disulfide **266**, and then oxidised to the acenaphthylene disulfide **264**.



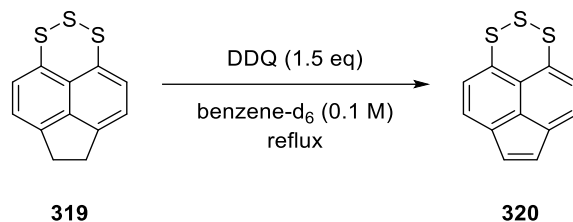


**Scheme 85** Synthesis of acenaphthylene disulfide **264**.

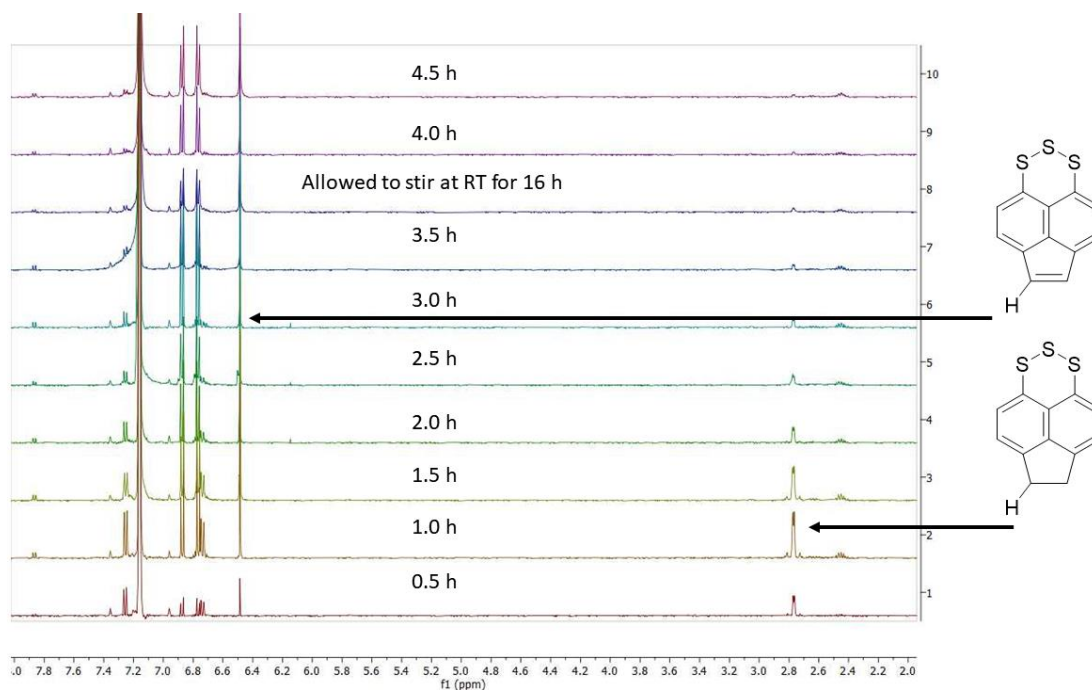
Further attempts to replicate the selective oxidation of acenaphthene trisulfide **319** to acenaphthylene trisulfide **320** were low yielding (~20%), even without rigorous work up. More extensive studies into the oxidation were therefore carried out. Literature procedures indicate the use of both benzene and toluene as the refluxing solvent in this reaction.<sup>126</sup> The reaction was performed in refluxing deuterated benzene (benzene- $d_6$ ) to allow  $^1\text{H}$  NMR aliquots to be taken to see the progression of the reaction and if any disulfide was synthesised.

To monitor reaction progress the carbon bridge protons were followed. For acenaphthene trisulfide **319** the integration of the  $\text{CH}_2$  peak at 2.77 ppm from the carbon bridge was followed. For acenaphthylene trisulfide **320** the integration of the  $\text{CH}$  peak at 6.49 ppm from the carbon bridge was followed. After 4.5 h, nearly all of the acenaphthene trisulfide **319** had been consumed (<10% remained) (**Table 2** and **Figure 7**).

**Table 2** DDQ oxidation of acenaphthene trisulfide in *d*<sub>6</sub>-benzene.



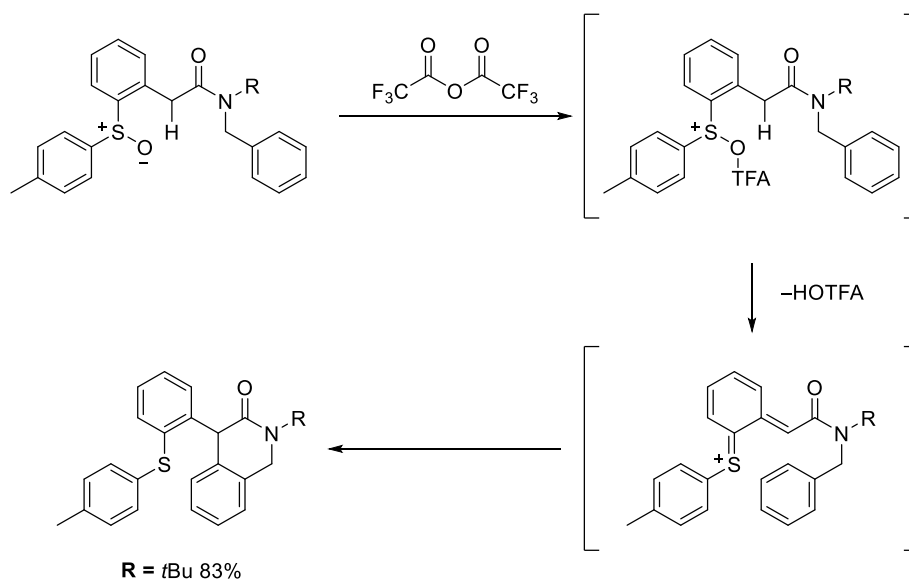
Time	Acenaphthene trisulfide 319 (2.77 ppm peak integration)	Acenaphthylene trisulfide 320 (6.49 ppm peak integration)	Acenaphthylene disulfide 264 (7.12 ppm peak integration)
0.5	2.75	1	-
1	1.26	1	-
1.5	0.78	1	-
2	0.57	1	-
2.5	0.41	1	-
3	0.33	1	-
3.5	0.22	1	-
RT overnight	0.24	1	-
4	0.29	1	-
4.5	0.20	1	-



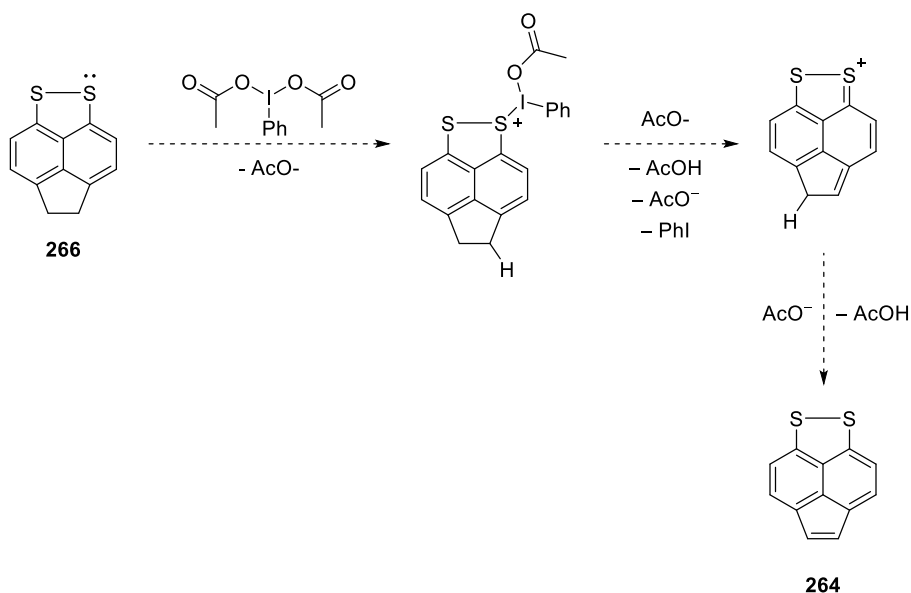
**Figure 7** Optimisation of the oxidation of acenaphthene trisulfide **319** to acenaphthylene trisulfide **320** by  $^1\text{H}$  NMR.

Having optimised the time and temperature of the reaction, the reaction was then performed in toluene (at the reflux temperature of benzene – 80 °C) to reduce the carcinogenicity of the reaction. Toluene gave identical reaction times and similar yields (~20 – 40%).

Other oxidation methods were attempted due to initially low yields. An interrupted Pummerer reaction was hypothesised (**Scheme 87**). A hypervalent iodine species oxidises the disulfide making the benzylic position *para*- more acidic allowing for deprotonation and eventually re-aromatisation. The Pummerer reaction is known to work through an aromatic system and subsequently substitute onto a benzylic position (**Scheme 86**).<sup>171</sup>



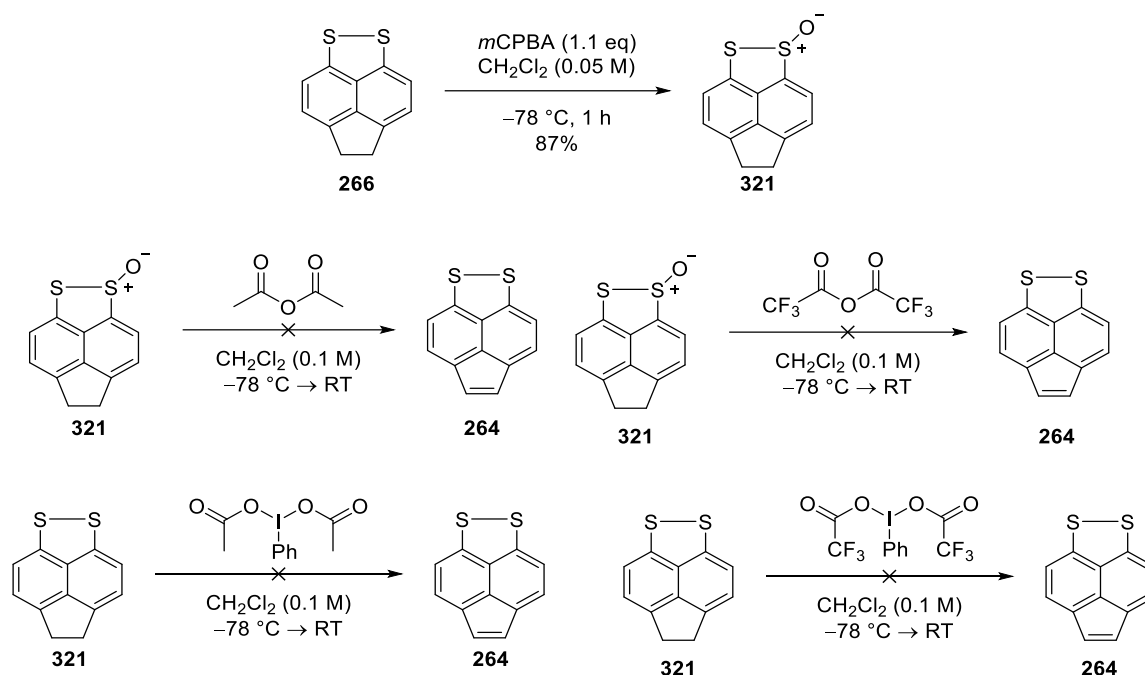
**Scheme 86** An example of a “through-aromatic” Pummerer reaction.



**Scheme 87** Proposed mechanism of the hypervalent iodine interrupted Pummerer reaction/Pummerer-like reaction to synthesise **264**.

Acenaphthene disulfide **266** was subjected to oxidation using *m*CPBA to yield acenaphthene thiosulfinate **321**.<sup>107</sup> Thiosulfinate **321** was subjected to Pummerer reaction conditions in an attempt to form the acenaphthylene disulfide. Using both acetic anhydride and trifluoroacetic anhydride in  $\text{CH}_2\text{Cl}_2$ , no reaction was observed. Refluxing thiosulfinate **321** in neat acetic

anhydride was another route to acenaphthylene disulfide **264** – the desired product was not found, only decomposition was observed (**Scheme 88**).

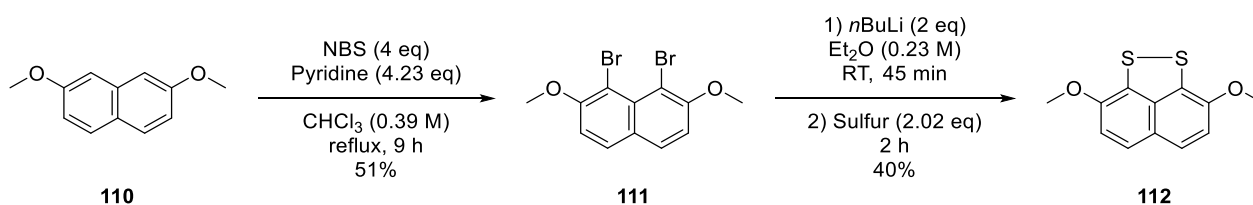


**Scheme 88** Alternative acenaphthylene disulfide **260** synthesis.

Hypervalent iodine species are known to directly activate sulfides in Pummerer-like reactions. Both (diacetoxy)iodobenzene and [bis(trifluoroacetoxy)iodo]benzene were trialed as oxidants. The disulfide performed a nucleophilic attack on the hypervalent iodine species however, no acenaphthylene was observed – indicating the interrupted Pummerer did not occur. Purification gave near full recovery of the starting material or the recovery of thiosulfinate **321** in trace amounts. If thiosulfinate **321** is being produced then an oxygen nucleophile must be present in the reaction system. Only three are possible – acetate that is released from the hypervalent iodine compound after S nucleophilic attack, water present in the solvents, or molecular oxygen. Oxygen was thought not to be the issue therefore, all the reactions were then attempted under dry conditions (freshly distilled reagents, solvents dried over 3 Å molecular sieves, argon atmosphere dried via silica column, glassware was either

flame-dried or oven-dried). Once again, the reaction did not produce the desired product, with only disulfide **266** recovered. Base was added to encourage the deprotonation step (triethylamine, DBU, Hünig's base and K<sub>2</sub>CO<sub>3</sub>) – all of which gave no reaction.

Considering the difficulty making the acenaphthylene disulfide, other naphthalene substituted cores were considered because it could potentially alter the UV properties of the naphthalene core. Therefore, electron-donating methoxy groups were added in the 2,7-positions. A different absorption profile could provide an alternative photochemical release mechanism for the reactive diatomic molecules. The synthesis of 2,7-dimethoxynaphthalene disulfide **112** was completed using a previously reported group method.<sup>43</sup> 2,7-Dimethoxynaphthalene **110** was subjected to 2,5-pyrrolidenone 1-bromopyridinium salt (made *in situ* by reacting pyridine and NBS) which gave 2,7-dimethoxynaphthalene dibromide **111** in a 50% yield (**Scheme 89**).<sup>43,172</sup> Dibromide **111** was treated with *n*BuLi (double lithium halogen exchange) in Et<sub>2</sub>O, to give the *peri*-substituted dilithio-species. The addition of sulfur quenches the dilithio-species which yielded the desired disulfide **112**.<sup>43,172,173</sup>

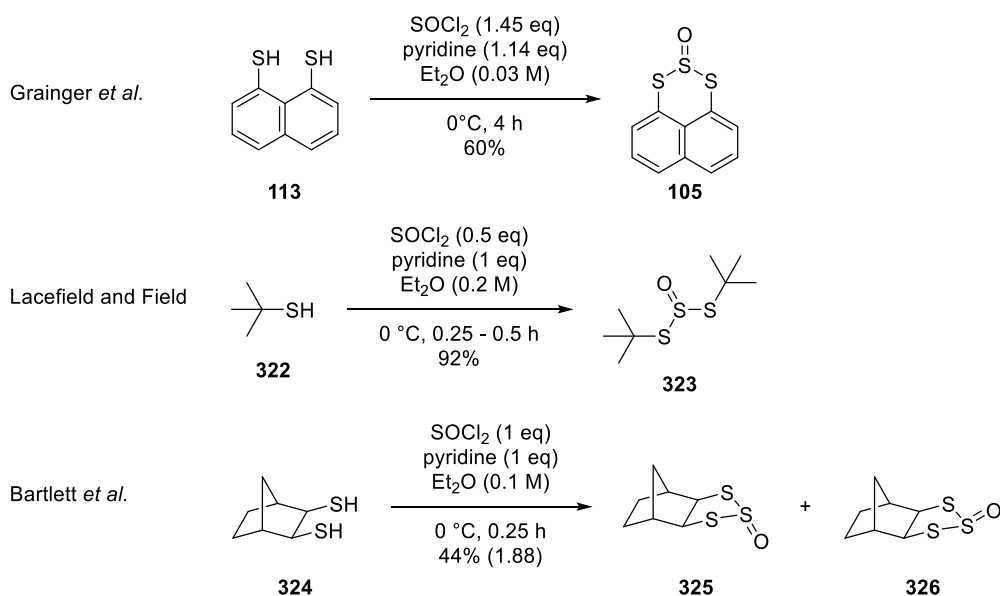


**Scheme 89** Synthesis of dimethoxynaphthalene disulfide **112**.<sup>43,172</sup>

### 2.3 Synthesis of the trisulfide-2-oxides

Fluorene trisulfide-2-oxide **301** was the first novel trisulfide-2-oxide to be synthesised (from the dithiol). After several attempts using the conditions previously used in the group, i.e. the use of pyridine and thionyl chloride on the dithiol, previous literature methods were revisited

(section 1.1.5).<sup>42,43</sup> Grainger and co-workers' conditions were inspired by Lacefield and Field who began the synthesis of trisulfide-2-oxides in 1966, using 1 equivalent of pyridine per thiol.<sup>174,175</sup> Bartlett used only 0.5 equivalents pyridine per thiol (**Scheme 90**) to synthesise norbornane derived cyclic trisulfide-2-oxides.



**Scheme 90** The prior syntheses of trisulfide-2-oxides using  $\text{SOCl}_2$ .<sup>42,43,174,175</sup>

All the above conditions yielded trisulfide-2-oxide **301** (**Table 3**). However, the group's previous conditions proved to be the best (**Table 3**, Entry 1).

**Table 3** Synthesis of fluorene trisulfide-2-oxide **301** using a variety of methods.

Entry	Source	SOCl <sub>2</sub> eq.	Pyridine eq.	Concentration / M	% Yield	Notes
1	Grainger	1.45	1.45	0.03	37	H <sub>2</sub> SO <sub>4</sub> work-up
2	Bartlett	1	1	0.1	6	H <sub>2</sub> SO <sub>4</sub> work-up
3	Lacefield	1	2	0.1	26	H <sub>2</sub> SO <sub>4</sub> work-up
4	Lacefield	1	2	0.1	0	HCl work-up



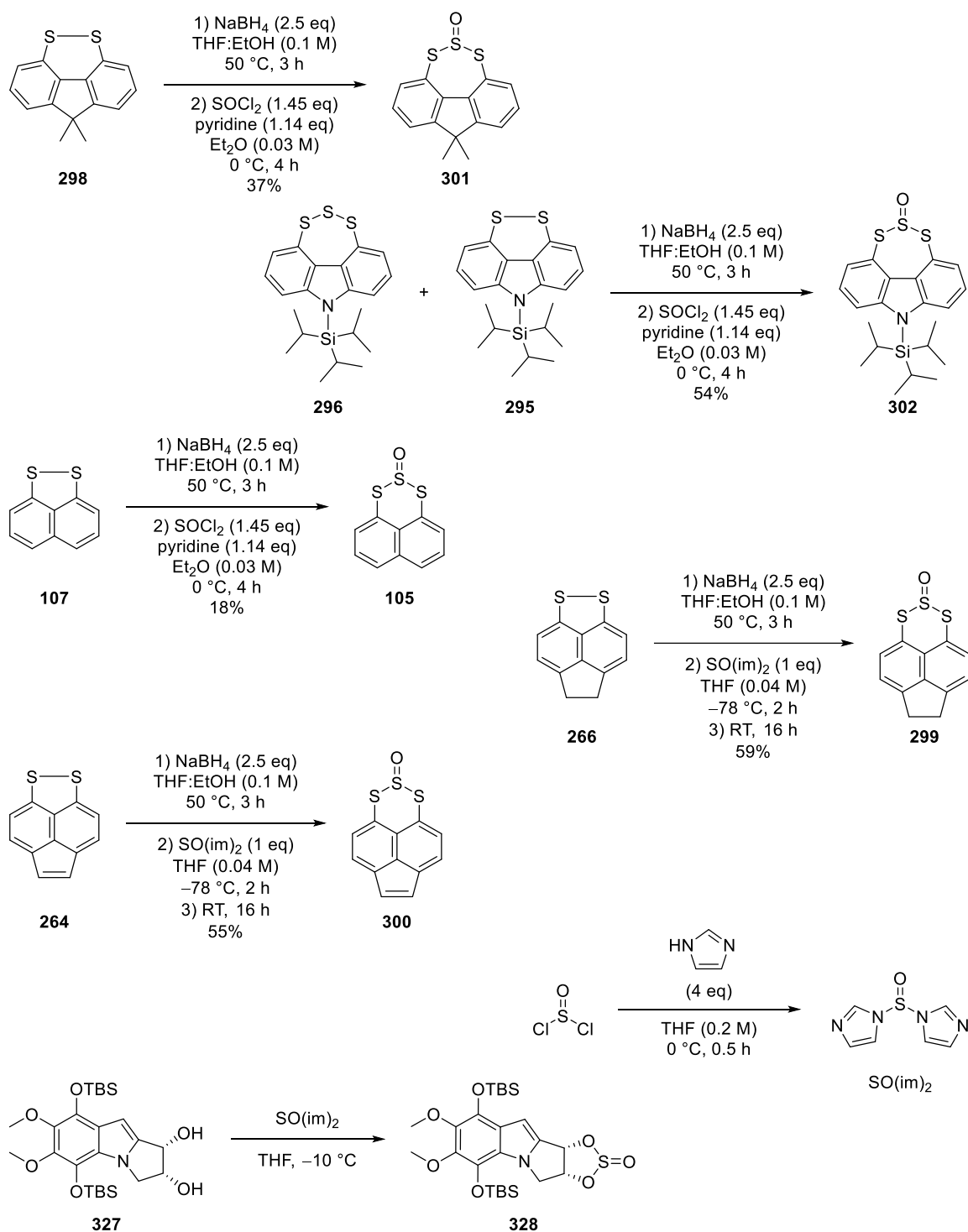
Alternative work-up conditions were trialled. Dilute HCl (0.01 M) was used instead of H<sub>2</sub>SO<sub>4</sub>. This allowed for a cleaner work up and removal of the pyridinium chloride salts from the ether layer; however, only starting material was recovered (**Table 3**, Entry 4). The chloride anion maybe acting as a nucleophile towards the trisulfide-2-oxide (at the sulfinyl). Switching back to a H<sub>2</sub>SO<sub>4</sub> work-up gave the desired product. The sulfate anion is less nucleophilic than chloride and does not attack the trisulfide-2-oxide.

Carbazole trisulfide-2-oxide **302** was synthesised in a similar manner to fluorene trisulfide-2-oxide **301**. However, the best yield came for the reduction of a mixture of carbazole disulfide **295** and trisulfide **296**. Once carbazole dithiol **310** had been synthesised the crude mixture was subjected to the standard Grainger conditions of SOCl<sub>2</sub>/pyridine to give carbazole trisulfide-2-oxide **302** in a 54% yield.

The fluorene and carbazole scaffolds were produced in slightly lower yields than the naphthalene scaffold, as reported in the literature (although the naphthalene scaffold was synthesised in much lower yield in my hands) (**Scheme 91**). An alternative trisulfide-2-oxide synthesis was proposed. Yang and Gu published a total synthesis in which they synthesised sulfite **328** using thionyl diimidazole (SO(im)<sub>2</sub>) (**Scheme 91**).<sup>176</sup> Using SO(im)<sub>2</sub> on naphthalene dithiol **113** gave a poor ratio of disulfide to trisulfide-2-oxide (9:1) by <sup>1</sup>H NMR of the crude reaction mixture. Therefore, the total theoretical yield was 10%. SO(im)<sub>2</sub> with fluorene and carbazole dithiol **306** and **310** returned only disulfide. This may be due to SO(im)<sub>2</sub> being larger than SOCl<sub>2</sub> and therefore not being able to insert efficiently into the closer dithiols. However, SO(im)<sub>2</sub> reacts with the acenaphthene **312** and acenaphthylene dithiol to yield the trisulfide-2-oxides **299** and **300** in excellent yields (58% and 55%, respectively). Alternatively, using

Grainger *et al.*'s conditions on acenaphthylene dithiol gave a poor yield of the trisulfide-2-oxide.

The difference in reactivity between the dithiols towards  $\text{SO}(\text{im})_2$  to give the trisulfide-2-oxides was hypothesised to be due to the close proximity effect. As the thiol groups get closer together, they are unable to undergo nucleophilic substitution at the thionyl group due to the size of the imidazole in comparison to the chloride. This may explain why higher yields were observed for  $\text{SO}(\text{im})_2$  over  $\text{SOCl}_2$  with the splayed thiols of the acenaphthene and acenaphthylene **299** and **300**.

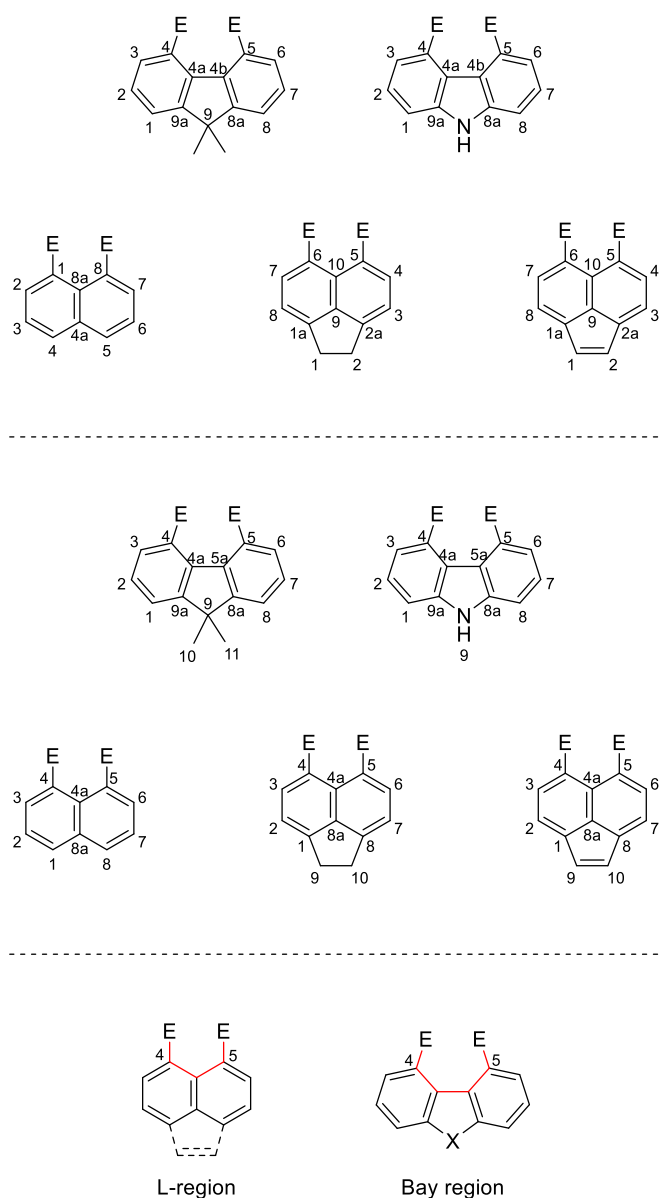


**Scheme 91** Synthesis of the fluorene **301**, carbazole **302**, naphthalene **105**, acenaphthene **299** and acenaphthylene **300** trisulfide-2-oxides. Yang and Gu's synthesis of sulfite **328** and how they synthesised SO(im)<sub>2</sub> is also shown at the bottom. SO(im)<sub>2</sub> is synthesised in situ and sulfite **328** is isolated but no yield is given as it is used directly in another reaction.

## 2.4 Structure analysis and characterisation

### 2.4.1 Peri-substitution analysis

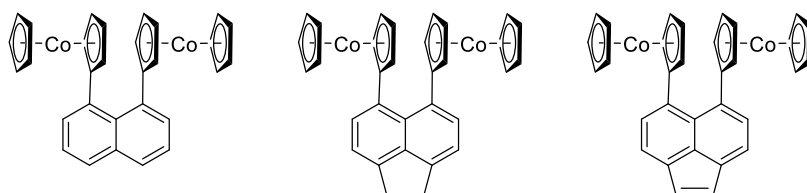
A few key definitions need to be outlined before the section is presented. First is the numbering of both the *peri*- and *peri*-like structures in order to be clear about which angles, and bonds are being described. In this section the standard IUPAC numbering for naphthalene, acenaphthene and acenaphthylene do not mirror one another. Therefore, an alternative numbering system has been used in order to make the comparisons easier for the reader. Naphthalene will be numbered in the reverse of its IUPAC numbering. There are several defined areas within polyaromatics. The L-region is defined as the region around the *peri*-positions. The bay region is defined as the positions across the *peri*-like positions of carbazole and fluorene.<sup>129,130</sup>



**Figure 8** Top) IUPAC numbering for fluorene, carbazole, naphthalene, acenaphthene and acenaphthylene. Middle) Numbering used in this thesis for fluorene, carbazole, naphthalene, acenaphthene and acenaphthylene. B) The definitions of the L-region and the bay-region.

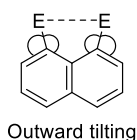
In 2020 Jürgen Heck and co-workers published their findings on the through-space and through-bond exchange pathways of bis-cobaltocenes and their potential as molecular spintronics.<sup>177</sup> In this publication they thoroughly analyse the crystal structures of their

molecules (**Figure 9**) and use excellent definitions of specific bond lengths, angles and twists in the molecules.



**Figure 9** Heck and co-workers' naphthalene, acenaphthene and acenaphthylene bis-cobaltacenes.<sup>177</sup>

They address two structural ideas that are relevant to this work: outward tilting and naphthalene torsion. For the purpose of these structural definitions E = any functionality.



**Figure 10** Outward tilting across the peri-positions in naphthalene.

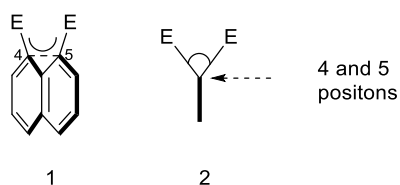
Outward tilting is a measure of the number of degrees the angle between the E groups have deviated from the value of the unsubstituted hydrocarbon. This gives the splay angle (**Equation 1**).

**Equation 1** Equation to calculate the splay angles and, therefore, the degree of outward tilting of a peri-substituted system.

$$\text{Splay Angle } ^\circ = \sum \text{Internal Bay Region Angles} - 360^\circ$$

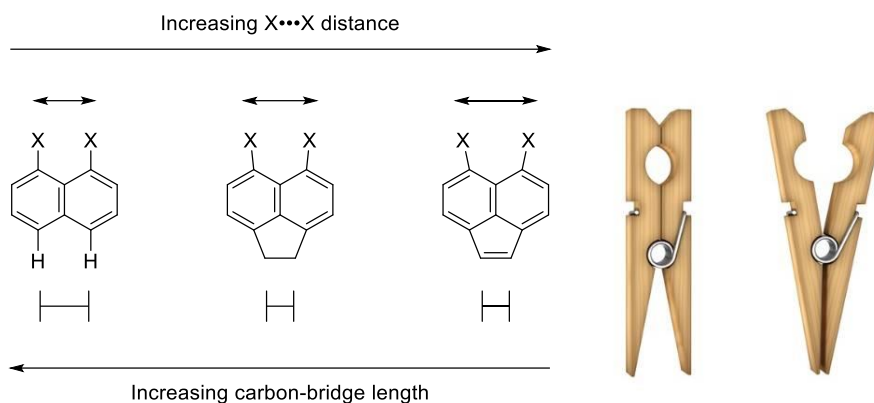
If the splay angle is positive there is an outward tilting effect. If the splay angle is negative the opposite is occurring, and there is an inward tilting effect.

Naphthalene torsion is another type of strain which can be measured. It is defined as the angle of the displacement between E1 and E2 out of the aromatic plane.<sup>177</sup> **Figure 11** explains this in further detail. In **Figure 11** it is clear that the two E groups are twisted out of the plane of aromaticity away from one another. The diagram shows the view looking down the aromatic plane, and the angle that is measured. Therefore, for the *peri*-substituted scaffolds the naphthalene torsion is the angle between E1-C4...C5-E2.



**Figure 11** Definition of naphthalene torsion.

In the comparison of naphthalene **258**, acenaphthene **265** and acenaphthylene **263** it is expected that the shorter the carbon bridge (C9-C10) across the C1...C8 positions, the greater the bond angles, distances, and bond lengths across the opposite L-region of the molecule. This is due to a “clothes peg”-like effect that should be experienced. This was explained by Heck and co-workers.<sup>177</sup> To explain this further an analysis of crystallographic data of the known dibromo- *peri*-substituted compounds (**Figure 12** and **Table 7**) is shown.



**Figure 12** The “clothes peg” effect: The effect of the carbon bridge on peri-substitution distance.

**Table 4** Crystallographic data for the dibromides of naphthalene **258**,<sup>178</sup> acenaphthene **265**,<sup>162</sup> and acenaphthylene **263**.<sup>126</sup>

Entry	Scaffold	Naphthalene <b>258</b>	Acenaphthene <b>265</b>	Acenaphthylene <b>263</b>	
				Molecule A	Molecule B
<b>1</b>	<b>Structure and Numbering</b>	<p style="text-align: center;"><math>C_{10}H_6Br_2</math><sup>178</sup></p>	<p style="text-align: center;"><math>C_{12}H_8Br_2</math><sup>162</sup></p>	<p style="text-align: center;"><math>C_{12}H_6Br_2</math><sup>126</sup></p>	
<b>2</b>	<b>Br1...Br2 distance / Å</b>	3.2019(17)	3.296(3)	3.3387(6)	3.3195(6)
<b>3</b>	<b>C4...C5 distance / Å</b>	2.4303(13)	2.620(2)	2.618(4)	2.639(4)
<b>4</b>	<b>C1...C8 distance / Å</b>	2.4152(13)	2.2928(19)	2.312(4)	2.320(4)
<b>5</b>	<b>C9-C10 bond length / °</b>	2.4563(13)	1.5120(13)	1.322(4)	1.359(5)
<b>6</b>	<b>Br1-C4-C4a angle / °</b>	129.093(16)	128.02(5)	124.0(2)	123.6(2)
<b>7</b>	<b>Br2-C5-C4a angle / °</b>	127.543(19)	125.13(5)	124.44(19)	123.4(2)
<b>8</b>	<b>C4-C4a-C5 angle / °</b>	122.42(3)	127.09(3)	133.3(2)	133.6(3)
<b>9</b>	<b>C1-C8a-C8 angle / °</b>	120.35(3)	112.80(4)	109.5(2)	109.5(3)
<b>10</b>	<b>C9-C1-C8a angle / °</b>	120.18(13)	108.95(3)	105.7(2)	106.2(3)



11	C10-C8-C8a angle / °	120.03(3)	108.78(6)	105.6(2)	106.3(3)
12	Splay Angle / °	19.893	20.24	-21.74	20.6
13	Naphthalene torsion angle / °	5.3(8)	4.7280(8)	-1.28(14)	-0.28(13)

*Note: When a X-ray diffraction pattern is observed and the structure solved and refined, the hydrogen positions are usually predicted. To gain an accurate position of the hydrogens a neutron diffraction pattern must be observed. Therefore, in naphthalene, the carbon bridge distance is inaccurate due to the predicted hydrogen positions being used.*

In dibromonaphthalene **258** (the H1...H8 distance is 2.4563(13) Å and the Br1...Br2 distance is 3.2019(17) Å. In dibromoacenaphthene **265** the carbon bridge is 1.5120(13) Å and the Br1...Br2 distance is 3.296(3) Å. In dibromoacenaphthylene **263** the carbon bridge is shortened again to 1.322(4) Å and 1.359(5) Å and the Br1...Br2 distances are 3.3387(6) Å and 3.2195(6) which is longer again (**Table 4**, Entries 2 and 5). It is clear from **Table 4** that the carbon bridge influences the opposite L-region, including the C4...C5 distances. The splay angles also increase as the carbon bridge bond length gets shorter. Consequently, the longer the carbon bridge (or the absence of the carbon bridge) the increased naphthalene torsion due to the bromine atoms repelling one another.

#### 2.4.2 Peri-like structural analysis

For the *peri*-like molecules there has never been an in-depth analysis of the different structural ideas that can affect the strain around the bay region. Therefore, definitions are proposed herein.

Like the *peri*-substituted molecules, the outward tilting can be measured on the *peri*-like systems. For the fluorene and carbazole systems the splay angles must be calculated differently to accommodate the extra carbon in the bay-region. The splay angle of the *peri*-like systems will also be determined as deviations from their parent hydrocarbons. For an accurate representation of the bay region angles the crystal should be analysed with neutron diffraction. With this being out of reach, 9,9-dimethylfluorene **307** and *N*-TIPS-carbazole **286** were crystallised and the bay angles determined using XRD. The final H4-C4-C4a and H5-C5-C5a angles were calculated, halving the C3-C4-C4a and C6-C5-C5a external angles to give the position of the hydrogens as a prediction. Below are the calculated total bay-region angles for fluorene and carbazole, respectively.

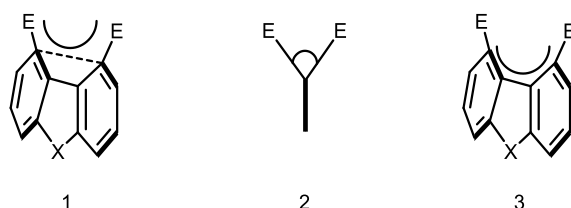
*Equation 2 Calculations for the bay region angles of fluorene and carbazole.*

$$\begin{aligned}
 & \text{Splay Angle of Peri-like system} / ^\circ \\
 &= \sum \text{bay region angles of substituted scaffold} \\
 &\quad - \sum \text{bay region angles of unsubstituted scaffold} \\
 \\
 &\sum \text{Bay region angles for fluorene} = 130.87 + 131.10 + 120.64 + 120.73 \\
 &\quad = \mathbf{503.34}^\circ \\
 \\
 &\sum \text{Bay region angles for carbazole} = 131.9 + 132.5 + 120.55 + 120.55 = \mathbf{505.50}^\circ
 \end{aligned}$$

If the value is positive, the angles are wider than the unsubstituted scaffold and there is an outward tilting effect that the E groups are experiencing. If the value is negative, the angles

are smaller than the unsubstituted scaffold and therefore the E groups are experiencing an inward tilting effect.

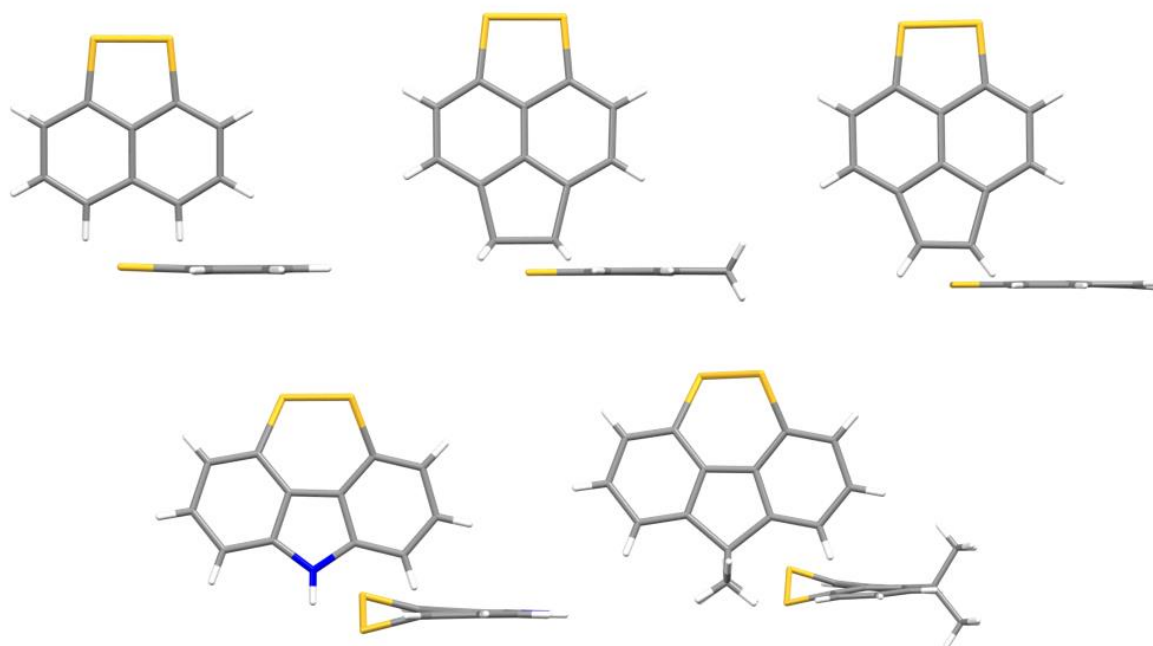
The idea of the naphthalene torsion angle can also be applied to the *peri*-like system. In these systems, like the *peri*-systems, the *peri*-like positions need to be used to calculate the aromatic out of plane distortion. It is defined as the angle between the E1-C4...C5-E2, when looking down the C4...C5 axis.



**Figure 13** Structure 1 shows the *peri*-like scaffold torsion. Structure 2 is a side-on profile of the *peri*-like systems. Structure 3 shows the deviation from planarity angle.

Often there is a deviation from planarity of the *peri*-like scaffolds. It is defined as the torsion angle about the C4-C4a-C5a-C5 bond when looking down the C4a-C5a bond. The final angle used to describe the strain of a system can only be related to other disulfides. The disulfide angle (i.e. C-S-S-C angle) for an unconstrained organic disulfide is typically 85 °. Distortion away from this value by the ring system can give an indication of how strained the system is.

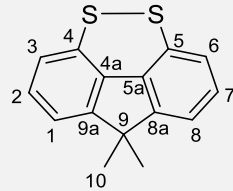
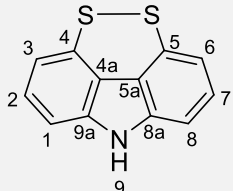
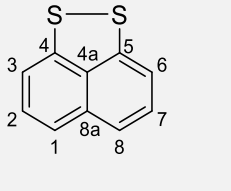
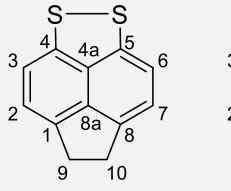
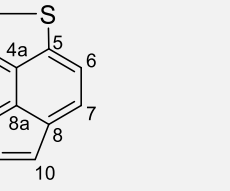
### 2.4.3 Disulfides



**Figure 14** The structures of the disulfides obtained by x-ray diffraction. All novel disulfides were collected at 100 K with Cu K $\alpha$  ( $\lambda = 1.54184$ ) as the radiation source and the crystals grown from slow vapour evaporation. Top left – naphthalene disulfide **107**;<sup>112</sup> Top centre – acenaphthene disulfide **266**;<sup>113</sup> Top right – acenaphthylene disulfide **264**;<sup>112</sup> Bottom left – carbazole disulfide **311** (this work); Bottom right – fluorene disulfide **300** (this work).

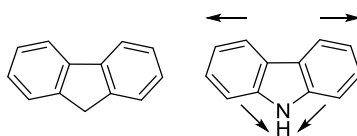
Woollins and co-workers previously synthesised naphthalene **107**, acenaphthene **266**, and acenaphthylene disulfides **264** and characterised them crystallographically. These data from the papers by Woollins and co-workers allows for a comparison of the *peri*-disulfides and the *peri*-like disulfides.

**Table 5** All novel disulfides were collected at 100 K with Cu K $\alpha$  ( $\lambda = 1.54184$ ) as the radiation source and the crystals grown from slow vapour evaporation. Crystallographic data of disulfides **300**, **311**, **107**, **266**, and **264**.

	Disulfide	Fluorene 298		Carbazole 311		Naphthalene 107		Acenaphthene 266	Acenaphthylene 264	
1	Structure and numbering									
2	Molecules in unit cell	A	B	A	B	A	B	—	A	B
3	S1-S2 bond length / Å	2.0779(8)	2.0772(8)	2.0819(6)	2.0883(6)	2.0879(8)	2.096(3)	2.1025(18)	2.0891(4)	2.0838(4)
4	Peri- or peri-like carbon distance (C4...C5)/ Å	3.184(3)	3.180(3)	3.209(2)	3.211(2)	2.431(3)	2.414(3)	2.464(7)	2.3929(4)	2.4241(4)
5	C4-S1-S2 bond angle / °	102.53(7)	101.34(7)	103.29(6)	103.23(6)	95.56(6)	96.25(14)	96.35(18)	98.375(16)	97.255(16)
6	C5-S2-S1 bond angle / °	102.24(7)	102.48(8)	102.86(6)	103.57(6)	95.62(6)	93.85(11)	95.49(17)	92.193(17)	94.401(17)
7	S1-C4-C4a bond angle / °	117.87(15)	117.24(15)	116.29(13)	117.12(13)	115.02(12)	114.02(18)	113.6(3)	113.688(11)	113.883(11)
8	S2-C5-C5a bond angle / °	118.11(16)	118.24(16)	116.71(13)	116.53(13)	—	—	—	—	—
9	C4-C4a-C5a bond angle / °	128.76(18)	128.37(18)	130.17(16)	129.92(16)	—	—	—	—	—
10	C5-C5a-C4a bond angle / °	128.16(18)	128.10(19)	129.69(16)	130.28(16)	—	—	—	—	—
11	C4-C4a-C5 bond angle (peri-substituted only) / °	—	—	—	—	118.65(16)	117.99(18)	120.2(5)	116.317(7)	118.770(7)
12	S2-C5-C4a bond angle (peri-substituted only) / °	—	—	—	—	115.11(14)	117.84(13)	114.4(4)	119.335(14)	115.671(15)
13	C1...C8 distance / Å	5.090(3)	5.101(3)	4.994(3)	4.992(3)	2.514(3)	2.517(4)	2.377(7)	2.4241(4)	2.3929(4)
14	C9-C9a bond length (C9a-N1) / Å	1.529(3)	1.525(3)	1.382(2)	1.383(2)	—	—	—	—	—

15	C9-C8a bond length (C8a-N1)/ Å	1.527(3)	1.532(3)	1.383(2)	1.388(2)	—	—	—	—	—
16	C9a...C8a distance / Å	2.365(3)	2.367(3)	2.259(3)	2.262(2)	—	—	—	—	—
17	C9a-C9-C8a (C9a-N1-C8a) bond angle / °	101.39(16)	101.47(17)	109.60(14)	109.48(15)	—	—	—	—	—
18	C9-C10 bond length (peri- substituted only) / Å	—	—	—	—	2.5903(3)	2.6151(2)	1.657(7)	1.3736(3)	1.3858(3)
19	C1-C8a-C8 bond angle (peri- substituted only) / °	—	—	—	—	124.91(16)	128.2(3)	114.9(5)	118.770(7)	116.317(7)
20	Disulfide angle / °	-48.66(10)	50.26(10)	47.65(8)	45.79(8)	0.16(8)	-1.92(15)	0.5(3)	2.3499(3)	-0.31611(4)
21	S1-C4...C5-S2 torsion angle / °	-32.88(11)	34.07(12)	31.98(9)	30.71(9)	0.14(9)	-1.66(14)	0.4(3)	2.0507(2)	-0.27162(3)
22	Disulfide twist out of the aromatic plane / °	-30.33(7)	31.66(7)	28.11(8)	27.04(8)	-0.09(7)	1.8(9)	-0.51(9)	1.6030(3)	-0.37117(7)
23	Planarity torsion C4-C4a-C5a- C5 / °	-12.2(3)	13.3(3)	11.4(2)	10.5(2)	—	—	—	—	—
24	Splay angle / °	-10.44	-11.39	-12.64	-11.65	-11.22	-10.15	-11.80	-10.667	-11.676

Naphthalene disulfide **107** and acenaphthylene disulfide **264** have very similar disulfide bond lengths (2.083 – 2.096 Å), whilst acenaphthene has a slightly longer disulfide bond (2.103 Å) (**Table 5**, Entry 3). Interestingly, all the *peri*-substituted disulfides have a similar C4...C5 distances (~2.4 Å) (**Table 5**, Entry 5). Likewise, the C1...C8 distances are also similar (**Table 5**, Entry 13). Acenaphthene has the shortest C1...C8 distance (2.377(7) Å), not acenaphthylene disulfide **264**, which can be attributed to it also the alkyl C9-C10 bond length. The disulfide appears to mitigate the distortion of the naphthalene core in acenaphthene **266** and acenaphthylene **264** disulfides. This gives acenaphthene **266** and acenaphthylene **264** an unusual set of bond angles and lengths (**Table 5**). The carbon bridge is only affecting the bond angles in its close proximity, and not the opposite L-region – unlike the dibromo-analogues (**Table 4**). Due to the sulfur atoms being in close proximity to one another, the disulfide bond forms over remaining as two thiols. It is thermodynamically favourable. This explains why the disulfides are formed, and why the mitigation of the carbon bridge strain is observed. All the disulfides have a negative splay angle, indicating that there is an inward tilting effect occurring. The disulfide bond is causing the *peri*-positions to distort inward.



**Figure 15** The effect of nitrogen vs carbon on carbazole vs fluorene scaffolds.

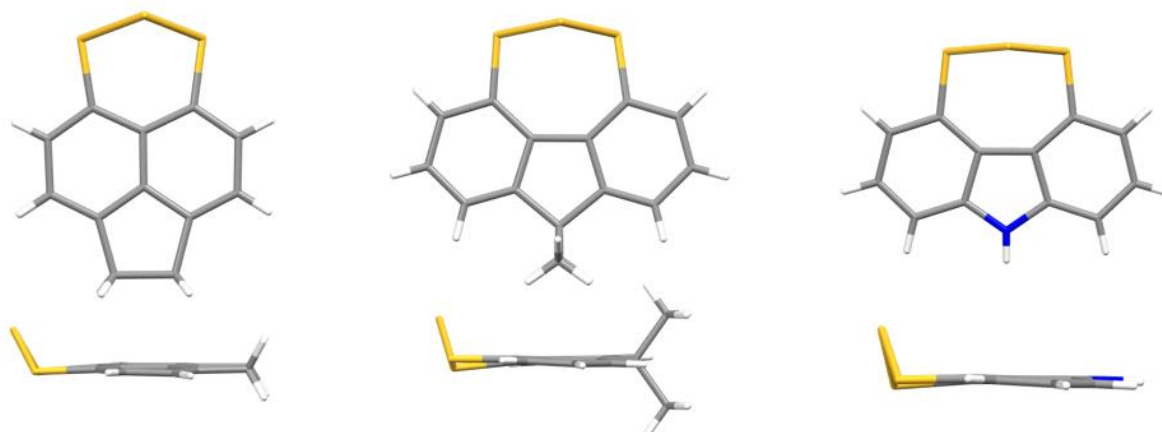
Fluorene and carbazole are the two *peri*-like systems that have been explored extensively during this work. The two structures are similar, however the nitrogen atom vs. carbon atom which connects the biphenyl rings, accounts for the slight changes between the two structures. When the C9a and C8a are pinched together the C4 and C5 positions move further apart – like a clothes peg. This can be applied to the fluorene/carbazole analogy. Due to the

electronegativity of the nitrogen atom, carbon-nitrogen bonds are shorter than carbon-carbon bonds. Therefore, carbazole's *peri*-like positions are further apart in comparison to the fluorene – this is proved in the crystallographic data (**Table 5**). In carbazole the bond distances of the C-N bonds are approximately 1.38 Å for all 4 bonds (2 molecules in the unit cell and 2 C-N bonds per molecule). However, the fluorene scaffold has a C-C bond length of approximately 1.53 Å for all 4 bonds (2 molecules in the unit cell and 2 C-C bonds per molecule) (**Table 5**, Entries 14 and 15). The crystallographic data displays that the C-N bonds are shorter, which has an effect on the strain of the 5 membered rings. The C8a...C9a distance for carbazole is 2.26 Å for both molecules in the unit cell, whilst for fluorene it is 2.37 Å (**Table 5**, Entry 16). The effect of the increased pull at the 5 membered ring is the difference in steric interactions at the *peri*-like positions and the overall strain in the heteroaromatic ring. This can be seen in the C4...C5 distance difference between the *peri*-like systems. In carbazole the C4...C5 distance is 3.21 Å whilst the fluorene scaffold is 3.18 Å (**Table 5**, Entry 4). Furthermore, the disulfide length and the subsequent twist out of the plane of aromaticity are also affected. In carbazole the disulfide bond length is slightly longer than fluorene (2.0819(6)/2.0883(6) Å vs 2.0779(8)/2.0772(8) Å) and the twist out of plane is smaller for carbazole than fluorene (30.11(5)/28.66(5) Å vs. 32.45(6)/34.08(7) Å respectively) (**Table 5**, Entry 3). The fluorene scaffold is more congested and strained in the *peri*-like region of the molecule.

Interestingly the *peri*-like scaffolds have a shorter S1-S2 bond length than the *peri*-substituted scaffolds (**Table 5**, Entry 3). Therefore if an atom is placed between them then the system would be more strained than the *peri*-substituted scaffolds.



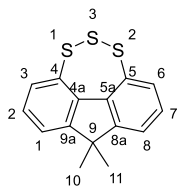
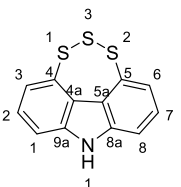
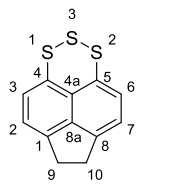
#### 2.4.4 Trisulfides



**Figure 16** All novel trisulfides were collected at 100 K with Cu K $\alpha$  ( $\lambda = 1.54184$ ) as the radiation source – except for trisulfide **309** where the radiation source was Mo K $\alpha$  ( $\lambda = 0.71075$ ). and the crystals grown from slow vapour evaporation – except for acenaphthene trisulfide **319**, which was grown by hot recrystallisation (reflux) from ethanol. The structures of the trisulfides obtained by x-ray diffraction. Left - acenaphthene trisulfide **319**; Centre - fluorene trisulfide **309**; Right - carbazole trisulfide **329**.

To study the structures of the new trisulfides prepared, crystals of **309**, **319** and **329** were grown by slow evaporation (trisulfides **329** and **309**) and recrystallisation from boiling ethanol (trisulfide **319**), and their x-ray diffraction data collected at 100 K and refined in the usual way.

**Table 6** All novel trisulfides were collected at 100 K with Cu K $\alpha$  ( $\lambda$  = 1.54184) as the radiation source – except for trisulfide **309** where the radiation source was Mo K $\alpha$  ( $\lambda$  = 0.71075). All crystals grown from slow vapour evaporation – except for acenaphthene trisulfide **319**, which was grown by hot recrystallisation (reflux) from ethanol. Crystallographic data for trisulfides **309**, **329** and **319**.

Entry	Trisulfide	Fluorene <b>309</b>	Carbazole <b>329</b>	Acenaphthene <b>319</b>
1		S1-S2-S3 group (75% of molecules) (Molecule A)		
2	Structure and Numbering	S1'-S2'-S3' group (25% of molecules) (Molecule B)		
				
3	S1-S3 bond length / Å	2.0405(17)	2.025(6)	2.0413(6)
4	S3-S2 bond length / Å	2.019(4)	2.026(15)	2.0404(7)
5	S1...S2 distance / Å	3.169(4)	3.165(14)	3.2012(7)
6	S1-S3-S2 bond angle / °	102.62(14)	102.8(4)	103.31(3)
7	Sulfur atom plane - Aromatic plane angle / °	106.45(10)	110.3(5)	106.19(5)
8	C4...C5 (Peri- or peri-like carbon) distance / Å	3.536(3)	3.536(3)	3.571(3)
9	C4-C4a-C5a bond angle (peri-like only) / °	136.13(15)	136.13(15)	138.23(17)

10	C5-C5a-C4a bond angle (peri-like only) / °	136.66(16)	136.66(16)	138.20(16)	—
11	S1-C4-C4a angle (peri-like only) / °	124.96(14)	132.9(2)	125.39(14)	
12	S2-C5-C5a angle (peri-like only) / °	129.89(18)	122.0(4)	125.96(13)	
13	C9-C8a bond length (N1-C8a) (peri-like only) / Å	1.510(2)	1.510(2)	1.368(2)	—
14	C9-C9a bond length (N1-C9a) (peri-like only) / Å	1.507(2)	1.507(2)	1.370(2)	—
15	C9a-C8a distance (peri-like only) / Å	2.334(3)	2.334(3)	2.242(3)	—
16	C8a-C9-C9a bond angle (C8a-N1-C9a) (peri-like only) / °	101.40(13)	101.40(13)	109.95(16)	—
17	C4-C4a-C5 bond angle (peri- only) / °	—	—	—	129.68(15)
18	S1-C4-C4a bond angle (peri- only) / °	—	—	—	124.06(13)
19	S2-C5-C4a bond angle (peri- only) / °	—	—	—	122.98(12)
20	C1...C8 distance / Å	4.986(3)	4.986(3)	4.892(3)	2.337(2)

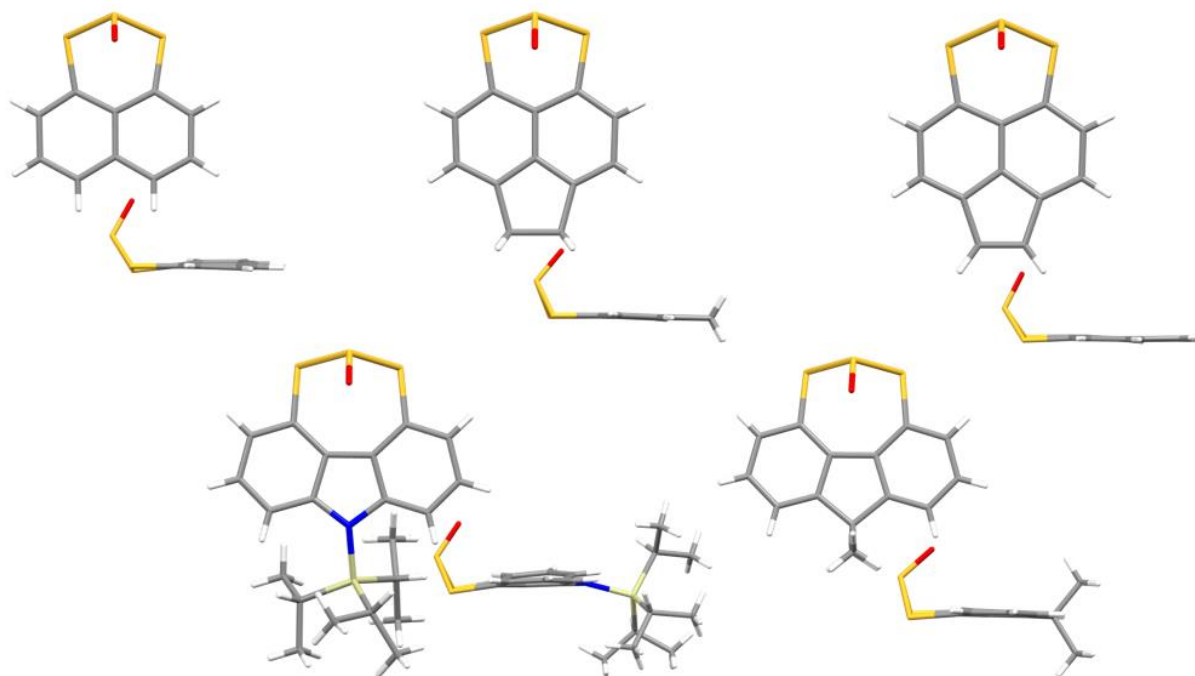
21	C4-C4a-C5 bond angle (peri-only)/ °	—	—	—	129.68(15)
22	C9-C10 bond length (acenaphthene only) / Å	—	—	—	1.553(3)
23	Splay angle	24.3	24.35	22.28	16.72
24	S1-C4...C5-S2 torsion angle / °	-6.47(18)	2.1(5)	-3.18(7)	-2.66(8)

All the trisulfides exhibit a kink out of the plane of aromaticity. The central sulfur atom is forced out of the plane, which is expected given the tetrahedral nature of the atom. The sulfur-sulfur bond lengths also decrease by a small amount in comparison to the respective disulfides. The fluorene and carbazole trisulfides have differences in structure due to the nature of the elemental composition of the 5 membered ring. It is clear from the crystallographic data that, like the disulfides, the decreased bond lengths from the carbon-nitrogen bond causes the greater separation of the *peri*-like positions. This inevitably influences the strain of the bay region. In carbazole trisulfide the C4...C5 distance is 3.571(3) Å which is larger than the fluorene trisulfide, 3.536(3) Å (**Table 6**, Entry 8). This inevitably influences the S1...S2 distance, which again is larger for the carbazole than the fluorene (3.2012(7) Å and 3.169(4)/3.165(14) Å respectively) (**Table 6**, Entry 5). The angle between the sulfur atom plane and the aromatic plane is calculated by drawing a plane between the sulfur atoms, then drawing plane for the aromatic scaffold, and calculating the angle between the two. The angle between the sulfur atom plane and the aromatic plane is not hugely different between carbazole trisulfide **325** and fluorene trisulfide **305**. The angle between the sulfur atom plane and the aromatic plane for carbazole is 106.19(5) °. The angle between the sulfur atom plane and the aromatic plane for fluorene is 106.45(10)° and 110.3(5)° (**Table 6**, Entry 7).

The sulfur atom plane-aromatic plane angle is lower for carbazole (106.19(5)°) than fluorene (106.45(10)° and 110.3(5)°). This is true for both conformations of fluorene trisulfide **309**. The difference is 0.26 ° or 4.16 °, respectively. The splay angle of the carbazole system is smaller than that of the fluorene (**Table 6**, Entry 23).

Structurally, the differences between the *peri*-like and *peri*-scaffolds are interesting as well. The *peri*-positions are much closer together than the *peri*-like system (simply due to the nature of the systems). For example, the C4...C5 distance on fluorene trisulfide **305** is 3.536(3) Å and the C4...C5 distance on carbazole trisulfide **325** is 3.571(3) Å. However, the C4...C5 distance on acenaphthene trisulfide **315** is 2.595(2) Å. Whilst the sulfur atoms in the *peri*-like systems are forced together by the structure, the *peri*-systems (e.g. acenaphthene trisulfide **315**) are not and the sulfur atoms are repelled by one another. This is clearly seen in the crystallographic data. The S1...S2 distance of acenaphthene trisulfide **319** is 3.1122(6) Å. This gives a clear deviation away from perpendicular *peri*- carbon-sulfur bonds, which is also evidenced by the splay angle. The splay angle of the acenaphthene trisulfide is 16.72 °. This is clearly a huge deviation from parallelism. The splay angles also show a repulsive interaction between the flanking sulfur atoms in comparison to the disulfides which have negative values indicating an attraction.

#### 2.4.5 Trisulfide-2-oxides



**Figure 17** All novel trisulfide-2-oxides were collected at 100 K with Cu K $\alpha$  ( $\lambda = 1.54184$ ) as the radiation source, except for trisulfide-2-oxide **300** where the radiation source was Mo K $\alpha$  ( $\lambda = 0.71075$ ). All crystals grown from slow vapour evaporation in the dark at 4 °C. The structures of the trisulfide-2-oxides obtained by x-ray diffraction. Top left – naphthalene trisulfide-2-oxide **105**<sup>43</sup>; Top centre – acenaphthene trisulfide-2-oxide **299**; Top right – acenaphthylene trisulfide-2-oxide **300**; Bottom left – carbazole trisulfide-2-oxide **302**; Bottom right – fluorene trisulfide-2-oxide **301**.

The trisulfide-2-oxides of acenaphthene, acenaphthylene, fluorene and carbazole have all been synthesised and the crystallographic data obtained. Crystals were grown from slow evaporation of CH<sub>2</sub>Cl<sub>2</sub> in a refrigerated environment (4 °C) whilst excluded from light. Trisulfide-2-oxide **105** is previously known in the literature. Trisulfide-2-oxide **299** has two polymorphs. Both were grown under the same conditions but indifferent vessels. One has crystallographic mirror symmetry and the other is not. Trisulfide-2-oxide **300** has two crystallographically unique structures in the asymmetric unit. Like trisulfides in the previous

section (Section 2.4.4), the trisulfide-2-oxides have a distinctive “kink” of the central sulfur atom out of the aromatic plane. The trisulfide-2-oxides can be analysed in a similar manner to the trisulfides.



**Table 7** All novel trisulfide-2-oxides were collected at 100 K with Cu K $\alpha$  ( $\lambda = 1.54184$ ) as the radiation source, except for trisulfide-2-oxide **300** where the radiation source was Mo K $\alpha$  ( $\lambda = 0.71075$ ). All crystals grown from slow vapour evaporation in the dark at 4 °C. The crystallographic data for trisulfide-2-oxides **105**, **299**, **300**, **301** and **302**.

Entry	Scaffold	Naphthalene <b>105</b> <sup>43</sup>	Acenaphthene <b>299</b>		Acenaphthylene <b>300</b>		Fluorene <b>301</b>	Carbazole <b>302</b>
			Polymorph 1	Polymorph 2	Molecule A	Molecule B		
<b>1</b>	<b>Structure and Numbering</b>							
<b>2</b>	<b>S1 ... S3 / Å</b>	3.0960(11)	3.1321(10)	3.1445(12)	3.1751(11)	3.1739(11)	3.136(14)	3.1815(8)
<b>3</b>	<b>S1 – S3 / Å</b>	2.0910(1)	2.1219(7)	2.1218(14)	2.1054(12)	2.1171(11)	2.1245(17)	2.1102(6)
<b>4</b>	<b>S2 – S3 / Å</b>	2.0964(11)	2.1219(7)	2.1112(12)	2.1080(12)	2.1133(11)	2.1088(13)	2.1011(7)
<b>5</b>	<b>S3 – O / Å</b>	1.474(3)	1.472(2)	1.472(3)	1.476(2)	1.475(2)	1.473(5)	1.4699(18)
<b>6</b>	<b>S1 – S3 – S2/ °</b>	95.53(4)	95.13(4)	95.95(5)	97.51(4)	97.50(5)	97.54(6)	98.13(3)
<b>7</b>	<b>C4 – S1 – S3/ °</b>	103.12(10)	98.56(7)	100.08(11)	102.57(11)	102.84(10)	128.1(3)	104.81(7)
<b>8</b>	<b>C5 – S2 – S3/ °</b>	100.46(10)	98.56(7)	100.59(11)	101.55(11)	101.86(10)	129.2(4)	103.39(7)
<b>9</b>	<b>S1 – S3 – O/ °</b>	109.71(11)	107.73(6)	108.75(14)	109.47(10)	108.93(10)	107.28(16)	110.05(7)
<b>10</b>	<b>S2 – S3 – O/ °</b>	108.43(10)	107.73(6)	108.21(13)	109.38(10)	107.95(10)	108.53(16)	109.89(7)
<b>11</b>	<b>S1 – C4 – C4a/ °</b>	125.7(2)	124.12(15)	124.5(2)	123.6(3)	125.2(2)	129.2(3)	126.31(15)
<b>12</b>	<b>S2 – C5 – C5a/ °</b>	124.8(2)	124.12(15)	129.4(3)	124.3(2)	123.9(2)	128.1(3)	128.93(15)

13	C4a-C5a-C5 / °	–	–	–	–	–	135.5(4)	136.40(17)
14	C4-C4a-C5a / °	–	–	–	–	–	135.8(4)	136.25(18)
15	C4-C4a-C5 / °	126.6(2)	129.4(2)	129.4(3)	130.7(3)	129.9(3)	–	–
16	C1-C8a-C8 / °	119.7(3)	111.9(2)	111.3(3)	109.7(2)	109.3(2)	–	–
17	C1...C8 distance / Å	2.452(4)	2.339(4)	2.335(4)	2.314(4)	2.312(4)	5.007(7)	4.905(3)
18	C4...C5 distance / Å	2.555(4)	2.589(4)	2.584(4)	2.598(4)	2.593(4)	3.516(6)	3.496(3)
19	C9 – C10 / Å (H1 – H8 distance for naphthalene)	2.42550(7)	1.559(5)	1.553(4)	1.368(4)	1.358(4)	–	–
20	Aromatic plane – sulfur atom plane angle / °	121.95(4)	114.92(5)	119.29(3)	124.38(4)	122.37(7)	105.75(9)	113.38(4)
21	Sulfur atom plane - O1 angle / °	119.03(11)	114.92(5)	119.29(3)	119.91(11)	119.04(11)	117.80(17)	121.41(7)
22	Splay angle / °	19.90	17.64	18.20	21.40	21.80	25.26	22.39
23	S1-C4...C5-S2 Torsion Angle / °	–6.22(13)	0.00(12)	–0.58(16)	1.42(14)	–0.04(15)	2.5(2)	–1.31(9)

*Note to reader: For comparisons between the trisulfides and trisulfide-2-oxides, please see **Table 8** and the discussion around them.*

In this chapter, it has been highlighted that a carbon bridge across the 1 and 8 positions of a naphthalene ring changes the distances and steric interactions of the functionality at the 4 and 5 positions. In the trisulfide-2-oxides this is no different. Naphthalene has no carbon bridge (C1...C8 distance = 2.452(4) Å) and the S1...S3 distance is the shortest (S1...S3 distance = 3.0960 Å). Acenaphthene (C9-C10 = -C<sub>2</sub>H<sub>4</sub>-) has the second shortest distance between the C1...C8 carbons (2.339(4) Å and 2.335(4) Å), the second shortest carbon bridge (C9-C10 distance = 1.559(5) Å and 1.553(4) Å) and the second longest S1...S3 distance (3.1321(10) Å and 3.1445(12) Å). Acenaphthylene (C9-C10 = -C<sub>2</sub>H<sub>2</sub>-) has the shortest distance between the C1...C8 carbons (2.314(4) Å and 2.312(4) Å), the shortest carbon bridge (C9-C10 distance = 1.368(4) Å and 1.358(4) Å), and the longest S1...S3 distance (3.1751(11) Å and 3.1739(11) Å). These distances indicate that a C9-C10 carbon bridge has an effect on the S1...S3 distance and C4...C5 distance.

The carbon bridge also influences the L-region angles. As the carbon bridge distance gets shorter, the L-region angles increase in size to accommodate this. This is observed in the C4-C4a-C5 angle, the S1-C4-C4a angle, and the S2-C5-C4a angle (**Table 7**, Entries 10, 11, and 14).

There appears to be no trend that links the carbon bridge to the sulfur plane to aromatic plane angle. Naphthalene has a sulfur plane to aromatic plane angle of 121.95(4)°, acenaphthene is 114.92(5)° and 119.29(3)°, and acenaphthylene is 124.38(4)° and 122.37(7)° (**Table 6**, Entry 20). Given that there is a drop in angle at acenaphthene, no trend can be observed.

From the disulfide crystallographic data both fluorene and carbazole disulfide have S-S bond lengths that are shorter than naphthalene disulfide. Therefore, adding an atom in between

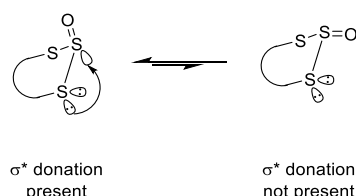
the flanking sulfur atoms in the *peri*-like scaffolds could increase the sterics more than the naphthalene scaffold. Therefore, the fluorene trisulfide-2-oxide **301** and carbazole trisulfide-2-oxide **302** will be more strained than previous naphthalene trisulfide-2-oxide **105**. In this case, the insertion of the sulfinyl group forces the outer sulfur atoms outwards. This makes the S1...S3 distance larger than that of the naphthalene trisulfide-2-oxide and the parent disulfide. However, when looking at the sulfur atom plane-aromatic plane fold angle the difference is much greater. The fold angle difference is 16.11° between naphthalene and fluorene, and 8.57° between carbazole and naphthalene. The naphthalene fold angle is 121.86° whilst the fluorene angle is 105.75° and the carbazole is 113.38° (**Table 7**, Entry 20). The *peri*-like scaffolds sulfur atom plane-aromatic plane angle is much sharper meaning the scaffolds are actively folding back on themselves further than the naphthalene system.

The N-C bonds in carbazole trisulfide-2-oxide **302** are smaller than the corresponding C-C in fluorene **297**. The C9-C8a and C9-C9a distances in fluorene **301** are 1.498(8) Å and 1.501(6) Å respectively. N1-C8a and N1-C9a distances are 1.401(3) Å and 1.404(2) Å respectively. The effects of the C vs N atom affect several other bond angles, bond lengths and distances between atoms. For example, C4...C5 distances and C1...C8 distances are shorter for the carbazole scaffold over the fluorene scaffold (**Table 7**, entry 16 and 17). Interestingly, even though the C4...C5 distance is shorter in carbazole over fluorene, S1...S3 is longer.

The *peri*-like scaffolds also show no significant twist in the S1-C4...C5-S2 torsion angle in comparison to the *peri*-scaffolds (**Table 7**, Entry 20). It was anticipated that the twist would be larger as the *peri*-like scaffolds are less ridged than the *peri*-scaffolds.

Trisulfide-2-oxides have been known to experience an “anomeric-like” effect. The central sulfinyl group, rather than being pseudo-equatorial to reduce the steric interactions, becomes

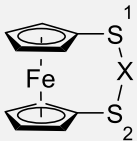
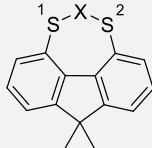
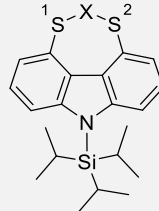
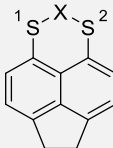
pseudo axial. This can be explained by the donation of the flanking sulfur atoms donating into the sulfinyl group's  $\sigma^*$  orbital (**Scheme 92**). This donation lowers the overall energy of the system.



**Scheme 92** Anomeric effect donation into the  $\sigma^*$  orbital in trisulfide-2-oxides.

The synthesis of the trisulfides of acenaphthene **319**, fluorene **309** and carbazole **329** gives a unique opportunity to explore the anomeric effect in trisulfide-2-oxides with a sterically locked aromatic backbone. If the anomeric effect is present, the S-S-O bond, in trisulfide-2-oxides should be shorter than the respective trisulfides, and the sulfinyl group should be pseudo-axial to accommodate the overlap and lower the energy of the system. The single crystal structures of carbazole, fluorene, acenaphthene, acenaphthylene and naphthalene show the sulfinyl group pointing in the pseudo-axial position. In the literature there are few examples of the crystal structures of both a trisulfide and trisulfide-2-oxide with the same functionality on the flanking sulfur atoms. One of which is ferrocenes **330** and **331**. The crystallographic data from the two ferrocene molecules give us another scaffold in which we can compare the bond lengths and angles.

**Table 8** A crystallographic comparison of trisulfides to trisulfide-2-oxides.

Entry	Scaffold	Ferrocene	Fluorene		Carbazole		Acenaphthene	
1	Structure and numbering							
2	Trisulfide or Trisulfide-2-oxide	<b>330</b> X = S <sup>179</sup>	<b>331</b> X = SO <sup>180</sup>	<b>309</b> X = S	<b>301</b> X = SO	<b>329</b> X = S (no TIPS)	<b>302</b> X = SO (with TIPS)	<b>319</b> X = S <b>299</b> X = SO
3	S1-S3 bond length / Å	2.050	2.118	2.0405(17) (molecule 1) 2.025(6) (molecule 2)	2.1087	2.0413	2.1101	2.0563    2.1218 (polymorph 1)
	S2-S3 bond length / Å	2.048	2.130	2.019(4) (molecule 1) 2.026(15) (molecule 2)	2.1245	2.0403	2.1011	2.0523    2.1218 (polymorph 1) 2.1218 2.1112 (polymorph 2)
4	Sulfur atom plane to aromatic plane angle / °	109.63	118.33	106.45(10) (molecule 1) 110.3(5) (molecule 2)	105.75(9)	106.19(5)	113.38(4)	119.28(3)    114.92(5) (polymorph 1) 119.29(3) (polymorph 2)

As seen from **Table 8** the S1-S3 and S2-S3 bond lengths increases throughout all the scaffolds from the trisulfides to the trisulfide-2-oxides. This goes against the hypothesis of a decreased S1-S3 and S2-S3 bond length in the trisulfide-2-oxides. Therefore, the increased bonding that is seen in the trisulfide-2-oxides has not been observed crystallographically. But the orientation on the sulfoxides all indicate that an anomeric effect is present. Freeman has previously reported that S-S bonds do get longer upon oxidation to the thiosulfinate. This would indicate our systems are experiencing similar effects.<sup>181</sup>

## 2.5 The controlled release of SO from trisulfide-2-oxides

The new trisulfide-2-oxides were all pyrolyzed in chlorobenzene (0.01 M) in the presence of 2,3-dimethyl-1,3-butadiene **18** (10 eq.); optimal conditions from previous group investigations.<sup>42,43</sup> Fluorene trisulfide-2-oxide **301** decomposed significantly quicker (3.5 h) than that of the reported decomposition time for naphthalene trisulfide-2-oxide **105** (10 h). Carbazole trisulfide-2-oxide **302** degraded faster again (3 h). Acenaphthene and acenaphthylene trisulfide-2-oxides **299** and **300** both degraded faster than naphthalene also (6 h and 3 h – respectively). Naphthalene trisulfide-2-oxide **105** appeared to be the most stable as it can withstand the pyrolysis for longer. This goes against the hypothesis of the acenaphthene and acenaphthylene trisulfide-2-oxides **299** and **300** being more stable due to the wider S1...S2 distances.

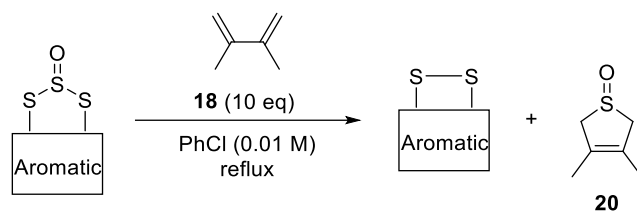
Naphthalene trisulfide-2-oxide **105** remained the best at the transfer of SO – both in terms of recovered disulfide and the resulting sulfoxide. Fluorene and carbazole both gave good yields of recovered disulfide (86% for both) and fast release of SO. However, the yield of sulfoxide **20** was significantly lower (fluorene trisulfide-2-oxide **301** release 32% and carbazole

trisulfide-2-oxide **302** release 58%). The sulfoxide yield from carbazole transfer is a moderate yield whilst the fluorene yield was poor. Acenaphthene and acenaphthylene both gave a poor recovery of the corresponding disulfide. Whilst acenaphthylene trisulfide-2-oxide **300** gives the most efficient transfer of SO out of the trisulfide-2-oxides studied in this work (65%), due to having such a poor yield of recovered disulfide, it is not recommended as a transfer reagent because of its difficult and low yielding synthesis. Acenaphthene trisulfide-2-oxide **299** transferred SO poorly to the diene (14%).

The poor recovery of disulfides from acenaphthene and acenaphthylene could be due to SO reacting with the resulting disulfides (which would explain the poor yields as of the acenaphthene SO transfer). This could be *via* hydrogen abstraction or reacting with the alkene.

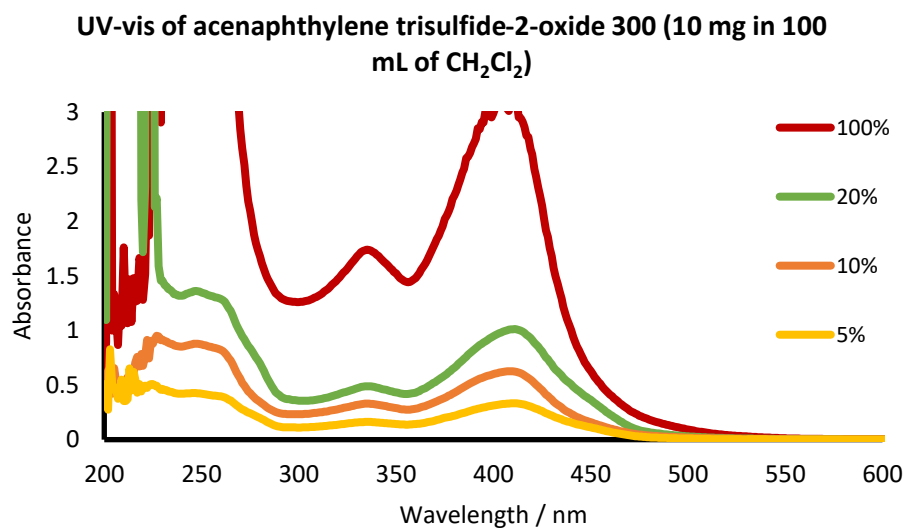
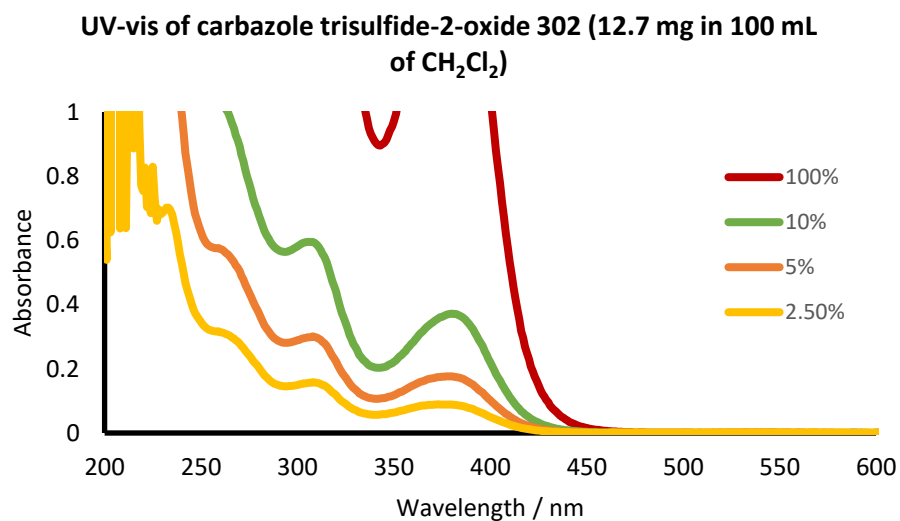
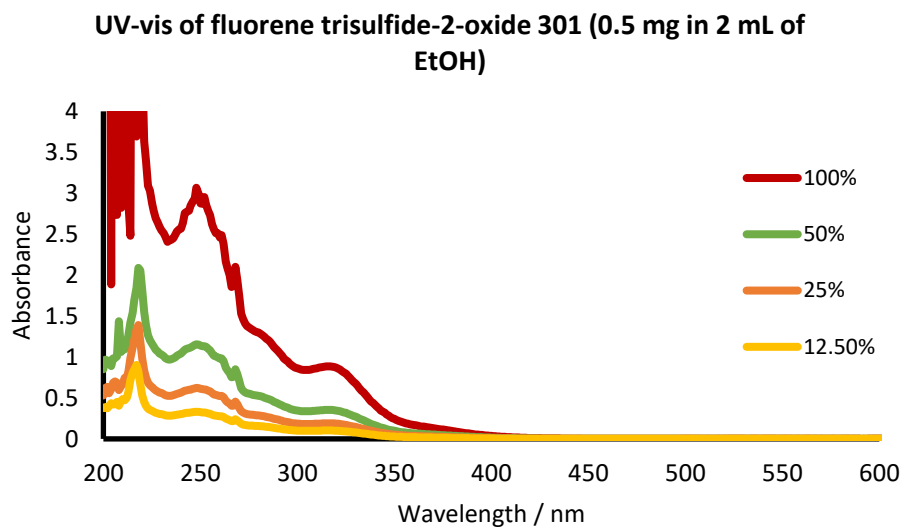


**Table 9** The thermal release of SO from trisulfides-2-oxides **105**, **295**, **296**, **297**, and **298** and the yields of disulfides **107**, **262**, **260**, **294**, and **291** and sulfoxide **20**.



Trisulfide-2-oxide	Time / h	Disulfide % yield	Sulfoxide <b>20</b> % yield
Naphthalene <b>105</b>	10	<b>107</b> 99	98
Acenaphthene <b>299</b>	6	<b>266</b> 39	14
Acenaphthylene <b>300</b>	3	<b>264</b> 16	65
Fluorene <b>301</b>	4	<b>300</b> 86	32
Carbazole <b>302</b>	3	<b>295</b> 86	58

Grainger *et al.* also demonstrated that naphthalene trisulfide-2-oxide **105** releases SO in the presence of light. Therefore, the novel trisulfide-2-oxides could also release SO photochemically. The UV-Vis spectra of fluorene trisulfide-2-oxide **301**, carbazole trisulfide-2-oxide **302** and acenaphthylene trisulfide-2-oxide **300** were measured. Each of the spectra show very different absorption patterns with distinct peaks. Fluorene trisulfide-2-oxide **301** has absorption peaks at 252, 269, and 322 nm. Interestingly, going from fluorene to carbazole trisulfide-2-oxide **302**, greatly changes the absorption peaks. Carbazole trisulfide-2-oxide **302** absorbs at 265, 312, and 384 nm. This could be due to the nitrogen playing a role in the aromaticity of the system. Finally, the acenaphthylene trisulfide-2-oxide **300** shows several absorption maxima too. Acenaphthylene trisulfide-2-oxide **300** absorbs at 253, 341, and 420 nm. The peak at 420 nm follows the classic absorption for an acenaphthylene double bond and the formation of the bis-radical.

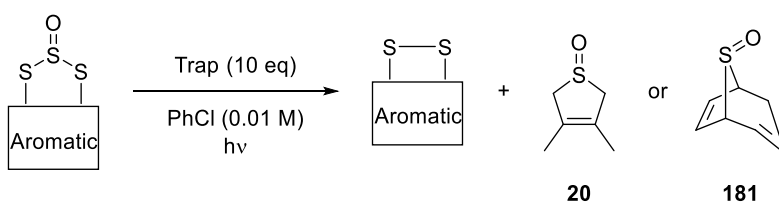


In the presence of light, fluorene trisulfide-2-oxide **301** was unstable. Therefore, to determine whether fluorene trisulfide-2-oxide **301** released SO photochemically, it was irradiated in the presence of 2,3-dimethyl-1,3-butadiene **18** (10 eq). The reaction was irradiated with a 400 W medium pressure mercury lamp in chlorobenzene (0.01 M) and decomposition to the disulfide **298** was observed with excellent recovery (90%), but no resulting sulfoxide **20** was identified by  $^1\text{H}$  NMR (**Table 10**). A sun lamp is a type of lamp which emits a broad spectrum of light similar to that of the sun. When a sun lamp was used, the trisulfide-2-oxide **301** decomposed and SO was successfully trapped in a 6% yield (sulfoxide **20**) – however this is much lower than naphthalene which yielded 55% sulfoxide **20**.<sup>43</sup> Fluorene trisulfide-2-oxide **297** was photolysed in PhCl in the presence of cycloheptatriene **35** in a semi-micro photochemical reactor at 254 nm. No cyclic sulfoxide **181** was detected by mass spec and IR (SO stretch).

Carbazole trisulfide-2-oxide **302** absorbs light at  $\lambda_{\text{max}} = 384$  nm and 312 nm. Irradiation of carbazole trisulfide-2-oxide **302** using a sun lamp in the presence of 2,3-dimethyl-1,3-butadiene **18** yielded the desired sulfoxide **20** in a 23% yield. This indicated that carbazole **302** allowed for a SO release pathway *via* irradiation. The reaction was set up again but in the presence of cycloheptatriene **35** (10 eq). The reaction yielded bridged sulfoxide **181** – but not cleanly. Mass spectrometry indicated the correct mass for the sulfoxide and IR confirmed there to be a sulfoxide peak (**Table 10**).

Therefore, carbazole trisulfide-2-oxide **302** appears to be the 3<sup>rd</sup> compound in the literature to yield singlet SO, and the 2<sup>nd</sup> to prove it experimentally. Due to the difficulty in synthesising the acenaphthylene trisulfide-2-oxide **300**, the photochemical release of SO was not performed.

**Table 10** The photochemical release of SO from trisulfide-2-oxides **105**, **301** and **302** and the yields of the corresponding disulfides **107**, **301**, and **302** and sulfoxide **20**.



Trisulfide-2-oxide	Time / h	Light source	Trap	Disulfide % yield	Sulfoxide yield	%
Naphthalene <b>105</b> <sup>43</sup>	3	Sun lamp	2,3-dimethyl-1,3-butadiene <b>18</b>	<b>107</b> 93	<b>20</b> 55	
Fluorene <b>301</b>	4	Sun lamp	2,3-dimethyl-1,3-butadiene <b>18</b>	<b>298</b> 90	<b>20</b> 6	
Fluorene <b>301</b>	4	254 nm	Cycloheptatriene <b>35</b>	<b>298</b> Identified by MS	-	
Carbazole <b>302</b>	1.5	Sun lamp	2,3-dimethyl-1,3-butadiene <b>18</b>	<b>295</b> 92	<b>20</b> 23	
Carbazole <b>302</b>	1.5	Sun lamp	Cycloheptatriene <b>35</b>	<b>295</b> 45	<b>181</b> Isolated but not clean	

## 2.6 Conclusions and future work

In conclusion, two novel disulfides, fluorene disulfide and carbazole disulfide have been synthesised in moderate yields (~50%). A new methodology has been displayed to access the 4,5-positions of carbazole. Also produced are the novel trisulfides, fluorene trisulfide **309**, carbazole trisulfide **329**, acenaphthene trisulfide **319**, and acenaphthylene trisulfide **320**. A new methodology to install sulfur atoms to the *peri*-positions of acenaphthene has been described (thanks to the work of Dr Ian A. Pocock). This new methodology increases the yields of previous methods by double (to 51%). The previously difficult-to-synthesise acenaphthene disulfide **262** and acenaphthylene disulfide **264** are now significantly less challenging.

Four novel trisulfide-2-oxides have also been synthesised – fluorene trisulfide-2-oxide **297** (37%), carbazole trisulfide-2-oxide **302** (54%), acenaphthene trisulfide-2-oxide **299** (59%), and acenaphthylene trisulfide-2-oxide **300** (55%). Acenaphthene trisulfide-2-oxide **299** and acenaphthylene trisulfide-2-oxide **300** are synthesised *via* a new methodology. SO(im)<sub>2</sub> is displayed the best yields for the synthesis. Fluorene trisulfide-2-oxide **301** and carbazole trisulfide-2-oxide **302** are both synthesised *via* previous literature conditions described by Grainger *et al.*

Each of the new trisulfide-2-oxides were evaluated as potential SO transfer reagents. None of the trisulfide-2-oxides performed as well as the previous naphthalene trisulfide-2-oxide **105** when subject to pyrolysis. Carbazole trisulfide-2-oxide **302** and fluorene trisulfide-2-oxide **301** displayed excellent recovery of disulfide (86% and 86%, respectively). However, significantly less sulfoxide **20** was isolated than the previous naphthalene trisulfide-2-oxide **105** (32% and

58%, respectively). Both acenaphthene trisulfide-2-oxide **299** and acenaphthylene trisulfide-2-oxide **300** gave poor disulfide recovery (39% and 16%, respectively). This included the poor yields of sulfoxide **20** (14% and 65%, respectively).

Grainger *et al.* displayed that naphthalene trisulfide-2-oxide **105** undergoes release of SO under photochemical conditions. Therefore, a UV-vis spectra of fluorene trisulfide-2-oxide **301**, carbazole trisulfide-2-oxide **302**, and acenaphthylene trisulfide-2-oxide **300** was taken. This gave an indication of which wavelength of light was required to irradiate the trisulfide-2-oxides. Photochemical release of fluorene trisulfide-2-oxide **301** displayed only a 6% yield of the sulfoxide **20**, but a 90% recovery of the disulfide **298**. Carbazole trisulfide-2-oxide **302** displayed a good recovery of disulfide **295** (92%) and a 23% yield of the desired sulfoxide **20**. Both fluorene trisulfide-2-oxide **301** and carbazole trisulfide-2-oxide **302** were irradiated in the presence of cycloheptatriene **35** to determine the state of the SO being released. For fluorene trisulfide-2-oxide **301** no cycloheptatriene dimer **36** was observed or, bridged sulfoxide **181**. However, carbazole trisulfide-2-oxide **302** yielded bridged sulfoxide **181**. This has been detected by mass spectrometry, IR and  $^1\text{H}$  NMR. However, the isolation of the compound was not clean. This does indicate, that carbazole trisulfide-2-oxide **302** may be the 3<sup>rd</sup> compound to release singlet SO, and the second to prove it using cycloheptatriene **35** as the trap.

In the future, carbazole trisulfide-2-oxide **302** needs to be irradiated in the presence of cycloheptatriene to gain a better understanding of the reactivity of the system. If the reaction was probed in a react IR instrument the IR peaks for the trisulfide-2-oxide **302**, SO, and sulfoxide **20** would be observed. This experiment may also give an indication to the proposed

chelotropic release of SO *via* dithione **304**. Acenaphthylene trisulfide-2-oxide would also need to be examined photochemically for the release of singlet SO.



*Chapter 3:* The design, synthesis, and application of carbon monochalcogenide reagents (CO and CS).

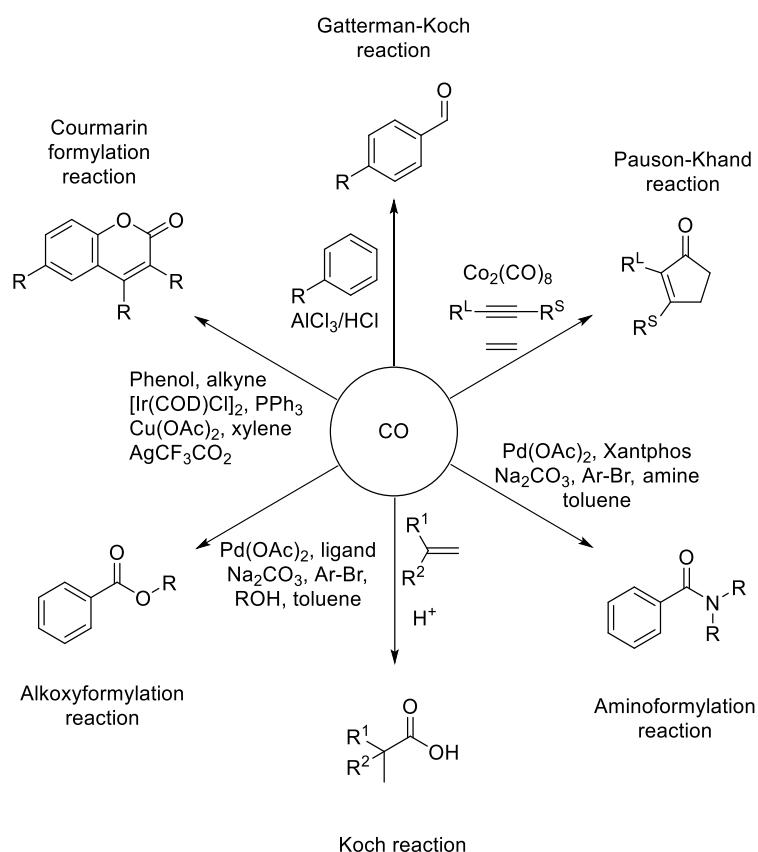
### 3 Carbon monochalcogenides

#### 3.1 Carbon monoxide

##### 3.1.1 Introduction to Carbon monoxide

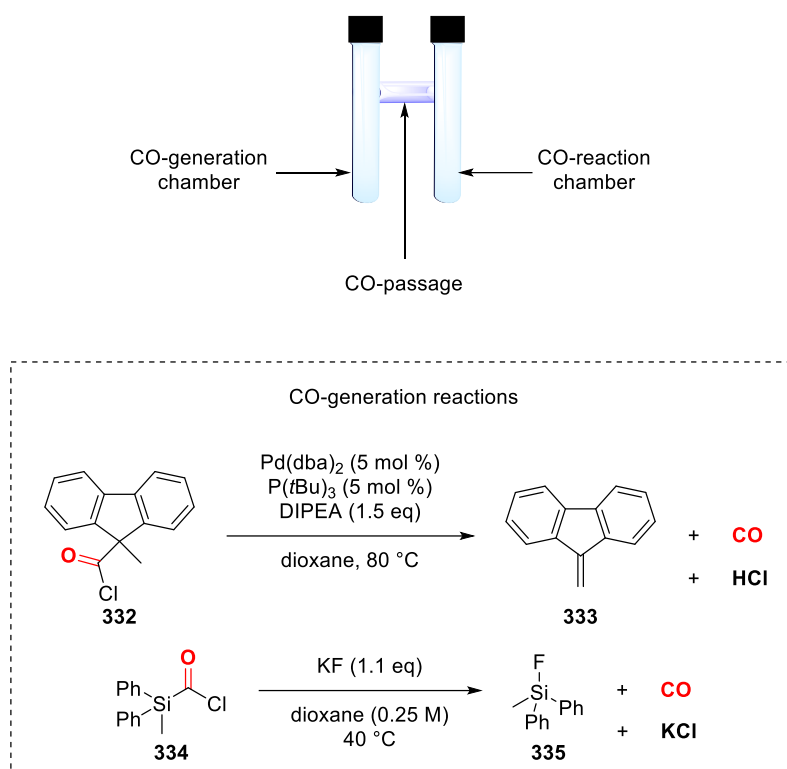
Carbon monoxide (CO) is a highly polarised reactive diatomic molecule. Its properties are well known and have been studied for centuries. In large doses it can cause poisoning and death by binding to haemoglobin, displacing oxygen. CO is colourless and has no smell. There are very few symptoms and therefore can be difficult to diagnose.<sup>182,183</sup>

CO has been used as a synthon in organic chemistry for a little over a century. A wide variety of reactions have been developed to install ketones, eneones, esters, amides, aldehydes and many more (**Scheme 93**).<sup>184–186</sup>



**Scheme 93** A representative summary of a variety of different reactions of CO to form various products.<sup>186–196</sup>

In more recent years there has been a drive to producing CO *in situ*, to avoid the use of a highly pressurised CO atmosphere (30 – 50 bar).<sup>197,198</sup> This will remove the potential for a CO gas leak which could harm or kill the experimentalist. The first report of an equimolar CO reaction was reported by Skrydstrup and co-workers in 2011.<sup>199,200</sup> These reagents are solid, stable at room temperature, easy to synthesise and now, commercially available. They are COgen **332** and silaCOgen **334** (Scheme 92).<sup>199</sup> The aim outlined by Skrydstrup and co-workers is to develop an *ex situ* CO reagent which could deliver an equimolar amount of CO to a second reaction. The CO would be released by a chemical reaction in one chamber which would in turn transfer into another chamber (Scheme 94).



**Scheme 94** Current methods to generate CO *in situ* and the designer glassware to facilitate the reaction.

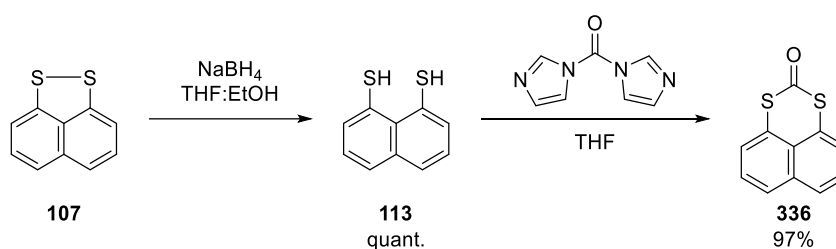
CO is an important biomolecule.<sup>182,201,202</sup> As mentioned before, CO is toxic due to the strong affinity of CO to bind to iron, including haemoglobin (245 times more than  $\text{O}_2$ ). However, it is naturally occurring in the body and has been proven to be a signalling molecule in the body. Haem is oxidised by haem oxygenase to give biliverdin,  $\text{Fe}^{2+}$  and CO.<sup>183,201,203–205</sup> CO has several uses in the body; notably as a signalling molecule, a neuroprotector against ROS in the brain, and as a muscle relaxant in the heart. It has been suggested that CO could be used in specific circumstances as a therapeutic in the body – and therefore there has been a drive to find biologically safe carbon monoxide release molecules (CORMs).

However, there are several challenges with CORMs that need to be overcome in order for them to be used in a pharmacological setting:

1. Both the CORM and the CORM products both need to be biologically compatible and have a method of excretion out of the body.
2. They need to be triggerable i.e. something must trigger the CO release once in the body (e.g. light, pH, heat, an enzyme).
3. They need to be bench stable and soluble in water.

Synthetically, it is also important that they are easily accessible and achievable in high yield in an analytically pure sample.

Building on the previous group work of SO release from trisulfide-2-oxides, it was proposed that CO could also be produced using *peri*-substituted disulfides. Naphthalene dithiocarbonate **332** has been previously synthesised by Ogura and co-workers to investigate the properties of binaphthol[1,8-d,e]-1,3-dithiin-2-ylidene as an electron donor. This provides a synthetic route to the desired precursor. Naphthalene disulfide was reduced to the corresponding dithiol which was subsequently reacted with 1,1'-carbonyldiimidazole (CDI) to yield naphthalene dithiocarbonate **336** (Scheme 95).<sup>105,114</sup>



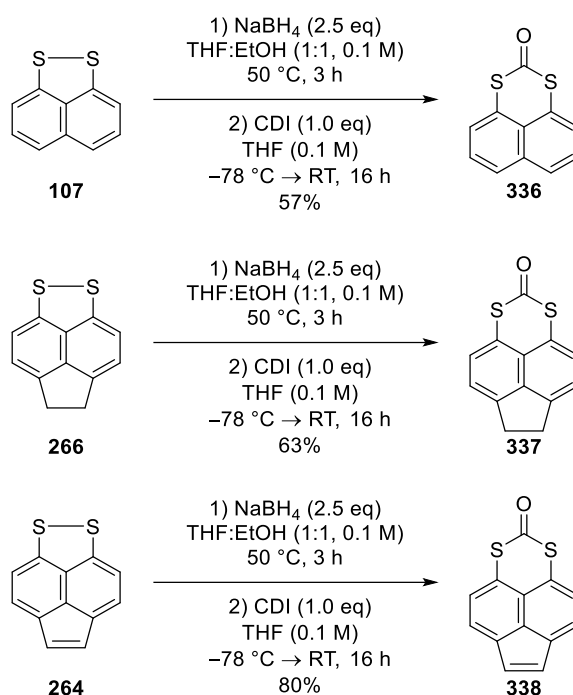
***Scheme 95** Ogura and co-workers work into the synthesis of naphthalene dithiocarbonate **336**.*

The aim of the present work is to synthesise a *peri*-dithiocarbonate that can release CO under triggerable conditions – most likely light due to the naphthalene chromophore. Once the

project progresses, the aim will be to be able to functionalise the core to make the system more soluble and easily to excrete from the body. This project is a fundamental principle idea, an investigation into whether CO can be released from a dithiocarbonate. If so, then a more biologically compatible compound could be pursued.

### 3.1.2 Synthesis of the dithiocarbonates

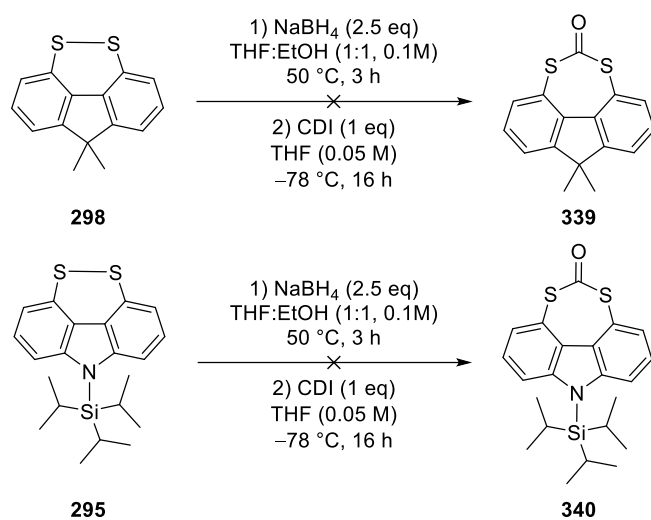
In the 1980s, Fumio Ogura and co-workers were working on synthesising new electron donor compounds.<sup>114,206</sup> The molecule they were attempting to synthesise was completed *via* accessing dithiocarbonate **336**. Taking naphthalene disulfide **107** they reduced it to the dithiol **113**. Dithiocarbonate **336** was synthesised by reacting dithiol **113** with CDI – insertion of the carbonyl group in between the sulfur atoms released 2 equivalents of imidazole. Taking inspiration from the work of Ogura (**Scheme 96**) we attempted the reaction; however, unlike, Ogura *et al.* a glove box was not used. Therefore, disulfide **107** was reduced to the dithiol **113** and the crude reaction mixture was reacted with CDI. The addition was carried out at –78 °C instead of –20 °C as it was easier to maintain the temperature.



**Scheme 96** Synthesis of the *peri*-substituted dithiocarbonates.<sup>114,206</sup>

The *peri*-substituted scaffold's dithiocarbonates were accessed first. Naphthalene dithiocarbonate **336**, acenaphthene dithiocarbonate **337**, and acenaphthylene dithiocarbonate **338** were all prepared in good yields (**Scheme 96**). The latter two had not previously been synthesised due to the difficulty accessing the scaffolds. The increase in yields from naphthalene to acenaphthene to acenaphthylene could be due to the thiols being more stable as the distance increases.

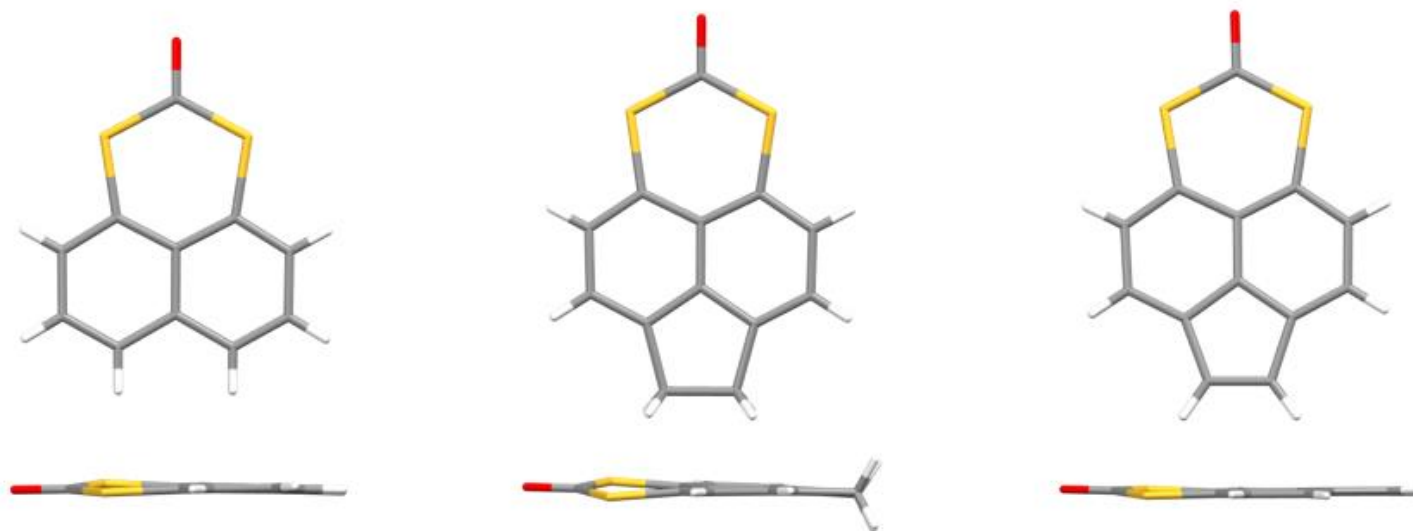
Synthesis of fluorene dithiocarbonate **339** and carbazole dithiocarbonate **340** were also attempted, but the reactions did not yield the desired product, but returned starting material. This may be due to the size of the CDI and therefore not being able to have the thiols access the carbonyl (**Scheme 97**).



**Scheme 97** Attempted synthesis of fluorene dithiocarbonate **339** and carbazole dithiocarbonate **340**.

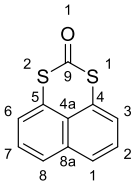
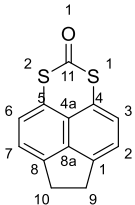
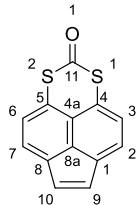
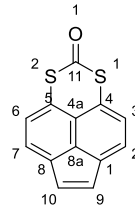


### 3.1.3 Dithiocarbonate structural analysis



**Figure 18** The structures of the dithiocarbonates obtained by X-ray diffraction at 100 K with Cu K $\alpha$  ( $\lambda = 1.54184$ ) as the radiation source – all structures were grown by slow solvent evaporation. Left – naphthalene dithiocarbonate **336**; Centre – dithiocarbonate **337**; Right – acenaphthylene dithiocarbonate **338**.

**Table 11** The structures of the dithiocarbonates obtained by X-ray diffraction at 100 K with Cu K $\alpha$  ( $\lambda = 1.54184$ ) as the radiation source – all structures were grown by slow solvent evaporation. Crystallographic data for dithiocarbonates **336**, **337** and **338**.

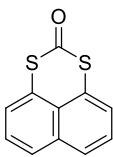
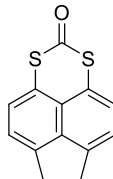
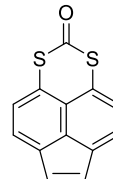
Entry	Scaffold	Naphthalene dithiocarbonate <b>336</b>	Acenaphthene dithiocarbonate <b>337</b>	Acenaphthylene dithiocarbonate <b>338</b>	
				A	B
<b>1</b>	Structure and numbering				
<b>2</b>	Carbon bridge	C <sub>11</sub> H <sub>6</sub> OS <sub>2</sub> -	C <sub>13</sub> H <sub>8</sub> OS <sub>2</sub> CH <sub>2</sub> CH <sub>2</sub>	C <sub>13</sub> H <sub>6</sub> OS <sub>2</sub> CH=CH	C <sub>13</sub> H <sub>6</sub> OS <sub>2</sub> CH=CH
<b>3</b>	C9-C10 length / Å	2.44603(5)	1.558(2)	1.372(14)	1.370(15)
<b>4</b>	S1...S2 distance / Å	3.0803(10)	3.1023(5)	3.113(3)	3.108(3)
<b>5</b>	S-C(O)-S Bond angle / °	123.75(15)	124.82(9)	125.1(5)	124.6(5)
<b>6</b>	S1-C4-C4a Bond angle / °	126.2(2)	124.32(11)	125.3(6)	123.5(7)
<b>7</b>	S2-C5-C4a Bond angle / °	126.15(19)	124.21(11)	125.2(7)	123.2(7)
<b>8</b>	C4-C4a-C5 bond angle / °	125.3(2)	128.68(13)	127.8(8)	130.5(8)
<b>9</b>	S1-C(O) bond length / Å	1.743(3)	1.7514(17)	1.735(10)	1.770(10)
<b>10</b>	S2-C(O) bond length / Å	1.750(3)	1.7489(17)	1.774(12)	1.740(10)
<b>11</b>	C1...C8 distance / Å	2.457(4)	2.340(2)	2.332(13)	2.328(16)

<b>12</b>	C4...C5 distance / Å	2.534(4)	2.560(2)	2.550(13)	2.584(14)
<b>13</b>	C1-C8a-C8 bond angle / °	120.2(2)	112.10(12)	110.2(8)	111.1(8)
<b>14</b>	Splay angle / °	17.64	17.22	18.3	17
<b>15</b>	S1-C4...C5-S2 torsion angle / °	4.72(13)	7.72(7)	3.7(4)	-1.2(4)
<b>16</b>	C=O bond length / Å	1.217(3)	1.2157(19)	1.222(10)	1.219(12)
<b>17</b>	S1-C=O bond angle / °	118.5(2)	117.63(13)	118.9(8)	117.9(8)
<b>18</b>	S2-C=O bond angle / °	117.7(2)	117.55(13)	116.1(7)	117.5(8)

The dithiocarbonates of three *peri*-substituted scaffolds were synthesised. As previously described for the corresponding dibromide, (section 2.4.1) the decreasing length of the carbon bridge has the associated effect of widening the opposite L-region. The C9-C10 bond length on acenaphthene dithiocarbonate is 1.558(2) Å whilst for acenaphthylene it is 1.372(14) Å on both molecules in the unit cell (**Table 11**, Entry 3). The naphthalene system has a C1...C8 distance of 2.457(4) Å, acenaphthene has a C1...C8 distance of 2.340(2) Å and acenaphthylene (two molecules in the unit cell) has a C1...C8 distance of 2.332(13)/2.328(16) Å (**Table 11**, Entry 11). This shows the gradual decrease in the C1...C8 distance with respect to the carbon bridge. The dithiocarbonate *peri*-positions (C4...C5 distance) are expected to have the greatest distance for acenaphthylene and the smallest in naphthalene – but this is not the case. The C4...C5 distance for naphthalene is 2.534(4) Å, acenaphthene is 2.560(2) Å and acenaphthylene is 2.550(13)/2.584(14) Å (**Table 11**, Entry 12). Clearly there is a large increase in the distance from naphthalene to acenaphthene, but in acenaphthylene there are two molecules in the unit cell. The C4...C5 distances are different, and one is larger, and the other is smaller than acenaphthene. The carbon bridge pinching effect influences the S1...S2 distances – 3.0803(10) Å, 3.1023(5) Å and 3.113(3)/3.108(3) Å for naphthalene, acenaphthene and acenaphthylene, respectively (**Table 11**, Entry 4). Whilst the trend is followed, it is not a large difference from the acenaphthene to acenaphthylene. However, the final reflection of the difference the carbon bridge makes can be seen in the angle S1-C(O)-S2 angle. Once again going from naphthalene to acenaphthene and acenaphthylene the angle changes from 123.75(15) °, 124.82(9) ° and 125.1(5)/124.6(5) °, respectively (**Table 11**, Entry 5).

The dithiocarbonate functionality was also investigated using IR and <sup>13</sup>C NMR spectroscopy. As the C9-C10 bond length gets shorter, and therefore the S1...S3 distance gets longer the wavenumber of the C=O stretch decreases and the <sup>13</sup>C NMR ppm also decreases

(Figure 19). This can be attributed to the decreased strain in the system from naphthalene dithiocarbonate **336**, to acenaphthene dithiocarbonate **337**, to acenaphthylene dithiocarbonate **338**. As with lactams and amides, as strain is released the IR peak decreases in shift. E.g. 4-membered lactams ( $1745\text{ cm}^{-1}$ ) > 5-membered lactams ( $1700\text{ cm}^{-1}$ ) > tertiary amides ( $1650\text{ cm}^{-1}$ ). The differences observed between dithiocarbonates **336**, **337**, and **338** are minimal and a further study into these compounds would be required to fully understand them.

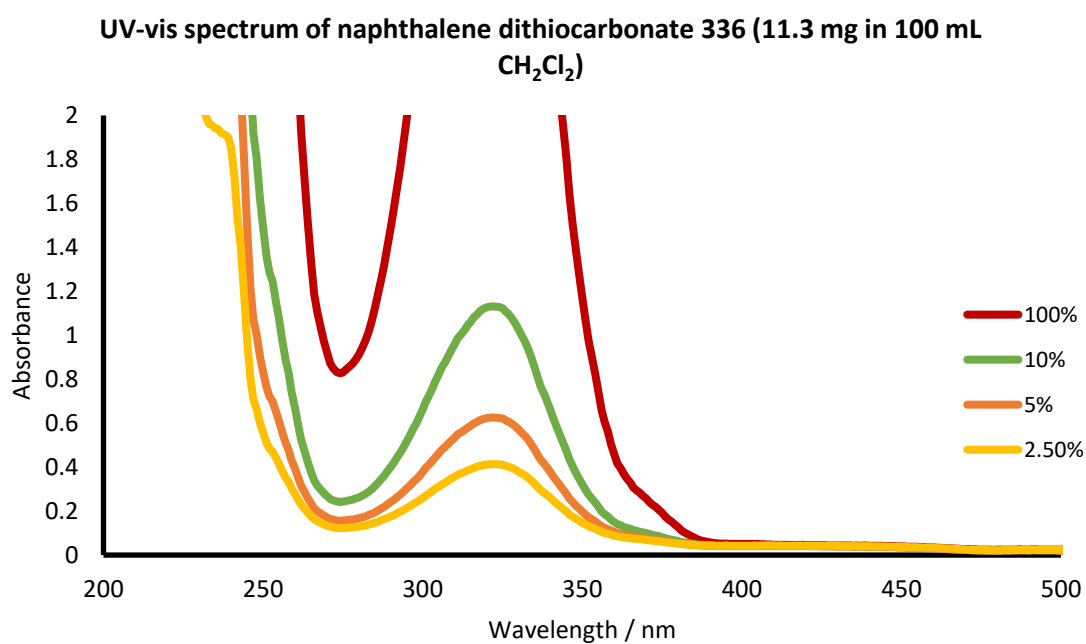
			
	<b>336</b>	<b>337</b>	<b>338</b>
C=O IR Shift / $\text{cm}^{-1}$	1623	1619	1615
C=O $^{13}\text{C}$ NMR Shift / ppm	185.2	184.9	182.8

**Figure 19** Comparison of the C=O IR shifts and  $^{13}\text{C}$  NMR shifts of naphthalene dithiocarbonate **336**, acenaphthene dithiocarbonate **337**, and acenaphthylene dithiocarbonate **338**.

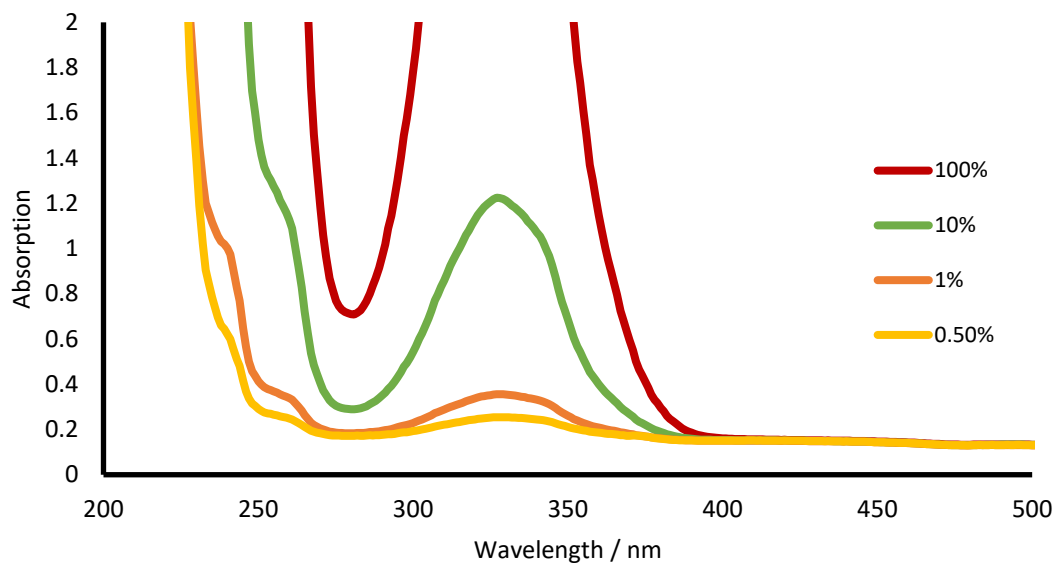
#### 3.1.4 The controlled release of CO from dithiocarbonates

Carbon monoxide has not previously been released from a *peri*-substituted system. Inspiration from previous group work for the release of SO was taken and applied to CO. Thermolysis of acenaphthylene dithiocarbonate **338** was attempted in chlorobenzene at reflux ( $132\text{ }^{\circ}\text{C}$ ). After 24 hours of reflux only decomposition to black powder was observed. Due to the unsuccessful thermolysis of acenaphthylene dithiocarbonate a different CO release trigger was required. Previous group work displayed that trisulfide-2-oxides undergo photolysis. Therefore, a UV-vis spectrum of naphthalene dithiocarbonate **336**, acenaphthene

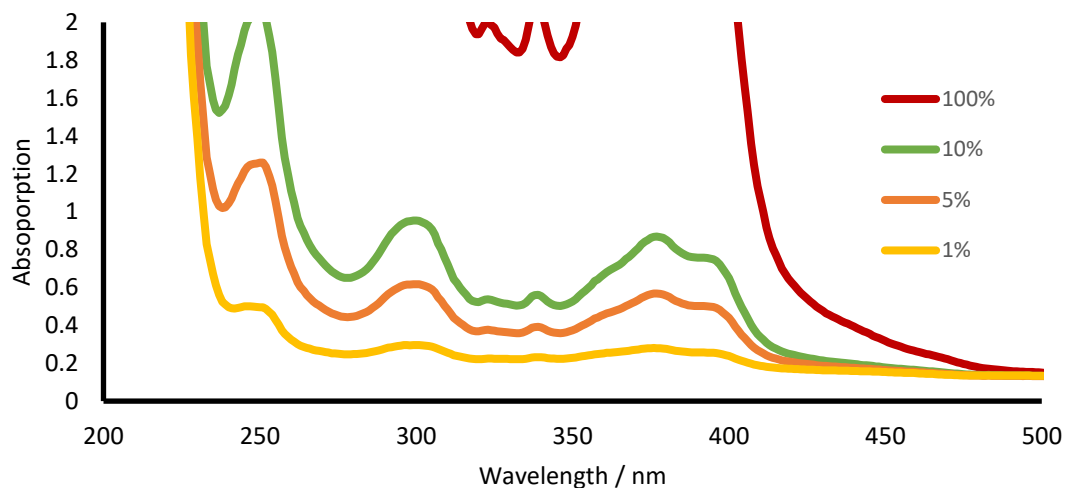
dithiocarbonate **337**, and acenaphthylene dithiocarbonate **338** was obtained. The UV-vis spectrum of naphthalene dithiocarbonate **336** indicated irradiation at ~325 nm was required. The UV-vis spectrum of acenaphthene dithiocarbonate **337** indicated irradiation at ~330 nm was required. Finally, the UV-vis spectrum of acenaphthylene dithiocarbonate **338** indicated irradiation at ~250 nm, ~300 nm, ~340 nm and ~380-400 nm was required.



UV-vis spectrum of acenaphthene dithiocarbonate **337** (10.6 mg in 100 mL of CH<sub>2</sub>Cl<sub>2</sub>)

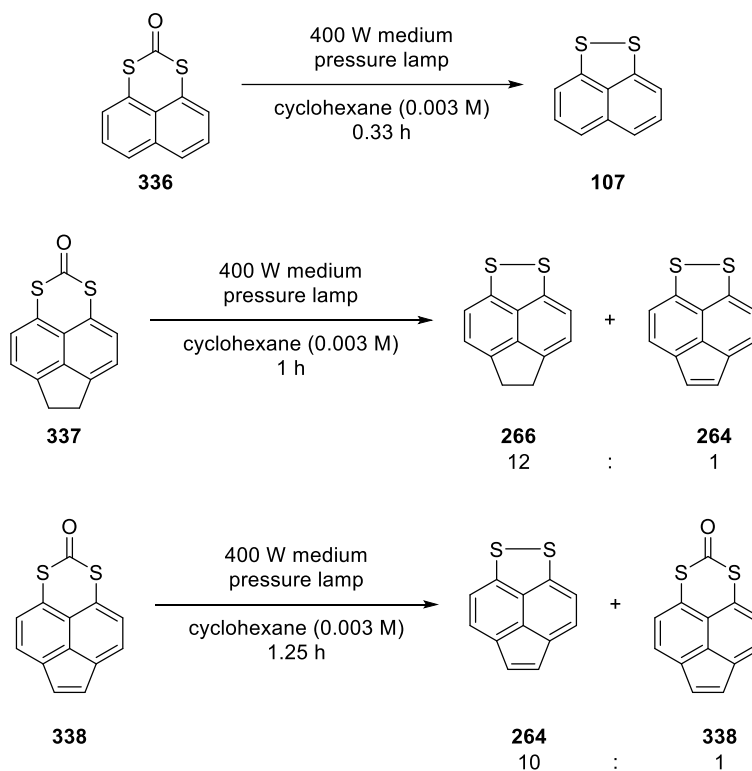


UV-vis spectrum of acenaphthylene dithiocarbonate **338** (10.2 mg in 100 mL of CH<sub>2</sub>Cl<sub>2</sub>)



Irradiation of acenaphthylene dithiocarbonate **338** in cyclohexane (0.003 M) using a 125 W medium pressure mercury lamp was attempted. After 1.25 h a 10:1 ratio of acenaphthylene disulfide to acenaphthylene dithiocarbonate (<sup>1</sup>H NMR ratios) was observed. Identical experiments were performed on acenaphthene dithiocarbonate **337** and naphthalene

dithiocarbonate **336**. This yielded a 12:1 ratio of acenaphthene to acenaphthylene disulfide (for the acenaphthene dithiocarbonate), respectively in 1 hour. It also gave the full conversion of naphthalene dithiocarbonate to naphthalene disulfide in 20 minutes (**Scheme 98**).



**Scheme 98** Irradiation of naphthalene dithiocarbonate **336**, acenaphthene dithiocarbonate **337**, and acenaphthylene dithiocarbonate **338** to the respective disulfides.

In this case, the acenaphthylene dithiocarbonate **338** releases CO at the slowest rate whilst naphthalene dithiocarbonate **337** is the fastest. This is in line with the hypothesis that the naphthalene dithiocarbonate **336** is more strained in the dithiocarbonate region and the acenaphthylene dithiocarbonate **338** is the least.



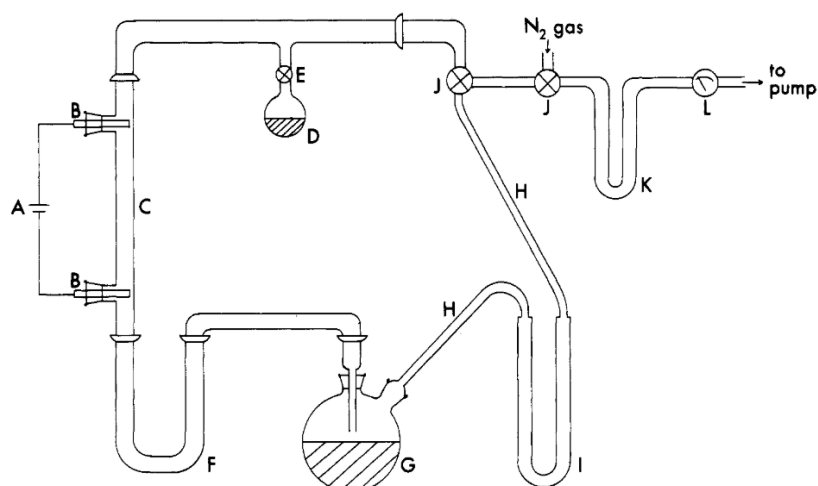
## 3.2 Carbon monosulfide

### 3.2.1 Introduction to carbon monosulfide

Carbon monosulfide (CS) has been known in the literature since 1911.<sup>207,208</sup> It was first generated via electrical discharge through a matrix of CS<sub>2</sub>. It is highly reactive with both itself and oxygen. CS reacts with itself to form a carbon/sulfur polymer and in the presence of O<sub>2</sub> it forms SCO.<sup>209,210</sup> This makes it extremely difficult to characterise and use as a reagent in synthesis.

Over the last few decades, characterisation of CS has determined the vibrational levels, rotational levels, the electronic, the mass, and even the dipole moment, despite the reactive nature of CS.<sup>7,211–213</sup>

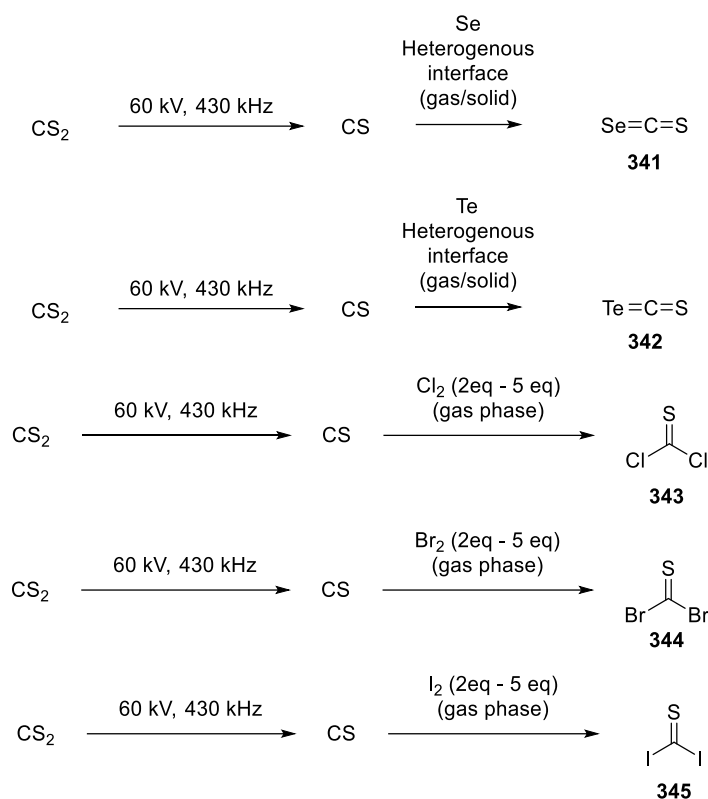
Despite advances in technology, CS is still generated by an energy intensive and dangerous method. It is produced by vaporising carbon disulfide (CS<sub>2</sub>, a toxic substance) by vacuum distillation into a discharge chamber.<sup>211,214</sup> In the discharge chamber is a pair of electrodes which then allows for an electrical discharge (**Figure 20**). The discharge causes the CS<sub>2</sub> to fission producing CS and sulfur. The conversion of CS<sub>2</sub> to CS is poor (~70% conversion to CS). Therefore, there is a synthetic need to produce CS in a safe, reliable manner that will allow it to be a useful reagent.



**Figure 1.** Key: A, power supply; B, brass electrodes; C, discharge tube; D, CS<sub>2</sub> container; E, needle valve; F, metal cold trap; G, reaction flask; H, rubber vacuum tubes; I, metal cold trap; J, three-way valves; K, glass cold trap; L, vacuum gauge.

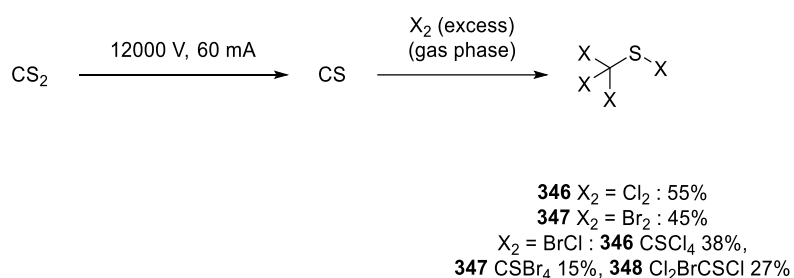
**Figure 20** Figure of the synthesis of CS gas via electrolysis.<sup>215</sup>

The use of CS in synthesis has been explored to make some very unusual structures. The carbene nature of CS makes it ideal as an insertion molecule into weak bonds. For example, the first purposeful reaction of CS was its reaction with Se, Te and dihalogens to form mixed carbon dichalcogens and thiocarbonyl halides by Steudel in 1966 (**Scheme 99**).<sup>216</sup>



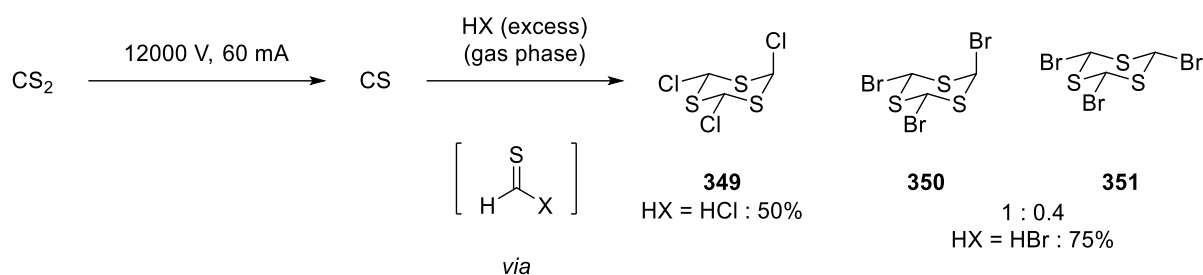
**Scheme 99** First known reactivity of CS with Se, Te, I<sub>2</sub>, Br<sub>2</sub> and Cl<sub>2</sub>.<sup>216,217</sup>

Following Stuedel's work, Klabunde and co-workers investigated the reactivity of CS with other halogen-related compounds. In the presence of excess halogens (X<sub>2</sub>) trihalomethane sulfenylhalides were formed in moderate yields (**Scheme 100**). Reactions with iodine suffered from poor solubility and poor stability.



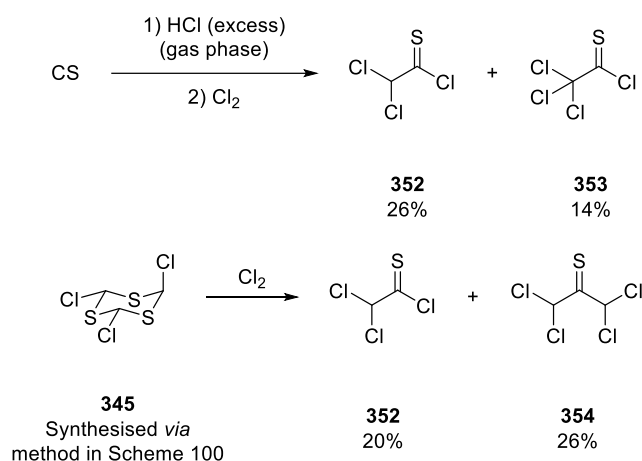
**Scheme 100** Reactivity of CS in the presence of excess halogens.

Klabunde and co-workers also reacted CS with HBr and HCl in an attempt to form thioformyl halides. However, upon warming the thioformyl halides produced 1,3,5-trithianes **349**, **350**, and **351** (**Scheme 101**).<sup>218</sup> HCl only gives selectively the *trans*-isomer, whilst HBr gives the *trans*- and *cis*-isomers in a 1 : 0.4 ratio (by <sup>1</sup>H NMR).



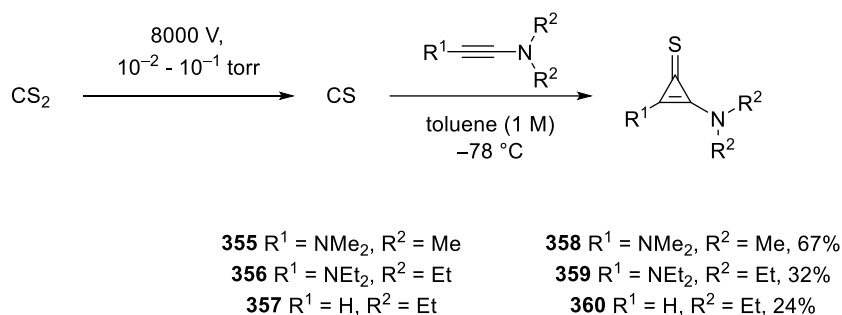
**Scheme 101** Reactivity of CS with excess hydrogen halide acids.

HCSCl was also reacted with chlorine to yield thioacylchlorides **352** in a 26% yield and **353** in a 14% yield (**Scheme 102**). Reaction of 2,4,6-trichloro-1,3,5-trithiane **349** with chlorine yielded thioacylchloride **352** in 20% yield and thione **354** in 26% yield (**Scheme 102**).



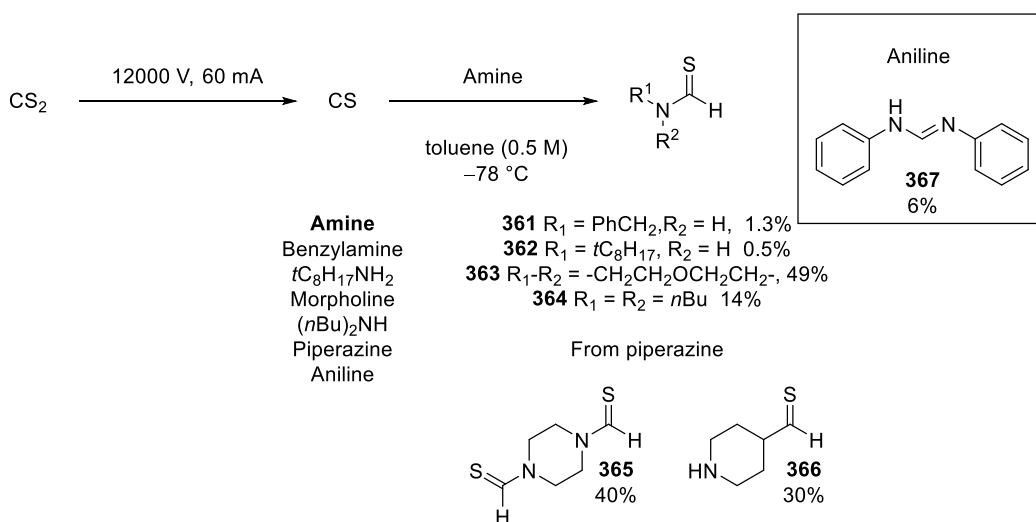
**Scheme 102** Reactivity of CS with excess HCl then reacting with Cl<sub>2</sub>.

The organic chemistry of CS was investigated by Krebs and co-workers in 1984.<sup>215</sup> Due to CS being a carbene, it undergoes [1+2] cycloadditions with ynamines and ynediamines to form bis(dialkylamino)cyclopropenethiones. An electrical discharge (8000V) was applied to a discharge tube containing CS<sub>2</sub> at a pressure of 10<sup>-2</sup> - 10<sup>-1</sup> torr. The gas was then passed over a 1 M solution of the alkyne in toluene at -78 °C (**Scheme 103**).



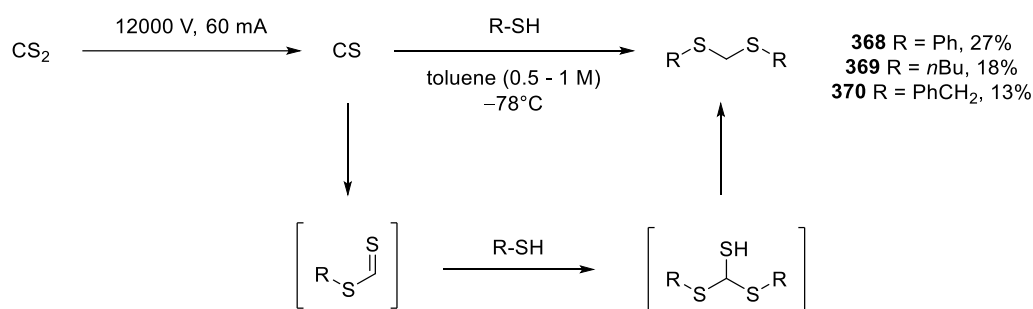
**Scheme 103** Reactivity of CS with ynamines to form cyclopropenethiones.

Senning and co-workers observed the reactivity of CS towards primary and secondary amines and thiols. The CS acts as a carbene and inserts into the weak N-H or S-H bond. When reacted with an amine a thioformamide is formed. Aniline, however, is an exception. Reaction of CS with aniline yields formamidine **367** (**Scheme 104**).<sup>218</sup>



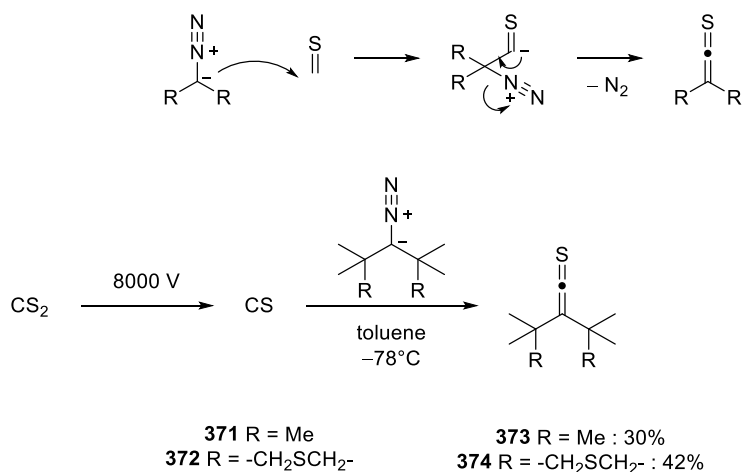
**Scheme 104** Reactivity of CS with amines to form thioformamides.

However, in the presence of a thiol, a thioacetal is formed. CS inserts into the S-H bond of a thiol to give a dithioformate. The dithioformate reacts with a second equivalent of thiol to yield a thiol, which degrades to thioacetals (**Scheme 105**).<sup>218</sup>



**Scheme 105** Reactivity of CS with thiols to form thioacetals.

Krebs and co-workers also explored the reactivity of CS with diazoalkanes.<sup>219</sup> They found that the reaction yields thioketenes. CS is an electrophile, and the proposed mechanism does not go *via* a carbene on either the CS or the diazoalkane (**Scheme 106**).

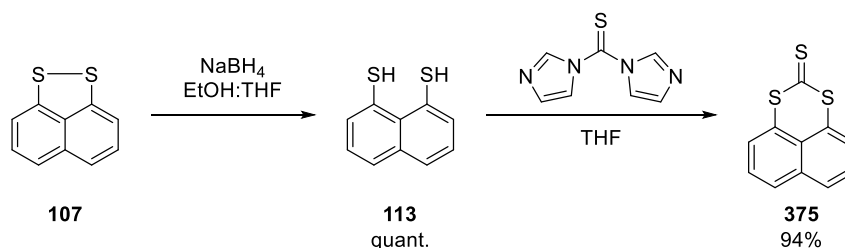


**Scheme 106** The reaction of diazoalkanes with CS to form thioketenes.

The known synthetic chemistry of CS is, therefore, relatively small in comparison to SO. Therefore, if a method is developed to generate CS then exploration of its reactivity can be explored further.

Therefore, the aim of this project is to identify whether a *peri*-substituted trithiocarbonate releases CS gas which can be trapped by a previously described method.

There are several objectives will help achieve the aim. Firstly, the synthesis of naphthalene trithiocarbonate from a modified procedure to that of Ogura *et al.* must be completed. In the same paper described to synthesise naphthalene dithiocarbonate **332** by Ogura *et al.* they synthesise naphthalene trithiocarbonate **375** (Scheme 107).

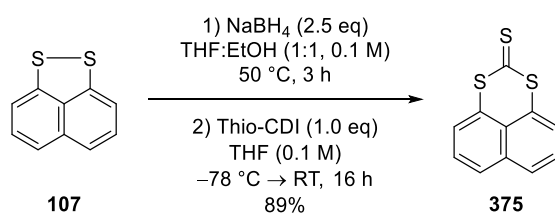


**Scheme 107** Ogura *et al.* synthesis of naphthalene trithiocarbonate **372**.

With naphthalene trithiocarbonate **375** in hand, a UV-vis spectrum will identify any peaks which need to be irradiated which may give a mechanism of CS release. Finally, if formal CS loss is observed, then a series of trapping experiments will be attempted to see if the trapping of CS from the naphthalene trithiocarbonate **375** is possible.

### 3.2.2 Synthesis of the trithiocarbonates

Analogous to the dithiocarbonates, trithiocarbonates can be synthesised using thiocarbonyl-1,1'-diimidazole (thio-CDI).<sup>114,206</sup> Firstly, naphthalene disulfide was successfully converted to naphthalene trithiocarbonate in excellent yield. This provided the opportunity to investigate a potential CS transfer reagent.

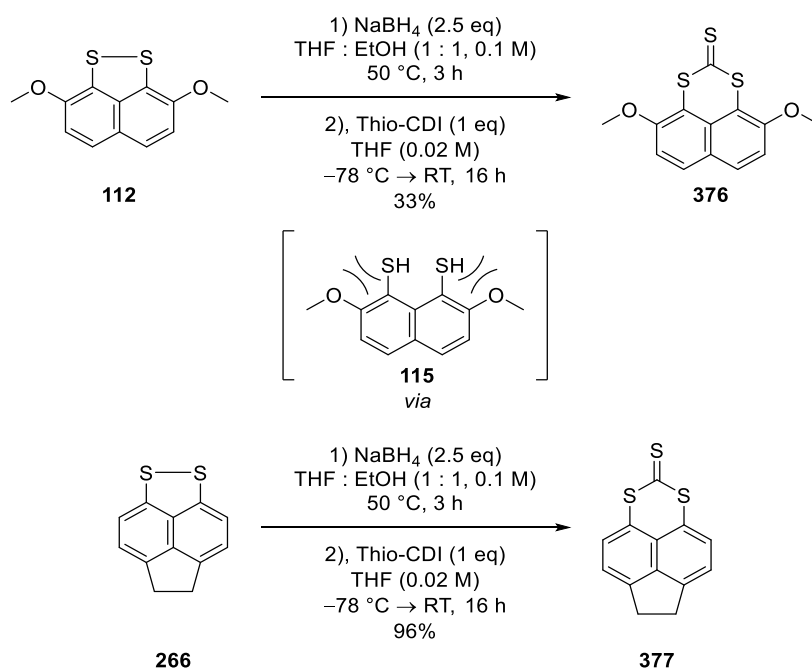


**Scheme 108** Synthesis of naphthalene trithiocarbonate **375**.<sup>114,206</sup>

To explore the effects of functionalising the naphthalene system, 2,7-dimethoxy-naphthalene trithiocarbonate **376** was also synthesised albeit in a lower yield. The methoxy groups increased steric bulk around the disulfide bond which make it less susceptible to reduction, using  $\text{NaBH}_4$ , to the dithiol **115**, required for the reaction with thiocarbonyl-1,1'-diimidazole. The methoxy groups also affects the proximity of the *peri*-thiols, potentially increasing the rate of oxidation to the disulfide (**Scheme 109**).

Acenaphthene trithiocarbonate **377** was also synthesised in excellent yield. This was completed in the same manner as the naphthalene trithiocarbonate **375** (**Scheme 109**). The synthesis of acenaphthylene trithiocarbonate was also attempted but was not isolated cleanly.

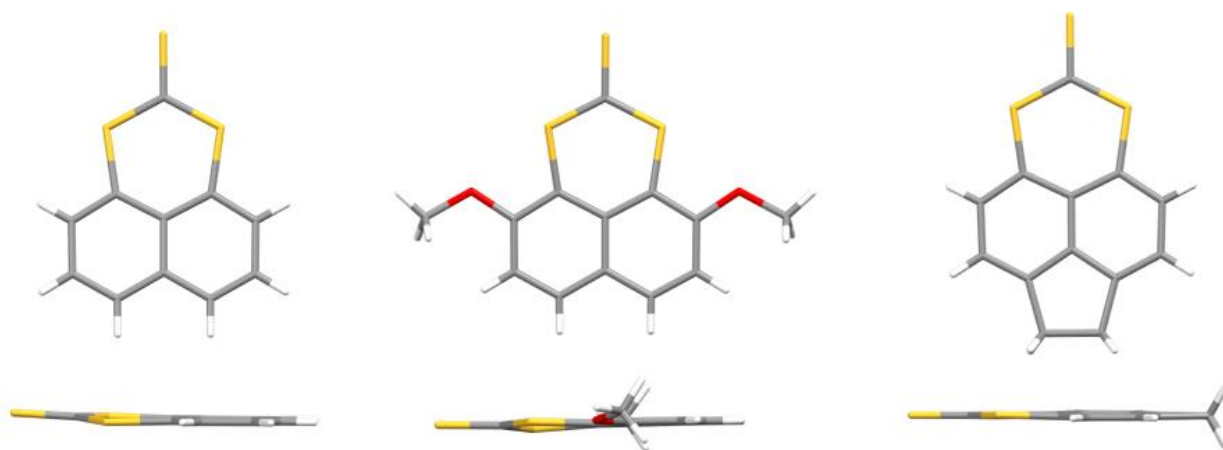




**Scheme 109** Synthesis of 2,7-dimethoxynaphthalene trithiocarbonate **376** and acenaphthene trithiocarbonate **377**.<sup>105,114</sup>

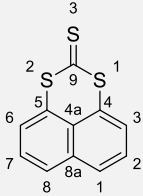
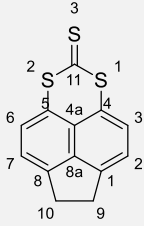
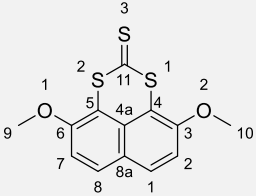
### 3.2.3 Trithiocarbonates structural analysis

The crystal structures for all the cleanly isolated trithiocarbonates were obtained.



**Figure 21** The structures of the trithiocarbonates obtained by X-ray diffraction at 100 K with Cu K $\alpha$  ( $\lambda = 1.54184$ ) as the radiation source – all structures were grown by slow solvent evaporation. Left - naphthalene trithiocarbonate **375**; Centre - 2,7-dimethoxynaphthalene trithiocarbonate **376**; Right - acenaphthene trithiocarbonate **377**.

**Table 12** The structures of the trithiocarbonates obtained by X-ray diffraction at 100 K with Cu K $\alpha$  ( $\lambda = 1.54184$ ) as the radiation source – all structures were grown by slow solvent evaporation. Crystal structure data for naphthalene trithiocarbonate **375**, acenaphthene trithiocarbonate **377** and 2,7-dimethoxynaphthalene trithiocarbonate **376**.

Entry	Scaffold	Naphthalene trithiocarbonate <b>375</b>	Acenaphthene trithiocarbonate <b>377</b>	2,7-dimethoxynaphthalene trithiocarbonate <b>376</b>
<b>1</b>	Structure and numbering			
		C <sub>11</sub> H <sub>6</sub> S <sub>3</sub>	C <sub>13</sub> H <sub>8</sub> S <sub>3</sub>	C <sub>13</sub> H <sub>10</sub> S <sub>3</sub> O <sub>2</sub>
<b>2</b>	Carbon bridge	H...H	CH <sub>2</sub> CH <sub>2</sub>	H...H
<b>3</b>	C9-C10 length / Å	2.45710(14)	1.562(5)	2.4400(2)
<b>4</b>	S1...S2 distance / Å	3.0369(8)	3.0615(12)	3.0582(8)
<b>5</b>	S-C(S)-S Bond angle / °	123.93(13)	125.5(2)	126.14(8)
<b>6</b>	S1-C4-C4a Bond angle / °	125.63(17)	123.6(2)	126.24(14)
<b>7</b>	S2-C5-C4a Bond angle / °	125.46(18)	123.6(2)	126.06(11)
<b>8</b>	C4-C4a-C5 bond angle / °	125.3(2)	128.9(3)	124.99(12)
<b>9</b>	S1-C(S) bond length / Å	1.715(2)	1.7215(17)	1.710(2)
<b>10</b>	S2-C(S) bond length / Å	1.725(3)	1.7215(17)	1.7201(19)
<b>11</b>	C4...C5 distance / Å	2.531(3)	2.566(5)	2.519(3)
<b>12</b>	C1...C8 distance / Å	2.464(3)	2.346(5)	2.457(3)
<b>13</b>	C1-C8a-C8 bond angle / °	120.5(2)	112.5(3)	120.78(13)
<b>14</b>	Splay angle / °	16.41(35)	16.17(00)	17.29(37)
<b>15</b>	S1-C4...C5-S2 torsion angle / °	2.78(11)	2.80(3)	5.43(10)
<b>16</b>	C=S bond length / Å	1.645(2)	1.652(4)	1.6518(14)
<b>17</b>	S1-C=S bond angle / °	118.38(14)	117.23(11)	117.16(10)

<b>18</b>	S2-C=S bond angle / °	117.66(13)	117.23(11)	116.70(12)
-----------	--------------------------	------------	------------	------------

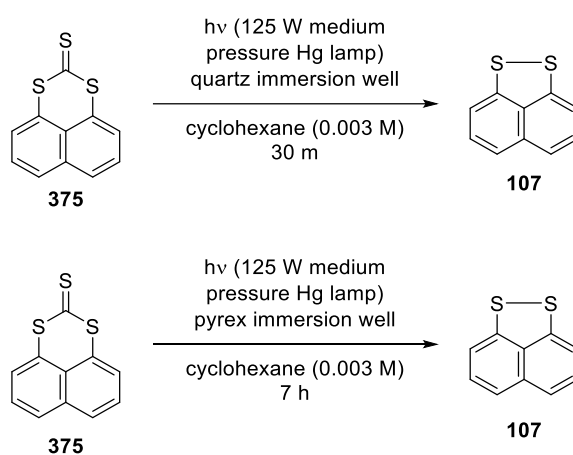
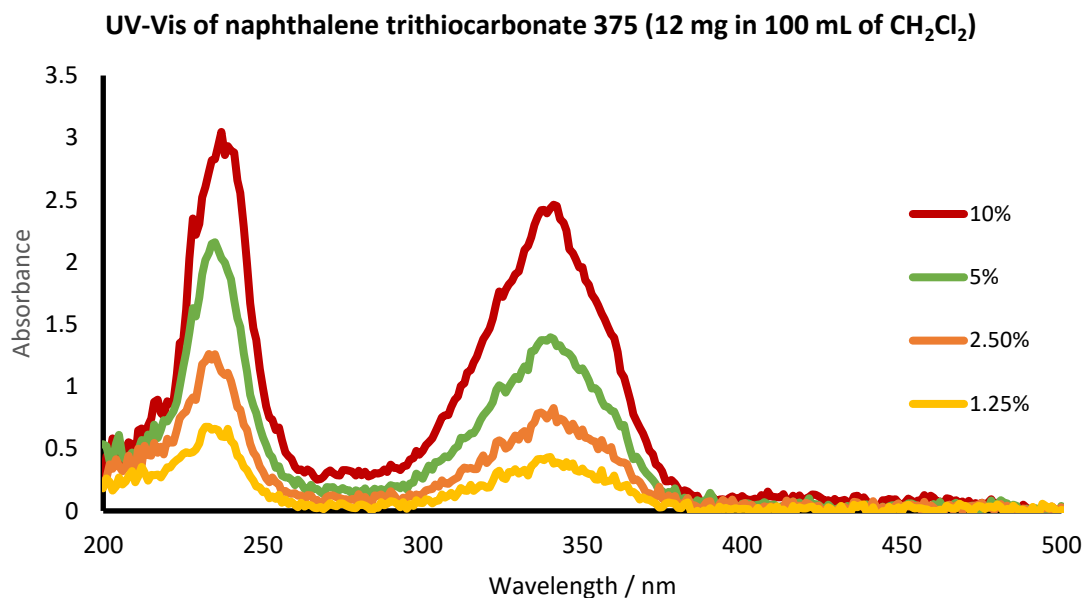
As with previous sections (section 2.4 and section 3.1.3), the insertion of the carbon bridge from naphthalene trithiocarbonate **376** to acenaphthene trithiocarbonate **377** causes the S1...S2 distance to slightly increase from 3.0369(8) Å to 3.0615(12) (Table 12, entry 4). This is also reflected in the slight increased S1-C(S) and S2-C(S) distances in acenaphthene trithiocarbonate **377**. The carbon bridge also effects the C1...C8 and C4...C5 distances of naphthalene trithiocarbonate **375** vs. acenaphthene trithiocarbonate **377**, 2.464(3) Å vs. 2.346(5) Å and 2.531(3) Å vs. 2.566(5) Å, respectively (Table 12, entries 11 and 12). As can be seen the C1...C8 distance decreases from naphthalene trithiocarbonate **375** to acenaphthene trithiocarbonate **377** and the C4...C5 distance increases, both of which are consistent with the “clothes peg” hypothesis (Section 2.4.1). What is interesting is the splay angle decreases from naphthalene to acenaphthene (16.41(35)° vs. 16.17(00)°) (Table 12, Entry 14). This is not expected especially, given the increased S1...S2 distance. However this can be explained by the torsion angles. The acenaphthene scaffold has a slightly larger naphthalene torsion (2.78(11)° vs. 2.80(3)°) (Table 12, Entry 15). This can therefore accommodate the increased S1...S2 distance and the decreased splay angle.

What is more interesting is the structural data of 2,7-dimethoxynaphthalene trithiocarbonate **373**. The S1...S2 distance (3.0582(8)) is larger than naphthalene trithiocarbonate **375** but just a little smaller than the acenaphthene trithiocarbonate **377** (Table 12, Entry 4). This is also reflected in the increased splay angle of the 2,7-dimethoxynaphthalene trithiocarbonate **376** (17.29(37)°) (Table 12, Entry 14). It could be hypothesised that the methoxy groups would push the S1...S2 atoms together, but the opposite is observed. The S1-C(S)-S2, S1-C4-C4a, and S2-C5-C4a angles are all larger in the 2,7-dimethoxynaphthalene trithiocarbonate **376** than both other trithiocarbonates. However, to accommodate these unusual increases, the 2,7-dimethoxynaphthalene trithiocarbonate **373** has an increased torsion angle (5.43(10)°) nearly

3 degrees larger than the other two scaffolds (**Table 12**, Entry 15). In fact, the methoxy groups do increase the strain of the system but not in the way the hypothesis outlines. The naphthalene torsion is significantly more which can accommodate the electrostatic repulsions from the O1/2 to the S1/2.

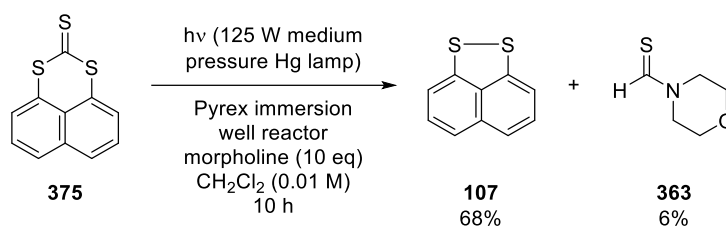
### 3.2.4 The controlled release of CS from trithiocarbonates

In contrast to the CO work (Section 3.1.4), a CS transfer reagent has never been reported – but it has been hypothesised to be a useful reagent for organic chemists. The initial idea was to see if CS was extruded from trithiocarbonates **375**, **376**, and **377**. Initially naphthalene trithiocarbonate **375** was heated in chlorobenzene at varying temperatures and the reaction was followed by TLC. The reaction was deemed to not occur thermally at 132 °C after no reaction was observed after 12 h. Therefore, photochemical release of CS was explored. The UV-vis spectrum of naphthalene trithiocarbonate was measured and the key absorption peak was found to be ~340 nm. As a preliminary result, a medium pressure mercury lamp was used to irradiate a solution of naphthalene trithiocarbonate in cyclohexane in a quartz immersion well reactor. TLC and then <sup>1</sup>H NMR, indicated the decomposition of the trithiocarbonate to the disulfide (**Scheme 110**). A brown solid was deposited on the outside of the photochemical immersion well, potentially CS polymer.<sup>220</sup> Interestingly naphthalene trithiocarbonate **375** degraded faster when irradiated with a quartz immersion well reactor vs. a Pyrex immersion well reactor. The 125 W medium pressure Hg lamp irradiates a broad range of wavelengths including 254 nm and 365 nm. The UV cut-off point for Pyrex is ~275 nm whilst quartz is below 200 nm. Therefore, the choice of immersion well reactor allowed for tailored irradiation. In the quartz reactor (irradiating at 254 nm and above) the reaction had gone to completion after 30 minutes. However, in a Pyrex reactor (~275 nm and above) the reaction took 7 h (**Scheme 110**). There could be an alternative degradation pathway at 254 nm vs. 365 nm.



**Scheme 110** Photochemical decomposition naphthalene trithiocarbonate **375** to naphthalene disulfide **107**.

The addition of morpholine (10 eq) produced no brown solid, unlike previous reactions without morpholine. <sup>1</sup>H NMR of the reaction mixture indicated the formation of thioformamide **363**. After column chromatography, naphthalene disulfide **107** was recovered in a 68% yield and thioformamide **363** was isolated in a 6% yield (**Scheme 111**).



**Scheme 111** Photochemical degradation of naphthalene trithiocarbonate with morpholine to naphthalene disulfide **107** and thioformamide **363**.

The targeted irradiation of the 340 nm peak was achieved by using LEDs. Photochemistry has moved towards using LEDs in the last 20 years due to the ability to selectively irradiate one wavelength, the reduced the power consumption (photochemical immersion well reactors are very energy intensive) and safety concerns (photochemical immersion well reactors emit harmful UV radiation across the full UV spectrum).

The initial irradiation took place in a 0.003 M solution in cyclohexane. Due to the poor solubility in cyclohexane,  $\text{CH}_2\text{Cl}_2$  was used instead.  $\text{CH}_2\text{Cl}_2$  was used as the reaction solvent to generate the thioformamide **363** (0.01 M concentration). A quick solvent screen of naphthalene trithiocarbonate **372** found that the best solubilities were in THF (0.02 M; 0.01 M was also trialled),  $\text{CH}_2\text{Cl}_2$  (0.01 M), DMF (0.01 M), PhCl (0.01 M), PhF (0.01 M) and toluene (0.01 M). These became the solvents to test the release of CS (for full details on the solubility study see the experimental).

Naphthalene trithiocarbonate was irradiated using a LED tape set up where a glass bowl was wrapped in foil and the lights. The lights were bought from *Downlights Direct*. The wavelength of irradiation is 365 nm. Even though the wavelength of irradiation is not 340 nm, the tail of the absorption peak was irradiated and therefore the same mechanism should occur.

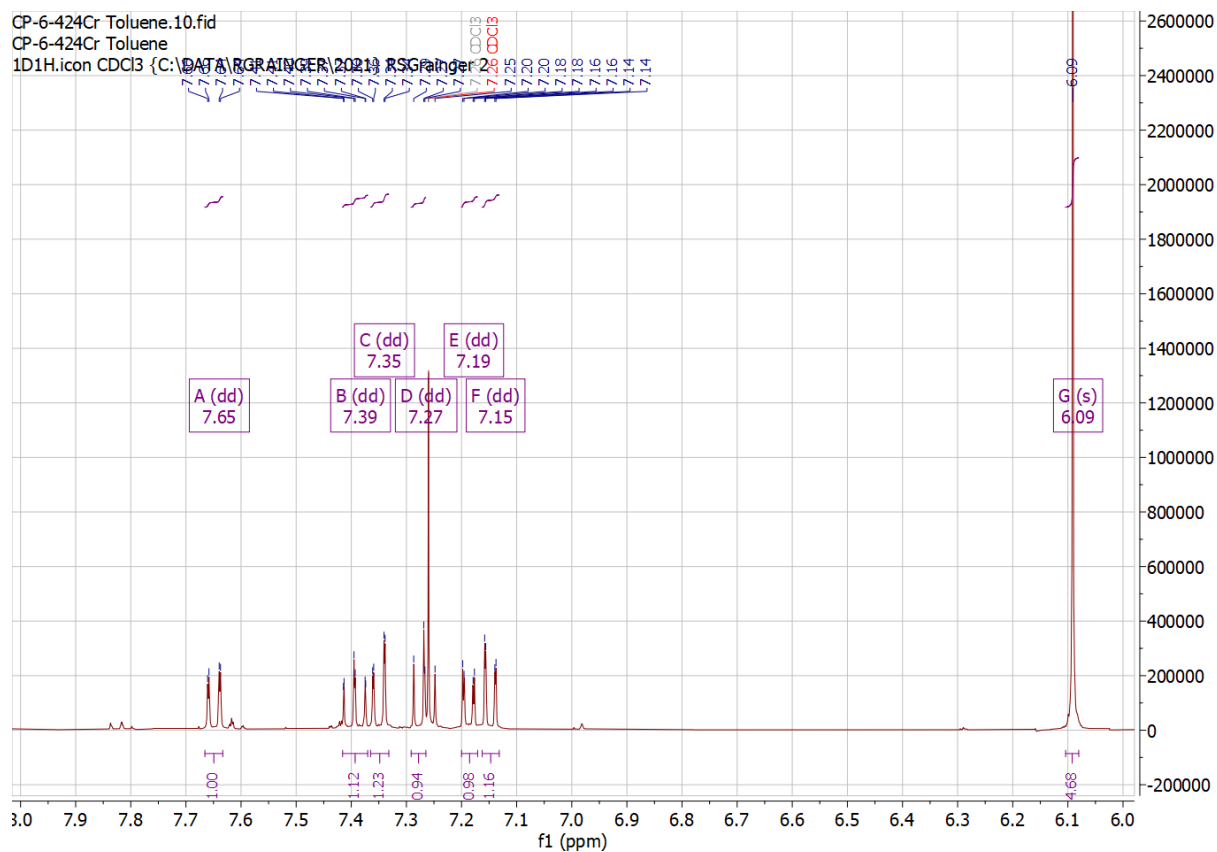
All the screening reactions were performed at a 0.01 M concentration in a solvent of choice, 10 equivalents of morpholine were added, wavelength of light was 365 nm, the distance



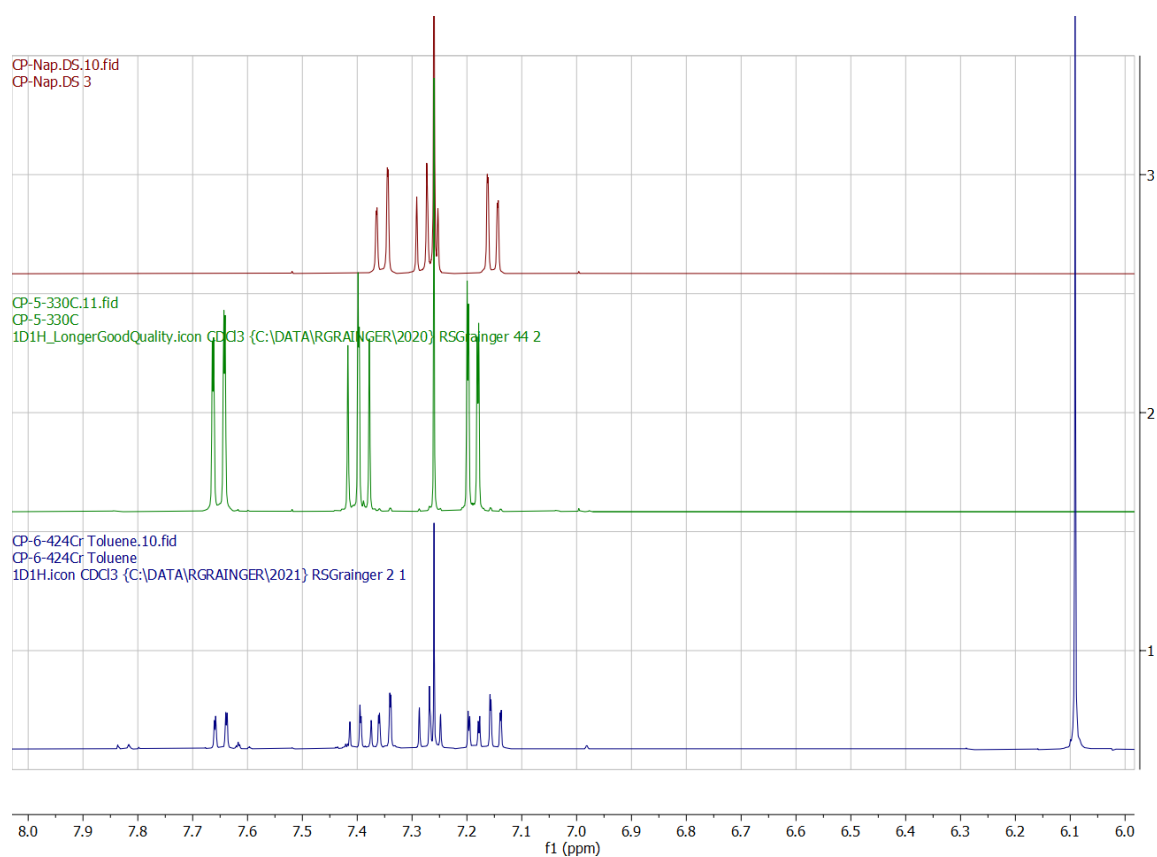
between the light source and the reaction vessel was 1 cm, all reaction were irradiated for 3 hours, and all reactions were deoxygenated for 5 minutes prior to the reaction using a stream of argon.

Once the 3-hour reaction time had finished, 17 mg of 1,3,5-trimethoxybenzene (1 eq) was added to each sample and concentrated under reduced.  $^1\text{H}$  NMR was then used to assess the yield of the reaction using the 1,3,5-trimethoxybenzene as an internal standard. In each case the desired thioformamide **363** was produced in trace amounts.

Each sample was analysed by  $^1\text{H}$  NMR and the corresponding peaks were used to determine the integration – trithiocarbonate **375** (7.19 ppm – dd), disulfide **107** (7.15 ppm – dd), thioformamide **363** (9.27 ppm – singlet), 1,3,5-trimethoxybenzene (6.09 ppm – s). All integrations and yields are with respect to an integration of 1 for the thioformamide **363** peak.



**Figure 22** Zoomed-in  $^1\text{H}$  NMR of the aromatic region (8.0 ppm - 6.0 ppm) for the decomposition of naphthalene trithiocarbonate **375** to naphthalene disulfide **107**.



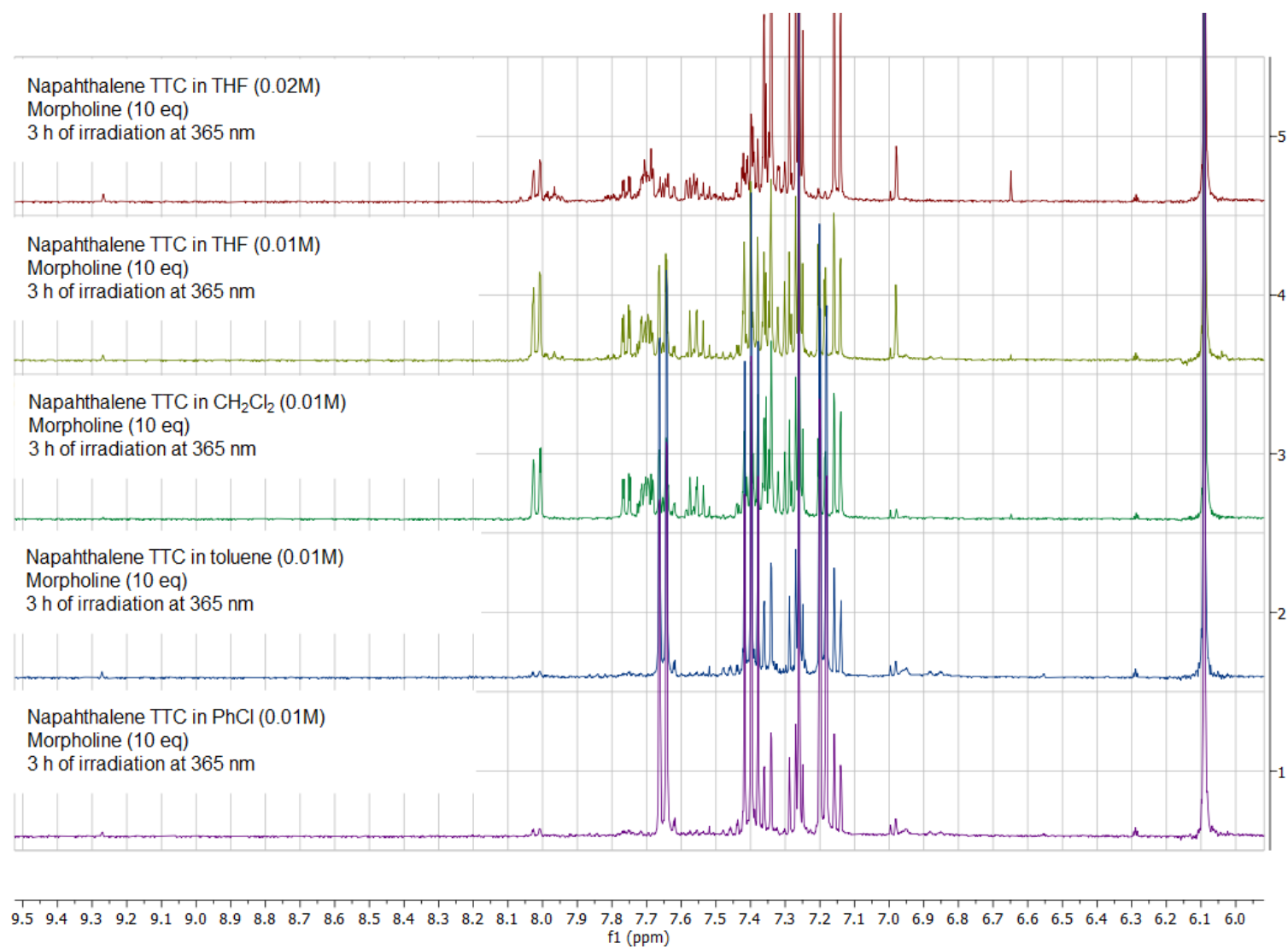
**Figure 23** Zoomed in  $^1\text{H}$  NMR of the aromatic region for the decomposition of naphthalene trithiocarbonate **375** to naphthalene disulfide **107**. Top)  $^1\text{H}$  NMR of pure naphthalene disulfide **107**. Middle)  $^1\text{H}$  NMR of pure naphthalene trithiocarbonate **375**. Bottom) Crude reaction mixture containing both.

**Table 13** Table of conditions and  $^1\text{H}$  NMR integrations and yields of the products with respect to trimethoxybenzene. TA – thioformamide **363**, TTC – trithiocarbonate **375**, DS – disulfide **107**, and TMB – trimethoxybenzene.

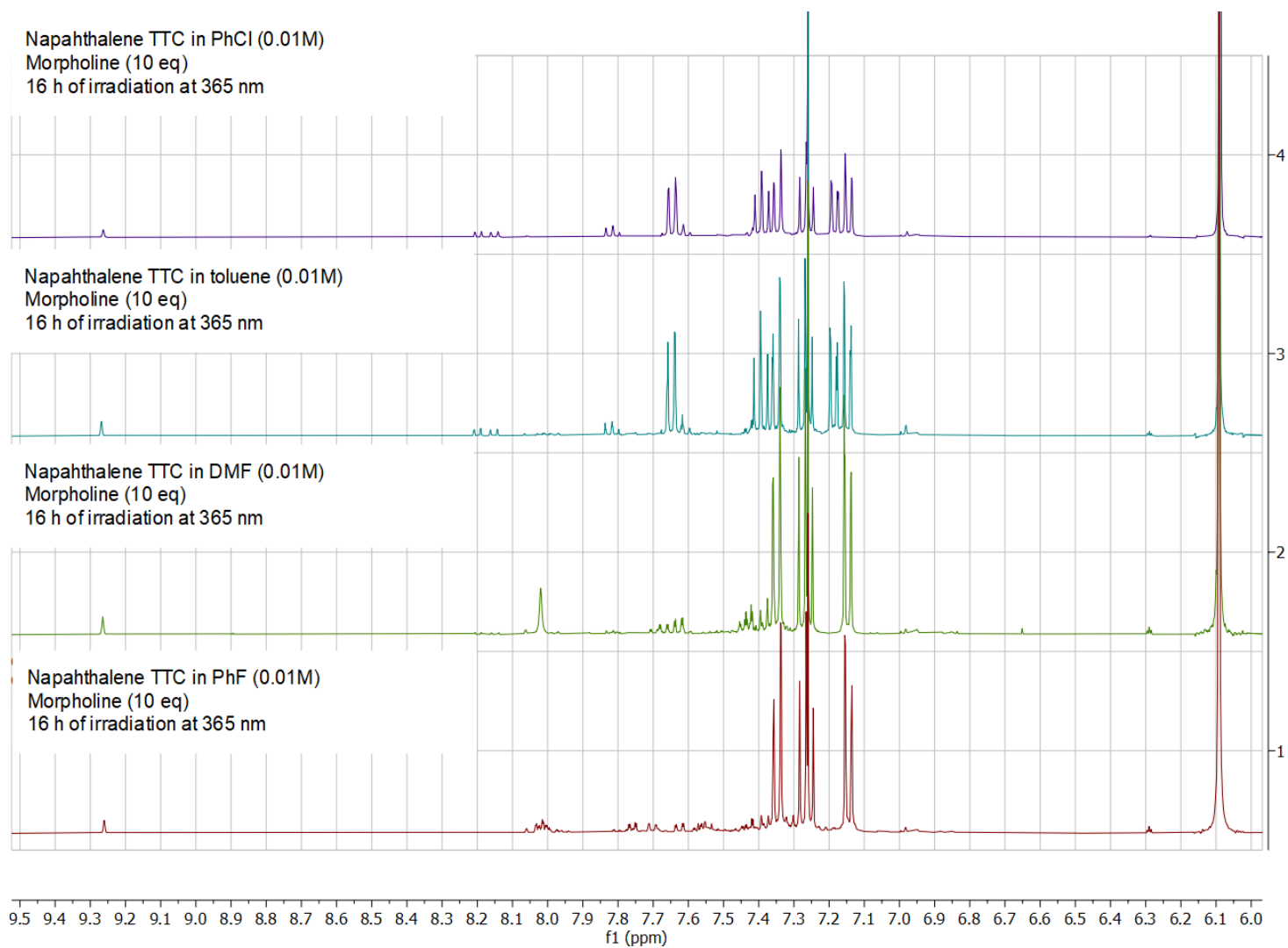
Entry	Solvent	Time / h	Conc. / M	TA 363 integral	TA 363 % yield	TTC 375 integral	TTC 375 % yield	DS 107 integral	DS 107 % yield	TMB integral
1	THF	3	0.02	1	2.2	3.91	4.3	39.10	42.9	136.62
2	THF	3	0.01	1	1.7	26.44	22.1	28.80	24.1	178.71
3	$\text{CH}_2\text{Cl}_2$	3	0.01	1	0.8	44.07	17.5	66.75	26.5	377.75
4	Toluene	3	0.01	1	1.7	81.01	68.5	18.90	16.0	177.51
5	PhCl	3	0.01	1	1.1	122.44	70.1	27.21	15.6	262.09

**Table 14** Table of conditions and  $^1\text{H}$  NMR integrations of the products with respect to trimethoxybenzene. TA – thioformamide **359**, TTC – trithiocarbonate **372**, DS – disulfide **107**, and TMB – trimethoxybenzene.

Entry	Solvent	Time / h	Conc. / M	TA 363 integral	TA 363 % yield	TTC 375 integral	TTC 375 % yield	DS 107 integral	DS 107 % yield	TMB integral
1	PhCl	16	0.01	1	4.8	12.35	29.4	14.81	35.2	63.05
2	Toluene	16	0.01	1	5.8	10.86	31.3	12.95	37.3	52.05
3	DMF	16	0.01	1	4.5	0	0	16.54	37.2	66.63
4	PhF	16	0.01	1	3.2	0	0	21.67	36.6	93.85



**Figure 24**  $^1\text{H}$  NMR data of the 3 h irradiation of naphthalene trithiocarbonate **375**.



**Figure 25**  $^1\text{H}$  NMR data of the 16 h irradiation of naphthalene trithiocarbonate **375**.

According to the data, the best conversion to the desired thioformamide was using THF at 0.02 M (4.3% of TTC remained. **Table 13**). However, the reaction had also progressed the furthest and therefore more starting material had been consumed, and potentially, more CS produced. Aromatic solvents provided the cleanest conversion and still gave good solubility, but the reaction proceeded the slowest.

The highest yielding reaction of the thioformamide **363** was in toluene after 16h (5.8%). However, not all naphthalene trithiocarbonate **375** had been consumed. Interestingly, the sum of the naphthalene disulfide **107** % yield and naphthalene trithiocarbonate **375** % yield does not equal 100% in any reaction. Therefore, either the naphthalene disulfide **107** degrades under the conditions or the naphthalene trithiocarbonate **375** decomposes to yield another product which was not identified by the  $^1\text{H}$  NMR.

As a control experiment, morpholine was removed and the reaction was repeated. The purpose of these controls was to determine if morpholine was a critical reagent for the release of CS. Reactions without morpholine yielded no thioformamide **363**. Only THF gave decomposition of naphthalene trithiocarbonate **375** to the disulfide **107** without morpholine. This would indicate that the amine is required in most solvents. It is possible that the naphthalene trithiocarbonate requires a sacrificial electron donor to release CS. This electron could be obtained from the morpholine or THF.

*tert*-Butylbenzene thiol was used as an alternative to morpholine. As previously mentioned (Section 3.2.1), thiols can also react with CS to form thioacetals. Disulfide **107** was produced, indicating that the thiol is also an additive that allows for the formal loss of CS – unfortunately no thioacetal was detected. DABCO was also tested and degradation of the trithiocarbonate

to disulfide was also observed. Indicating that even tertiary amines can also cause the photodegradation of naphthalene trithiocarbonate **375**.

### 3.3 Conclusions and future work

The synthesis and characterisation of three dithiocarbonates have been completed; naphthalene dithiocarbonate **336**, acenaphthene dithiocarbonate **337** and acenaphthylene dithiocarbonate **338**. The acenaphthene **337** and acenaphthylene **338** dithiocarbonates are novel and have not been previously synthesised. Each of the dithiocarbonates were crystallised and the structures studied. The “clothes peg” trend analogy is followed. Each of the dithiocarbonates were irradiated using a 125 W Hg medium pressure lamp and each one yielded the corresponding disulfide with naphthalene dithiocarbonate **336** being the fastest decomposition time. To excel this work towards a potential CORM material, head space mass spectrometry or IR would have to be completed in order to detect if CO has been formally released from the system. Then the solubility of the naphthalene core would have to be developed. E.g. putting PE(G) chains onto the scaffold or making the dithiocarbonate into an organic salt. However, wavelength that would require to be irradiated is still too high and would damage DNA. Therefore, naphthalene dithiocarbonate would not be a useful CORM unless the absorption profile is red shifted.

The synthesis and characterisation of naphthalene, acenaphthene and 2,7-dimethoxynaphthalene trithiocarbonates **375**, **377**, and **376** have been completed. A simple solvent screen on naphthalene trithiocarbonate **375** found that aromatic solvents, chlorinated solvents, and THF tended to have the highest solubility. The properties of naphthalene trithiocarbonate **375** have been studied and it has been confirmed to release CS



in small quantities but only photochemically. Thermal release was attempted but no reaction occurred and starting material was returned. Unfortunately, the electrolysis of CS<sub>2</sub> vapour is still the most reliable way to release CS at the present time. The best solvents to release CS in are aromatic solvents – particularly toluene. To observe photodegradation an amine, thiol or THF is required. Studies have begun into the photochemical degradation pathway by investigating the absorbance and emission spectra as well as the cyclic voltammetry. This will give us an insight into whether an excited state or the ground state undergoes decomposition to release CS or whether it is a radical anion or radical cation which causes CS to be released. It is clear that the reaction so far requires a source of sacrificial electrons. Therefore, our working thought is that the reaction undergoes an electron transfer to the trithiocarbonate

**375.**

## **4 Experimental**

### General Experimental:

All solvents and reagents were purchased from standard suppliers and used without further purification unless otherwise stated. CDI and Thio-CDI were stored in a refrigerated environment at 4 °C until required. All anhydrous solvents were collected from a pure Solv-MD solvent purification system or dried over 4 Å molecular sieves and purged under argon for 15 min prior to use. All reactions were performed in flame-dried or oven-dried glassware and under an argon atmosphere, unless otherwise stated. Solutions of *n*butyllithium in hexanes (*n*BuLi) were purchased from Sigma Aldrich at 2.5 M concentration and titrated in

THF (anhydrous) with menthol in the presence of 1-(biphenyl-4-yl)-3-phenyl-2-azapropene ("Blue").<sup>221</sup> *N,N,N',N'*-TMEDA was distilled from calcium hydride over KOH pellets. Elemental sulfur was recrystallised from hot toluene and dried under vacuum. When sulfur is used in the experimental, the molar amount was calculated from 32.07 g·mol<sup>-1</sup> (the atomic weight of a single atom of sulfur). Sulfur will react in its S<sub>8</sub> ring form, however. "10% H<sub>2</sub>SO<sub>4</sub>" is defined as aqueous solution where 10% of the solution is concentrated H<sub>2</sub>SO<sub>4</sub> by volume. When NaBH<sub>4</sub> is used to reduce a disulfide or trisulfide the number of equivalents is always 2.5 equivalents per S-S.

All temperature readings equal to and above 0 °C are external readings (stirrer hot plate or an independent thermometer) and all temperatures below 0 °C are internal temperatures, except -78 °C which is also external.

All column chromatography was performed under pressure (flash column chromatography – FCC) with Sigma-Aldrich silica gel, 60 Å pore size, 230 – 400 mesh, 40 – 63 µm. All compounds were dry-loaded onto silica on the minimum amount of silica that was required (minimum amount refers the minimum amount of silica required in order for the silica to be free flowing when doped with the compound). All TLC analysis was performed using silica gel on Merck aluminium TLC silica gel plates, 60 with 254 nm fluorescent indicator, with visualisation using 254 nm UV light or KMnO<sub>4</sub> solution.

Nuclear magnetic resonance (<sup>1</sup>H and <sup>13</sup>C) was detected by a Bruker Avance NEO 400 or Bruker 300 MHz AVIII spectrometer (<sup>1</sup>H – 400 MHz and <sup>13</sup>C 101 MHz). All spectra were recorded in CDCl<sub>3</sub> and referenced to the residual CHCl<sub>3</sub> (<sup>1</sup>H – 7.26 ppm and <sup>13</sup>C – 77.16 ppm) unless otherwise stated. Chemical shifts are reported in ppm and coupling constants, *J*, are reported in Hz. The following abbreviations are used to describe multiplicity; s – singlet, d – doublet,

dd – double doublet, ddd – double double doublet, t – triplet, q – quartet, hept – heptet, m – multiplet, app – apparent and st – stack. All coupling constants are reported as observed not averaged. All assignments were made using analysis of 2D NMR (COSY, NOESY, HSQC, HMBC). Mass spectrometry was recorded using GCMS on a Water micro mass GC-ToF Premier/Agilent 7890A with a Phenomenex ZB-5 column 30 m × 0.25 mm ID × 0.25 μm film thickness or ASAPs Waters Xevo G2-XSToF and are reported as (m/z%). IR spectra were recorded neat, unless otherwise specified, on a Perkin Elmer spectrum 100 FT-IR spectrometer.

<sup>1</sup>H NMR integration comparisons are either done as a conversion from starting material to product identifying specific peaks in both (peaks will be made clear in the relevant sections). In some cases, 1,3,5-trimethoxybenzene (an internal standard, 0.1 mmol, 1 eq) was added to the reaction mixture upon either completion of the reaction by TLC or after a specified time window, to measure the <sup>1</sup>H NMR integrations between the internal standard and the desired compounds. The equation for determining the yield from <sup>1</sup>H NMR integration is shown.

*% yield of thioformylamide **363***

$$= \left( \frac{\left( \frac{\text{NMR integration of peak at 9.27 ppm}}{1} \right)}{\left( \frac{\text{NMR integration of TMB peak at 6.09}}{3} \right)} \right) \times 100$$

*% yield of naphthalene disulfide **107***

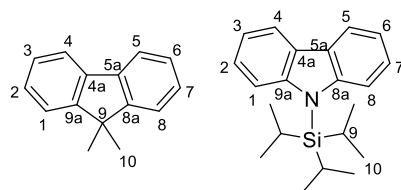
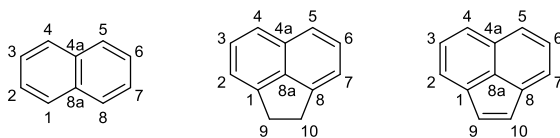
$$= \left( \frac{\left( \frac{\text{NMR integration of peak at 7.15 ppm}}{2} \right)}{\left( \frac{\text{NMR integration of TMB peak at 6.09}}{3} \right)} \right) \times 100$$

*% yield of naphthalene trithiocarbonate **375***

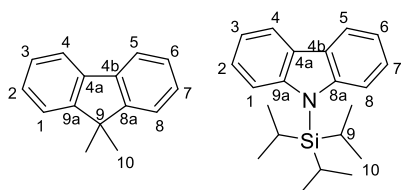
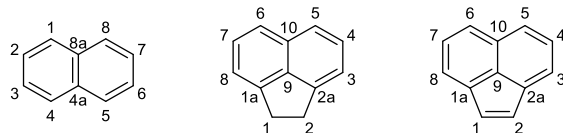
$$= \left( \frac{\left( \frac{\text{NMR integration of peak at 7.19 ppm}}{2} \right)}{\left( \frac{\text{NMR integration of TMB peak at 6.09}}{3} \right)} \right) \times 100$$

Defined scaffold numbering:

Self-designed numbering for the scaffolds used in the thesis

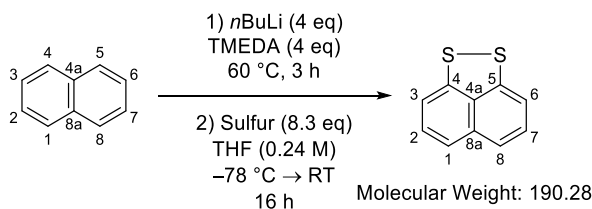


IUPAC Numbering for the scaffolds in this thesis



## Chapter 2 experimental

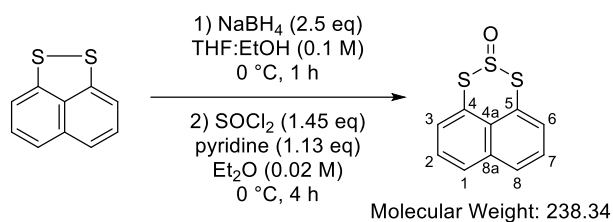
### Synthesis of naphtho[1,8-*cd*][1,2]dithiole 107



Naphtho[1,8-*cd*][1,2]dithiole was synthesised using a literature procedure.<sup>120</sup>

*n*BuLi (47.78 mL, 93.64 mmol, 1.96 M, 4 eq.) was added to a solution of naphthalene (3.00 g, 23.41 mmol) in TMEDA (14.04 mL, 93.64 mmol, 4 eq.) and the reaction mixture was heated at 60 °C for 3 h. After 3 h, the reaction mixture was cooled to -78 °C and diluted with anhydrous THF (98 mL, 0.24 M). Sulfur (6.23 g, 194.30 mmol, 8.3 eq.) was added in one portion. The reaction mixture was allowed to equilibrate to room temperature over 16 h. 1 M HCl(aq) (50 mL) was added, and the reaction was allowed to stir open to the atmosphere for 1 h. The reaction mixture was extracted with CH<sub>2</sub>Cl<sub>2</sub> (100 mL × 3). The combined organics were washed with water (50 mL) and brine (50 mL), dried over MgSO<sub>4</sub>, filtered, and concentrated under reduced pressure to yield a red/brown oil. The oil was dry loaded onto silica and purified by FCC (100% *n*hexane) to yield a red solid (1.37 g, 31%). *R*<sub>f</sub> 0.56 (*n*hexane); δH (400 MHz, CDCl<sub>3</sub>, 7.26 ppm) 7.35 (2H, dd, *J* = 8.3 Hz, 0.8 Hz, H-3/H-5), 7.28 (2H, app. t, *J* = 7.4 Hz H-2/H-7), 7.15 (2H, dd, *J* = 7.5, 0.9 Hz, H-1/H-8); δC (101 MHz, CDCl<sub>3</sub>, 77.16 ppm) 144.2 (CH, C-1/C-8), 135.9 (C, C-4a), 132.8 (C, C-8a), 128.1 (CH, C-3/C-6), 121.8 (CH, C-2/C-7), 116.1 (CS, C-4/C-5); *m/z* (LRMS, EI+) Found 191.89 (9), 190.90 (11), ([M]<sup>+</sup> 189.88). Data matches that by Grainger and co-workers.<sup>42,43</sup>

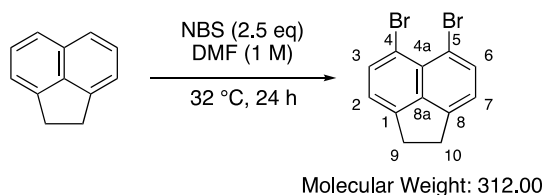
## Synthesis of naphtho[1,8-*de*][1,2,3]trithiane-2-oxide **105**



Naphtho[1,8-*de*][1,2,3]trithiane-2-oxide **105** was synthesised using a literature procedure.<sup>42,43</sup>

NaBH<sub>4</sub> (31 mg, 0.8 mmol) was dissolved in EtOH (0.32 mL, 2.5 M WRT NaBH<sub>4</sub>) and was added to naphthalene disulfide **107** (100 mg, 0.53 mmol) in THF (0.32 mL, 1.66 M) at 0 °C. The reaction mixture was stirred at 0 °C for 1 h. The reaction mixture was quenched with 10% (wt/wt) HCl(aq) (10 mL) and extracted with CH<sub>2</sub>Cl<sub>2</sub> (10 mL × 3). The combined organics were washed with water (10 mL × 3), dried over MgSO<sub>4</sub>, filtered, and concentrated under reduced pressure to yield a white solid. The oil was dissolved in Et<sub>2</sub>O (anhydrous, 17.6 mL), and pyridine (anhydrous, 0.05 mL) was added. SOCl<sub>2</sub> (freshly distilled, 0.06 mL) in Et<sub>2</sub>O (anhydrous, 6.91 mL) was added to a pressure-equalising dropping-funnel and was added to the dithiol solution at 0 °C over 15 min. The reaction was allowed to equilibrate to room temperature over 4 h. A white solid precipitated and the solution turned yellow. The reaction mixture was quenched with 10% H<sub>2</sub>SO<sub>4</sub>(aq) (20 mL) and the aqueous layer was extracted with Et<sub>2</sub>O (10 mL × 3). The combined organics were washed with brine (10 mL × 3), dried over MgSO<sub>4</sub>, filtered, and concentrated under reduced pressure. The reaction mixture was dry-loaded onto silica and purified by FFC (*n*hexane:Et<sub>2</sub>O, 7:3) to yield a yellow solid (22 mg, 18%). *R<sub>f</sub>* 0.31 (*n*hexane:Et<sub>2</sub>O, 7:3); *v*<sub>max</sub>(neat)/cm<sup>-1</sup>; δH (400 MHz, CDCl<sub>3</sub>, 7.26 ppm) 7.94 (2H, dd, *J* = 7.9, 1.7 Hz), 7.62 (2H, dd, *J* = 7.3, 1.7 Hz), 7.57 (2H, app. t, *J* = 7.3 Hz, H-2/H-7). Data matches that by Grainger and co-workers.<sup>42,43</sup>

## Synthesis of 5,6-dibromo-1,2-dihydroacenaphthylene **265**



5,6-dibromo-1,2-dihydroacenaphthylene **265** was synthesised using a literature procedure.<sup>169</sup>

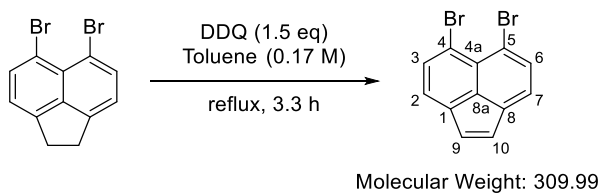
*For convenience, the reaction was split into 2 × 1 L flasks. Below are the amounts for one flask. The yield is of both flasks together.*

Acenaphthene (50 g, 324.3 mmol) was dissolved in DMF (325 mL, 1 M) and NBS (144.28 g, 810.64 mmol) was added. The reaction temperature was raised to 32 °C. After 24 h, a yellow precipitate had formed and was filtered using a sinter funnel. The precipitate was washed with MeOH (500 mL) and *n*hexane (200 mL) and dried under vacuum to yield an off-white solid (49.7 g, 25% - for the combined flasks). The product was used without further purification. An analytical standard sample was produced via recrystallisation from CHCl<sub>3</sub>.; *R<sub>f</sub>* 0.25 (*n*hexane);  $\nu_{\text{max}}(\text{neat})/\text{cm}^{-1}$  3064 w, 3011 w, 2972 w, 2958 w, 2919 w, 2865 w, 1439 m;  $\delta\text{H}$  (400 MHz, CDCl<sub>3</sub>, 7.26 ppm) 7.80 (2H, d, *J* = 7.4 Hz, H-3/H-6), 7.10 (2H, d, *J* = 7.4 H-2/H-7), 3.31 (4H, s, H-9/H-10);  $\delta\text{C}$  (101 MHz, CDCl<sub>3</sub>, 77.16 ppm) 147.2 (CBr, C-4/C-5), 142.1 (C, C-1/C-8), 136.0 (CH, C-3/C-6), 128.0 (C, C-4a), 121.1 (CH, C-2/C-7), 114.6 (C, C-8a), 30.2 (CH<sub>2</sub>, C-9/C-10); *m/z* (LRMS, ASAP+) 314.90 (25%), 313.90 (48), 312.90 (49), 311.90 ([M]<sup>+</sup>, 100%, <sup>79</sup>Br and <sup>81</sup>Br), 310.91 (22), 309.90 (50); (HRMS, ASAP+) Found [M]<sup>+</sup> 311.8983. C<sub>12</sub>H<sub>8</sub><sup>79</sup>Br<sup>81</sup>Br requires [M] 311.8973.

Data matched that by Woollins and co-workers.<sup>126</sup>



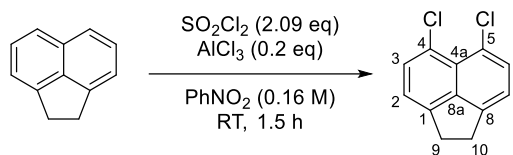
### Synthesis of 5,6-dibromoacenaphthylene **263**



5,6-Dibromo-1,2-dihydroacenaphthylene **265** (551 mg, 1.765 mmol) and DDQ (601 mg, 2.647 mmol, 1.5 eq) were dissolved in toluene (10.26 mL). The reaction mixture was allowed to reflux for 3.3 h. The reaction mixture was filtered through of celite pad and concentrated under reduced pressure to yield an orange solid. The solid was dry-loaded onto silica and purified by FFC (*n*hexane) to yield a yellow solid (104 mg, 19%).

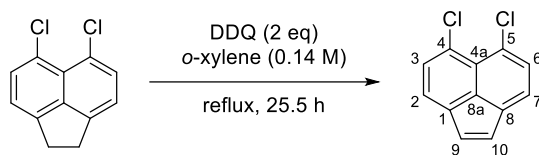
$\delta$ H (400 MHz, CDCl<sub>3</sub>, 7.26 ppm) 7.89 (2H, d,  $J$  = 7.4 Hz), 7.43 (2H, d,  $J$  = 7.4 Hz), 6.95 (2H, s, H-9/H-10);  $m/z$  (LRMS, EI<sup>+</sup>) 150.1 (67), 307.9 (60), 309.9 (100%), 311.9 (58), 312.9 (11). Data matches reports from Woollins and co-workers.<sup>126</sup>

### Synthesis of 5,6-dichloro-1,2-dihydroacenaphthylene 313



$\text{AlCl}_3$  (0.884 g, 6.63 mmol, 0.2 eq) and acenaphthene (5.110 g, 33.14 mmol) were dissolved in anhydrous nitrobenzene (21 mL, 0.16 M).  $\text{SO}_2\text{Cl}_2$  (5.62 mL, 69.26 mmol, 2.09 eq) was added dropwise over 20 min. The reaction mixture was allowed to stir at room temperature for 1.5 h. The reaction mixture was quenched with a sat. solution of  $\text{Na}_2\text{CO}_3(\text{aq})$  (50 mL). The aqueous layer was extracted with  $\text{Et}_2\text{O}$  (100 mL). The combined organics were washed with a sat. solution of  $\text{Na}_2\text{CO}_3(\text{aq})$  (50 mL) and brine (50 mL), dried over  $\text{MgSO}_4$ , filtered, and concentrated under reduced pressure. The brown solid was dry-loaded onto silica and purified by FFC (*n*hexane:EtOAc, 99:1) to yield a white solid (3.140 g, 42%).  $\delta\text{H}$  (400 MHz,  $\text{CDCl}_3$ , 7.26 ppm) 7.52 (2H, d,  $J = 7.4$  Hz), 7.18 (2H, d,  $J = 7.5$  Hz), 3.36 (4H, t,  $J = 0.9$  Hz, H-9/H-10);  $\delta\text{C}$  (101 MHz,  $\text{CDCl}_3$ , 77.16 ppm) 145.4, 142.3, 132.3, 127.2, 125.9, 121.4, 32.6 ( $\text{CH}_2$ , C-9/C-10). Data matches that by Corić and co-workers.<sup>222</sup>

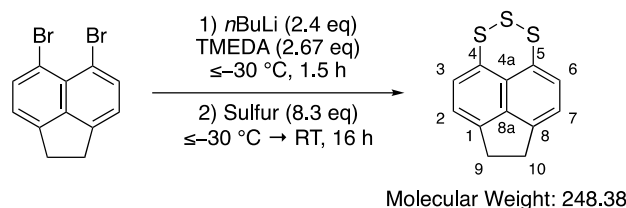
### Synthesis of 5,6-dichloroacenaphthylene **316**



5,6-Dichloroacenaphthene **313** (1.501 g, 6.72 mmol) and DDQ (2.297 g, 10.09 mmol, 1.5 eq) was dissolved in *o*-xylene (48 mL, 0.14 M) and brought to reflux. After 8 h, DDQ (0.764 g, 3.37 mmol) in *o*-xylene (10 mL) was added. The reaction was maintained at reflux for 17.5 h. The reaction mixture was allowed to equilibrate to room temperature before being passed through a silica pad. The filtrate was dry-loaded onto silica and purified by FCC (*n*hexane) to yield a yellow solid (647 mg, 43%).

$\delta$ H (400 MHz, CDCl<sub>3</sub>, 7.26 ppm) 7.59 (2H, d,  $J$  = 7.4 Hz), 7.52 (2H, d,  $J$  = 7.4 Hz), 6.97 (2H, s, H-9/H-10);  $m/z$  (LRMS, EI<sup>+</sup>) 150.05 (45), 185.02 (32), 219.99 (100%), 221.99 (70), 223.98 (15); Data matches that from Bhaven Patel's PhD thesis.<sup>223</sup>

## Synthesis of 6,7-dihydroacenaphtho[5,6-*de*][1,2,3]trithiane **319**



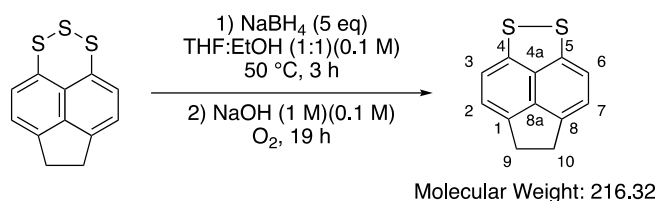
6,7-Dihydroacenaphtho[5,6-*de*][1,2,3]trithiane **319** is a novel compound and was synthesised from a modified literature procedure.<sup>128,169</sup>

5,6-Dibromoacenaphthene **265** (4.68 g, 15.00 mmol) was suspended in Et<sub>2</sub>O (anhydrous, 500 mL, 0.03 M) and cooled to  $\leq -30$  °C. *n*BuLi (17.31 mL, 36.00 mmol, 2.08 M, 2.40 eq.) and TMEDA (6.00 mL, 40.10 mmol, 2.67 eq.) were added to a dropping funnel and aged for 15 min. The *n*BuLi/TMEDA solution was added to the suspension dropwise over 15 min, ensuring the temperature did not rise above  $-30$  °C. The reaction mixture was allowed to stir at  $\leq -30$  °C for a further 1.5 h. Sulfur (3.99 g, 124.50 mmol, 8.3 eq.) was added in one portion and the reaction temperature was maintained at  $\leq -30$  °C for a further 30 min. The cooling bath was removed, and reaction mixture was allowed to equilibrate to room temperature over 16 h. The reaction mixture was quenched with 1M HCl(aq) (200 mL) and allowed to stir open to the atmosphere for 1 h. The biphasic reaction mixture was filtered through a pad of celite. The aqueous layer was separated and extracted with Et<sub>2</sub>O (100 mL), and the combined organics were washed with water (100 mL) and brine (100 mL), dried over MgSO<sub>4</sub>, filtered, and concentrated under reduced pressure. The orange solid was dry loaded onto silica and purified by FCC (100% *n*hexane) to yield a yellow solid (1.78 g, 48 %); *R*<sub>f</sub> 0.55 (*n*hexane); m.p. 135 – 137 °C (EtOH, obtained by I. A. Pocock);  $\nu_{\text{max}}(\text{neat})/\text{cm}^{-1}$  3033 w, 2924 m, 2869 w, 2826 w, 1861 m, 1589 m;  $\delta$ H (400 MHz, CDCl<sub>3</sub>, 7.26 ppm) 7.57 (2H, d, *J* = 7.1 Hz, H-3/H-6), 7.30 (2H, d, *J* = 7.2, H-2/H-7), 3.42 (4H, m, H-9/H-10);  $\delta$ C (101 MHz, CDCl<sub>3</sub>, 77.16 ppm) 148.5, 140.6 (C,

C-1/C-8), 129.6 (CH, C-3/C-6), 124.7 (C, C-8a), 124.5, 119.3 (CH, C-2/C-7), 30.6 (CH<sub>2</sub>, C-9/C-10);

m/z (HRMS, ASAP+) Found [M]<sup>+</sup> 247.9788. C<sub>12</sub>H<sub>8</sub>S<sub>3</sub> requires 247.9788 [M].

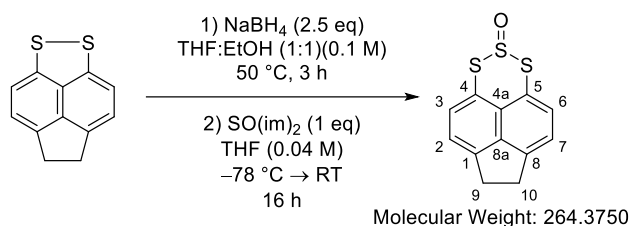
## Synthesis of 5,6-dihydroacenaphtho[5,6-*cd*][1,2]dithiole **266**



5,6-Dihydroacenaphtho[5,6-*cd*][1,2]dithiole **266** was synthesised from a modified literature procedure.<sup>42,43,224</sup>

Acenaphthene trisulfide **319** (523 mg, 2.11 mmol) was dissolved in THF:EtOH (1:1, 21 mL, 0.1 M) and NaBH<sub>4</sub> (398 mg, 10.53 mmol, 5 eq.) was added in one portion. Once effervescence had ceased, the reaction mixture was heated at 50 °C for 3 h. The reaction mixture was allowed to equilibrate to room temperature and was quenched with 1 M NaOH(aq) (20 mL, 0.1 M WRT the reaction mixture). The reaction mixture was allowed to stir open to the atmosphere for 19 h. The reaction mixture was extracted with CH<sub>2</sub>Cl<sub>2</sub> (50 mL × 3), and the combined organics were washed water (50 mL) and brine (50 mL), dried over MgSO<sub>4</sub>, filtered, and concentrated under reduced pressure to yield a red solid (418 mg, 92%). *R*<sub>f</sub> 0.58 (*n*hexane); *v*<sub>max</sub>(neat)/cm<sup>-1</sup> 2919 w, 2835 w, 1561 m, 1396 s; δH (400 MHz, CDCl<sub>3</sub>, 7.26 ppm) 7.80 (2H, d, *J* = 7.4 Hz, H-3/H-6), 7.10 (2H, d, *J* = 7.4 H-2/H-7), 3.31 (4H, s, H-9/H-10); δC (101 MHz, CDCl<sub>3</sub>, 77.16 ppm) 141.5 (CS, C-4/C-5), 140.4 (C, C-1/C-8), 138.4 (CH, C-3/C-6), 134.4 (C, C-4a), 121.2 (CH, C-2/C-7), 117.0 (C, C-8a), 30.8 (CH<sub>2</sub>, C-9/C-10); *m/z* (LRMS, ASAP+) 219.01 (10), 218.02 (19), 217.01 ([M + H]<sup>+</sup>, 100%), 216.0072 ([M]<sup>+</sup>, 70%) *m/z* (HRMS, ASAP+) Found [M]<sup>+</sup> 216.0072. C<sub>12</sub>H<sub>8</sub>S<sub>2</sub> requires [M]<sup>+</sup> 216.0067. Data matched that by Woollins and co-workers.<sup>108</sup>

## Synthesis of 6,7-dihydroacenaphtho[5,6-*de*][1,2,3]trithiine-2-oxide **299**



6,7-Dihydroacenaphtho[5,6-*de*][1,2,3]trithiine-2-oxide **299** is a novel compound and was synthesised from a modified literature procedure.<sup>43,176</sup>

### Reaction A:

Acenaphthene disulfide **266** (175 mg, 0.81 mmol) was dissolved in THF:EtOH (1:1, 8.1 mL, 0.1 M) and  $\text{NaBH}_4$  (78 mg, 2.01 mmol, 2.5 eq.) was added. Once effervescence had ceased the reaction mixture was heated at 50 °C for 3 h. The reaction was quenched with 1 M  $\text{HCl}(\text{aq})$  (20 mL) and extracted with  $\text{CH}_2\text{Cl}_2$  (3  $\times$  20 mL). The combined organics were washed with water (20 mL) and brine (20 mL), dried over  $\text{MgSO}_4$ , filtered, and concentrated under reduced pressure to yield a white solid.

### Reaction B:

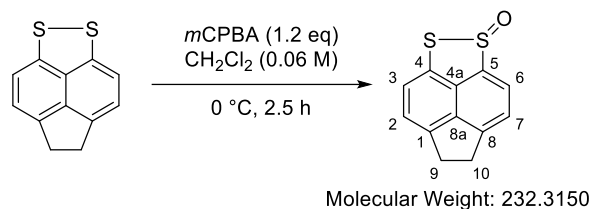
*Begin 1.5 h into the reduction in reaction A.*

Imidazole (221 mg, 3.24 mmol, 4 eq.) was dissolved in anhydrous THF (4.1 mL). The solution was cooled to 0 °C and  $\text{SOCl}_2$  (0.06 mL, 0.81 mmol, 1 eq.) was added dropwise over 2 min. A white precipitate formed. The reaction mixture was allowed to stir at 0 °C for a further 30 min, then the cooling bath was removed, and the reaction mixture was stirred at room temperature for a further 1.5 h.

Reaction mixture B was cooled to  $-78\text{ }^{\circ}\text{C}$ , then the dithiol (white solid from reaction A) was dissolved in THF (anhydrous, 16.0 mL) and added dropwise over the course of 10 min. The reaction mixture was stirred at  $-78\text{ }^{\circ}\text{C}$  for 2 h, then was allowed equilibrate to room temperature for 16 h (cooling bath was not removed). The reaction mixture was washed with 10%  $\text{H}_2\text{SO}_4(\text{aq})$  (20 mL  $\times$  2), water (20 mL) and brine (20 mL), dried over  $\text{MgSO}_4$ , filtered, and concentrated under reduced pressure. The reaction mixture was dry-loaded onto silica and purified by FCC (*n*hexane:EtOAc, 8:2) to yield an orange solid (127 mg, 59%).  $R_f$  0.13 ( $\text{CH}_2\text{Cl}_2$ :*n*hexane, 1:1); m.p.  $136 - 140\text{ }^{\circ}\text{C}$  (from *n*hexane: $\text{CH}_2\text{Cl}_2$ );  $\nu_{\text{max}}(\text{neat})/\text{cm}^{-1}$  3076 w, 1461 m, 1415 m, 1101 s (S=O), 1082 s;  $\delta\text{H}$  (400 MHz,  $\text{CDCl}_3$ , 7.26 ppm) 7.53 (2H, d,  $J = 7.2\text{ Hz}$ , H-2/H-7), 7.42 (2H, d,  $J = 7.2$ , H-3/H-6), 3.45 (4H, s, H-9/H-10);  $\delta\text{C}$  (101 MHz,  $\text{CDCl}_3$ , 77.16 ppm) 149.5, 139.7, 133.5, 122.0, 121.4, 117.6, 30.7 ( $\text{CH}_2$ , C-9/C-10);  $m/z$  (HRMS, ASAP+)  $[\text{M} + \text{H}]^+$  264.9799.  $\text{C}_{12}\text{H}_9\text{S}_3\text{O}$  requires  $[\text{M} + \text{H}]$  264.9815.

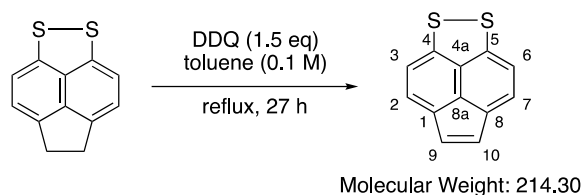


## Synthesis of 5,6-dihydroacenaphtho[5,6-*cd*][1,2]dithiole-1-oxide **321**



A solution of *m*CPBA (284 mg, 1.40 mmol, 85% purity) in CH<sub>2</sub>Cl<sub>2</sub> (8 mL) was added dropwise to a solution of acenaphthene disulfide **266** (252 mg, 1.16 mmol) in CH<sub>2</sub>Cl<sub>2</sub> (10 mL) at 0 °C over 30 m. The reaction mixture was allowed to stir for 2 h at 0 °C. After 2 h, the reaction mixture was removed from the cooling bath and allowed to stir at room temperature for a further 2.5 h. The reaction mixture was quenched with a sat. solution of NaHCO<sub>3</sub>(aq) (10 mL). The aqueous layer was extracted with CH<sub>2</sub>Cl<sub>2</sub> (10 mL × 3) and the combined organics were washed with water (10 mL), brine (10 mL), dried over MgSO<sub>4</sub>, filtered and concentrated under reduced pressure to yield a yellow solid. The solid was dried loaded onto silica and purified by FFC (*n*hexane:Et<sub>2</sub>O, 6:4) to yield a yellow solid. The solid was further purified by recrystallisation from boiling *n*hexane to yield yellow crystals (234 mg, 87%).  $\nu_{\max}(\text{neat})/\text{cm}^{-1}$  2916 w, 1567, 1483, 1397, 1066 (S=O) s;  $\delta_{\text{H}}$  (400 MHz, CDCl<sub>3</sub>, 7.26 ppm) 8.13 (1H, d,  $J$  = 7.3 Hz), 7.59 (1H, dt,  $J$  = 7.3, 1.3 Hz), 7.51 (1H, d,  $J$  = 7.3 Hz), 7.48 – 7.41 (1H, m), 3.55 (4H, st, H-9/H-10);  $\delta_{\text{C}}$  (101 MHz, CDCl<sub>3</sub>, 77.16 ppm) 151.8, 143.9, 143.3, 139.8, 132.4, 129.5, 128.7, 122.9, 122.1, 121.4, 31.9, 31.0;  $m/z$  (LRMS, ASAP+) 152.06 (15), 178.16 (80), 233.01 ([M + H]<sup>+</sup>, 100%);  $m/z$  (HRMS, ASAP+) Found [M]<sup>+</sup> 233.0106. C<sub>12</sub>H<sub>8</sub>S<sub>2</sub> requires [M+H]<sup>+</sup> 232.0095.

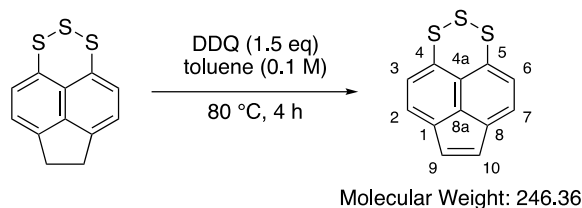
## Synthesis of acenaphtho[5,6-*cd*][1,2]dithiole **264**



Acenaphtho[5,6-*cd*][1,2]dithiole **264** was synthesised from a modified literature procedure.<sup>126</sup>

Acenaphthene disulfide **266** (201 g, 0.92 mmol) and DDQ (316 g, 1.39 mmol) were dissolved in toluene (9.2 mL, 0.1 M) and brought to reflux. After 27 h the reaction mixture was allowed to equilibrate to room temperature and the reaction mixture was filtered and washed with EtOAc (30 mL). The filtrate was concentrated under reduced pressure to yield a red solid. The red solid was redissolved in EtOAc (30 mL) and washed with 1 M NaOH(aq) (10 mL  $\times$  3), water (10 mL) and brine (10 mL), dried over MgSO<sub>4</sub>, filtered, and concentrated under reduced pressure to yield a red solid. The red solid was dry-loaded onto silica and purified by silica plug (100% *n*hexane) to yield a red solid (66 mg, 33%).  $R_f$  0.58 (*n*hexane);  $\nu_{\max}(\text{neat})/\text{cm}^{-1}$  2954 w, 2919 m, 2850 m, 1395 m, 1369 m;  $\delta H$  (400 MHz, CDCl<sub>3</sub>, 7.26 ppm) 7.90 (2H, d,  $J$  = 7.5 Hz), 7.57 (2H, d,  $J$  = 7.5 Hz), 7.25 (2H, s, H-9/H-10);  $\delta C$  (101 MHz, CDCl<sub>3</sub>, 77.16 ppm) 143.6 (CS, C-4/C-5), 133.1, 131.0, 128.8, 125.9 (CH), 125.7 (CH), 116.2 (CH, C-9/C-10);  $m/z$  (HRMS, EI<sup>+</sup>) [M]<sup>+</sup> 213.9916. C<sub>12</sub>H<sub>6</sub>S<sub>2</sub> requires [M] 213.9911. Data matches that by Woollins and co-workers.<sup>112</sup>

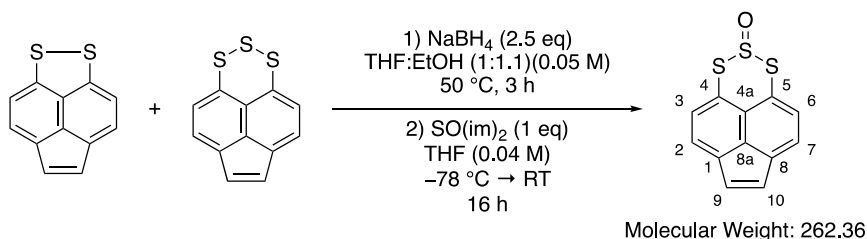
## Synthesis of acenaphtho[5,6-*de*][1,2,3]trithiane **320**



Acenaphtho[5,6-*de*][1,2,3]trithiane **320** is a novel compound and was synthesised from a modified literature procedure.<sup>126</sup>

Acenaphthene trisulfide **319** (1.00 g, 4.03 mmol) and DDQ (1.37 g, 6.04 mmol) were dissolved in toluene (40 mL, 0.1 M) and brought to 80 °C. After 4.5 h the reaction mixture was allowed to equilibrate to room temperature, diluted with *n*hexane (10 mL) and the reaction mixture was dry-loaded onto silica and purified by FCC to yield an orange solid (160 mg, 16%);  $R_f$  0.55 (*n*hexane);  $\nu_{\max}(\text{neat})/\text{cm}^{-1}$  3069 w, 3033 w, 2956 w, 1461 m, 1415 m;  $\delta_H$  (400 MHz,  $\text{CDCl}_3$ , 7.26 ppm) 7.41 (2H, d,  $J = 7.2$  Hz, C-3/C-6), 7.39 (2H, d,  $J = 7.2$ , C-2/C-7), 6.84 (2H, s, C-9/C-10);  $\delta_C$  (101 MHz,  $\text{CDCl}_3$ , 77.16 ppm) 141.4 (C, C-1/C-8), 131.3 (CS, C-4/C-5), 130.8 (C, C-4a), 129.9 (CH, C-9/C-10), 128.3 (CH, C-2/C-7), 123.7 (CH, C-3/C-6);  $m/z$  (ASAP+) 246.9632 ( $M^+$ , 57%).

## Synthesis of acenaphtho[5,6-*de*][1,2,3]trithiane-2-oxide **300**



Acenaphtho[5,6-*de*][1,2,3]trithiane-2-oxide **300** is a novel compound and was synthesised from a modified literature procedure.<sup>43,176</sup>

### Reaction A:

A mixture of acenaphthylene trisulfide **320**/disulfide **264** (1:0.33, 158 mg, 0.50 mmol [trisulfide]: 0.17 mmol [disulfide]) was dissolved in THF (6.7 mL, 0.1 M) and EtOH (6.1 mL, 0.11 M) and NaBH<sub>4</sub> (114 mg, 3.01 mmol, 2.5 eq.) was added. Once effervescence had ceased the reaction mixture was heated at 50 °C for 3 h. The reaction was quenched with 1 M HCl(aq) (10 mL) and extracted with CH<sub>2</sub>Cl<sub>2</sub> (3 × 10 mL). The combined organics were washed with water (10 mL) and brine (10 mL), dried over MgSO<sub>4</sub>, filtered, and concentrated under reduced pressure to yield a yellow solid.

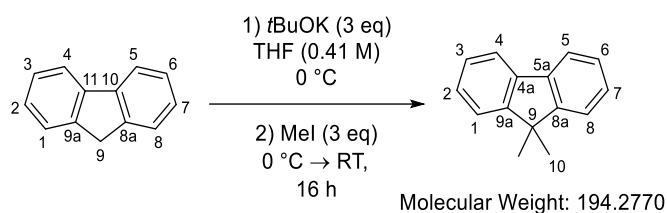
### Reaction B:

*Begin 1.5 h into the reduction in reaction A.*

Imidazole (182 mg, 2.68 mmol, 4 eq.) was dissolved in anhydrous THF (3.4 mL). The solution was cooled to 0 °C and SOCl<sub>2</sub> (50 µL, 0.67 mmol, 1 eq.) was added dropwise over 1 min. The reaction mixture was allowed to stir at 0 °C for a further 30 min, then the cooling bath was removed, and the reaction mixture was stirred at room temperature for a further 1.5 h.

Reaction mixture B was cooled to  $-78\text{ }^{\circ}\text{C}$ , then dithiol (yellow solid from reaction A) was dissolved in anhydrous THF (13.4 mL) and added dropwise over the course of 10 min. The reaction mixture was allowed equilibrate to room temperature for 16 h without the removal of the cooling bath. The reaction mixture was concentrated under reduced pressure and was separated with EtOAc (20 mL) and 10%  $\text{H}_2\text{SO}_4(\text{aq})$  (20 mL). The aqueous layer was extracted with EtOAc (20 mL  $\times$  2). The combined organics were washed with water (20 mL) and brine (20 mL), dried over  $\text{MgSO}_4$ , filtered, and concentrated under reduced pressure. The reaction mixture was dry-loaded onto silica and purified by FCC (*n*hexane:EtOAc, 9:1) to yield an orange solid (97 mg, 55%).  $R_f$  0.38 (*n*hexane:EtOAc, 9:1); m.p.  $140 - 144\text{ }^{\circ}\text{C}$ ;  $\lambda_{\text{max}}$  ( $\text{CH}_2\text{Cl}_2$ ) / nm 409 ( $\epsilon$  /  $\text{dm}^3\text{mol}^{-1}\text{cm}^{-1}$  13376), 336 (4229);  $\nu_{\text{max}}(\text{neat})/\text{cm}^{-1}$  3076 w, 1461 m, 1415 m, 1101 s (S=O), 1082 s;  $\delta\text{H}$  (400 MHz,  $\text{CDCl}_3$ , 7.26 ppm) 7.60 (2H, d,  $J = 7.2\text{ Hz}$ , H-2/H-7), 7.45 (2H, d,  $J = 7.2\text{ Hz}$ , H-3/H-6), 6.94 (2H, s, H-9/H-10);  $\delta\text{C}$  (101 MHz,  $\text{CDCl}_3$ , 77.16 ppm) 141.7, 131.6 (CH, C-3/C-6), 130.1 (CH, C-9/C-10), 129.6, 125.5 (CH, C-2/C-7), 123.0, 119.3;  $m/z$  (ASAP+, M+H, 262.9659).

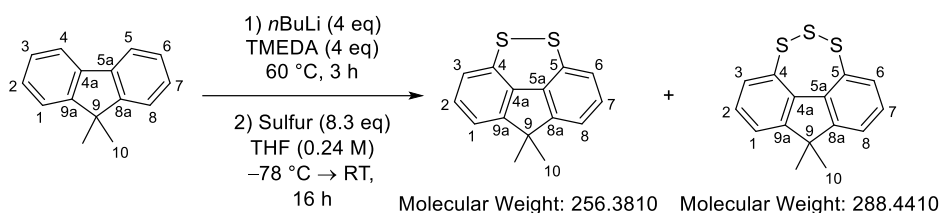
## Synthesis of 9,9-dimethyl-9H-fluorene **307**



9,9-dimethyl-9H-fluorene **307** was synthesised using a modified literature procedure.<sup>159</sup>

Fluorene **308** (15.00 g, 90.24 mmol) was dissolved in THF (220.1 mL, 0.41 M) and cooled to 0 °C. *t*BuOK (30.36 g, 270.70 mmol, 3 eq.) was added portion-wise over 5 min. Once all the *t*BuOK had been added, the reaction was stirred for a further 5 min at 0 °C, before the cooling bath was removed and the reaction mixture allowed to equilibrate to room temperature for 1 h. The orange solution was then cooled to 0 °C, MeI (38.42 g, 16.85 mL, 270.7 mmol, 3 eq.) was added. The reaction mixture turned turquoise, and a significant amount of KI precipitated out. The reaction mixture was stirred for a further 15 min at 0 °C before the cooling bath was removed and the reaction mixture allowed to equilibrate to room temperature for 16 h. The reaction mixture was filtered through a silica pad and the filtrate was concentrated under reduced pressure yielding an orange solid. The orange solid was dry-loaded onto silica and purified by FCC (100% *n*hexane) to yield a crystalline white solid (15.03 g, 86%). *R*<sub>f</sub> 0.36 (100% *n*hexane); *v*<sub>max</sub>(neat)/cm<sup>-1</sup> 3065 w, 3026 w, 2957 w, 2971 w (aromatic C-H), 2864 w, 1439 m; δH(400 MHz, CDCl<sub>3</sub>, 7.26 ppm) 7.75 – 7.72 (2H, m, H-2/H-7), 7.46 – 7.43 (2H, m, H-3/H-6), 7.37 – 7.29 (4H, st, H-1/H-8 and H-4/H-5), 1.50 (6H, s, H-10); δC (101 MHz, CDCl<sub>3</sub>, 77.16 ppm) 153.7 (C, C-9a/C-8a), 139.3 (C, C-4a/C-5a), 127.4 (CH, C-1/C-8 or C-4/C-5), 127.1 (CH, C-1/C-8 or C-4/C-5), 122.7 (CH, C-3/C-6), 120.1 (CH, C-2/C-7), 47.0 (C, C-9), 27.3 (CH<sub>3</sub>, C-10); *m/z* (LRMS, ASAP+) 195.11 (22), 194.1095 ([M + H]<sup>+</sup>, 100%); *m/z* (HRMS, ASAP+) Found [M + H]<sup>+</sup> 194.1096. C<sub>15</sub>H<sub>14</sub> requires [M + H] 194.1095. Data matches that by Skabara and co-workers.<sup>159</sup>

**Synthesis of 9,9-dimethyl-9H-fluoreno[4,5-*cde*][1,2]dithiine **298** and 4,4-dimethyl-4H-fluoreno[4,5-*def*][1,2,3]trithiine **309****



9,9-Dimethyl-9H-fluoreno[4,5-*cde*][1,2]dithiine **298** and 4,4-dimethyl-4H-fluoreno[4,5-*def*][1,2,3]trithiine **309** are both novel compounds and were synthesised using a literature procedure.<sup>130,144</sup>

*n*BuLi (2.02 M, 25.48 mL, 51.47 mmol, 4 eq.) was added to a solution of 9,9-dimethyl fluorene **307** (2.51 g, 12.91 mmol) in TMEDA (7.72 mL, 51.47 mmol, 4 eq.). The reaction mixture was heated at 60 °C for 3 h. The reaction mixture was allowed to equilibrate to room temperature over 15 min, before further cooling to -78 °C and dilution with THF (53.6 mL, 0.24 M) and addition of sulfur (3.68 g, 114.63 mmol). After 1 h at -78 °C the cooling bath was removed and the reaction allowed to equilibrate to room temperature for 16 h. The reaction mixture was quenched with 1M HCl(aq) (30 mL) and opened to the atmosphere (air) and allowed to stir for 2 h. The reaction mixture was portioned between water (30 mL) and Et<sub>2</sub>O (30 mL). The aqueous phase was extracted with Et<sub>2</sub>O (30 mL × 2), and the combined organics were washed with brine (30 mL × 3), dried over MgSO<sub>4</sub>, filtered, and concentrated under reduced pressure yielding a brown oil. The brown oil was dry-loaded onto silica and purified by FCC (100% *n*hexane) yielding a yellow solid (1.83 g, 55%). <sup>1</sup>H NMR indicated it to be a 1:0.16 ratio of fluorene disulfide **298**:trisulfide **309**. *R*<sub>f</sub> 0.52 (100% *n*hexane); m.p. 77 – 80 °C (from *n*hexane); *v*<sub>max</sub>(neat)/cm<sup>-1</sup> 3033 w br, 2961 w, 2919 w, 2859 w, 1451 m, 1451 m, 1431 m, 1408 m, 1398 m; δH (400 MHz, CDCl<sub>3</sub>, 7.26 ppm) 7.23 (2H, app. t, *J* = 7.5 Hz, H-2/H-7), 7.20 (2H, dd, *J* = 7.6,

1.4 Hz, H-1/H-8), 7.06 (2H, dd,  $J = 7, 1.5$  Hz, H-3/H-6), 1.47 (6H, s, H-10);  $\delta C$  (101 MHz,  $CDCl_3$ , 77.16 ppm) 153.3 (C, C-9a/C-8a), 135.7 (C-S, C-4/C-5), 129.6 (CH, C-2/C-7), 125.5 (C, C-4a/C-5a), 123.9 (CH, C-3/C-6), 121.4 (CH, C-1/C-8), 48.5 (C, C-9), 26.2 ( $CH_3$ , C10);  $m/z$  (LRMS, ASAP+) 258.04 (10), 257.04 (13), 256.04 (100%);  $m/z$  (HRMS, ASAP+) Found  $[M]^+$  256.0387.  $C_{15}H_{12}S_2$  requires  $[M]^+$  256.0381.

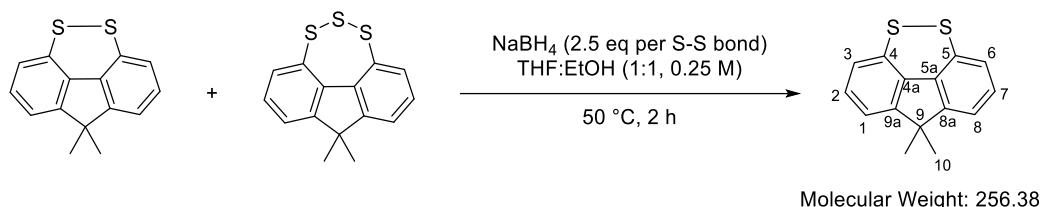
**Also isolated from the disulfide synthesis 4,4-dimethyl-4*H*-fluoreno[4,5-*def*][1,2,3]trithiepine 309**

$R_f$  0.52 (100% *n*hexane); m.p. 92 – 96 °C (from *n*hexane);  $\nu_{max}(neat)/cm^{-1}$  3042 w br, 2961 m, 2919 m, 2859 m, 1397 m;  $\delta H$  (400 MHz,  $CDCl_3$ , 7.26 ppm) 7.45 (2H, dd,  $J = 6.5, 1.3$  Hz), 7.43 (2H, dd,  $J = 6.8$  Hz + 1.1 Hz), 7.28 (2H, dd,  $J = 6.8$  Hz + 6.5 Hz, H-2/H-7), 1.53 (6H, s, H-10);  $\delta C$  (101 MHz,  $CDCl_3$ , 77.16 ppm) 157.6 (C, C-9a/C-8a), 138.9 (C, C-4/C-5), 138.7 (CH, C-2/ C-7), 128.5 (C, C-4a/C-5a), 126.5 (CH, C-3/C-6), 122.0 (CH, C-1/C-8), 46.6 (C, C-9), 28.1 ( $CH_3$ , C-10), 27.9 ( $CH_3$ , C-10');  $m/z$  (LRMS, ASAP+) 290.01 (12), 289.01 (15), 288.05 (10), 288.01 ( $[M]^+$  100%);  $m/z$  (HRMS, ASAP+) Found  $[M]^+$  288.0107.  $C_{15}H_{12}S_3$  requires  $[M]^+$  288.0101.

Disulfide **298**:Trisulfide **309** (1:0.16).

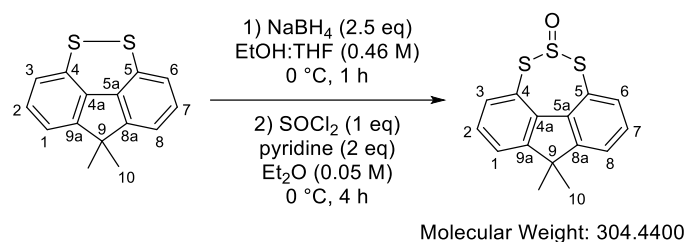


Reduction of 9,9-dimethyl-9*H*-fluoreno[4,5-*cde*][1,2]dithiine **298**/4,4-dimethyl-4*H*-fluoreno[4,5-*def*][1,2,3]trithiine **309** mixture to 9,9-dimethyl-9*H*-fluoreno[4,5-*cde*][1,2]dithiine **298**



A solution of fluorene disulfide **298**/trisulfide **309** mixture (1.927 g, 17.8:1, 7.04 mmol of disulfide and 0.42 mmol of trisulfide) in THF (15 mL) was added to a solution of  $\text{NaBH}_4$  (0.747 g, 19.70 mmol, 2.5 eq per S-S bond) at room temperature. The reaction mixture was heated at 50 °C for 2 h open to the atmosphere. The reaction mixture was allowed to equilibrate to room temperature and stirred for a further 2 days. The reaction mixture was quenched with 1 M  $\text{HCl(aq)}$  (50 mL) and stirred for a further 12 hours open to the atmosphere. The reaction mixture was then extracted with  $\text{CH}_2\text{Cl}_2$  (50 mL  $\times$  2). The combined organics were washed with brine (50 mL  $\times$  3), dried over  $\text{MgSO}_4$ , filtered and concentrated under reduced pressure to yield a yellow solid. The yellow solid was dry-loaded onto silica and purified by FCC (*n*hexane) to yield a yellow solid (1.764 g, 92%). Data matched the data as reported previously.

## Synthesis of 4,4-dimethyl-4*H*-fluoreno[4,5-*def*][1,2,3]trithiepine-9-oxide **301**

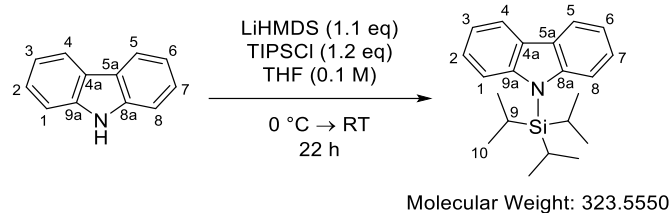


4,4-dimethyl-4*H*-fluoreno[4,5-*def*][1,2,3]trithiepine-9-oxide **301** is a novel compound and synthesised using a literature procedure.<sup>42,43</sup>

A solution of NaBH<sub>4</sub> (509 mg, 13.5 mmol) in EtOH (6.31 mL) was added in one portion to a solution of 9,9-dimethyl fluorene disulfide **298** (1.36 g, 5.30 mmol) in THF (5.30 mL) at 0 °C (Large quantities of gas formed – a bleed needle is required in order to reduce pressure). Once effervescence had ceased, the reaction mixture was stirred at 0 °C for 1 h. The reaction was quenched with 1M HCl(aq) (60 mL). CH<sub>2</sub>Cl<sub>2</sub> (50 mL) was added, the aqueous separated, and further extracted with CH<sub>2</sub>Cl<sub>2</sub> (50 mL × 2) and the combined organics were washed with brine (50 mL × 3), dried over MgSO<sub>4</sub>, filtered, and concentrated under reduced pressure yielding an off-white oil (**WARNING**: Dithiol – **STENCH!**). The resulting dithiol was immediately dissolved in Et<sub>2</sub>O (177 mL) and added to a dropping funnel containing pyridine (0.48 mL, 5.99 mmol). The mixture was added dropwise to a solution of SOCl<sub>2</sub> (0.56 mL, 7.69 mmol) in Et<sub>2</sub>O (480 mL) over 20 min at 0 °C. A white solid precipitated and the solution turned yellow. The reaction mixture was stirred at 0 °C for 4 h. The reaction was quenched with 10% H<sub>2</sub>SO<sub>4</sub> (50 mL) and separated. The aqueous layer was extracted with Et<sub>2</sub>O (50 mL × 3), and the combined organics were washed sequentially with water (50 mL), then brine (50 mL), dried over MgSO<sub>4</sub>, filtered, and concentrated under reduced pressure to yield a pale-yellow solid. The solid was purified by FCC (*n*hexane) to afford disulfide. Further elution (*n*hexane:Et<sub>2</sub>O, 7:3) afforded a pale-

yellow solid (605 mg, 37%).  $R_f$  0.26 (1:1 *n*hexane:CH<sub>2</sub>Cl<sub>2</sub>); m.p. 91 – 95 °C (neat);  $\lambda_{\max}$  (EtOH) / nm 324 ( $\epsilon$  / dm<sup>3</sup>mol<sup>-1</sup>cm<sup>-1</sup> 1008), 249 (3742);  $\nu_{\max}$ (neat)/cm<sup>-1</sup> 3056 w br, 2958 w, 2919 w, 2863 w, 1101 m (SO stretch) ;  $\delta$ H (400 MHz, CDCl<sub>3</sub>, 7.26 ppm) 7.55 (2H, dd,  $J$  = 7.1, 1.6 Hz, H-1/H-8), 7.44 (2H, app. t,  $J$  = 7.8, 7.1 Hz, H-2/H-7), 7.40 (2H, dd,  $J$  = 7.8, 1.6 Hz, H-3/H-6), 1.57 (3H, s, H-10/H-10'), 1.54 (3H, s, H-10/H-10');  $\delta$ C (101 MHz, CDCl<sub>3</sub>, 77.0 ppm) 156.9, 140.0, 132.2, 128.5, 123.9, 123.1, 46.3 (C, C-9), 28.1 (CH<sub>3</sub>, C-10), 27.8 (C-10'); m/z (HRMS, ASAP+) Found [M + H]<sup>+</sup> 305.0122. C<sub>15</sub>H<sub>13</sub>S<sub>3</sub>O requires [M + H]<sup>+</sup> 305.0129.

## Synthesis of 9-(triisopropylsilyl)-9*H*-carbazole **286**

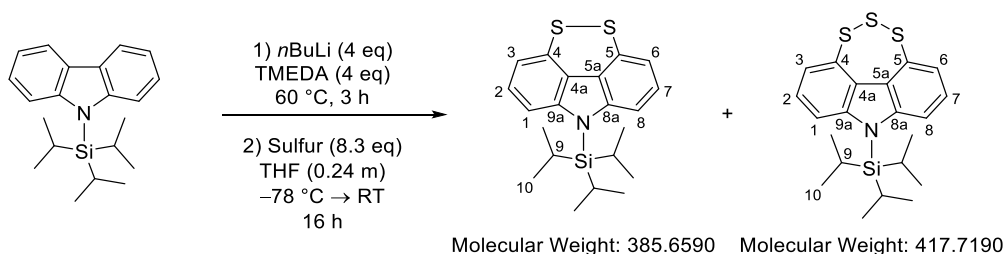


9-(triisopropylsilyl)-9*H*-carbazole **286** was synthesised using a literature procedure.<sup>225</sup>

A solution of LiHMDS in THF (1.3 M, 25.3 mL, 32.9 mmol) was added dropwise to a solution of carbazole (5.00 g, 29.9 mmol) in anhydrous THF (300 mL) at 0 °C over 5 min. The reaction mixture was allowed to stir at 0 °C for 15 min. TIPSCl (7.7 mL, 35.9 mmol) was added in one portion and the reaction mixture was allowed to stir at 0 °C for a further 15 min. The cooling bath was removed, and the reaction was stirred for 22 h at room temperature. The reaction mixture was concentrated under reduced pressure and redissolved in EtOAc (50 mL) and separated with water (50 mL). The aqueous layer was extracted with EtOAc (50 mL × 2), and the combined organics were washed with water (50 mL) and brine (50 mL), dried over MgSO<sub>4</sub>, filtered, and concentrated under reduced pressure to yield a beige solid. The reaction mixture was dry-loaded onto silica and purified by FCC to yield a white solid (9.00 g, 93%). *R<sub>f</sub>* 0.25 (*n*hexane); m.p. 88 – 90 °C (from *n*hexane);  $\nu_{\text{max}}$ (neat)/cm<sup>-1</sup> 3061 w br, 2960 w, 2945 w, 2890 w, 2867 w, 1442 s;  $\delta$ H (400 MHz, CDCl<sub>3</sub>, 7.26 ppm) 8.07 (2H, ddd, *J* = 7.7, 1.4, 0.7 Hz, H-4/H-5), 7.70 (2H, app. dt, *J* = 8.5 Hz, 0.8 Hz, H-1/H-8), 7.36 (2H, ddd, *J* = 8.5, 7.1, 1.5 Hz, H-2/H-7), 7.23 (2H, ddd, *J* = 7.8, 7.1, 0.8 Hz H-3/H-6) 2.01 (3H, hept, *J* = 7.5 Hz, H-9), 1.20 (18H, d, *J* = 7.5 Hz, H-10);  $\delta$ C (101 MHz, CDCl<sub>3</sub>, 77.16 ppm) 145.2 (C, C-9a/C-8a), 126.6 (C, C-4a/C-5a), 125.4 (CH, C-2/C-7), 119.8 (CH, C-4/C-5), 119.6 (CH, C-3/C-6), 114.2 (CH, C-1/C-8), 18.8 (CH, C-9), 14.0 (CH<sub>3</sub>, C-10); *m/z* (HRMS, ASAP+) 326.2165 (10), 325.2180 (22), 324.2155 ([*M* + *H*]<sup>+</sup>, 100%);

m/z (HRMS, ASAP+) Found [M + H]<sup>+</sup> 324.2155. C<sub>21</sub>H<sub>29</sub>NSi requires [M + H] 324.2148. Data matched that by Baran and co-workers.<sup>225</sup>

**Synthesis of 9-(triisopropylsilyl)-9H-[1,2]dithiino[3,4,5,6-*def*]carbazole **295** and 4-(triisopropylsilyl)-4H-[1,2,3]trithiepine[4,5,6,7-*def*]carbazole **296****



9-(triisopropylsilyl)-9H-[1,2]dithiino[3,4,5,6-*def*]carbazole **295** and 4-(triisopropylsilyl)-4H-[1,2,3]trithiepine[4,5,6,7-*def*]carbazole **292** are novel compounds and were synthesised from a modified literature procedure.<sup>129,144</sup>

*n*BuLi (1.68 M, 3.68 mL, 6.18 mmol, 4 eq.) was added to a solution of TIPS-carbazole **286** (502 mg, 1.55 mmol) in TMEDA (0.93 mL, 6.18 mmol, 4 eq) and the reaction mixture was heated at 60 °C for 3 h. The reaction mixture allowed to equilibrate to room temperature over 15 min, before further cooling to −78 °C and dilution with anhydrous THF (6.4 mL, 0.24 M). Sulfur (412 mg, 12.8 mmol, 8.3 eq.) was added. After 1 h at −78 °C, the reaction allowed to equilibrate to room temperature for 16 h. The reaction mixture was quenched with 1M HCl(aq) (30 mL) and opened to the atmosphere (air) and air was forcefully bubbled through the reaction mixture for 1 h. The reaction mixture was extracted using CH<sub>2</sub>Cl<sub>2</sub> (50 mL × 3) and the combined organics were washed with brine (50 mL × 3), dried over MgSO<sub>4</sub>, filtered, and concentrated under reduced pressure yielding a brown oil. The brown oil was dry-loaded onto silica and purified by FCC (100% *n*hexane) yielding a yellow solid (327 mg, 55%). *R*<sub>f</sub> 0.46 (*n*hexane); m.p. 142 – 146 °C (from *n*hexane, lit = 141 – 143 °C); *v*<sub>max</sub>(neat)/cm<sup>−1</sup> 2946 m, 2865 m, 1425 s, 1253 s;  $\delta$ H (400 MHz, CDCl<sub>3</sub>, 7.26 ppm) 7.47 (2H, dd, *J* = 8.5, 0.5 Hz, H-3/H-6), 7.30

(2H, dd,  $J = 8.5, 7.5$  Hz, H-2/H-7), 7.00 (2H, dd,  $J = 7.4, 0.5$  Hz, H-1/H-8), 1.95 (3H, hept,  $J = 7.6$  Hz, H-9) 1.19 (18H, d,  $J = 7.6$  Hz, H-10);  $\delta C$  (101 MHz,  $CDCl_3$ , 77.16 ppm) 144.2 (C, C-9a/C-8a), 127.5 (CH, C-2/C-7), 124.3 (CS, C-4/C-5), 123.6 (C, C-4a/C-5a), 117.0 (CH, C-1/C-8), 113.8 (CH, C-3/C-6), 18.6 ( $CH_3$ , C-10), 13.9 (CH, C-9);  $m/z$  (LRMS, ASAP+) 388.14 (15), 387.15 (30), 386.14 ( $[M + H]^+$ , 100%)  $m/z$  (HRMS, ASAP+) Found  $[M + H]^+$  386.1436.  $C_{21}H_{27}S_2NSi$  requires  $[M + H]$  386.1432. Data matches that by Grainger and co-workers.<sup>129</sup>

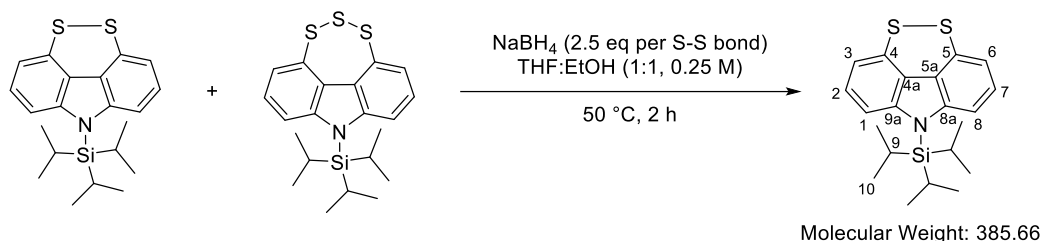
**Also isolated from the disulfide synthesis Synthesis of 4-(triisopropylsilyl)-4H-[1,2,3]trithiepine[4,5,6,7-*def*]carbazole **296****

$nBuLi$  (2.39 M, 20.69 mL, 49.45 mmol, 4 eq.) was added to a solution of TIPS-carbazole **282** (4.00 g, 12.36 mmol) in TMEDA (7.41 mL, 49.45 mmol, 4 eq) and the reaction mixture was heated at 60 °C for 3 h. The reaction mixture allowed to equilibrate to room temperature over 15 min, before further cooling to -78 °C and dilution with THF (52 mL, 0.24 M). Sulfur (3.29 g, 102.59 mmol, 8.3 eq.) was added. After 1 h at -78 °C the reaction allowed to equilibrate to room temperature for 16 h. The reaction mixture was quenched with 1M HCl(aq) (60 mL) and opened to the atmosphere (air) and air was forcefully bubbled through the reaction mixture for 1 h. The reaction mixture was extracted with  $CH_2Cl_2$  (50 mL  $\times$  3), and the combined organics were washed with water (50 mL) and brine (50 mL), dried over  $MgSO_4$ , filtered, and concentrated under reduced pressure yielding a brown oil. The brown oil was dry-loaded onto silica and purified by FCC (100% *n*hexane) yielding a yellow solid (3.28g).  $^1H$  NMR indicated it to be a 1:0.27 ratio of trisulfide **296**:disulfide **295**. 65%.  $R_f$  0.46 (*n*hexane);  $\nu_{max}(\text{neat})/cm^{-1}$  2946 m, 2866 m, 1410 s, 1274 s;  $\delta H$  (400 MHz,  $CDCl_3$ , 7.26 ppm) 7.77 (2H, dd,  $J = 8.2, 1.3$  Hz, H-3/H-6), 7.35 (2H, dd,  $J = 7.5, 1.2$  Hz, H-1/H-8), 7.31 (2H, dd,  $J = 8.2, 7.5$  Hz, H-2/H-7), 2.02 (3H, hept,  $J = 7.5$  Hz, H-9) 1.19 (18H, d,  $J = 7.5$  Hz, H-10);  $\delta C$  (101 MHz,  $CDCl_3$ , 77.16 ppm) 147.6

(C, C-9a/C-8a), 137.0 (CS, C-4/C-5), 125.5 (C, C-4a/C-5a), 124.2 (CH, C-2/C-7), 121.5 (CH, C-1/C-8), 113.6 (CH, C-3/C-6), 18.8 (CH<sub>3</sub>, C-10), 14.1 (CH, C-9); m/z (LRMS, ASAP+) 420.11 (20), 419.12 (27), 418.12 ([M + H]<sup>+</sup>, 100%), 417.11 (8) m/z (HRMS, ASAP+) Found [M + H]<sup>+</sup> 418.1150. C<sub>21</sub>H<sub>27</sub>S<sub>3</sub>NSi requires [M + H] 418.1153. Data matches that by Grainger and co-workers.<sup>129</sup>

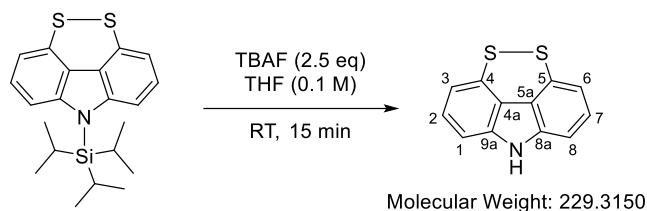


Reduction of 9-(triisopropylsilyl)-9*H*-[1,2]dithiino[3,4,5,6-*def*]carbazole **295**/4-(triisopropylsilyl)-4*H*-[1,2,3]trithiepine[4,5,6,7-*def*]carbazole **296** mixture to 9-(triisopropylsilyl)-9*H*-[1,2]dithiino[3,4,5,6-*def*]carbazole **295**



A solution of TIPS-carbazole disulfide **295**/trisulfide **296** mixture (3.040 g, 1.98 mmol of disulfide and 5.50 mmol of trisulfide) in THF (20 mL) was added to a solution of NaBH<sub>4</sub> (1.238 g, 32.72 mmol, 2.5 eq per S-S bond) in EtOH (65 mL) at room temperature. Once effervescence had ceased, the reaction mixture was heated at 50 °C for 2 h. The reaction mixture was allowed to equilibrate to room temperature. The reaction mixture was quenched with 1 M NaOH(aq) (50 mL) and a force flow of air was bubbled through the reaction mixture for 1.5 h. The reaction mixture was extracted with CH<sub>2</sub>Cl<sub>2</sub> (50 mL × 2). The combined organics were washed with water (50 mL), brine (50 mL), dried over MgSO<sub>4</sub>, filtered, and concentrated under reduced pressure to yield a yellow solid (2.198 g, 76%). No purification was required. Data matches that by Grainger and co-workers.<sup>129</sup>

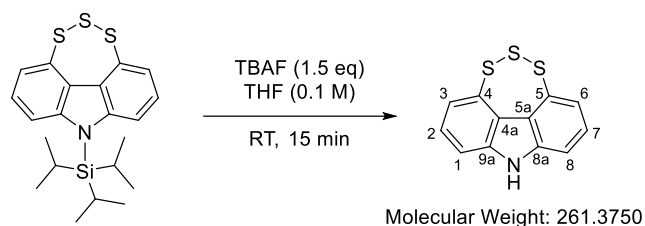
## Synthesis of 9H-[1,2]dithiino[3,4,5,6-def]carbazole **311**



9H-[1,2]dithiino[3,4,5,6-def]carbazole **31** is a novel compound and was prepared from a modified literature procedure.<sup>226</sup>

TBAF in THF (1 M, 6.48 mL, 6.48 mmol, 2.5 eq.) was added in one portion to a solution of TIPS-carbazole disulfide **295** (1.00 g, 2.59 mmol) in THF (26 mL, 0.1 M). The reaction mixture immediately turned from yellow to red. The reaction mixture was concentrated under reduced pressure and redissolved in CH<sub>2</sub>Cl<sub>2</sub> (50 mL). The organics were washed with water (2 × 20 mL) and brine (20 mL), dried over MgSO<sub>4</sub>, filtered, and concentrated under reduced pressure to yield a red solid. The reaction mixture was dry loaded onto silica and purified by FCC (Et<sub>2</sub>O: *n*hexane, 1:1) to yield a yellow solid (389 mg, 66%). *R<sub>f</sub>* 0.25 (*n*hexane);  $\nu_{\text{max}}$ (neat)/cm<sup>-1</sup> 3425.66 m (N-H), 3402 w, 3356 w br, 1433 m;  $\delta$ H (400 MHz, CDCl<sub>3</sub>, 7.26 ppm) 8.01 (1H, br. s, N-H), 7.33 (2H, dd, *J* = 8.2, 7.4 Hz, H-2/H-7), 7.23 (2H, dd, *J* = 8.2, 0.6 Hz, H-3/H-6), 6.99 (2H, dd, *J* = 7.4, 0.6 Hz, H-1/H-8);  $\delta$ C (101 MHz, CDCl<sub>3</sub>, 77.0 ppm) 138.0 (C, C-9a/C-8a), 128.2 (CH, C-2/C-7), 124.5 (CS, C-4/C-5), 120.9 (C, C-4a/C-5a), 116.5 (CH, C-1/8), 110.2 (CH, C-3/C-6); *m/z* (LRMS, ASAP+) 233.14 (8), 232.01 (11), 231.01 (20), 230.01 (68), 229.00 ([M]<sup>+</sup>, 100%); *m/z* (HRMS, ASAP+) Found [M]<sup>+</sup> 229.0031. C<sub>12</sub>H<sub>7</sub>S<sub>2</sub>N requires [M]<sup>+</sup> 229.0020. Found [M + H]<sup>+</sup> 230.0098. C<sub>12</sub>H<sub>7</sub>S<sub>2</sub>N requires [M + H] 229.0098. Data matches that by Grainger and co-workers.<sup>129</sup>

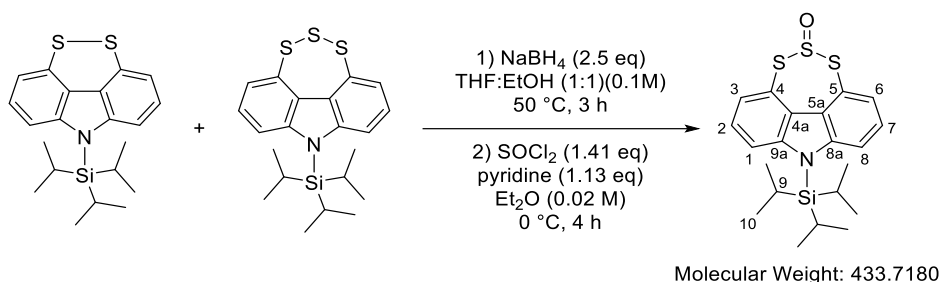
## Synthesis of 4*H*-[1,2,3]trithiepino[4,5,6,7-*def*]carbazole **329**



4*H*-[1,2,3]trithiepino[4,5,6,7-*def*]carbazole **329** is a novel compound and was prepared from a modified literature procedure.<sup>226</sup>

TBAF in THF (1 M, 0.36 mL, 0.36 mmol, 1.5 eq.) was added in one portion to a solution of TIPS-carbazole trisulfide **296** (101 mg, 0.242 mmol) in THF (2.4 mL, 0.1 M). The reaction mixture immediately turned from yellow to red. The reaction mixture was concentrated under reduced pressure and redissolved in CH<sub>2</sub>Cl<sub>2</sub> (20 mL) and separated with water (20 mL). The aqueous layer was extracted with CH<sub>2</sub>Cl<sub>2</sub> (3 × 10 mL). The combined organics were washed with water (2 × 10 mL), dried over MgSO<sub>4</sub>, filtered, and concentrated under reduced pressure to yield a red solid. The reaction mixture was dry loaded onto silica and purified by FCC (Et<sub>2</sub>O:*n*hexane, 1 :1) to yield a yellow solid (54 mg, 86%); *R*<sub>f</sub> 0.08 (9:1, *n*hexane:EtOAc); m.p. 141 – 151 °C;  $\nu_{\text{max}}$ (neat)/cm<sup>-1</sup> 3391 m br (N-H), 3053 w, 1421 m, 1318 m;  $\delta$ H (400 MHz, CDCl<sub>3</sub>, 7.26 ppm) 8.56 (1H, br. s, N-H), 7.45 (2H, dd, *J* = 7.6, 1.5 Hz, H-1/H-8), 7.37 (2H, app. t, *J* = 7.6 Hz, H-2/H-7), 7.33 (2H, dd, *J* = 7.4, 1.5 Hz, C-3/C-6);  $\delta$ C (101 MHz, CDCl<sub>3</sub>, 77.16 ppm) 141.4 (C-9a/8a), 137.8 (C-4/C-5), 125.3 (C-2/C-7), 122.5 (C-4a/C-5a), 120.8 (C-3/C-6), 110.2 (C-1/C-8); *m/z* (M<sup>+</sup>, 260.9751), (M+H, 261.9864). *m/z* (HRMS, ASAP+) Found [M]<sup>+</sup> 260.9751 and [M + H]<sup>+</sup> 261.9864. C<sub>12</sub>H<sub>7</sub>S<sub>3</sub>N requires [M]<sup>+</sup> 260.9741 and [M + H] 261.9819.

## Synthesis of 4-(triisopropylsilyl)-4*H*-[1,2,3]trithiepine[4,5,6,7-*def*]carbazole-9-oxide **302**

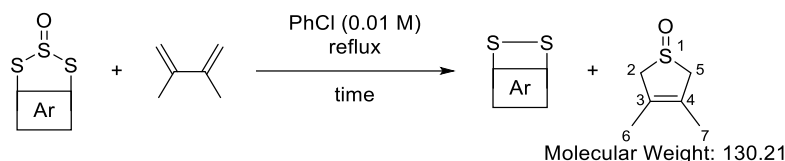


4-(triisopropylsilyl)-4*H*-[1,2,3]trithiepine[4,5,6,7-*def*]carbazole-9-oxide **302** is a novel compound and was synthesised using a literature procedure.<sup>42,43</sup>

TIPS-carbazole trisulfide **296**/disulfide **295** (661 mg, 1:0.72, 0.684 mmol [disulfide] and 0.951 mmol [trisulfide]) was dissolved in THF:EtOH (16 mL, 1:1, 0.1 M). NaBH<sub>4</sub> (245 mg, 6.465 mmol, 2.5 eq per S-S bond) was added. Once effervescence had ceased, the reaction was heated at 50 °C for 3 h. The reaction mixture was quenched with 1 M HCl(aq) (10 mL) and extracted with CH<sub>2</sub>Cl<sub>2</sub> (3 × 15 mL). The combined organics were washed with water (10 mL) and brine (10 mL), dried over MgSO<sub>4</sub>, filtered, and concentrated under reduced pressure to yield an off-white oil. The oil was dissolved in Et<sub>2</sub>O (anhydrous, 55 mL) and pyridine (anhydrous, 0.15 mL, 1.9 mmol, 1.13 eq.) was added. SOCl<sub>2</sub> (0.17 mL, 2.3 mmol) in Et<sub>2</sub>O (anhydrous, 27 mL) was added to a pressure-equalising dropping-funnel and was added to the dithiol solution at 0 °C over 30 min. The reaction was allowed to equilibrate to room temperature over 4 h. A white solid crashed out and the solution turned yellow. The reaction mixture was washed with 10% H<sub>2</sub>SO<sub>4</sub>(aq) (30 mL), water (30 mL) and brine (30 mL), dried over MgSO<sub>4</sub>, filtered, and concentrated under reduced pressure to yield a yellow solid. The yellow solid was dry-loaded onto silica and purified by FFC (*n*hexane:CH<sub>2</sub>Cl<sub>2</sub>, 1:1) to yield a yellow solid (386 mg, 54%).

$R_f$  0.25 (*n*hexane:CH<sub>2</sub>Cl<sub>2</sub>) (1:1); m.p. 117 – 120 °C;  $\lambda_{\max}$  (CH<sub>2</sub>Cl<sub>2</sub>) / nm 381 ( $\epsilon$  / dm<sup>3</sup>mol<sup>-1</sup>cm<sup>-1</sup> 13074), 304 (20276);  $\nu_{\max}$ (neat)/cm<sup>-1</sup> 2939 m, 2857 m, 1596 w, 1571 m, 1411 m, 1272 m, 1101 s (SO stretch);  $\delta$ H (400 MHz, CDCl<sub>3</sub>, 7.26 ppm) 7.87 (2H, dd,  $J$  = 8.5, 1.5 Hz), 7.46 (2H, dd,  $J$  = 8.4, 7.5 Hz, H-2/H-7), 7.34 (2H, dd,  $J$  = 7.6, 0.9 Hz), 2.04 (3H, hept.,  $J$  = 7.5 Hz, H-9), 1.21 (18H, d,  $J$  = 7.5 Hz, H-10);  $\delta$ C (101 MHz, CDCl<sub>3</sub>, 77.16 ppm) 147.1 (C, C-9a/C-8a), 126.5, 125.8 (C-2/C-7), 125.2, 122.5, 114.8, 18.8 (C-10), 14.1 (C-9); m/z (HRMS, ASAP+) Found [M + H]<sup>+</sup> 434.1115. C<sub>21</sub>H<sub>27</sub>S<sub>3</sub>NOSi requires [M + H] 434.1102.

## Synthesis of 3,4-dimethyl-2,5-dihydrothiophene-1-oxide **20** (Pyrolysis of trisulfide-2-oxides)

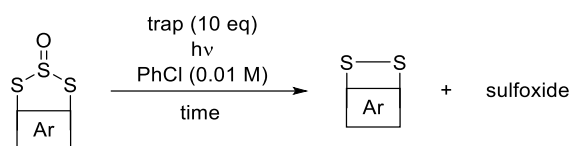


3,4-Dimethyl-2,5-dihydrothiophene-1-oxide **20** was synthesised from a modified literature procedure.<sup>42,43</sup>

Trisulfide-2-oxide was dissolved in PhCl (0.01 M) and degassed with argon for 15 min. 2,3-dimethyl-1,3-butadiene (10 eq) was added, and the reaction mixture was refluxed. Once trisulfide-2-oxide has disappeared by TLC, the reaction mixture was cooled to room temperature and the reaction mixture was concentrated under reduced pressure. The brown solid was dry loaded onto silica and purified by FFC (100% *n*hexane – elution of disulfide, then 50% CH<sub>2</sub>Cl<sub>2</sub> in *n*hexane, then 100% CH<sub>2</sub>Cl<sub>2</sub>, then 5% MeOH in CH<sub>2</sub>Cl<sub>2</sub> – elution of sulfoxide). *R<sub>f</sub>* 0.31 MeOH:CH<sub>2</sub>Cl<sub>2</sub> (5:95),  $\delta$ H(400 MHz, CDCl<sub>3</sub>, 7.26 ppm) 3.80 (2H, d, *J* = 15.9 Hz, H *cis*-to sulfoxide H-2/H-5), 3.43 (2H, d, *J* = 17.0 Hz, H *trans*-to sulfoxide H-2/H-5), 1.76 (6H, s, **CH<sub>3</sub>**, H-6/H-7);  $\delta$ C (101 MHz, CDCl<sub>3</sub>, 77.16 ppm) 126.2 (alkene C), 64.4 (CH<sub>2</sub>) and 14.6 (CH<sub>3</sub>).

Trisulfide-2-oxide	Time / h	Disulfide % yield	Sulfoxide <b>20</b> % yield
Naphthalene <b>105</b>	10	<b>105</b> 99	98
Acenaphthene <b>299</b>	6	<b>266</b> 39	14
Acenaphthylene <b>300</b>	3	<b>264</b> 16	65
Fluorene <b>301</b>	4	<b>298</b> 86	32
Carbazole <b>302</b>	3	<b>295</b> 86	58

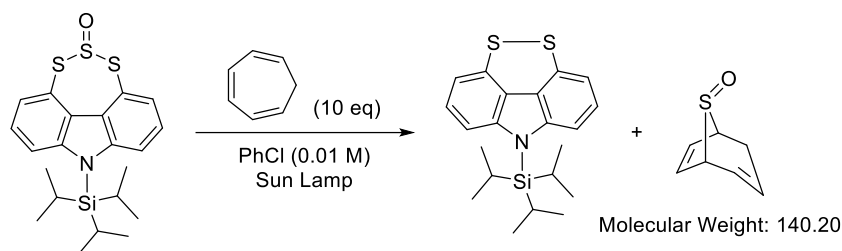
## Synthesis of 3,4-dimethyl-2,5-dihydrothiophene-1-oxide 20 (Photolysis of trisulfide-2-oxides)



Trisulfide-2-oxide was dissolved in PhCl (0.01 M) and degassed with argon for 15 min. A trap (10 eq) was added, and the reaction mixture was irradiated with a light source. Once the reaction had gone to completion by TLC, the reaction mixture was allowed to cool to room temperature and then dry-loaded onto silica and purified by FCC (100% *n*hexane – elution of disulfide, then 50% CH<sub>2</sub>Cl<sub>2</sub> in *n*hexane, then 100% CH<sub>2</sub>Cl<sub>2</sub>, then 5% MeOH in CH<sub>2</sub>Cl<sub>2</sub> – elution of sulfoxide).

Trisulfide-2-oxide	Time / h	Light source	Trap	Disulfide % yield	Sulfoxide % yield
Naphthalene 105	103	Sun lamp	2,3-dimethyl-1,3-butadiene	107 93	55
Fluorene 301	4	Sun lamp	2,3-dimethyl-1,3-butadiene	298 90	6
Fluorene 301	4	Sun lamp	Cycloheptatriene	298 90	-
Carbazole 302	1.5	Sun lamp	2,3-dimethyl-1,3-butadiene	295 92	23
Carbazole 302	1.5	Sun lamp	Cycloheptatriene	295 45%	Isolated but not clean

## Synthesis of (1R,5S,8R)-8lambda4-thiabicyclo[3.2.1]octa-2,6-dien-8-one **181**

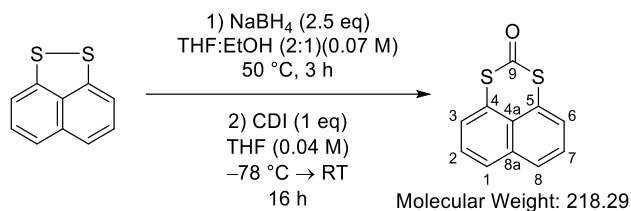


TIPS-carbazole trisulfide-2-oxide **302** (130 mg, 0.30 mmol) was dissolved in PhCl (30 mL, 0.01 M), added to a water-jacketed photochemical reactor and degassed by bubbling a stream of argon through the reaction mixture for 15 m. Cycloheptatriene **35** (0.31 mL, 10 eq.) was added, and the reaction mixture was irradiated with a sun lamp. Once the reaction had gone to completion by TLC, the reaction mixture was allowed to cool to room temperature and then dry-loaded onto silica and purified by FCC (100% *n*hexane) to yield TIPS-carbazole disulfide **291** (52 mg, 45%), (*n*hexane:CH<sub>2</sub>Cl<sub>2</sub>, 1:1, then 100% CH<sub>2</sub>Cl<sub>2</sub>, then CH<sub>2</sub>Cl<sub>2</sub>:MeOH, 95:5) to yield sulfoxide **178** as a brown oil (7 mg).  $\nu_{\text{max}}$ (neat)/cm<sup>-1</sup> 3400 br, 2923, 1718, 1079 s (S=O);  $\delta$ H(400 MHz, CDCl<sub>3</sub>, 7.26 ppm) 6.35 (1H, dd, *J* = 7.1, 4.5 Hz), 5.81 – 5.71 (1H, m), 3.60 (1H, dd, 7.0, 4.5 Hz), 3.37 (1H, d, *J* = 4.2 Hz), 2.70 (1H, dddd, *J* = 19.7, 4.4, 3.4, 2.1 Hz), 2.09 (1H, dt, *J* = 4.1, 2.2 Hz). All other peaks which are known in the literature are stacked with impurity peaks. *m/z* (HRMS, ASAP+) Found [M]<sup>+</sup> 251.0232. C<sub>12</sub>H<sub>10</sub>O<sub>2</sub>S<sub>2</sub> requires [M] 250.0122. IR and mass spectrometry data marches that by Nakayama and co-workers. The <sup>1</sup>H NMR data matches for the most part.<sup>14</sup>



## Chapter 3 experimental

### Synthesis of naphtho[1,8-*de*][1,3]dithiin-2-one **336**

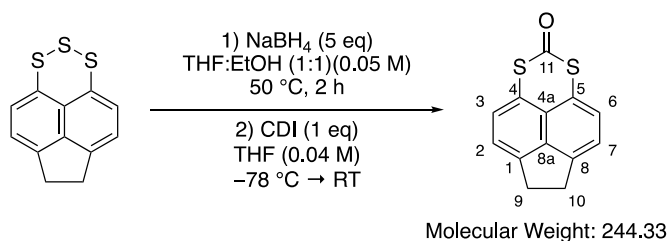


Naphtho[1,8-*de*][1,3]dithiin-2-one **336** was synthesised from a modified literature procedure.<sup>105,114</sup>

Naphthalene disulfide **107** (100 mg, 0.53 mmol) was dissolved in THF (5.3 mL, 0.1M) and EtOH (2.6 mL, 0.5 M) and  $\text{NaBH}_4$  (50 mg, 1.31 mmol) was added in one portion. Once effervescence had ceased, the reaction mixture was heated at 50 °C for 3 h. After 3 h the reaction mixture was allowed to equilibrate to room temperature and was quenched with 1 M HCl(aq) (20 mL) and separated with EtOAc (20 mL). The aqueous layer was extracted with EtOAc (20 mL  $\times$  2), and the combined organics were washed with water (20 mL) and brine (20 mL), dried over  $\text{MgSO}_4$ , filtered, and concentrated under reduced pressure. The resulting white solid was dissolved in THF (anhydrous, 8.8 mL), cooled to -78 °C and a solution of CDI (86 mg, 0.53 mmol) in THF (anhydrous, 4.4 mL) was added dropwise over 10 min. The reaction mixture was allowed to equilibrate to room temperature over 16 h. The reaction mixture was concentrated under reduced pressure to yield an off-white solid. The solid was dry-loaded onto silica and purified by FCC (100% *n*hexane until elution of disulfide, then 20% EtOAc in *n*hexane) to yield a white solid (65 mg, 57%).  $R_f$  0.28 (*n*hexane:EtOAc, 8:2); m.p. 127 – 132 °C;  $\lambda_{\text{max}}$  ( $\text{CH}_2\text{Cl}_2$ ) / nm 322 ( $\epsilon$  /  $\text{dm}^3\text{mol}^{-1}\text{cm}^{-1}$  18582);  $\nu_{\text{max}}$ (neat)/ $\text{cm}^{-1}$  3218 w, 3040 w, 1623 s (C=O stretch), 1551 s, 1206 m;  $\delta\text{H}$  (400 MHz,  $\text{CDCl}_3$ , 7.26 ppm) 7.68 (2H, dd,  $J$  = 8.4, 1.0 Hz), 7.40 (2H, dd,  $J$  = 8.2, 7.3 Hz, H-2/H-7), 7.25 (2H, dd,  $J$  = 7.3, 1.1 Hz);  $\delta\text{C}$  (101 MHz,  $\text{CDCl}_3$ , 77.16

ppm) 185.2 (SC(O)S, C-9), 135.3 , 130.6, 128.4, 126.9 (CH, C-2/C-7), 124.4, 122.2; m/z (M+H, 218.9940).

## Synthesis of 6,7-dihydroacenaphtho[5,6-*de*][1,3]dithiin-2-one **337**



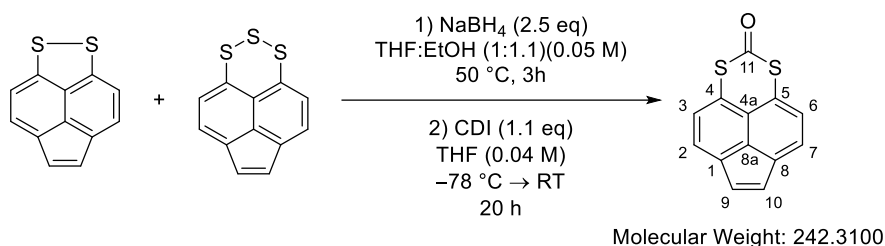
6,7-Dihydroacenaphtho[5,6-*de*][1,3]dithiin-2-one **337** is a novel compound and was synthesised from a modified literature procedure.<sup>105,114</sup>

Acenaphthene trisulfide **319** (201 mg, 0.81 mmol) was dissolved in THF:EtOH (1:1, 16.0 mL, 0.05 M) and NaBH<sub>4</sub> (156 mg, 4.05 mmol, 5 eq.) was added in one portion. Once effervescence had ceased, the reaction mixture was heated at 50 °C for 2. The reaction mixture was allowed to equilibrate to room temperature and was quenched with 1 M HCl(aq) (20 mL). The reaction mixture was extracted with Et<sub>2</sub>O (20 mL × 3). The combined organics were washed with water (20 mL) and brine (20 mL), dried over MgSO<sub>4</sub>, filtered, and concentrated under reduced pressure. The resulting white solid was dissolved in THF (anhydrous, 13.0 mL), cooled to –78 °C and a solution of CDI (132 mg, 0.81 mmol) in THF (anhydrous, 7.0 mL) was added dropwise over 10 min. The reaction mixture was allowed to equilibrate to room temperature over 16 h. The reaction mixture was concentrated under reduced pressure, dry-loaded onto silica and purified by FCC (*n*hexane:Et<sub>2</sub>O, 9:1) to yield a white solid (159 mg, 82%). *R<sub>f</sub>* 0.10 (*n*hexane); m.p. 170 – 172 °C (from *n*hexane:CH<sub>2</sub>Cl<sub>2</sub>);  $\lambda_{\text{max}}$  (CH<sub>2</sub>Cl<sub>2</sub>) / nm 327 ( $\epsilon$  / dm<sup>3</sup>mol<sup>–1</sup>cm<sup>–1</sup> 23183);  $\nu_{\text{max}}$ (neat)/cm<sup>–1</sup> 2920 w, 1619 s (C=O stretch);  $\delta$ H (400 MHz, CDCl<sub>3</sub>, 7.26 ppm) 7.41 (2H, d, *J* = 7.41 Hz, H-2/H-7), 7.06 (2H, d, *J* = 7.3 Hz, H-3/H-6), 3.33 (4H, s, H-9/H-10);  $\delta$ C (101 MHz, CDCl<sub>3</sub>, 77.16 ppm) 184.9 (C(O), C-11), 146.0 (C, C-4a), 140.1 (C, C-8a), 125.3 (C, C-1/C-8), 124.6 (CH, C-3/C-6), 121.0 (CH, C-2/C-7), 119.5 (CS, C-4/C-5), 30.5 (CH<sub>2</sub>, C-9/C-10); *m/z* (LRMS, ASAP+)

247.00 (8), 246.01 (11), 245.01 ( $[M + H]^+$ , 100%);  $m/z$  (HRMS, ASAP+) Found  $[M + H]^+$  245.0099.

$C_{13}H_8S_2O$  requires  $[M + H]$  245.0095.

## Synthesis of acenaphtho[5,6-*de*][1,3]dithin-2-one **338**

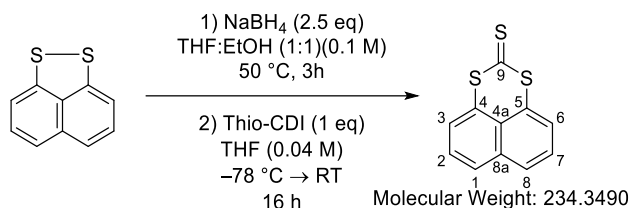


Acenaphtho[5,6-*de*][1,3]dithin-2-one **338** is a novel compound and was synthesised from a modified literature procedure.<sup>105,114</sup>

NaBH<sub>4</sub> (139 mg, 3.68 mmol, 2.5 eq.) was added in one portion to a solution of acenaphthylene disulfide **264**/trisulfide **320** mixture (0.33:1, 201 mg, 0.84 mmol) in THF (8.4 mL) and EtOH (7.4 mL). Once effervescence had ceased, the reaction mixture was heated at 50 °C for 3 h. The reaction mixture was separated using EtOAc (20 mL) and 1 M HCl(aq) (20 mL). The aqueous layer was extracted using EtOAc (20 mL). The combined organics were washed with water (20 mL), then brine (20 mL) and dried over MgSO<sub>4</sub>, filtered, and concentrated under reduced pressure to yield a yellow solid. The yellow solid was dissolved in THF (anhydrous, 14 mL) and placed under an argon atmosphere. The solution was cooled to -78 °C and a solution of CDI (149 mg, 0.92 mmol) in THF (anhydrous, 7.6 mL) was added dropwise over 15 min. The reaction mixture was allowed to equilibrate to room temperature over 20 h. The reaction mixture was concentrated under reduced pressure to yield an orange solid. The reaction mixture was dry-loaded onto silica and purified by FCC (100% *n*hexane) until elution of the disulfide **260**/trisulfide **316**, (*n*hexane:EtOAc, 8:2) then the second compound eluted to yield a yellow solid (163 mg, 80%). *R*<sub>f</sub> 0.61 (*n*hexane:Et<sub>2</sub>O, 9:1); m.p. 160 – 169 °C; λ<sub>max</sub> (CH<sub>2</sub>Cl<sub>2</sub>) / nm 396 (ε / dm<sup>3</sup>mol<sup>-1</sup>cm<sup>-1</sup> 12814), 377 (15529), 339 (8674), 301 (17272); ν<sub>max</sub>(neat)/cm<sup>-1</sup> 3197 w, 3042 w, 2926 w, 1615 s (C=O), 1420 s, 1083 s; δ<sub>H</sub> (400 MHz, CDCl<sub>3</sub>, 7.26 ppm) 7.71 (2H, d,

$J = 7.4$  Hz, C-3/C-6), 7.36 (2H, d,  $J = 7.4$  Hz, C-2/C-7), 7.12 (2H, s, C-9/C-10);  $\delta$ C (101 MHz,  $\text{CDCl}_3$ , 77.16 ppm) 182.8 (C(O), C-11), 138.8, 131.2, 128.9, 128.6, 125.4, 123.7, 115.5;  $m/z$  (LRMS, ASAP+) 244.99 (12), 244.00 (13), 242.99 ( $[\text{M} + \text{H}]^+$ , 100%);  $m/z$  (HRMS, ASAP+) Found  $[\text{M} + \text{H}]^+$  242.9944.  $\text{C}_{13}\text{H}_6\text{S}_2\text{O}$  requires  $[\text{M} + \text{H}]$  242.9938.

### Synthesis of naphtho[1,8-*de*][1,3]dithiine-2-thione **378**



naphtho[1,8-*de*][1,3]dithiine-2-thione **378** was synthesised from a modified literature procedure.<sup>105,114</sup>

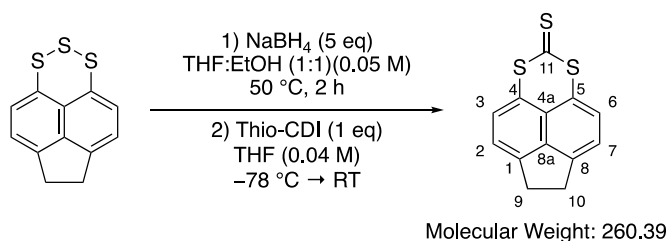
Naphthalene disulfide **107** (1.00 g, 5.26 mmol) was dissolved in THF:EtOH (1:1, 52 mL, 0.1 M) and NaBH<sub>4</sub> (497 mg, 13.14 mmol, 2.5 eq.) was added in one portion. Once effervescence had ceased, the reaction mixture was heated at 50 °C for 3 h. After 3 h the reaction mixture was allowed to equilibrate to room temperature and was quenched with 1 M HCl(aq) (50 mL). The reaction mixture was extracted with CH<sub>2</sub>Cl<sub>2</sub> (50 mL × 3). The combined organics were washed with water (50 mL) and brine (50 mL), dried over MgSO<sub>4</sub>, filtered, and concentrated under reduced pressure to yield a white solid. The resulting white solid was dissolved in THF (anhydrous, 88 mL), cooled to -78 °C and a solution of thio-CDI (937 mg, 5.26 mmol) in THF (anhydrous, 35 mL) was added dropwise over 10 min. The reaction mixture was allowed to gradually warm to room temperature over 16 h (cooling bath was not removed). The reaction mixture was concentrated under reduced pressure, redissolved in CH<sub>2</sub>Cl<sub>2</sub> (200 mL), washed with 1 M HCl(aq) (50 mL × 2) and brine (50 mL), dried over MgSO<sub>4</sub>, filtered, and concentrated under reduced pressure to yield a yellow solid (1.10 g, 89 %).

*If further purification is required dry load the solid onto silica and purify by FCC (nhexane:CH<sub>2</sub>Cl<sub>2</sub>, 8:2).*

$R_f$  0.25 (*n*hexane:CH<sub>2</sub>Cl<sub>2</sub>, 2:1); m.p. 168 – 172 °C (from *n*hexane:CH<sub>2</sub>Cl<sub>2</sub>);  $\lambda_{\max}$  (CH<sub>2</sub>Cl<sub>2</sub>) / nm 342 ( $\epsilon$  / dm<sup>3</sup>mol<sup>-1</sup>cm<sup>-1</sup> 46122) $\nu_{\max}$ (neat)/cm<sup>-1</sup> 3053 w, 2921 w, 1933 w, 941 s (C=S);  $\delta$ H (400 MHz, CDCl<sub>3</sub>, 7.26 ppm) 7.65 (2H, dd,  $J$  = 8.5, 0.9 Hz), 7.40 (2H, dd,  $J$  = 8.2, 7.3 Hz, C-3/C-6), 7.19 (2H, dd,  $J$  = 7.3, 1.1 Hz);  $\delta$ C (101 MHz, CDCl<sub>3</sub>, 77.16 ppm) 211.1 (S-C(S)-S, C-9), 135.0, 132.1, 128.6, 127.1, 121.6, 121.6;  $m/z$  (HRMS, ASAP+) Found [M + H]<sup>+</sup> 234.9715. C<sub>11</sub>H<sub>6</sub>S<sub>3</sub> requires [M + H] 234.9710.



## Synthesis of 6,7-dihydroacenaphtho[5,6-*de*][1,3]dithiine-2-thione **378**

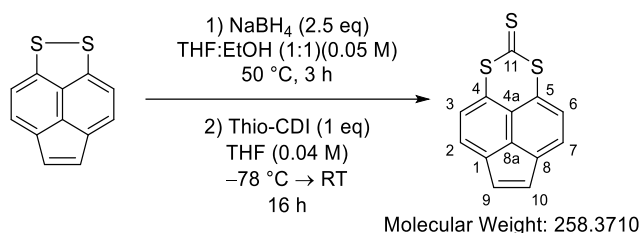


6,7-Dihydroacenaphtho[5,6-*de*][1,3]dithiine-2-thione **378** is a novel compound and was synthesised from a modified literature procedure.<sup>105,114</sup>

Acenaphthene trisulfide **319** (637 mg, 2.56 mmol) was dissolved in THF:EtOH (1:1, 25.6 mL, 0.1 M) and NaBH<sub>4</sub> (485 mg, 12.8 mmol, 2.5 eq per S-S bond) was added in one portion. Once effervescence had ceased, the reaction mixture was heated at 50 °C for 3 h. The reaction mixture was allowed to equilibrate to room temperature and was quenched with 1 M HCl(aq) (50 mL). The reaction mixture was extracted with CH<sub>2</sub>Cl<sub>2</sub> (50 mL × 2). The combined organics were washed with water (50 mL) and brine (50 mL), dried over MgSO<sub>4</sub>, filtered, and concentrated under reduced pressure. The resulting white solid was dissolved in THF (anhydrous, 46 mL), cooled to -78 °C and a solution of thio-CDI (457 mg, 2.56 mmol, 1 eq.) in THF (anhydrous, 17 mL) was added dropwise over 10 min. The reaction mixture was allowed to equilibrate to room temperature over 16 h. The reaction mixture was concentrated under reduced pressure, redissolved in CH<sub>2</sub>Cl<sub>2</sub> (200 mL) and separated with 1 M HCl(aq) (100 mL). The aqueous layer was extracted with CH<sub>2</sub>Cl<sub>2</sub> (100 mL × 2). The combined organics were washed with 1 M HCl(aq) (100 mL × 2), dried over MgSO<sub>4</sub>, filtered, and concentrated under reduced pressure to yield an orange solid (637 mg, 96%). *R*<sub>f</sub> 0.16 (*n*hexane:CH<sub>2</sub>Cl<sub>2</sub>, 4:1); m.p. 180 – 183 °C (decomp.); *v*<sub>max</sub>(neat)/cm<sup>-1</sup> 2914 m, 1568 m, 1417 m, 1000 m, 831 s (C=S); δH(400 MHz, CDCl<sub>3</sub>, 7.26 ppm) 7.18 (2H, d, *J* = 7.2 Hz, H-2/H-7), 7.03 (2H, d, *J* = 7.2 Hz, H-3/H-6), 3.34

(4H, s, H-9/H-10);  $\delta$ C (101 MHz, CDCl<sub>3</sub>, 77.16 ppm) 211.4 (C=S), 146.8 (C, C-4a), 139.9, 127.1, 122.1 (CH, C-3/C-6), 121.2 (CH, C-2/C-7), 119.3 (C-S, C-4/C-5) 30.5 (CH<sub>2</sub>, C-9/C-10); m/z (HRMS, ASAP+) Found [M + H]<sup>+</sup> 260.9871. C<sub>13</sub>H<sub>9</sub>S<sub>3</sub> requires 260.9866 [M + H].

## Synthesis of acenaphtho[5,6-*de*][1,3]dithiine-2-one **379**

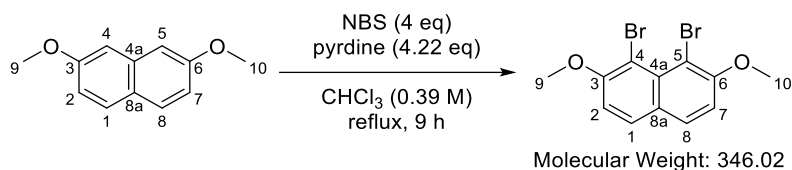


Acenaphtho[5,6-*de*][1,3]dithiine-2-one **375** is a novel compound and was synthesise from a modified literature procedure.<sup>105,114</sup>

Acenaphthylene disulfide **264** (41 mg, 0.19 mmol) was dissolved in THF:EtOH (1:1, 8 mL, 0.05 M) and NaBH<sub>4</sub> (18 mg, 0.48 mmol) was added in one portion. Once effervescence had ceased, the reaction mixture was heated at 50 °C for 3 h. The reaction mixture was allowed to equilibrate to room temperature and was quenched with 1 M HCl(aq) (20 mL). The reaction mixture was extracted with CH<sub>2</sub>Cl<sub>2</sub> (20 mL × 2). The combined organics were washed with water (10 mL) and brine (10 mL), dried over MgSO<sub>4</sub>, filtered, and concentrated under reduced pressure. The resulting yellow solid was dissolved in THF (anhydrous, 3.2 mL), cooled to -78 °C and a solution of thio-CDI (34 mg, 0.19 mmol) in THF (anhydrous, 1.26 mL) was added dropwise over 10 min. The reaction mixture was allowed to equilibrate to room temperature over 16 h. The reaction mixture was concentrated under reduced pressure, redissolved in CH<sub>2</sub>Cl<sub>2</sub> (50 mL), and separated with 1 M HCl(aq) (20 mL). The aqueous layer was extracted with CH<sub>2</sub>Cl<sub>2</sub> (10 mL × 2). The combined organics were washed with 1 M HCl(aq) (10 mL), water (10 mL), brine (10 mL) dried over MgSO<sub>4</sub>, filtered, and concentrated under reduced pressure to yield an orange solid. The orange solid was dry-loaded onto silica and was purified by FCC (*n*hexane:CH<sub>2</sub>Cl<sub>2</sub>, 8:2, twice) to yield an orange solid 17 mg. *R<sub>f</sub>* 0.16 (*n*hexane:CH<sub>2</sub>Cl<sub>2</sub>, 4:1); m.p. 180 – 183 °C (decomp.); *v*<sub>max</sub>(neat)/cm<sup>-1</sup> 2914 w, 1417 m, 1000 m, 831 s (C=S), 809 s; *δ*H (400

MHz, CDCl<sub>3</sub>, 7.26 ppm) 7.76 (2H, d,  $J = 7.4$  Hz, H-3/C-6), 7.37 (2H, d,  $J = 7.4$  Hz, H-2/H-7), 7.19 (2H, s, H-9/H-10),  $\delta$ C (101 MHz, CDCl<sub>3</sub>, 77.16 ppm),  $m/z$  (LRMS, ASAP+) 260.98 (25), 259.97 (20), 258.97 (100%);  $m/z$  (HRMS, ASAP+) Found  $[M + H]^+$  258.9714. C<sub>13</sub>H<sub>6</sub>S<sub>3</sub> requires  $[M + H]$  258.9710. Found  $[M + OH]^+$  274.9664. C<sub>13</sub>H<sub>6</sub>S<sub>3</sub> requires  $[M + OH]$  274.9659.

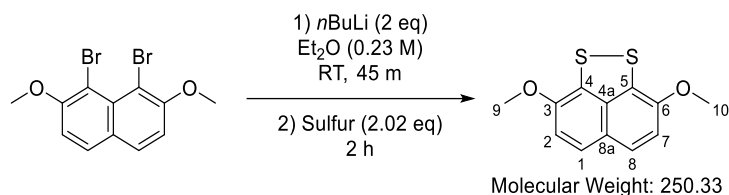
## Synthesis of 1,8-dibromo-2,7-dimethoxynaphthalene **111**



1,8-Dibromo-2,7-dimethoxynaphthalene **111** was prepared using a literature procedure.<sup>43</sup>

*N*-bromosuccinimide (1890 mg, 10.62 mmol, 4 eq.) was dissolved in CHCl<sub>3</sub> (26 mL, 0.39 M) and pyridine (0.91 mL, 11.25 mmol, 4.23 eq.) was added. The reaction mixture was brought to reflux. After 1 h at reflux, 2,7-dimethoxynaphthalene **110** (500 mg, 2.66 mmol) in CHCl<sub>3</sub> (3.9 mL) was added dropwise over 10 min. The reaction mixture was refluxed for a further 9 h. The reaction mixture was allowed to equilibrate to room temperature over 14 h. The reaction mixture was dry-loaded onto silica and purified by FCC (*n*hexane:EtOAc, 9:1) to yield an off-white solid (468 mg, 51%). *R*<sub>f</sub> 0.56 (4:1, *n*hexane:EtOAc); *v*<sub>max</sub>(neat)/cm<sup>-1</sup> 3008 w, 2975 w, 2936 w, 2838 w, 1610 m, 1501 s, 1262 s (C-O), 1239 s (C-O);  $\delta$ H (400 MHz, CDCl<sub>3</sub>, 7.26 ppm) 7.73 (2H, d, *J* = 9 Hz), 7.15 (2H, d, *J* = 9 Hz), 4.01 (6H, s, HC-9/H-10);  $\delta$ C (101 MHz, CDCl<sub>3</sub>, 77.16 ppm) 156.5 (CH, C-2/C-7), 131.7, 130.2, 127.5 (CBr, C-4/C-5), 111.7, 106.1, 57.3 (CH<sub>3</sub>, C-9/C-10); *m/z* (HRMS, ASAP+) Found [M + H]<sup>+</sup> 346.9108 C<sub>12</sub>H<sub>11</sub>O<sub>2</sub>Br<sub>2</sub> requires 346.9106 [M + H]. Data matches that by Grainger and co-workers.<sup>43</sup>

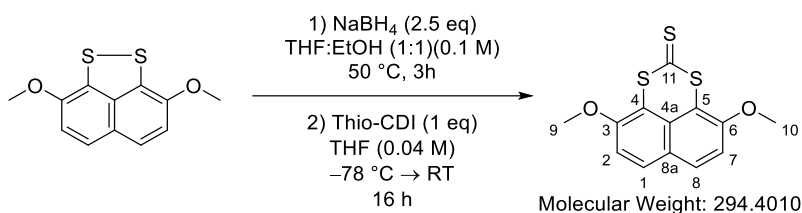
## Synthesis of 3,8-dimethoxynaphtho[1,8-*cd*][1,2]dithiole **112**



3,8-Dimethoxynaphtho[1,8-*cd*][1,2]dithiole **112** was synthesised using a literature procedure.<sup>43</sup>

1,8-dibromo-2,7-dimethoxynaphthalene **111** (400 mg, 1.16 mmol) was suspended in Et<sub>2</sub>O (anhydrous, 5.00 mL, 0.23 M). *n*BuLi (0.97 mL, 2.38 M, 2.31 mmol, 2 eq.) was added dropwise over 10 min and the reaction went from a white suspension to a grey suspension. The grey suspension was stirred for a further 45 min. Sulfur (75 mg, 2.34 mmol, 2.02 eq.) was added in one portion and the reaction mixture was allowed to stir for a further 2 h. 1 M HCl(aq) (20 mL) was added to the reaction mixture and the organic layer was washed with water (10 mL) and brine (10 mL), dried over MgSO<sub>4</sub>, filtered, and concentrated under reduced pressure. The resulting orange oil was dry loaded onto silica and purified by FCC (*n*hexane:EtOAc, 9:1) to yield a red solid (115 mg, 40%). *R*<sub>f</sub> 0.34 (*n*hexane:EtOAc, 9:1); *v*<sub>max</sub>(neat)/cm<sup>-1</sup>;  $\delta$ H (400 MHz, CDCl<sub>3</sub>, 7.26 ppm) 7.18 (2H, d, *J* = 7.2 Hz, H-3/H-6), 7.03 (2H, d, *J* = 7.2 Hz, H-2/H-7), 3.34 (4H, s, H-9/H-10);  $\delta$ C (101 MHz, CDCl<sub>3</sub>, 77.16 ppm) 145.7 (C4a), 139.9 (C-1/C-8 or C-8a), 127.1 (C-1/C-8 or C-8a), 122.1 (CH, C-3/C-6), 121.2 (CH, C-2/C-7), 119.3 (C-S, C-4/C-5), 30.5 (OCH<sub>3</sub>, C-9/C-10); *m/z* (HRMS, ASAP+) Found [M]<sup>+</sup> 251.0232. C<sub>12</sub>H<sub>10</sub>O<sub>2</sub>S<sub>2</sub> requires [M] 250.0122. Data matches that by Grainger and co-workers.<sup>43</sup>

## Synthesis of 4,9-dimethoxynaphtho[1,8-*de*][1,3]dithiine-2-thione **376**



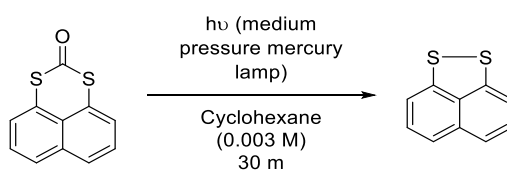
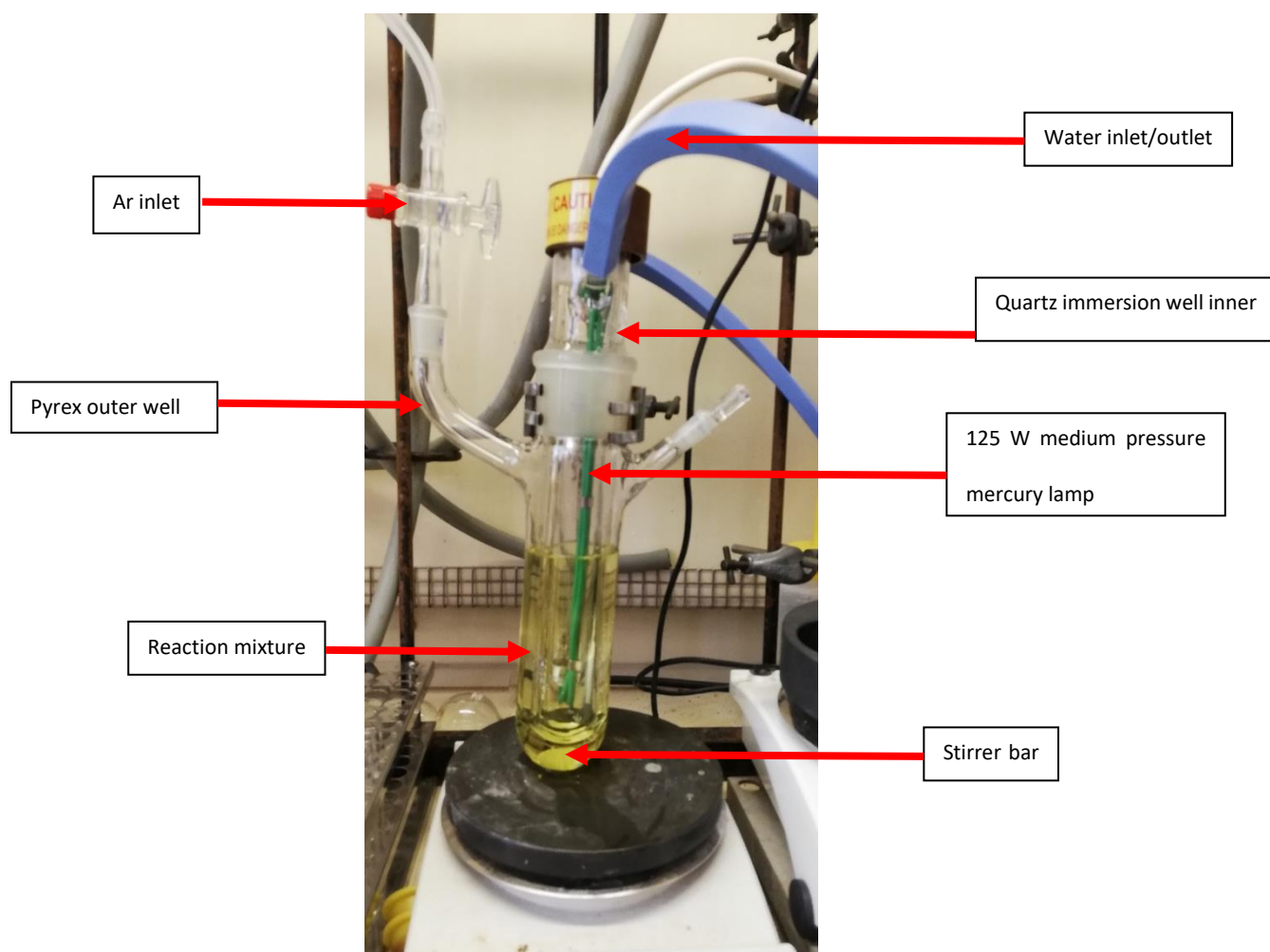
4,9-Dimethoxynaphtho[1,8-*de*][1,3]dithiine-2-thione **376** is a novel compound and was synthesised from a modified literature procedure.<sup>105,114</sup>

1,8-disulfide-2,7-dimethoxynaphthalene **112** (94 mg, 0.38 mmol) was dissolved in THF:EtOH (1:1, 4.00 mL, 0.01 M) and  $\text{NaBH}_4$  (36 mg, 0.94 mmol, 2.5 eq.) was added in one portion. Once effervescence had ceased, the reaction mixture was heated at 50 °C for 3 h. The reaction mixture was allowed to equilibrate to room temperature and 1 M  $\text{HCl(aq)}$  (20 mL) was added. The reaction mixture was extracted with  $\text{CH}_2\text{Cl}_2$  (10 mL  $\times$  2), and the combined organics were washed with water (10 mL) and brine (10 mL), dried over  $\text{MgSO}_4$ , filtered, and concentrated under reduced pressure to yield a red solid. The red solid was dissolved in THF (anhydrous, 7 mL) cooled to -78 °C. Thio-CDI (71 mg, 0.40 mmol) was dissolved in THF (anhydrous, 3 mL) and added dropwise to the dithiol over 10 min. After 2 h at -78 °C, the reaction mixture was allowed to equilibrate to room temperature over 16 h. The solvent was removed under reduced pressure, redissolved in  $\text{CH}_2\text{Cl}_2$  (20 mL), and washed with 1 M  $\text{HCl(aq)}$  (20 mL) and brine (20 mL), dried over  $\text{MgSO}_4$ , filtered, and concentrated under reduced pressure to yield an orange solid. The orange solid was dry-loaded onto silica and purified by FCC (*n*hexane:EtOAc, 9:1 $\rightarrow$ 1:1). A lot of orange solid was left on the dry-load. The column was flushed with *n*hexane: $\text{CH}_2\text{Cl}_2$  (1:1). An orange solid was isolated (36 mg, 33%). m.p. 230 – 232 °C (decomp);  $\nu_{\text{max}}$ (neat)/ $\text{cm}^{-1}$ ;  $\delta\text{H}$  (400 MHz,  $\text{CDCl}_3$ , 7.26 ppm) 7.62 (2H, d,  $J$  = 9.1 Hz), 7.10 (2H, d,  $J$  = 9.1 Hz), 3.99 (6H, s, H-9/H-10);  $\delta\text{C}$  (101 MHz,  $\text{CDCl}_3$ , 77.16 ppm) 212.1, 150.3, 129.0,

125.5, 122.9, 115.6, 111.7, 57.1; m/z (HRMS, ASAP+) Found  $[M + H]^+$  294.9921.  $C_{13}H_{11}S_3O_2$   
requires  $[M + H]$  294.9924.



## Photolysis of dithiocarbonates (CO release)

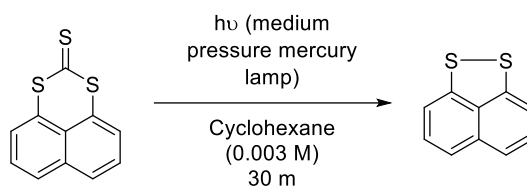


This is a novel procedure discovered by the Grainger Group.

Dithiocarbonate (0.252 mmol) was dissolved in cyclohexane (84 mL, 0.003 M) and was degassed for 15 min in a quartz immersion well photochemical reactor. The reaction mixture was irradiated with a 125 W medium pressure mercury lamp. The lamp was turned off when the reaction appeared to be complete by TLC. The reaction mixture was concentrated under reduced pressure and  $^1\text{H}$  NMR was taken.

Entry	Scaffold	Time / h	Dithiocarbonate <sup>1</sup> H NMR integration ratio	Disulfide <sup>1</sup> H NMR integration ratio	Other
1	Naphthalene dithiocarbonate <b>336</b>	0.33	0	107 1	-
2	Acenaphthene dithiocarbonate <b>337</b>	1	0	.266 12	Acenaphthylene disulfide <b>264</b> ratio = 1
3	Acenaphthylene dithiocarbonate <b>338</b>	1.25	1	264 10	-

### Photolysis of naphtho[1,8-*de*][1,3]dithiine-2-thione **372** (CS transfer)



This is a novel procedure discovered by the Grainger Group.

Naphthalene trithiocarbonate **375** (60 mg, 0.252 mmol) was added to a quartz immersion well photochemical reactor and dissolved in cyclohexane (84 mL, 0.003 M). The reaction mixture was irradiated in 10-minute intervals until completion by TLC. After 30 min the reaction vessel was washed with  $\text{CH}_2\text{Cl}_2$  (50 mL) and concentrated under reduced pressure to yield a brown solid.

$^1\text{H}$  NMR data indicated full conversion to naphthalene disulfide. Data matched that to Grainger and co-workers.<sup>43</sup>

### Solubility study of naphtho[1,8-*de*][1,3]dithiine-2-thione **375**

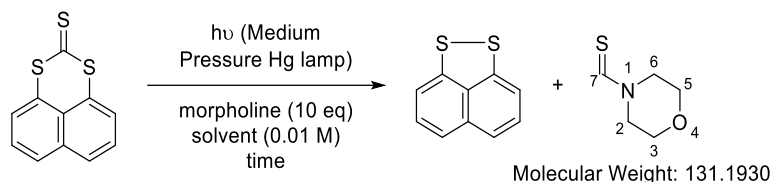
A solubility study was performed on naphthalene trithiocarbonate **375** to see which solvent allowed for the highest concentration:

Naphthalene trithiocarbonate (23 mg, 0.1 mmol) was dissolved in a solvent in the below increments of solubility. After the addition of solvent at each increment, the vial was vigorously shaken and allowed to stand for 5 min, before the dilution was continued.

Table 15 Solubility study of naphthalene trithiocarbonate **375** in various solvents. X = soluble. - + not soluble.

Concentration / mmol·mL <sup>-1</sup>	<i>n</i> hexane	Et <sub>2</sub> O	EtOAc	Acetone	Toluene	THF	DMF	PhCl	PhF	(CF <sub>3</sub> ) <sub>2</sub> CHOH	CF <sub>3</sub> CH <sub>2</sub> OH
<b>0.1</b>	-	-	-	-	-	-	-	-	-	-	-
<b>0.05</b>	-	-	-	-	-	-	-	-	-	-	-
<b>0.04</b>	-	-	-	-	-	-	-	-	-	-	-
<b>0.03</b>	-	-	-	-	-	-	-	-	-	-	-
<b>0.02</b>	-	-	-	-	-	X	-	-	-	-	-
<b>0.01</b>	-	-	-	X	X	X	X	X	X	-	-

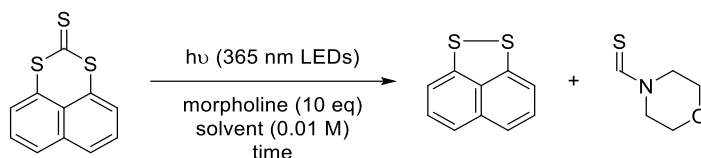
**Synthesis of morpholine-4-carbothialdehyde **363** (Photolysis of naphtho[1,8-*de*][1,3]dithiine-2-thione **375** in the presence of morpholine – Medium Pressure Mercury Lamp)**



This is a novel procedure discovered by the Grainger Group.

Naphthalene trithiocarbonate **375** (197 mg, 0.84 mmol) dissolved in  $\text{CH}_2\text{Cl}_2$  (84 mL) and morpholine (0.72 mL, 8.40 mmol) were added to a Pyrex immersion well photochemical reactor and degassed with argon for 15 min. The light inlet was then attached, and the head space purged with argon. The reaction mixture was irradiated using a medium pressure mercury lamp. After 10 h, the reaction mixture was concentrated under reduced pressure to yield a yellow/brown solid. The reaction mixture was purified by FCC (100% *n*hexane) to elute naphthalene disulfide **107** (109 mg, 68%), then ( $\text{CH}_2\text{Cl}_2$ :*n*hexane, 2:8), then (100%  $\text{CH}_2\text{Cl}_2$ ) and finally (MeOH: $\text{CH}_2\text{Cl}_2$ , 5:95) to yield a white solid (6 %).  $R_f$  0.42 ( $\text{CH}_2\text{Cl}_2$ :MeOH, 95:5);  $\delta\text{H}$  (400 MHz,  $\text{CDCl}_3$ , 7.26 ppm) 9.27 (1H, s, C-7), 4.11 (2H, m), 3.77 (4H, m), 3.68 (2H, m);  $m/z$  (HRMS, ASAP+) Found  $[\text{M} + \text{H}]^+$  132.0494  $\text{C}_5\text{H}_{10}\text{NOS}$  requires 132.0483 (M+H). Data matches that by Asai and Murai.<sup>227</sup>

**Synthesis of morpholine-4-carbothialdehyde **363** (Photolysis of naphtho[1,8-*de*][1,3]dithiine-2-thione **375** in the presence of morpholine – LEDs):**



This is a novel procedure discovered by the Grainger Group.

Naphthalene trithiocarbonate **375** (23 mg, 0.01 mmol) dissolved in solvent (10 mL) and morpholine (0.11 mL, 0.1 mmol) was added to a Pyrex vial. The vial was sealed using a trimmed B19 Suba-seal and degassed using argon gas for 5 min. The vial was blue-tacked to a LED (365 nm) lined dish, 1 cm from the light bulbs. The reaction mixture was irradiated for 3 h. Once the reaction was complete, 1,3,5-trimethoxybenzene was added to the reaction mixture and was concentrated under reduced pressure.  $^1\text{H}$  NMR yields were taken.

Entry	Solvent	Disulfide 107 integral	Trithiocarboante 375 integral	Comments
1	Toluene	0	1	No decomposition observed
2	PhCl	0	1	No decomposition observed
3	PhF	0	1	No decomposition observed
4	DMF	0	1	No decomposition observed
5	THF	0.11	1	Some decomposition



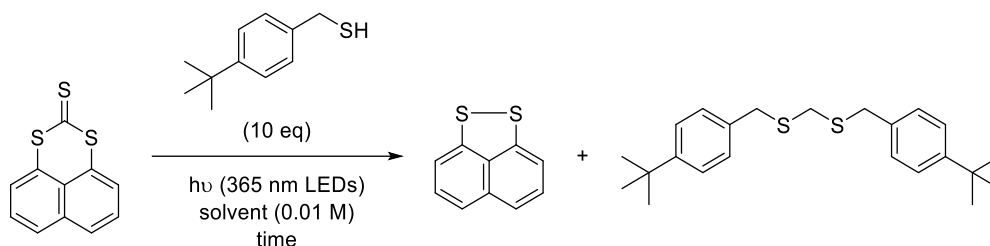
**Table 16** Table of conditions and  $^1\text{H}$  NMR integrations and yields of the products with respect to trimethoxybenzene. TA – thioformamide **363**, TTC – trithiocarbonate **375**, DS – disulfide **107**, and TMB – trimethoxybenzene.

Entry	Solvent	Time / h	Conc. / M	TA 363 integral	TA 363 % yield	TTC 375 integral	TTC 375 % yield	DS 107 integral	DS 107 % yield	TMB integral
1	THF	3	0.02	1	2.2	3.91	4.3	39.10	42.9	136.62
2	THF	3	0.01	1	1.7	26.44	22.1	28.80	24.1	178.71
3	$\text{CH}_2\text{Cl}_2$	3	0.01	1	0.8	44.07	17.5	66.75	26.5	377.75
4	Toluene	3	0.01	1	1.7	81.01	68.5	18.90	16.0	177.51
5	PhCl	3	0.01	1	1.1	122.44	70.1	27.21	15.6	262.09

**Table 17** Table of conditions and  $^1\text{H}$  NMR integrations and yields of the products with respect to trimethoxybenzene. TA – thioformamide **363**, TTC – trithiocarbonate **375**, DS – disulfide **107**, and TMB – trimethoxybenzene.

Entry	Solvent	Time / h	Conc. / M	TA 363 integral	TA 363 % yield	TTC 375 integral	TTC 375 % yield	DS 107 integral	DS 107 % yield	TMB integral
1	PhCl	16	0.01	1	4.8	12.35	29.4	14.81	35.2	63.05
2	Toluene	16	0.01	1	5.8	10.86	31.3	12.95	37.3	52.05
3	DMF	16	0.01	1	4.5	0	0	16.54	37.2	66.63
4	PhF	16	0.01	1	3.2	0	0	21.67	36.6	93.85

**Photolysis of naphtho[1,8-*de*][1,3]dithiine-2-thione **375** in the presence of 4-*tert*-butylbenzylmercaptan – LEDs**



This is a novel procedure discovered by the Grainger Group.

Naphthalene trithiocarbonate **375** dissolved in toluene (0.01 M) and 4-*tert*-butylbenzylmercaptan (10 eq) was added to a Pyrex vial. The vial was sealed using a trimmed B19 Suba-seal and degassed using argon gas for 5 min. The vial was blue-tacked to a LED (365 nm) lined dish, 1 cm from the light bulbs. The reaction mixture was irradiated for XX h. Once the reaction was complete, the reaction mixture was concentrated under reduced pressure.  $^1\text{H}$  NMR integrations are measured. No thioacetal was found.

*Table 18 Decomposition of naphthalene trithiocarbonate **375** in the presence of *t*Bu-benzene thiol*

Entry	Solvent	Conc. / M	Additive	Equivalents of additive	Time / h	Disulfide 107 integral	Trithiocarbonate 375 integral	Comments
1	Toluene	0.01	<i>t</i> Bu-benzene-thiol	10	3	-	-	Degradation
2	Toluene	0.01	<i>t</i> Bu-benzene-thiol	10	1	-	1	No light

## 5 References

- 1 M. Yu. Zolotov and B. Fegley, *Icarus*, 1998, **132**, 431–434.
- 2 C. Y. Na, L. W. Esposito, W. E. McClintock and C. A. Barth, *Icarus*, 1994, **112**, 389–395.
- 3 C. Y. Na, L. W. Esposito and T. E. Skinner, *J. Geophys. Res.*, 1990, **95**, 7485.
- 4 B. N. Frandsen, P. O. Wennberg and H. G. Kjaergaard, *Geophys. Res. Lett.*, 2016, **43**, 11146–11155.
- 5 C. T. Russell and M. G. Kivelson, *Science*, 2000, **287**, 1998–1999.
- 6 P. W. Schenk and R. Steudel, *Angew. Chem., Int. Ed. Engl.*, 1965, **4**, 402–409.
- 7 E. V. Martin, *Phys. Rev.*, 1932, **41**, 167–193.
- 8 W. A. Schenk, *Dalton Trans.*, 2011, **40**, 1209–1219.
- 9 R. M. Dodson and R. F. Sauers, *Chem. Commun. (London)*, 1967, 1189.
- 10 R. M. Dodson and J. P. Nelson, *J. Chem. Soc. D, Chem. Commun.*, 1969, 1159–1160.
- 11 A. Battaglia, A. Dondoni, G. Maccagnani and G. Mazzanti, *J. Chem. Soc., Perkin Trans. 2*, 1974, 609.
- 12 B. F. Bonini, G. Maccagnani, G. Mazzanti, C. N. R. Laboratorio, C. Organica and V. Risorgimento, *Tetrahedron Lett.*, 1977, **18**, 1185–1186.
- 13 W. A. Schenk and U. Karl, *Z. Naturforsch. B*, 1989, **44**, 988–989.

- 14 J. Nakayama, Y. Tajima, P. Xue-hua and Y. Sugihara, *J. Am. Chem. Soc.*, 2007, **129**, 7250–7251.
- 15 M. Joost, M. Nava, W. J. Transue, M. A. Martin-Drumel, M. C. McCarthy, D. Patterson and C. C. Cummins, *Proc. Natl. Acad. Sci. U. S. A.*, 2018, **115**, 5866–5871.
- 16 G. E. Hartzell and J. N. Paige, *J. Am. Chem. Soc.*, 1966, **88**, 2616–2617.
- 17 G. E. Hartzell and J. N. Paige, *J. Org. Chem.*, 1967, **32**, 459–460.
- 18 N. P. Neureiter, *J. Am. Chem. Soc.*, 1966, **88**, 558–564.
- 19 K. Kondo, M. Matsumoto and A. Negishi, *Tetrahedron Lett.*, 1972, **13**, 2131–2134.
- 20 S. Saito, *Tetrahedron Lett.*, 1968, **9**, 4961–4964.
- 21 H. Uehara, *Bull. Chem. Soc. Jpn.*, 1969, **42**, 886–889.
- 22 P. Chao and D. M. Lemal, *J. Am. Chem. Soc.*, 1973, **95**, 920–922.
- 23 W. G. L. Aalberberg and K. P. C. Vollhardt, *J. Am. Chem. Soc.*, 1977, **8**, 2792–2794.
- 24 R. S. Glass and W. Jung, *Sulfur Letters*, 1994, **17**, 183–188.
- 25 D. M. Lemal and P. Chao, *J. Am. Chem. Soc.*, 1973, **95**, 922–924.
- 26 R. Grigg, G. J. Reimer and A. R. Wade, *J. Chem. Soc., Perkin Trans. 1*, 1983, 1929–1935.
- 27 A. G. Anastassiou, J. C. Wetzel and B. Y. H. Chao, *J. Am. Chem. Soc.*, 1975, **97**, 1124–1132.
- 28 L. D. Quin, N. S. Rao and J. Szewcysk, *Tetrahedron Lett.*, 1985, **26**, 6293–6296.
- 29 Y. L. Chow, J. N. S. Tam, J. E. Blier and H. H. Szmant, *J. Chem. Soc. D, Chem. Commun.*, 1970, 1604–1605.

- 30 I. A. Abu-Yousef and D. N. Harpp, *Tetrahedron Lett.*, 1995, **36**, 201–204.
- 31 I. A. Abu-Yousef and D. N. Harpp, *J. Org. Chem.*, 1997, **62**, 8366–8371.
- 32 B. F. Bonini, G. Maccagnani and G. Mazzanti, *J. Chem. Soc., Chem. Commun.*, 1976, 431.
- 33 B. F. Bonini, G. Maccagnani, G. Mazzanti, P. Pedrini and P. Piccinelli, *J. Chem. Soc., Perkin Trans. 1*, 1979, 1720–1722.
- 34 K. S. Arulsamy, K. K. Pandey and U. C. Agarwala, *Inorganica Chim. Acta*, 1981, **54**, L51.
- 35 K. Kondo and A. Negishi, *Tetrahedron*, 1971, **27**, 4821–4830.
- 36 W. A. Schenk, J. Leissner and C. Burschka, *Angew. Chem., Int. Ed. Engl.*, 1984, **23**, 806–807.
- 37 I.-P. Lorenz, J. Messelhäuser, W. Hiller and K. Haug, *Angew. Chem., Int. Ed. Engl.*, 1985, **24**, 228–229.
- 38 W. A. Schenk and S. Müssig, *J. Organomet. Chem.*, 1987, **320**, C23–C25.
- 39 O. Heyke, A. Neher and I.-P. Lorenz, *Z. Anorg. Allg. Chem.*, 1992, **608**, 23–27.
- 40 O. Heyke, G. Beuter and I. P. Lorenz, *J. Organomet. Chem.*, 1992, **440**, 197–205.
- 41 M. Breitenstein, R. Schulz and A. Schweig, *J. Org. Chem.*, 2002, **47**, 1979–1980.
- 42 R. S. Grainger, A. Procopio and J. W. Steed, *Org. Lett.*, 2001, **3**, 3565–3568.
- 43 R. S. Grainger, B. Patel, B. M. Kariuki, L. Male and N. Spencer, *J. Am. Chem. Soc.*, 2011, **133**, 5843–5852.
- 44 R. Huang and J. H. Espenson, *J. Org. Chem.*, 1999, **64**, 6374–6379.
- 45 A. Battaglia, A. Dondoni, P. Giorgianni, G. Maccagnani and G. Mazzanti, *J. Chem. Soc. B*, 1971, 1547.

- 46 J. Nakayama, S. Yoshida, Y. Sugihara and A. Sakamoto, *Helv. Chim. Acta*, 2005, **88**, 1451–1471.
- 47 A. Ishii, M. Ohishi, K. Matsumoto and T. Takayanagi, *Org. Lett.*, 2006, **8**, 91–94.
- 48 A. Ishii, M. Nakabayashi and J. Nakayama, *J. Am. Chem. Soc.*, 1999, **121**, 7959–7960.
- 49 J. Nakayama and Y. Sugihara, *Sulfur reports*, 1997, **19**, 349–375.
- 50 J. Nakayama, *Bull. Chem. Soc. Jpn.*, 2000, **73**, 1–17.
- 51 J. Nakayama, *Sulfur reports*, 2000, **22**, 123–149.
- 52 J. Nakayama, T. Yu, Y. Sugihara and A. Ishii, *Chem. Lett.*, 1997, **26**, 499–500.
- 53 T. Otani, J. Takayama, Y. Sugihara, A. Ishii and J. Nakayama, *J. Am. Chem. Soc.*, 2003, **125**, 8255–8263.
- 54 S. Suwabe, A. Okuhara, T. Sugahara, K. Suzuki, K. Kunimasa, T. Nakajima, Y. Kumafuji, Y. Osawa, T. Yoshimura and H. Morita, *Tetrahedron Lett.*, 2009, **50**, 1381–1384.
- 55 L. E. Longobardi, V. Wolter and D. W. Stephan, *Angew. Chem. Int. Ed.*, 2015, **54**, 809–812.
- 56 S. Chan and H. Goldwhite, *Phosphorous Sulfur Relat. Elem.*, 1978, **4**, 33–34.
- 57 F. Buß, P. Rotering, C. Mück-Lichtenfeld and F. Dielmann, *Dalton Trans.*, 2018, **47**, 10420–10424.
- 58 P. Holtkamp, T. Glodde, D. Poier, B. Neumann, H. Stammeler and N. W. Mitzel, *Angew. Chem. Int. Ed.*, 2020, **59**, 17388–17392.
- 59 M. Malischewski and K. Seppelt, *Angew. Chem. Int. Ed.*, 2017, **56**, 16495–16497.

- 60 H. C. Böttcher, M. Graf, K. Merzweiler and C. Wagner, *Inorganica Chim. Acta*, 2003, **350**, 399–406.
- 61 C. Bianchini, C. Mealli, A. Meli and M. Sabat, *J. Chem. Soc., Chem. Commun.*, 1985, 1024–1025.
- 62 A. Muller, E. Krickemeyer, R. Jostes, H. Bogge, E. Diemann and U. Bergmann, *Z. Naturforsch. B*, 1985, **40 b**, 1715–1718.
- 63 L. Markó, B. Markó-Monostory, T. Madach and H. Vahrenkamp, *Angew. Chem., Int. Ed. Engl.*, 1980, **19**, 226–227.
- 64 I.-P. Lorenz and J. Messelhäuser, *Z. Naturforsch. B*, 1984, 39, 403–404.
- 65 W. A. Schenk, *Angew. Chem., Int. Ed. Engl.*, 1987, **26**, 98–109.
- 66 W. A. Schenk, U. Karl, M. R. Horn and S. Müssig, *Z. Naturforsch. B*, 1990, **45**, 239–244.
- 67 J. K. Gong, P. E. Fanwick and C. P. Kubiak, *J. Chem. Soc., Chem. Commun.*, 1990, 1190–1191.
- 68 T. Chihara, T. Tase, H. Ogawa and Y. Wakatsuki, *Chem. Commun.*, 1999, 279–280.
- 69 C. MinhTuong, W. K. Hammons, A. L. Howarth, K. E. Lutz, A. D. Maduvu, L. B. Haysley, B. R. T. Allred, L. K. Hoyt, M. S. Mashuta and M. E. Noble, *Inorg. Chem.*, 2009, **48**, 5027–5038.
- 70 A. Neher and I.-P. Lorenz, *Angew. Chem., Int. Ed. Engl.*, 1989, **28**, 1342–1343.
- 71 R. Wei, X. Chen and Y. Gong, *Inorg. Chem.*, 2019, **58**, 11801–11806.
- 72 W. A. Schenk and J. Leißner, *Z. Naturforsch. B*, 1987, **42b**, 967–971.



- 73 A. Mayr, C. M. Bastos, G. D. Stucky, F. A. Cotton, B. Hong, A. Sobkowiak, H.-C. Tung, D. T. Sawyer, M. Witt, H. W. Roesky, K. K. Pandey and C. D. Hoff, *Progress in Inorganic Chemistry*, John Wiley & Sons, Inc., New York, Chichester, Brisbane, Toronto, Singapore, 1st Ed., 1992, vol. 40.
- 74 R. Wang, M. S. Mashuta, J. F. Richardson and M. E. Noble, *Inorg. Chem.*, 1996, **35**, 3022–3030.
- 75 W. A. Schenk, J. Leißner and C. Burschka, *Z. Naturforsch. B*, 1985, **40**, 1264–1273.
- 76 W. A. Schenk and J. Leißner, *Z. Naturforsch. B*, 1987, **42**, 799–800.
- 77 J. D. Kendall and N. S. Simpkins, *Synlett*, 1998, 391–392.
- 78 C. Hervieu, M. S. Kirillova, T. Suárez, M. Müller, E. Merino and C. Nevado, *Nat. Chem.*, 2021, **13**, 327–334.
- 79 T. Sephton, J. M. Large, S. Butterworth and M. F. Greaney, *Org. Lett.*, 2022, **24**, 1132–1135.
- 80 J. Barluenga, J. F. López-Ortiz, M. Tomás and V. Gotor, *J. Chem. Soc., Perkin Trans. 1*, 1981, 1891–1895.
- 81 I. S. Kondratov, N. A. Tolmachova and G. Haufe, *Eur. J. Org. Chem.*, 2018, 3618–3647.
- 82 D. M. Lemal, M. Akashi, Y. Lou and V. Kumar, *J. Org. Chem.*, 2013, **78**, 12330–12337.
- 83 H. Kato, Y. Arikawa, M. Hashimoto and M. Masuzawa, *J. Chem. Soc., Chem. Commun.*, 1983, 938.
- 84 C. Song and T. M. Swager, *J. Org. Chem.*, 2010, **75**, 999–1005.
- 85 R. Fu, X. Xu, Q. Dang, F. Chen and X. Bai, *Org. Lett.*, 2007, **9**, 571–574.

- 86 P. R. Christensen, B. O. Patrick, É. Caron and M. O. Wolf, *Angew. Chem. Int. Ed.*, 2013, **52**, 12946–12950.
- 87 M. Murata, Y. Murata and K. Komatsu, *J. Am. Chem. Soc.*, 2006, **128**, 8024–8033.
- 88 F. S. Ehrenhauser, *Polycycl. Aromat. Compd.*, 2015, **35**, 161–176.
- 89 V. Balasubramaniyan, *Chem. Rev.*, 1966, **66**, 567–641.
- 90 O. Minge, S. Nogai and H. Schmidbaur, *Z. Naturforsch. B*, 2004, **59b**, 153–160.
- 91 D. J. Press and T. G. Back, *Org. Lett.*, 2011, **13**, 4104–4107.
- 92 A. Zweig and A. K. Hoffmann, *J. Org. Chem.*, 1965, **30**, 3997–4001.
- 93 K. M. Rabanzo-Castillo, M. Hanif, T. Söhnle and E. M. Leitao, *Dalton Trans.*, 2019, **48**, 13971–13980.
- 94 T. Mizuta, T. Nakazono and K. Miyoshi, *Angew. Chem. Int. Ed.*, 2002, **41**, 3897–3898.
- 95 R. D. Jackson, S. James, A. G. Orpen and P. G. Pringle, *J. Organomet. Chem.*, 1993, **458**, C3–C4.
- 96 A. Karaçar, H. Thönnissen, P. G. Jones, R. Bartsch and R. Schmutzler, *Chem. Ber.*, 1997, **130**, 1485–1489.
- 97 W. Neugebauer, T. Clark and P. von Ragué Schleyer, *Chem. Ber.*, 1983, **116**, 3283–3292.
- 98 C. Ganesamoorthy, S. Heimann, S. Hölscher, R. Haack, C. Wölper, G. Jansen and S. Schulz, *Dalton Trans.*, 2017, **46**, 9227–9234.
- 99 P. Prabhakaran, V. G. Puranik, J. N. Chandran, P. R. Rajamohanan, H.-J. Hofmann and G. J. Sanjayan, *Chem. Commun.*, 2009, 3446.

- 100 L. Nilakantan, D. R. McMillin and P. R. Sharp, *Organometallics*, 2016, **35**, 2339–2347.
- 101 W. B. Price and S. Smiles, *J. Chem. Soc.*, 1928, 2372–2374.
- 102 E. W. Miller, S. X. Bian and C. J. Chang, *J. Am. Chem. Soc.*, 2007, **129**, 3458–3459.
- 103 R. Dong, M. Pfeiffermann, D. Skidin, F. Wang, Y. Fu, A. Narita, M. Tommasini, F. Moresco, G. Cuniberti, R. Berger, K. Müllen and X. Feng, *J. Am. Chem. Soc.*, 2017, **139**, 2168–2171.
- 104 C. Figliola, L. Male, P. N. Horton, M. B. Pitak, S. J. Coles, S. L. Horswell and R. S. Grainger, *Organometallics*, 2014, **33**, 4449–4460.
- 105 K. Yui, Y. Aso, T. Otsubo and F. Ogura, *Bull. Chem. Soc. Jpn.*, 1988, **61**, 953–959.
- 106 L. Zhang, S. M. Fakhouri, F. Liu, J. C. Timmons, N. A. Ran and A. L. Briseno, *J. Mater. Chem.*, 2011, **21**, 1329–1337.
- 107 R. S. Grainger, B. Patel and B. M. Kariuki, *Angew. Chem. Inter. Ed.*, 2009, **48**, 4832–4835.
- 108 C. G. M. Benson, C. M. Schofield, R. A. M. Randall, L. Wakefield, F. R. Knight, A. M. Z. Slawin and J. D. Woollins, *Eur. J. Inorg. Chem.*, 2013, 427–437.
- 109 M. R. Garrett, M. J. Durán-Peña, W. Lewis, K. Pudzs, J. Užulis, I. Mihailovs, B. Tyril, J. Shine, E. F. Smith, M. Rutkis and S. Woodward, *J. Mater. Chem. C*, 2018, **6**, 3403–3409.
- 110 P. Hu, X. He, M. Ng, J. Ye, C. Zhao, S. Wang, K. Tan, A. Chaturvedi, H. Jiang, C. Kloc, W. Hu and Y. Long, *Angew. Chem. Inter. Ed.*, 2019, **58**, 13513–135.
- 111 P. Kilian, F. R. Knight and J. D. Woollins, *Coord. Chem. Rev.*, 2011, **255**, 1387–1413.
- 112 L. M. Diamond, F. R. Knight, D. B. Cordes, A. C. C. Ward, A. M. Z. Slawin and J. D. Woollins, *Polyhedron*, 2015, **85**, 395–404.

- 113 S. M. Aucott, H. L. Milton, S. D. Robertson, A. M. Z. Slawin, G. D. Walker and J. D. Woollins, *Eur. J. Chem.*, 2004, **10**, 1666–1676.
- 114 K. Yui, Y. Aso, T. Otsubo and F. Ogura, *Chem. Lett.*, 1986, **15**, 551–554.
- 115 D. Manna, S. Mondal and G. Mugesh, *Eur. J. Chem.*, 2015, **21**, 2409–2416.
- 116 S. Mondal and G. Mugesh, *Org. Biomol. Chem.*, 2016, **14**, 9490–9500.
- 117 D. Manna and G. Mugesh, *J. Am. Chem. Soc.*, 2011, **133**, 9980–9983.
- 118 L.-Y. Chiang and J. Meinwald, *Tetrahedron Lett.*, 1980, **21**, 4565–4568.
- 119 D. Dauplaise, J. Meinwald, J. C. Scott, H. Temkin and J. Clardy, *Ann. N. Y. Acad. Sci.*, 1978, **313**, 382–394.
- 120 A. J. Ashe, J. W. Kampf and P. M. Savla, *Heteroat. Chem.*, 1994, **5**, 113–119.
- 121 W. Bauer, T. Clark and P. v. R. Schleyer, *J. Am. Chem. Soc.*, 2002, **109**, 970–977.
- 122 U. Schubert, W. Neugebauer and P. Von Ragué Schleyer, *J. Chem. Soc., Chem. Commun.*, 1982, **4**, 1184–1185.
- 123 H. Mayer and J. Sauer, *Tetrahedron Lett.*, 1983, **24**, 4091–4094.
- 124 J. C. Koziar and D. O. Cowan, *J. Am. Chem. Soc.*, 1976, **98**, 1001–1007.
- 125 S. M. Aucott, H. L. Milton, S. D. Robertson, A. M. Z. Slawin and J. D. Woollins, *Heteroat. Chem.*, 2004, **15**, 530–542.
- 126 L. M. Diamond, F. R. Knight, K. S. Athukorala Arachchige, R. A. M. Randall, M. Bühl, A. M. Z. Slawin and J. D. Woollins, *Eur. J. Inorg. Chem.*, 2014, 1512–1523.

- 127 H. Miyamoto, K. Yui, Y. Aso, T. Otsubo and F. Ogura, *Tetrahedron Lett.*, 1986, **27**, 2011–2014.
- 128 Y. Aso, K. Yui, T. Miyoshi, T. Otsubo, F. Ogura and J. Tanaka, *Bull. Chem. Soc. Jpn.*, 1988, **61**, 2013–2018.
- 129 I. A. Pocock, A. M. Alotaibi, K. Jagdev, C. Prior, G. R. Burgess, L. Male and R. S. Grainger, *Chem. Commun.*, 2021, **57**, 7252–7255.
- 130 K. Jagdev, D. Tanini, J. W. Lownes, C. Figliola, L. Male, A. Capperucci and R. S. Grainger, *Org. Biomol. Chem.*, 2021, **19**, 10565–10569.
- 131 M. Ballester, C. Molinet and J. Castañer, *J. Am. Chem. Soc.*, 1960, **82**, 4254–4258.
- 132 R. C. Mansfield and C. J. Schmidle, *J. Org. Chem.*, 2003, **21**, 698–699.
- 133 T. V. Mezhenkova, V. V. Komarov, V. M. Karpov, I. V. Beregovaya and Y. V. Zonov, *J. Fluor. Chem.*, 2020, **237**, 109615.
- 134 T. V. Mezhenkova, V. M. Karpov and Y. V. Zonov, *J. Fluor. Chem.*, 2018, **207**, 59–66.
- 135 F. Marchetti, F. Marchetti, F. Masi, G. Pampaloni, V. Passarelli, A. Sommazzi and S. Spera, *J. Fluor. Chem.*, 2009, **130**, 341–347.
- 136 F. Calderazzo, F. Masi, G. Pampaloni, V. Passarelli, R. Santi, A. Sommazzi, S. Spera and F. Tumminia, *J. Organomet. Chem.*, 2005, **690**, 4886–4898.
- 137 K. Ohkubo, Y. Sakamoto, T. Suzuki, T. Tsuzuki, D. Kumaki and S. Tokito, *Eur. J. Chem.*, 2008, **14**, 4472–4474.
- 138 L. Juliá, M. Ballester, J. Riera, J. Castañer, J. L. Ortin and C. Onrubia, *J. Org. Chem.*, 1988, **53**, 1267–1273.

- 139 M. A. Fox, E. Gaillard and C.-C. Chen, *J. Am. Chem. Soc.*, 1987, **109**, 7088–7094.
- 140 M. Ballester, J. Castañer, J. Riera, G. de la Fuente and M. Camps, *J. Org. Chem.*, 2002, **50**, 2287–2292.
- 141 R. Filler, A. E. Fiebig and M. Y. Pelister, *J. Org. Chem.*, 2002, **45**, 1290–1295.
- 142 R. Filler and A. E. Fiebig, *Chem. Commun.*, 1968, 606.
- 143 L. Horner and D. W. Baston, *Justus Liebigs Ann. Chem.*, 1973, 910–935.
- 144 V. D. B. Bonifácio, J. Morgado and U. Scherf, *Synlett*, 2010, 1333–1336.
- 145 J. Yin, Y. Ma, G. Li, M. Peng and W. Lin, *Coord. Chem. Rev.*, 2020, **412**, 213257.
- 146 G. Yaqub, E. A. Hussain, M. A. Rehman and B. Mateen, *Asian J. Chem.*, 2009, **21**, 2485–2520.
- 147 W. Gao, Y. Su, Z. Wang, Y. Zhang, D. Zhang, P. Jia, C. Yang, Y. Li, R. Ganguly and Y. Zhao, *ACS Appl Mater. Interfaces*, 2019, **11**, 47162–47169.
- 148 A. Kimoto, J.-S. Cho, M. Higuchi and K. Yamamoto, *Macromolecules*, 2004, **37**, 5531–5537.
- 149 S. Kato, H. Noguchi, A. Kobayashi, T. Yoshihara, S. Tobita and Y. Nakamura, *J. Org. Chem.*, 2012, **77**, 9120–9133.
- 150 G. Sathiyar, E. K. T. Sivakumar, R. Ganesamoorthy, R. Thangamuthu and P. Sakthivel, *Tetrahedron Lett.*, 2016, **57**, 243–252.
- 151 A. Hallberg and A. R. Martin, *J. Heterocycl. Chem.*, 1984, **21**, 837–840.
- 152 A. R. Katritzky, G. W. Rewcastle and L. M. Vazquez de Miguel, *J. Org. Chem.*, 1988, **53**, 794–799.

- 153 United States Patent Office, 4,273,711, 1981, 1–3.
- 154 J. A. Leitch, C. J. Heron, J. McKnight, G. Kociok-Köhn, Y. Bhonoah and C. G. Frost, *Chem. Commun.*, 2017, **53**, 13039–13042.
- 155 IUPAC, *Blackwell Scientific Publications, Oxford*, 2014, 1670.
- 156 E. Block, *Phosphorus, Sulfur Silicon Relat. Elem.*, 1999, **153–154**, 173–192.
- 157 F. Freeman, D. S. H. L. Kim and E. Rodriguez, *Sulfur reports*, 1989, **9**, 207–247.
- 158 A. J. Ashe, J. W. Kampf and P. M. Savla, *J. Org. Chem.*, 1990, **55**, 5558–5559.
- 159 N. Lardi, I. Romeo, E. Cerrada and P. J. Skabara, *Dalton Trans.*, 2007, 5329–5338.
- 160 K. Albrecht, K. Matsuoka, K. Fujita and K. Yamamoto, *Angew. Chem. Int. Ed.*, 2015, **54**, 5677–5682.
- 161 S. J. Cristol, F. R. Stermitz and P. S. Ramey, *J. Am. Chem. Soc.*, 1956, **78**, 4939–4941.
- 162 N. Jaiboon, *Sci.*, 2002, **28**, 271–275.
- 163 V. F. Anikin, V. V Veduta and A. Merz, *Monatsh. Chem.*, 1999, **130**, 681–690.
- 164 Y. Fei, Y. Fu, X. Bai, L. Du, Z. Li, H. Komber, K. H. Low, S. Zhou, D. L. Phillips, X. Feng and J. Liu, *J. Am. Chem. Soc.*, 2021, **143**, 2353–2360.
- 165 L. Testaferri, M. Tiecco, M. Tingoli, D. Chianelli and M. Montanucci, *Synthesis (Stuttg)*, 1983, 751–755.
- 166 L. Testaferri, M. Tingoli and M. Tiecco, *Tetrahedron Lett.*, 1980, **21**, 3099–3100.
- 167 M. A. G. M. Tinga, G. Schat, O. S. Akkerman, F. Bickelhaupt, E. Horn, H. Kooijman, W. J. J. Smeets and A. L. Spek, *J. Am. Chem. Soc.*, 1993, **115**, 2808–2817.

- 168 M. A. G. M. Tinga, G. Schat, O. S. Akkerman, F. Bickelhaupt, W. J. J. Smeets and A. L. Spek, *Chem. Ber.*, 1994, **127**, 1851–1856.
- 169 N. Tanaka and T. Kasai, *Bull. Chem. Soc. Jpn.*, 1981, **54**, 3020–3025.
- 170 F. R. Knight, L. M. Diamond, K. S. Athukorala Arachchige, P. Sanz Camacho, R. A. M. Randall, S. E. Ashbrook, M. Bühl, A. M. Z. Slawin and J. D. Woollins, *Eur. J. Chem.*, 2015, **21**, 3613–3627.
- 171 K. S. Feldman, *Tetrahedron*, 2006, **62**, 5003–5034.
- 172 D. J. Press, T. G. Back and T. C. Sutherland, *Tetrahedron Lett.*, 2012, **53**, 1603–1605.
- 173 C. Thirsk, G. E. Hawkes, K. R. Liedl, T. Loerting, R. Nasser, R. G. Pritchard, M. Steele, J. E. Warren and A. Whiting, *J. Chem. Soc., Perkin Trans. 2*, 2002, **9**, 1510–1519.
- 174 L. Field and W. B. Lacefield, *J. Org. Chem.*, 1966, **31**, 3555–3561.
- 175 Tirthankar. Ghosh and P. D. Bartlett, *J. Am. Chem. Soc.*, 1988, **110**, 7499–7506.
- 176 Q.-S. Gu and D. Yang, *Angew. Chem. Int. Ed.*, 2017, **56**, 5886–5889.
- 177 S. Puhl, T. Steenbock, C. Herrmann and J. Heck, *Angew. Chem. Int. Ed.*, 2020, **59**, 2407–2413.
- 178 R. C. Haltiwanger, P. T. Beurskens, J. M. J. Vankan and W. S. Veeman, *J. Crystallogr. Spectrosc. Res.*, 1984, **14**, 589–597.
- 179 B. R. Davis and I. Bernal, *J. Cryst. Mol. Struct.*, 1972, **2**, 107–114.
- 180 Ralf Steudel, and Karin Hassenberg and J. Pickardt, *Organometallics*, 1999, **18**, 2910–2911.



- 181 F. Freeman, *Chem. Rev.*, 1984, **84**, 117–135.
- 182 L. Wu and R. Wang, *Pharmacol. Rev.*, 2005, **57**, 585–630.
- 183 B. Olas, *Chem. Biol. Interact.*, 2014, **222**, 37–43.
- 184 J. B. Peng, H. Q. Geng and X. F. Wu, *Chem*, 2019, **5**, 526–552.
- 185 H. W. Lee and F. Y. Kwong, *Eur. J. Org. Chem.*, 2010, 789–811.
- 186 I. Omae, *Coord. Chem. Rev.*, 2011, **255**, 139–160.
- 187 P. L. Pauson, *Tetrahedron*, 1985, **41**, 5855–5860.
- 188 S. E. Gibson and N. Mainolfi, *Angew. Chem. Int. Ed.*, 2005, 44, 3022–3037.
- 189 S. T. Ingate and J. Marco-Contellers, *Org. Prep. Proced. Int.*, 1998, **30**, 121–143.
- 190 T. Shibata, *Adv. Synth. Catal.*, 2006, **348**, 2328–2336.
- 191 S. E. Gibson and A. Stevenazzi, *Angew. Chem. Int. Ed.*, 2003, 42, 1800–1810.
- 192 E. L. Niedzielski and F. F. Nord, *J. Org. Chem.*, 1943, **8**, 147–152.
- 193 J. Li, N. Wang, W. T. Liu, H. L. Ding, Y. An and C. W. Lü, *New J. Chem.*, 2017, **41**, 12225–12230.
- 194 Z. Wang, in *Comprehensive Organic Name Reactions and Reagents*, ed. Z. Wang, John Wiley & Sons, Inc., Hoboken, NJ, USA, 1st Ed., 2010, pp. 1209–1212.
- 195 R. Naigre, T. Chenal, I. Ciprés, P. Kalck, J. C. Daran and J. Vaissermann, *J. Organomet. Chem.*, 1994, **480**, 91–102.
- 196 J. Voss, R. Edler and G. Adiwidjaja, *Phosphorus, Sulfur Silicon Relat. Elem.*, 2007, **182**, 1893–1905.

- 197 J. Demaerel, C. Veryser and W. M. De Borggraeve, *React. Chem. Eng.*, 2020, **5**, 615–621.
- 198 C. Veryser, S. Van Mileghem, B. Egle, P. Gilles and W. M. De Borggraeve, *React. Chem. Eng.*, 2016, **1**, 142–146.
- 199 S. D. Friis, A. T. Lindhardt and T. Skrydstrup, *Acc. Chem. Res.*, 2016, **49**, 594–605.
- 200 A. T. Lindhardt, R. Simonssen, R. H. Taaning, T. M. Gøgsig, G. N. Nilsson, G. Stenhagen, C. S. Elmore and T. Skrydstrup, *J. Label. Compd. Radiopharm.*, 2012, **55**, 411–418.
- 201 H. P. Kim, S. W. Ryter and A. M. K. Choi, *Ann. Rev. Pharmacol. Toxicol.*, 2006, **46**, 411–449.
- 202 A. K. Gilbert, Y. Zhao, C. E. Otteson and M. D. Pluth, *Journal of Organic Chemistry*, 2019, **84**, 14469–14475.
- 203 F. Yang and G. N. Phillips, *J. Mol. Biol.*, 1996, **256**, 762–774.
- 204 A. Verma, D. J. Hirsch, C. E. Glatt, G. V. Ronnett and S. H. Snyder, *Science*, 1993, **259**, 381–384.
- 205 M. Bilban, A. Haschemi, B. Wegiel, B. Y. Chin, O. Wagner and L. E. Otterbein, *J. Mol. Med.*, 2008, **86**, 267–279.
- 206 K. Yui, Y. Aso, T. Otsubo and F. Ogura, *Bull. Chem. Soc. Jpn.*, 1988, **61**, 953–959.
- 207 J. Dewar and H. J. Jones, *Proc. R. Soc. London*, 1910, **83**, 526–529.
- 208 J. Dewar and H. O. Jones, *Proc. R. Soc. London*, 1910, **83**, 408–413.
- 209 R. J. Richardson, *J. Phys. Chem.*, 1975, **79**, 1153–1158.
- 210 N. D. Sze and M. K. W. Ko, *Geophys. Res. Lett.*, 1981, **8**, 765–768.
- 211 N. Djeu, H. S. Pilloff and S. K. Searles, *Appl. Phys. Lett.*, 1971, **18**, 538–540.

- 212 G. Winnewisser and R. L. Cook, *J. Mol. Spectrosc.*, 1968, **28**, 266–268.
- 213 G. P. Raine, H. F. Schaefer and R. C. Haddon, *J. Am. Chem. Soc.*, 1983, **105**, 194–198.
- 214 E. K. Moltzen, K. J. Klabunde and A. Senning, *Chem. Rev.*, 1988, **88**, 391–406.
- 215 A. Krebs, A. Güntner, A. Senning, E. K. Moltzen, K. J. Klabunde and M. P. Kramer, *Angew. Chem., Int. Ed. Engl.*, 1984, **23**, 729–729.
- 216 R. Steudel, *Angew. Chem. Int. Ed. Engl.*, 1967, **6**, 635–635.
- 217 K. J. Klabunde, C. M. White and H. F. Efner, *Inorg. Chem.*, 1974, **13**, 1778–1781.
- 218 K. J. Klabunde and K. Voska, *Phosphorus Sulfur Silicon Relat. Elem.*, 1989, **43**, 47–61.
- 219 E. K. Moltzen, A. Senning, H. Luetjens and A. Krebs, *J. Org. Chem.*, 2002, **56**, 1317–1318.
- 220 F. Cataldo, *Inorganica Chim. Acta*, 1995, **232**, 27–33.
- 221 A. F. Burchat, J. M. Chong and N. Nielsen, *J. Organomet. Chem.*, 1997, **542**, 281–283.
- 222 J. Dhankhar, E. González-Fernández, C. C. Dong, T. K. Mukhopadhyay, A. Linden and I. Čorić, *J. Am. Chem. Soc.*, 2020, **142**, 19040–19046.
- 223 B. Patel, University of Birmingham, 2009.
- 224 J. A. Burns and G. M. Whitesides, *J. Am. Chem. Soc.*, 2002, **112**, 6296–6303.
- 225 Y. Feng, D. Holte, J. Zoller, S. Umemiya, L. R. Simke and P. S. Baran, *J. Am. Chem. Soc.*, 2015, **137**, 10160–10163.
- 226 K. Jarowicki and P. Kocienski, *J. Chem. Soc., Perkin Trans. 1*, 1999, 1589–1615.
- 227 T. Murai and F. Asai, *J. Am. Chem. Soc.*, 2007, **129**, 780–781.



## 6 Appendix

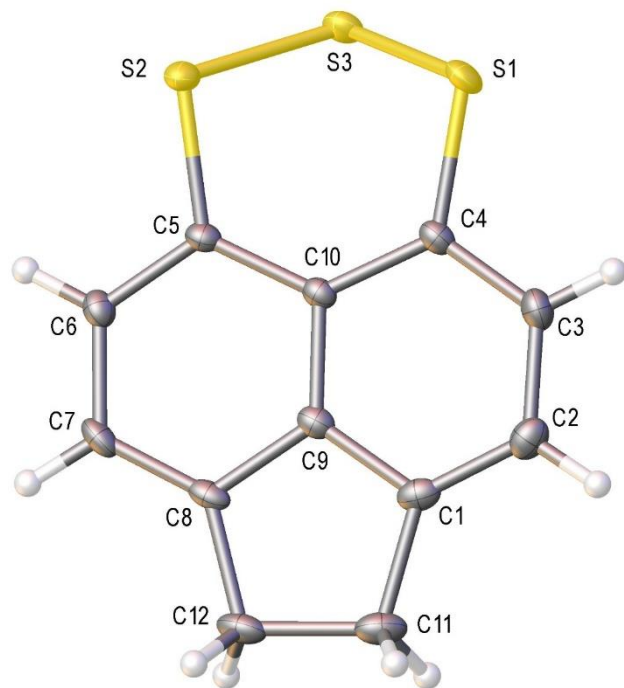
### Crystal structure of 6,7-dihydroacenaphtho[5,6-*de*][1,2,3]trithiane 319

#### IP-002

Table 1 Crystal data and structure refinement for IP-002.

Identification code	IP-002
Empirical formula	C <sub>12</sub> H <sub>8</sub> S <sub>3</sub>
Formula weight	248.36
Temperature/K	100.01(10)
Crystal system	orthorhombic
Space group	Pbca
a/Å	7.7708(2)
b/Å	15.1206(5)
c/Å	17.6993(6)
$\alpha$ /°	90
$\beta$ /°	90
$\gamma$ /°	90
Volume/Å <sup>3</sup>	2079.65(11)
Z	8
$\rho_{\text{calc}}/\text{g/cm}^3$	1.586
$\mu/\text{mm}^{-1}$	6.153
F(000)	1024.0
Crystal size/mm <sup>3</sup>	0.24 × 0.086 × 0.073
Radiation	CuK $\alpha$ ( $\lambda$ = 1.54184)
2 $\theta$ range for data collection/°	9.996 to 149.096
Index ranges	-6 ≤ h ≤ 9, -18 ≤ k ≤ 18, -15 ≤ l ≤ 21
Reflections collected	5140
Independent reflections	2067 [ $R_{\text{int}}$ = 0.0233, $R_{\text{sigma}}$ = 0.0252]
Data/restraints/parameters	2067/0/136
Goodness-of-fit on F <sup>2</sup>	1.055
Final R indexes [ $ I  \geq 2\sigma(I)$ ]	$R_1$ = 0.0266, $wR_2$ = 0.0667
Final R indexes [all data]	$R_1$ = 0.0304, $wR_2$ = 0.0698
Largest diff. peak/hole / e Å <sup>-3</sup>	0.47/-0.25

IP-002.jpg: Crystal structure of IP-002 with ellipsoids drawn at the 50 % probability level.



**Notes:**

All hydrogen atoms were fixed as riding models with the isotropic thermal parameters ( $U_{\text{iso}}$ ) based on the  $U_{\text{eq}}$  of the parent atom.

The IP-002\_Tables.html report contains tables of bond lengths, angles and torsion angles with standard deviations given in brackets.

Crystals were grown from a saturated solution of the compound in boiling EtOH before being allowed to equilibrate to room temperature.

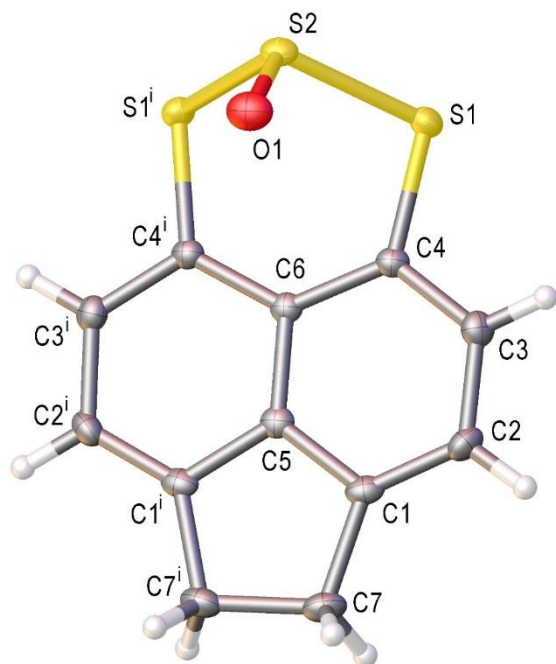
**CP-5-376B**

Table 1 Crystal data and structure refinement for CP-5-376B.

Identification code	CP-5-376B
Empirical formula	C <sub>12</sub> H <sub>8</sub> OS <sub>3</sub>
Formula weight	264.36
Temperature/K	99.9(2)
Crystal system	orthorhombic
Space group	Pnma
a/Å	8.5226(8)
b/Å	12.4656(12)
c/Å	9.8305(9)
α/°	90
β/°	90
γ/°	90
Volume/Å <sup>3</sup>	1044.39(17)
Z	4
ρ <sub>calc</sub> /cm <sup>3</sup>	1.681
μ/mm <sup>-1</sup>	6.242
F(000)	544.0
Crystal size/mm <sup>3</sup>	0.153 × 0.148 × 0.061
Radiation	CuKα (λ = 1.54184)
2θ range for data collection/°	11.464 to 146.008
Index ranges	-10 ≤ h ≤ 10, -11 ≤ k ≤ 15, -11 ≤ l ≤ 11
Reflections collected	2583
Independent reflections	1060 [R <sub>int</sub> = 0.0230, R <sub>sigma</sub> = 0.0233]
Data/restraints/parameters	1060/0/79
Goodness-of-fit on F <sup>2</sup>	1.113
Final R indexes [I ≥ 2σ (I)]	R <sub>1</sub> = 0.0301, wR <sub>2</sub> = 0.0789
Final R indexes [all data]	R <sub>1</sub> = 0.0333, wR <sub>2</sub> = 0.0826
Largest diff. peak/hole / e Å <sup>-3</sup>	0.36/-0.41

CP-5-376B.jpg: Crystal structure of CP-5-376B with ellipsoids drawn at the 50 % probability level.

Symmetry code used to generate equivalent atoms: \$1 x, ½-y, z.



**Notes:**

The molecule lies on a mirror plane running through S(2), O(1), C(6) and C(5) such that only half the molecule is crystallographically-unique.

The hydrogen atoms were fixed as riding models with the isotropic thermal parameters ( $U_{iso}$ ) based on the  $U_{eq}$  of the parent atom.

The CP-5-376B\_Tables.html report contains tables of bond lengths, angles and torsion angles with standard deviations given in brackets.

Crystals were grown from a saturated solution of  $\text{CH}_2\text{Cl}_2$  *via* slow diffusion in a refrigerated environment (4 °C) and wrapped in foil as to exclude light.

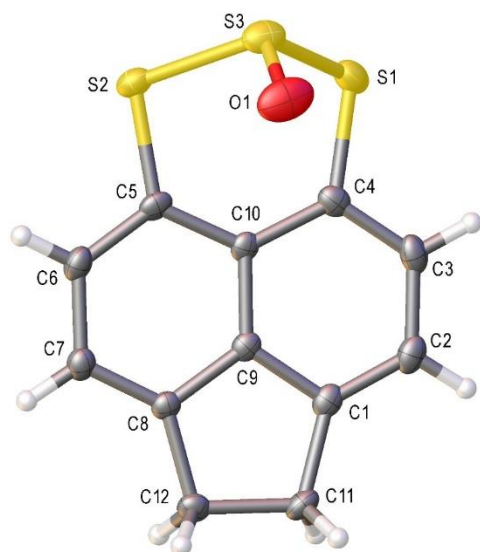


**CP-6-447C**

Table 1 Crystal data and structure refinement for CP-6-447C.

Identification code	CP-6-447C
Empirical formula	C <sub>12</sub> H <sub>8</sub> OS <sub>3</sub>
Formula weight	264.36
Temperature/K	100.01(10)
Crystal system	monoclinic
Space group	P2 <sub>1</sub> /n
a/Å	7.6195(5)
b/Å	8.2285(5)
c/Å	17.2251(11)
α/°	90
β/°	99.920(6)
γ/°	90
Volume/Å <sup>3</sup>	1063.82(12)
Z	4
ρ <sub>calc</sub> /g/cm <sup>3</sup>	1.651
μ/mm <sup>-1</sup>	6.128
F(000)	544.0
Crystal size/mm <sup>3</sup>	0.148 × 0.051 × 0.041
Radiation	Cu Kα (λ = 1.54184)
2θ range for data collection/°	10.428 to 145.67
Index ranges	-9 ≤ h ≤ 8, -6 ≤ k ≤ 9, -21 ≤ l ≤ 21
Reflections collected	3783
Independent reflections	2052 [R <sub>int</sub> = 0.0385, R <sub>sigma</sub> = 0.0535]
Data/restraints/parameters	2052/0/145
Goodness-of-fit on F <sup>2</sup>	1.037
Final R indexes [I ≥ 2σ (I)]	R <sub>1</sub> = 0.0474, wR <sub>2</sub> = 0.1226
Final R indexes [all data]	R <sub>1</sub> = 0.0595, wR <sub>2</sub> = 0.1331
Largest diff. peak/hole / e Å <sup>-3</sup>	0.93/-0.52

CP-6-447C\_YellowNeedle.jpg: Crystal structure of the yellow needle crystals in CP-6-447C with ellipsoids drawn at the 50 % probability level.



**Notes:**

The hydrogen atoms were fixed as riding models with the isotropic thermal parameters ( $U_{\text{iso}}$ ) based on the  $U_{\text{eq}}$  of the parent atom.

The CP-6-447C\_YellowNeedle\_Tables.html report contains tables of bond lengths, angles and torsion angles with standard deviations given in brackets.

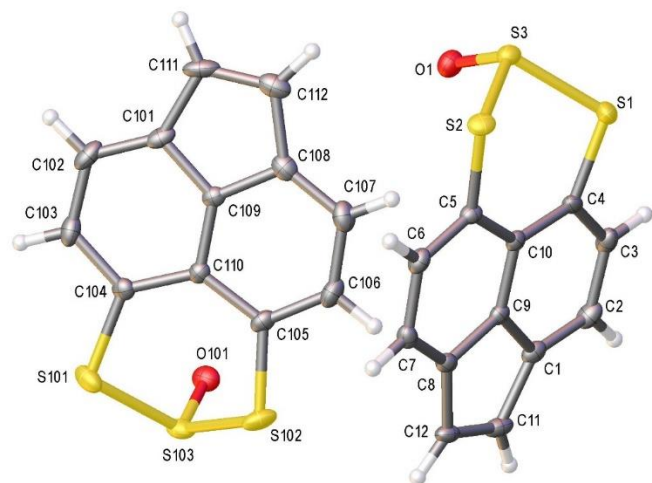
Crystals were grown from a saturated solution of  $\text{CH}_2\text{Cl}_2$  *via* slow diffusion in a refrigerated environment (4 °C) and wrapped in foil as to exclude light.

**CP-4-298B**

Table 1 Crystal data and structure refinement for CP-4-298B.

Identification code	CP-4-298B
Empirical formula	C <sub>12</sub> H <sub>6</sub> OS <sub>3</sub>
Formula weight	262.35
Temperature/K	100.15
Crystal system	orthorhombic
Space group	Pna2 <sub>1</sub>
a/Å	15.2201(2)
b/Å	7.84070(10)
c/Å	17.8587(2)
$\alpha/^\circ$	90
$\beta/^\circ$	90
$\gamma/^\circ$	90
Volume/Å <sup>3</sup>	2131.19(5)
Z	8
$\rho_{\text{calc}}/\text{cm}^3$	1.635
$\mu/\text{mm}^{-1}$	0.665
F(000)	1072.0
Crystal size/mm <sup>3</sup>	0.16 × 0.14 × 0.015
Radiation	MoK $\alpha$ ( $\lambda$ = 0.71075)
2 $\theta$ range for data collection/ $^\circ$	4.562 to 54.958
Index ranges	-19 ≤ h ≤ 19, -10 ≤ k ≤ 10, -23 ≤ l ≤ 23
Reflections collected	89714
Independent reflections	4888 [ $R_{\text{int}}$ = 0.0339, $R_{\text{sigma}}$ = 0.0116]
Data/restraints/parameters	4888/1/289
Goodness-of-fit on F <sup>2</sup>	1.080
Final R indexes [ $ I  \geq 2\sigma(I)$ ]	$R_1$ = 0.0250, $wR_2$ = 0.0717
Final R indexes [all data]	$R_1$ = 0.0254, $wR_2$ = 0.0719
Largest diff. peak/hole / e Å <sup>-3</sup>	0.38/-0.17
Flack parameter	0.215(15)

CP-4-298B.jpg: Crystal structure of CP-4-298B with ellipsoids drawn at the 50 % probability level.



**Notes:**

The data were collected by the UK National Crystallography Service, under the code 2020NCS0047r.

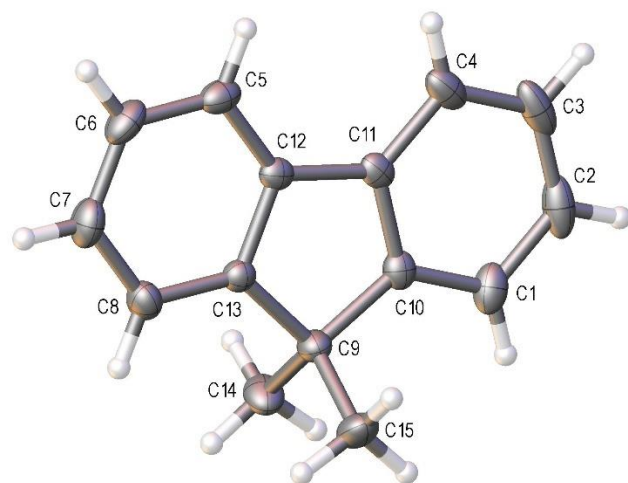
The hydrogen atoms were fixed as riding models with the isotropic thermal parameters ( $U_{\text{iso}}$ ) based on the  $U_{\text{eq}}$  of the parent atom.

The CP-4-298B\_Tables.html report contains tables of bond lengths, angles and torsion angles with standard deviations given in brackets.

**Dimethyl Fluorene**

Table 1 Crystal data and structure refinement for Dimethyl Fluorene.

Identification code	Dimethyl Fluorene
Empirical formula	C <sub>15</sub> H <sub>14</sub>
Formula weight	194.26
Temperature/K	99.9(2)
Crystal system	tetragonal
Space group	I4 <sub>1</sub> /a
a/Å	21.5292(5)
b/Å	21.5292(5)
c/Å	9.6610(4)
$\alpha$ /°	90
$\beta$ /°	90
$\gamma$ /°	90
Volume/Å <sup>3</sup>	4477.9(3)
Z	16
$\rho_{\text{calc}}/\text{cm}^3$	1.153
$\mu/\text{mm}^{-1}$	0.485
F(000)	1664.0
Crystal size/mm <sup>3</sup>	0.305 × 0.264 × 0.163
Radiation	CuK $\alpha$ ( $\lambda$ = 1.54184)
2 $\theta$ range for data collection/°	8.214 to 146.174
Index ranges	-23 ≤ h ≤ 21, -13 ≤ k ≤ 26, -9 ≤ l ≤ 11
Reflections collected	4943
Independent reflections	2190 [ $R_{\text{int}}$ = 0.0196, $R_{\text{sigma}}$ = 0.0206]
Data/restraints/parameters	2190/0/138
Goodness-of-fit on F <sup>2</sup>	1.058
Final R indexes [ $ I  \geq 2\sigma(I)$ ]	$R_1$ = 0.0384, $wR_2$ = 0.0986
Final R indexes [all data]	$R_1$ = 0.0416, $wR_2$ = 0.1026
Largest diff. peak/hole / e Å <sup>-3</sup>	0.27/-0.19



**Notes:**

The hydrogen atoms were fixed as riding models with the isotropic thermal parameters ( $U_{\text{iso}}$ ) based on the  $U_{\text{eq}}$  of the parent atom.

The Dimethyl Fluorene\_Tables.html report contains tables of bond lengths, angles and torsion angles with standard deviations given in brackets.

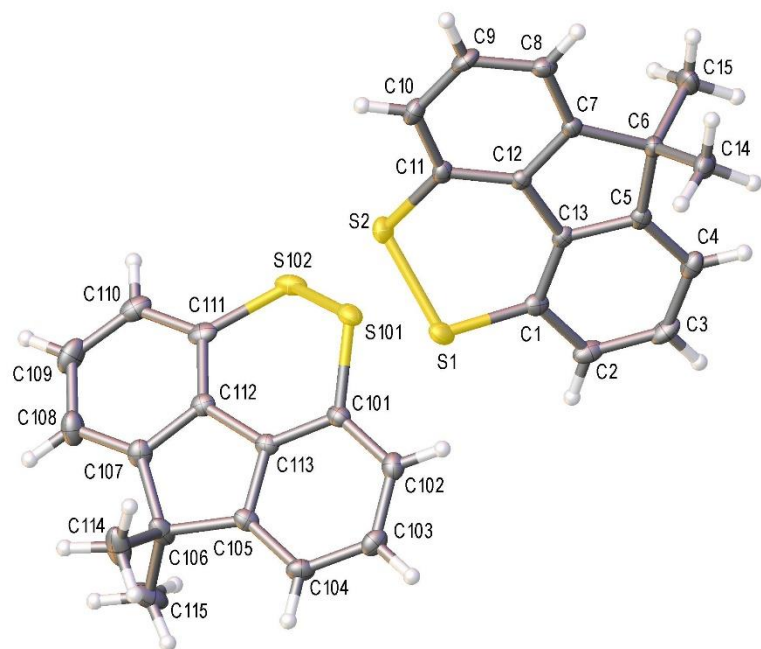
Crystals were grown from a saturated solution of the compound in boiling *n*hexane before being allowed to cool to room temperature.

Crystal structure of **9,9-dimethyl-9H-fluoreno[4,5-*cde*][1,2]dithiine 298**

**CP-1-37A**

Table 1 Crystal data and structure refinement for CP-1-37A.

Identification code	CP-1-37A
Empirical formula	C <sub>15</sub> H <sub>12</sub> S <sub>2</sub>
Formula weight	256.37
Temperature/K	100.01(10)
Crystal system	orthorhombic
Space group	P2 <sub>1</sub> 2 <sub>1</sub> 2 <sub>1</sub>
a/Å	12.25373(14)
b/Å	12.39979(13)
c/Å	16.53362(16)
α/°	90
β/°	90
γ/°	90
Volume/Å <sup>3</sup>	2512.18(4)
Z	8
ρ <sub>calc</sub> /g/cm <sup>3</sup>	1.356
μ/mm <sup>-1</sup>	3.597
F(000)	1072.0
Crystal size/mm <sup>3</sup>	0.198 × 0.145 × 0.081
Radiation	CuKα (λ = 1.54184)
2θ range for data collection/°	8.914 to 144.16
Index ranges	-13 ≤ h ≤ 15, -15 ≤ k ≤ 15, -20 ≤ l ≤ 20
Reflections collected	23988
Independent reflections	4942 [R <sub>int</sub> = 0.0251, R <sub>sigma</sub> = 0.0172]
Data/restraints/parameters	4942/0/311
Goodness-of-fit on F <sup>2</sup>	1.051
Final R indexes [I ≥ 2σ (I)]	R <sub>1</sub> = 0.0220, wR <sub>2</sub> = 0.0567
Final R indexes [all data]	R <sub>1</sub> = 0.0225, wR <sub>2</sub> = 0.0572
Largest diff. peak/hole / e Å <sup>-3</sup>	0.40/-0.17
Flack parameter	-0.003(4)



**Notes:**

The structure contains two crystallographically-independent molecules.

All hydrogen atoms are fixed as riding models.

The CP-1-37A\_Tables.html report contains tables of bond lengths, angles and torsion angles with standard deviations given in brackets.

Crystals were grown from a saturated solution of the compound in Et<sub>2</sub>O *via* slow diffusion at room temperature.

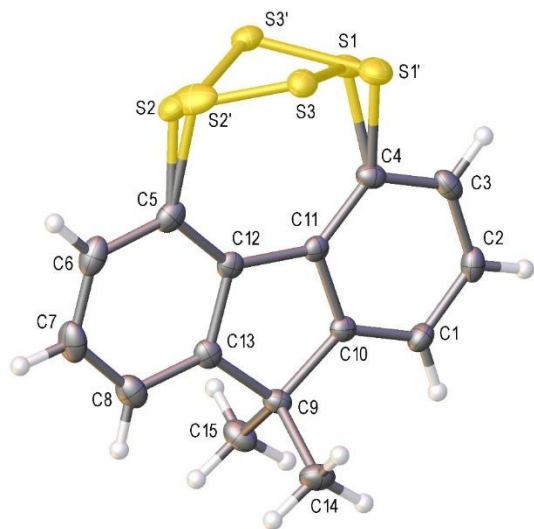


**CP-3-148A**

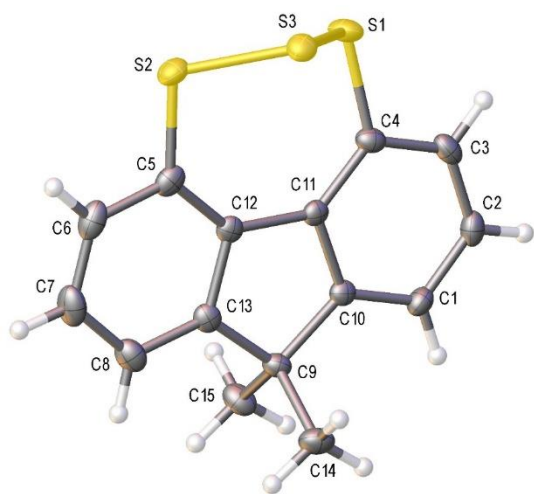
Table 1 Crystal data and structure refinement for CP-3-148A.

Identification code	CP-3-148A
Empirical formula	C <sub>15</sub> H <sub>12</sub> S <sub>3</sub>
Formula weight	288.43
Temperature/K	100.01(10)
Crystal system	monoclinic
Space group	P2 <sub>1</sub> /n
a/Å	8.0341(4)
b/Å	9.7990(6)
c/Å	17.0480(9)
$\alpha$ /°	90
$\beta$ /°	95.954(5)
$\gamma$ /°	90
Volume/Å <sup>3</sup>	1334.88(13)
Z	4
$\rho_{\text{calc}}$ /g/cm <sup>3</sup>	1.435
$\mu$ /mm <sup>-1</sup>	0.532
F(000)	600.0
Crystal size/mm <sup>3</sup>	0.343 × 0.194 × 0.163
Radiation	MoK $\alpha$ ( $\lambda$ = 0.71073)
2 $\theta$ range for data collection/°	7.184 to 56.882
Index ranges	-9 ≤ h ≤ 9, -9 ≤ k ≤ 12, -22 ≤ l ≤ 17
Reflections collected	7119
Independent reflections	2869 [ $R_{\text{int}}$ = 0.0292, $R_{\text{sigma}}$ = 0.0407]
Data/restraints/parameters	2869/0/193
Goodness-of-fit on F <sup>2</sup>	1.057
Final R indexes [ $ I  \geq 2\sigma(I)$ ]	$R_1$ = 0.0368, $wR_2$ = 0.0839
Final R indexes [all data]	$R_1$ = 0.0459, $wR_2$ = 0.0915
Largest diff. peak/hole / e Å <sup>-3</sup>	0.34/-0.29

CP-3-148A\_Complete\_Labelled.jpg / : CP-3-148A\_Complete\_Unlabelled.jpg Crystal structure of CP-3-148A with ellipsoids drawn at the 50 % probability level. The S<sub>3</sub> group (S(1)-S(3) / S(1')-S(3')) is disordered over two positions at a refined percentage occupancy ratio of 75.18 (16) : 24.82 (16).

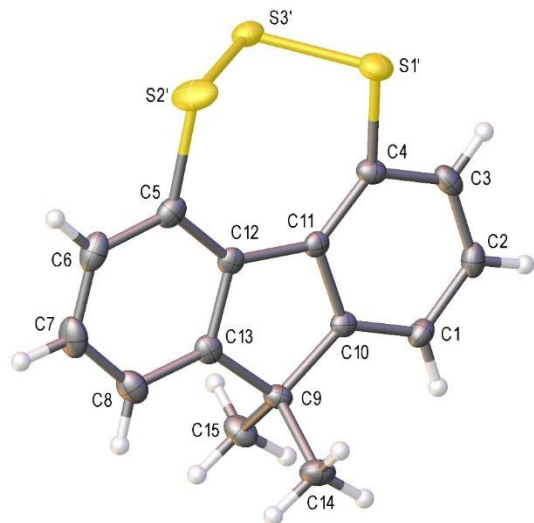


CP-3-148A\_MajorComponent\_Labelled.jpg / : CP-3-148A\_Complete\_Unlabelled.jpg Crystal structure of CP-3-148A with ellipsoids drawn at the 50 % probability level. The  $S_3$  group (S(1)-S(3) / S(1')-S(3')) is disordered over two positions at a refined percentage occupancy ratio of 75.18 (16) : 24.82 (16), with only the major position shown.



CP-3-148A\_MinorComponent\_Labelled.jpg / : CP-3-148A\_Complete\_Unlabelled.jpg Crystal structure of CP-3-148A with ellipsoids drawn at the 50 % probability level. The  $S_3$  group (S(1)-S(3)

/ S(1')-S(3')) is disordered over two positions at a refined percentage occupancy ratio of 75.18 (16) : 24.82 (16), with only the minor position shown.



#### Notes:

The S<sub>3</sub> group (S(1)-S(3) / S(1')-S(3')) is disordered over two positions at a refined percentage occupancy ratio of 75.18 (16) : 24.82 (16).

All hydrogen atoms were fixed as riding models with the isotropic thermal parameters ( $U_{iso}$ ) based on the  $U_{eq}$  of the parent atom.

The CP-3-148A \_Tables.html report contains tables of bond lengths, angles and torsion angles with standard deviations given in brackets.

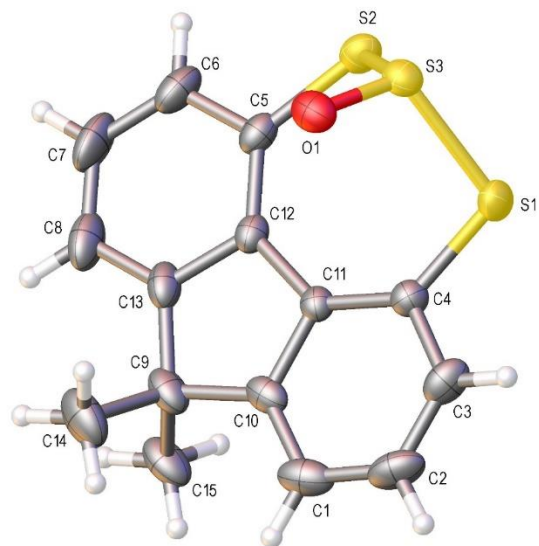
Crystals were grown from a saturated solution of the compound in CH<sub>2</sub>Cl<sub>2</sub> *via* slow diffusion at room temperature.

**CP-2-116AA**

Table 1 Crystal data and structure refinement for CP-2-116AA.

Identification code	CP-2-116AA
Empirical formula	C <sub>15</sub> H <sub>12</sub> OS <sub>3</sub>
Formula weight	304.43
Temperature/K	100.00(10)
Crystal system	trigonal
Space group	R3c
a/Å	27.9546(9)
b/Å	27.9546(9)
c/Å	9.1011(4)
$\alpha/^\circ$	90
$\beta/^\circ$	90
$\gamma/^\circ$	120
Volume/Å <sup>3</sup>	6159.3(5)
Z	18
$\rho_{\text{calc}}/\text{g cm}^{-3}$	1.477
$\mu/\text{mm}^{-1}$	4.843
F(000)	2844.0
Crystal size/mm <sup>3</sup>	0.221 × 0.07 × 0.039
Radiation	CuK $\alpha$ ( $\lambda$ = 1.54184)
2 $\theta$ range for data collection/ $^\circ$	10.964 to 148.966
Index ranges	-34 ≤ h ≤ 34, -32 ≤ k ≤ 34, -11 ≤ l ≤ 10
Reflections collected	28254
Independent reflections	2777 [ $R_{\text{int}}$ = 0.0546, $R_{\text{sigma}}$ = 0.0236]
Data/restraints/parameters	2777/1/174
Goodness-of-fit on $F^2$	1.066
Final R indexes [ $ I  \geq 2\sigma(I)$ ]	$R_1$ = 0.0378, $wR_2$ = 0.1007
Final R indexes [all data]	$R_1$ = 0.0395, $wR_2$ = 0.1024
Largest diff. peak/hole / e Å <sup>-3</sup>	0.26/-0.57
Flack parameter	0.003(13)

CP-2-116AA.jpg: Crystal structure of CP-2-116AA with ellipsoids drawn at the 50 % probability level.



### Notes:

The structure occupies a trigonal, non-centrosymmetric, non-chiral space group and the Flack parameter is 0.003(13), meaning that the absolute structure has been determined from the diffraction data.

The angle of bond S(3)-O(1) with the mean plane containing S(1)-S(3) is 117.81 (17)°.

All hydrogen atoms are fixed as riding models.

The CP-2-116AA\_Tables.html report contains tables of bond lengths, angles and torsion angles with standard deviations given in brackets.

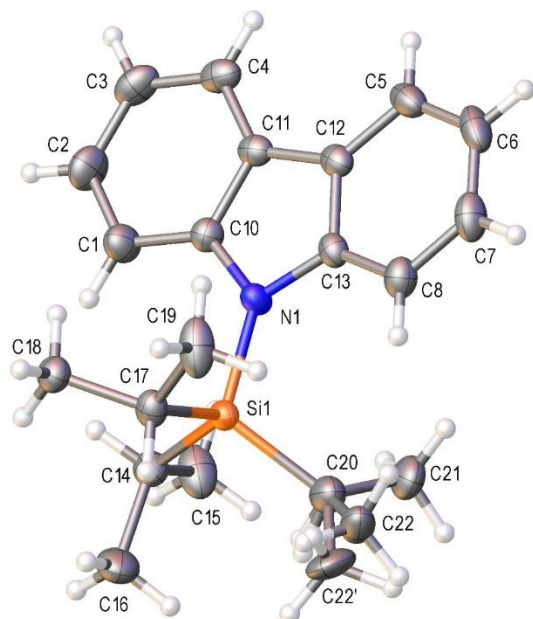
Crystals were grown from a saturated solution of CH<sub>2</sub>Cl<sub>2</sub> *via* slow diffusion in a refrigerated environment (4 °C) and wrapped in foil as to exclude light.

**CP-14-3-19**

Table 1 Crystal data and structure refinement for CP-14-3-19.

Identification code	CP-14-3-19
Empirical formula	C <sub>21</sub> H <sub>29</sub> NSi
Formula weight	323.54
Temperature/K	100.01(10)
Crystal system	monoclinic
Space group	P2 <sub>1</sub> /c
a/Å	9.3498(4)
b/Å	7.3678(3)
c/Å	27.1186(10)
$\alpha$ /°	90
$\beta$ /°	98.469(4)
$\gamma$ /°	90
Volume/Å <sup>3</sup>	1847.76(12)
Z	4
$\rho_{\text{calc}}$ /g/cm <sup>3</sup>	1.163
$\mu$ /mm <sup>-1</sup>	1.093
F(000)	704.0
Crystal size/mm <sup>3</sup>	0.241 × 0.049 × 0.031
Radiation	CuK $\alpha$ ( $\lambda$ = 1.54184)
2 $\theta$ range for data collection/°	9.564 to 140.102
Index ranges	-11 ≤ h ≤ 10, -8 ≤ k ≤ 6, -23 ≤ l ≤ 33
Reflections collected	6721
Independent reflections	3490 [ $R_{\text{int}}$ = 0.0354, $R_{\text{sigma}}$ = 0.0476]
Data/restraints/parameters	3490/0/225
Goodness-of-fit on $F^2$	1.052
Final R indexes [ $ I  \geq 2\sigma(I)$ ]	$R_1$ = 0.0581, $wR_2$ = 0.1456
Final R indexes [all data]	$R_1$ = 0.0679, $wR_2$ = 0.1522
Largest diff. peak/hole / e Å <sup>-3</sup>	0.38/-0.50

CP-14-3-19.jpg: Crystal structure of CP-14-3-19 with ellipsoids drawn at the 50 % probability level. The methyl group C(22) / C(22') is disordered over two positions at a refined percentage occupancy ratio of 84 (2) : 16 (2).



**Notes:**

The methyl group C(22) / C(22') is disordered over two positions at a refined percentage occupancy ratio of 84 (2) : 16 (2).

All hydrogen atoms were fixed as riding models with the isotropic thermal parameters ( $U_{iso}$ ) based on the  $U_{eq}$  of the parent atom.

The CP-14-3-19\_Tables.html report contains tables of bond lengths, angles and torsion angles with standard deviations given in brackets.

Crystals were grown from a saturated solution of the compound in  $CH_2Cl_2$  *via* slow diffusion at room temperature.

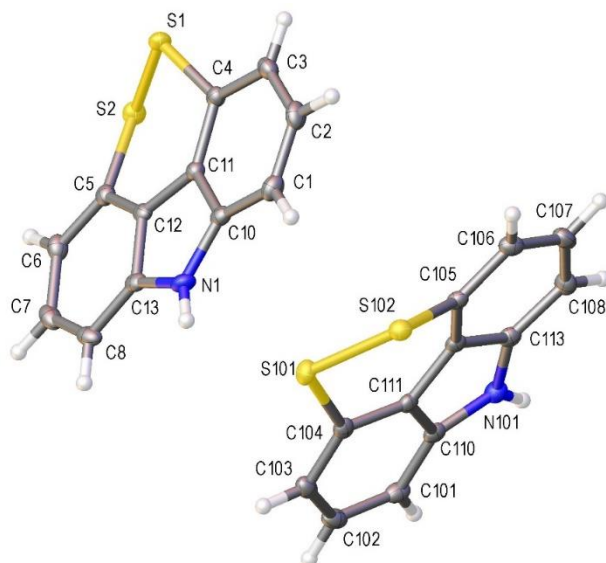
**CP-3-190A**

Table 1 Crystal data and structure refinement for CP-3-190A.

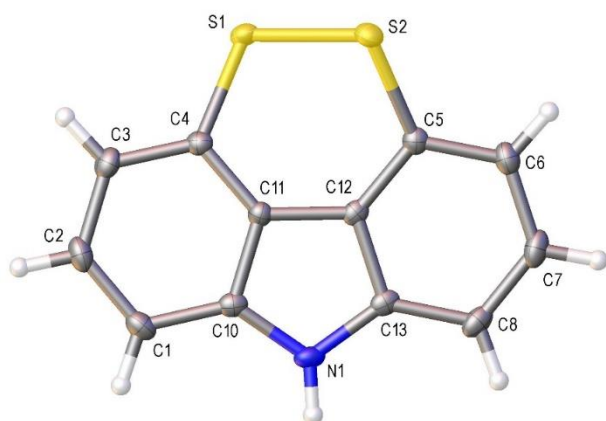
Identification code	CP-3-190A
Empirical formula	C <sub>12</sub> H <sub>7</sub> NS <sub>2</sub>
Formula weight	229.31
Temperature/K	100.00(10)
Crystal system	triclinic
Space group	P-1
a/Å	9.3372(6)
b/Å	10.5025(6)
c/Å	10.6156(6)
$\alpha$ /°	92.683(4)
$\beta$ /°	108.926(5)
$\gamma$ /°	91.966(5)
Volume/Å <sup>3</sup>	982.30(10)
Z	4
$\rho_{\text{calc}}$ /g/cm <sup>3</sup>	1.551
$\mu$ /mm <sup>-1</sup>	4.559
F(000)	472.0
Crystal size/mm <sup>3</sup>	0.18 × 0.141 × 0.058
Radiation	CuK $\alpha$ ( $\lambda$ = 1.54184)
2 $\theta$ range for data collection/°	8.44 to 149.248
Index ranges	-10 ≤ h ≤ 11, -9 ≤ k ≤ 12, -13 ≤ l ≤ 9
Reflections collected	6804
Independent reflections	3862 [ $R_{\text{int}}$ = 0.0234, $R_{\text{sigma}}$ = 0.0301]
Data/restraints/parameters	3862/0/279
Goodness-of-fit on F <sup>2</sup>	1.047
Final R indexes [ $ I  \geq 2\sigma(I)$ ]	$R_1$ = 0.0292, $wR_2$ = 0.0741
Final R indexes [all data]	$R_1$ = 0.0335, $wR_2$ = 0.0776
Largest diff. peak/hole / e Å <sup>-3</sup>	0.37/-0.32

CP-3-190A\_Complete.jpg: Crystal structure of CP-3-190A with ellipsoids drawn at the 50 % probability level. The structure contains two crystallographically-independent molecules.

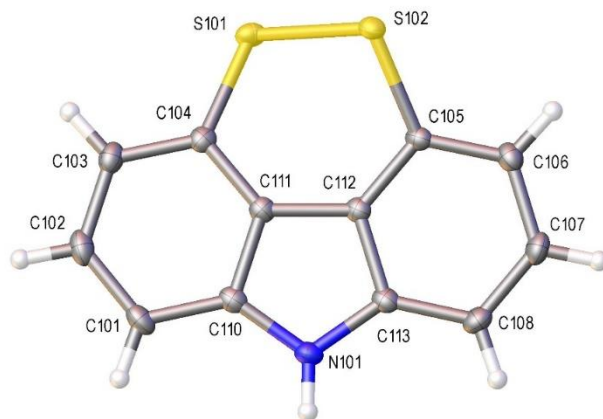




CP-3-190A\_Molecule1.jpg: Crystal structure of molecule 1 of CP-3-190A with ellipsoids drawn at the 50 % probability level. The structure contains two crystallographically-independent molecules of which only one is shown for clarity.



CP-3-190A\_Molecule2.jpg: Crystal structure of molecule 2 of CP-3-190A with ellipsoids drawn at the 50 % probability level. The structure contains two crystallographically-independent molecules of which only one is shown for clarity.



**Notes:**

The structure contains two crystallographically-independent molecules.

The hydrogen atoms bonded to N(1) and N(101) were located in the electron density and freely refined. All remaining hydrogen atoms were fixed as riding models with the isotropic thermal parameters ( $U_{iso}$ ) based on the  $U_{eq}$  of the parent atom.

Hydrogen bonding is detailed in Table 6 of the CP-3-190A\_Tables.html report.

The CP-3-190A\_Tables.html report contains tables of bond lengths, angles and torsion angles with standard deviations given in brackets.

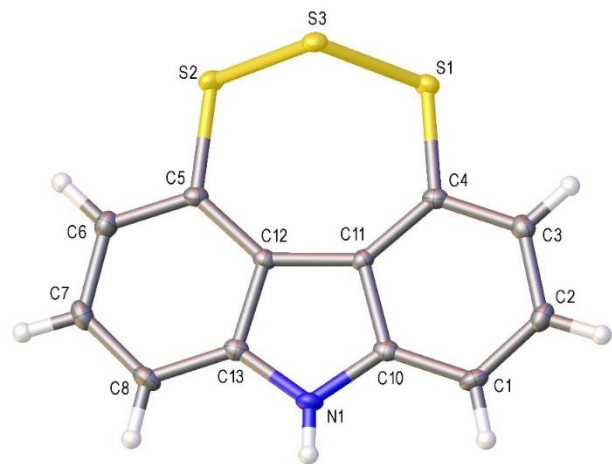
Crystals were grown from a saturated solution of the compound in Et<sub>2</sub>O *via* slow diffusion at room temperature.

**CP-3-210**

Table 1 Crystal data and structure refinement for CP-3-210.

Identification code	CP-3-210
Empirical formula	C <sub>12</sub> H <sub>7</sub> NS <sub>3</sub>
Formula weight	261.37
Temperature/K	100.01(10)
Crystal system	monoclinic
Space group	P2 <sub>1</sub> /c
a/Å	7.6019(3)
b/Å	8.7842(5)
c/Å	15.5542(7)
α/°	90
β/°	94.998(4)
γ/°	90
Volume/Å <sup>3</sup>	1034.71(9)
Z	4
ρ <sub>calc</sub> /cm <sup>3</sup>	1.678
μ/mm <sup>-1</sup>	6.250
F(000)	536.0
Crystal size/mm <sup>3</sup>	0.254 × 0.126 × 0.048
Radiation	CuKα (λ = 1.54184)
2θ range for data collection/°	11.58 to 149.034
Index ranges	-5 ≤ h ≤ 9, -10 ≤ k ≤ 10, -19 ≤ l ≤ 18
Reflections collected	3946
Independent reflections	2043 [R <sub>int</sub> = 0.0205, R <sub>sigma</sub> = 0.0264]
Data/restraints/parameters	2043/0/149
Goodness-of-fit on F <sup>2</sup>	1.087
Final R indexes [I ≥ 2σ (I)]	R <sub>1</sub> = 0.0277, wR <sub>2</sub> = 0.0692
Final R indexes [all data]	R <sub>1</sub> = 0.0318, wR <sub>2</sub> = 0.0727
Largest diff. peak/hole / e Å <sup>-3</sup>	0.38/-0.29

CP-3-210.jpg: Crystal structure of CP-3-210 with ellipsoids drawn at the 50 % probability level.



**Notes:**

The hydrogen atom bonded to N(1) was located in the electron density and freely refined. All remaining hydrogen atoms were fixed as riding models with the isotropic thermal parameters ( $U_{\text{iso}}$ ) based on the  $U_{\text{eq}}$  of the parent atom.

Hydrogen bonding is detailed in Table 6 of the CP-3-210\_Tables.html report.

The CP-3-210\_Tables.html report contains tables of bond lengths, angles, torsion angles and hydrogen bonding with standard deviations given in brackets.

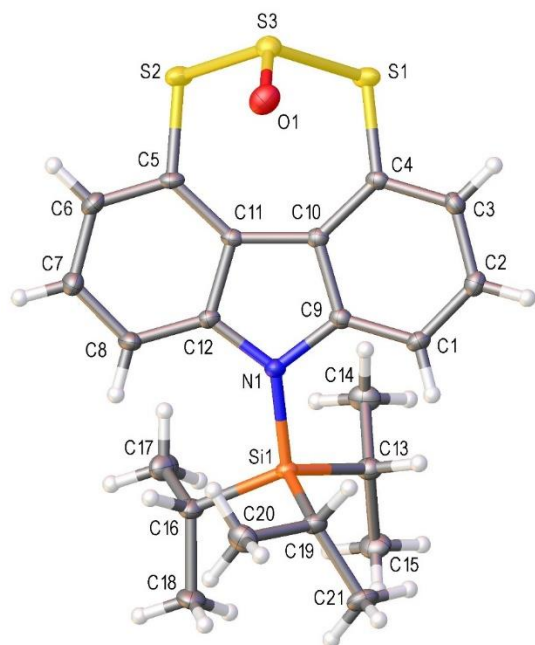
Crystals were grown from a saturated solution of the compound in  $\text{CH}_2\text{Cl}_2$  *via* slow diffusion at room temperature.

**CP-6-438B**

Table 1 Crystal data and structure refinement for CP-6-438B.

Identification code	CP-6-438B
Empirical formula	C <sub>21</sub> H <sub>27</sub> NOS <sub>3</sub> Si
Formula weight	433.70
Temperature/K	100.01(10)
Crystal system	monoclinic
Space group	P2 <sub>1</sub> /n
a/Å	11.7378(2)
b/Å	14.8810(3)
c/Å	12.2904(2)
α/°	90
β/°	96.299(2)
γ/°	90
Volume/Å <sup>3</sup>	2133.81(7)
Z	4
ρ <sub>calc</sub> /cm <sup>3</sup>	1.350
μ/mm <sup>-1</sup>	3.798
F(000)	920.0
Crystal size/mm <sup>3</sup>	0.184 × 0.108 × 0.072
Radiation	CuKα (λ = 1.54184)
2θ range for data collection/°	9.366 to 145.912
Index ranges	-13 ≤ h ≤ 14, -18 ≤ k ≤ 18, -15 ≤ l ≤ 15
Reflections collected	40094
Independent reflections	4241 [R <sub>int</sub> = 0.0394, R <sub>sigma</sub> = 0.0177]
Data/restraints/parameters	4241/0/250
Goodness-of-fit on F <sup>2</sup>	1.059
Final R indexes [I ≥ 2σ (I)]	R <sub>1</sub> = 0.0387, wR <sub>2</sub> = 0.1002
Final R indexes [all data]	R <sub>1</sub> = 0.0411, wR <sub>2</sub> = 0.1024
Largest diff. peak/hole / e Å <sup>-3</sup>	1.52/-0.51

Crystal structure of 4*H*-[1,2,3]trithiepine[4,5,6,7-*def*]carbazole-9-oxide with ellipsoids drawn at the 50 % probability level.



#### Notes:

The hydrogen atoms were fixed as riding models with the isotropic thermal parameters ( $U_{\text{iso}}$ ) based on the  $U_{\text{eq}}$  of the parent atom.

The CP-6-438B\_Tables.html report contains tables of bond lengths, angles and torsion angles with standard deviations given in brackets.

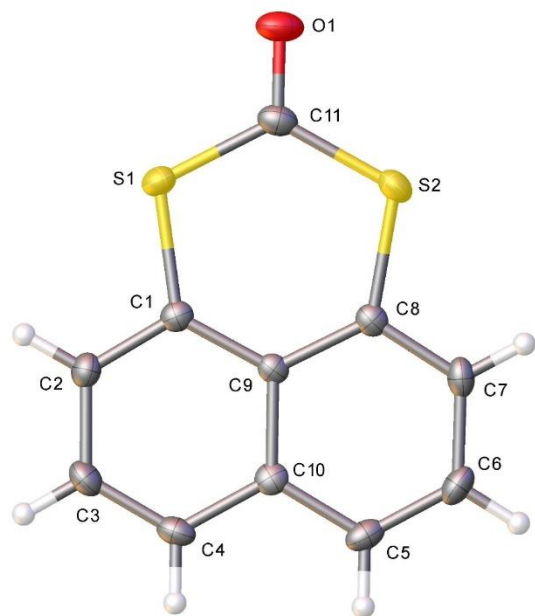
Crystals were grown from a saturated solution of  $\text{CH}_2\text{Cl}_2$  *via* slow diffusion in a refrigerated environment (4 °C) and wrapped in foil as to exclude light.

**CP-4-259B\_NAPHTHALENE DITHIOCARBONATE**

Table 1 Crystal data and structure refinement for CP-4-259B\_NAPHTHALENE DITHIOCARBONATE.

Identification code	CP-4-259B_NAPHTHALENE DITHIOCARBONATE
Empirical formula	C <sub>11</sub> H <sub>6</sub> OS <sub>2</sub>
Formula weight	218.28
Temperature/K	100.00(10)
Crystal system	orthorhombic
Space group	Pna2 <sub>1</sub>
a/Å	13.6325(4)
b/Å	17.5885(5)
c/Å	3.85100(10)
$\alpha/^\circ$	90
$\beta/^\circ$	90
$\gamma/^\circ$	90
Volume/Å <sup>3</sup>	923.37(4)
Z	4
$\rho_{\text{calc}}/\text{g cm}^{-3}$	1.570
$\mu/\text{mm}^{-1}$	4.868
F(000)	448.0
Crystal size/mm <sup>3</sup>	0.319 × 0.073 × 0.049
Radiation	CuK $\alpha$ ( $\lambda$ = 1.54184)
2 $\theta$ range for data collection/ $^\circ$	8.206 to 136.502
Index ranges	-16 ≤ h ≤ 16, -21 ≤ k ≤ 21, -4 ≤ l ≤ 4
Reflections collected	8287
Independent reflections	1651 [ $R_{\text{int}}$ = 0.0318, $R_{\text{sigma}}$ = 0.0207]
Data/restraints/parameters	1651/1/127
Goodness-of-fit on $F^2$	1.055
Final R indexes [ $I \geq 2\sigma(I)$ ]	$R_1$ = 0.0254, $wR_2$ = 0.0647
Final R indexes [all data]	$R_1$ = 0.0264, $wR_2$ = 0.0656
Largest diff. peak/hole / e Å <sup>-3</sup>	0.21/-0.19
Flack parameter	-0.025(18)

Crystal structure of naphtho[1,8-*de*][1,3]dithiin-2-one with ellipsoids drawn at the 50 % probability level.



**Notes:**

The Naphthalene dithiocarbonate\_Tables.html report contains tables of bond lengths, angles and torsion angles with standard deviations given in brackets.

Crystals were grown from a saturated solution of the compound in CH<sub>2</sub>Cl<sub>2</sub> *via* slow diffusion.

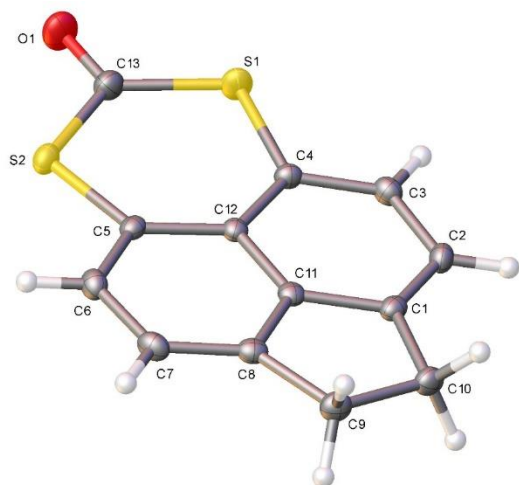


## CP-3-235B

Table 1 Crystal data and structure refinement for CP-3-235B.

Identification code	CP-3-235B
Empirical formula	C <sub>13</sub> H <sub>8</sub> OS <sub>2</sub>
Formula weight	244.31
Temperature/K	100.00(10)
Crystal system	monoclinic
Space group	P2 <sub>1</sub> /c
a/Å	8.6942(2)
b/Å	10.8592(2)
c/Å	11.1683(2)
α/°	90
β/°	101.228(2)
γ/°	90
Volume/Å <sup>3</sup>	1034.24(4)
Z	4
ρ <sub>calc</sub> /cm <sup>3</sup>	1.569
μ/mm <sup>-1</sup>	4.416
F(000)	504.0
Crystal size/mm <sup>3</sup>	0.203 × 0.174 × 0.054
Radiation	CuKα (λ = 1.54184)
2θ range for data collection/°	10.374 to 149.33
Index ranges	-10 ≤ h ≤ 10, -13 ≤ k ≤ 13, -13 ≤ l ≤ 13
Reflections collected	19284
Independent reflections	2104 [R <sub>int</sub> = 0.0348, R <sub>sigma</sub> = 0.0145]
Data/restraints/parameters	2104/0/145
Goodness-of-fit on F <sup>2</sup>	1.073
Final R indexes [I ≥ 2σ (I)]	R <sub>1</sub> = 0.0288, wR <sub>2</sub> = 0.0725
Final R indexes [all data]	R <sub>1</sub> = 0.0306, wR <sub>2</sub> = 0.0742
Largest diff. peak/hole / e Å <sup>-3</sup>	0.63/-0.32

CP-3-235B.jpg: Crystal structure of CP-3-235B B with ellipsoids drawn at the 50 % probability level.



**Notes:**

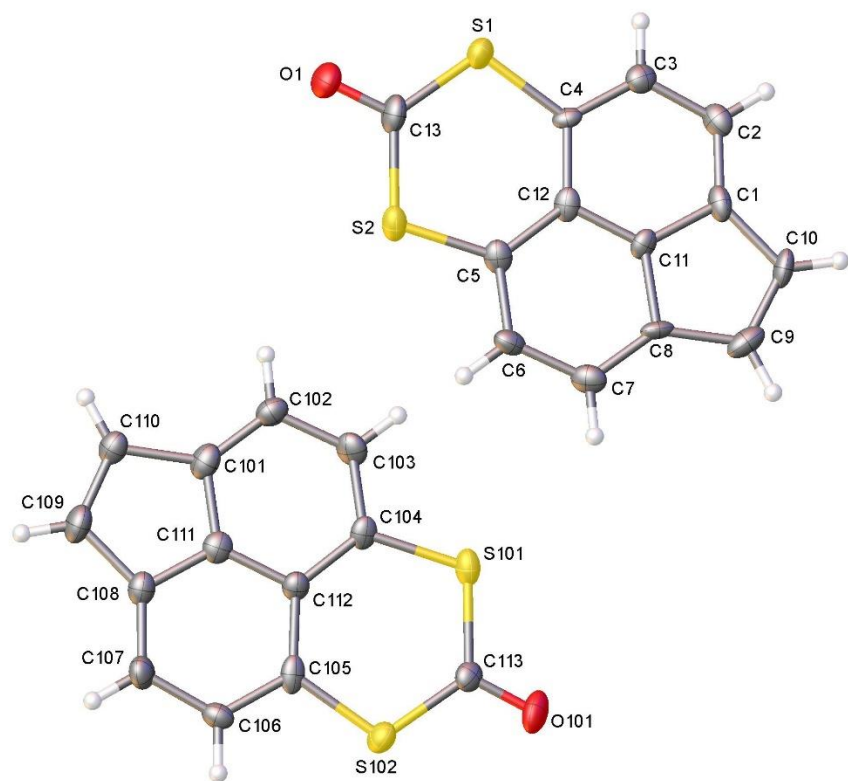
Crystals were grown from a saturated solution of  $\text{CH}_2\text{Cl}_2$  *via* slow diffusion.

**CP-4-245B**

Table 1 Crystal data and structure refinement for CP-4-245B.

Identification code	CP-4-245B
Empirical formula	C <sub>13</sub> H <sub>6</sub> OS <sub>2</sub>
Formula weight	242.30
Temperature/K	100.00(10)
Crystal system	orthorhombic
Space group	Pca2 <sub>1</sub>
a/Å	19.5898(10)
b/Å	3.8640(2)
c/Å	26.4840(12)
α/°	90
β/°	90
γ/°	90
Volume/Å <sup>3</sup>	2004.71(17)
Z	8
ρ <sub>calc</sub> /cm <sup>3</sup>	1.606
μ/mm <sup>-1</sup>	4.556
F(000)	992.0
Crystal size/mm <sup>3</sup>	0.128 × 0.107 × 0.048
Radiation	CuKα (λ = 1.54184)
2θ range for data collection/°	9.028 to 136.46
Index ranges	-23 ≤ h ≤ 23, -4 ≤ k ≤ 4, -31 ≤ l ≤ 28
Reflections collected	6369
Independent reflections	3133 [R <sub>int</sub> = 0.0406, R <sub>sigma</sub> = 0.0520]
Data/restraints/parameters	3133/1/290
Goodness-of-fit on F <sup>2</sup>	1.066
Final R indexes [I ≥ 2σ (I)]	R <sub>1</sub> = 0.0755, wR <sub>2</sub> = 0.1909
Final R indexes [all data]	R <sub>1</sub> = 0.0788, wR <sub>2</sub> = 0.1963
Largest diff. peak/hole / e Å <sup>-3</sup>	2.01/-0.53
Flack parameter	0.30(6)

CP-4-245B.jpg: Crystal structure of CP-4-245B with ellipsoids drawn at the 50 % probability level.



**Notes:**

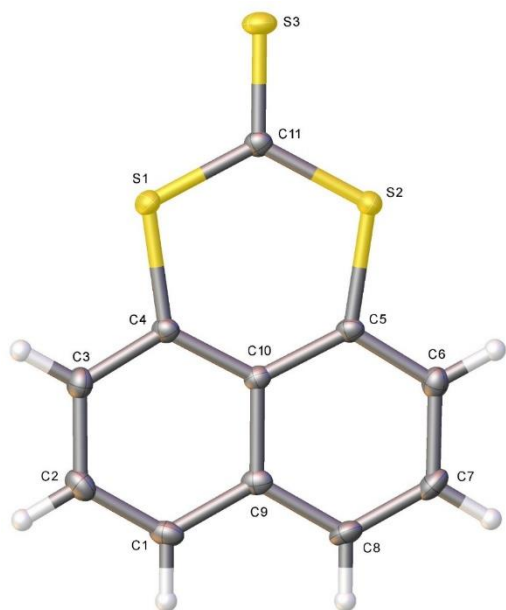
Crystals were grown from a saturated solution of  $\text{CH}_2\text{Cl}_2$  *via* slow diffusion.

**CP-5-330C**

Table 1 Crystal data and structure refinement for CP-5-330C.

Identification code	CP-5-330C
Empirical formula	C <sub>11</sub> H <sub>6</sub> S <sub>3</sub>
Formula weight	234.34
Temperature/K	100.01(10)
Crystal system	monoclinic
Space group	P2 <sub>1</sub> /c
a/Å	12.1432(8)
b/Å	3.8846(3)
c/Å	20.2421(12)
$\alpha$ /°	90
$\beta$ /°	95.363(6)
$\gamma$ /°	90
Volume/Å <sup>3</sup>	950.67(11)
Z	4
$\rho_{\text{calc}}/\text{cm}^3$	1.637
$\mu/\text{mm}^{-1}$	6.691
F(000)	480.0
Crystal size/mm <sup>3</sup>	0.292 × 0.11 × 0.094
Radiation	Cu K $\alpha$ ( $\lambda$ = 1.54184)
2 $\theta$ range for data collection/°	7.312 to 146.024
Index ranges	-13 ≤ h ≤ 15, -2 ≤ k ≤ 4, -24 ≤ l ≤ 24
Reflections collected	3143
Independent reflections	1845 [ $R_{\text{int}}$ = 0.0258, $R_{\text{sigma}}$ = 0.0328]
Data/restraints/parameters	1845/0/127
Goodness-of-fit on F <sup>2</sup>	1.078
Final R indexes [ $ I  \geq 2\sigma(I)$ ]	$R_1$ = 0.0383, $wR_2$ = 0.1031
Final R indexes [all data]	$R_1$ = 0.0432, $wR_2$ = 0.1087
Largest diff. peak/hole / e Å <sup>-3</sup>	0.52/-0.68

Crystal structure of naphtho[1,8-*de*][1,3]dithiin-2-thione with ellipsoids drawn at the 50 % probability level.



Crystals were grown from a saturated solution of the compound in  $\text{CH}_2\text{Cl}_2$  *via* slow diffusion.

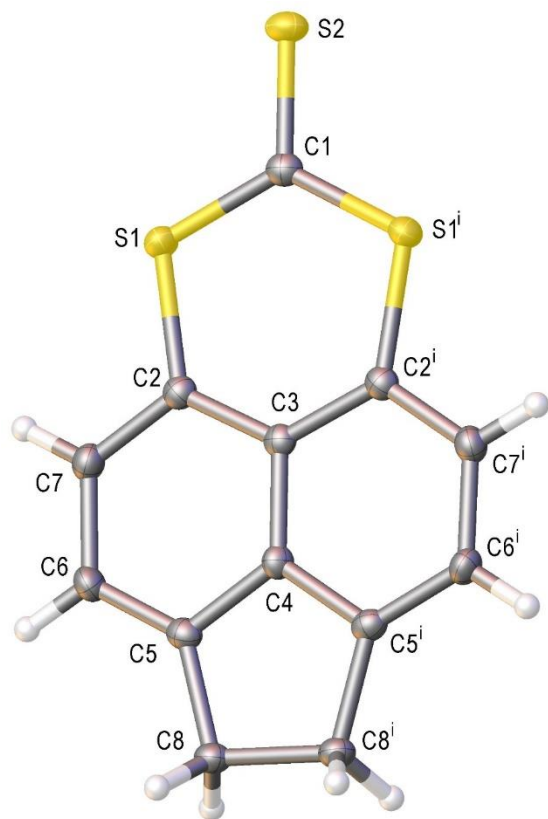
## CP-3-235B

Table 1 Crystal data and structure refinement for CP-3-235B.

Identification code	CP-3-235B
Empirical formula	C <sub>13</sub> H <sub>8</sub> OS <sub>2</sub>
Formula weight	244.31
Temperature/K	100.00(10)
Crystal system	monoclinic
Space group	P2 <sub>1</sub> /c
a/Å	8.6942(2)
b/Å	10.8592(2)
c/Å	11.1683(2)
α/°	90
β/°	101.228(2)
γ/°	90
Volume/Å <sup>3</sup>	1034.24(4)
Z	4
ρ <sub>calc</sub> /cm <sup>3</sup>	1.569
μ/mm <sup>-1</sup>	4.416
F(000)	504.0
Crystal size/mm <sup>3</sup>	0.203 × 0.174 × 0.054
Radiation	CuKα (λ = 1.54184)
2θ range for data collection/°	10.374 to 149.33
Index ranges	-10 ≤ h ≤ 10, -13 ≤ k ≤ 13, -13 ≤ l ≤ 13
Reflections collected	19284
Independent reflections	2104 [R <sub>int</sub> = 0.0348, R <sub>sigma</sub> = 0.0145]
Data/restraints/parameters	2104/0/145
Goodness-of-fit on F <sup>2</sup>	1.073
Final R indexes [I ≥ 2σ (I)]	R <sub>1</sub> = 0.0288, wR <sub>2</sub> = 0.0725
Final R indexes [all data]	R <sub>1</sub> = 0.0306, wR <sub>2</sub> = 0.0742
Largest diff. peak/hole / e Å <sup>-3</sup>	0.63/-0.32

CP-5-355A.jpg: Crystal structure of CP-5-355A with ellipsoids drawn at the 50 % probability level.

Symmetry code used to generate equivalent atoms: \$1 1-x, y, 1.5-x.



**Notes:**

The molecule lies on a 2-fold rotation axis running through C(1), C(3), C(4) and S(2) such that only half the molecule is crystallographically-unique.

The hydrogen atoms were fixed as riding models with the isotropic thermal parameters ( $U_{iso}$ ) based on the  $U_{eq}$  of the parent atom.

The CP-5-355A\_Tables.html report contains tables of bond lengths, angles and torsion angles with standard deviations given in brackets.



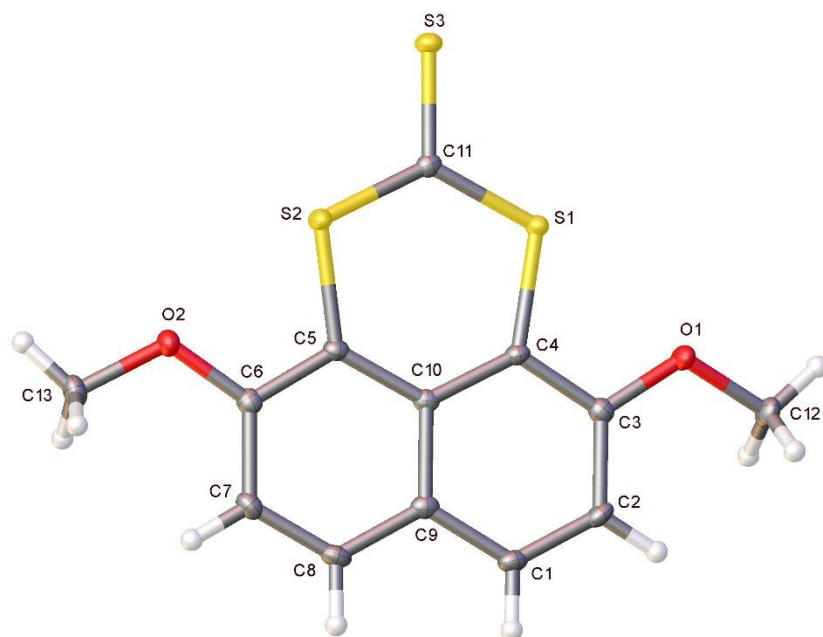
## CP-Dimethoxynaphthalene TTC

Table 1 Crystal data and structure refinement for CP-Dimethoxynaphthalene TTC.

Identification code	CP-Dimethoxynaphthalene TTC
Empirical formula	C <sub>13</sub> H <sub>10</sub> O <sub>2</sub> S <sub>3</sub>
Formula weight	294.39
Temperature/K	100.00(10)
Crystal system	triclinic
Space group	P-1
a/Å	7.8677(7)
b/Å	9.0231(8)
c/Å	9.9377(8)
α/°	112.088(8)
β/°	97.194(7)
γ/°	108.017(8)
Volume/Å <sup>3</sup>	597.84(10)
Z	2
ρ <sub>calc</sub> /cm <sup>3</sup>	1.635
μ/mm <sup>-1</sup>	5.584
F(000)	304.0
Crystal size/mm <sup>3</sup>	0.09 × 0.084 × 0.026
Radiation	Cu Kα (λ = 1.54184)
2θ range for data collection/°	9.988 to 145.942
Index ranges	-7 ≤ h ≤ 9, -9 ≤ k ≤ 10, -12 ≤ l ≤ 9
Reflections collected	3912
Independent reflections	2296 [R <sub>int</sub> = 0.0251, R <sub>sigma</sub> = 0.0382]
Data/restraints/parameters	2296/0/165
Goodness-of-fit on F <sup>2</sup>	1.053
Final R indexes [I ≥ 2σ (I)]	R <sub>1</sub> = 0.0291, wR <sub>2</sub> = 0.0666
Final R indexes [all data]	R <sub>1</sub> = 0.0341, wR <sub>2</sub> = 0.0703
Largest diff. peak/hole / e Å <sup>-3</sup>	0.32/-0.31

CP-5-355A.jpg: Crystal structure of CP-5-355A with ellipsoids drawn at the 50 % probability level.

Symmetry code used to generate equivalent atoms: \$1 1-x, y, 1.5-x\$.



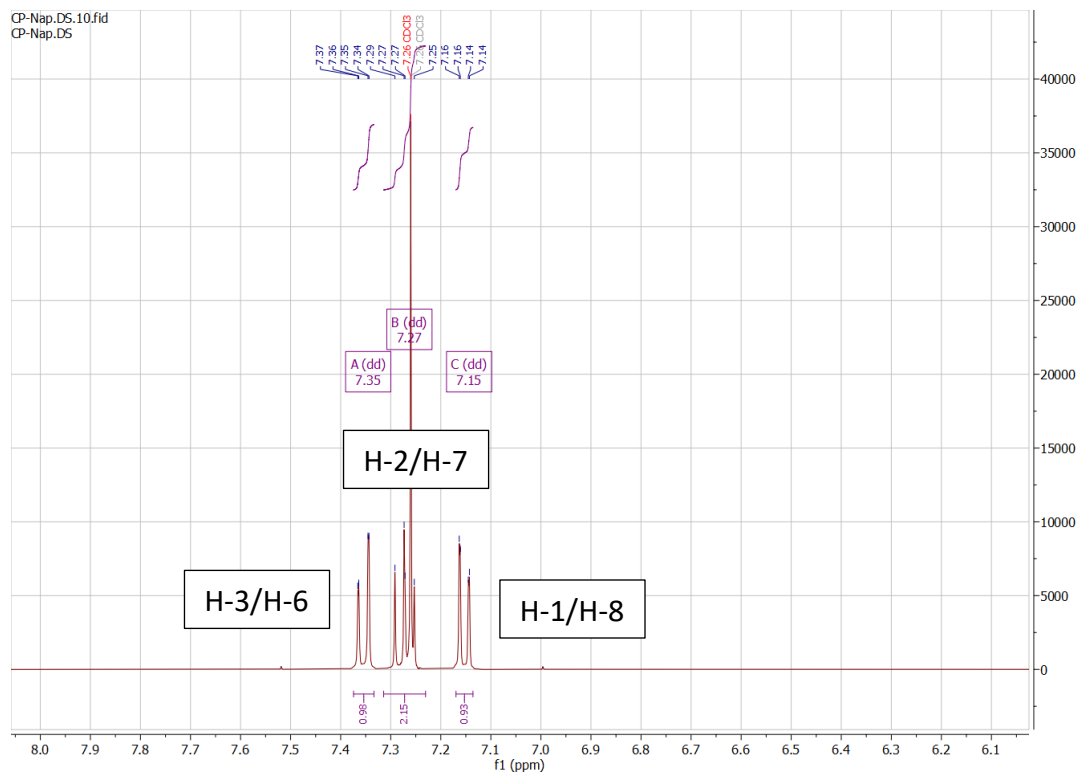
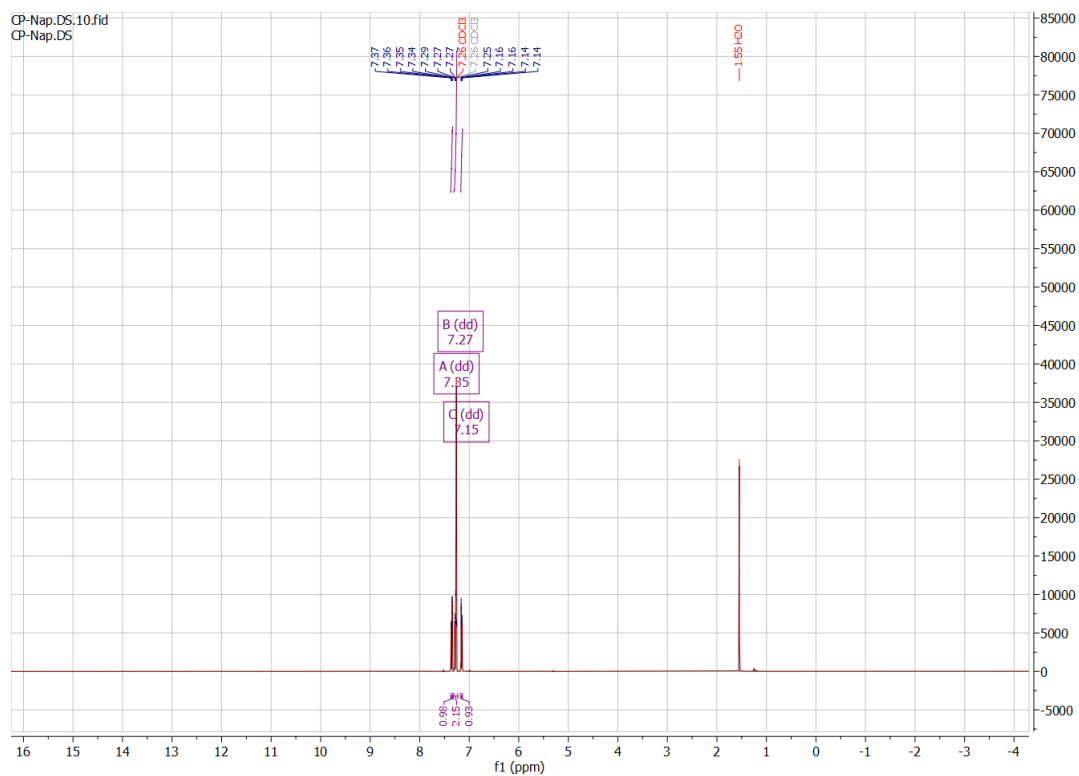
**Notes:**

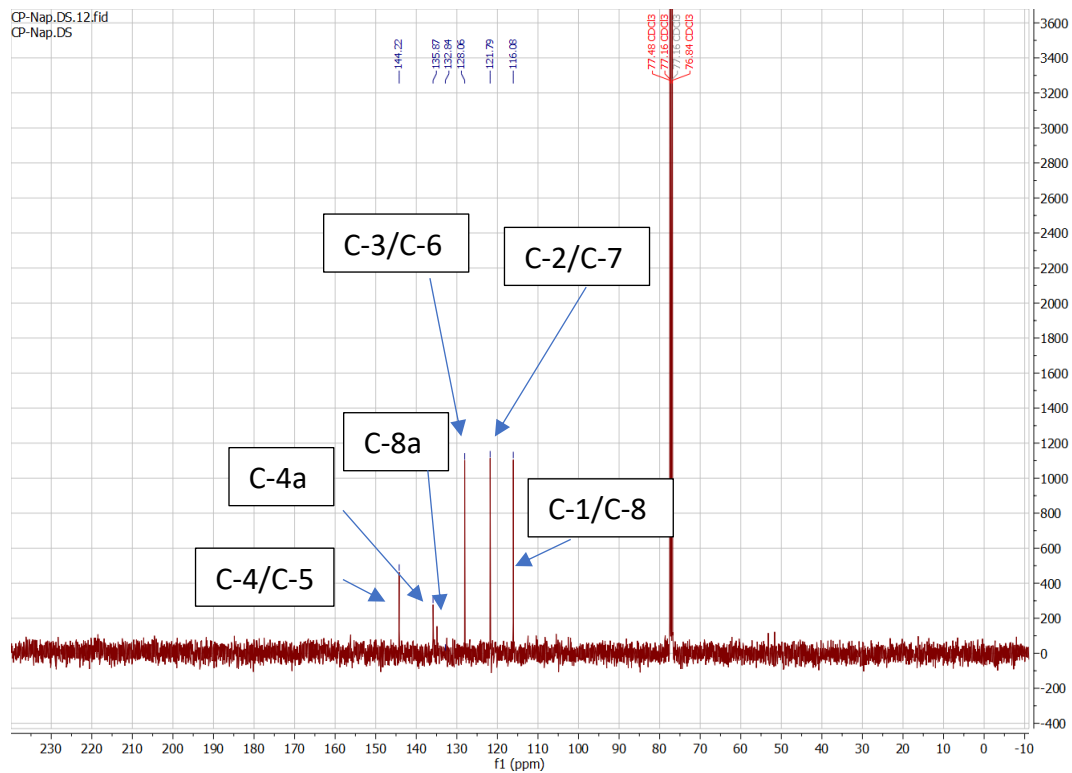
The molecule lies on a 2-fold rotation axis running through C(1), C(3), C(4) and S(2) such that only half the molecule is crystallographically-unique.

The hydrogen atoms were fixed as riding models with the isotropic thermal parameters ( $U_{iso}$ ) based on the  $U_{eq}$  of the parent atom.

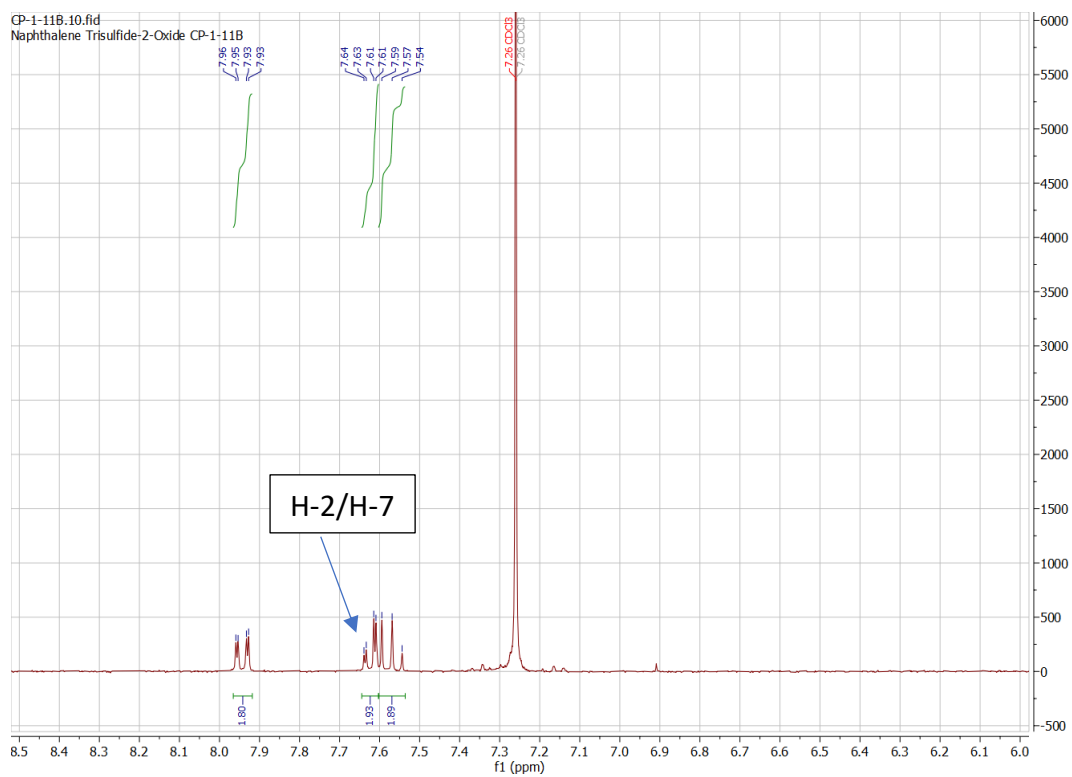
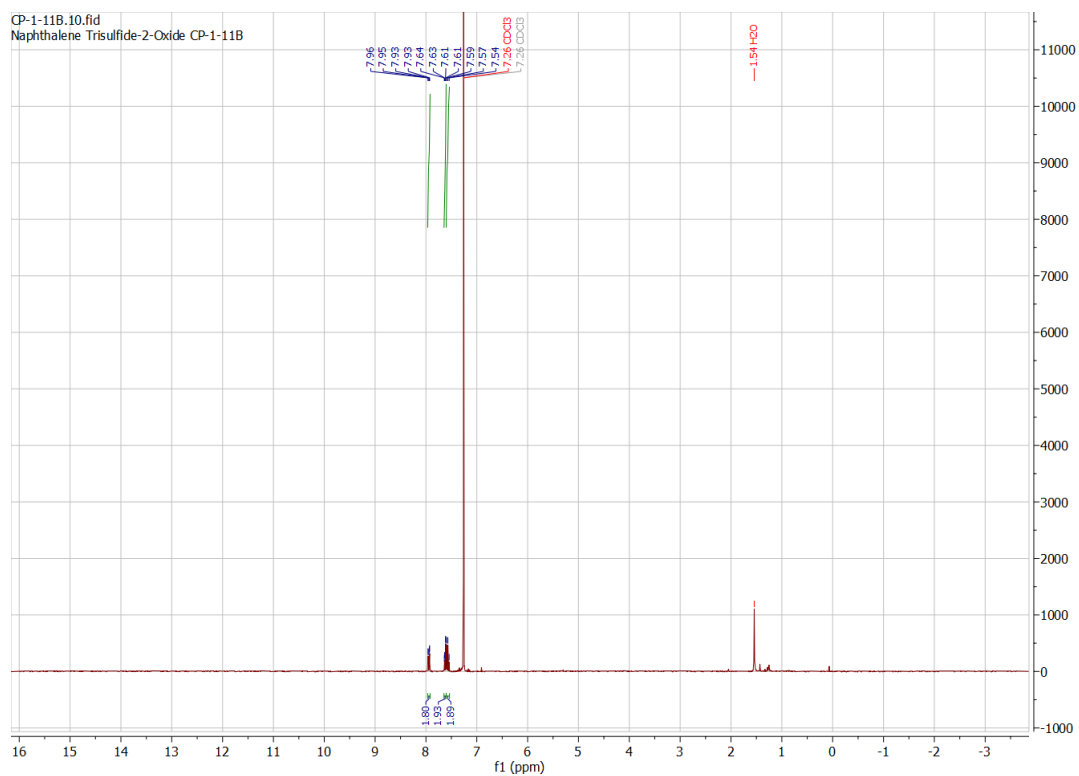
The CP-5-355A\_Tables.html report contains tables of bond lengths, angles and torsion angles with standard deviations given in brackets.

# NMR data for naphtho[1,8-cd][1,2]dithiole 107

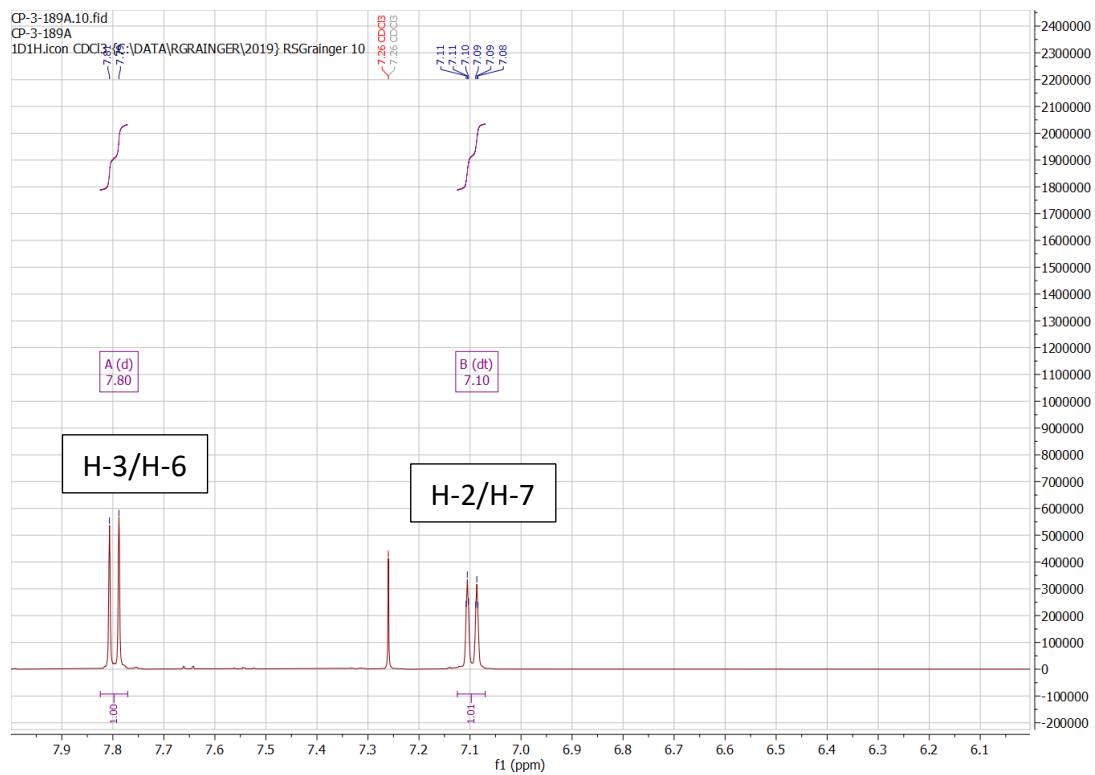
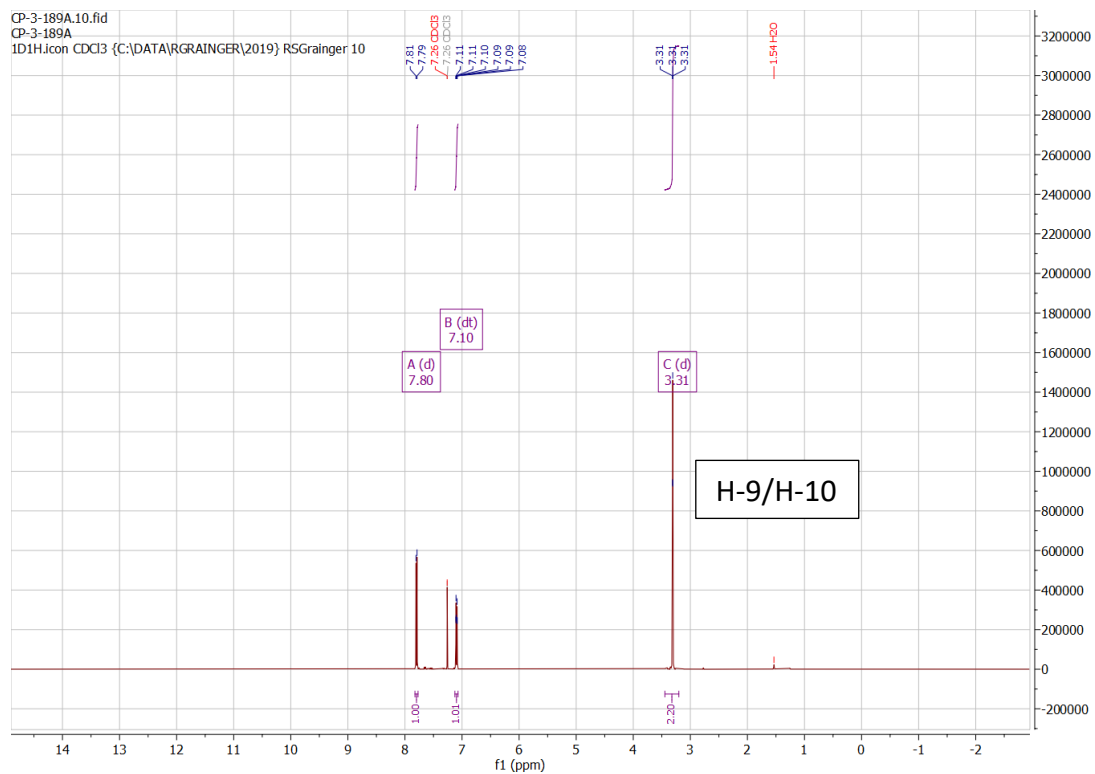


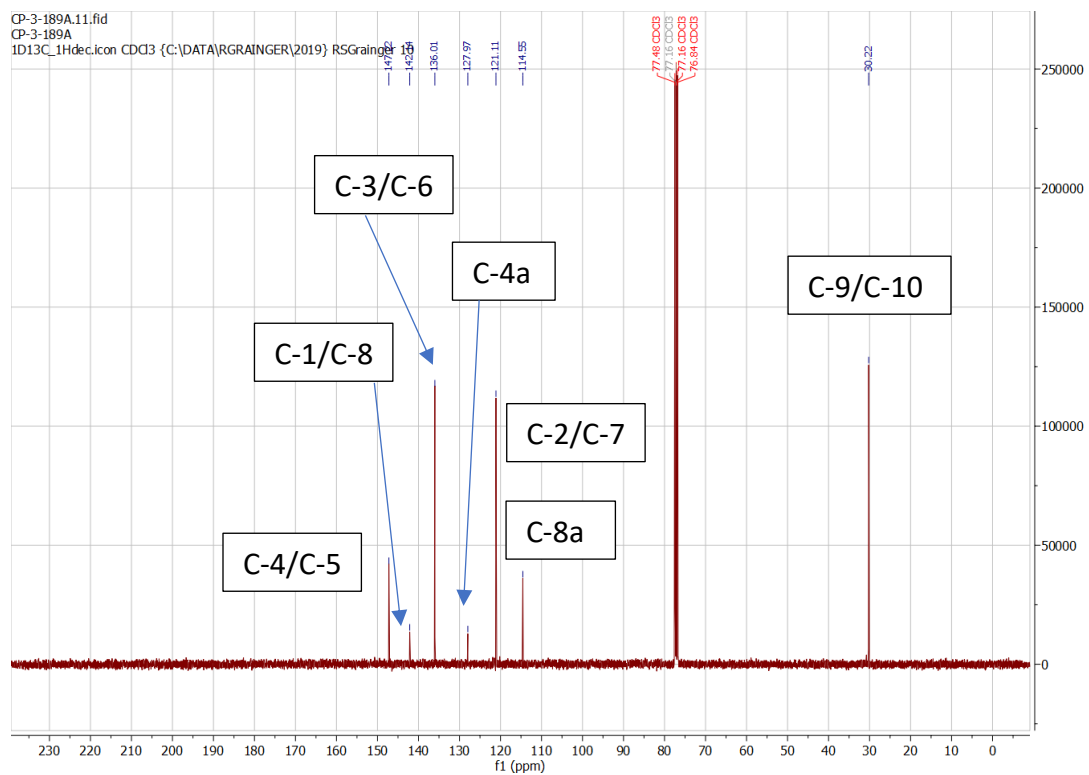


# NMR data for naphtho[1,8-*de*][1,2,3]trithiane-2-oxide 105

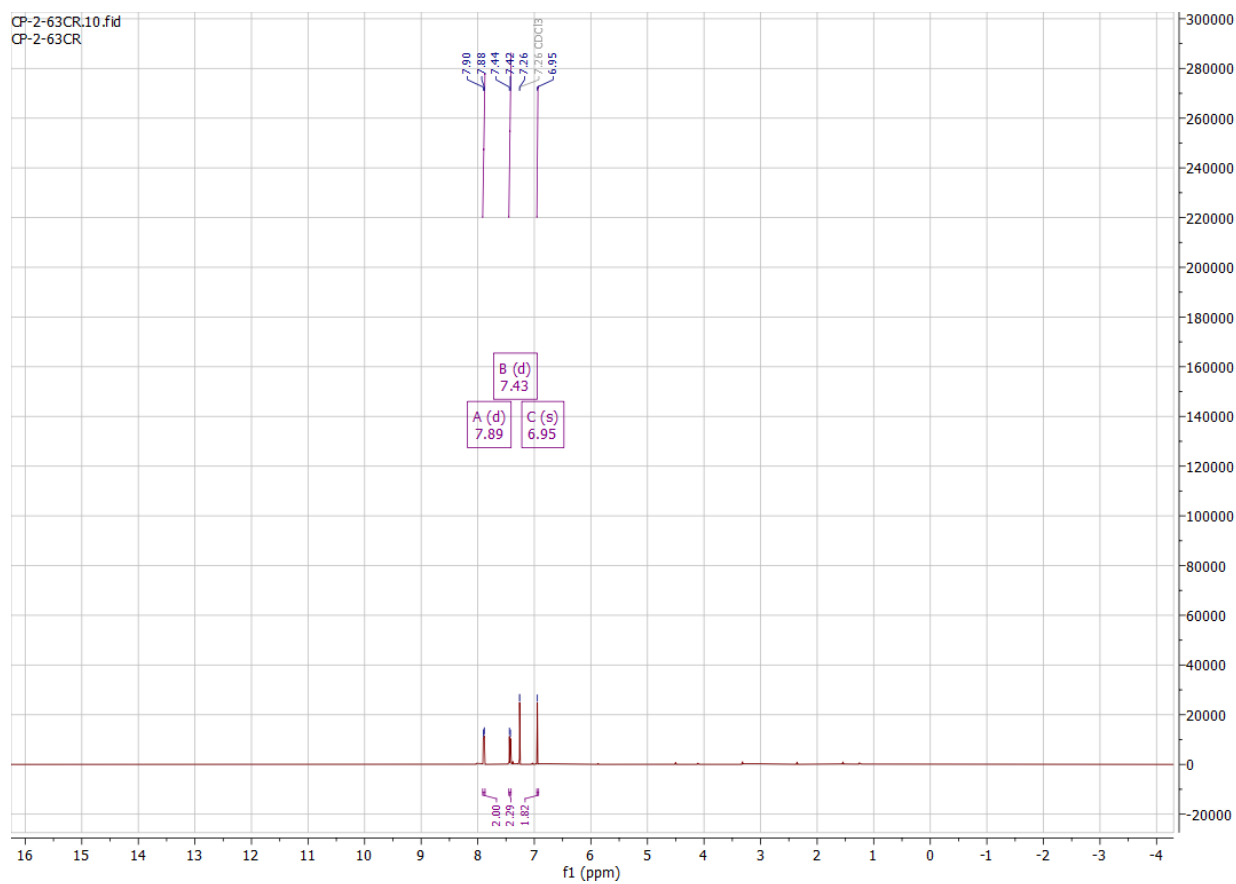


# NMR data for 5,6-dibromo-1,2-dihydroacenaphthylene 265

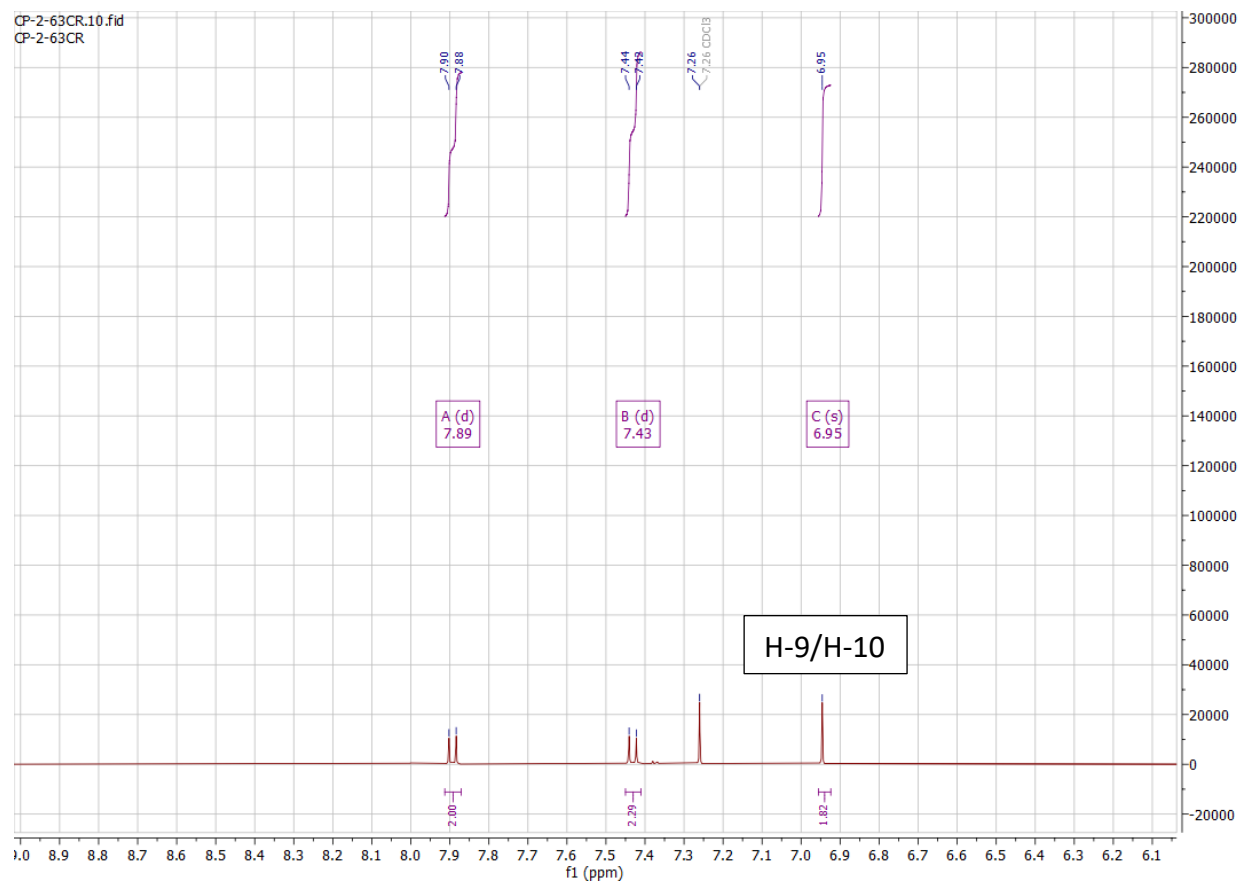




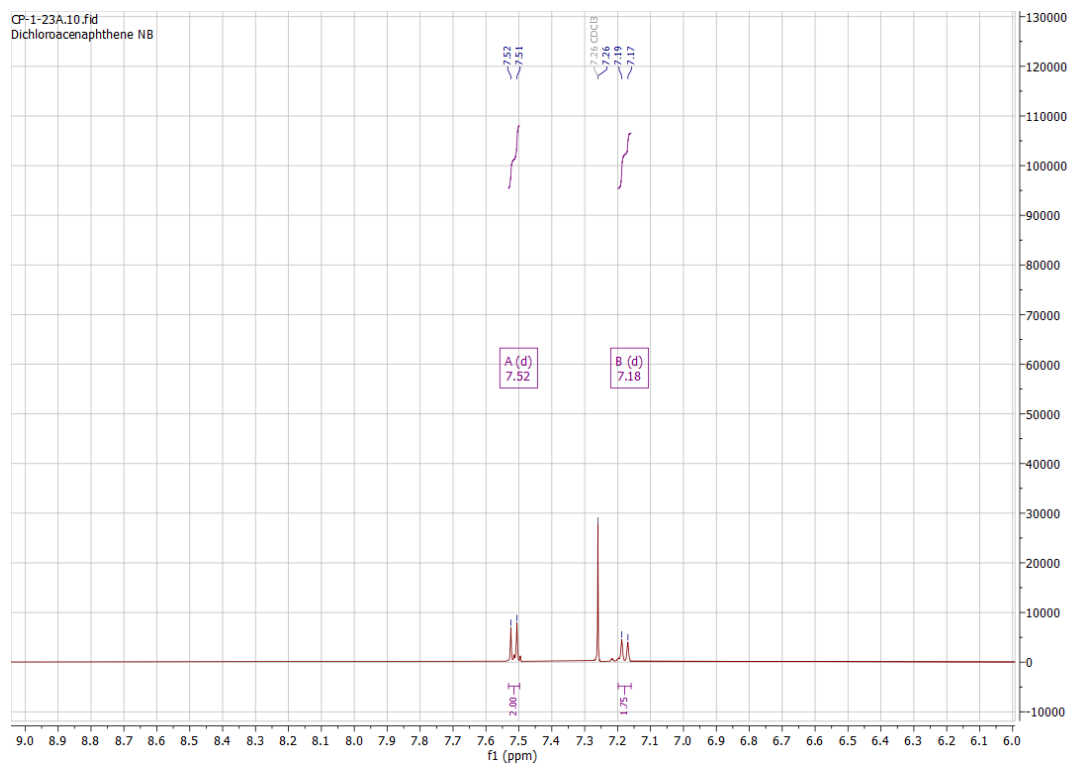
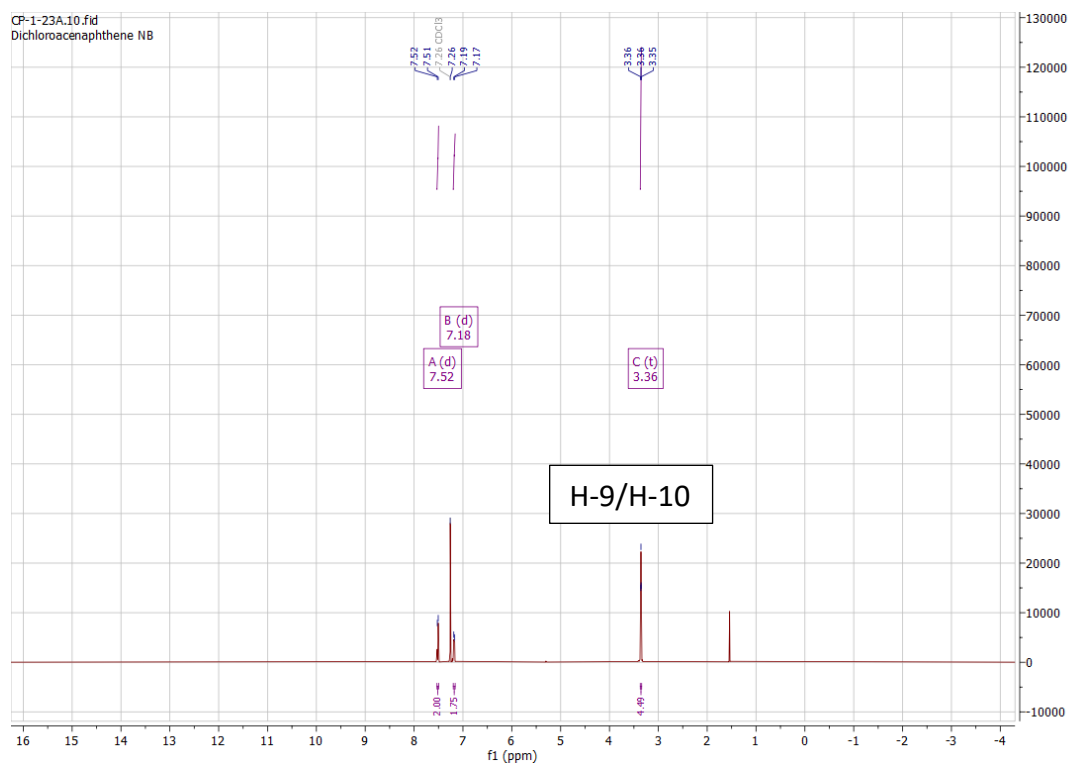
# NMR data for 5,6-dibromoacenaphthylene 293



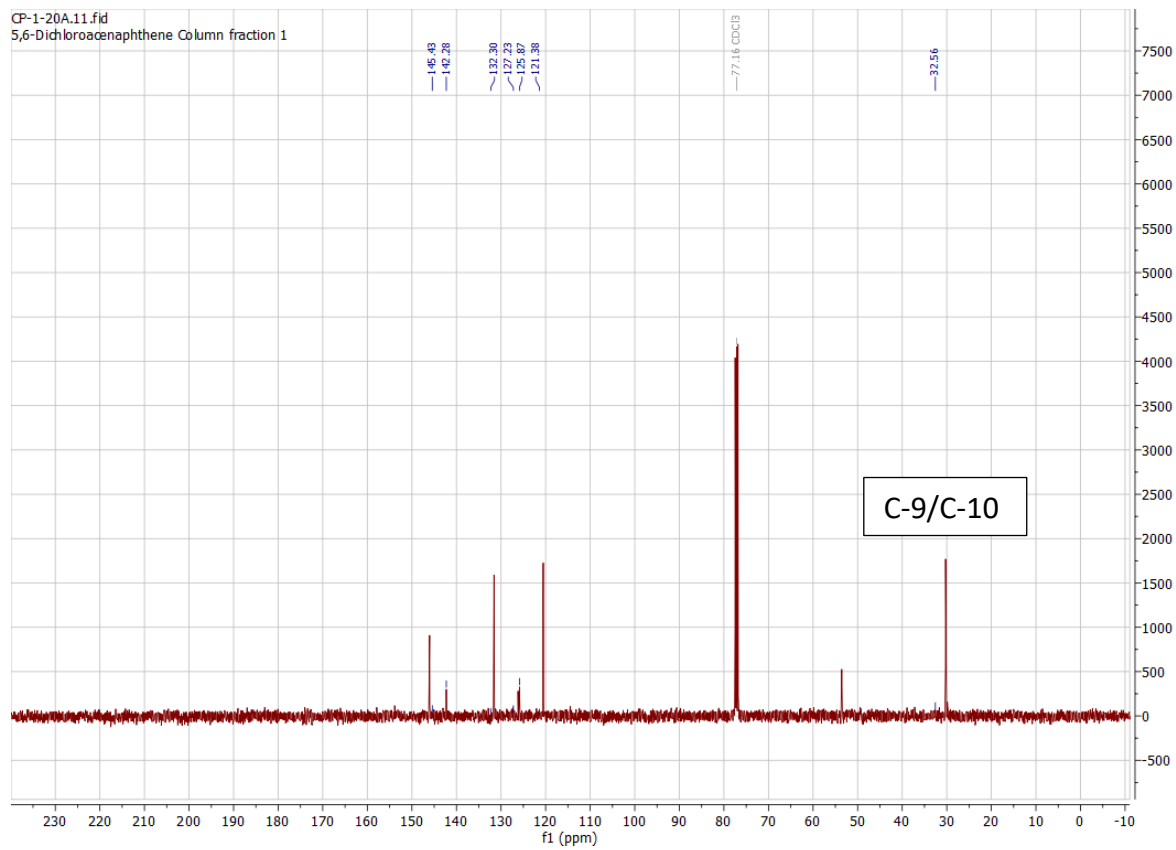




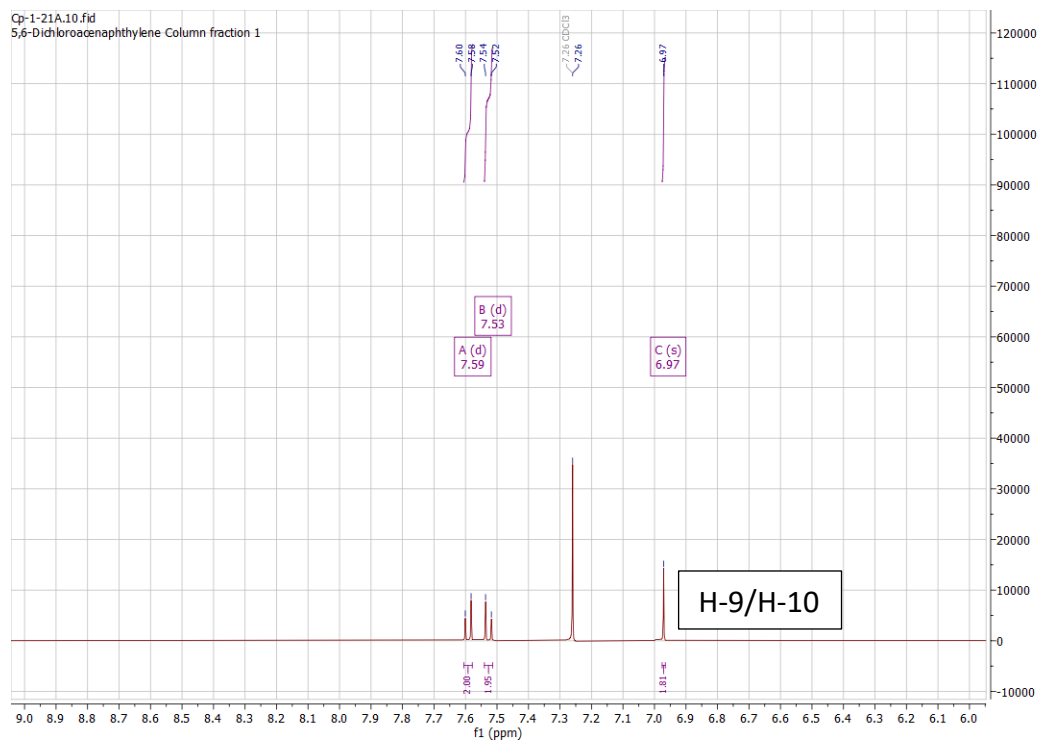
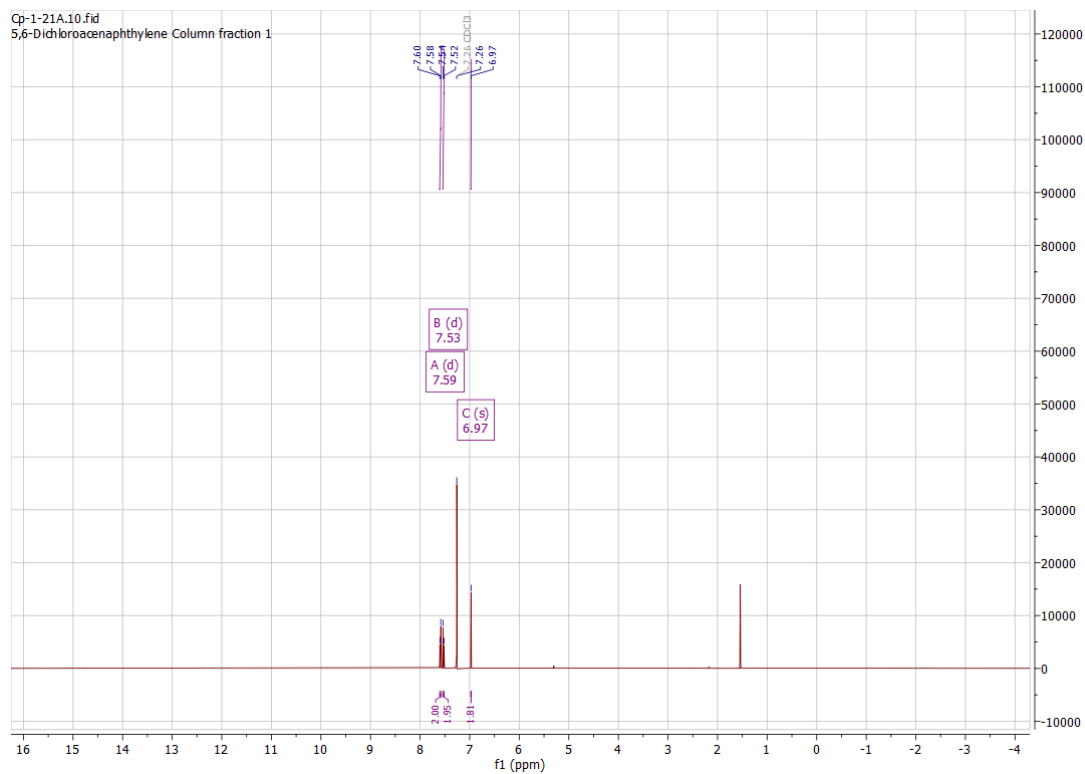
# NMR data for 5,6-dichloro-1,2-dihydroacenaphthylene 265



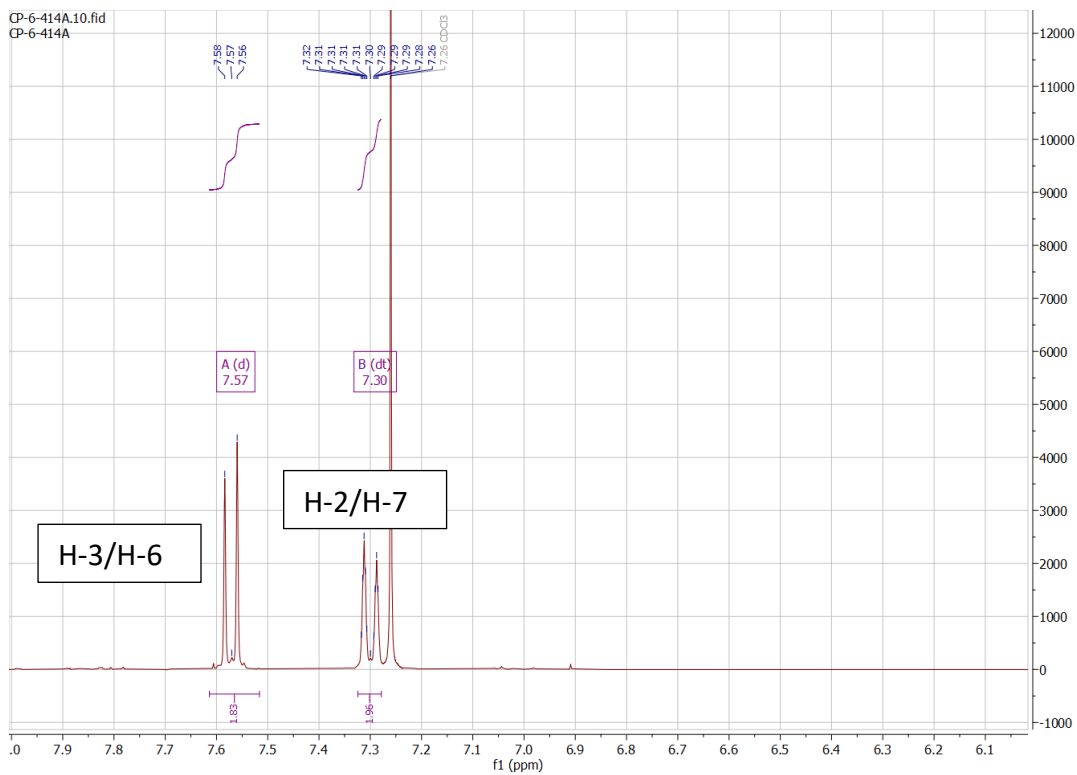
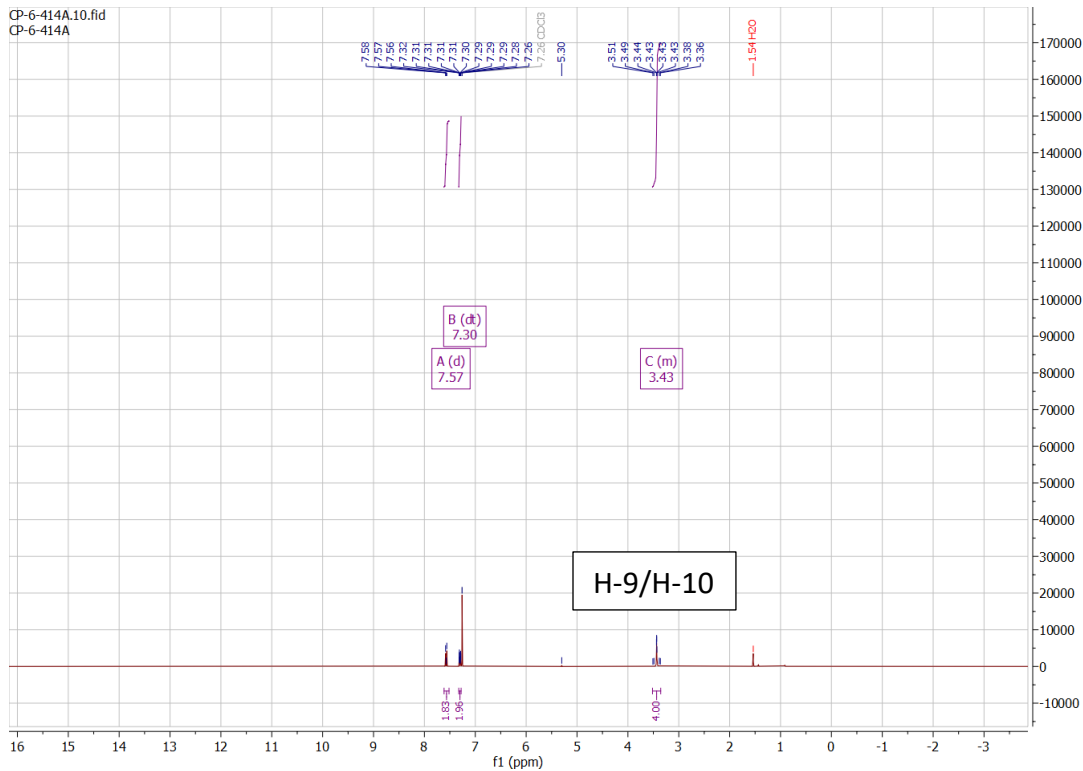
CP-1-20A.11.fid  
5,6-Dichloronaphthene Column fraction 1



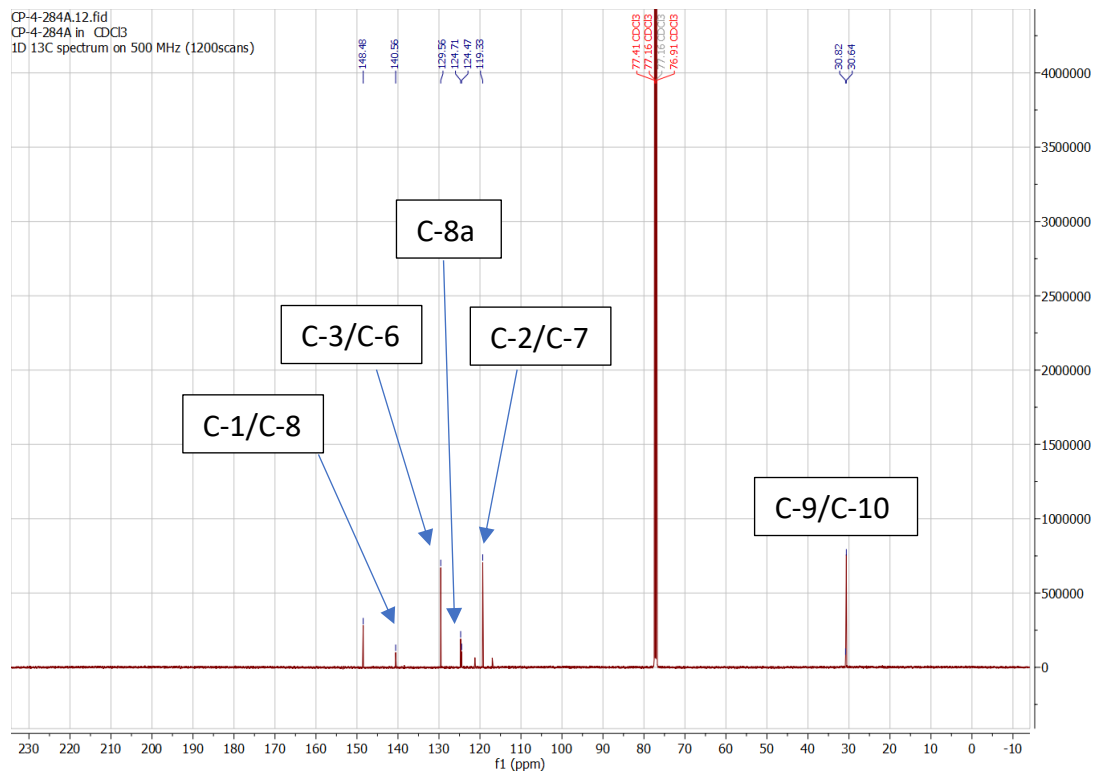
# NMR data for 5,6-dichloroacenaphthylene 316



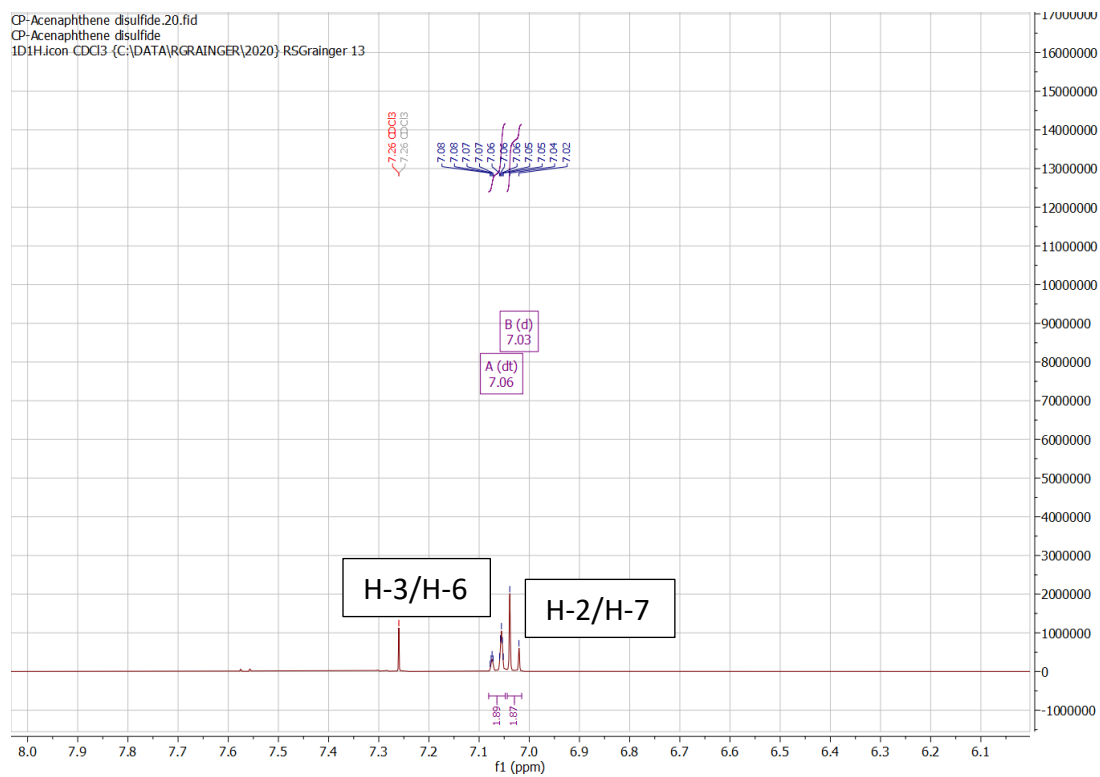
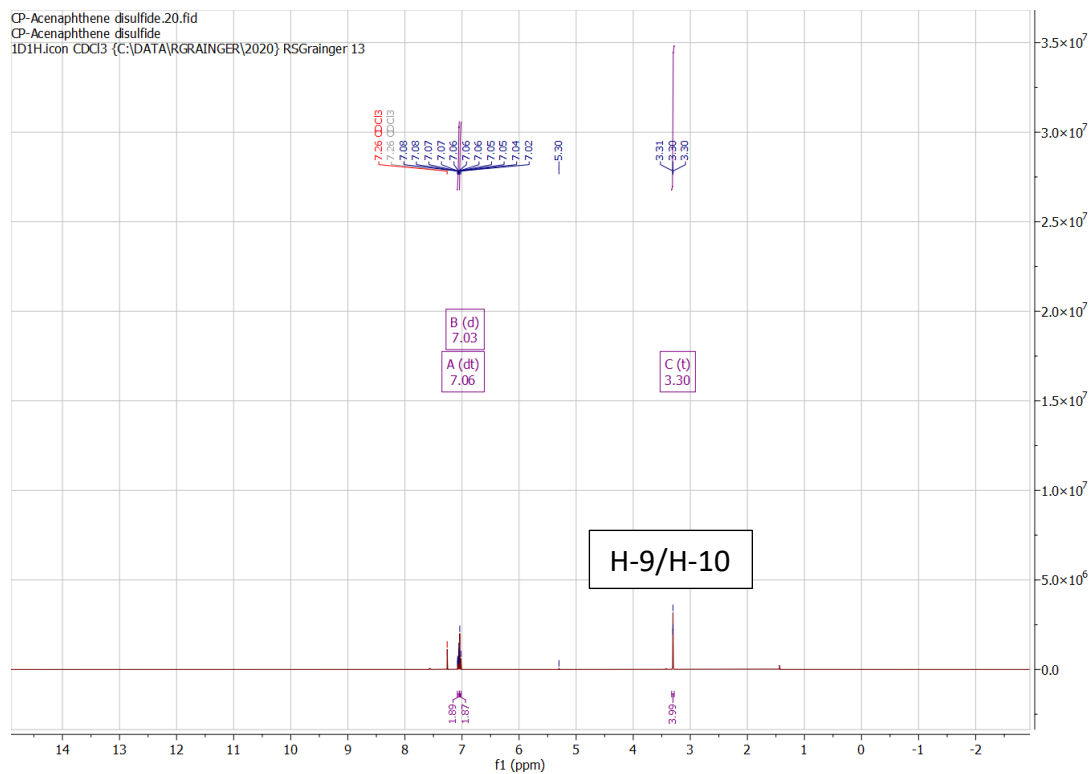
NMR data for **6,7-dihydroacenaphtho[5,6-*de*][1,2,3]trithiane 319**

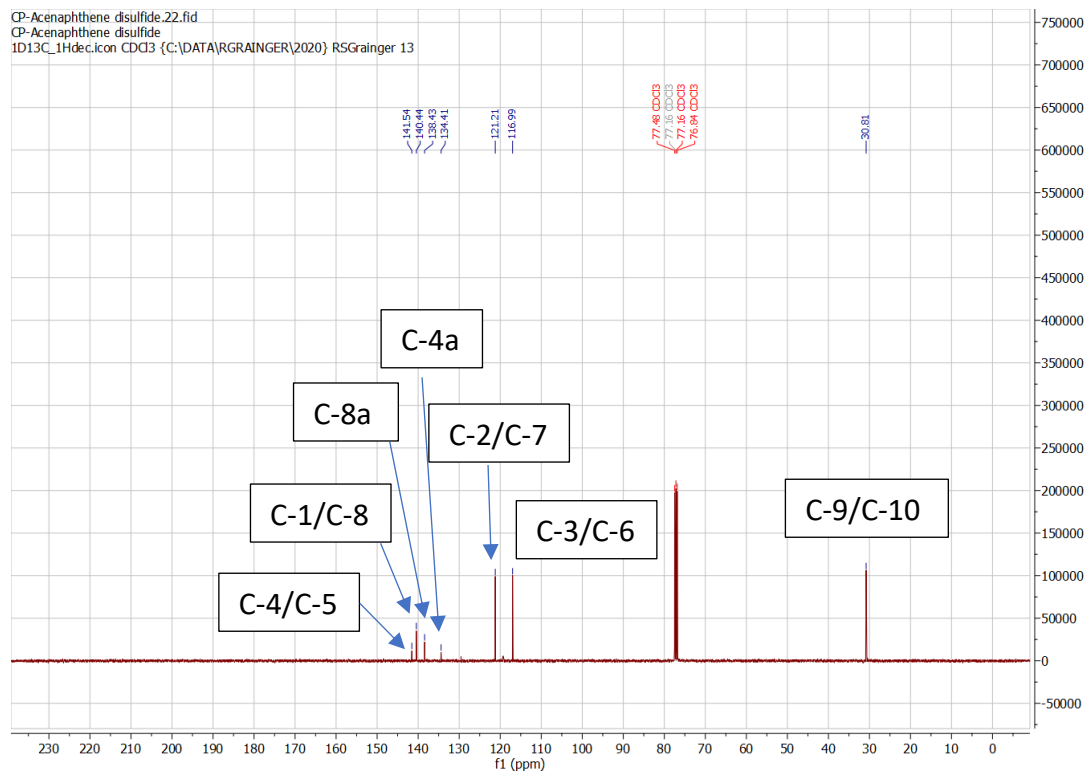


CP-4-284A.12.fid  
CP-4-284A in CDCl<sub>3</sub>  
1D 13C spectrum on 500 MHz (1200scans)



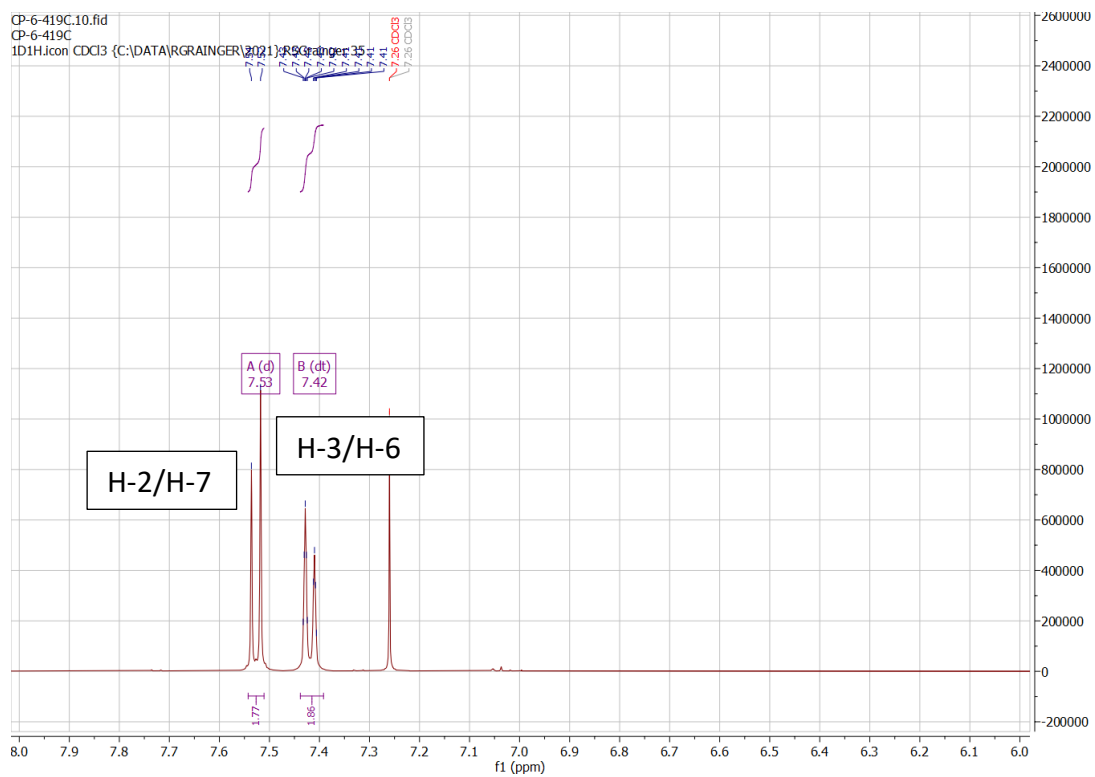
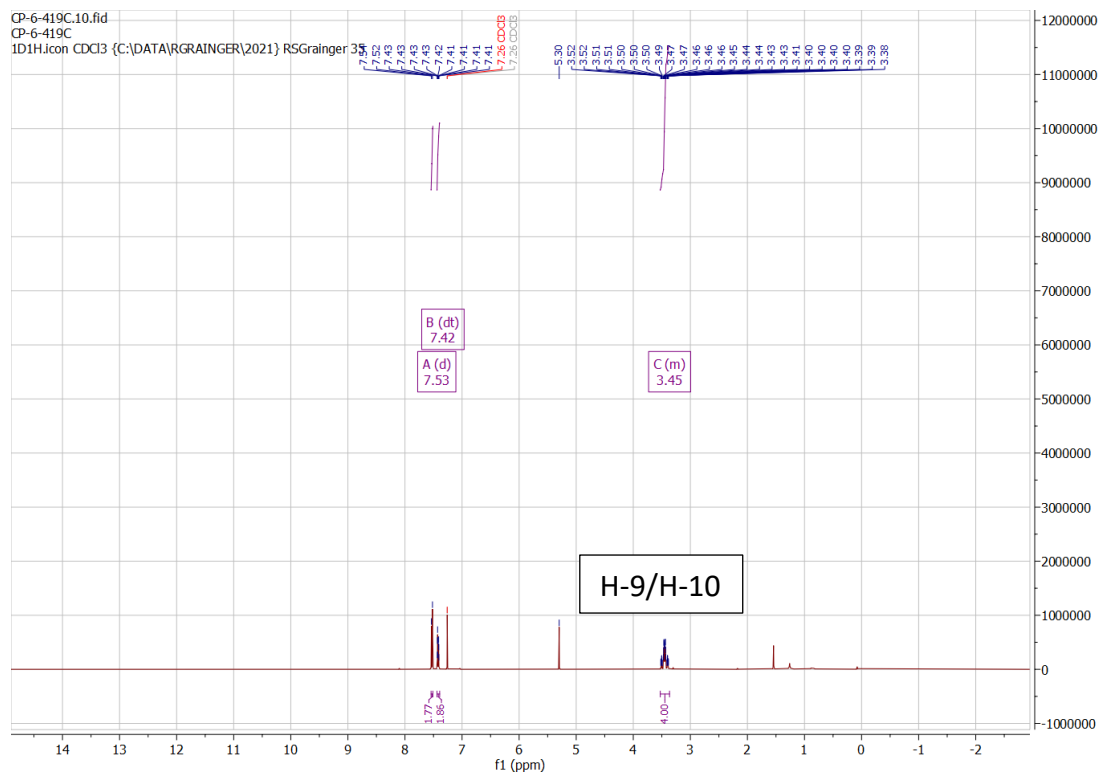
# NMR data for 5,6-dihydroacenaphtho[5,6-*cd*][1,2]dithiole 266

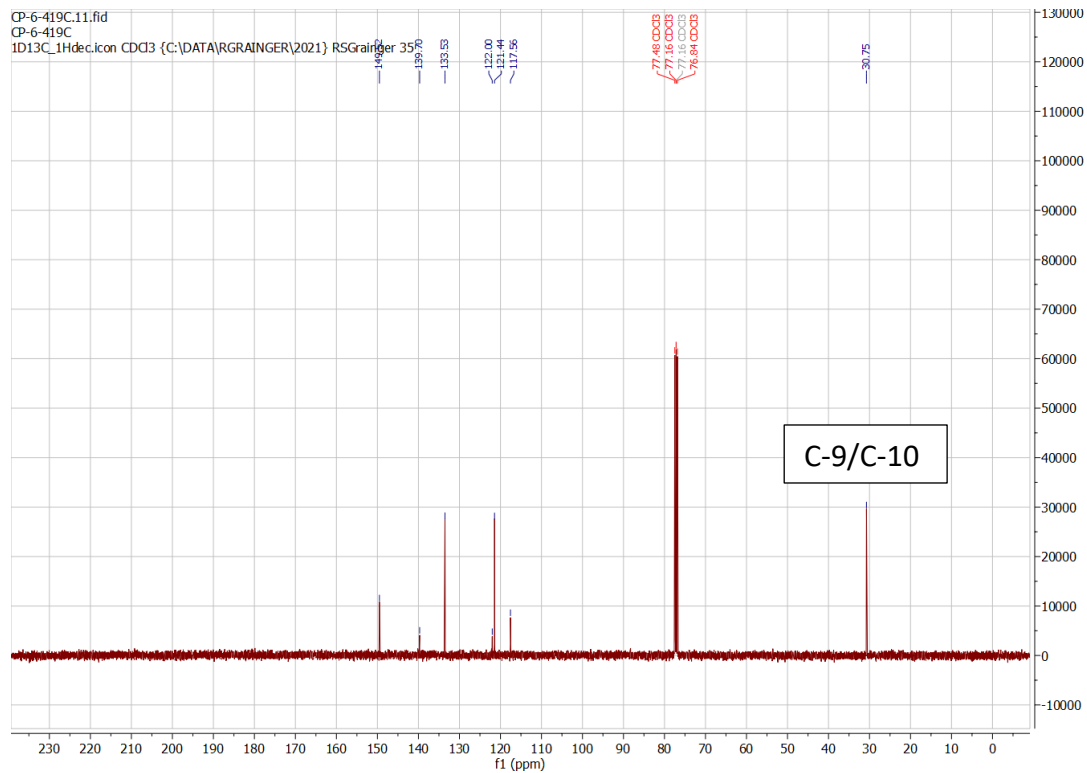






# NMR data for 6,7-dihydroacenaphtho[5,6-*de*][1,2,3]trithiine-2-oxide 299





CP-3-234A recryst hex.10.fid  
CP-3-234A recryst hex

8.14  
8.13  
8.11  
7.61  
7.60  
7.58  
7.58  
7.57  
7.56  
7.55  
7.50  
7.46  
7.46  
7.44  
7.43  
7.43  
7.41  
7.26 CDCl3  
7.26 CDCl3  
3.59  
3.58  
3.57  
3.57  
3.56  
3.56  
3.55  
3.54  
3.54  
3.53  
3.53  
3.52  
3.51  
3.50  
1.54H2O

A (d)  
8.13

B (dt)  
7.59

D (m)  
7.45

C (d)  
7.5

E (qt)  
3.55

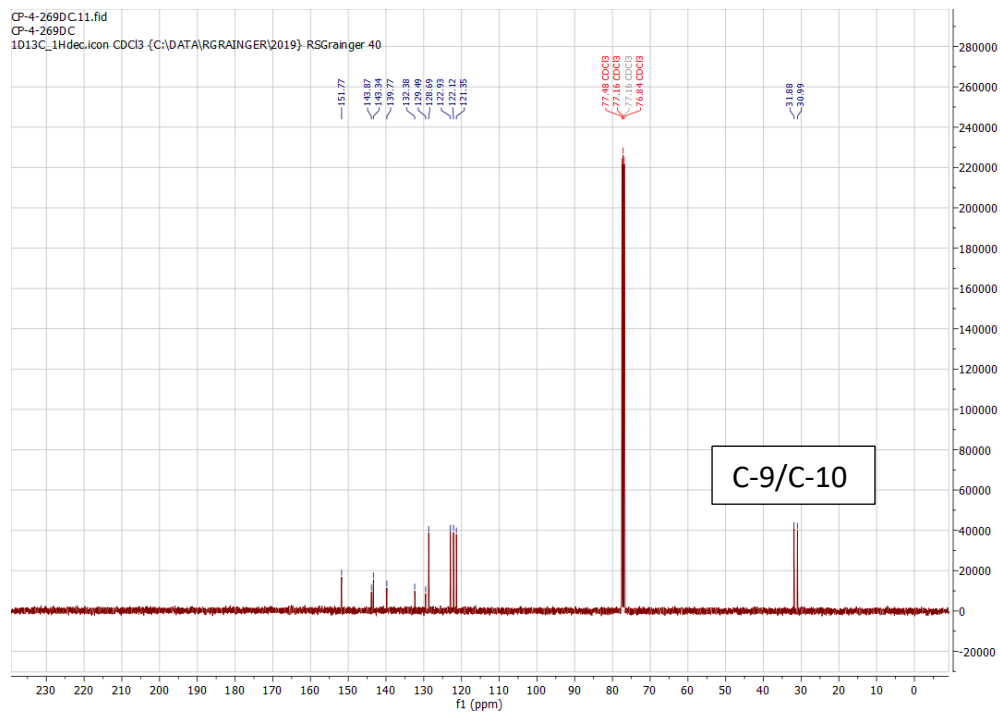
154H2O

H-9/H-10

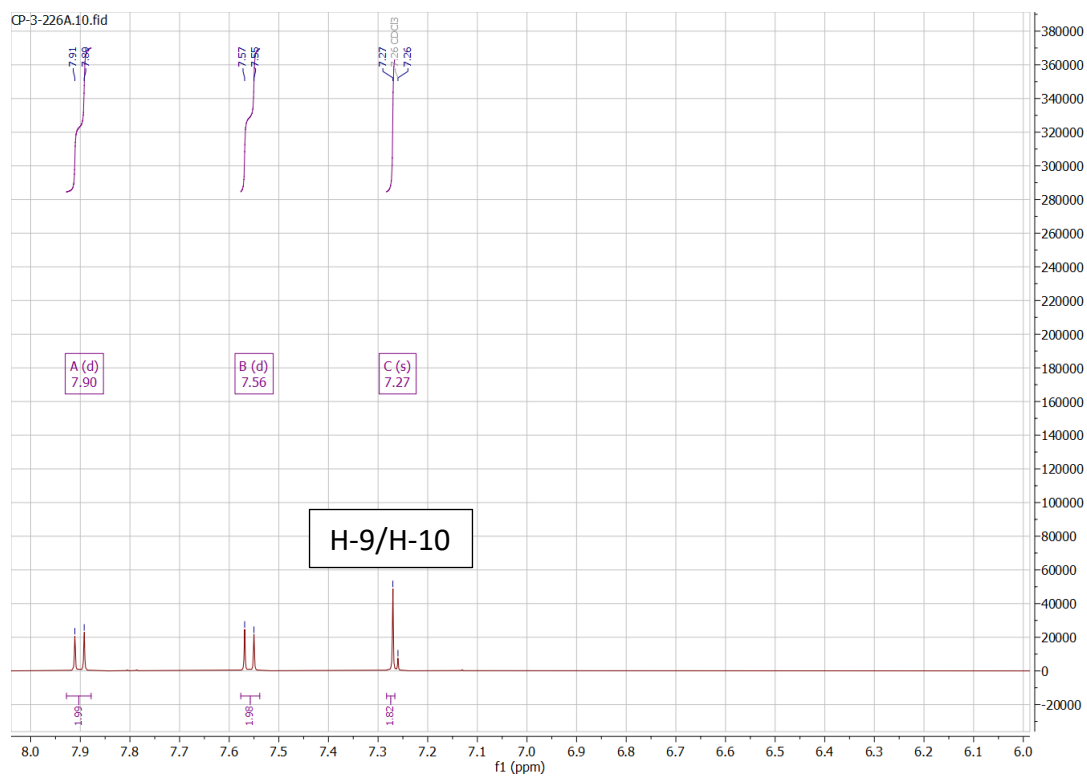
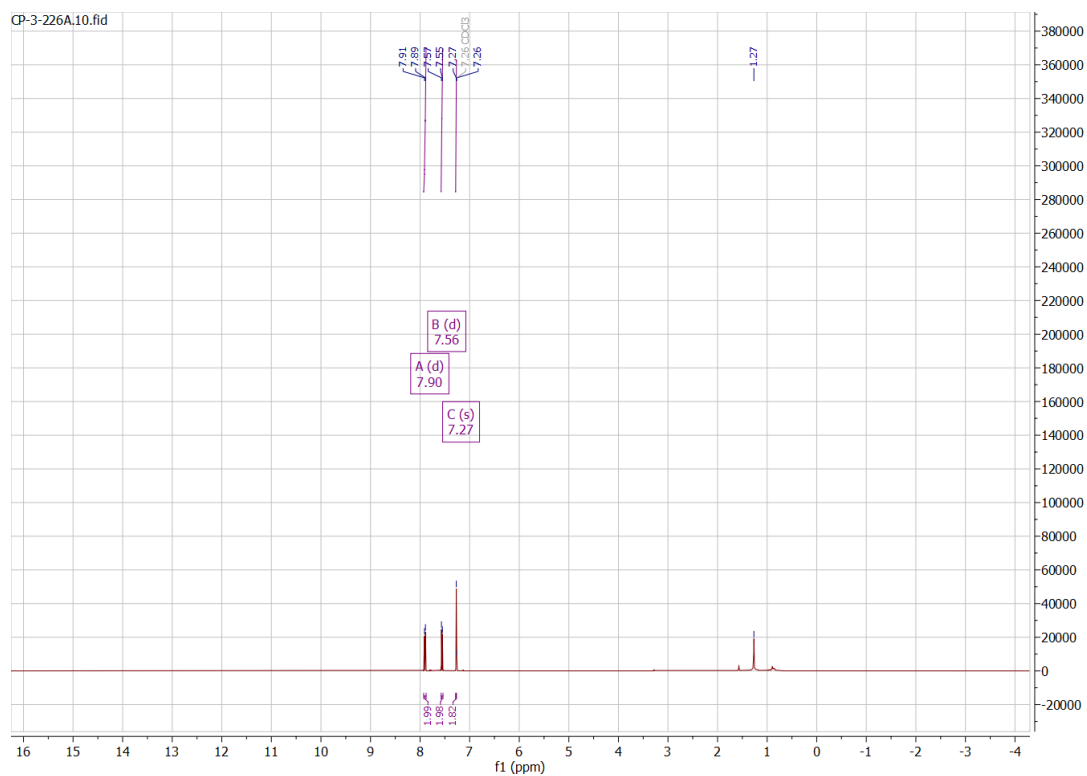
0.85  
0.93  
0.88  
1.02  
4.00

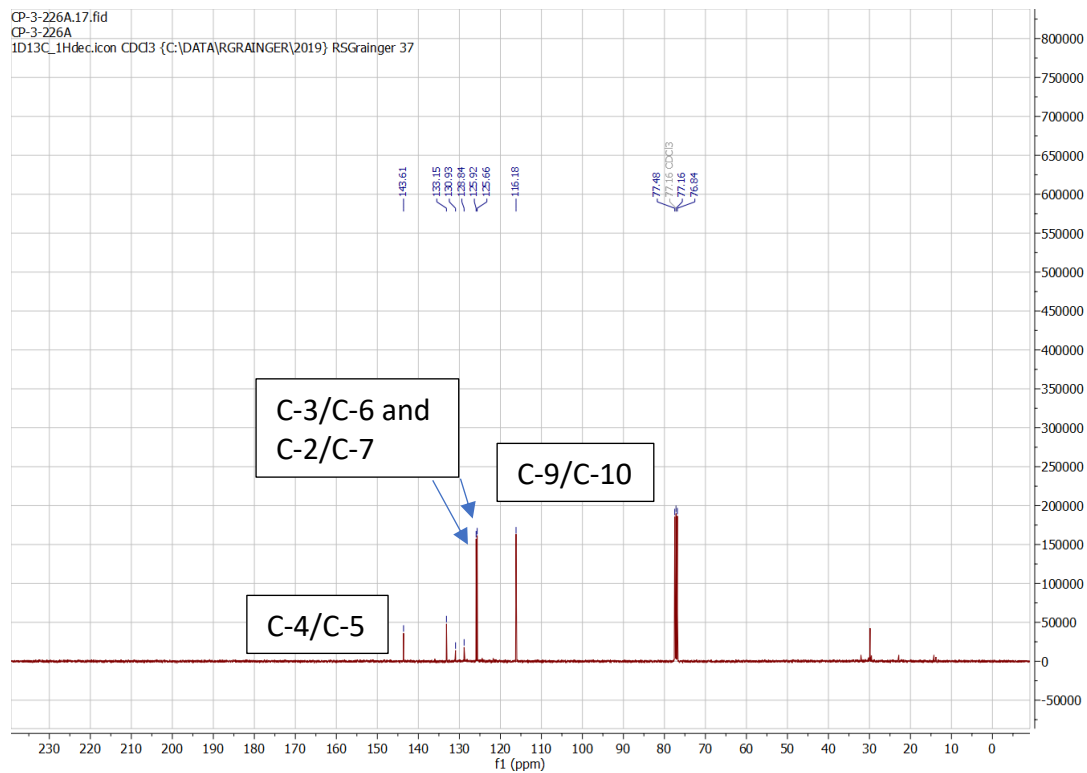
f1 (ppm)



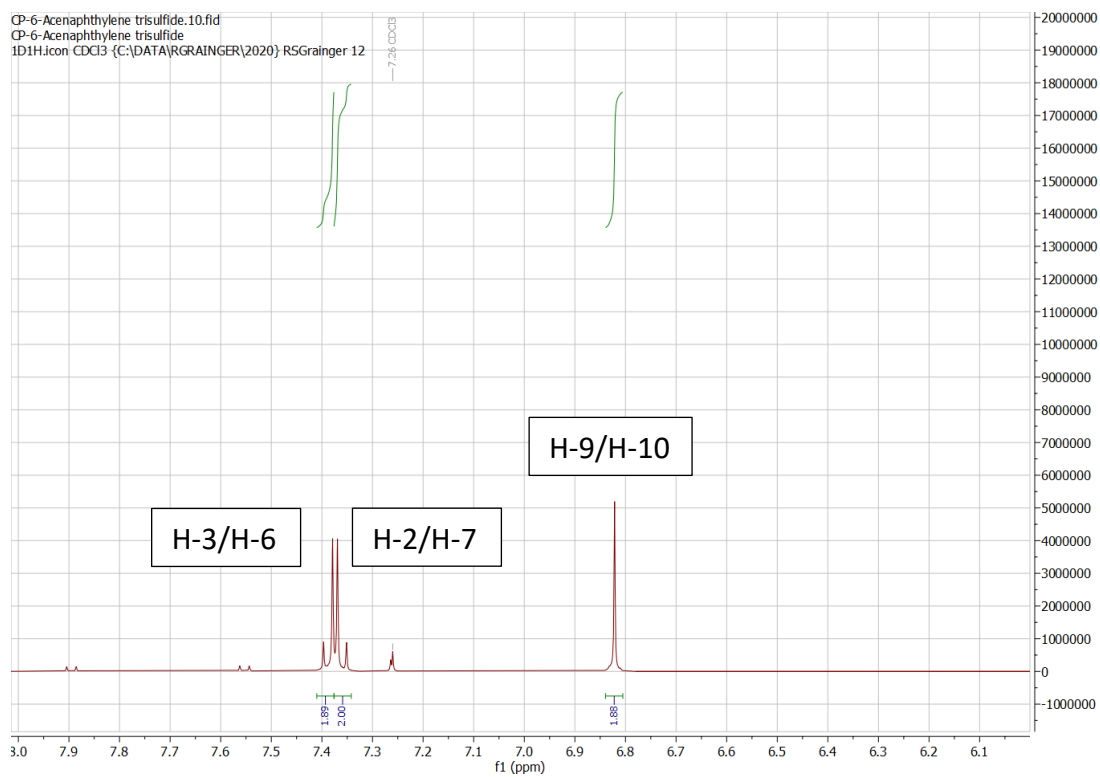
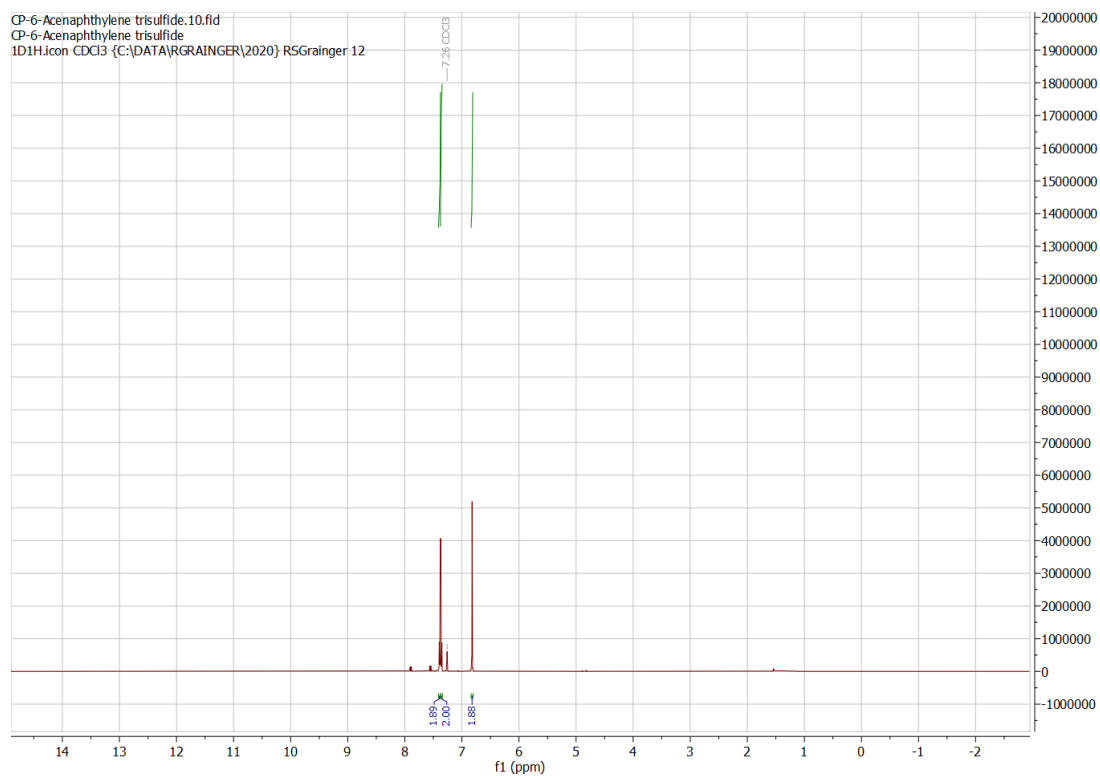


# NMR data for acenaphtho[5,6-*cd*][1,2]dithiole 264





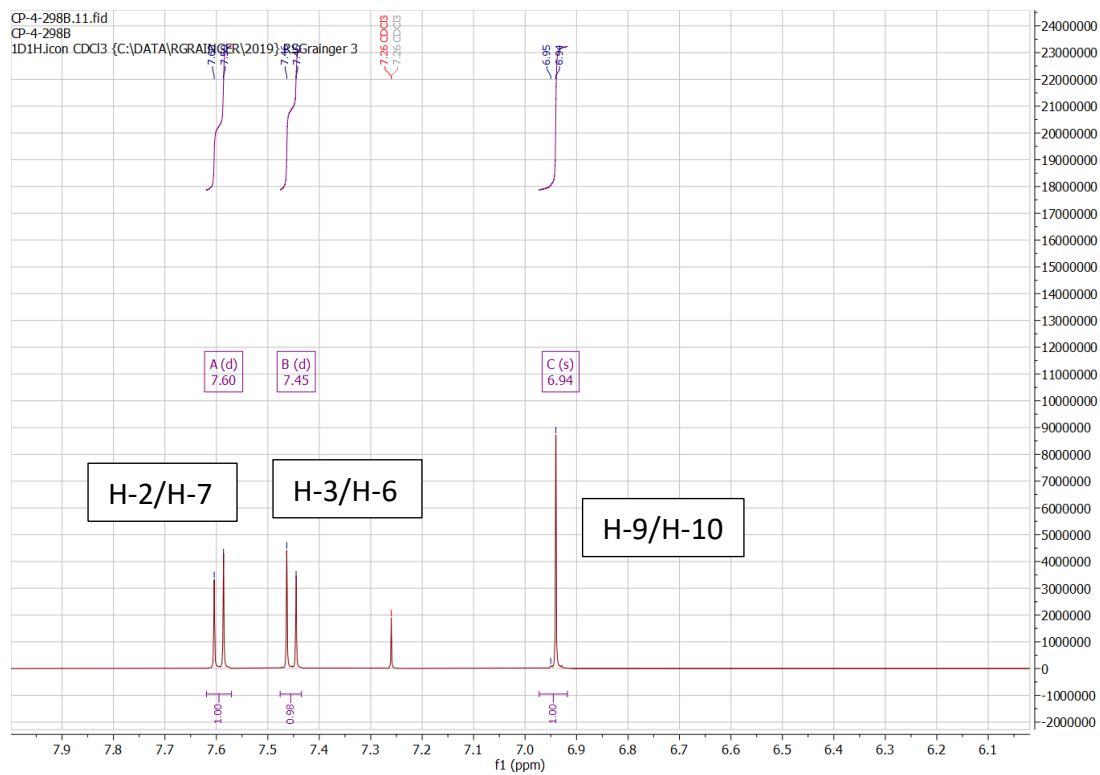
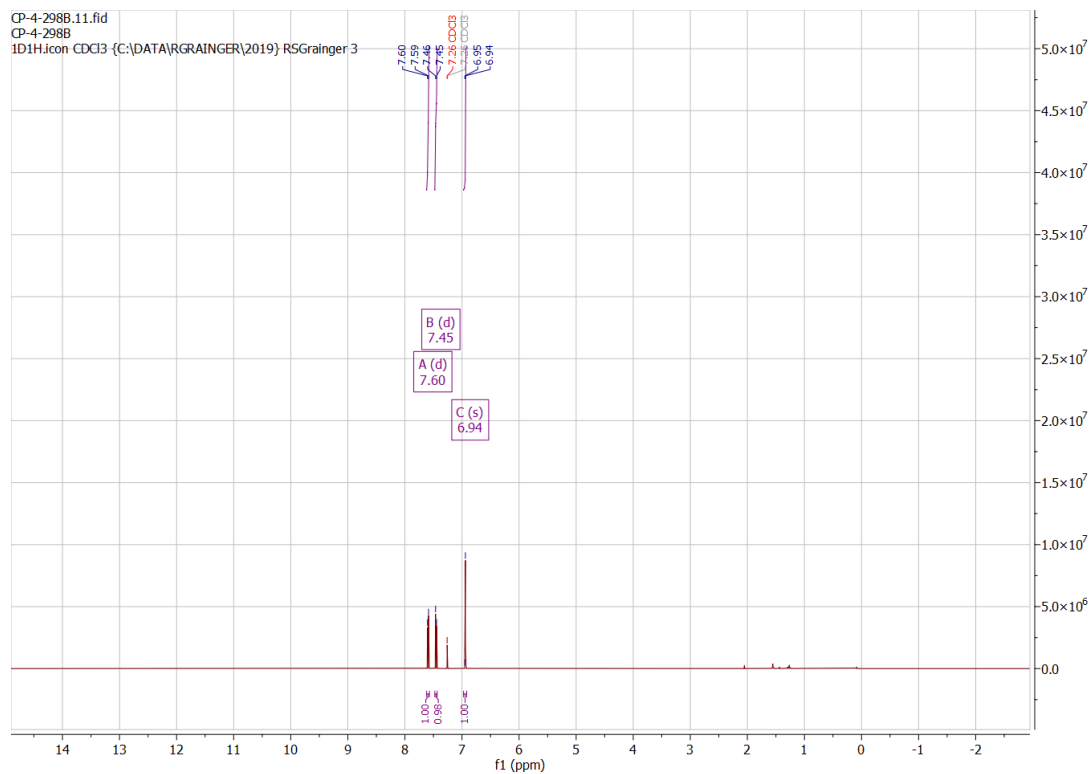
# NMR data for acenaphtho[5,6-*de*][1,2,3]trithiane 320

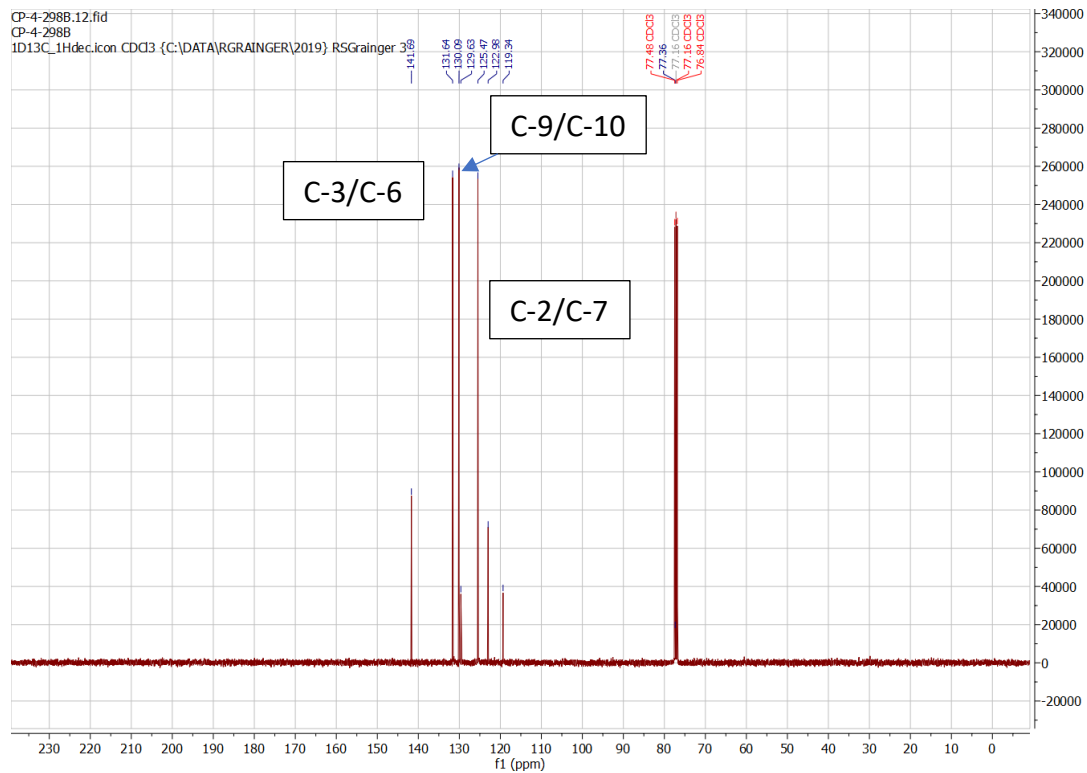






# NMR data for acenaphtho[5,6-*de*][1,2,3]trithiane-2-oxide 300





CP-9,9-dimethylfluorene.10.fid  
CP-9,9-dimethylfluorene

7.75  
7.74  
7.74  
7.73  
7.73  
7.72  
7.72  
7.72  
7.66  
7.65  
7.65  
7.63  
7.63  
7.62  
7.58  
7.56  
7.55  
7.34  
7.34  
7.33  
7.33  
7.32  
7.32  
7.30  
7.29  
7.26 CDCl<sub>3</sub>

C (m)  
7.44

B (m)  
7.73

D (m)  
7.33

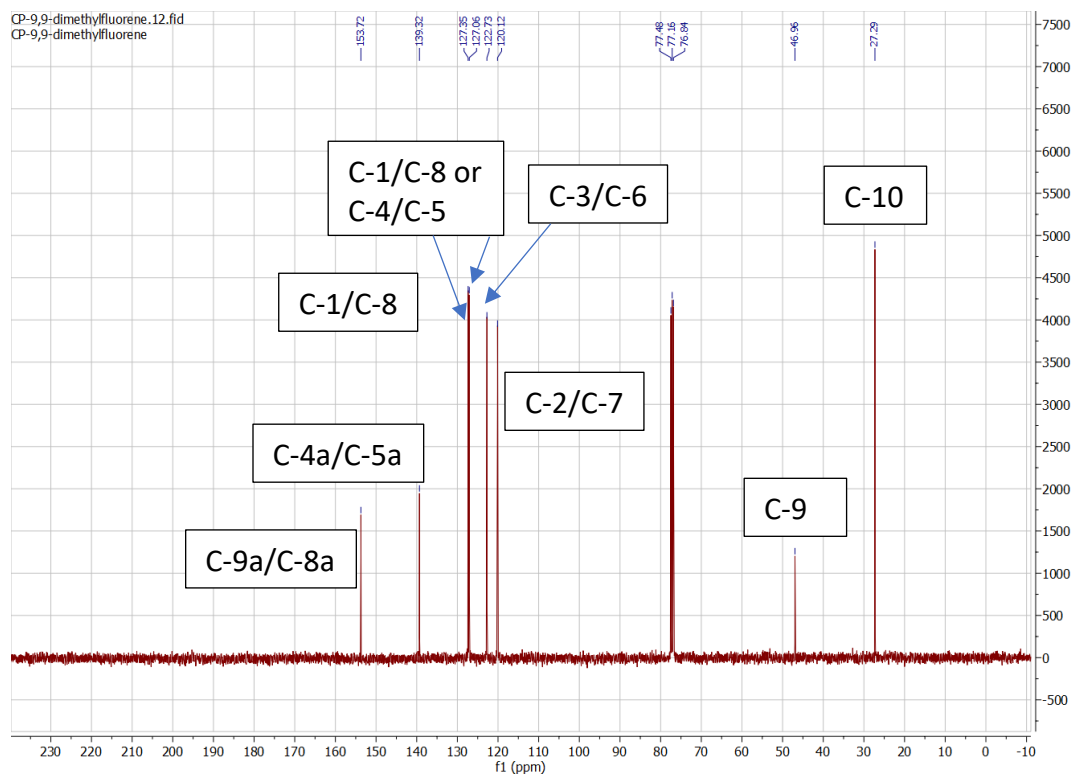
A (s)  
1.50

H-10

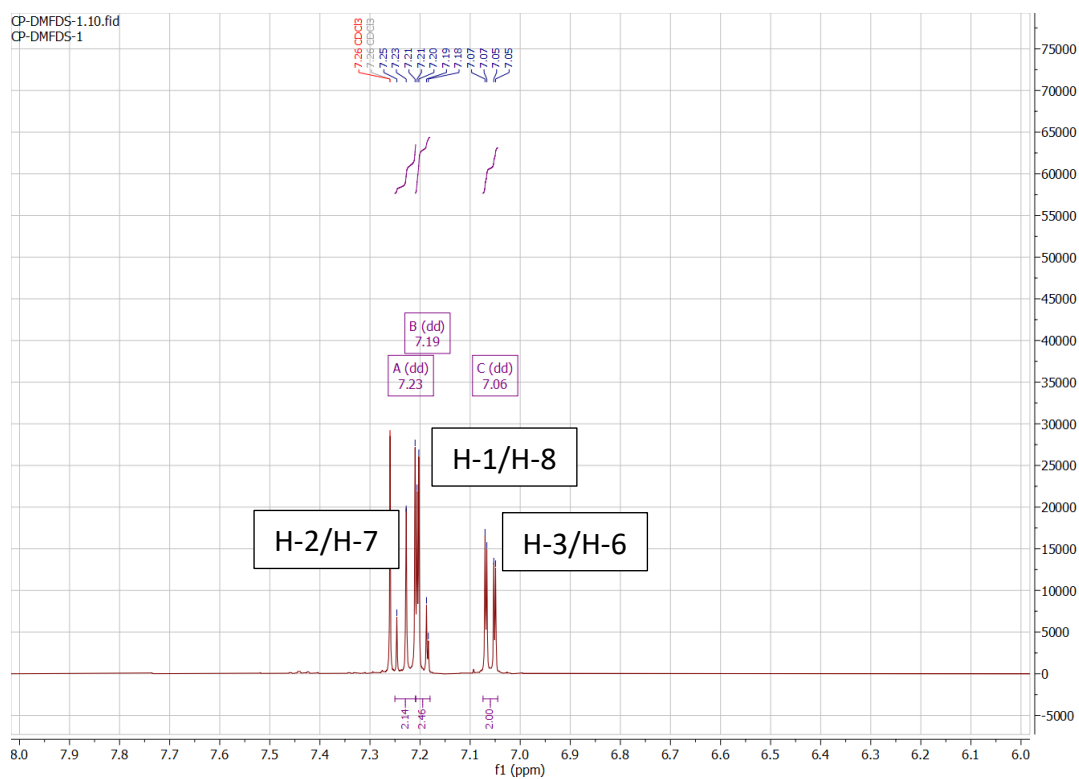
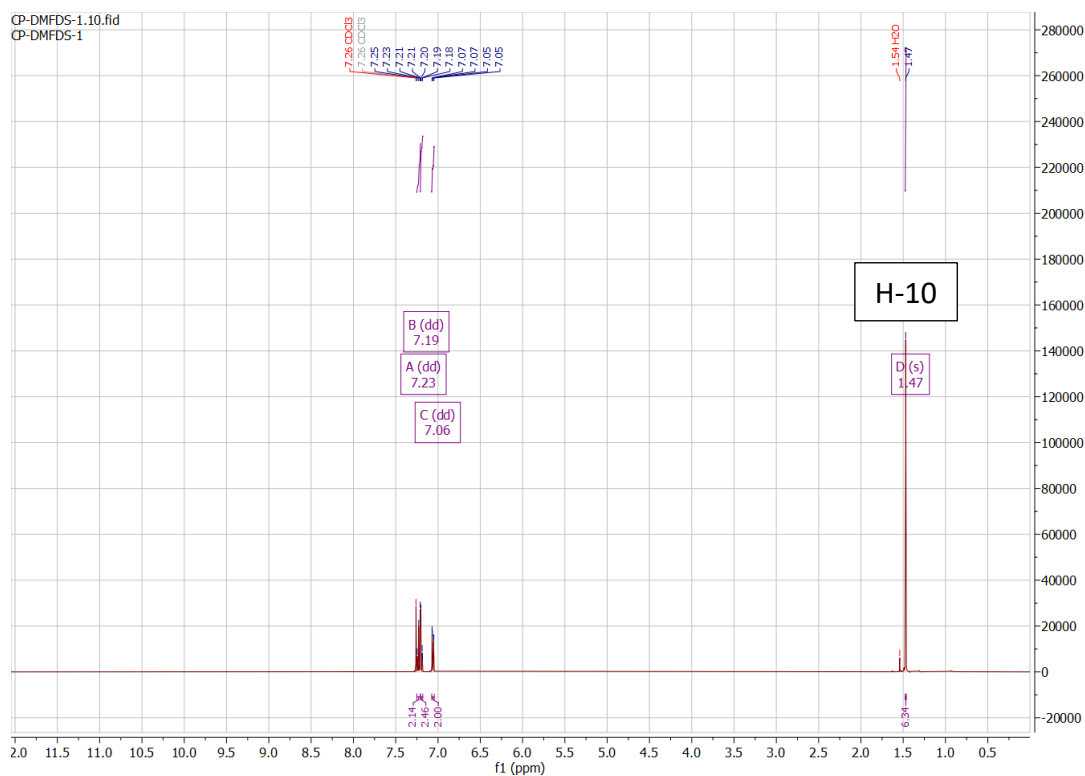
1.81  
1.85  
1.86  
6.00

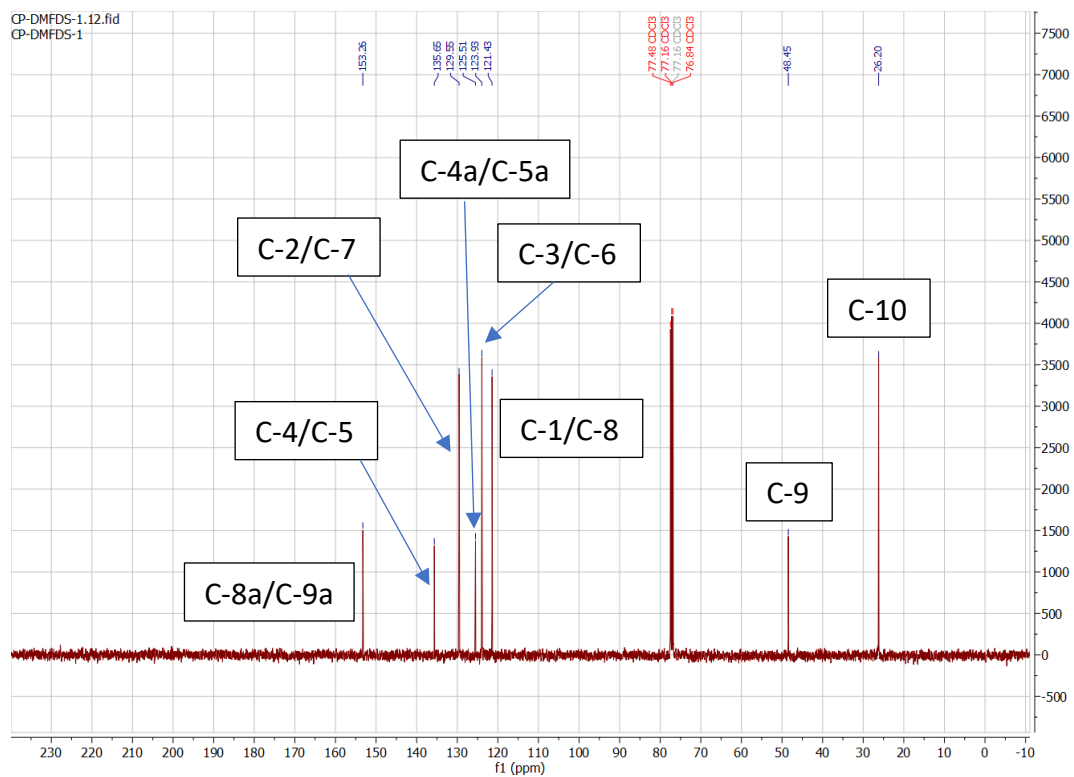
f1 (ppm)



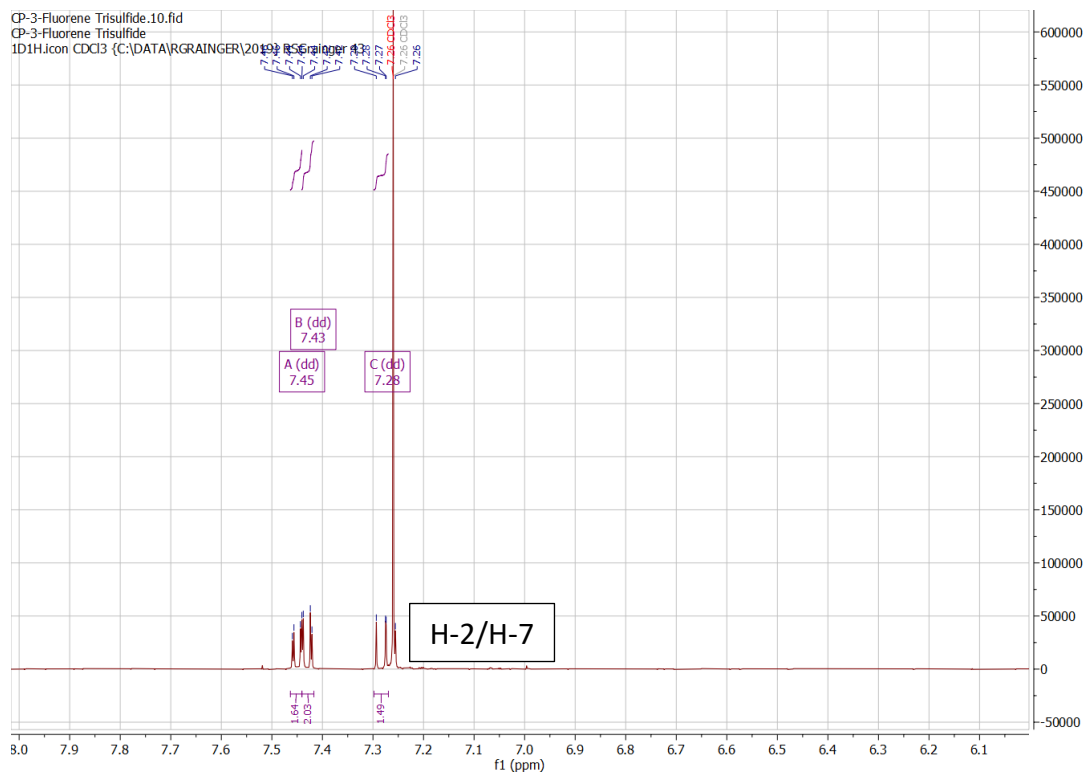
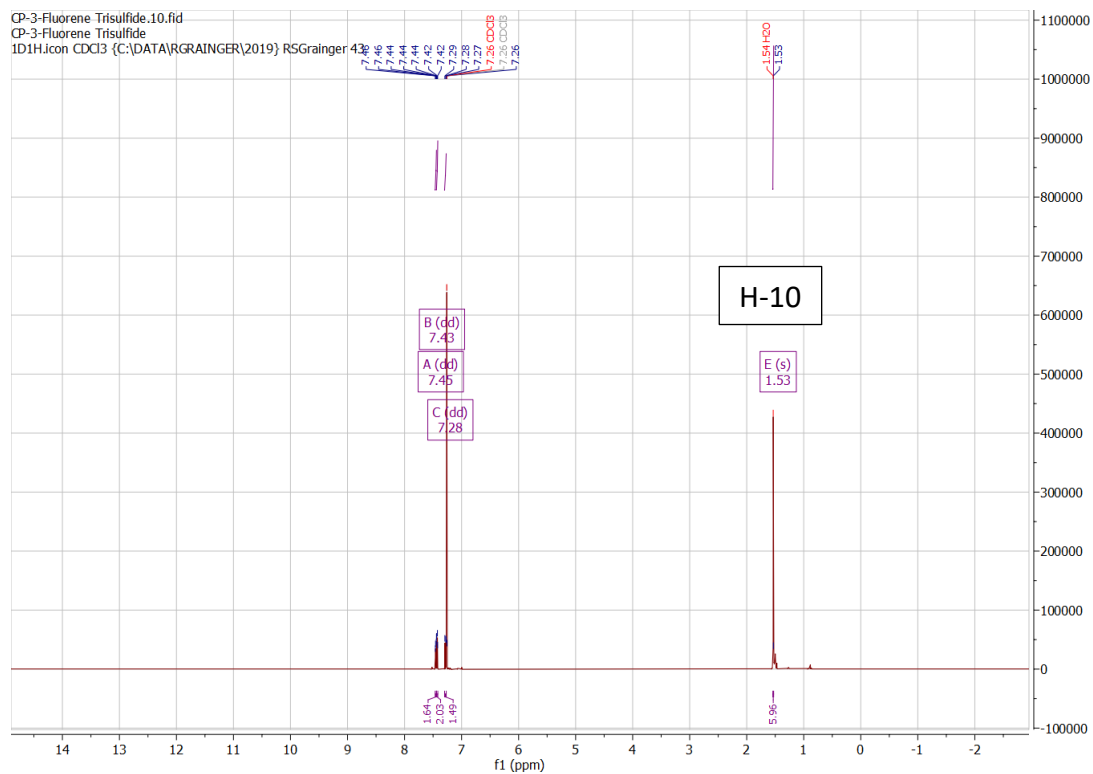


# NMR data for 9,9-dimethyl-9H-fluoreno[4,5-cde][1,2]dithiine 298

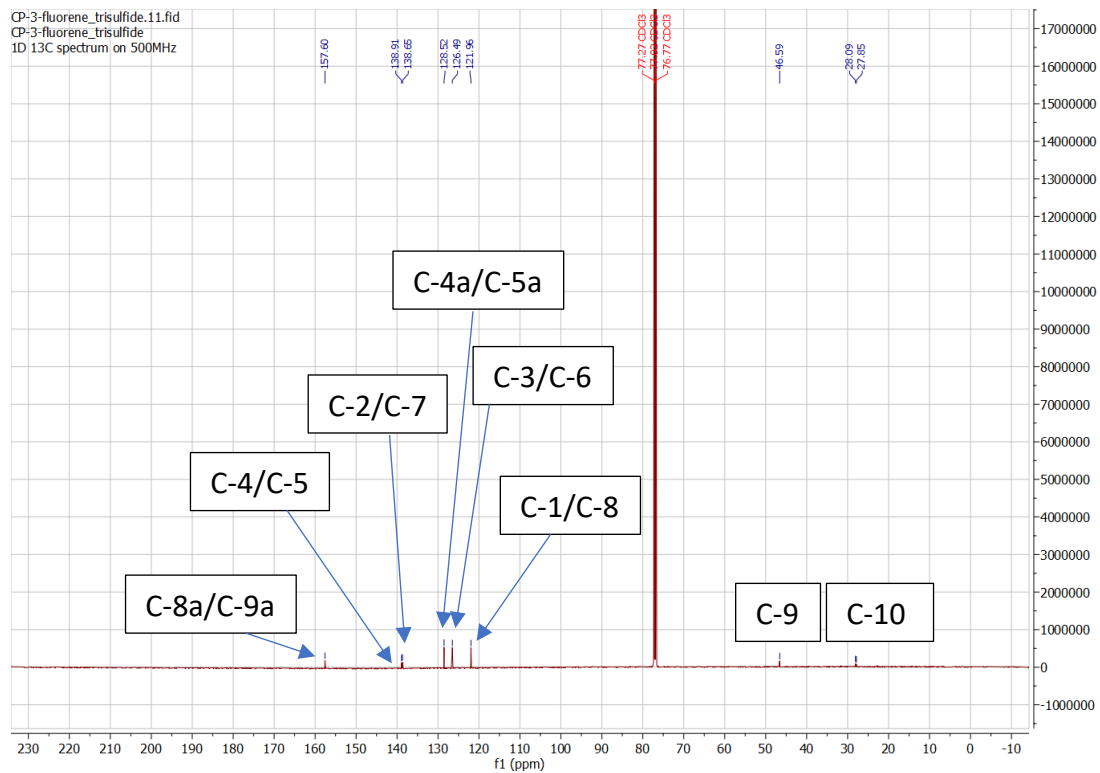




# NMR data for 4,4-dimethyl-4*H*-fluoreno[4,5-*def*][1,2,3]trithiepine 309

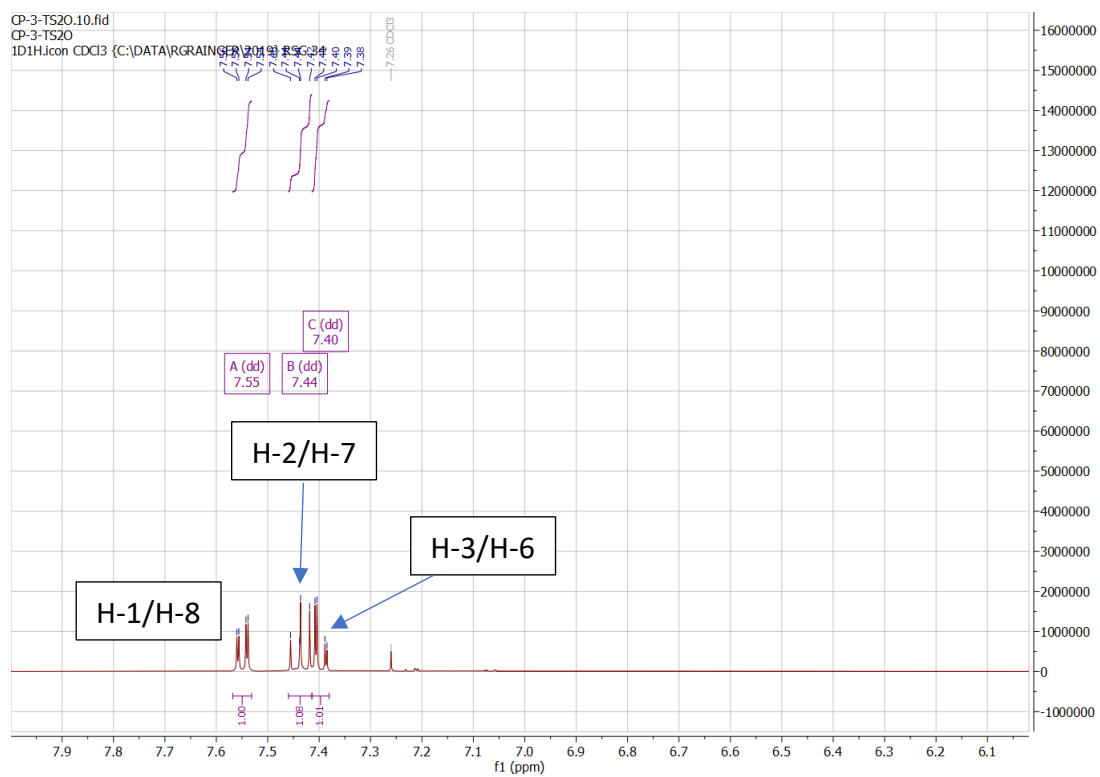
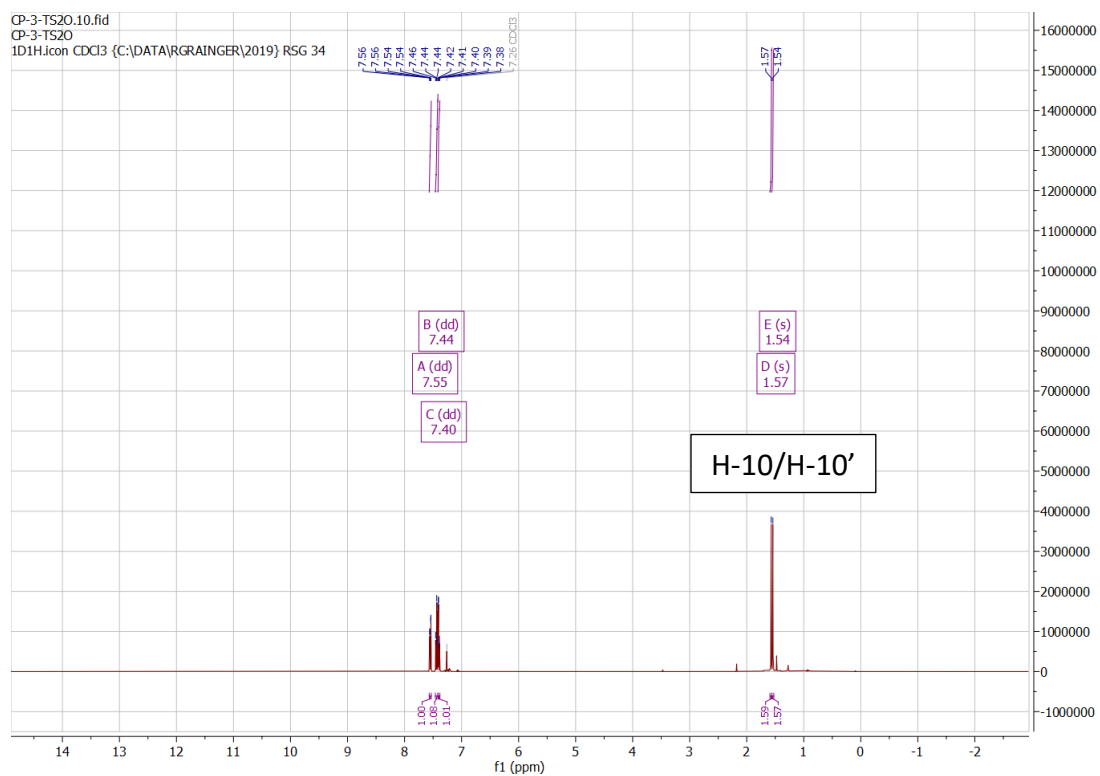


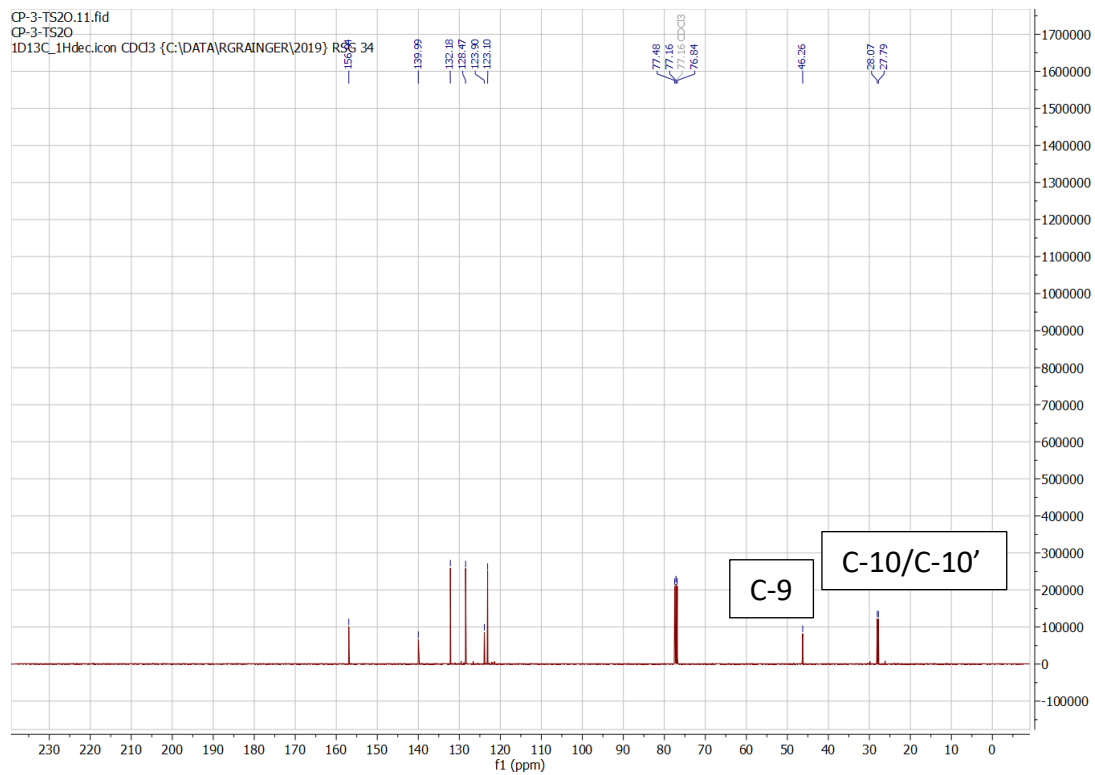
CP-3-fluorene\_trisulfide.11.fid  
 CP-3-fluorene\_trisulfide  
 1D 13C spectrum on 500MHz





# NMR data for 4,4-dimethyl-4*H*-fluoreno[4,5-*def*][1,2,3]trithiepine-9-oxide 301





CP-TIPS-Carbazole:10.fid  
 CP-TIPS-Carbazole  
 1D1H Icon CDCl3 (C:\DATA\GRAINGER\2020\BSC\cplg10.fid)

Chemical shift (ppm): 14, 13, 12, 11, 10, 9, 8, 7, 6, 5, 4, 3, 2, 1, 0, -1, -2

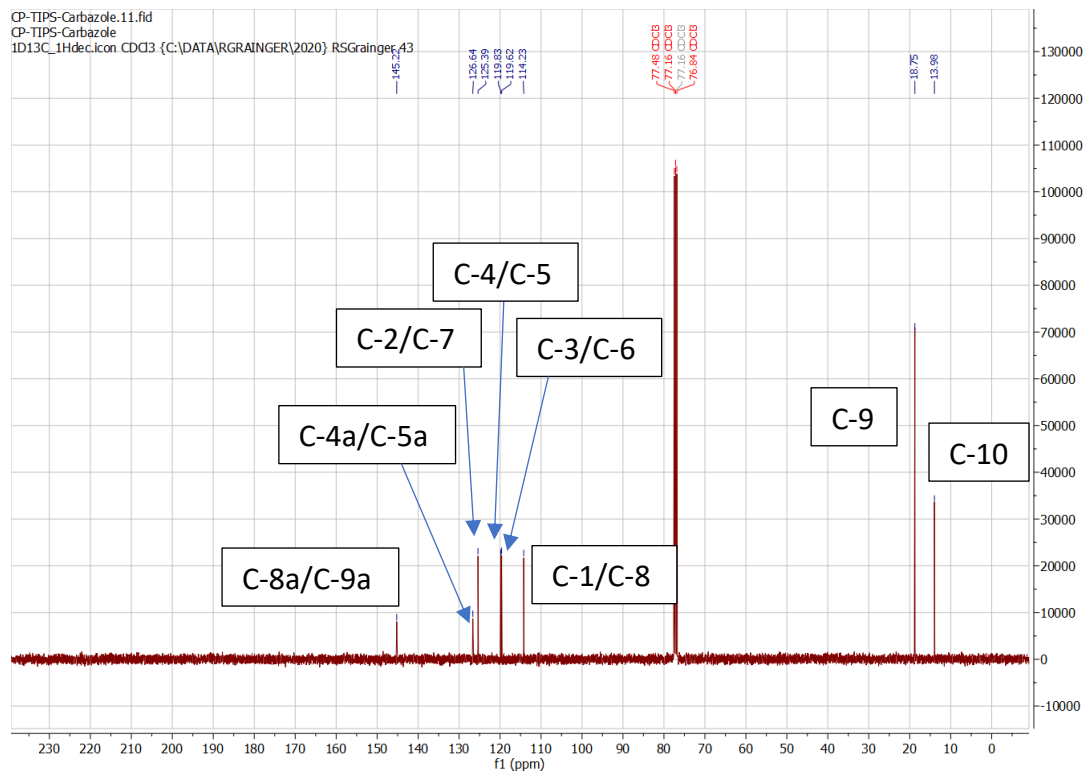
Integration values: 1.46, 1.96, 1.97, 1.97, 3.03, 18.00

Peak assignments and integrations:

- A (ddd) 8.07
- B (dt) 7.70
- C (ddd) 7.36
- D (ddd) 7.23
- E (h) 2.01
- F (d) 1.20

Labels: H-9, H-10



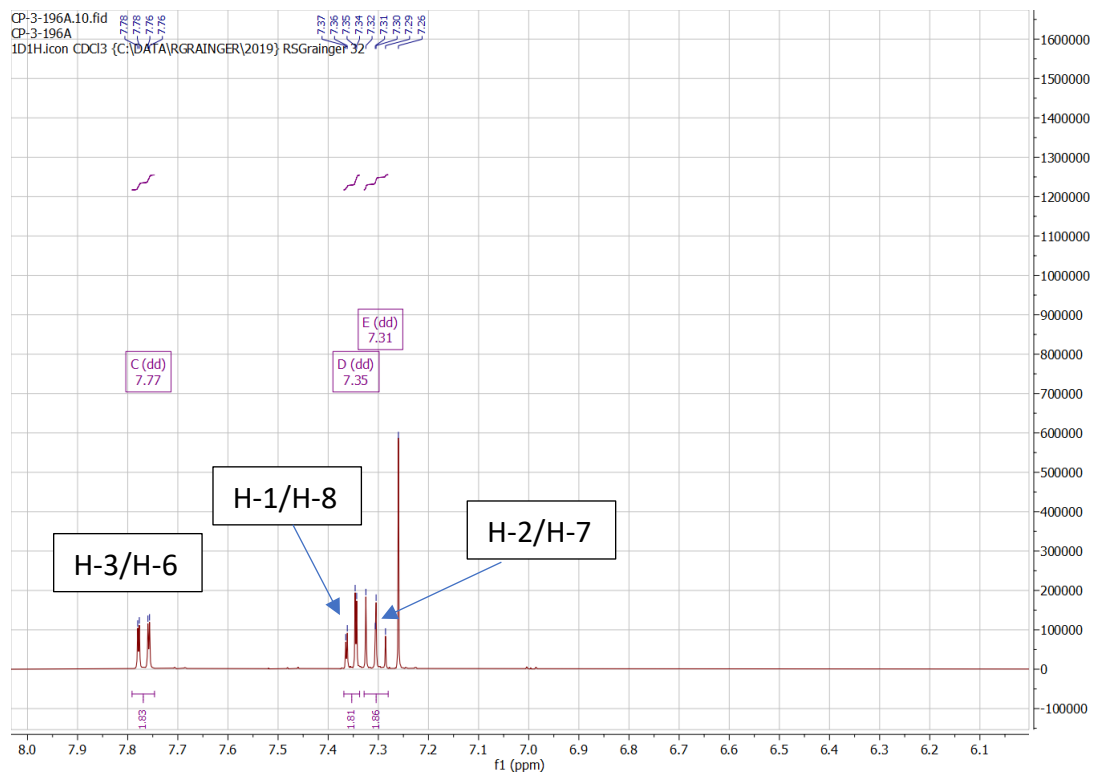
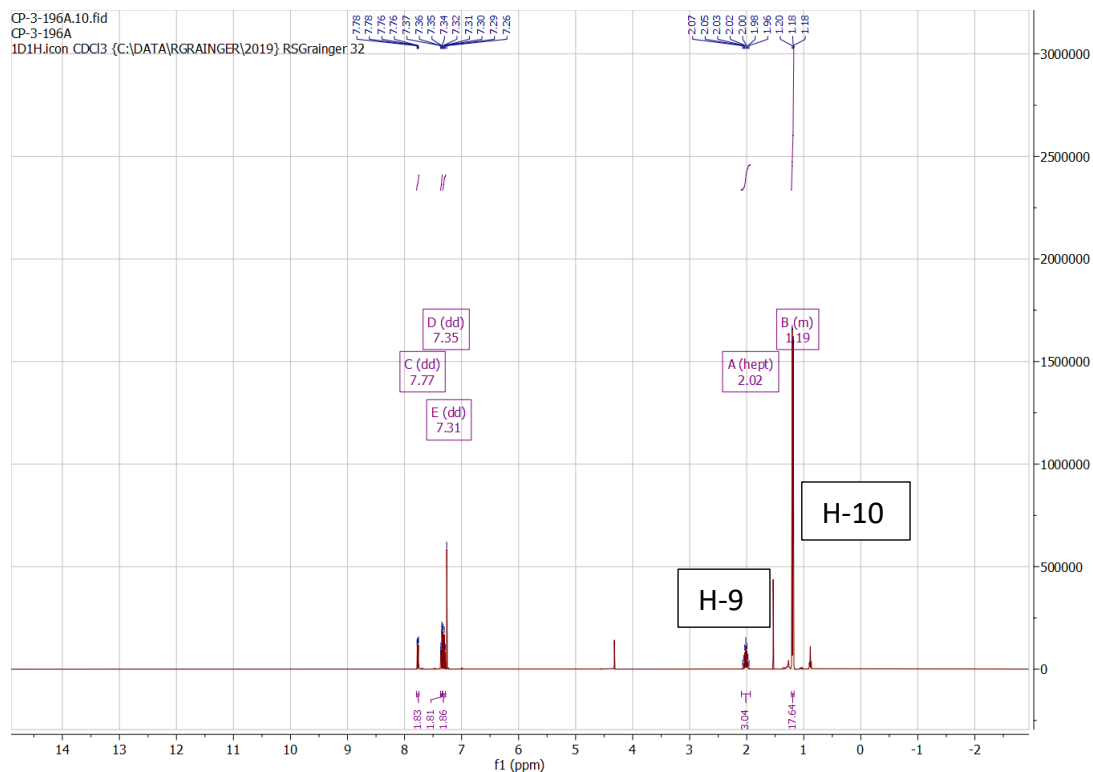


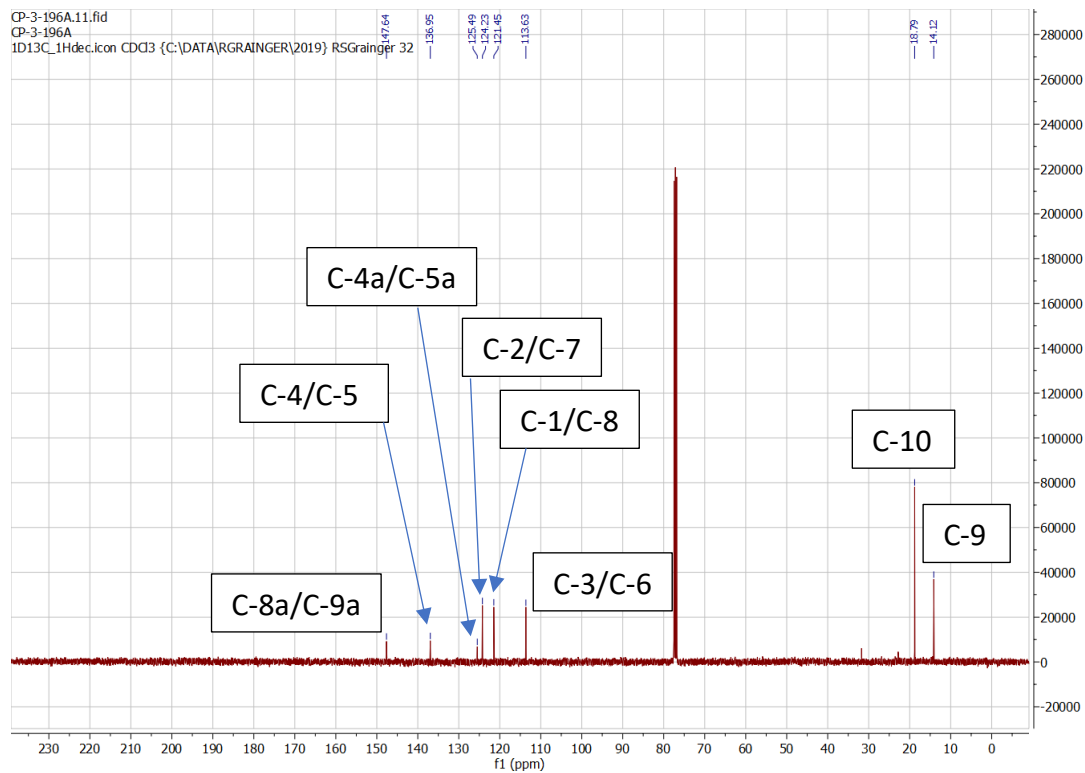
**1D<sup>1</sup>H NMR Spectrum of Compound 17**

Assignment	Chemical Shift (ppm)	Multiplicity	Integration
H-2/H-7	~7.3	dd	1.80
H-3/H-6	~7.4	dd	2.79
H-1/H-8	~7.0	dd	1.76
H-9	~1.9	hept	3.00
H-10	~1.2	d	16.00

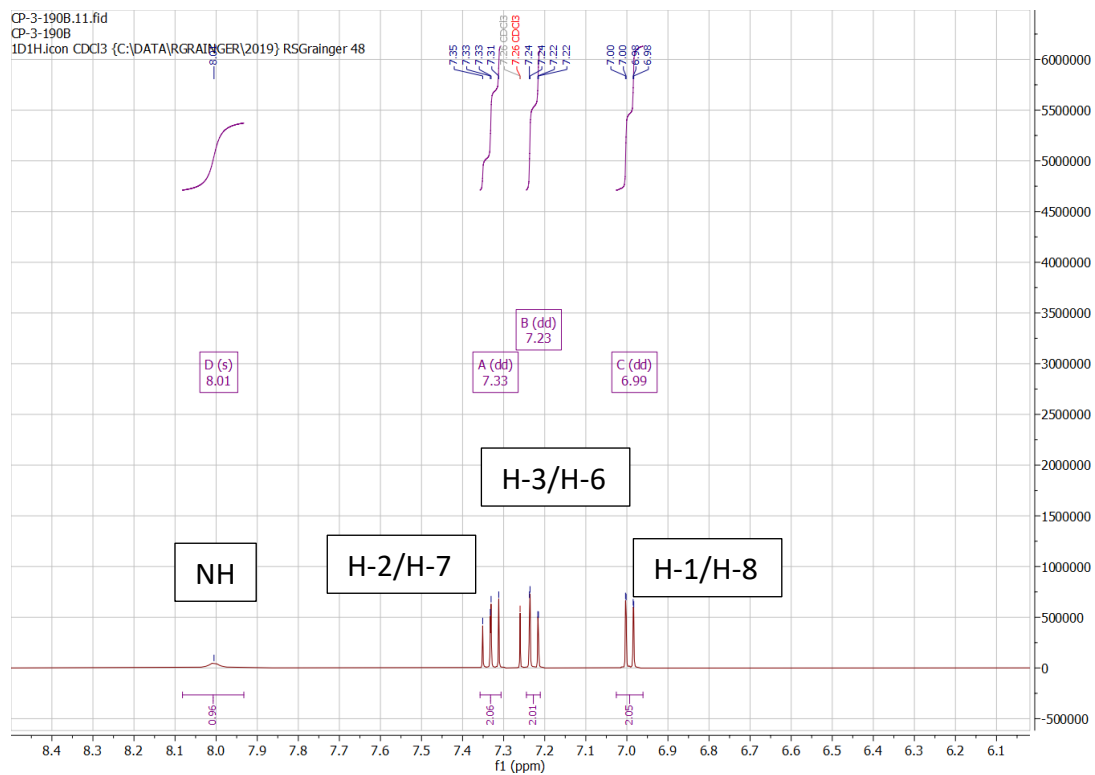
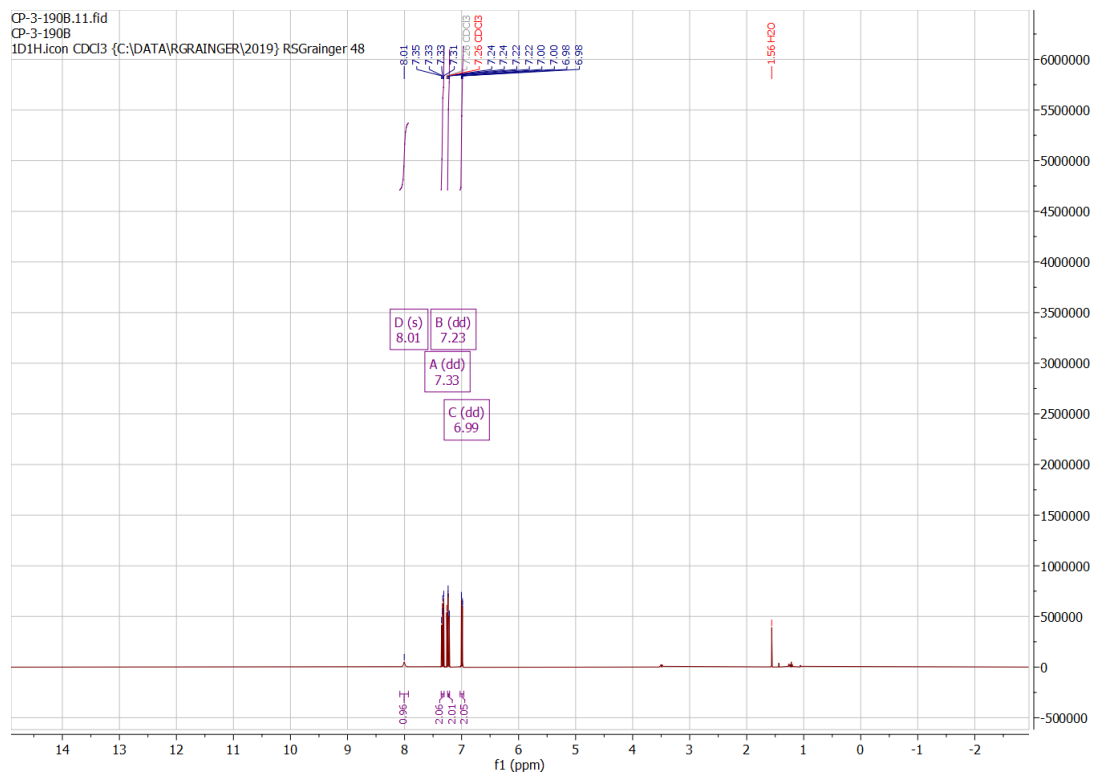


# NMR data for 4-(triisopropylsilyl)-4H-[1,2,3]trithiepine[4,5,6,7-def]carbazole 296

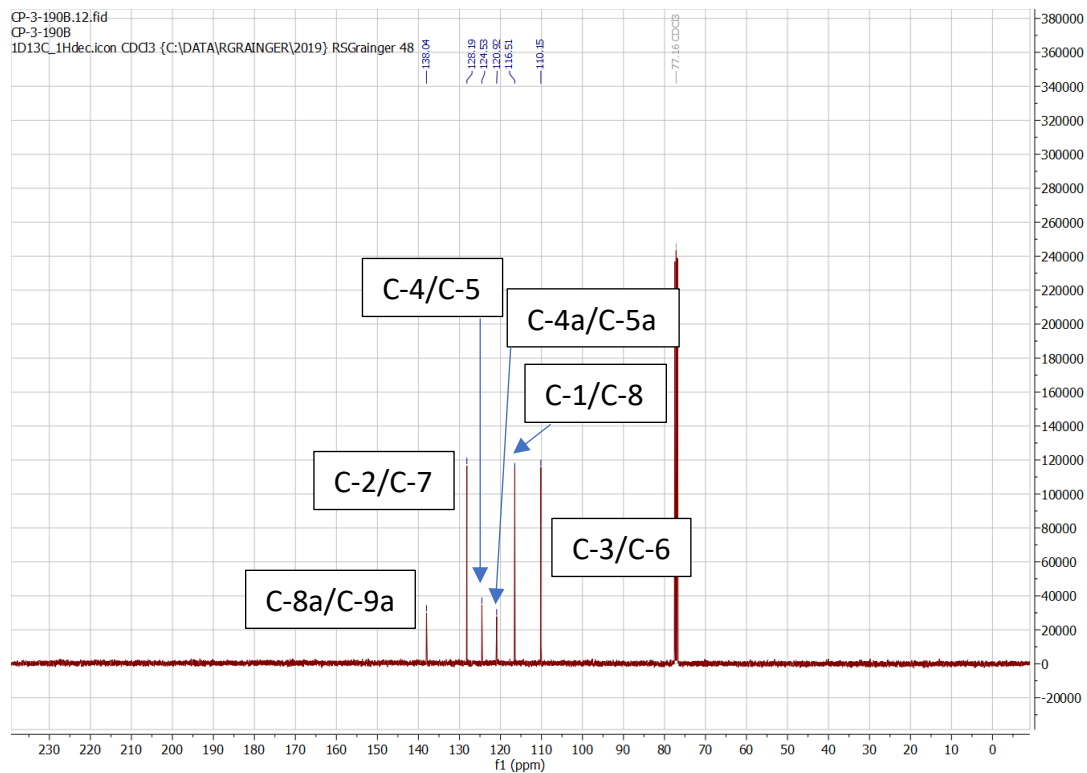




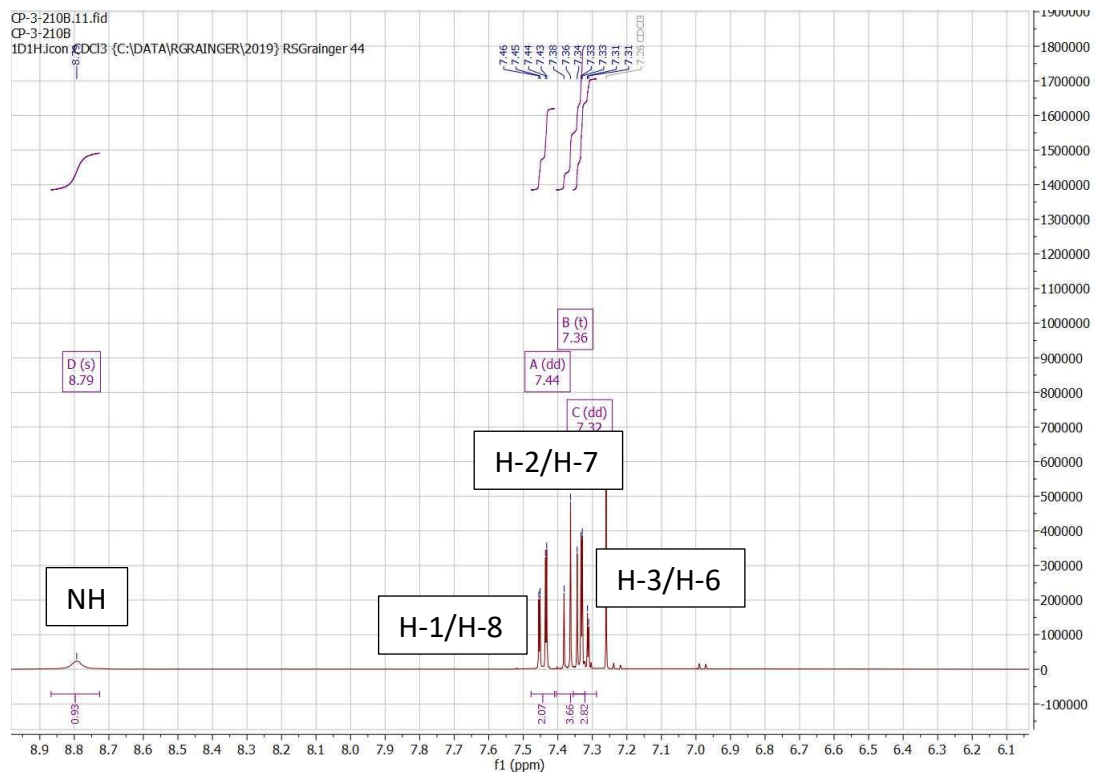
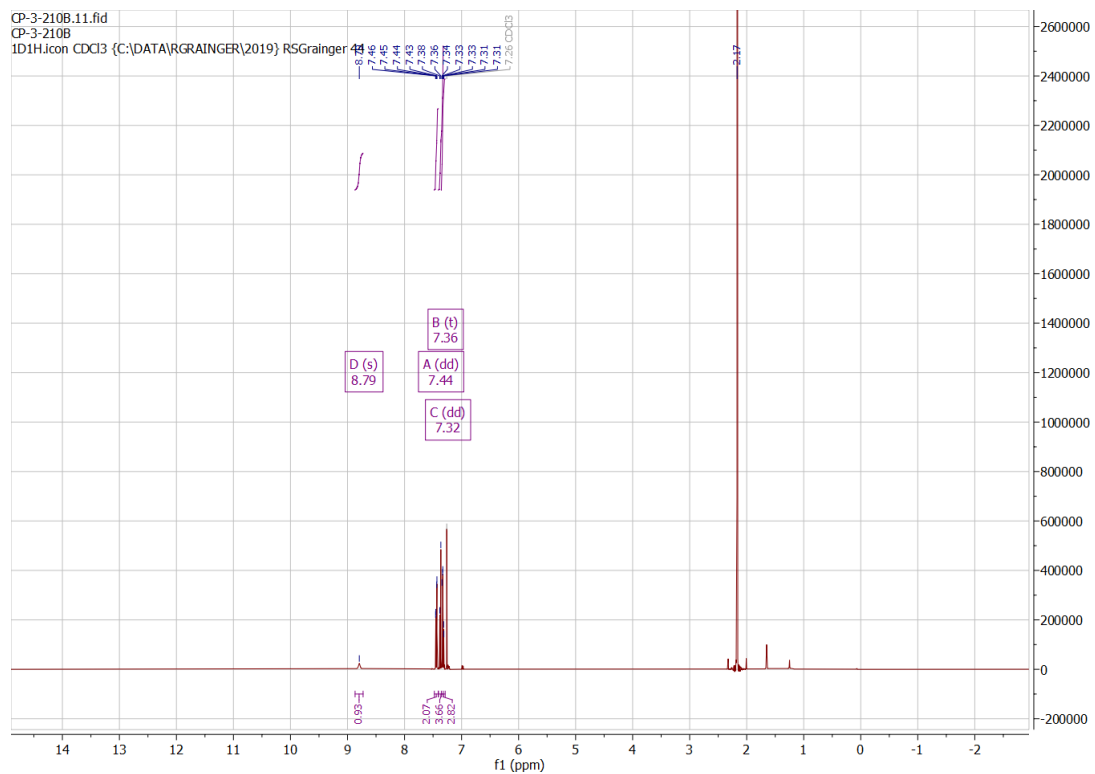
# NMR data for **9H-[1,2]dithiino[3,4,5,6-def]carbazole 311**

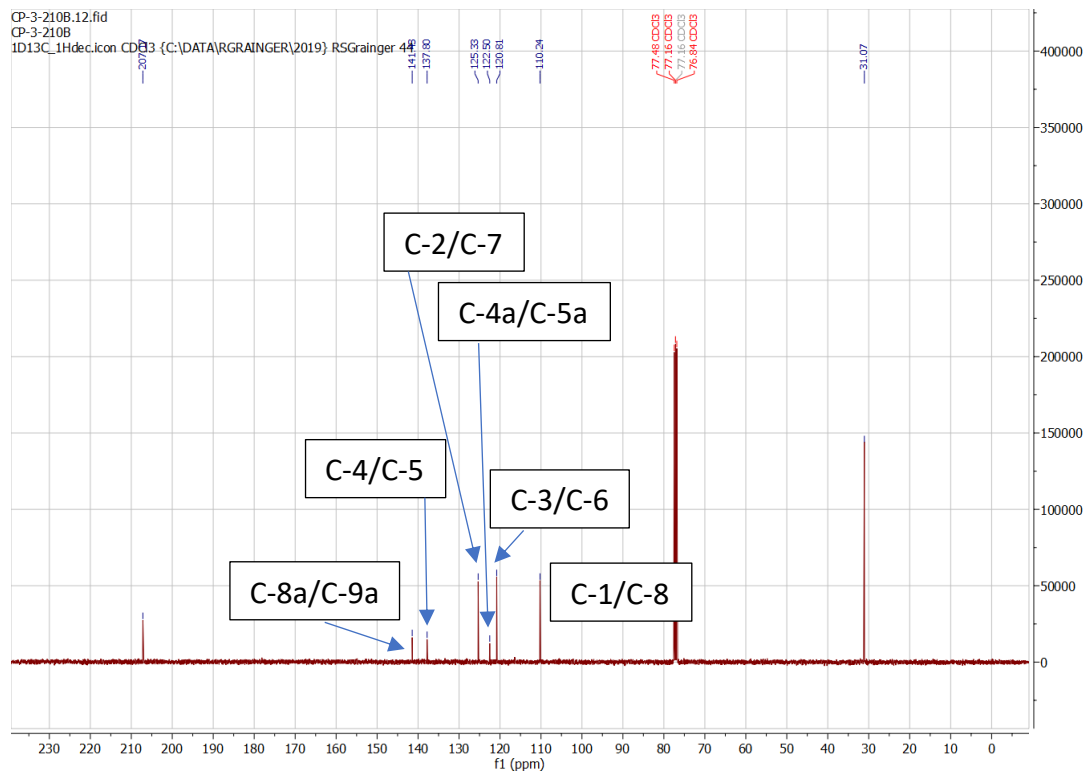




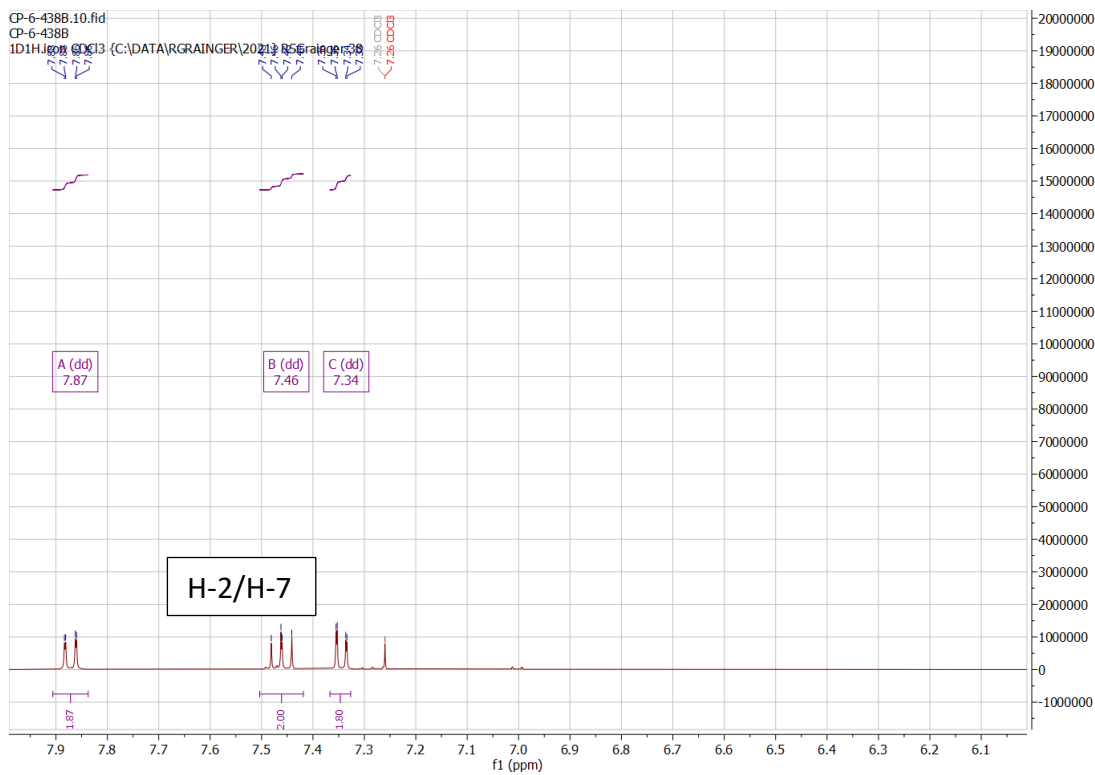
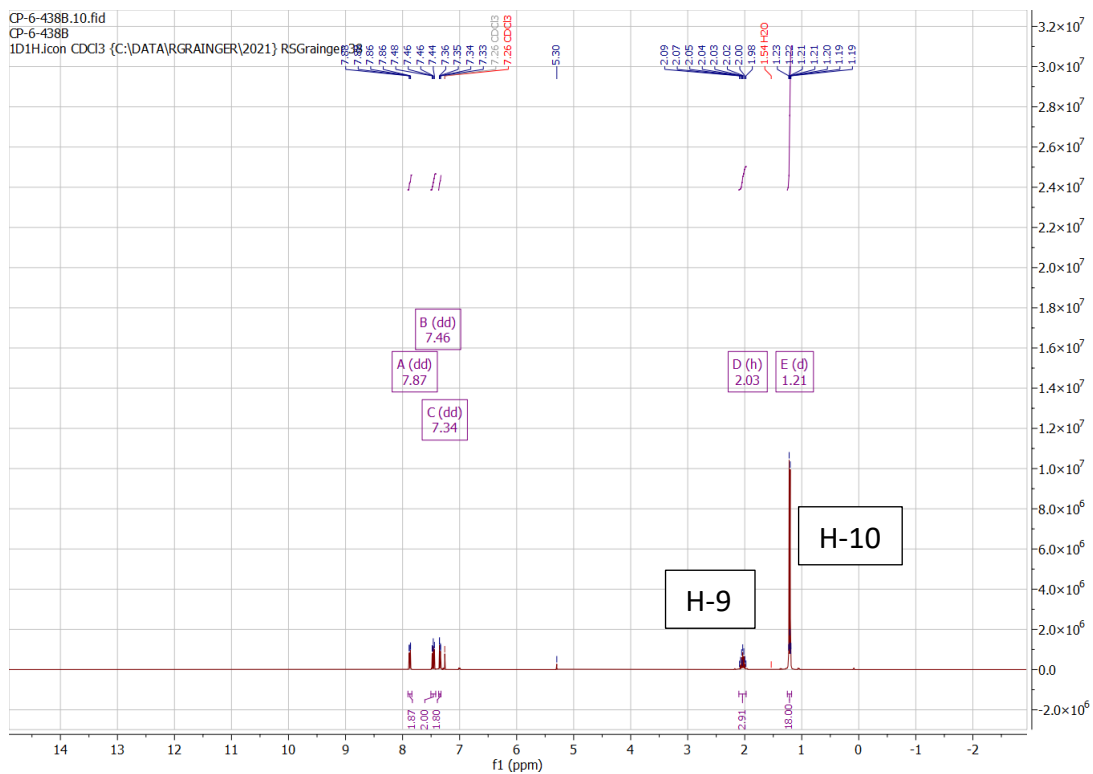


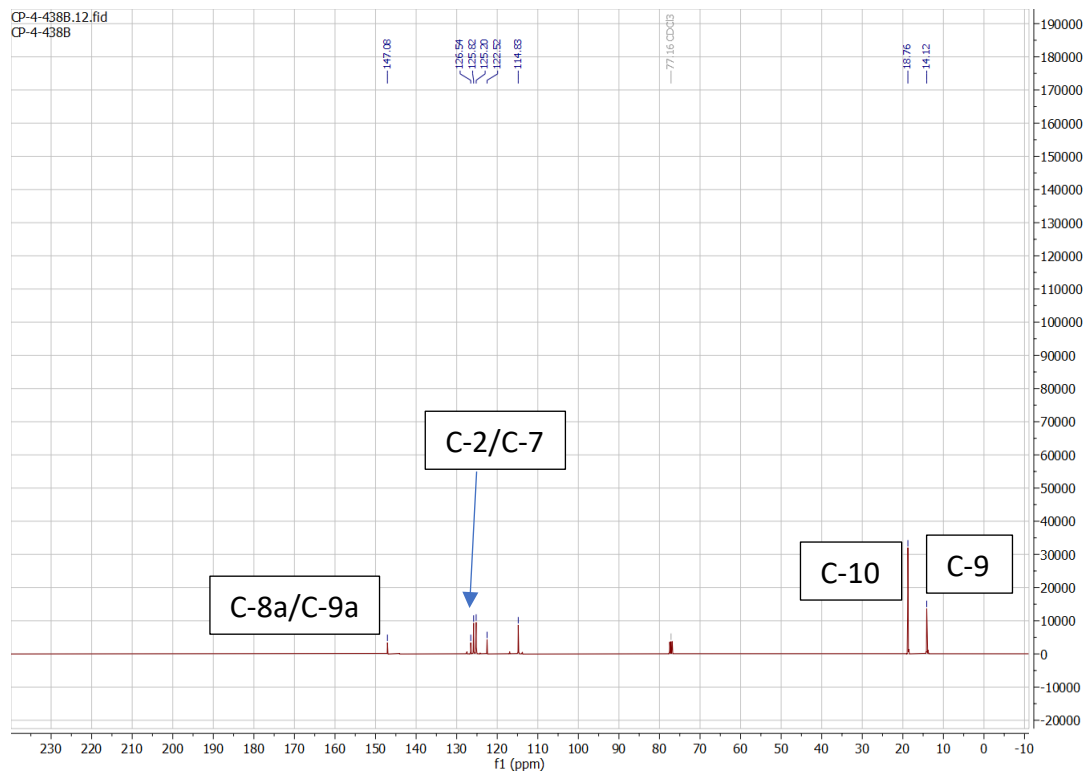
# NMR data for **4H-[1,2,3]trithiepine[4,5,6,7-def]carbazole 329**



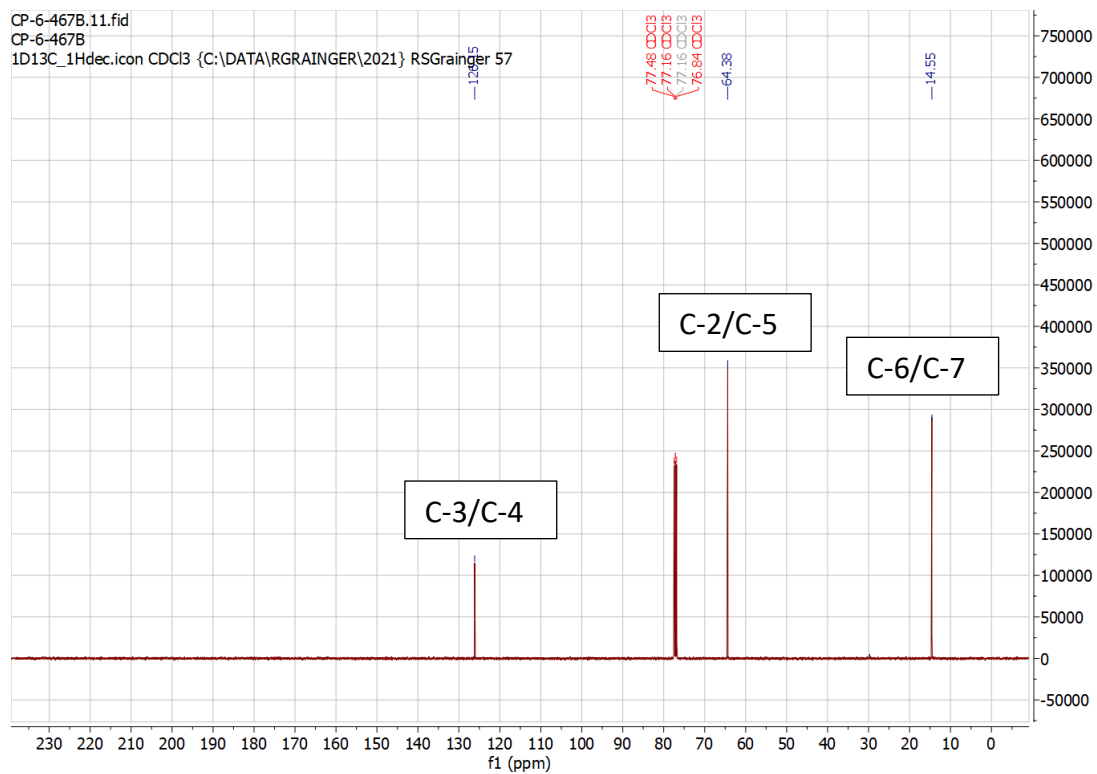


# NMR data for 4-(triisopropylsilyl)-4H-[1,2,3]trithiepine[4,5,6,7-def]carbazole-9-oxide 302

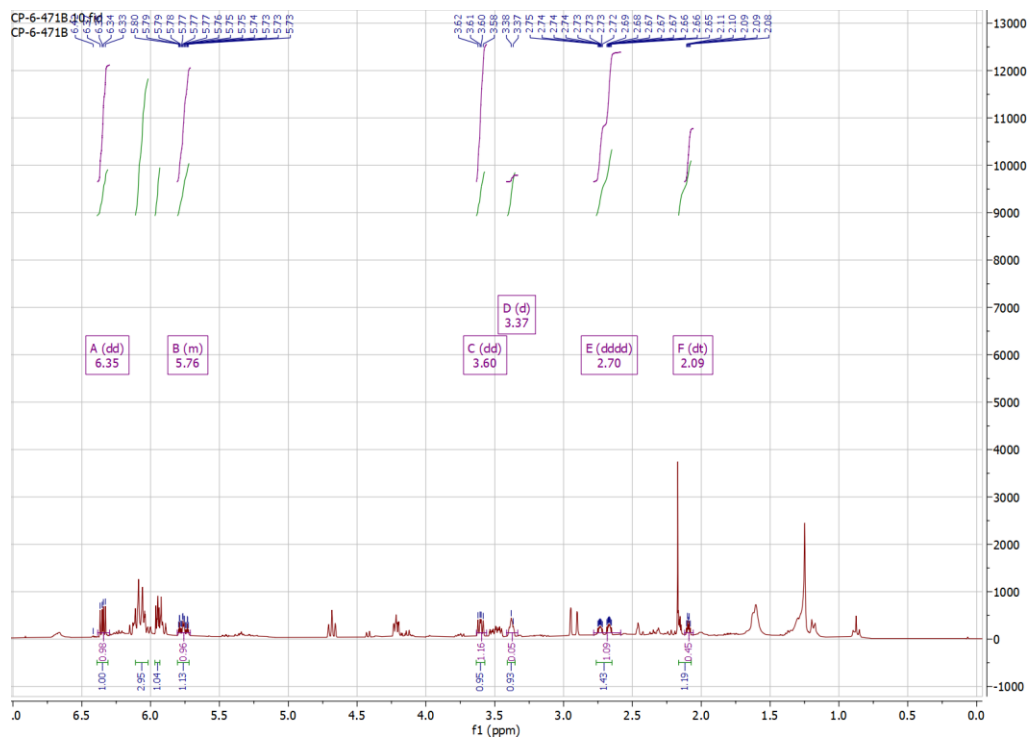
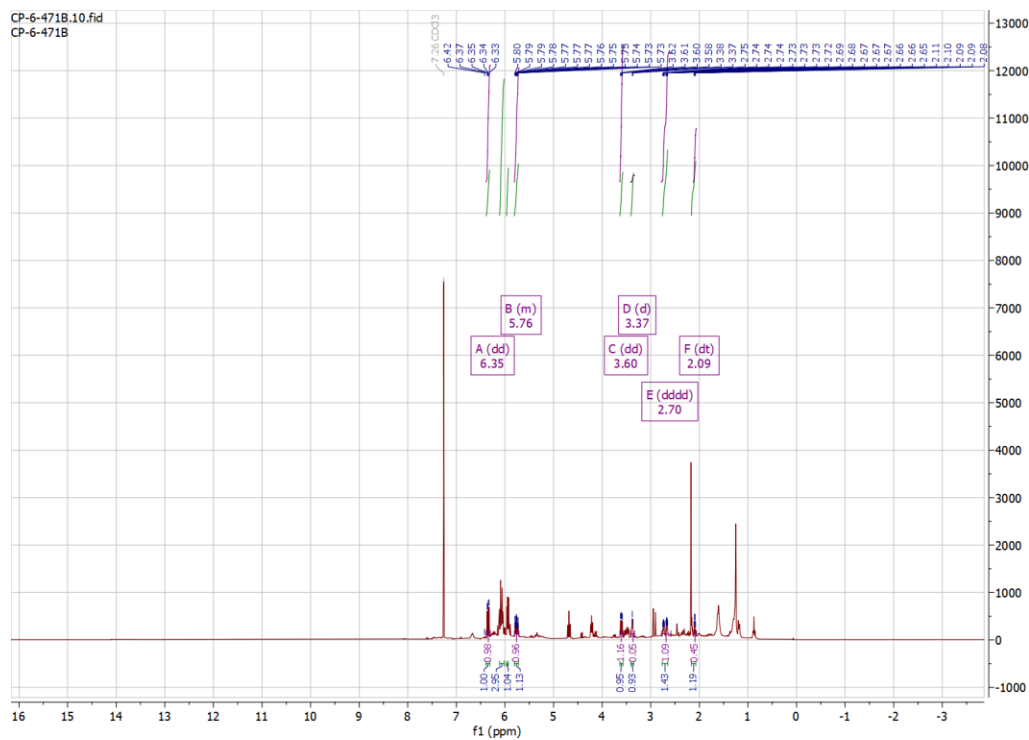






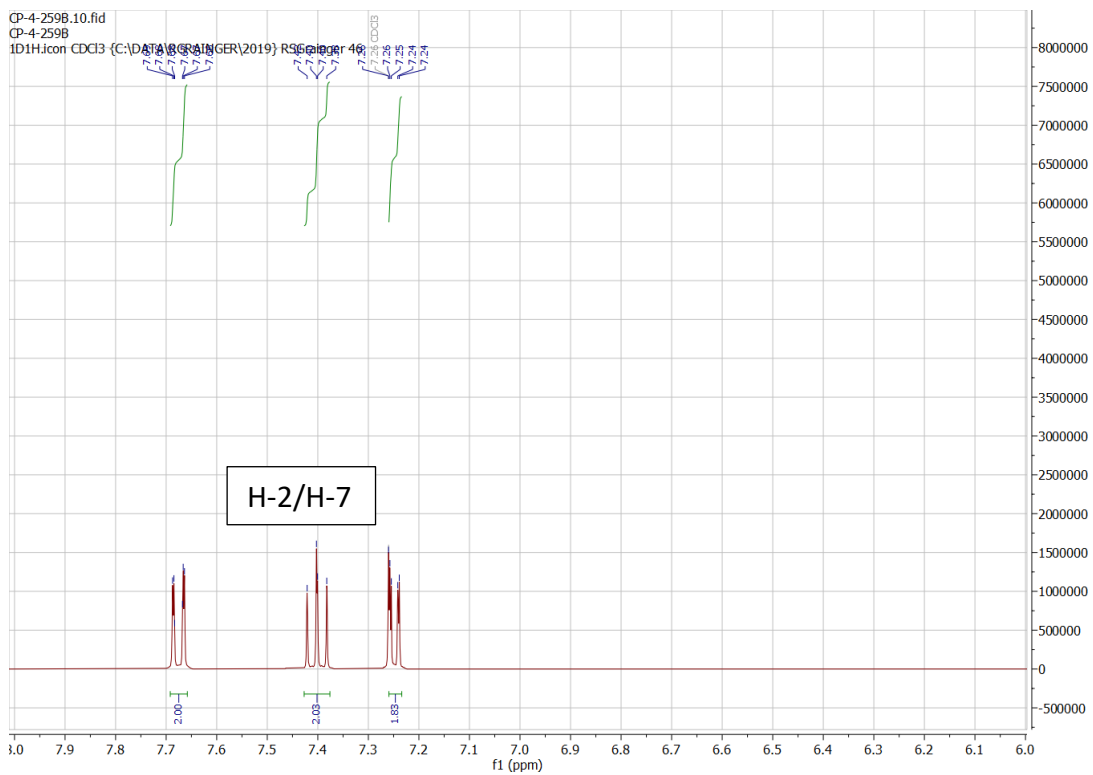
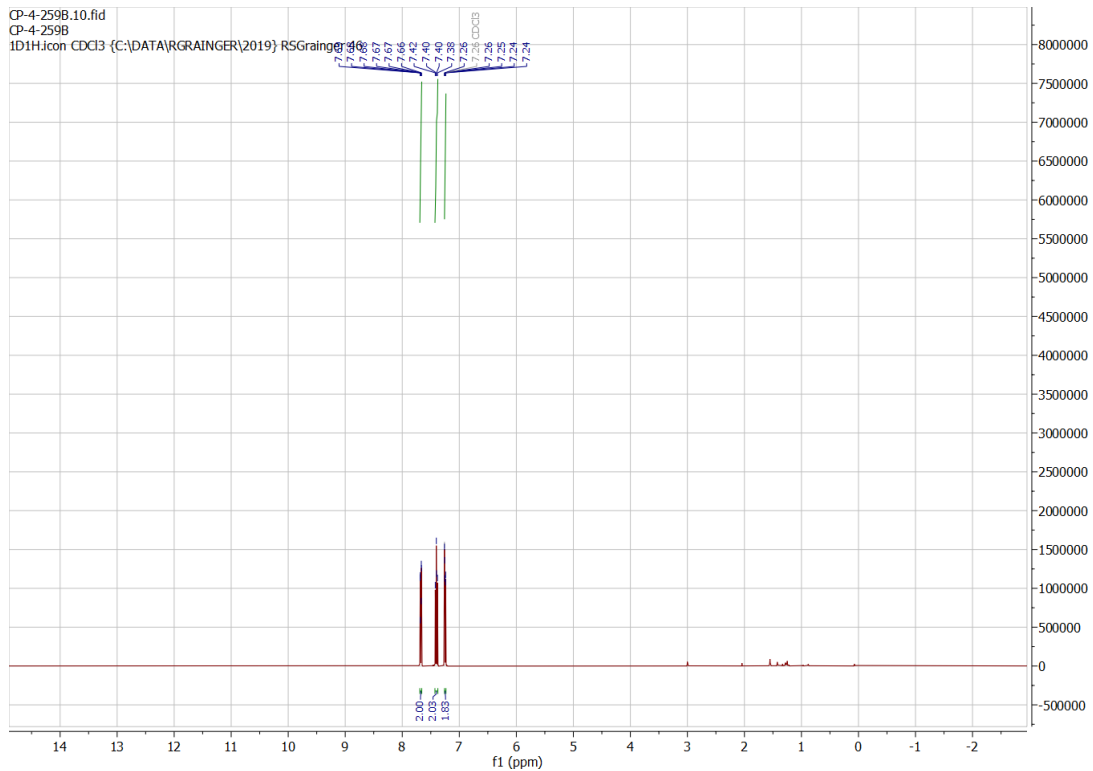


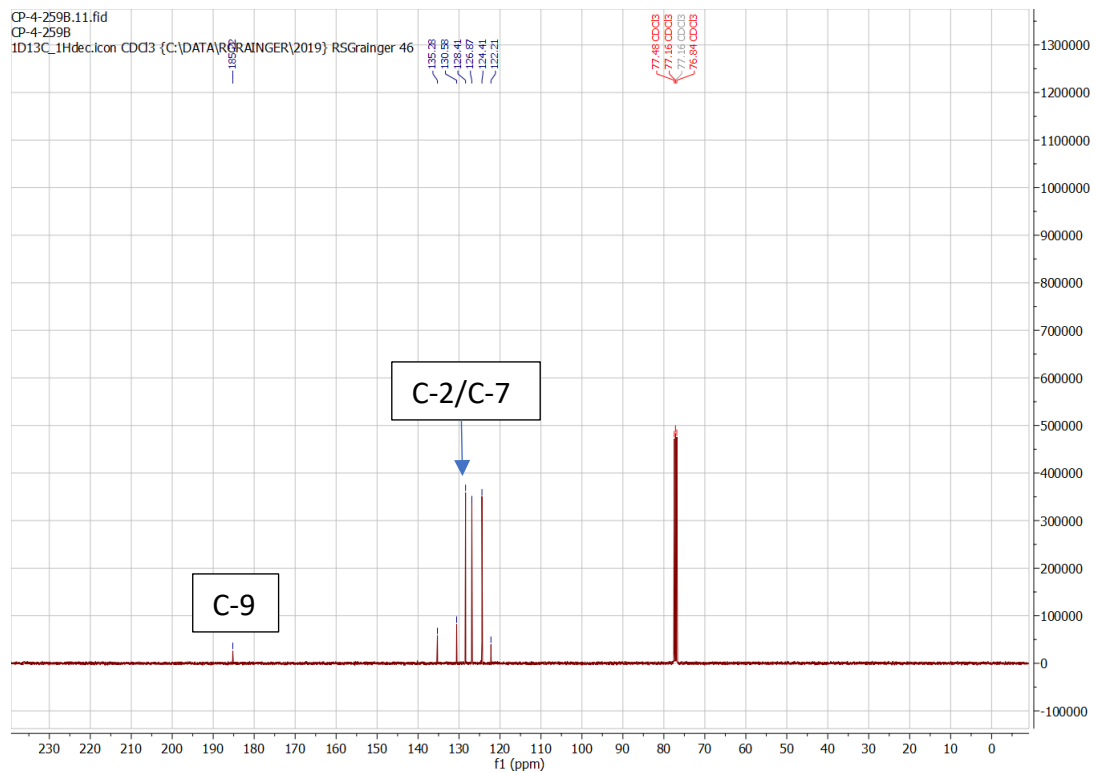
# NMR data for **1R,5S,8R)-8lambda4-thiabicyclo[3.2.1]octa-2,6-dien-8-one 181**



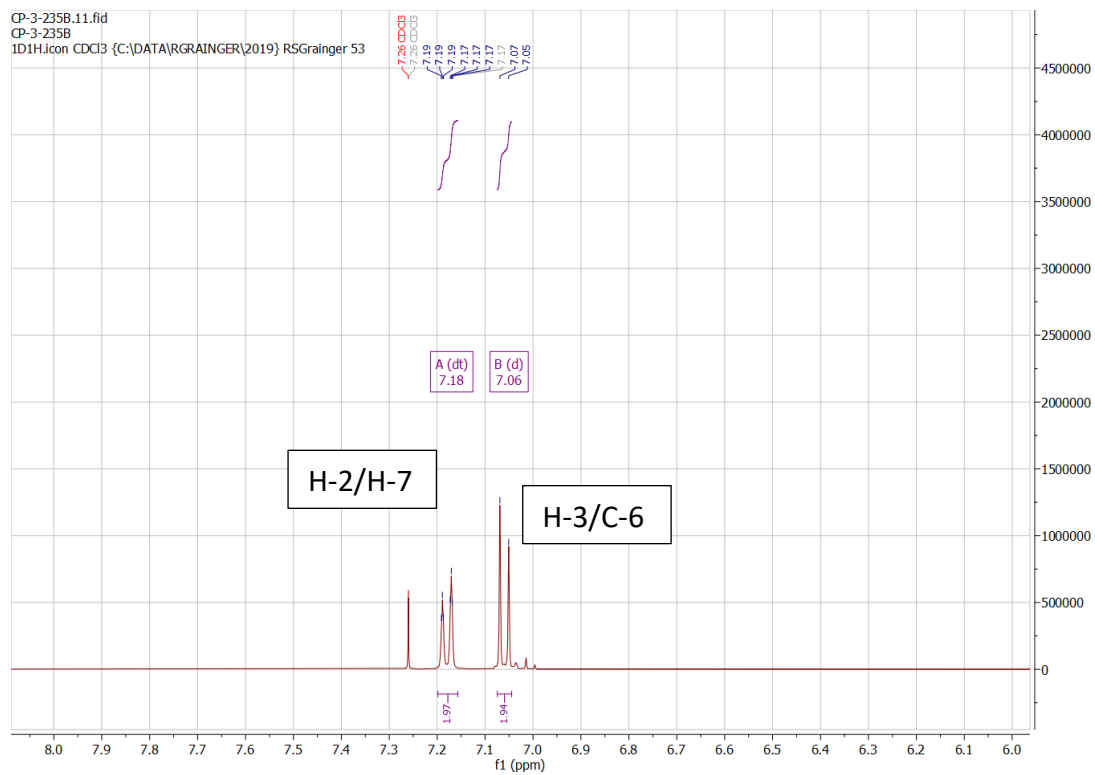
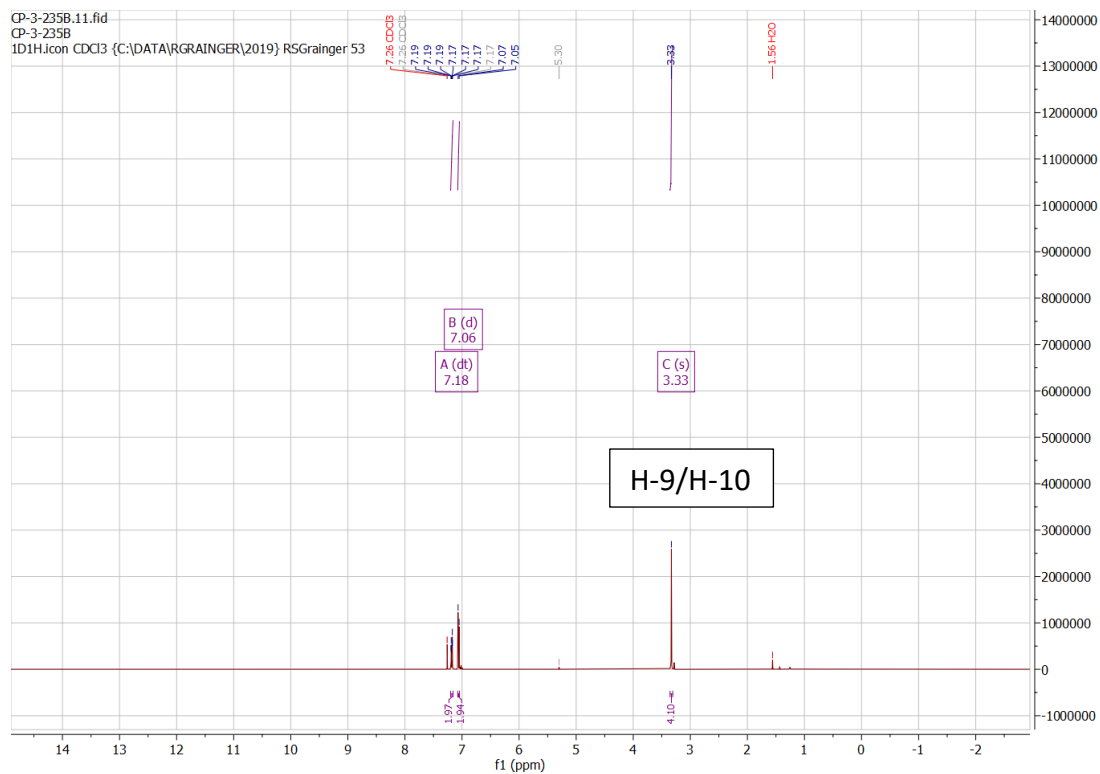


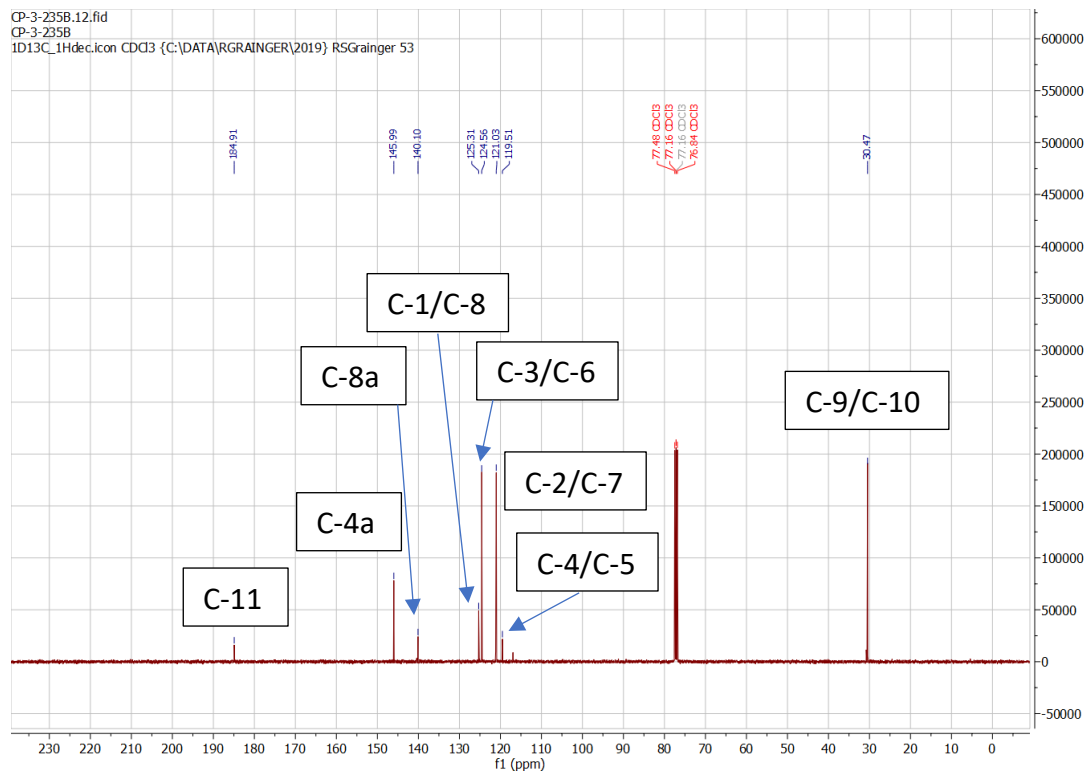
NMR data for **naphtho[1,8-*de*][1,3]dithiin-2-one 336**



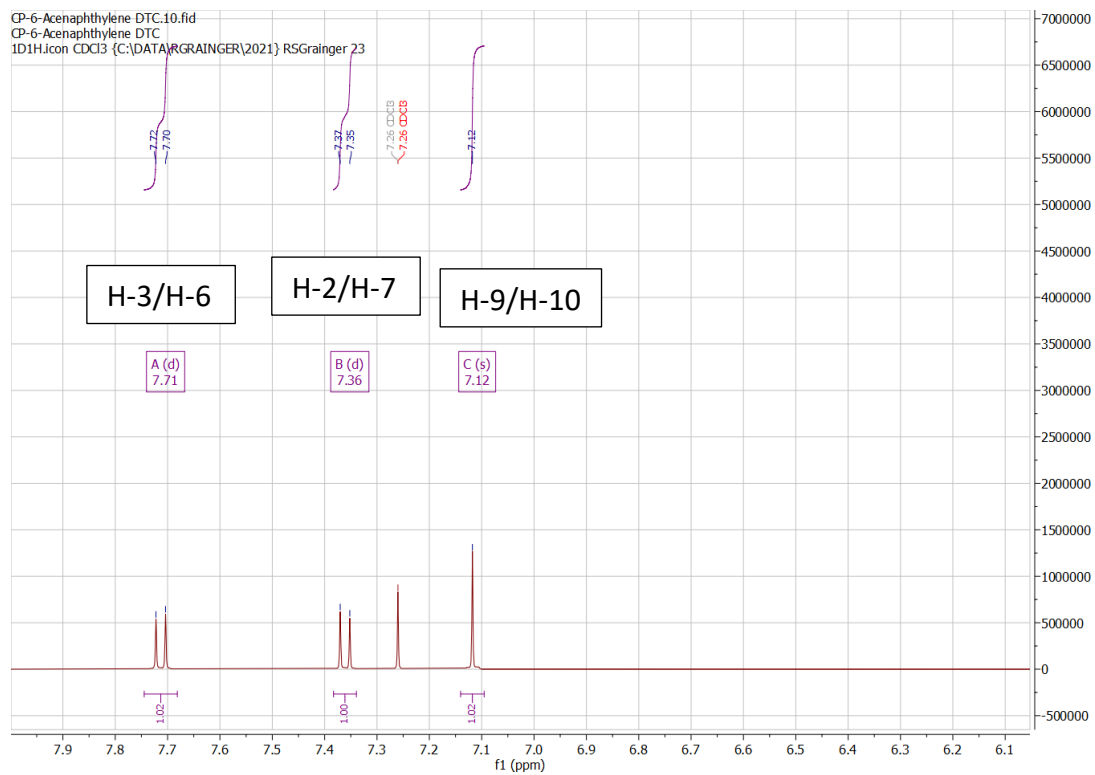
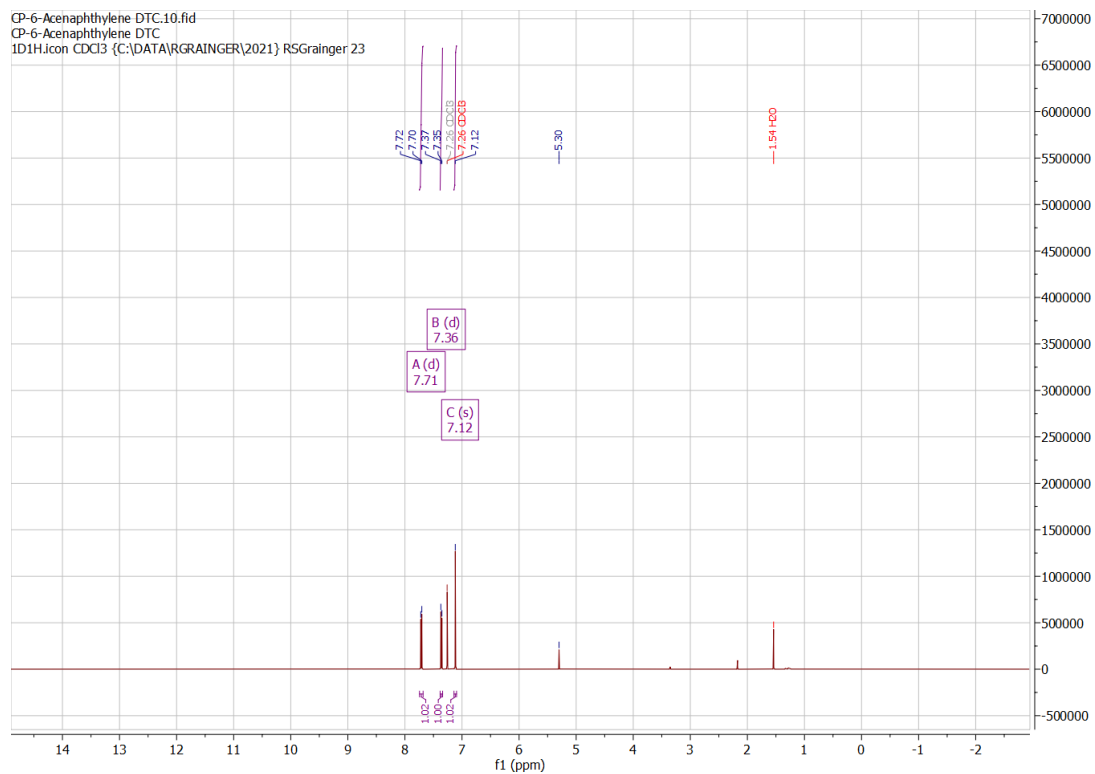


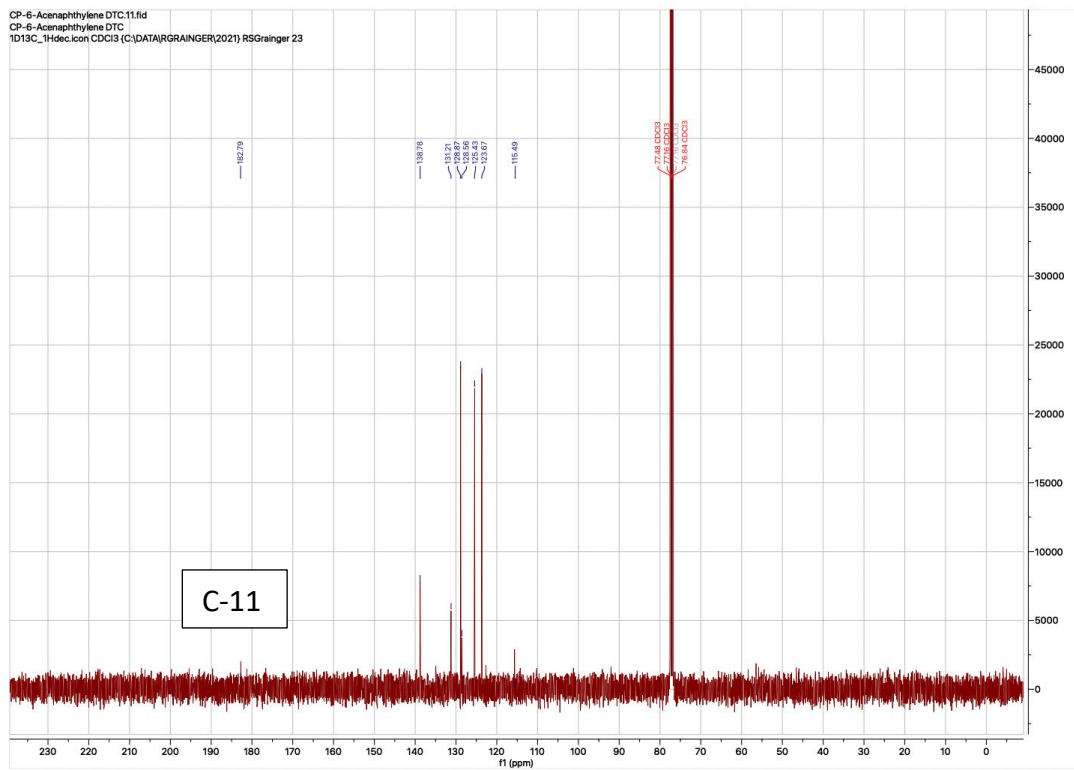
# NMR data for 6,7-dihydroacenaphtho[5,6-*de*][1,3]dithiin-2-one 337





# NMR data for acenaphtho[5,6-*de*][1,3]dithin-2-one 338



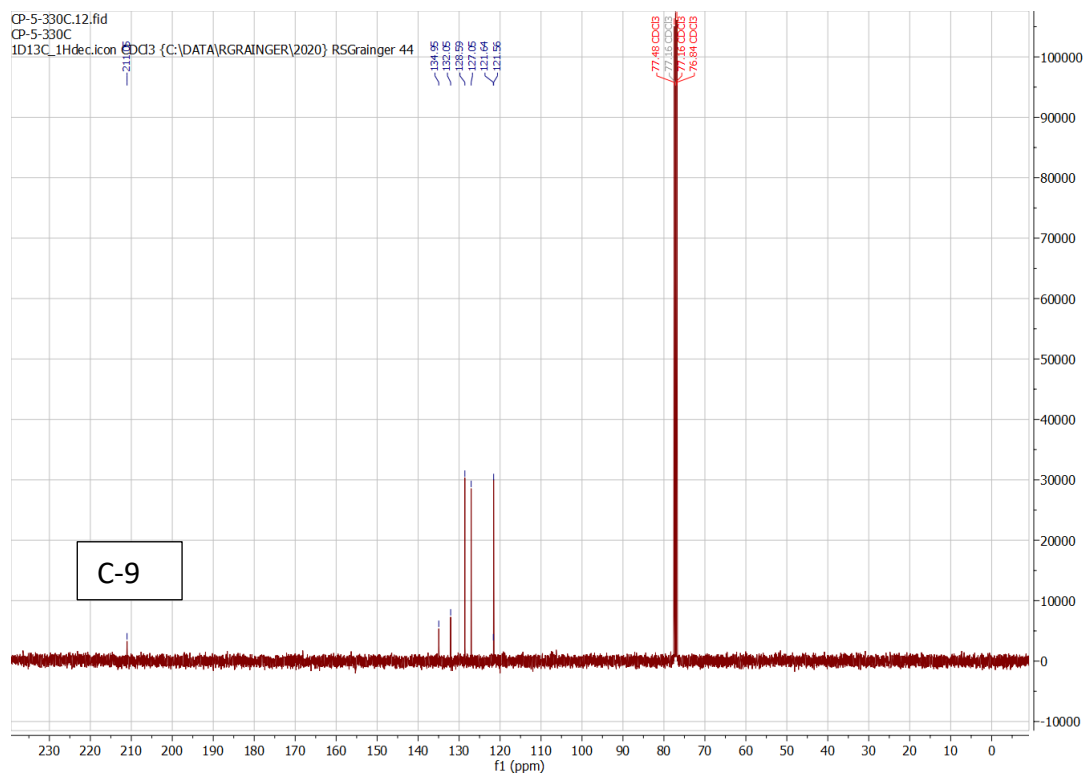


**1D  ${}^1\text{H}$  NMR Spectrum**

Solvent:  $\text{CDCl}_3$

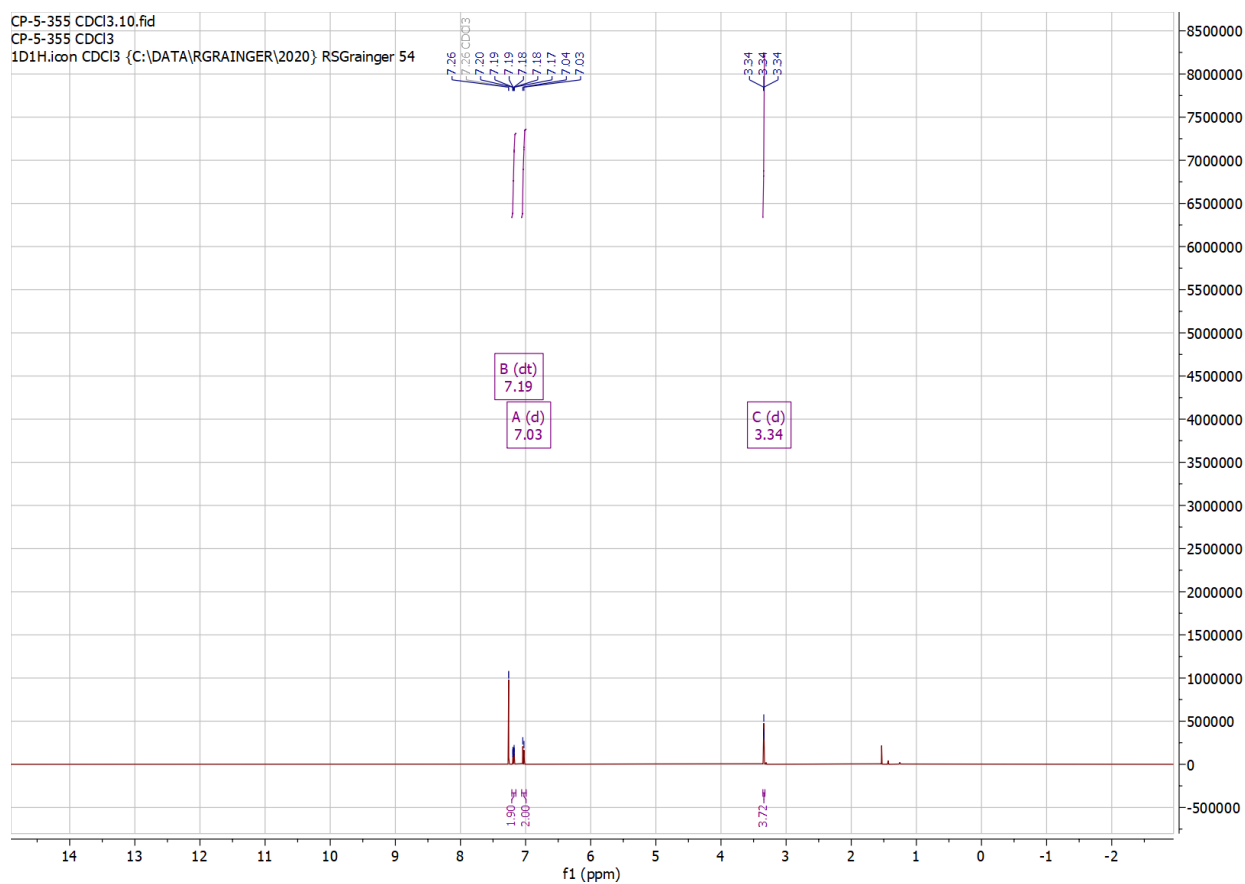
Chemical Shift (ppm)	Multiplicity	Integration
~7.19	dd	1.00
~7.65	m	0.98
~7.40	dd	0.98
1.54	s	-



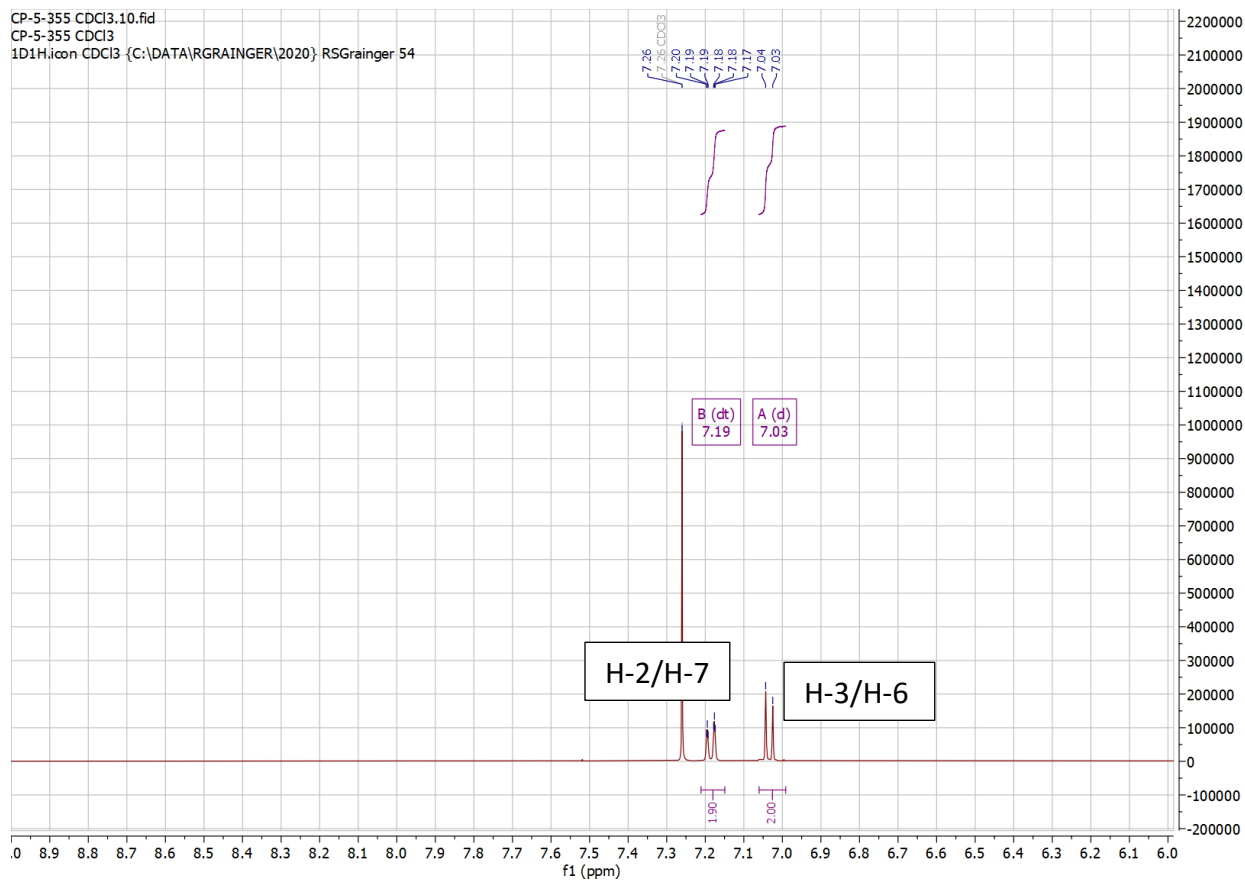


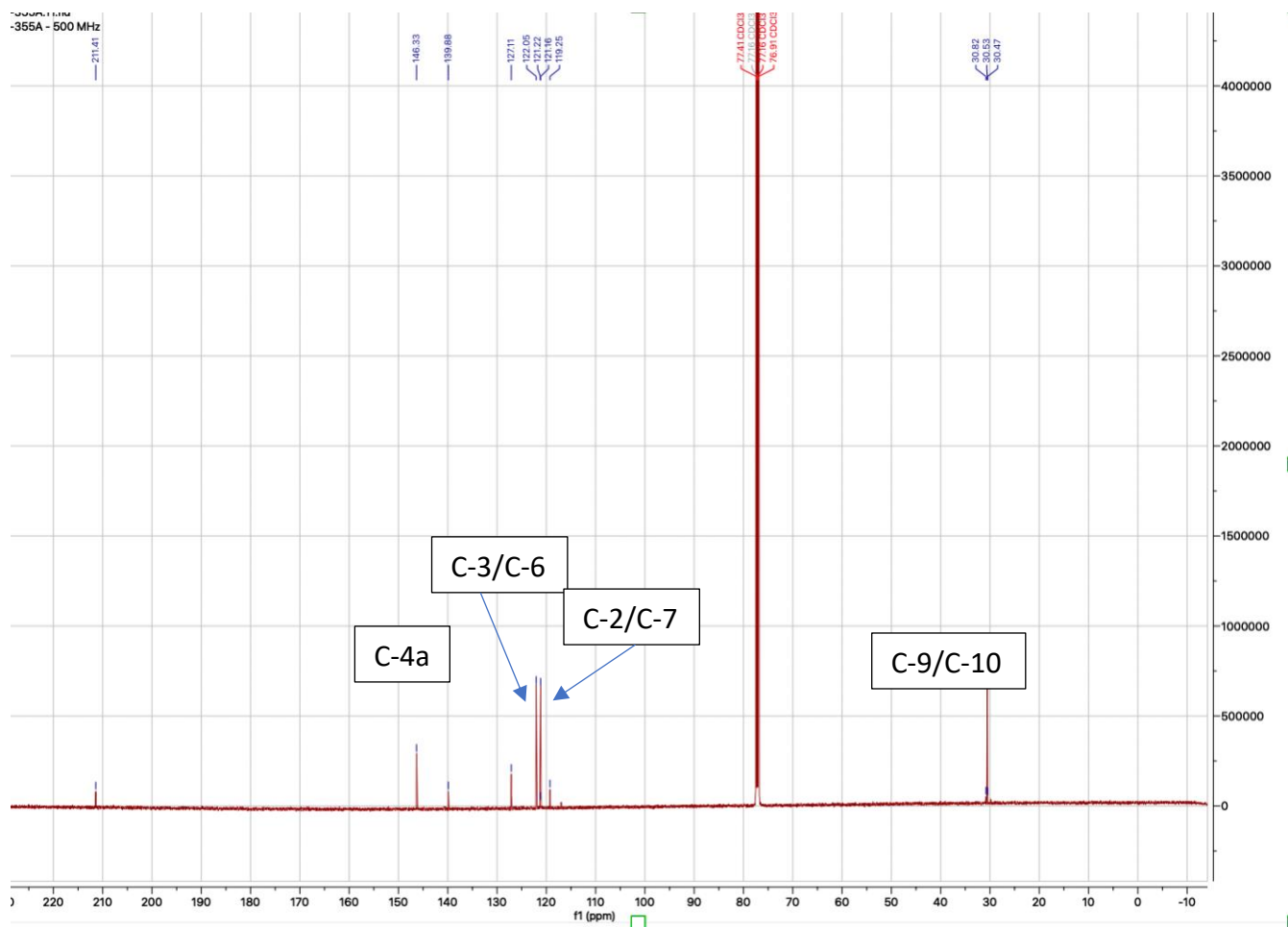


# NMR data for 6,7-dihydroacenaphtho[5,6-*de*][1,3]dithiine-2-thione 378

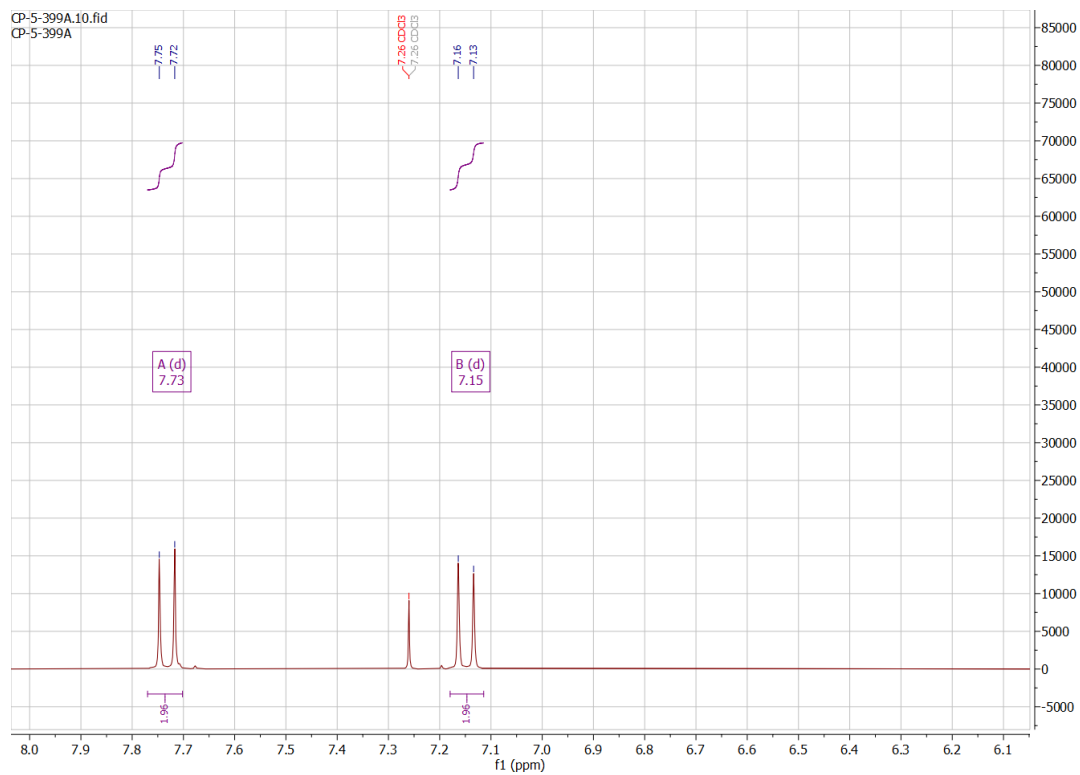
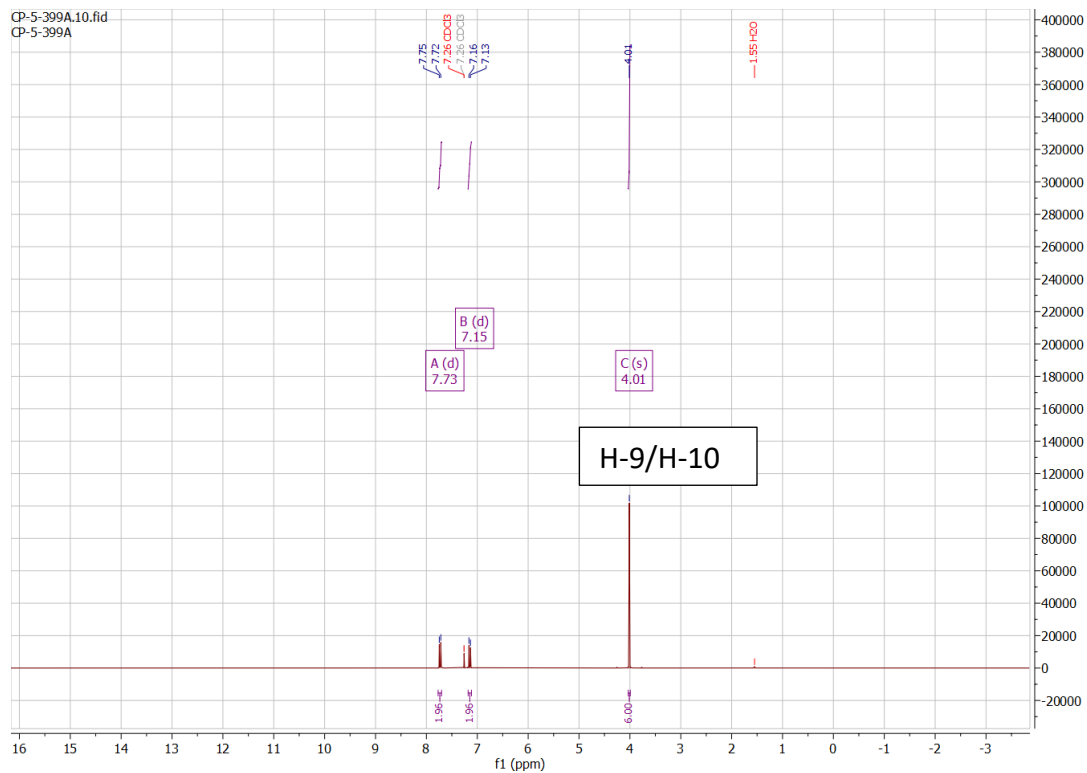


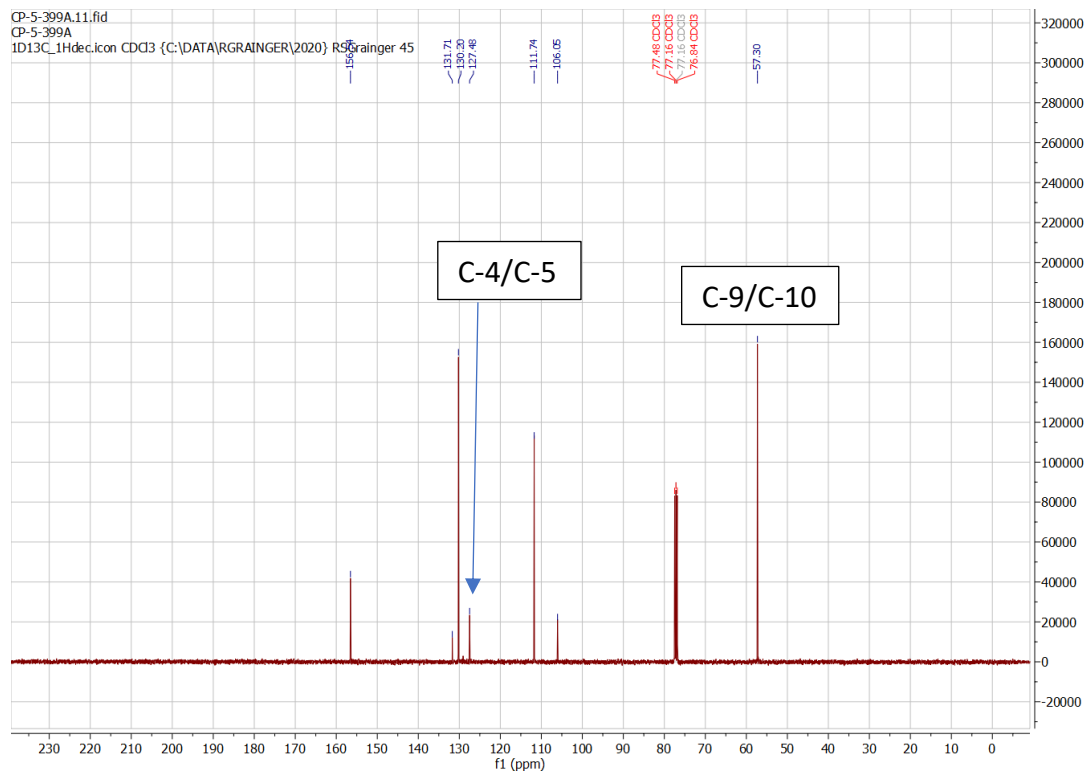
CP-5-355 CDCl3.10.fid  
CP-5-355 CDCl3  
1D1H.icon CDCl3 {C:\DATA\RGRAINER\2020} RSGranger 54



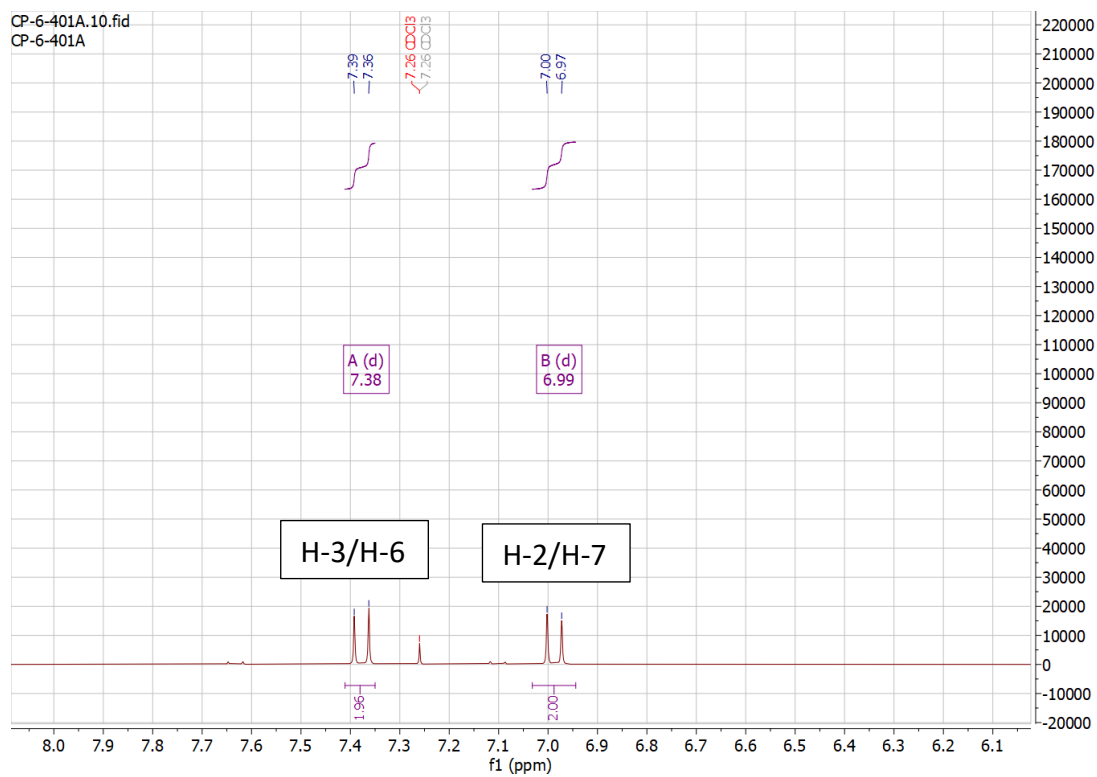
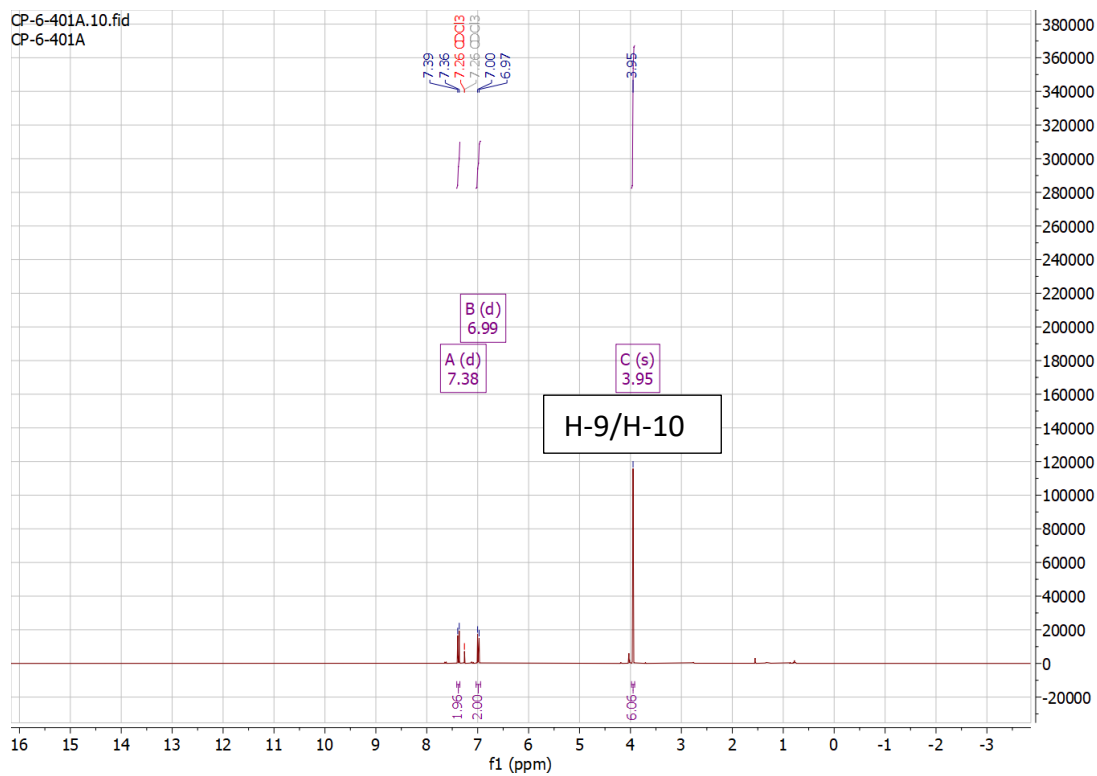


NMR data for **2,7-dimethoxy-1,8-dibromonaphthalene 111**





# NMR data for 3,8-dimethoxynaphtho[1,8-*cd*][1,2]dithiole 112



CP-6-404C.10.fid  
CP-6-404C  
1D1H.icon CDC3 {C:\DATA\RGRAINGER\2020} RS Granger 24

2.11  
2.16  
6.00

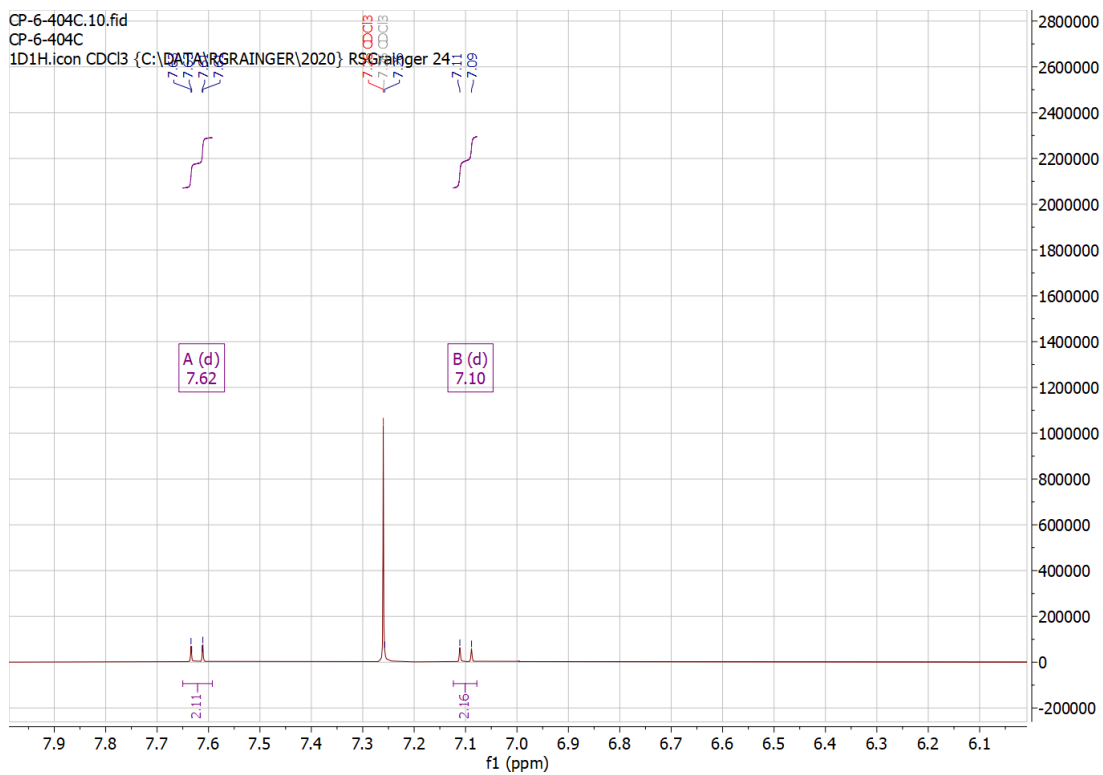
A (d)  
7.62

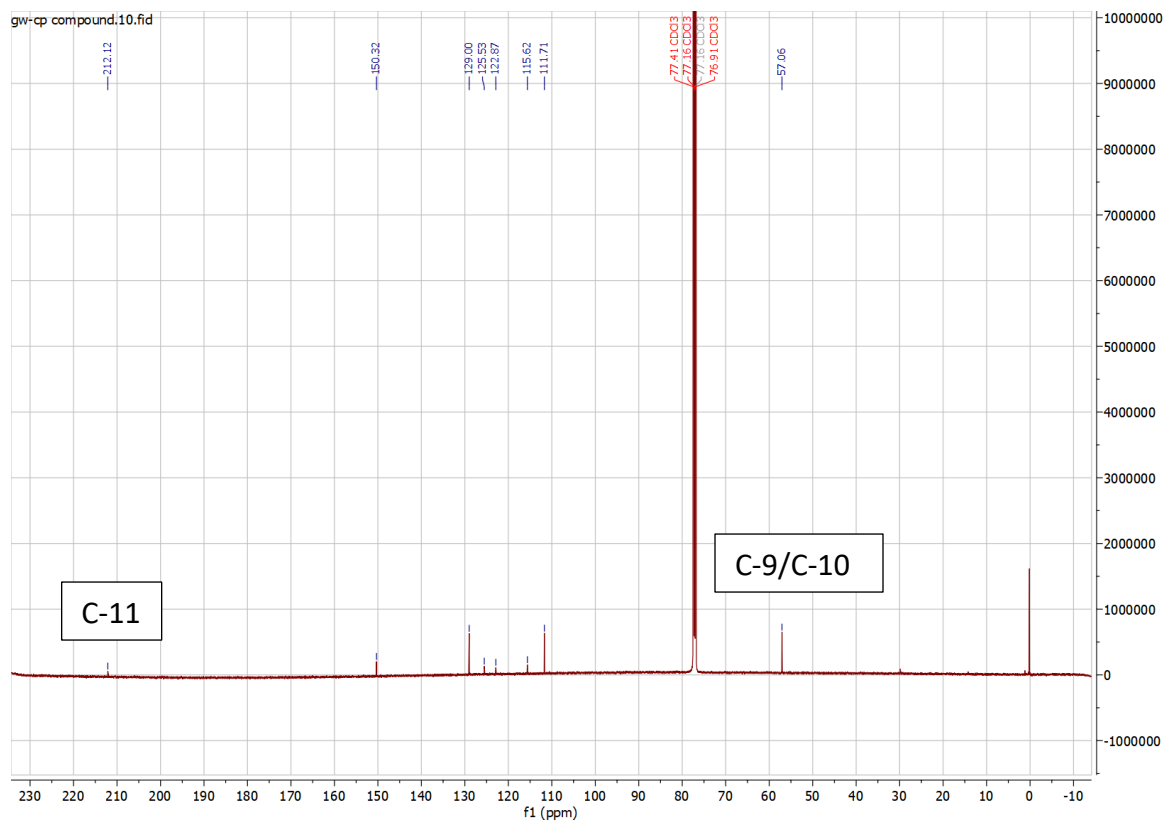
B (d)  
7.10

C (s)  
3.99

H-9/H-10

f1 (ppm)







# NMR data for **thioformamide 363**

